



**UNIVERSIDAD
DE GRANADA**

DEPARTAMENTO DE FARMACIA Y TECNOLOGÍA FARMACÉUTICA,
FACULTAD DE FARMACIA - UNIVERSIDAD DE GRANADA

Tesis Doctoral con Mención Internacional

**Aplicaciones farmacéuticas de aluminosilicatos
mesoporosos: estudio de arcillas fibrosas (sepiolita y
palygorskita) en geles con agua mineromedicinal**

* * *

**Pharmaceutical applications of mesoporous
aluminosilicates: studies of fibrous clay minerals (sepiolite
and palygorskite) in spring water hydrogels**

Fátima García Villén

Programa de Doctorado en Farmacia

Granada, noviembre de 2020

Editor: Universidad de Granada. Tesis Doctorales
Autor: Fátima García Villén
ISBN: 978-84-1306-711-7
URI: <http://hdl.handle.net/10481/65331>

La presente Tesis Doctoral ha sido financiada por el proyecto del Plan Nacional de I+D+i CGL2016-80833-R, proyecto de la junta de Andalucía P18-RT-3786 y por el Grupo de Investigación CTS-946 de la Junta de Andalucía. La doctoranda ha disfrutado de una beca FPU del plan nacional convocatoria 2015 (FPU15/01577). El trabajo ha sido desarrollado en los laboratorios del Departamento de Farmacia y Tecnología Farmacéutica de la Universidad de Granada y del Dipartimento di Scienze del Farmaco de la Università di Pavia (Italia).

*Agradezco profundamente a César, mi director de Tesis, mi tutor, mi puerta hacia la investigación, la puerta de mi carrera. A Carola, por su sabiduría y disponibilidad, pero sobre todo por su generosidad y tremendo cariño. A Pilar, una líder excepcional, luchadora incansable en favor de los intereses de los que estamos abajo. A mis compañeras Rita y Ana, con las que he compartido los mejores momentos de este camino. A Giuseppina, che mi ha spalancato le porte del suo laboratorio durante il mio soggiorno in Italia. Junto con ella, especial agradecimiento a Angela, Dalila y Barbara, che sono state il mio supporto tecnico... e anche le mie amiche. A mis amigos de siempre, por estar a mi lado y alegrarse de mis alegrías y llorar por mis penas. A Pablo. Y principalmente, a mi familia, el centro de mi Universo, el pilar de mi vida. A **papá**, a mamá, que siempre me llevarán de la mano.*

Índice

ÍNDICE

INTRODUCCIÓN

Chapter 1 - Clay Minerals and Skin.....	6
1.1. Clay Minerals in Drug Delivery Systems.....	11
1.1.1. Layered Clay Minerals.....	13
1.1.2. Tubular and Fibrous Clay Minerals	30
1.1.3. Future Trends	47
1.2. Clay Minerals in Skin Drug Delivery	48
1.2.1. Skin Anatomy and Physiology.....	49
1.2.2. Routes and targets on, into, and through skin drug delivery .50	
1.2.3. Quality and Performance of Topical Drug Products.....	51
1.2.4. Clay Minerals Functions in Topical Products	53
1.2.5. Summary and Outlook.....	68
1.3. Natural Inorganic Ingredients in Wound Healing	69
1.3.1. Functions of Inorganic Ingredients in Wound Healing	74
1.3.2. Clay Minerals for Wound Healing	78
1.3.3. Other Inorganic Materials for Wound Healing.....	96
1.3.4. Conclusions.....	109
1.4. Abbreviations	110
References	114
Chapter 2 - Layered Clay Minerals in Wound Healing.....	145
2.1. Characterisation of Andalusian Peats for Skin Health Care Formulations.....	149
2.1.1. Materials and Methods.....	150
2.1.2. Results and Discussion.....	153
2.1.3. Conclusions.....	161
2.2. Montmorillonite-Norfloxacin Nanocomposite Intended for Healing of Infected Wounds.....	162
2.2.1. Materials and Methods.....	164

2.2.2.	Results and Discussion	168
2.2.3.	Conclusions	179
2.3.	Abbreviations	180
References		181

OBJETIVOS

Chapter 3 - Objetivos y Plan de Trabajo		188
3.1.	Objetivos de la Tesis	190
3.1.1.	Objetivos específicos	192
3.1.2.	Plan de Trabajo	193
Referencias		195

RESULTADOS Y DISCUSIÓN

Chapter 4 - Fibrous Clays in Wound Healing		198
4.1.	Design and Characterization of Spring Water Hydrogels with Natural Inorganic Excipients.....	203
4.1.1.	Materials and Methods	205
4.1.2.	Results and Discussion	210
4.1.3.	Conclusions	237
4.2.	Wound Healing Activity of Nanoclay/Spring Water Hydrogels	239
4.2.1.	Materials and Methods	242
4.2.2.	Results and Discussion	247
4.2.3.	Conclusions	266
4.3.	Safety of Nanoclay/Spring Water Hydrogels: Assessment and Mobility of Hazardous Elements.....	267
4.3.1.	Materials and Methods	271
4.3.2.	Results	276
4.3.3.	Discussion.....	279
4.3.4.	Conclusions	287



4.4.	Correlation between Elemental Composition/Mobility and Skin Cell Proliferation of Fibrous Nanoclay/Spring Water Hydrogels	289
4.4.1.	Materials and Methods.....	290
4.4.2.	Results	294
4.4.3.	Discussion.....	299
4.5.	Abbreviations.....	311
References	313

CONCLUSIONES

Chapter 5 - Conclusiones	340
---------------------------------	-------	------------

ANEXOS

Anexo A - Material adicional del Capítulo 4	346
Figura	347
Tabla	348
Anexo B - Indicios de Calidad de las Publicaciones	350

Resumen

RESUMEN

Los aluminosilicatos son un amplio grupo de materiales mesoporosos en los que se incluyen tanto sustancias naturales como sintéticas y que presentan numerosas aplicaciones, muchas de ellas derivadas de sus características superficiales, y en particular de su porosidad y elevada superficie específica. Entre estos materiales, ocupan un lugar relevante los de origen natural, incluyendo, entre otros, las zeolitas naturales y algunos minerales de la arcilla. En nuestro caso, los aluminosilicatos de estudio pertenecen a las denominadas “arcillas especiales”, concretamente a las arcillas fibrosas, que son usadas como excipientes. En concreto, estas arcillas fibrosas son usadas en la formulación de hidrogeles de administración tópica empleados en distintos tratamientos. Un tipo particular de estos hidrogeles inorgánicos son aquellos en que el agua es mineromedicinal. Las acciones bioquímicas de estos hidrogeles con aguas mineromedicinales dependerán de la cantidad y velocidad con que los componentes disueltos penetran y/o permean a través de la piel. Los estudios centrados en la presencia de iones metálicos susceptibles de tener efectos biológicos (positivos o negativos) cuando se aplican estos geles son escasos y hasta la fecha poco concluyentes. Paralelamente, los materiales inorgánicos han demostrado ser útiles en el tratamiento de heridas de difícil curación.

Con estas premisas, el objetivo general de la tesis fue diseñar sistemas de tipo hidrogel constituidos por arcillas fibrosas y agua mineromedicinal destinados a su aplicación en heridas de difícil curación. En primer lugar, se hizo una profunda revisión del empleo de las arcillas especiales en sistemas de liberación modificada, con especial atención en formas farmacéuticas tópicas. Asimismo, se revisó el potencial de estos materiales inorgánicos en la curación de heridas. Se puso a punto la metodología específica necesaria para establecer la estabilidad, seguridad y eficacia de hidrogeles inorgánicos, así como para evaluar específicamente los efectos en heridas. De esta forma, se diseñaron hidrogeles preparados con dos aguas mineromedicinales y dos arcillas fibrosas (sepiolita y palygorskita). Tanto los excipientes como los hidrogeles fueron ampliamente caracterizados empleando difracción de rayos X, fluorescencia de rayos X, análisis térmicos, espectroscopía infrarroja, microscopía electrónica, estudios reológicos y ensayos específicos de

velocidad de enfriamiento. Especial atención se prestó a la pureza de las arcillas (identidad, pureza y riqueza del excipiente empleado) y al comportamiento reológico y estabilidad de las formulaciones semisólidas. Conocidos estos parámetros técnicos, se estudió la biocompatibilidad *in vitro* de los hidrogeles, así como la actividad *in vitro* de los hidrogeles en la curación de heridas empleando cultivos celulares de fibroblastos y ensayos de cierre de heridas. Algunas formulaciones demostraron una alta eficacia terapéutica, por lo que se profundizó en el estudio de los mecanismos implicados en estos efectos. En concreto se llevaron a cabo estudios de liberación de elementos presentes en los hidrogeles mediante celdas de Franz, evaluando tanto los potenciales efectos adversos asociados a determinados componentes como aquellos que permiten explicar la actividad terapéutica sobre la piel, y más concretamente sobre la curación de heridas. La cuantificación de los elementos liberados se hizo mediante espectrometría de plasma de acoplamiento inductivo (ICP), tanto óptico como de masas, alcanzando sensibilidades de partes por trillón.

Los resultados del estudio realizado permiten concluir que formulaciones de tipo hidrogel constituidas por arcillas de elevada pureza y agua mineromedicinal muestran efectos terapéuticos relevantes en la curación de heridas, determinados por la presencia de elementos químicos que son liberados desde el hidrogel a la piel. En particular, el calcio, sodio, potasio y magnesio en determinadas concentraciones favorecen la proliferación y movilidad de fibroblastos. Otros elementos como el zinc en determinada proporción con el calcio presentaban efectos proliferativos. La seguridad de las formulaciones fue evaluada para asegurar la ausencia de liberación de elementos que pueden comprometer el empleo, tales como metales pesados, que están de forma natural en los componentes de los hidrogeles inorgánicos estudiados.

ABSTRACT

Aluminosilicates are a wide group of mesoporous materials of natural or synthetic origin. Aluminosilicates have numerous uses and applications mainly due to their surface properties such as porosity and high specific surface. Natural ones are those with higher relevance, such as natural zeolites and clay minerals. In the present study, “special clays” and, more particularly, fibrous clays (sepiolite and palygorskite) are used as excipients of topical hydrogels. A particular case of clay hydrogels are those prepared with natural spring water (mineromedicinal water). Biochemical activity depends on the amount and rate of release and permeation of the dissolved components. Studies dealing with therapeutic effects (either positive or negatives) ascribed to chemical elements in the formulation are currently scarce and inconclusive. Nonetheless, inorganic materials have proven to be useful in wound healing treatments.

All that being said, the general objective of this PhD thesis was the design of hydrogels made of fibrous clays and spring waters as wound healing formulations. Firstly, a deep and detailed review of clay minerals as drug delivery systems, both in general and for topical formulations specifically, was performed. Moreover, the roles and uses of natural inorganic ingredients have also been reviewed. Secondly, the specific methodology for the study of stability, safety, hydrogel efficacy and wound healing activity were optimized. Therefore, fibrous clays/spring water hydrogels were prepared. Both clays, sepiolite and palygorskite, were deeply characterised by means of X-ray diffraction, X-ray fluorescence, thermal analysis, infrared spectroscopy, electronic microscopy, rheology and cooling kinetics. Special attention was paid to the purity of clay minerals (identity, purity and richness) and to the rheology and stability of the semisolid formulations. All the previous known and optimized, the *in vitro* biocompatibility was assessed together with the activity of hydrogels during *in vitro* wound closure (often known as “scratch assay”), all of the studies performed with fibroblasts cultures. Some systems demonstrated to have a high therapeutic activity, which incited to delve into the possible mechanisms of action. More particularly, release studies of elements present in the hydrogels were performed by means of Franz cells. Potential effects, either positive (elements

potentially involved in wound healing) or negative (evaluation of the release of hazardous elements), were addressed. To do so, released elements were quantified by means of inductively coupled plasma spectrometry (ICP-OES and ICP-MS), which allowed a sensitivity of parts per trillion.

The results of the present study led to conclude that hydrogels semisolid formulations made of high purity clay minerals and spring waters shown relevant wound healing therapeutic effects. Those effects have been ascribed to the presence and release of certain chemical elements. In particular, calcium, sodium, potassium and magnesium are released in concentrations able to improve wound healing. Other elements such as zinc, released in a certain amount and with a certain Zn:Ca ratio, enhanced fibroblasts proliferation. The safety of the hydrogels was also confirmed due to the low or absent release of hazardous elements (such as heavy metals), even if most of them are naturally present in the pristine ingredients.

Resumen

Chapter 1

Clay Minerals and Skin

1.1. Clay Minerals in Drug Delivery Systems

Prólogo

El uso farmacéutico de recursos naturales es el área de trabajo del grupo de investigación en el que ha sido realizada esta tesis doctoral. En particular, de entre las materias primas que son estudiadas en el grupo, el trabajo se ha centrado en las arcillas especiales, un tipo específico de materiales cuyo contenido en determinados minerales y propiedades que resultan les confieren un interés industrial elevado. Estos sólidos inorgánicos naturales han sido usados en la elaboración de medicamentos y cosméticos desde la antigüedad y siguen teniendo un papel fundamental, principalmente como excipientes. Entre ellos destaca el talco, que a día de hoy sigue siendo uno de los diez excipientes más usados. Otras arcillas especiales permiten el diseño y desarrollo de nuevas formas farmacéuticas.

El primer capítulo de la tesis profundiza precisamente en el conocimiento de los materiales arcillosos usados en el desarrollo de sistemas de liberación de fármacos. Muchos de los estudios revisados en esta primera sección no están directamente enfocados a una vía de administración determinada (sección 1.1). Como quiera que el objetivo final de la tesis está centrado en una vía de administración (tópica) y una patología (heridas de difícil curación), la sección 1.2 profundiza específicamente en los sistemas farmacéuticos con arcillas de administración tópica, mientras que la tercera (sección 1.3) está específicamente centrada en los usos de materiales inorgánicos naturales (tales como arcillas y zeolitas) en la curación de heridas.

Finalmente, y siguiendo la normativa establecida por la Escuela de Doctorado en Farmacia, se indican los indicios de calidad de las publicaciones científicas que conforman el presente capítulo:

Sección 1.1.

García-Villén, F., Carazo, E., Borrego-Sánchez, A., Sánchez-Espejo, R., Cerezo, P., Viseras, C., Aguzzi, C. Clay minerals in drug delivery systems. In: *Modified Clay and Zeolite Nanocomposite Materials*; Mercurio, M., Sarkar, B., Langella, A., Eds.; Elsevier Inc., 2019 ISBN 978-0-12-814617-0.

1.1. Clay Minerals in Drug Delivery Systems

Indicios de calidad de la publicación:

- Capítulo de libro – Editorial Elsevier
- Scholarly publishers indicators (general SPI): Q1. ICEE = 319 (2018).

Sección 1.2.

Viseras, C., Carazo, E., Borrego-Sánchez, A., García-Villén, F., Sánchez-Espejo, R., Cerezo, P., Aguzzi, C. **Clay minerals in skin drug delivery**. Clays and Clay Minerals, 2019, 67, 59–71. " fl ¶

Indicios de calidad de la publicación:

- Artículo científico
- Indexada en JCR: [CLAY CLAY MINER](#)
- Factor de impacto 2019: 1.507
- Ranking: Q3 (geosciences, multidisciplinary).

Sección 1.3.

García-Villén, F., Souza, I.M.S., de Melo Barbosa, R., Borrego-Sánchez, A., Sánchez-Espejo, R., Ojeda-Riascos, S., Viseras, C. **Natural inorganic ingredients in wound healing**. Current Pharmaceutical Design, 2020, 26. " fl

Indicios de calidad de la publicación:

- Artículo científico
- Indexada en JCR: [CURR PHARM DESIGN](#)
- Factor de impacto 2019: 2.208
- Ranking: Q3 (pharmacology & pharmacy).



1.1. Clay Minerals in Drug Delivery Systems

Drug delivery is the first step occurring once a medicine is administered to the body, and must guarantee the maintenance of a safe and effective drug concentration in the site of action during the treatment. Drug bioavailability, i.e., the rate and fraction at which the administered dose reaches the site of action, greatly depends on the design of the drug delivery system (DDS). All pharmaceutical dosage forms may be considered DDS, as they transport, protect and deliver a drug through the proper route of administration to obtain a therapeutic effect. Conventional dosage forms lead to possible overdosing or underdosing periods in plasma concentrations (Figure 1.1).

Modified drug delivery systems (MDDSs) are designed to improve drug bioavailability and/or minimize adverse effects, by changing the rate and/or time and/or site of drug release in comparison with conventional dosage forms. MDDSs are considered as useful strategies to ameliorate patient compliance (Sastry et al., 2000), and MDDSs include prolonged-release systems, delayed-release systems, and site-specific systems (Ph.Eur.9th., 2017). Prolonged-release systems are those in which the drug is released within a more extended period, compared with conventional dosage forms. Delayed-release systems are able to delay drug release for a certain time lapse, after which it occurs in a conventional way. Site-specific dosage forms perform drug delivery at the diseased tissue/organ or in the physiological drug receptor location.

The design of an MDDS depends as much on the method of preparation as on the excipients employed. In this regard, clay minerals have been proposed as useful MDDS excipients, due to their effective interactions with drug molecules, inertness, swelling capacity, abundance, and low toxicity (Aguzzi et al., 2007; Viseras et al., 2010, 2015; Rodrigues et al., 2013; Fakhrullina et al., 2015; Yang et al., 2016b; Jafarbeglou et al., 2016; Sandri et al., 2016; Carazo et al., 2018a). In certain cases it may be necessary to improve some clay properties, such as specific surface area, type of exchangeable cations, hydrophilic nature, zeta potential, interlayer space, or porosity, to engineer their performance as drug carriers and delivery systems. Raw clay minerals are usually treated to eliminate impurities and/or obtain homoionic

clay minerals (i.e., sodium derivatives). These are frequently named as natural excipients in contrast to those prepared by more specific treatments. In this regard, organic functionalization of clays, pillarization, or combination with polymers are highlighted as the most used clay modification strategies (Aguzzi et al., 2007; Viseras et al., 2008, 2010, 2015; Rodrigues et al., 2013; Liu et al., 2014; Yang et al., 2016b; Nazir et al., 2016; Meirelles and Raffin, 2017). This chapter focuses on the last decade's advances in the use of natural and functionalized clay minerals as well as clay/polymer nanocomposites in drug delivery.

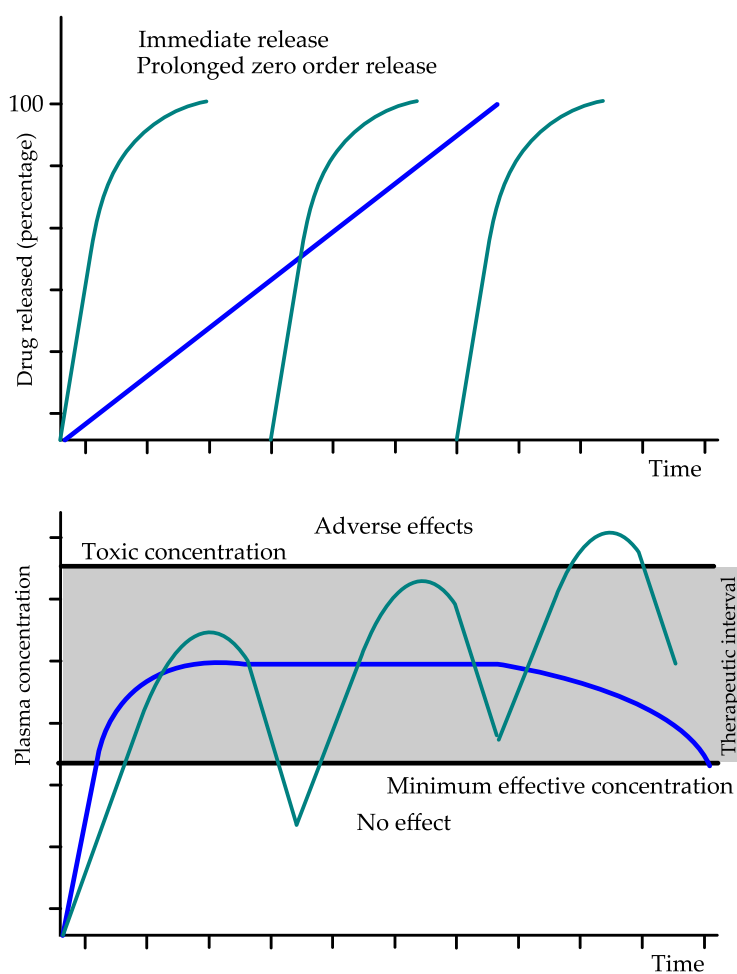


Figure 1.1. Schematic representation of the correlation established between drug release profiles and plasma concentrations. Modified from (Viseras et al., 2010)

1.1.1. Layered Clay Minerals

Two groups of layered clay minerals are frequently used as MDDS excipients: smectites (2:1 phyllosilicates) and kaolin (1:1 phyllosilicate).

Smectites are a group of layered clay minerals including montmorillonite (MMT), saponite, hectorite, beidellite, and nontronite, among others. As pharmaceutical excipients, these minerals are included in two pharmacopeial monographs: bentonite (mainly composed of MMT) and magnesium aluminium silicate (mainly composed of saponite and MMT) (Ph.Eur.9th., 2017). Other smectites are used in the design of MDDS once modified (e.g., disteardimonium hectorite, stearalkonium hectorite, quaternium-18 hectorite).

MMT is the most commonly used smectite in pharmaceutical applications. It possesses a dioctahedral structure in which Si(IV) atoms coordinate with oxygen, thus forming tetrahedral sheets that confine an octahedral sheet formed by Al(III) atoms also coordinated with oxygen. Typical Al isomorphic substitutions include Mg(II) and Fe(II), thus giving the structure a negative charge that is compensated by metal cations in the interlayer space. Ideal chemical structure of MMT has been defined as $\text{Si}_8\text{Al}_{3.5}\text{Mg}_{0.5}\text{O}_{20}(\text{OH})_4$ (Schoonheydt and Jonhston, 2006). The incorporation of a drug between MMT interlayers, which sometimes can even produce clay mineral exfoliation, can be easily detected by X-ray diffraction (XRD) analysis by observing a characteristic shift in the d-001 value of the mineral. Both natural and functionalized MMT have been widely used in drug delivery (Aguzzi et al., 2007; Park et al., 2016). However, the combination of MMT with polymers is one of the most currently extended strategies, leading to MMT-polymer nanocomposites (Viseras et al., 2008).

Kaolinite is the most common clay mineral of the kaolin group. It possesses a 1:1 structure, and it is composed of repetitive units of SiO_4 tetrahedral layers bonded to $\text{Al}(\text{O},\text{OH})_6$ octahedral layers through apically shared oxygen atoms. In relation to DDSs, and compared with other types of clay minerals, kaolinite is not as widely used as MMT or palygorskite. Nevertheless, studies performed with kaolinite on drug delivery issues

showed promising results, and have been focused on basic drugs (Holešová et al., 2014).

1.1.1.1. Natural Layered Clay Minerals

Table 1.1 summarizes examples of some most recent clay-based MDDS. In most cases, MMT, sometimes activated or functionalized or in combination with saponite, was used.

Diclofenac sodium is one of the most prescribed nonsteroidal antiinflammatory (NSAID) drugs, though extensive side effects are reported due to the frequent doses needed and short half-life of the active ingredient. Prolonged-release systems would help to minimize such problems with diclofenac sodium. MMT demonstrated an effective control of diclofenac release (76% (w/w) of loaded drug was dissolved in phosphate buffer medium (pH 7.4) after 8 h) (Kaur and Datta, 2014).

Chlorhexidine is a bacteriostatic and bactericidal agent widely used for sterilizing purposes since it is active against Gram-positive and Gram-negative bacteria, molds, yeasts, and viruses. Chlorhexidine dosage forms usually show erratic release profiles, and may result in toxicity to human dermal fibroblasts when topically applied. Na⁺-MMT was chosen as a chlorhexidine carrier in systems intended to be used as topical DDS with improved release properties (Saha et al., 2014a).

Na⁺-MMT was also demonstrated to be able to protect labile molecules from external agents such as light. Promethazine is a photolabile antihistamine topically administered to treat insect bites and erythema. Its degradation, when exposed to light, could cause cutaneous photoreactions. After MMT intercalation, photostability and diffusion-prolonged release of promethazine in *in vitro* Franz cell tests were accomplished (Ambrogi et al., 2014). The authors attributed the enhanced photostability to the confined space in which the drug was located after intercalation within MMT. This formulation consequently reduced the mobility of free electrons and oxygen species, avoiding drug alterations

Intercalation of anticancer drug paclitaxel in a Na⁺-MMT was optimized by Bothiraja and co-workers. Subsequently, the resultant system was coated with a natural polysaccharide (chitosan, CS). Results showed a

1.1. Clay Minerals in Drug Delivery Systems

controlled release of paclitaxel and an improvement of its *in vitro* anticancer activity (Bothiraja et al., 2014).

Gallic acid is a natural molecule extracted from gallnut, tea, cherries, and other plants. It is widely known by its antioxidant activity and also some antimutagenic, anticarcinogenic, antiinflammatory, and antimicrobial activities. Nevertheless, it is also a molecule with poor solubility, permeability, high instability, and fast metabolism. Rabiei and co-workers suggested the necessity of an MDDS to overcome these problems. They recently loaded gallic acid into MMT, and the adsorption/desorption of the active substance was evaluated in terms of pH and contact time. The measured lower loading capacity of MMT in neutral pH was ascribed to the formation of gallate anions. The authors claimed that, according to thermogravimetric analyses, stronger linkages existed between gallic acid adsorbed at neutral pH than acidic pH. On the other hand, release studies were conducted in simulated human cell fluid at pH 7.4, and no differences were found: ~70% (w/w) of gallic acid was released in 1 h, and total dissolution was obtained after 6 h for both the drug/clay hybrids prepared at acidic and neutral pH values (Rabiei et al., 2016).

Treatment of first grade burn wounds should be addressed by antibacterial, moisturizing, and analgesic compounds. With this objective, dermal patches made of Na⁺-MMT, silver, lidocaine, and betaine hydrochloride were prepared (Rangappa et al., 2017). Silver would act as a prophylactic antimicrobial agent, and lidocaine would minimize the pain. MMT would act as a skin smoothening agent and control the release of the drug. *In vitro* results showed that lidocaine was released in considerable and gradual amounts, and was also able to penetrate the skin due to its lipophilic nature. Nevertheless, the authors claimed that the *in vivo* model used in the study was limited, and further studies are needed to confirm the effectiveness of the clay-based dermal patch.

Metformin, an oral antidiabetic drug, has been recently intercalated in Na⁺-MMT to evaluate the usefulness of the resultant system in the control release of the drug (Rebitski et al., 2018). The authors aimed to create a dosage form able to maintain effective doses over prolonged periods to reduce doses and, therefore, side effects. *In vitro* release results showed that drug release

depended highly on the pH of the medium, although authors stated the necessity of further studies since the amount of drug released in an acidic environment (pH 1.2) was too high and fast (40%-50% (w/w) total metformin amount released in 2 h).

Silver and titanium dioxide were proposed as useful antibacterial agents with low toxicity levels. These two agents were loaded onto Na⁺-MMT by a thermal decomposition method (Krishnan and Mahalingam, 2017). On this occasion, *Staphylococcus aureus* and *Escherichia coli* were chosen as Gram-positive and Gram-negative bacteria, respectively. MMT-Ag-TiO₂ possessed an enhanced antibacterial activity, and the material was more intense against *E. coli* than *S. aureus*.

5-Aminosalicylic acid (mesalazine) is widely used for treating Crohn's disease and ulcerative colitis. Therapeutic amounts of the drug should reach the colon for the treatment to be effective. However, 5-aminosalicylic acid is mainly absorbed in the upper part of the gastrointestinal tract. MMT was used as a mesalazine carrier to prolong the drug release, and the system was then encapsulated in alginate (ALG) beads able to further reduce the drug dissolution in the acidic environment of the stomach (Hong et al., 2017). The MMT-mesalazine system immediately released more than 25% (w/w) of mesalazine in the gastric solution, while ALG-MMT-mesalazine beads released, 5% (w/w) of the total amount of drug in the same medium.

Acid activation of Na⁺-MMT generates pores and discontinuities on the clay layered structure, which effectively improves the clay surface area, along with interlayer charge modifications. MMT, treated with HCl at different concentrations, was evaluated as a ciprofloxacin carrier (Wu et al., 2017). Results showed that acidic treatment allowed a significant reduction of the drug release rate, being slower at a higher HCl concentration during the acid treatment of MMT. This effect was due to the amount of charges in the MMT interlayer spaces: a stronger interaction with ciprofloxacin molecules was established at a higher concentration of HCl, thus retarding the drug release process. Consequently, this study demonstrated the possibility to control drug release rates by defining the interlayer charge behaviours of a smectite clay.

1.1. Clay Minerals in Drug Delivery Systems

Table 1.1. Most recent layered clay/drugs combinations as drug delivery systems

	Clay Mineral	Interaction Methodology	Drug	Ref
Natural MMT	MMT	Intercalation solution	Diclofenac sodium	(Kaur and Datta, 2014)
			Chlorhexidine	(Saha et al., 2014a)
			Promethazine	(Ambrogi et al., 2014)
			Paclitaxel	(Bothiraja et al., 2014)
			Gallic acid	(Rabiei et al., 2016)
			Silver, lidocaine	(Rangappa et al., 2017)
			Praziquantel	(Borrego-Sánchez et al., 2017)
			Metformin	(Rebitski et al., 2018)
		Intercalation solution + thermal treatment	Silver and titanium dioxide	(Krishnan and Mahalingam, 2017)
		Intercalation solution + ALG coating	Mesalazine	(Hong et al., 2017)
	Acid-treated MMT	Intercalation solution	Ciprofloxacin	(Wu et al., 2017)
			AgNP	(Phukan et al., 2017)
			AgNP	(Roy et al., 2017)
Others	MMT-saponite	Intercalation solution	Tetracycline	(Aguzzi et al., 2014a, 2014b)
			Gentamicin	(Rapacz-Kmita et al., 2017a, 2017b)
			Theophylline	(Trivedi et al., 2018)
	Kaolinite		Ciprofloxacin	(Hamilton et al., 2014)
Functionalized	Pillared MMT	Intercalation solution	Nitric oxide	(Fernandes et al., 2013)
	Silica pillared MMT		Acetylsalicylic acid	(Mao et al., 2014)
			Ibuprofen	(Mao et al., 2016)
	Kaolinite		Doxorubicin	(Zhang et al., 2017)

In a recent work, silver nanoparticles were loaded in an activated Na⁺-MMT by an intercalation process (Phukan et al., 2017). According to the authors, silver nanoparticles were loaded inside the newly formed pores by

acid activation of Na⁺-MMT. No *in vitro* release studies were performed for this system, although the antibacterial activity was tested against *S. aureus* (Gram-positive) and *Proteus vulgaris* (Gram-negative) bacteria. Bigger inhibition zones were found in the case of *S. aureus* than for *P. vulgaris*, which led the authors to think a stronger activity of the clay hybrid against Gram-positive bacteria. A similar recent study by Roy and co-workers compared the loading capacity and the antibacterial activity of the resultant MMT-silver hybrids by using both non-acid activated Na⁺-MMT and acid-activated one (Roy et al., 2017). Silver nanoparticle loading capacity of acid-activated MMT was higher than non-acid activated MMT due to an improved cation exchange capacity (CEC) of the acid-activated material. Moreover, in comparison with the non-acid activated system, the acid activated MMT-silver system showed a more effective antibacterial activity against *E. coli* and *S. aureus*, ascribable to the smaller sized silver nanoparticles obtained in the MMT-silver hybrid.

Veegum[®] HV is a pharmaceutical excipient made of pharmaceutical grade MMT and saponite, and has been used as a tetracycline (antibiotic drug) carrier (Aguzzi et al., 2014a). Successful intercalation of the drug was achieved in the clay minerals. The drug release rate in simulated gingival fluid could allow the use of the resultant drug/clay hybrid as a periodontal extended release system. Chitosan gel was used as mucoadhesive base for application of the hybrid into the periodontal pocket, and the drug release results were compatible with a once-weekly administration regimen (Aguzzi et al., 2014b).

Veegum[®] F is also a pharmaceutical excipient composed of a mixture of natural smectites, specifically saponite and MMT. It was used to load gentamicin, an aminoglycoside antibiotic. Rapacz-Kmita and co-workers studied the intercalation of gentamicin in Veegum[®] F by a solution intercalation method at different temperatures (20 °C, 50 °C, and 80 °C) for 24 h to establish the optimum intercalation conditions. Moreover, they evaluated the antibacterial activity of the resultant composite against *E. coli*. Temperature was demonstrated to have influence on the drug loading efficiency, with 50 °C being optimal. All systems provided a sustained release of the drug up to 8 days, and thus high antibacterial effects, according to inhibitory zone tests (Rapacz-Kmita et al., 2017a). The subsequent release study of gentamicin loaded onto Veegum F composite at 50 °C showed a fast

1.1. Clay Minerals in Drug Delivery Systems

release within the first 12 h followed by a sustained release until reaching a plateau after 2 days (Rapacz-Kmita et al., 2017b).

Theophylline is a drug used in the treatment of asthma and chronic obstructive pulmonary disease due to its bronchodilator activity. The acidic environment of the stomach induces premature drug absorption and produces variable plasmatic drug levels and undesirable gastric side effects. Theophylline was loaded into Veegum® F with two objectives: avoid gastric drug absorption and perform a sustained drug release once in the intestine (Trivedi et al., 2018). The protonated cationic form of theophylline established electrostatic interactions with the anionic clay layers, which was improved with a drop in pH of the environment. Because of that, no detectable amount of drug was released at pH 1.2 during 72 h. On the other hand, in an alkaline environment, the drug was released in a sustained manner during the whole period.

Kaolin-ciprofloxacin systems showed higher *in vitro* antibacterial activity against *Staphylococcus epidermidis* and *Propionibacterium acnes* compared with similar ciprofloxacin systems prepared with two synthetic clays (MMT-K10 and Laponite) (Hamilton et al., 2014). The authors ascribed this effect to weaker Drug-clay interactions, which allowed easier ciprofloxacin release. No antibacterial effect was shown by kaolinite itself, thus guaranteeing that the antibacterial activity was solely due to the drug.

1.1.1.2. Functionalized Layered Clay Minerals

Organic functionalization of smectites is usually carried out by grafting the clay mineral with cationic surfactants (i.e., exchanging the interlayer cations with a quaternary ammonium compound). Another type of functionalization to which Na⁺-MMT can be subjected includes the exchange between interlayer Na⁺ cations by monomeric cations such as 4-(dimethylamino)-1-(4-vinylbenzyl) pyridinium chloride and 1-methyl-3-(4-vinylbenzyl) imidazolium chloride (Mahkam et al., 2015). These functionalized layered clay minerals have been proposed in MDDS (Table 1.1).

Pillared clays are a type of functionalized layered phyllosilicates characterized by an increased permanent porosity. They are obtained by

exchanging interlayered cations by bulky inorganic compounds, which are subsequently calcinated. This technique allows to increase the interlayer space of the clay as well as to create micro and mesoporosity. Consequently, pillarization produces specific surface area enlargement and potential drug adsorption, thus the pillared minerals could hold bulky molecules. A pillared interlayered MMT was synthesized by different procedures and their nitric oxide adsorption/desorption studied (Fernandes et al., 2013). Results claimed that simple MMT pillarization procedures were a promising alternative for nitric oxide storage and release. Pillarization of Ca^{2+} -MMT in the presence of Fe^{2+} and Fe^{3+} led to a product with mesoporous structure and magnetic properties, and the system was loaded with acetylsalicylic acid (Mao et al., 2014). The investigators claimed a sustained release of the drug, which reached its maximum at about 20 h. Magnetic properties of this kind of nanocomposite would permit site-specific releases.

Natural MMT was magnetically functionalized with Fe_3O_4 to create a silica-pillared clay, and ibuprofen was loaded into the composite (Mao et al., 2016). Release profiles under magnetic field influence were compared with release profiles of the corresponding nanocomposites without magnetic influence. A clear delay in ibuprofen release was measured under magnetic field. This effect was related to the aggregation of the composite under magnetic influence.

Natural kaolin platelets were functionalized with different products to increase the interlayer space of the kaolinite: dimethyl sulfoxide, methanol, 3-aminopropyltriethoxy silane (APTES), medium-chain hexylamine, and long-chain dodecylamine. Then, doxorubicin was loaded by an intercalation method in a phosphate buffer solution (Zhang et al., 2017). All the functionalized kaolinites loaded over 87% (w/w) of the drug and showed pH-responsive release behaviour and therapeutic effect against 10 different cancer cell lines.

1.1.1.3. Layered Clay/Polymer Nanocomposites

Examples of some most recent layered clay mineral/polymer nanocomposites are summarized in Table 1.2. In most nanocomposites, MMT

1.1. Clay Minerals in Drug Delivery Systems

(natural or functionalized) was combined with both natural and synthetic polymers.

Veegum[®] HS (pharmaceutical excipient made of MMT) was combined with CS as a potential MDDS of 5-aminosalicylic acid (Aguzzi et al., 2010). Results showed an effective interaction between the clay and the polymer. Both components showed to have a synergistic effect over 5-aminosalicylic acid loading and release control (higher loading capacity and slower drug release rate), compared with the corresponding CS/drug and MMT/drug interaction products.

Veegum[®] HS was also combined with CS to prepare an oxytetracycline carrier (Salcedo et al., 2014). Oxytetracycline is a broad-spectrum bacteriostatic agent that should be administered in high doses to compensate its oral absorption variations. The study by Salcedo and co-workers aimed to improve oral bioavailability of the drug. The authors found that permeation rate of the drug through Caco-2 cell cultures proceeded linearly and constantly. Moreover, cellular internalization of the nanocomposite was found, which suggested that the absorbed drug was able to elude the efflux transporter P-glycoprotein system, thus improving oxytetracycline oral bioavailability (Salcedo et al., 2014).

CS/Na⁺-MMT films were proposed as chlorhexidine release systems (Ambrogi et al., 2017). The authors studied how to reduce chlorhexidine cytotoxicity to human fibroblasts and to perform a topical controlled release of the drug. Prepared films performed a sustained release. MMTs presence in clay-polymer composites induced a reduction of the drug release profile and burst release step. Cytotoxicity results were in agreement with the dissolution profile, and sustained release composites were not cytotoxic. Moreover, toxicity was correlated with the amount of loaded drug in the system.

Silver sulfadiazine is the main drug to treat topical burns. Nonetheless, cytotoxicity was reported, which delays the wound healing processes. In an attempt to reduce this drawback, silver sulfadiazine was successfully loaded into Veegum[®]HS/CS glutamate composites (Aguzzi et al., 2014a). Electrostatic interactions between the cationic polymer and MMT were reported. The presence of the drug in the nanocomposite was confirmed by high-resolution transmission electron microscopy (TEM) and elemental

analysis. Both biocompatibility and *in vitro* wound healing properties of this nanocomposite were assessed and confirmed (Sandri et al., 2014). Additionally, antimicrobial activity of the drug was not affected but actually improved against *Pseudomonas aeruginosa*.

Table 1.2. Most recent layered clay/polymer nanocomposites used in drug delivery

	Components	Interaction Methodology	Drug	Ref
Natural MMT	MMT/CS	Intercalation solution	Mesalazine	(Aguzzi et al., 2010)
			Oxytetracycline	(Salcedo et al., 2014)
			Chlorhexidine	(Ambrogi et al., 2017)
	MMT/CS-glutamate		Silver sulfadiazine	(Aguzzi et al., 2014a)
			Silver sulfadiazine	(Sandri et al., 2014)
	MMT/Guar gum		Ibuprofen	(Dziadkowiec et al., 2017)
	MMT/ALG	Ionotropic gelation	Venlafaxine	(Jain and Datta, 2016)
	MMT/ALG/XG	Intercalation solution	Olanzapine	(Oliveira et al., 2017)
	MMT/CMC		Curcumin	(Madusanka et al., 2015)
	MMT/PC/MC		Ketorolac	(Saha et al., 2016)
	MMT/PLLA		6-mercaptopurine	(Kevadiya et al., 2013)
	MMT/P(AAm-MA)		Caffeine	(Dadkhah et al., 2014)
	MMT/polyamide		Diazoles	(Salahuddin et al., 2014)
	MMT/silica based copolymers	Emulsion solvent evaporation	Doxorubicin, methotrexate, ciprofloxacin	(Bazmi Zeynabad et al., 2015)
			Dexamethasone	(Jain and Datta, 2015)
			Atenolol	(Lal and Datta, 2015)
MMT/PLGA		Insulin	(Lal et al., 2017)	

Guar gum, a galactomannan biopolymer extracted from the guar plant's seeds, was proposed as a nanocomposite ingredient with MMT to control the delivery of ibuprofen (Dziadkowiec et al., 2017). Nanocomposites provided a slow release rate of the drug, which could be useful in reducing

1.1. Clay Minerals in Drug Delivery Systems

ibuprofen side effects in the intestinal tract. Burst releases were also reduced by these formulations.

Sodium ALG was crosslinked with venlafaxine and MMT in CaCl₂ to obtain beads (Jain and Datta, 2016). Venlafaxine is a third generation antidepressive drug. The posology involves the administration of 2-3 daily doses, compromising patient compliance. MMT/ALG provides no more than 25% of venlafaxine released within 30 h in both media. Prolonged release was definitely obtained, although the amounts of drug released could be considered to be low.

Table 1.2. (Continued, part II)

	Components	Interaction Methodology	Drug	Ref
Natural MMT	MMT/PCLA-PEG-PCLA	Intercalation solution	Gemcitabine	(Phan et al., 2016)
	MMT/PLA	Nano-precipitation	Paracetamol	(Othman et al., 2016)
	MMT/HEMA	<i>In situ</i> radical polymerization	Paracetamol	(Bounabi et al., 2016)
	MMT/PEG750/5000-PE	Intercalation solution	Doxorubicin	(Kohay et al., 2017)
Functiona-lized MMT	Organomodi-fication MMT/Epoxy resin	<i>In situ</i> reduction	Copper nanoparticles	(Das et al., 2014)
	Organomodi-fication MMT/MAA	Intercalation solution	Naproxen	(Mahkam et al., 2015)
	Organomodified MMT/PCL	Nano-precipitation	Curcumin	(Bakre et al., 2016)
	Organomodi-fication MMT/PVP K30	Intercalation solution	Copaiba oil resin	(de Almeida Borges et al., 2016)
Others	MMT-Saponite/CS	Casting/solvent evaporation	Nicotine	(Pongjanyakul et al., 2013)
	Kaolinite-urea-chlorhexidine	Intercalation solution	Chlorhexi-dine	(Holešová et al., 2014)
	Kaolinite-PVP-sodium lauryl sulfate		Hetero-poly-oxometalate of tungsten	(Bayaumy and Darwish, 2016)
	HNT/PVA/CS	Swelling	5-FU	(Reddy et al., 2016)

ALG and xanthan gum (XG) were used to entrap sodium Cloisite®/olanzapine hybrids (Oliveira et al., 2017). Olanzapine is a poorly

water soluble and highly permeable drug used in schizophrenia and bipolar disorder. Release profile of the drug was compared with a commercial tablet, ALG-XG/olanzapine beads, and ALG-XG/Cloisite/olanzapine beads at different pHs (Figure 1.2). Commercial tablet showed a fast and complete release of drug within 30 min at acidic pH. ALG-XG/olanzapine beads showed remarkable olanzapine controlled release, reaching 100% (w/w) at 6 h. The addition of Cloisite allowed an even more marked control of drug release. This complex material utilizes the Cloisite-OLZ and the biopolymer blend of ALG-XG to produce a more controlled release of OLZ.

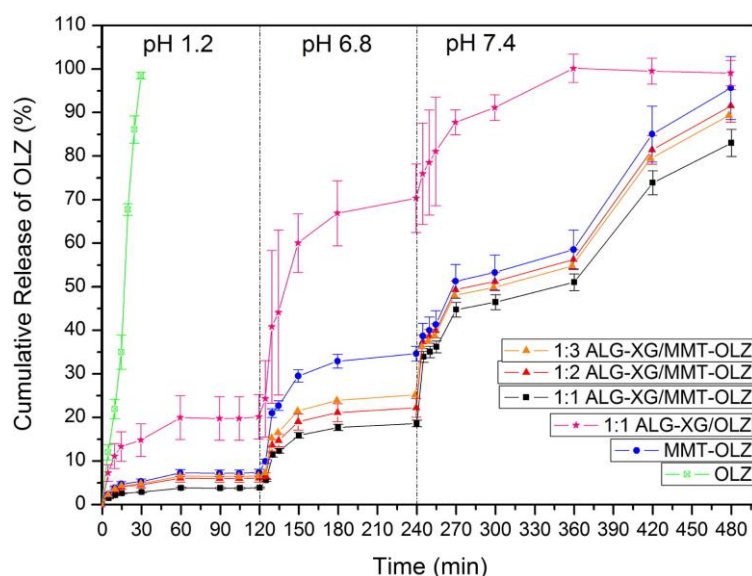


Figure 1.2. Cumulative release of olanzapine from hybrid materials at different pH values. Figure extracted from Oliveira et al. (2017)

Curcumin, extracted from the rhizome of *Curcuma longa*, is widely used as a food spice. It was demonstrated to have antibacterial, antioxidant, antiinflammatory, and anticancer properties. Curcumin aqueous solubility in acidic/neutral pH is remarkably low. Curcumin dispersed in carboxymethyl cellulose (CMC) was intercalated in MMT (Madusanka et al., 2015). The presence of CMC improved the dispersion of curcumin in aqueous environments prior to its intercalation into MMT. Despite curcumin's low solubility in acidic medium, the release rate of the drug in acidic pH conditions was significantly increased from the MMT/CMC nanocomposite.

1.1. Clay Minerals in Drug Delivery Systems

Nanocomposite films made of MMT, methyl cellulose and pectin in different proportions were prepared by Saha and co-workers. Ketorolac (an NSAID) was loaded on these films aiming to prepare a transdermal DDS. All the formulations performed ketorolac burst releases ascribable to the amount of drug located on the surface of the nanocomposite films. Nevertheless, the release rate decreased as the amount of MMT increased, thus demonstrating the useful effect of the clay mineral in terms of controlled release (Saha et al., 2016).

The anticancer drug 6-mercaptopurine was successfully intercalated into Na⁺-MMT prior to the formation of poly(L-lactide) acid (PLA) microspheres (Kevadiya et al., 2013). Microspheres containing MMT performed faster and had higher release rate of 6-mercaptopurine in comparison with microspheres prepared without MMT. The authors ascribed this behaviour to the low permeability of the polymer and low water solubility of the drug. Moreover, the presence of the clay mineral controlled drug release, as well as improved 6-mercaptopurine water solubility.

Poly(acrylamide-co-maleic acid) is a synthetic polymer considered to have a pH-dependent swelling behaviour (higher swelling at higher pH). This system would allow pH-dependent drug release when used as a drug carrier. Drug release mechanism was sensitive to hydrogel composition and was swelling-controlled for low concentrations of poly(acrylamide-co-maleic acid) and showed Fickian diffusion for high concentrations of the polymer (Thakur et al., 2012). In an attempt to improve poly(acrylamide-co-maleic acid) performance, MMT was added during in situ polymerization and caffeine loading/release was evaluated (Dadkhah et al., 2014). The authors claimed that the addition of small amounts of MMT (<5%, w/w) exerted a significant control during caffeine release, especially when pH of the release medium was changed from gastric to intestinal conditions. Burst release effect during pH change was also reduced.

1,3,4-Oxa(thia)diazoles were loaded into polyamide, and subsequently intercalated into Na⁺-MMT by ion exchange process (Salahuddin et al., 2014). Diazole derivatives are very versatile molecules in terms of therapeutic activities, since they can act as antibiotic, vasodilator, antifungal, cytotoxic, antiinflammatory, and analgesic agents. *In vitro* release

studies indicated that the resultant nanocomposites could be used as prolonged oral DDSs. Antimicrobial activity results were contradictory since no antimicrobial activity was detected *in vitro*, while *in vivo* experiments produced good results.

Two anticancer drugs, doxorubicin and methotrexate, together with the antibacterial molecule ciprofloxacin were combined with a silica based polymer/Na⁺-MMT to create a nanocomposite able to perform a site-specific release, mainly determined by the acidic pH of tumours (Bazmi Zeynabad et al., 2015). Burst releases were minimal in all *in vitro* release tests performed. Methotrexate and doxorubicin performed similar release profiles at pH 4 and 5.8 reaching ~80%-100% w/w of drug release within 25 days. In this period, the three drugs evaluated performed a prolonged release at pH 7.4, and ~20% (w/w) of total amount of drug was released. The difference between ciprofloxacin release profile at pH 5.8 and 4 was very distinct: at pH 5.8, the total amount of drug released within the total time lapse was less than 40% (w/w), whereas at pH 7.4 was less than 20% (w/w), and at pH 4 was close to 100% (w/w).

Poly(lactic-co-glycolic) acid (PLGA) is a safe, biodegradable, and biocompatible polymer extensively used and approved by the Food and Drug

Administration. PLGA/MMT were used as carriers of both dexamethasone (Jain and Datta, 2015) and atenolol (Lal and Datta, 2015). Atenolol molecule has short half-life and low intestinal permeability leading to low oral bioavailability and variable plasma concentrations during long-term treatments. An MDDS able to maintain effective doses of the drug for longer time would minimize the aforementioned problems. Atenolol was emulsified with PLGA, and then added to MMT to form a double emulsion (w/o/w) followed by solvent evaporation. Results showed the effective intercalation of PLGA-atenolol inside MMT layers in combination with a partial MMT exfoliation. In comparison with pure atenolol and commercial formulation, the MMT-PLGA-atenolol nanocomposites reduced the dissolution rate of the active substance in both acidic and alkaline media. In particular, the strongest change occurred in the acidic medium, where no burst release was reported (4% (w/w) of atenolol released within 30 min). The authors postulated that the presence of MMT imposed a longer path through

1.1. Clay Minerals in Drug Delivery Systems

which drug molecules should migrate before their release, thus explaining the modification in release profiles (Lal and Datta, 2015). Dexamethasone is a hydrophobic molecule, which clearly hinders its aqueous solubility. High doses are therefore required to achieve effective plasma concentration, and side effects such as osteoporosis can be encountered during long-term treatments of rheumatoid arthritis or bronchospasm. Emulsion solvent evaporation was used to intercalate the drug within MMT interlayer spaces in MMT/PLGA nanocomposites (Jain and Datta, 2015). *In vitro* drug release studies showed a high influence of the clay mineral during the dissolution of the active substance. The drug released steadily at acidic pH values, with a less remarkable burst effect in comparison with the pure drug, and reached 100% (w/w) before 25 h. Dissolution profile in simulated intestinal fluid reached approximately 60% (w/w) of total release in 30 h. No burst release was observed under these conditions, which strongly contrasted with pure dexamethasone.

The acid stability of MMT and its mucoadhesive properties could be useful to protect labile molecules such as proteins. A double emulsion solvent evaporation procedure was used to load insulin in MMT/PLGA nanocomposites (Lal et al., 2017). Successful intercalation of the drug was obtained according to XRD results, and the loaded nanocomposites did not influence the normal growth on HEK-293 cells. *In vitro* release studies showed that the presence of the clay mineral induced more sustained release profiles: insulin should travel a longer path before its dissolution. The amount of insulin released was higher in simulated intestinal fluid than in simulated gastric fluid, demonstrating the potential protective role of MMT.

Gemcitabine is an anticancer drug widely used in the treatment of solid tumours. It possesses a short half-life due to a fast metabolism, meaning frequent and high doses were needed. Among all strategies proposed within the past few years, intercalation of gemcitabine into MMT was found to be an effective way to control the drug release. In particular, a gemcitabine-MMT composite was combined with PCLA-PEG-PCLA triblock copolymer hydrogel to make it compatible with intravenous administration as well as to reduce side effects (Phan et al., 2016). The presence of MMT in the nanocomposite significantly controlled the release of the anticancer drug by

reducing burst release. *In vivo* experiments showed that therapeutic concentrations were maintained for several days, and this suppressed tumor growth without remarkable side effects.

Commercial organomodified MMT Cloisite 30B was combined with poly(D,L-lactide) to form nanoparticles able to carry and release paracetamol. During this synthesis, microfluidic mixing/precipitation was used (Othman et al., 2016). PLA is considered to be biodegradable and bioresorbable inside the human body. This composite was synthesized by mixing aqueous and organic phase in a glass capillary device. The inclusion of MMT increased the size of the resulting nanoparticles and improved the amount of drug encapsulated. In all cases, a burst release occurred, due to the high solubility of the drug in aqueous solution, followed by a very slow release, which was more pronounced as a higher proportion of clay was added.

Paracetamol dissolution profile was also intended to be modified by Na⁺-MMT/poly(2-hydroxyethyl methacrylate) (HEMA) nanocomposite (Bounabi et al., 2016). Combination of HEMA with MMT significantly decreased the burst release in comparison with the HEMA/paracetamol formulation.

PEG750/5000-PE polymer was combined with doxorubicin and then loaded over Na⁺-MMT (Kohay et al., 2017). As these nanocomposites were thought to be site-specific release systems, nanocomposite cellular internalization was tested. Polymers delayed the internalization but improved cytotoxicity due to the interruption of the P-gp pumps, which expel the drug outside of the cell.

Nanocomposites prepared with octadecylamine functionalized MMT and an epoxy resin were coated with copper nanoparticles by Das and co-workers. Enhanced antibacterial activity of the obtained material was thus reported (Das et al., 2014).

Functionalized MMT was polymerized with methacrylic acid, and naproxen was chosen as a drug model to evaluate drug loading capacity and release profiles. In acidic pH, all composites prepared showed a naproxen release <30% (w/w). On the other hand, at pH 7.4, the nanocomposite acquired

1.1. Clay Minerals in Drug Delivery Systems

a deprotonated stage, which generated electrostatic repulsions with the drug, thus explaining a higher release rate (Mahkam et al., 2015).

An organomodified MMT with (*n*-cetyl-*N,N,N*-trimethylammonium bromide) was combined with PCL to obtain a nanocomposite. Curcumin was included, and release studies were done in simulated intestinal fluid (Bakre et al., 2016). The MMT ratio in the nanocomposite influenced the amount of drug released in an indirect manner (the higher the MMT proportion, the lower the amount of curcumin released).

Copaiba oleoresin (COPA) is a natural molecule obtained from *Copaifera langsonii* able to reduce cyst size and increase apoptosis in endometrial explants. It is widely used in Brazil to treat endometriosis. Organomodified commercial MMT was combined with polyvinylpyrrolidone (PVP) K-30 to encapsulate COPA (de Almeida Borges et al., 2016). Nanocomposites showed a burst release profile, ascribable to the presence of adsorbed COPA to the nanocomposite surface. At acidic pH (1.2), the amount of COPA dissolved was 60% (w/w) within 15 min, and increased progressively during the rest of the test.

Veegum® HV was used to obtain nanocomposites with CS (Pongjanyakul et al., 2013). A direct relationship between the amount of clay and the nicotine loading capacity of the composites was found. Moreover, the presence of the clay was the main factor controlling the release profile of the drug. More particularly, as the ratio of clay increased in the composite, the mucosal permeation rate of the drug decreased.

One of the kaolinite optimization strategies to intercalate bulky substances inside kaolinite platelets is the use of polar molecules to expand the clay, and therefore, break the interlayer hydrogen bonds. With this method Holešová and co-workers prepared an antibacterial kaolinite/urea/chlorhexidine system. Minimum inhibitory concentration after antibacterial tests revealed that the hybrid provided an improved antibacterial effect: less concentration of chlorhexidine was needed to produce the same growth inhibition in comparison with the pure drug (Holešová et al., 2014).

PVP and sodium lauryl sulphate were used to exfoliate and functionalize kaolinite clay platelets. Then, heteropolyoxometalate of tungsten (HPW) was added as an active substance to treat schistosomiasis (Bayaumy and Darwish, 2016). *In vitro* HPW release occurred in a sustained manner and pilot *in vivo* studies results were also promising.

5-Fluorouracil (5-FU) is a rapidly metabolized drug and its oral absorption is very variable. 5-FU was recently encapsulated in a polymeric composite made of polyvinyl alcohol (PVA), CS, and MMT (Reddy et al., 2016). Results indicated that the higher was the amount of clay in the composite, the higher was the loading efficiency and the fraction of drug released.

1.1.2. Tubular and Fibrous Clay Minerals

Halloysite (Hal) is a clay mineral of the kaolin group, with dioctahedral 1:1 structure. In terms of chemistry, halloysite composition is the same as kaolinite though water is present between halloysite monolayers, thus it is known as the hydrated kaolinite phase (Brigatti et al., 2006). Hal particles can adopt different morphologies such as tubes, fibers, spheres, plates, laths, etc. The tubular morphology of halloysite is the most common one. Tube dimensions range from 0.2 to 2 μm in length; inner and outer diameters range from 10 to 40 nm and 40 to 70 nm (Liu et al., 2014). They are considered biocompatible, naturally abundant, and environmentally friendly materials. Tubular conformation causes aluminols (Al-OH) groups normally located in the interior of the tubes, while most of the silanols (Si-O-Si) are located in the outer part. This particularity explains why the outer surface of halloysite nanotubes is negatively charged and the inner surface is positive. The charges maintain at physiological pH (>2) (Qi et al., 2013; Tu et al., 2013). Hal nanotubes (HNTs) shape and properties make them very versatile in terms of drug carrying and drug release applications, including proteins as active substances (Lvov et al., 2014; Aguzzi et al., 2016; Lvov et al., 2016a, 2016b; Ariga et al., 2017; Minullina et al., 2017; Yendluri et al., 2017b). These substances can also be loaded into the lumen of HNTs under vacuum or using immersion techniques. HNTs have numerous advantages benefiting their interactions with chemically and biologically active molecules. Nevertheless,

1.1. Clay Minerals in Drug Delivery Systems

functionalizing HNTs could exert a huge difference to enhance their final properties, making them even able to interact with polymers and to form diverse nanocomposites. Functionalization processes could, however, reduce the biocompatibility, something that should be checked before human administration.

Besides HNTs, some other ribbon-shaped clay minerals are also used in drug delivery. In particular, fibrous phyllosilicates (palygorskite (Pal) and sepiolite (Sep)) show inverted tetrahedral arrangements that form ribbons and discontinuous octahedral sheets (Guggenheim and Krekeler, 2011). The resultant zeolitic channels are 3.7x6.4 Å (Pal) and 3.7x-10.6 Å (Sep) in diameter. Their use in drug delivery was reviewed previously (López-Galindo et al., 2011; Viseras et al., 2015).

In the following sections, the most recent progress in the use of tubular and fibrous clay minerals as advanced excipients in MDDS will be reviewed (Table 1.3) along with the nanocomposites prepared with these clay minerals (Table 1.4).

1.1.2.1. Natural Tubular and Fibrous Clay Minerals

5-Amino salicylic acid was encapsulated inside HNTs and over the nanotube surfaces (Viseras et al., 2008, 2009). The release of the drug was fitted to a novel kinetic model based on drug adsorption-desorption equilibrium. The superficially adsorbed drug released faster, while the drug located in the lumen of the tubes performed a more controlled and progressive release (Aguzzi et al., 2013b).

(Wang et al., 2014b) evaluated the effect of acid and heat treatment of HNTs and the influence of these treatments over ofloxacin loading and release behaviours. Under acidic conditions, HNTs maintained their crystallinity, though exchangeable cations were leached as HCl concentration increased. This caused weaker electrostatic interactions with ofloxacin, which led to a faster drug release. Temperatures higher than 400 °C caused dehydroxylation of aluminol groups, leading to a decrease in the drug adsorption capacity and faster drug release.

Table 1.3. Most recent tubular and fibrous clays/drugs combinations as drug delivery systems

	Clay Mineral	Methodology	Active Ingredient	Ref
Natural	HNT	Intercalation solution	5-Aminosallyclic acid	(Viseras et al., 2008, 2009; Aguzzi et al., 2013b)
			Ofloxacin	(Wang et al., 2014b)
			Tetracycline, ciprofloxacin, chlorpheniramine, diphenhydramine	(Jiang et al., 2016)
			Isoniazid	(Carazo et al., 2017b)
			Binase	(Khodzhaeva et al., 2017)
		Vacuum cycle	Breviscapine	(Gao et al., 2017)
		Intercalation solution, vacuum cycle	Vancomicin	(Pan et al., 2017)
		Vacuum cycle + PLGA coating	Tetracycline hydrochloride	(Qi et al., 2010, 2013)
		Vacuum cycle + CS/PLGA coating	Amoxicilin	(Tohidi et al., 2016)
		Vacuum cycle + PMMM coating	Paclitaxel	(Yendluri et al., 2017a)
	Pal	Intercalation solution	Ofloxacin	(Wang et al., 2014a)
			Isoniazid	(Carazo et al., 2018b)
		Vapor intercalation	Carvacrol	(Tenci et al., 2017)
	Sep	Intercalation solution	Praziquantel	(Borrego-Sánchez et al., 2017)
Pal or Sep	Melting intercalation + CD coground	Oxaprozín	(Mura et al., 2016)	

Drug loading capacities of HNTs and the mechanisms influencing drug loading processes of tetracycline, ciprofloxacin, chlorpheniramine, and diphenhydramine were investigated by (Jiang et al., 2016). CEC was determined to be the main factor controlling the drug loading. The pH of the medium influenced the drug loading process since it determined the ionization of the active substances (Jiang et al., 2016).

1.1. Clay Minerals in Drug Delivery Systems

Table 1.3. (Continued, part II)

	Clay Mineral	Methodology	Active Ingredient	Ref
Functionalized	Triazole-functionalized HNT	Intercalation solution	Curcumin	(Riela et al., 2014)
	APTES-functionalized HNT		Ag	(Zhang et al., 2013)
			AgNP	(Jana et al., 2017)
			Ibuprofen	(Tan et al., 2014)
			Vancomycin	(Kurczewska et al., 2017)
		Vacuum cycle	Metronidazole	(Xue et al., 2015)
	APTES-functionalized HNT/ALG/CS	Vacuum cycle	Ibuprofen	(Li et al., 2016a)
	Thiol-functionalized HNT	Vacuum cycle, intercalation solution	Silibin, curcumin	(Massaro et al., 2016b)
	Cysteamine hydrochloride-functionalized HNTs	Chemical reactions	Curcumin	(Massaro et al., 2016a)
AZPES-functionalized HNT	Condensation, vacuum cycle	Trolox, quercetin	(Massaro et al., 2016)	

Recent studies performed by (Carazo et al., 2017b, 2017a) explored the equilibrium and thermodynamic aspects of isoniazid adsorption onto HNTs. Isoniazid is one of the first-line drugs used to treat tuberculosis. Its presence on HNTs was confirmed by a fully comprehensive TEM study coupled with energy dispersive X-ray analysis (Figure 1.3). It was also shown that the isoniazid loading process occurred spontaneously since it increased the thermodynamic stability of the resultant system.

Specific anticancer treatments are focused on genetic treatments. Binase is an RNase enzyme of *Bacillus pumilus*, which triggers apoptosis in cancer cells expressing rat sarcoma oncogene. The immobilization of the enzyme in HNT and the resultant activity were studied by (Khodzhaeva et al., 2017). Optimal HNT-binase ratio was worked out and the resultant anticancer activity reported to be enhanced by the complex.

Unmodified HNTs were proposed as a potential sustained DDS of breviscapine, a short half-life, natural cerebrovascular drug extracted from *Erigeron breviscapinus*. The drug was loaded inside HNTs lumen by vacuum cycles, and *in vitro* phosphate buffer release was tested (Gao et al., 2017). HNT-breviscapine nanocomposite showed a slight reduction of the initial burst effect. Another drug vancomycin was loaded within the lumen of HTNs applying vacuum cycles (Pan et al., 2017). The resultant system released drug during a period of 33 days (a burst release occurred within the first 3 days). High antibacterial activity was also reported during the whole period against *S. aureus* and *B. streptococcus*.

A double drug loading process involving vacuum was used to load tetracycline and amoxicillin on HNTs, which were then coated with PLGA and CS polymers by electrospun technique (Qi et al., 2010, 2013; Tohidi et al., 2016). (Qi et al., 2010, 2013) reported that the cationic form of the drug, tetracycline hydrochloride, in solution interacted with the negative outer surface of HNTs, but it could also enter within the positively charged lumen of HNTs due to the applied vacuum during the drug loading process. The influence of the dissolution medium in which the drug and the clay mineral interacted with each other was crucial in terms of drug loading efficiency and release kinetics. In both experiments, the combination of PLGA and HNT allowed a sustained drug release since the initial burst weakened and no plateau was reached during the experiment (Qi et al., 2010, 2013). The combination of PLGA and CS with HNT-amoxicillin achieved via electrospun technique supported the aforementioned results in terms of controlled release behaviour (Tohidi et al., 2016). The authors highlighted the performance of HNT during amoxicillin release: CS and PLGA released amoxicillin faster than HNT-amoxicillin and HNT-CS-PLGA formulations. Burst release was remarkably prevented with the two latter formulations, confirming the importance of the clay mineral in the controlled delivery system.

1.1. Clay Minerals in Drug Delivery Systems

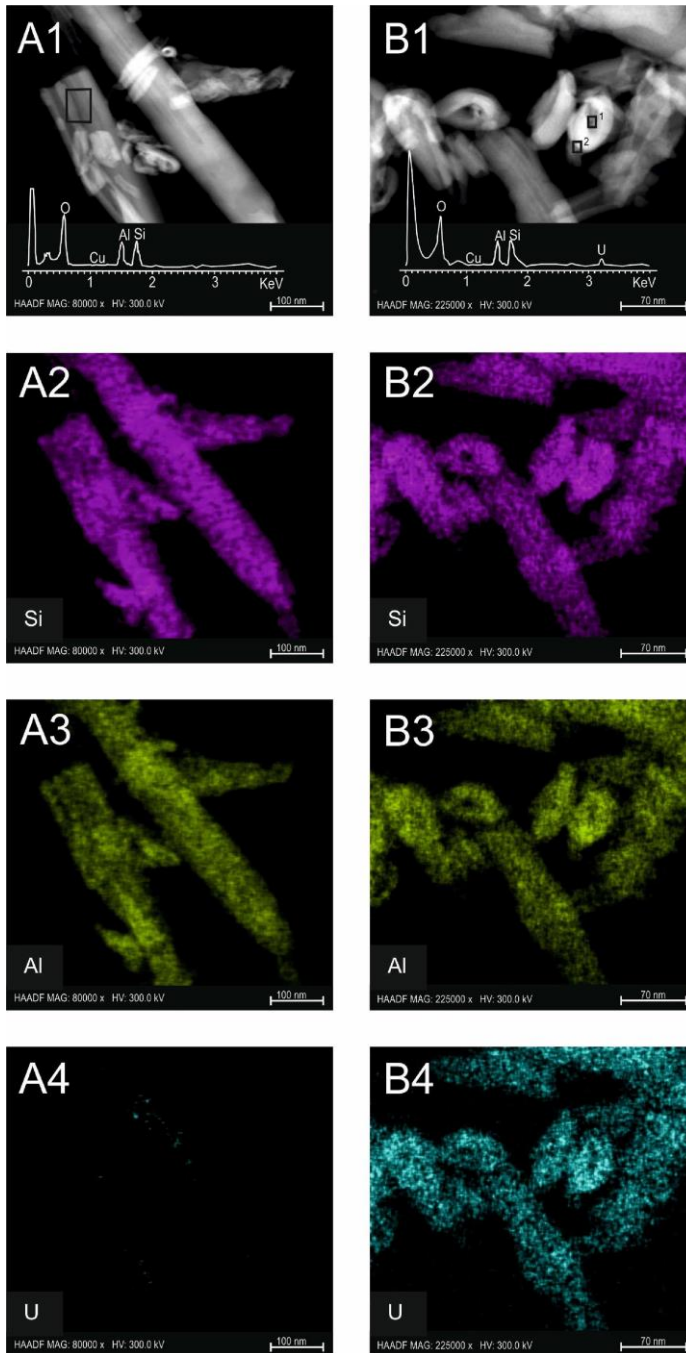


Figure 1.3. High-resolution transmission electron microscopy, energy dispersive X-ray spectroscopy (XEDS), and X-ray maps of unloaded HNTs (A) and HNTs loaded with isoniazid (B). Extracted from (Carazo et al., 2017b)

Paclitaxel-loaded HNTs were coated with poly(methyl methacrylate-co-methacrylic acid) as a pH-responsive polymer (Yendluri et al., 2017a). An increase in pH produced a triggered drug release, and a high therapeutic anticancer effect was observed for the aforementioned hybrid.

Palygorskite (Pal) particles interact with each other due to van der Waals forces (inter-particle forces) forming aggregates. This property could limit Pal's usefulness in drug delivery due to a reduction of the effective surface available to interact with organic molecules. Freeze-drying was proposed to reduce such particle aggregation problems (Wang et al., 2014a).

Adsorption of isoniazid active substance onto Pal was performed by (Carazo et al., 2018b). The antimicrobial molecule interacted through hydrogen bonds with superficial OH groups on the clay mineral surface and zeolitic water inside Pal channels. Isoniazid retention capacity in Pal increased as intercalation temperature increased.

Carvacrol is a natural, volatile, phenolic compound extracted from *Origanum vulgare* essential oil. Its antioxidant, antifungal, and antimicrobial properties make it useful for the treatment of infected skin lesions. To prevent carvacrol evaporation, its adsorption into MMT, HNT, and Pal was evaluated, and Pal showed the highest drug loading and prevented its evaporation without hindering its therapeutic activities (Tenci et al., 2017).

Praziquantel is used as a first-line drug in the treatment of schistosomiasis, and it possesses low water solubility and high permeability. Veegum HS and sepiolite were combined with praziquantel by Borrego-Sánchez and co-workers. The resultant hybrids improved drug dissolution profiles both in acidic and basic environment (Figure 1.4). The total amount of drug dissolved increased by 20% (w/w) with respect to the pristine praziquantel phosphate buffer dissolution profile. In acidic medium, the total amount of drug dissolved did not improve, although a high dissolution rate was found: ~50% (w/w) of total amount of drug was dissolved in less than 20 min compared with ~20% (w/w) in the case of pure praziquantel (Borrego-Sánchez et al., 2017).

1.1. Clay Minerals in Drug Delivery Systems

Table 1.4. Most recent tubular and fibrous clay/polymer nanocomposites used in drug delivery

	Clay Mineral	Interaction methodology	Drug	Ref	
Natural	HNT/CS	Intercalation solution	Doxorubicin	(Yang et al., 2016a)	
			Aspirin	(Li et al., 2016b)	
			CS	(Sandri et al., 2017)	
	HNT/Cellulose		Curcumin	(Huang et al., 2017a)	
	HNT/ALG, HNT/ALG/Gelatin		Vancomycin	(Kurczewska et al., 2017)	
	HNT/PEGm		Hydrocortisone	(Ghebour et al., 2016)	
	HNT/PEGdm		Hydrocortisone		
	HNT/PC		Vacuum cycle	Rosemary essential oil	(Gorrasi, 2015)
	HNT/hyaluronate/poly(HEMA)			5-FU	(Rao et al., 2014)
	HNT/PLL/PAA		Intercalation solution and vacuum cycle	Curcumin	(Dionisi et al., 2016)
	HNT/PVA	Sodium D-pantothenate		(Lee et al., 2016)	
	HNT/HPMCAS	Immersion	Atorvastatin	(Li et al., 2017)	
			Celecoxib		
	HNT/SBMP resin	Vacuum cycle	Doxycycline	(Feitosa et al., 2014; Palasuk et al., 2017)	
	HNT/PEI	Self-assembly	pDNA	(Long et al., 2017)	
	HNT/LIP	Intercalation solution	Doxorubicin	(Li et al., 2018a)	
	Pal/CS	Adsorption/entrapment	Diclofenac sodium	(Wu et al., 2014)	
		Intercalation solution	5-Aminosalicylic acid	(Santana et al., 2017)	
	Pal/PPy	In situ electropolymerization	Aspirin	(Kong et al., 2014)	
	SEP/CS	Intercalation solution	Tetracycline	(Gür et al., 2015)	
SEP/CS/PVA	Cefazolin		(Mahdavinia et al., 2016)		
Functionalized	APTES-functionalized HNT/CS	Vacuum cycle	Curcumin	(Liu et al., 2016)	
	AZPES-functionalized HNTs/Fmoc-F		Camptothecin	(Rizzo et al., 2017)	

Oxaprozin is an NSAID molecule used in the treatment of inflammatory disorders, typically osteoarthritis and rheumatoid arthritis. Oxaprozin bioavailability is hindered by its low solubility and permeability. Hybrids of Pal or Sep with modified cyclodextrins were proposed by (Mura et al., 2016) as dissolution enhancers of oxaprozin. The combination of cyclodextrin with the clay minerals allowed to achieve higher oxaprozin dissolution rates.

1.1.2.2. Functionalized Tubular and Fibrous Clay Minerals

HNTs functionalized with triazolium salts were proved to perform site-specific drug delivery of curcumin (Riela et al., 2014). Results demonstrated that curcumin was preferentially adsorbed over functionalized HNT surfaces, though small amounts were also detected inside the nanotube lumen. The release highly depended on the pH: higher and faster release at lower pH of the medium. In acidic environment, both curcumin and triazolium-functionalized HNTs acquired positive charges, which caused repulsion and promoted curcumin release.

Trimethoxy(propyl)silane and triethoxy(octyl)silane were used to functionalize HNTs (Sánchez-Fernández et al., 2014). Biocompatibility and cytotoxicity were tested on C6 Rat glioblastoma cells. HNTs were biocompatible, but functionalized materials induced cell apoptosis, probably due to the nature of the functionalizing organosilanes selected. Consequently, functionalization conditions should be carefully selected to obtain the desired HNT performances, and further studies are needed in this area.

HNT modified with [3-(2-aminoethyl) aminopropyl] trimethoxysilane was used to carry and release silver nanoparticles by electrostatic interactions over the surface of the clay mineral (Zhang et al., 2013). The higher antibacterial activity of Ag loaded HNTs compared with pure Ag nanoparticles could be related to the homogeneous dispersion of Ag particles over halloysite surfaces, which led to superior specific surface area, hence better antibacterial properties. APTES allowed to immobilize silver nanoparticles over the surface of HNTs, giving resultant antibacterial activity against *E. coli*, as reported by (Jana et al., 2017). APTES-modified HNTs also carried ibuprofen drug, which was located both in the lumen and onto the

external surface of nanotubes, in its crystalline form (Tan et al., 2014). In unmodified HNTs, ibuprofen established hydrogen bonds; while in APTES-HNT the drug interacted stronger due to electrostatic bonds. These divergences explained the slow release rate performed for ibuprofen from APTES-HNTs (up until 50 h). Coating through layer-by-layer technique of drug-APTES-HNT hybrids with CS and ALG extended ibuprofen release for longer than 110 h with a first-order release kinetic (Li et al., 2016a). (Xue et al., 2015) also functionalized HNT with APTES to be used as an ingredient in the formulation of guided tissue regeneration/guided bone regeneration membranes. Electrospinning technique was used to synthesize the membrane, and metronidazole was selected as an antibacterial drug aiming to prevent infections of anaerobic microorganisms. Hal improved the mechanical properties of the film, allowed further sustained release and reduced the initial burst.

Vancomycin was also loaded on HNTs previously functionalized with APTES (Kurczewska et al., 2017). In comparison with non-modified HNT and acid-activated HNT carrying vancomycin, the APTES-functionalized clay mineral avoided burst release effect and provided a prolonged release of drug for more than 70 h. This result could be justified by the strong electrostatic interactions established between vancomycin and functionalized-HNT.

Cyclodextrins, cyclic oligosaccharides composed of α -D-glucopyranose units, and functionalized HNTs were combined as dual drug-loaded systems for silibinin and curcumin. Both drugs are anionic molecules, and silibinin was loaded inside HNTs, while curcumin was located inside the cyclodextrin to improve its water solubility. The complex nanohybrid showed antiproliferative activity as well as high propensity to cross the cell membranes and performed a site-specific release (Massaro et al., 2016b). Curcumin was also bonded to HNT surfaces, thanks to HNTs functionalized with cysteamine hydrochloride, thus providing imine bonding with curcumin molecules (Massaro et al., 2016a). HNTs increased curcumin stability in alkaline/basic environment and lowered drug release rates. Due to the disulphide bond established between HNTs and curcumin, the drug release significantly increased in acidic and glutathione rich environments. These

latter conditions corresponded to the typical microenvironment of cancer cells.

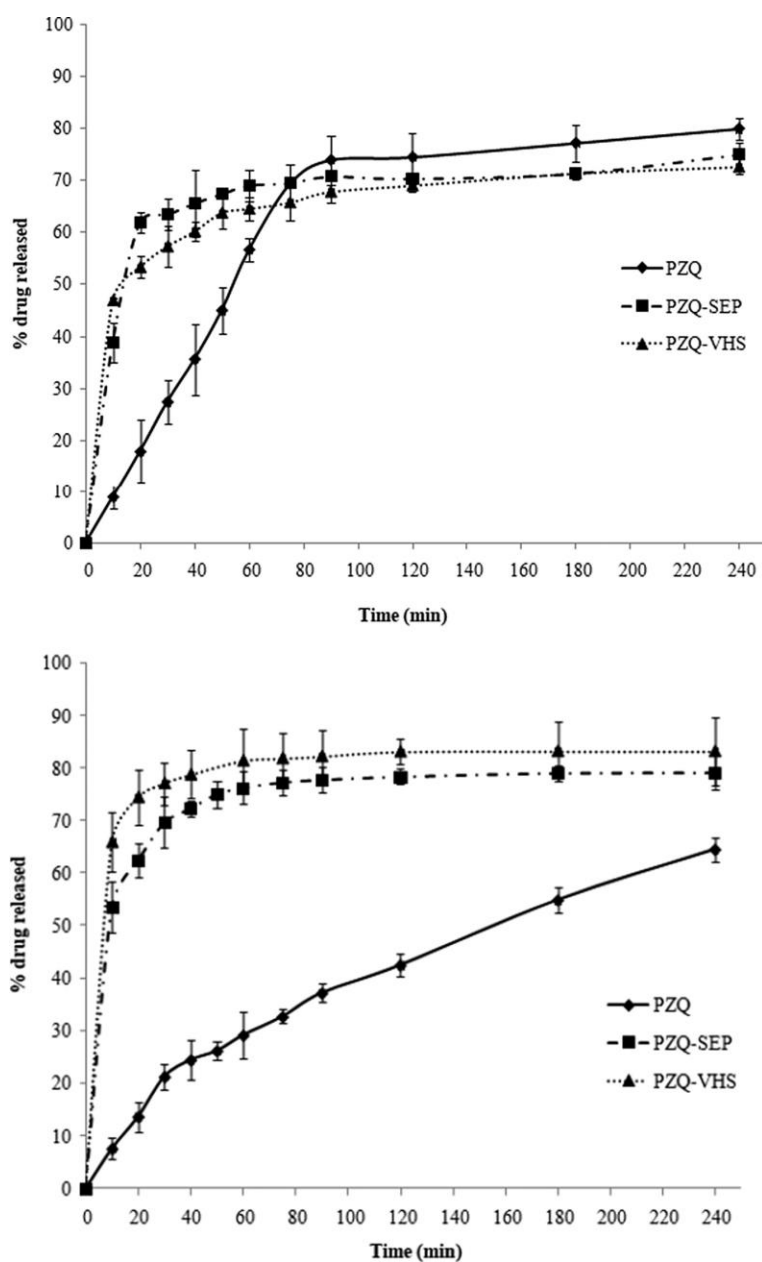


Figure 1.4. Praziquantel in vitro drug release profiles in HCl (up) and simulated intestinal fluid (down) from sepiolite, Veegum HS composites and pure praziquantel. Extracted from (Borrego-Sánchez et al., 2017)

1.1. Clay Minerals in Drug Delivery Systems

Trolox and quercetin, typically used as potent antioxidants, were loaded into HNT after surface functionalization of the clay nanotubes (Massaro et al., 2016). Particularly, functionalization was started by 3-azidopropyltrimethoxysilane reaction (AZPES). Once the functionalization was performed, trolox reacted by condensation and formed an amide bond in the external surface of HNTs. Subsequently, quercetin was loaded into the clay lumen by vacuum cycles. The antioxidant activity improved significantly due to synergistic effects between trolox and quercetin. Moreover, the presence of quercetin in HNT lumens implied a controlled release of this substance, hence a prolonged antioxidant activity.

1.1.2.3. Tubular and Fibrous Clay-Polymer Nanocomposites

CS-grafted HNTs were loaded with doxorubicin (Yang et al., 2016a) and curcumin (Liu et al., 2016). The functionalization of HNTs with APTES and its combination with CS allowed higher adsorption capacities of hydrophobic drugs such as curcumin (Liu et al., 2016). Moreover, they showed specific toxicity toward cancer cells. HNT loaded with curcumin was covered with poly-L-lysine as positive electrolyte and poly-acrylic acid as negative electrolyte using layer-by-layer technique, thus creating three layers of polymers. Polymer coated HNT-curcumin nanocomposite showed a much more slow release (<20% (w/w) of drug in 24 h) in comparison with free curcumin (>90% (w/w) of curcumin in 24 h) and uncoated HNT-curcumin (>40% (w/w) in 24 h) (Dionisi et al., 2016). CS-grafted HNTs with doxorubicin were internalized by human breast cells and effectively induced cell apoptosis (Yang et al., 2016a).

Physical adsorption between curcumin and cellulose-modified MMT also showed good biocompatibility, thus demonstrating the promising applications in cancer DDSs and wound dressings (Huang et al., 2017a)

Crosslinked PVA nanofibers with HNTs were prepared as a sodium D-pantothenate DDS (Lee et al., 2016). Significant changes occurred in drug release patterns due to the presence of the clay mineral. Burst releases were not avoided, although the second step of release occurred more slowly and total amount of drug release was smaller in comparison with the corresponding PVA-sodium D-pantothenate fibers.

Hydroxypropyl methylcellulose acetate succinate (HPMCAS) is insoluble in acidic conditions but highly soluble in neutral-alkaline conditions. Colon cancer is mainly treated with drugs such as atorvastatin and celecoxib, which are administered together due to their synergistic action. These drugs were loaded in HNT-HPMCAS microspheres prepared by a microfluidic flow-focusing oil-in-water emulsion technique, schematically represented in Figure 1.5. In comparison with pure celecoxib and atorvastatin, HNT-HPMCAS loaded microspheres did not release any drug at $\text{pH} \leq 6.5$, while a complete release occurred within 30 min at $\text{pH} > 6.8$. The immediate and complete release of both the drugs increased their permeability across the intestinal membranes inhibiting colon cancer cell proliferation in a more effective way (Li et al., 2017).

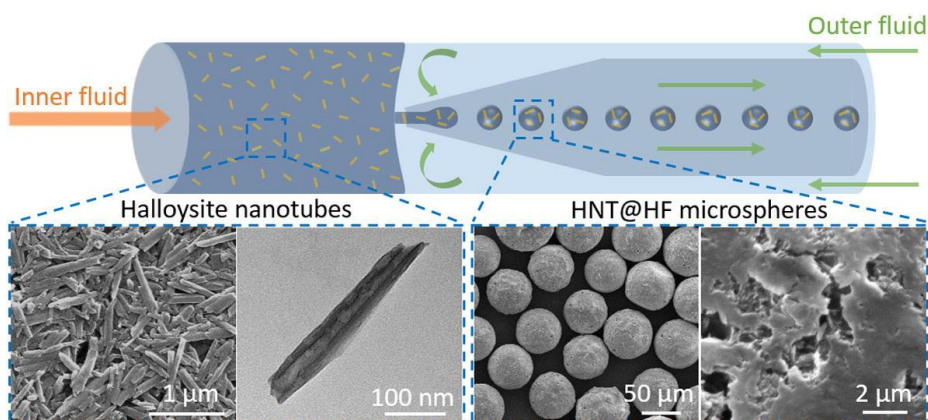


Figure 1.5. Preparation of pH-responsive nanocomposite of HNT and HPMCAS. Extracted from (Li et al., 2017)

HNTs functionalized with AZPES were condensed with fluoromethoxycarbonyl-L-phenylalanine (Fmoc-F) (Rizzo et al., 2017). Fmoc-F is able to create high density hydrogels. Camptothecin was loaded by intercalation solution and vacuum cycles. Oral administration of the drug is hindered by low solubility and low stability. AZPES-functionalized HNTs/Fmoc-F nanocomposites allowed the total dissolution of the drug in phosphate buffer solution.

Vacuum method was also used to prepare HNTs/pectin nanocomposites to carry rosemary essential oil (Gorrasi, 2015). The aim of the study was to obtain a nanocomposite film with biodegradable and

1.1. Clay Minerals in Drug Delivery Systems

antibacterial properties in which the release of the active substance proceeded in a sustained manner.

HNTs were combined with CS to prepare microspheres. Both materials were kept in contact for 12 h right after their dispersion/dissolution. Microspheres were prepared through an emulsification process with oleic acid (Li et al., 2016b). Aspirin was selected as a model drug. The partial dissolution of aspirin in the acidic environment of the stomach produces the adhesion of aspirin crystals over the gastric mucosa, which can pose gastric diseases. To minimize this problem, (Li et al., 2016b) proposed the preparation of the aforementioned microspheres to control aspirin release. The encapsulation efficiency was improved by HNT/CS microspheres, and the dissolution profile showed a lower release of aspirin in simulated gastric fluid, leading to a reduction of accumulation of the drug, and consequently minimizing the possible gastric side effects.

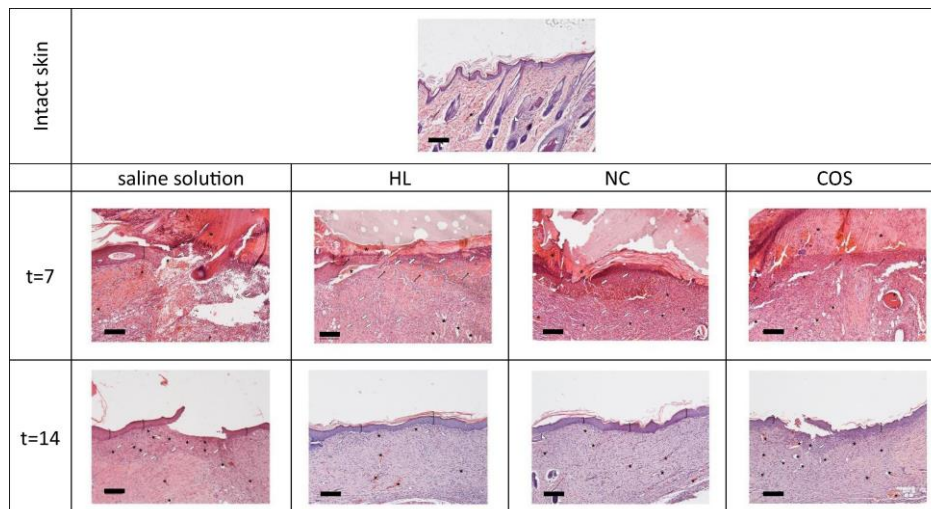


Figure 1.6. Light microphotographs of haematoxylin and eosin stained skin sections after 7 and 18 days of treatment with saline solution (negative controls), HNTs, chitosan oligosaccharide/HNTs nanocomposite and chitosan oligosaccharide. Intact tissue section is also reported. Skin structures are labelled as follows: epidermis = bracket; vessel = star; granulation tissue = pentagons; hair follicle = triangle; platelets = white arrow; necrotic tissue = asterisk; muscular fibers = arrow. Scale bar = 200 μ m. Extracted from (Sandri et al., 2016)

CS oligosaccharides, homo- or hetero-oligomers of N-acetylglucosamine and D-glucosamine, accelerate wound healing by enhancing the

activity of inflammatory and repairing cells. Sandri et al., (2017) used these oligomers and HNTs to obtain nanocomposites able to enhance healing in the treatment of chronic wounds. The results showed good *in vitro* biocompatibility with normal human dermal fibroblasts and enhanced *in vitro* fibroblast motility, promoting both cellular proliferation and migration. The HTNs/chitosan oligosaccharide nanocomposites allowed better skin re-epithelialization and reorganization than HNTs or CS, separately (Figure 1.6).

HNTs embedded inside hydrogels sensitive to pH changes were demonstrated to be a good strategy for the encapsulation of the anticancer drug 5-FU (Rao et al., 2014). This drug is used in colon cancer therapies, although its intravenous administration poses remarkable side effects. An oral dosage form would be a more convenient one for these kind of treatments. In this case, sodium hyaluronate and poly(HEMA) were crosslinked by free radical redox polymerization with and without the presence of HNTs (Rao et al., 2014). Vacuum cycles were performed to entrap the drug both inside the hydrogel network and in HNT lumen. The resultant nanocomposites practically avoided drug release in acidic pH (<10% (w/w) when HNTs were added), while in neutral environment 5-FU was successfully released.

A commercial adhesive resin used in dentin implants was modified by including HNTs loaded with doxycycline, a matrix metalloproteinases-inhibiting drug. Metalloproteinases are enzymes able to destroy connective tissue during certain issues such as periodontitis, hepatitis, atherosclerosis, asthma, skin and dental photoaging. The incorporation of HNTs and doxycycline inside dental resin (Scotchbond Multi-Purpose) was proposed to improve the adhesively bonded resin composite restorations (Feitosa et al., 2014; Palasuk et al., 2017). Doxycycline was successfully encapsulated within the system, and released in such a controlled manner that metalloproteinases were inhibited in subantimicrobial concentrations. Additionally, the biocompatibility of the system was not compromised.

Polyethylene glycol methacrylate (PEGm) and polyethylene glycol dimethacrylate (PEGdm) were proposed as HNT pH-sensitive modifying polymers (Ghebaur et al., 2016). The drug/clay ratio was the only factor influencing the adsorption of hydrocortisone, while polymers exerted a

1.1. Clay Minerals in Drug Delivery Systems

negligible impact on drug loading. Sustained releases were found in all cases, even with the absence of polymers (HNT/hydrocortisone).

APTES-functionalized HNTs were combined with ALG and gelatin, and vancomycin as an antibacterial drug was loaded to design a wound healing nanocomposite (Kurczewska et al., 2017). Nanocomposites showed sustained release of the drug in phosphate buffer medium, without any burst release.

HNT/cellulose-curcumin nanocomposite was tested and compared with a cellulose-curcumin system (Huang et al., 2017a). HNTs improved the amount of drug loaded and provided sustained release of curcumin without burst releases: ~15% (w/w) of drug in approximately 2.5 h reaching more than ~50% (w/w) after 20 h during *in vitro* release study.

APTES-HNTs were grafted with polyethyleneimine (PEI) to load pDNA and create a non-viral vector able to deliver pDNA into determined cells as a strategy to treat diseases such as cancer (Long et al., 2017). The complex with HNTs showed less *in vitro* toxicity than the one without HNTs. Likewise, the transfection efficiency of the clay-based nanocomposite was higher, being able to deliver the pDNA into the cellular nucleus.

Doxorubicin loading efficiency increased by increasing HNT proportion in HNT/soybean phospholipid nanocomposites (Li et al., 2018a). At neutral pH, doxorubicin was released in a sustained way, without burst release and reaching approximately 15% (w/w) of drug after 4 days. On the other hand, at acidic pH (5.4), the release profile possessed two stages: a burst release step in which 20% (w/w) of drug was released within the first 10 min followed by a more sustained and prolonged release to 25% (w/w) of total amount of drug released in 4 days.

Pal was mixed with polypyrrole (PPy) to improve physicochemical properties of the polymer as a drug carrier (Kong et al., 2014). Polypyrrole is a biocompatible polymer able to change its oxidation state under electrical potential, thus promoting drug release. In comparison with polypyrrole alone, Pal-polypyrrole composites showed higher drug loading capacities ascribable to the presence of the clay mineral. Pal-PPy-aspirin composites

were demonstrated to be a promising implantable DDS, which could help to release drugs according to patient convenience under electric stimulus.

Organo-modification of Pal with hexadecyl betaine was combined with CS through crosslinking reaction to create beads able to carry drugs such as diclofenac sodium (Wu et al., 2014). The organo-modification of the clay mineral improved chemical interactions with the polymer. Additionally, the presence of the clay mineral increased the swelling properties of the beads and modified drug release. Beads with 10%-20% (w/w) of organomodified Pal showed slower drug release and burst release reduction. Beads with 30% (w/w) of palygorskite performed faster release, even higher than pure CS-diclofenac beads.

Pal/CS as drug carrier was recently addressed (Santana et al., 2017). The model drug chosen in this study was 5-aminosalicylic acid. CS and Pal interacted through electrostatic interactions and intermolecular hydrogen bonds. The use of basic pH during Pal/CS interaction highly influenced the interactions between these components and influenced the drug loading capacity. At pH 11, the CS protonation decrease favoured the interaction with Pal but contributed to reduce 5-aminosalicylic acid adsorption due to low available drug interaction sites.

Sep and CS were combined by (Gür et al., 2015) to form a nanocomposite carrying tetracycline drug. A clear dependence of Sep ratio on the amount of drug released was found. Burst releases were also found in all the *in vitro* release studies performed, and were attributed to a fast swelling of the gel.

Sep was also combined with CS and PVA, and loaded with cefazolin, a broad-spectrum antibacterial drug (Mahdavinia et al., 2016). Drug release profile and antibacterial activity (*Bacillus cereus*, *Proteus* bacteria, and *E. coli*) were evaluated. CS improved swelling capacity of the nanocomposite. PVA decreased the amount of drug released since higher crosslinking occurred, consequently creating smaller hydrogel pore sizes that could hinder the diffusion of cefazolin. Effective growth inhibition areas were found except for the nanocomposite without cefazolin. The highest antimicrobial activity was reported against *B. cereus*.

1.1.3. Future Trends

Ten years have passed since Aguzzi and co-workers published their review article titled "Use of clays as drug delivery systems: Possibilities and limitations" (Viseras et al., 2007). During this time span the number of studies focused on this subject have increased exponentially. In this chapter, current advances are addressed, MMT and halloysite being the main clay minerals used in the design of new DDS. Recent results confirm that the usefulness of clay minerals will go beyond their conventional uses in pharmaceutical applications, thanks to multidisciplinary research efforts. The developments in biotechnology and nanomedicine research make us think that a possible future use of clay minerals would be focused on MMDS of biopharmaceuticals, including gene and protein delivery. Consequently, the number of patents and commercial pharmaceutical products will be increased, ultimately improving many pharmacological therapies.

1.2. Clay Minerals in Skin Drug Delivery

The aim of this review was to provide a summary of recent research on clay mineral uses in advanced skin drug delivery; a future perspective is included to discuss challenges and prospects. Because of their healing properties and global accessibility, use of clay minerals in the therapy of skin pathologies goes back to prehistoric times and continues to play a crucial role in the design of skin-addressed drug delivery systems. Clay minerals are used in conventional medicinal products as excipients or actives (Cornejo, 1990; A. López-Galindo and Viseras, 2004; Carretero et al., 2006; Viseras et al., 2007; López-Galindo et al., 2011) as well as advanced materials developed to modify drug delivery features (Aguzzi et al., 2007, 2016; Viseras et al., 2008, 2010, 2015; Sandri et al., 2016; Carazo et al., 2018a). Clay minerals were likely used in the very first prehistoric remedies, probably including geophagy and wound treatments. Clay minerals have continued to be essential ingredients in medicinal products during human history. In Europe, ancient western medicine used “Terra sigillata” (Λημυία Γη) or Stamped earth with “trade mark” denominations (*terra Armenica*, *Terra Florentina*, *terra Hierosolymitanae*, *terra Hispanica*, *terra Lemnia*, *terra Portugallica*, *terra Silesiaca*, among others) (Mantle et al., 2001; Macgregor, 2013). Clay minerals were mentioned in at least half of the most important historical texts constituting the European *Materia Medica* since the “Hippocratic Corpus” (5th–4th century BC) (De Vos, 2010). During the nineteenth century, the presence of clay “simples” in western medicine continued (Medicamentarius, 1866). In the first half of the twentieth century, the major Western pharmacopoeias included clay minerals in the substances used in medicinal products. Nowadays, the terms “Bentonite,” “Magnesium trisilicate,” “Magnesium aluminum silicate” (or “Aluminium Magnesium silicate”), and “Attapulgit” have their own monographs in the most important worldwide pharmacopoeias (*USP42 - NF37*, 2019; *BP*, 2018; *RFE*, 2015).

Clay minerals have been classically used in the elaboration of topical semisolid products as pastes, poultices, or liniments. Two examples, still in vogue, are “Calamine Lotion,” indicated for treatment of skin irritations that include 25% w/w of “Bentonite magma” and “Titanium dioxide paste” formulated with 10% w/w of kaolin (*USP42 - NF37*, 2019; *BP*, 2018; *RFE*, 2015).

1.2. Clay Minerals in Skin Drug Delivery

Clay minerals are currently used mainly as excipients (any constituent of a medicinal product other than the active substance and the packaging material). Excipients represent the largest part of the medicines (up to 95%) and determine drug release and bioavailability. More than 1200 excipients from many origins (animal, vegetable, or mineral) are used in medicines. Clays account for ~5% of the global market for inorganic excipients. Most of the advances in pharmaceutical science and technology are related directly to inorganic excipients, the market for which should reach \$433.7 million by 2020 (BCC, 2016).

1.2.1. Skin Anatomy and Physiology

In order to understand fully the design and development of skin pharmaceuticals, the structure, composition, and functions of human skin must be reviewed. The skin, which is considered the largest organ of the human body, is a multi-stratified structure (epidermis, dermis, and hypodermis) with essential functions as temperature control and barrier against physical, chemical, and thermal aggressions (Ng and Lau, 2015). The presence of appendages (hair follicles, sweat, and sebaceous glands) leads to several interesting properties. Human skin has an average surface area of 1.8 m² and constitutes a cellular layer, named dermis or true skin, sandwiched between the epidermis (outer layer and boundary with the exterior) and hypodermis (inner layer). The thickness of the epidermis varies between 0.05 mm on the eyelids to 1.55 mm on palms and soles. The epidermis is divided into *basale*, *spinosum*, *granulosum*, *lucidum* (only in palms and soles), and *corneum* strata. Continuous cell renewal in the stratum *basale* generates different cell types, mainly keratinocytes, melanocytes, and merkel cells (associated with terminal filaments of cutaneous nerves). Replication rates (normal full skin renewal requires ~28 days) increase during inflammation or injury. Keratinocytes move through the strata to reach the *stratum corneum* as corneocytes. The *stratum spinosum* contains a large concentration of keratin filaments appearing as a “spiny” area where Langerhans cells (antigen-presenting cells with an immunologic role) are also frequent. Langerhans cells and melanocytes are connected to adjacent cells by desmosomes in the same way keratinocytes are connected to one another. In the *stratum granulosum* the

keratinocytes become flattened, lose their nuclei, and secrete their contents to form a lipid barrier. One of the most determining layers of the skin in terms of permeation by control drugs is the *stratum corneum* (SC). The SC is the hardest barrier of the skin, comprising rows of corneocytes (matured keratinocytes lacking nuclei and having elongated and flattened shapes) organized on a “brick and mortar” structure: corneocytes (“bricks”) immersed in a lipid matrix (“mortar”) (Prow et al., 2011). The space between adjacent corneocytes is occupied by a mesophase (lyotropic liquid crystal) formed by phospholipid bilayers and with the presence of proteins. The dermis layer is much thicker than the epidermis. Blood vessels, nerves, and various appendages (sweat glands, hair follicles, and sebaceous glands) are also found, providing nutritional and structural support to the epidermis. The hypodermis obeys the main functions of energy supply and thermal insulation.

1.2.2. Routes and targets on, into, and through skin drug delivery

Delivery of drugs on/into/through the skin enables either local or systemic actions and improvement of poor biopharmaceutics profiles of drugs administered via other administration paths, and becomes a useful strategy in situations in which other administration routes are not possible or inadvisable (Aulton and Taylor, 2013). With these backgrounds, the main goals of advanced skin drug delivery systems are improving drug biopharmaceutics and pharmacokinetics and obtaining targeted drug delivery based on interaction with skin appendages and skin lipids leading to a facilitated, sustained, and/or stimuli-induced release.

While all topical and transdermal compounds are applied to the skin, it is necessary to accentuate the fact that skin drug delivery can provide local (topical) or systemic (transdermal) therapeutic effects. The two principal routes of penetration are transappendageal (via the pores and shafts embracing sweat glands and hair follicles with their associated sebaceous glands) and transepidermal (diffusion through the stratum corneum). The transappendageal pathway is minor but preferred by ions and large polar molecules because the stratum corneum is not involved, whereas the transepidermal route is the dominant one and comprises two routes:

transcellular, also known as intracellular, and intercellular (Figure 1.7). Via the intracellular route, drug molecules repeatedly diffuse through corneocytes (keratin-filled; of an aqueous environment) and then partition into the intercellular lipid domains. This pathway is preferred by hydrophilic molecules. In contrast, the intercellular route implies that drug molecules diffuse via a tortuous route within the continuous lipid domain. Lipophilic molecules opt for this route. All drug molecules might use the three available routes; their physicochemical properties, however, determine the preferred pathway for finally reaching the capillaries at the epidermal–dermal junction.

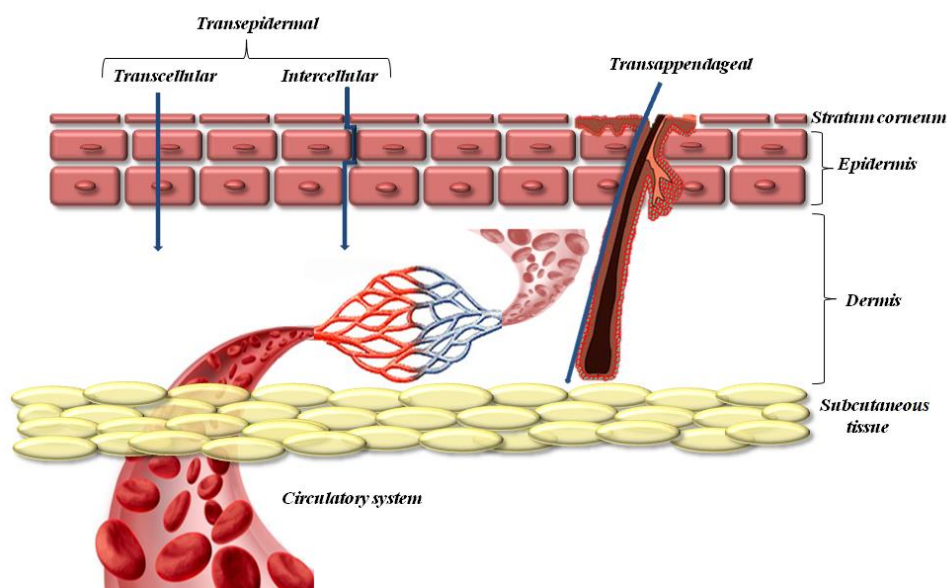


Figure 1.7. Skin layers and diverse routes of penetration

1.2.3. Quality and Performance of Topical Drug Products

Topically administered drug products include those applied for local action (exert their actions on the stratum corneum and/or modulate the function of the epidermis and/or the dermis) and those applied for systemic effects (transdermal drug delivery systems). Topical dosage forms include solutions (for which release testing is not indicated), suspensions, emulsions (e.g., lotions), semisolids (e.g., foams, ointments, pastes, creams, and gels), solids (e.g., powders), and sprays (e.g., aerosols).

Two categories of tests, product quality tests and product performance tests, are performed with topical drug products. Product quality tests are performed to assess attributes such as assay, identification, content uniformity, pH and microbial limits.

Product performance tests are conducted to assess drug release from the finished dosage form.

Quality tests ensure safety and efficacy (ICH, 2000) and includes general tests such as identification, assay, content uniformity, impurities, pH, water content, microbial limits, antimicrobial preservative content, antioxidant preservative content, and sterility (in some cases), and specific test such as viscosity and particle size determinations (*USP42 - NF37*, 2019; *BP*, 2018; *RFE*, 2015).

Particularly interesting are performance tests, aimed to measure drug release from the finished dosage form and detect changes in drug release related to formulation and manufacturing variables as well as storage and aging effects.

Intercellular route represents the principal mode of entry for permeation of both, hydrophilic and lipophilic drugs. A drug that penetrates the SC can reach the dermis and enter the bloodstream by passive diffusion, which is considered the rate-limiting step for the transdermal transport of drug molecules and depends on the physicochemical properties of the substance (Couto et al., 2014). This transport can be described by Fick's First Law of Diffusion (Eq. 1.1),

$$J = -D \frac{\delta C}{\delta x} \quad \text{Eq. 1.1}$$

where J is the flux, C is the concentration of diffusing drug, x is the space coordinate and D is the diffusion coefficient of the drug. Fick's Law assumes that diffusion occurs through an isotropic material, with same structural and diffusional properties in all directions. However, skin is heterogeneous structure so Fickian diffusion laws lead to approximations from transdermal drug delivery data.

In vitro protocols are aimed to mimic the *in vivo* situation. Several diffusion-type cell devices have been proposed as potential apparatus for

drug release testing from topical drug products. However, only vertical diffusion cell system (VDC, also named Franz Cells), have been normalized to measuring drug release from semisolid dosage forms (USP, 2018).

VDC are made of a membrane (synthetic, animal or human epidermis) separating two compartments. The drug in a vehicle is then applied to the uppermost membrane surface (“donor” solution). The other compartment contains a “receptor” solution that provides sink conditions (near zero concentration) allowing a concentration gradient to exist between the donor and receptor phase which is required for diffusion across the membrane.

1.2.4. Clay Minerals Functions in Topical Products

Inorganic excipients and in particular clay minerals may be used to overcome the traditional difficulties derived from topical drug administration and provide advanced functionalities (Carazo et al., 2018a). Clay minerals have been traditionally included in topical products to improve technical properties; increase emulsions stabilities and suspensions viscosities (Viseras et al., 2007). Besides, clay minerals show advanced functionalities that made them essential ingredients in anti-inflammatory, antibacterial and wound healing products. Clay minerals also provide specific functions in some dermocosmetics products. Figure 1.8 attempts to shed light on the different locations, pathways, and advanced functions of clay minerals in topical products. Table 1.5 compiles the scope and uses of clay minerals administered on/into/through the skin which are further explained in the text.

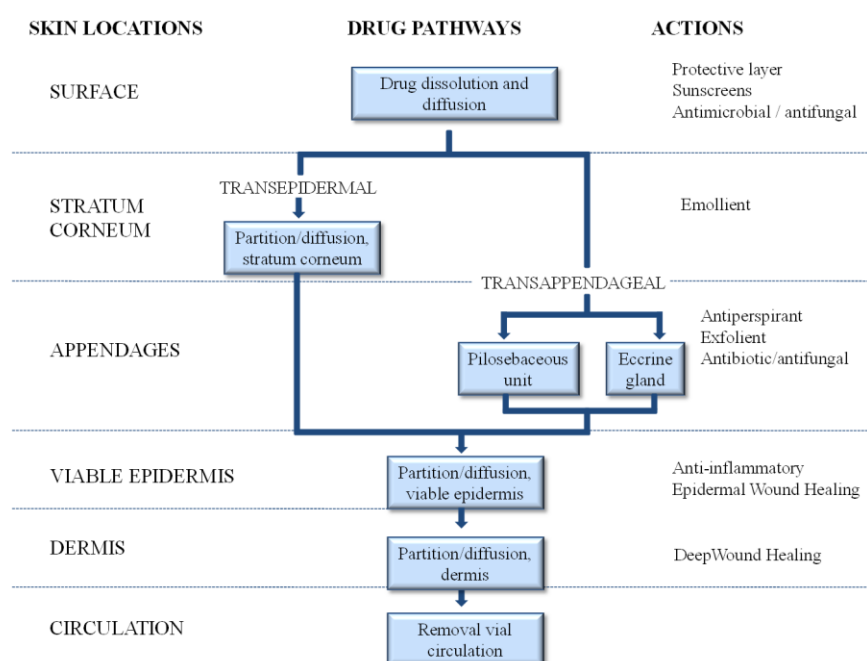


Figure 1.8. Places and routes of skin treatments and penetration with examples of clay mineral functions (modified from Barry, 1983)

1.2.4.1. Anti-inflammatory

Pelotherapy consists on the topical administration of hot-muds termed peloids. Peloids are inorganic gels with optimal rheological and thermal properties composed by clay minerals and mineral-medicinal water aimed to treat arthro-rheumatic issues, bone-muscle traumatic damage and dermatological pathologies. The optimum characteristics of the peloids depend on the required treatment and is related with not only the components of the peloid (mineromedicinal water and clay minerals) but also with the process of maturation (contact between the solid and water medium during a prolonged time period) (Veniale et al., 2007). Baschini and co-workers claimed the use of natural peloids from Copahue, "clayey-sulphurous mud", a special type of therapeutic muds, whose thermal properties are similar to those of other peloids but with special possibilities for the treatment of various pathologies due to the presence of sulphur (Baschini et al., 2010). Portuguese clayey materials for medical hydrology applications, were selected as candidates to be used in the preparation of tailored peloids (Rebelo et al.,

2011). Regulations and quality criteria for suitable therapeutic applications of peloids were reviewed (Quintela et al., 2012). The influence of “maturation” conditions (time and agitation) on aggregation states, gel structure and rheological behaviour of peloids made with a pharmaceutical-grade smectite and a sepiolite and a medicinal mineral water from an Spanish thermal spring (Graena, Granada, Spain) were investigated (Aguzzi et al., 2013a). A concise definition and a classification of peloids as well as a complete glossary of the whole mud-therapy terms were proposed to compile the different terminology used in the course of time (Gomes et al., 2013). Five clay samples used in various spa centres of southern European/Mediterranean were subjected to ethnopharmaceutic research aimed to ascertain the compositional characters that allow establishing quality attributes and corresponding requirements for peloids including identity, purity, richness and safety (Sánchez-Espejo et al., 2014a). Besides, the suitability of eleven clay samples (green and brown) from five Tunisian medina markets, traditionally used in home-made mud-packs was fully investigated (Khiari et al., 2014). It was found that maturation increased the release of cations from therapeutic muds but did not improve their thermal properties, allowing to assess that maturation could explain the differential chemical effects associated with the use of therapeutic muds compared to other thermotherapeutic agents (Sánchez-Espejo et al., 2015). Therefore, it was determined that the bacterial community in peloids changed mostly on the early stages of maturation and it reached stability after two months (Pesciaroli et al., 2016). The potentiality of seven selected kaolinite-rich samples from Egyptian Carboniferous sedimentary deposits to use them in medicinal semisolid formulations as peloids focusing on the effect of particle geometry and kaolinite crystallite size were studied (Awad et al., 2017). Peloids prepared with kaolin and saponite and medicinal mineral waters from Lanjarón Spa (Granada, Spain) were prepared and the optimum maturation time was investigated (Fernández-González et al., 2017).

Table 1.5. Clay minerals applications in skin drug delivery

Action	Outcomes	Ref
Anti-inflammatory	Optimum characteristics of peloids	Veniale et al., 2007
	Advanced uses of "clayey-sulphurous muds"	Baschini et al., 2010
	Portuguese tailored peloids	Rebelo et al., 2011
	Regulations and quality criteria for suitable therapeutic applications of peloids	Quintela et al., 2012
	The influence of "maturation" conditions on peloids behavior	(Aguzzi et al., 2013a)
	Definition, classification and glossary of "mud-therapy" terms	Gomes et al., 2013
	Establishment of quality attributes and requirements for peloids	Sánchez-Espejo et al., 2014
	Suitability of Tunisian clay samples for pelotherapy	Khiari et al., 2014
	Maturation time increased the release of cations	Sánchez-Espejo et al., 2015
	Bacterial community in peloids changed mostly on the early stages of maturation	Pesciaroli et al., 2016
	Suitability of kaolinite-rich samples from Egypt for pelotherapy	Awad et al., 2017
	Optimum maturation time of peloids from Lanjarón spa (Granada, Spain)	Fernández-González et al., 2017

1.2. Clay Minerals in Skin Drug Delivery

Table 1.5. (continued, part II)

Action	Outcomes	Ref
Wound healing and treatment of skin lesions	Revision of the role of clay minerals in the design of advanced wound dressings	Sandri et al., 2016
	Ability of clays to physically adsorb and remove bacterial cells, toxins, and debris from the wound	Otto et al., 2016
	Epidermal growth factor immobilized on montmorillonite stimulate cell growth and migration	Vaiana et al., 2011
	Montmorillonite-chitosan nanocomposite with silver sulfadiazine: bacteriostatic and bactericidal properties	Sandri et al., 2014
	Solid state characterization of montmorillonite-chitosan-silver sulfadiazine nanocomposite	(Aguzzi et al., 2014b)
	Brasilian clay allowed greater formation of collagen fibers when tested in rat animal models	Dário et al., 2014
	Functionalized layered clays with aminoacids promoted fibroblast proliferation	Ghadiri et al., 2014
	Antibacterial activity of clay-ciprofloxacin composites	Hamilton et al., 2014
	Methyl cellulose-sodium alginate-montmorillonite bionanocomposite films	Mishra et al., 2014
	Polymers/clay minerals composite scaffolds used for skin tissue engineering	Ninan et al., 2015
	Montmorillonite-chitosan films loaded with chlorhexidine for wound dressing	Ambrogi et al., 2017
	Silicate (tourmaline)/chitosan composite films for wound healing applications	Zou et al., 2017
	Chitosan oligosaccharide/halloysite nanocomposite with re-epithelialization activity	Sandri et al., 2017
	Carvacrol/clay hybrid for skin ulcer treatment	Tenci et al., 2017
	Montmorillonite-betaine hydrochloride silver nitrate for burn wounds	Rangappa et al., 2017
Poly (vinyl alcohol)/chitosan/honey/clay nanocomposite hydrogel as novel wound dressing	Noori et al., 2018	
Burn ointment including montmorillonite for tissue regeneration and skin growth	Zhang et al., 2018	
Sunscreens	Bentonite and hectorite as sunscreens	Ghadiri et al., 2015; Mattioli et al., 2016
	Mineral-based sunscreen containing activated clay with UVB/UVA protection	Timothy et al., 2015
	UV shielding of formulations with clay minerals	Ijiri et al., 2015

Table 1.5. (continued, part III)

Action	Outcomes	Ref
Cell adhesion, proliferation and differentiation: skin engineering and regenerative medicine	Cell proliferation and adhesion properties of clay minerals	Sandri et al., 2016
	Clay nanoparticles on cellular adhesion, proliferation and differentiation	Mousa et al., 2018
	Sepiolite-collagen complexes and fibroblast proliferation from explants	Lizarbe et al., 1987; Olmo et al., 1987
	Fibroblast attachment and spreading improved by montmorillonite and halloysite	Kommireddy et al., 2006
	The addition of montmorillonite to chitosan enhanced the adhesion of osteoblasts (a) and fibroblasts (b)	Katti et al., 2008; Popryadukhin et al., 2012
	Biocompatible and biodegradable retinal scaffold based on montmorillonite/polyurethane nanocomposite	Da Silva et al., 2013
	Biocompatibility and cell proliferation of montmorillonite	Sandri et al., 2014
	Montmorillonite-silk fibroin nanocomposite for bone tissue formation	Mieszawska et al., 2011
	Composite scaffold based on chitosan-gelatin/nanohydroxyapatite-montmorillonite for tissue engineering	Olad and Farshi-Azhar, 2014
	Montmorillonite -reinforced hydrogels, for the osteo-induction of osteoblast precursor cells	Mauro et al., 2017
	Chitosan-montmorillonite-triclosan loaded films compatibility towards human dermal fibroblasts	Chen et al., 2018
	Sr2+/chitosan/montmorillonite composite with enhanced properties to be used in bone tissue engineering	Demir et al., 2018
	Halloysite nanotubes in tissue engineering	Lvov et al., 2016b
	Alginate-halloysite composite scaffolds with enhanced fibroblasts attachment and proliferation	Liu et al., 2015
	Chitosan-gelatin-agarose doped halloysite scaffolds for tissue engineering	Naumenko et al., 2016
	A tri-component hydrogel, based on gellan gum, glycerol, and halloysite nanotubes for soft tissue engineering	Bonifacio et al., 2017
	Laponite cross-linked: adhesion and proliferation of HepG2, skin fibroblast, and human endothelial cells	Haraguchi et al., 2006; Liu et al., 2012
	Laponite- (a) and attapulgite- (b) poly(lactic-co-glycolic acid) nanofibers: fibroblast adhesion and proliferation	Wang et al., 2012, 2015
Carboxymethyl chitosan, gelatin, and laponite biocomposite scaffold with potential use in bone tissue engineering	Tao et al., 2017	
General cosmetic uses	Clay minerals as dermatological active ingredients and excipients of dermocosmetic products	López-Galindo et al., 2007; Viseras et al., 2007
	Dermocosmetic applications of clays are related with their surface, physical and mechanical properties	Moraes et al., 2017

1.2. Clay Minerals in Skin Drug Delivery

Table 1.5. (continued, part IV)

Action	Outcomes	Ref
Natural antibacterial clays	Natural antibacterial clays able to kill human pathogens including antibiotic resistant strains	Morrison et al., 2016
	Clays used for the treatment of cutaneous bacterial infections	Carretero, 2002; Williams et al., 2004, 2008, 2011; Ferrell, 2008; Friedlander et al., 2015
	Biotic and abiotic actions responsible of antibacterial activity of natural clay minerals	Otto et al., 2013
	Biotic activity of the Jordan red clays	Falkinham et al., 2009
	Abiotic processes involved in antibacterial activity of clay minerals	Otto and Haydel, 2013a
	Antibacterial activity of some natural clays depend on microbicidal activities of desorbed metal ions	Otto and Haydel, 2013b
Antibiotics-loaded nanoclays	Natural zeolite exchanged with inorganic Zn ²⁺ -erythromycin	Cerri et al., 2004; Bonferoni et al., 2007
	Chlorhexidine/montmorillonite inhibited the growth of Staphylococcus aureus and Escherichia coli	Saha et al., 2014b
	Organo-modified bentonite for gentamicin topical application	Iannuccelli et al., 2018
	Topical ointment consisting on smectite, illite, rectorite to treat skin infections and skin diseases	Tuba, 2018
	Smectite-zwitterion-silver-analgesic system with antimicrobial and pain relieving properties has been patented	Rangappa et al., 2017
	Chitosan-montmorillonite nanocomposite film loaded with triclosan	Chen et al., 2018
Other clay-based cosmetic products	A wide range of cosmetic products containing clay minerals have been designed and have their patent registered	Viseras et al., 2007
	Use of clays as emulgents or emulsifiers in cosmetic products	Alexander, 1973; Gabriel, 1973; Carter, 1940; Sarfaraz, 2004
	Optimization of a peel-off facial mask formulation containing green clay and aloe vera	Beringhs et al., 2013
	Dry shampoo comprising an smectite clay, natural starches, and a natural oil absorbent	Perfitt and Carimbocas, 2017
	An emulsion of bio-minerals more stable, and requiring less energy and time to prepare	Rochette et al., 2017

1.2.4.2. Wound Healing and Treatment of Skin Lesions

The protective functions of the skin are compromised by injury. A wound can be defined as a defect or a break in the skin, resulting from a

mechanical or thermal damage, or the consequence of an underlying medical or physiological condition.

Wound healing is a dynamic process in which the collaborative efforts of many different tissues and cell lines are required to recover the integrity of damaged tissue and replace lost tissue. It occurs in four stages: inflammation, migration, proliferation, and maturation. Healing is considered to be complete when the skin surface has reformed and re-established its tensile strength.

- a) Inflammation: it is the body's initial response to injury and involves both cellular and vascular responses resulting in vasodilation, increased capillary permeation and stimulation of pain receptors. It occurs within a few minutes to 24 h of injury.
- b) Migration: growth factors in the wound exudate promote the growth and migration of epithelial cells, fibroblasts and keratinocytes to the injured area to replace damaged and lost tissue. It lasts for 2–3 days.
- c) Proliferation: it involves the development of new tissue and occurs simultaneously or just after the migration phase. The network is important for developing the tensile strength of the skin. As the proliferation continues, further epithelial cell migration across the wound takes place, providing closure and visible wound contraction. During the proliferation stage, the wound is typically beefy red in colour and moist, but not exuding.
- d) Maturation: this final phase of wound healing (also called the "remodelling phase") involves the diminution of the vasculature and enlargement of collagen fibres, which increase the tensile strength of the repair.

The need for regenerating rapidly and effectively the injured skin has stimulated the research of advanced therapies for wound care. Advanced wound dressings are designed to control the environment for wound healing. Role of clay minerals in the design of advanced wound dressings has been thoroughly reviewed (Sandri et al., 2016). Besides, it had been previously assessed that not only the use of clay minerals as nanocarriers of antimicrobial agents was important for treating cutaneous bacterial infections, but also the

ability of the clays to physically adsorb and remove bacterial cells, toxins, and debris from the wound provided additional benefits aimed to wound healing (Otto and Haydel, 2013a, 2013b).

A functionalized montmorillonite with epidermal growth factor (EGF) demonstrated that EGF immobilized on montmorillonite can stimulate cell growth and migration *in vitro* required in the proliferation step of the wound healing process (Vaiana et al., 2011). A nanocomposite based on montmorillonite and chitosan loaded with silver sulfadiazine was developed and its abilities not only to protect fibroblasts from the cytotoxic action of the drug but also the improvement of its bacteriostatic and bactericidal properties, especially against *Pseudomonas aeruginosa* were successfully assessed aimed to be used as an advanced wound dressing (Sandri et al., 2014). A comprehensive and detailed structural study of the aforementioned montmorillonite-chitosan-silver sulfadiazine nanocomposite and the interactions involved was also reported (Aguzzi et al., 2014b). It was observed that the treatment made with a Brazilian clay allowed greater formation of collagen fibers and consequent regeneration of the deep dermis and re-epithelialization and continuous formation of granulation tissue when tested in rat animal models (Dário et al., 2014). Functionalized layered clays with aminoacids (arginine, lysine and leucine) promoted fibroblast proliferation and can be potentially applied as a wound dressing to promote the wound healing process (Ghadiri et al., 2014a). Antibacterial activity of clay-ciprofloxacin composites against the common skin bacteria *Staphylococcus epidermidis* and *Propionibacterium acnes* was demonstrated as potential delivery systems for ciprofloxacin molecules aimed to design novel wound dressings (Hamilton et al., 2014). A methyl cellulose-sodium alginate-montmorillonite bionanocomposite films with interesting wound healing properties based both on its property to inhibit the growth of *Enterococcus faecium* and *Pseudomonas aeruginosa* and its potential wound closure activities (Mishra et al., 2014). A detailed review of the possibilities offered by various natural polymers/clay minerals composite scaffolds used for skin tissue engineering due to their enhanced wound healing properties was reported (Ninan et al., 2015b). The potential use of montmorillonite-chitosan films loaded with chlorhexidine as a potential wound dressing material to prevent

microbial colonization in wounds was assayed and all prepared films showed good antimicrobial activity (Ambrogi et al., 2017). A silicate (tourmaline)/chitosan composite films for wound healing applications was obtained with improved cell adhesion and proliferation, higher number of newly-formed, and mature blood vessels, as well as fastest regeneration of dermis when tested in porcine burn wounds (Zou et al., 2017). A nanocomposite made of chitosan oligosaccharide/halloysite was successfully prepared and characterized by advanced electron microscopy techniques. It was found to be biocompatible *in vitro* towards normal human dermal fibroblasts, the results of an *in vitro* wound healing test showed that it enhanced *in vitro* cell proliferation (cells in S-phase) rather than simple fibroblast migration. *In vivo* wound healing murine model results were in agreement with the previous *in vitro* results providing an early re-epithelialization process and an advanced degree of haemostasis and angiogenesis (Sandri et al., 2017). Polymer films loaded with a carvacrol/clay hybrid for skin ulcer treatment were investigated. Different clays were considered: montmorillonite, halloysite and palygorskite and finally a pharmaceutical-grade palygorskite was selected due to its ability to reduce carvacrol volatility and preservation of its antioxidant properties. The hybrid system provided improved antimicrobial properties against *Staphylococcus aureus* and *Escherichia coli* and cytocompatibility towards human fibroblasts (Tenci et al., 2017). A new clay based dermal patch system based on montmorillonite-betaine hydrochloride silver nitrate for potential use in first degree burn wounds and its anti-nociceptive activity was evaluated (Rangappa et al., 2017). A novel responsive nanocomposite hydrogel based on poly(vinyl alcohol)/chitosan/honey/clay was designed and successfully evaluated aimed to become a novel wound dressing. (Noori et al., 2018). The preparation method of a burn ointment including montmorillonite aimed to promote tissue regeneration and skin growth has been recently patented (Zhang et al., 2018).

1.2.4.3. Cell Adhesion, Proliferation and Differentiation: Skin Engineering and Regenerative Medicine

Cell adhesion and proliferation on biomaterials are crucial points in tissue engineering and biotechnology. Studies aimed to assess cell proliferation and adhesion to clay minerals are a current matter of interest. The most studied clay minerals are laponite, montmorillonite, cloisite, and halloysite (Sandri et al., 2016). Mousa and co-workers have recently reviewed and compiled the beneficial effects of clay nanoparticles on cellular adhesion, proliferation, differentiation, and their attractive mechanical or rheological properties highlighted the striking potential of clays for the creation and development of new bioactive scaffolds to be used in skin regenerative medicine (Mousa et al., 2018). Early studies on sepiolite-collagen complexes observed normal fibroblast proliferation and outgrowth of skin fibroblasts from explants (Lizarbe et al., 1987; Olmo et al., 1987). Fibroblast attachment and spreading was improved by montmorillonite and halloysite and allowed cells to maintain their phenotype (Kommireddy et al., 2006). The addition of montmorillonite to chitosan enhanced the adhesion of osteoblasts (Katti et al., 2008) and fibroblasts (Popriadukhin et al., 2011). Da Silva and co-workers developed a biocompatible and biodegradable retinal scaffold based on montmorillonite/polyurethane nanocomposites (Da Silva et al., 2013). The biocompatibility and cell proliferation of montmorillonite have been evaluated in cultured normal human dermal fibroblasts (Sandri et al., 2014). A nanocomposite based on montmorillonite and silk fibroin has been developed as biomaterial for bone tissue formation (Mieszawska et al., 2011). A novel composite scaffold based on chitosan–gelatine and nanohydroxyapatite–montmorillonite with improved properties for use in tissue engineering applications was accurately prepared (Olad and Farshi-Azhar, 2014). Montmorillonite-reinforced hydrogels, based on a peptidomimetic polyamidoamine carrying guanidine pendants were successfully used as substrates for the osteo-induction of osteoblast precursor cells (Mauro et al., 2017). Cell viability tests showed that newly developed chitosan-montmorillonite triclosan loaded films are compatible with human dermal fibroblasts (Chen et al., 2018). A strontium (Sr^{2+}) modified chitosan/montmorillonite composite scaffold has been recently developed

with enhanced properties to be used in bone tissue engineering (Demir et al., 2018). A full and comprehensive study of the features provided by halloysite nanotubes in tissue engineering was reported (Fakhrullin and Lvov, 2016). Alginate-halloysite composite scaffolds were prepared with enhanced fibroblasts attachment and proliferation attributed to the increase in the surface roughness due to the incorporation of halloysite (Liu et al., 2015). Chitosan–gelatine–agarose doped halloysite scaffolds prepared were promising candidates for tissue engineering applications due to their *in vitro* and *in vivo* biocompatibility and their ability to enable the neo-vascularization in newly formed connective tissue placed near the scaffold that allowed the complete restoration of blood flow (Naumenko et al., 2016). A tri-component hydrogel, based on gellan gum, glycerol, and halloysite nanotubes was designed for soft tissue engineering applications (Bonifacio et al., 2017). Laponite cross-linked was able to maintain both the adhesion and proliferation of HepG2, skin fibroblast, and human umbilical vein endothelial in a manner strongly associated with the concentration of clay in the hydrogel (Haraguchi et al., 2006; Liu et al., 2012). Wang and co-workers, used Laponite to develop poly(lactic-co-glycolic acid; PLGA) nanofibers with promoted fibroblast adhesion and proliferation (Wang et al., 2012). Similarly, attapulgitite was included in PLGA nanofibers as a scaffolding material for osteogenic differentiation of stem cells (Wang et al., 2015). A biocomposite scaffold composed of carboxymethyl chitosan, gelatin, and laponite nanoparticles via freeze-drying was prepared with potential use in bone tissue engineering (Tao et al., 2017).

1.2.4.4. Antibacterial Purposes

As above mentioned, skin acts as a physical barrier to avoid the invasion of external pathogens. The desiccated, nutrient-poor, acidic environment, contributes to the adversity that microorganisms must deal with to colonize human skin (Byrd et al., 2018). Besides, topical antimicrobial therapy emerges as an attractive route for the treatment of infectious diseases due to the increased resistance to oral-administered systemic antimicrobial therapy (Lam et al., 2018).

Natural Antibacterial Clays

Natural antibacterial clays when hydrated and applied topically are able to kill human pathogens including antibiotic resistant strains proliferating worldwide. Only certain clays are bactericidal (Morrison et al., 2016). Examples of clays and soils being used for the treatment of cutaneous bacterial infections are well known (Carretero, 2002; Williams et al., 2004, 2008, 2011; Ferrell, 2008; Friedlander et al., 2015). Antibacterial activity of natural clay minerals is the result of two types of actions: biotic and abiotic (Otto and Haydel, 2013a, 2013b). To be highlighted as example of biotic activity is the case of the Jordan red clays whose antimicrobial activity is explained by the proliferation of bacteria naturally present within the clay and their concomitant production of antimicrobial compounds (Falkinham et al., 2009). Other biotic influences, including protozoan or mycobacterial predation, lytic microorganisms, and bacteriophages, may also be responsible for controlling bacterial growing. Besides, abiotic processes are also responsible for the antimicrobial activity of some clays (Otto and Haydel, 2013a). Clays bind toxic metals to their surface due to their net negative charge and then release those exchangeable metal ions from the clay surface. Hence, antibacterial activity of these natural clays is dependent on microbicidal activities of the desorbed metal ions (Otto and Haydel, 2013b).

Antibiotic-Loaded Nanoclays

Clays act as topical delivery agents for various antimicrobial products. A natural zeolite was exchanged with inorganic Zn^{2+} and subsequently charged the micronized composite with erythromycin to investigate its antimicrobial efficacy against erythromycin-resistant *Propionibacterium* strains obtaining a 99.5% reduction in *P. acnes* viability was observed (Cerri et al., 2004; Bonferoni et al., 2007). Furthermore, chlorhexidine was intercalated onto a montmorillonite aimed to be useful in skin pathologies due to its successful inhibition of the growth of a wide range of microorganisms including both *Staphylococcus aureus* and *Escherichia coli* (Saha et al., 2014b). An organo-modified bentonite for gentamicin topical application was developed with sustained antibacterial activity and enhanced drug permeation rate (Iannuccelli et al., 2018). A topical ointment consisting

on smectite, illite, rectorite clay minerals alone or in combination has been recently patented to treat bacterially-caused skin infections and skin diseases (Tuba, 2018). Thus, a multifunctional smectite-zwitterion-silver-analgesic system with both antimicrobial and pain relieving properties has been patented (Rangappa et al., 2017). A chitosan-montmorillonite nanocomposite film was loaded with the antibiotic triclosan and an intelligent pH responsive long-term release was obtained. High sterilization efficiency of the films was found by means of *Staphylococcus aureus*, *Escherichia coli* and *Staphylococcus epidermidis*. Furthermore, cell biocompatibility measurements toward L929 fibroblasts and human lens epithelial cells showed no adverse effects of the multilayer film (Chen et al., 2018).

1.2.4.5. Dermocosmetics

Clay minerals are part of a large variety of dermocosmetic products, such as facial creams, sunscreen, products for skin cleansing, shampoos, and makeup items (liquid and powder foundations, eye shadow, facial masks, lipsticks, etc.) either as dermatological active ingredients or as excipients (López-Galindo et al., 2007; Viseras et al., 2007).

Most important properties attributed to clays for dermocosmetic applications are related with their surface properties: (surface area, cation exchange capacity, layer charge among others); rheological properties: (thixotrophy, rheopexy, viscosity, plasticity), and other physical and mechanical properties including particle size, shape, colour, softness, opacity, reflectance, iridescence, and so on (Moraes et al., 2017).

Sunscreens

The detrimental effects of ultraviolet A and B radiations (UVA and UVB) on the skin can lead to the development of malignant carcinomas in the cutaneous tissue. Hence, sunscreens are dermocosmetic products of great importance to the skin health. Thanks to their excellent properties, some clay minerals have been included in dermocosmetic formulations of sunscreens, acting as a barrier that blocks the solar radiation and thus protects the cellular nucleic acids. Clay minerals must have high index of refraction and optimal light dispersion properties to be used as sunscreens. Bentonite and hectorite meet the required specifications and are already being used as sunscreen

(Ghadiri et al., 2015; Mattioli et al., 2016). A mineral-based sunscreen containing activated clay combined with a dispersing agent and one or more inorganic sunscreen actives was patented resulting in a mineral sunscreen having high UVB/UVA protection and exceptional spreadability that is non-whitening (Timothy et al., 2015). Besides, a composition for cosmetics is provided, which has a UV shielding effect and good dispersibility including microparticulate titanium dioxide, magnesium, and/or calcium hydroxide and a clay mineral. The clay mineral suitable for the present invention, no limitation is posed upon it, so long as it can be used as a powder to be employed in ordinary cosmetics. For example, there are boron nitride, sericite, natural mica, calcined mica, synthetic mica, synthetic sericite, alumina, mica, talc, kaolin, bentonite, smectite (Ijiri et al., 2015).

Other Clay-Based Cosmetic Products

A wide range of cosmetic products containing clay minerals in their composition have been designed throughout time and most of them have their patent registered (Viseras et al., 2007). Use of clays as emulgents or emulsifiers in cosmetic products is well-known. To be highlighted is the use of talc as emulgent in “make-up preparations” because of its high surface area (Gabriel, 1973). Besides, bentonite was used as emulsifier in a nail-enamel remover (Carter, 1940), in oil-in-water make-up (Gabriel, 1973), vanishing low oil-content creams (Alexander, 1973), and in cleansing lotions (Sarfaraz, 2004). The optimization of a peel-off facial mask formulation containing green clay and aloe vera was studied (Beringhs et al., 2013). More recently a dry shampoo composition comprising an smectite clay, natural starches, and a natural oil absorbent was developed and subsequently its patent was registered (Perfitt and Carimbocas, 2017). An emulsion of bio-minerals (phyllosilicate, inosilicate, cyclosilicate, tectosilicate, neosilicate or sorosilicate) created using unique process steps that allows the combination of ingredients to be emulsified in a cold, chemical-free environment to create a product that is more stable, and requires less energy and time to prepare was registered (Rochette et al., 2017).

1.2.5. Summary and Outlook

Topical and transdermal products including clay minerals have a long history and remain key formulations for delivering drugs not only onto the skin for local purposes, but also through it for systemic action. Skin is a widely used route of delivery for local and systemic drugs and is potentially a route for their delivery as nanoparticles. Among the wide range of nanoparticles available, clay minerals have been used since ancient times both as actives and excipients in the treatment of skin illness. Besides, use of nanoclays alone and/or in combination with biopolymers and/or drug in treating local skin and systemic diseases is a current matter of concern. Therefore, in this review we discuss recent work in the field of clay minerals-based nanoparticle delivery to the skin, and future directions currently being explored. Once this attempt to summarise and highlight the possibilities offered by clay minerals in advanced skin drug delivery finished, our final goal is to provide a greater understanding of the countless benefits derived from both this administration path and this kind of nanosystems.

1.3. Natural Inorganic Ingredients in Wound Healing

The skin is the largest organ of the human body, with an average surface area of 1.8 m². It is in charge of multiple functions such as temperature control and defence against physical, chemical and thermal aggressions. Additionally, the presence of other appendages such as hair follicles, sweat and sebaceous glands provide additional functions and properties. Histologically speaking, the skin is a stratified structure formed by the epidermis, the dermis and the hypodermis (from outer to inner stratum). Along the human body, the skin thickness varies majorly from 0.5 to 2 mm, reaching 4 mm in the nape region (Ng and Lau, 2015).

The epidermis is the most external stratum and it is divided into *basale*, *spinosum*, *granulosum*, *lucidum* and *corneum strata*. In the stratum basale, cell renewal is continuous and produces keratinocytes, melanocytes, Merkel and Langerhans cells. Keratinocytes are the predominant cells of the epidermis and they organize forming 4 or 5 cell strata, depending on the corresponding thickness of the skin along the different parts of the body. Normally, full skin renewal requires about 28 days, though this rate increases during inflammation, injury or other conditions. Keratinocytes move through the strata to reach the *stratum corneum* as corneocytes. The *stratum spinosum* contains keratin filaments appearing as a “spiny” area, more frequented by Langerhans cells (dendritic, antigen-presenting cells with the remarkable immunologic role). Melanocytes are responsible for pigment production.

The dermis stratum is much thicker than the epidermis and is divided into *papilar* and *reticularis* strata. Blood vessels, nerves, hair follicles, sweat and sebaceous glands are found in this stratum, thus providing nutritional and structural support. Dendritic cells, macrophages, fibroblasts and mast cells are the cells constituting this stratum. Fibroblasts synthesize/degrade extracellular matrix proteins; Langerhans cells and masts are involved in immunologic reactions together with macrophages, though the latter one is also involved in coagulation and remodelling processes. The hypodermis obeys the main functions of energy supply and thermal insulation, formed by three strata (superficial, intermediate and deep) but without well-defined limits.

Physical injuries or skin diseases altering skin normal composition and/or functioning can compromise skin integrity and, therefore, skin functions. A wound is a defect or a break in the skin, with or without loss of connective tissue. Injuries or wounds are described in different ways: based on its aetiology, anatomical location, depending on the method of healing, on the symptoms, etc. They can be the consequence of mechanical or thermal damage or be the consequence of an underlying medical or physiological condition. Injuries that do not achieve anatomic and functional integrity after approximately six weeks of standard medical treatment are defined as chronic wounds.

Wound healing is a dynamic and coordinated process in which the collaborative efforts of many different tissues and cell lines are required, both to recover the integrity of the damaged tissue and to replace the lost one. Growth factors, chemokines, cytokines, extracellular matrix molecules, cell adhesion molecules, among others are the main molecules allowing crosstalk between multiple cell types involved during healing. Despite the complexity of the process, it can be divided into four stages that overlap in time and space (inflammation, migration, proliferation and maturation) and is completed when skin surface is fully reformed and recovers its tensile strength. An additional step, haemostasis, is considered if the injury happens beyond the epidermis (reaching capillary or bigger blood vessels) and entails bleeding.

- During inflammation, vasodilation increased capillary permeation and stimulation of pain receptors are mainly involved as a first response toward the injury. The inflammatory response initiates by the production of pro-inflammatory cytokines and the secretion of prostaglandins and chemotactic substances such as complement factors, interleukin-1, TNF- α and TGF- β . It occurs within the first moments and it can last for 24 h without complications. Nevertheless, necrotic or infected injuries maintain inflammation for longer periods (Burns et al., 2003; Eming et al., 2007; Demidova-Rice et al., 2012).
- When migration step initiates, growth factors in the wound exudate promote the growth and migration of epithelial cells, fibroblasts and keratinocytes to the injured area to replace damaged and lost tissue.

1.3. Natural Inorganic Ingredients in Wound Healing

It lasts for 2-3 days and most of the time is difficult to differentiate from the proliferation stage, since they occurs simultaneously.

- Proliferation involves the development of new tissue by re-epithelialization, matrix and collagen deposition and angiogenesis. Epithelial-cell migration takes place across the wound, providing closure and visible wound contraction.
- Maturation or “remodelling phase” is the final stage in a normal skin healing process. In this step, vasculature and enlargement of collagen fibers take place, allowing tensile strength improvement. It is the result of an equilibrium process between synthesis and degradation of the extracellular matrix, mainly regulated by fibroblasts and can last even for a year.

Multiple factors can cause impaired wound healing by affecting one or more phases of the healing process, especially with underlying disease states such as diabetes. Different medical approaches and therapeutic choices can affect wound healing and skin remodelling. If wound healing does not progress normally, a chronic wound may result, which is a significant burden to the patient and the medical system. Chronic wounds such as diabetic foot, venous leg ulcers and pressure ulcers have common features such as prolonged or excessive inflammation, persistent infections, a formation of drug-resistant microbial biofilms, and an inability of the dermal and/or epidermal cells to respond to repair stimuli (Tenci et al., 2017). Chronic wounds are a current health problem with devastating consequences for patients and they contribute to major costs to healthcare systems and societies (Olsson et al., 2017; Nussbaum et al., 2018). Treatment costs for chronic wounds are substantial and are estimated to account for up to 6% of total healthcare expenditure in developed countries. In the United States, it has been reported that wounded patients cost over \$25 billion annually (Sen et al., 2009). Hospitalization costs of patients with chronic ulcers range from US\$12,851 to US\$16,267 (Olsson et al., 2017). With these premises, the development and implementation of new wound healing management strategies and healthcare products are imperative. Adequate and comprehensive discussions on wound healing advances require basic notions of the different types of wounds and specific treatments for each of them.

The use of natural inorganic materials such as clay minerals in skin pathologies therapy goes back to prehistoric times and they continue to play a crucial role in the design of new drug delivery systems. They were used in the very first prehistoric remedies, including oral (geophagy) and skin treatments. The first historical evidence of the use of clay for therapeutic purposes appears around 2500 BC in a Sumerian-Mesopotamian tablet (Biggs, 2013). In Europe and Mediterranean countries, the pharmaceutical ancient historical text of Greek, Roman, Byzantine and Medieval periods include clays as “simples” (De Vos, 2010). Most of “simples” were herbal but also animal parts and minerals (Sánchez-Espejo et al., 2017). Particularly, reports inform that they were used as therapeutic agents during wound healing and to stop bleeding. Cleopatra used Dead Sea mud as a natural cosmetic product and “Nubian earth” was identified as anti-inflammatory (Gomes and Silva, 2007). Natural inorganic products were widely mentioned in the important historical texts constituting the *European materia medica* since the “Hippocratic Corpus” (5th-4th century BC) (De Vos, 2010).

Besides clays, other inorganic ingredients have been widely used in classical skin formulations. Paradigmatic example is the use of silver, as silver nitrate or silver sulfadiazine applied as liquids (solutions), semisolid (creams and pastes) and solid (pencils) forms to treat infections and chronic wounds, such as ulcers and burns (Demling, 2001; Dunn and Edwards-Jones, 2004; Fong, 2005). Together with its well-established antimicrobial effects, new studies have focused on the potential effects of silver nanoparticles (as well as other transition metals) in the healing process.

Today, natural inorganic materials such as clay minerals continue to play an important role in conventional pharmaceutical formulations (Viseras et al., 2019). Together, clay minerals are ingredients in complementary and alternative medicinal products (Sánchez-Espejo et al., 2014b). Clay minerals also play a noteworthy role in the development of innovative drug delivery systems (Fakhrullina et al., 2015; Viseras et al., 2015; Aguzzi et al., 2016; Yang et al., 2016b; Jafarbeglou et al., 2016; Sandri et al., 2016; Carazo et al., 2018a; García-Villén et al., 2019a).

Clay minerals are classical but also advanced excipients. They are used in formulations designed to be administered by oral, but also topical

1.3. Natural Inorganic Ingredients in Wound Healing

route (López-Galindo et al., 2011; García-Villén et al., 2019b). Skin is the preferred route of administration in several pathologies and topical and transdermal products are formulated to deliver drugs onto the skin for both local and systemic treatments. Particularly, clay minerals are a classical compound in the elaboration of topical semisolid products and they form pastes, poultices or liniments. For instance, currently, it is possible to find formulations such as “Calamine Lotion” in some of the most important Pharmacopoeias (BP, 2018; RFE, 2015; USP42-NF37, 2019). Calamine lotion, used for skin irritation treatment, includes zinc oxide as active and montmorillonite as an excipient in most of these regulatory procedures.

Future uses of clays and other natural inorganic ingredients in skin-directed preparations will arise from their abilities to resolve skin pathologies and/or to improve the transport of active ingredients to the skin. Particularly, their use in wound healing treatments would be determined by their activity through *in vitro* tests. Briefly, *in vitro* wound healing tests are methods to evaluate and study cellular proliferation and migration. They are based on the creation of an artificial gap (scratch) inside a single layer of confluence cell culture. This cell gap can be done by physical exclusion or by removing cells from the test area with mechanical, thermal or chemical damage methods (Jonkman et al., 2014). If tested cells found a favourable ambience, they will move toward the gap and proliferate in order to cover it. These tests can be done with epithelial (fibroblasts and keratinocytes being the main ones) and endothelial cells (Bindschadler and McGrath, 2007; Liang et al., 2007). These cells have a “collective migration” called “sheet migration” since they move in two dimensions while maintaining cellular contact. Cellular sheet migration occurs during cancer metastasis, embryonic morphogenesis and tissue injury (Jonkman et al., 2014). One of the techniques to create cell gaps is to perform a straight scratch in the middle of the confluent culture by using pipette tips and similar instruments (Liang et al., 2007; Kar et al., 2014; Abduljawwad and Ahmed, 2019). Because of that, “scratch assay” or “scratch wound healing assay” is a common terminology among researches and widely used in the scientific literature. Nonetheless, this method is subjected to high variability since the creation of the gap is affected by a wide variety of factors. Currently, it is possible to use specific culture dishes, in which the gap

is delimited by a silicon insert. Cells are seeded inside two “growth” spaces marked by the silicon insert and left to grow until confluence. Then, the silicon insert is removed, leaving two cells cultures separated by a well-defined, reproducible gap (Sandri et al., 2014, 2017; Saporito et al., 2017).

The rate of gap closure (speed of the collective motion of cells to close the gap) is the main information extracted from *in vitro* wound healing tests. Microscopic and imaging techniques are usually employed to visualize, record, photograph and/or measure the remaining gap during the process. Alterations of the extracellular matrix composition, environmental condition changes and culture medium modifications are some of the strategies that can be performed to study certain wound healing mechanisms.

Once a wound healing agent has demonstrated its potential by *in vitro* test, *in vivo* wound healing experiments are performed over animals such as rats or mice and should be approved by Animal Care and Use Committees. Animals are wounded following a proper protocol, which includes anaesthesia, hair-shave and injury creation. The wound healing process is monitored in a continuous manner. Depending on the scope of the study, different substances or objects can be applied over the injury in order to address their influence during the whole process or some healing stages. Equivalent data to “rate of gap closure” is obtained by *in vivo* wound healing by measuring the animal wound diameter as time passes. For that purpose, digital photographs should be taken at predetermined times, always placing the animal in the same way and maintaining camera settings and height fixed. Frequently, *in vivo* wound healing tests are accompanied by histopathological analyses of the wounded area, which can be harvested at different time points of the healing process after animal euthanasia (Ganguli-Indra, 2014).

The aim of this review is to provide a comprehensive summary of the most recent advances and studies implying natural inorganic ingredients (clay minerals, metal cations, zeolites, etc) in wound healing, both as active ingredients and as excipients bestowing enhancing properties.

1.3.1. Functions of Inorganic Ingredients in Wound Healing

The participation of inorganic ingredients in wound healing strategies are supported by the already demonstrated biocompatibility of

1.3. Natural Inorganic Ingredients in Wound Healing

substances such as clay minerals with different types of skin cells (Lizarbe et al., 1987; Olmo et al., 1987; Kommireddy et al., 2006) but also, and mainly because they offer a wide variety of active functions. In the last years, they have demonstrated to be useful in cellular adhesion, proliferation and differentiation and therefore in tissue engineering and biotechnology strategies (Sandri et al., 2016; Mousa et al., 2018).

Interactions between natural inorganic ingredients and living organisms lead to different biomedical applications, based on the establishment of either a negative or a positive haemostatic interaction between the inorganic ingredient and the living organism (antibacterial or haemostatic effects, respectively).

1.3.1.1. Antimicrobial Effects

Wounds compromised the barrier effect of the skin and constitute an ideal environment for infections. Consequently, wound treatments always require prophylaxis and/or treatment of microorganism. Numerous skin conditions (i.e. ulcers, comedones, acne, seborrheic dermatitis, among others) can be ameliorated by using clay minerals since they are able to adsorb liquids, oiliness, toxins, sebum, bacteria and other wound debris (Figure 1.9) (Meier et al., 2012; Adusumilli and Haydel, 2016).

Natural inorganic ingredients such as clay minerals have demonstrated to kill human pathogens, including the antibiotic-resistant strains (Morrison et al., 2014, 2016; Williams, 2017). On the other hand, phyllosilicates possess additional physical properties such as high adsorption capacity (due to high specific surface areas) and negative net surface charges. These properties have also been related to antimicrobial properties due to the adsorption of both bacteria and/or toxins from the infected sites.

Examples of clays and soils being used for the treatment of cutaneous bacterial infections are well known and due to biotic or abiotic actions (Carretero, 2002; Ferrell, 2008; Petkewich, 2008; Williams et al., 2008, 2011; Otto and Haydel, 2013a; Otto et al., 2014; Friedlander et al., 2015). Biotic antimicrobial action is ascribed to the presence of intrinsic microorganisms growing in the midst of the inorganic material (bacteria, protozoan, mycobacteria, bacteriophages, etc). For instance, Jordan red clay presents a

kind of bacteria that naturally produces antimicrobial compounds, which are responsible for the antimicrobial performance of the solid system (Falkinham et al., 2009). Abiotic antimicrobial activities of natural inorganic ingredients are those performed by the mineral itself. In particular, clay minerals (negative net-surface charge) can adsorb and release toxic metals with antimicrobial effects (Otto et al., 2014, 2016). For instance, Fe^{3+} leachate from a natural clay formed by illite-smectite, pyrite, plagioclase and quartz proved effective against Gram-positive and Gram-negative bacteria, including resistant strain (Caflisch et al., 2018).

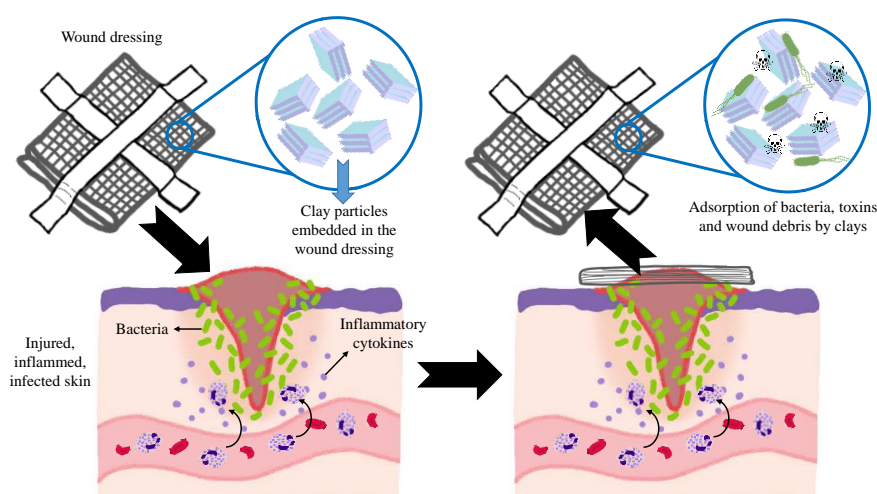


Figure 1.9. Schematic representation of bacteria and toxins adsorption from infected wounds by clay mineral particles. The inclusion of inorganic materials such as clay minerals in wound dressings increase the adsorption capacity of the dressing, thus helping to eliminate wound debris like bacteria (green) or toxins (☞☞)

Some authors claimed that the relationship between antibacterial activity and exchangeable cations of clay minerals should be interpreted with precaution since not all the exchangeable ions are effective as antimicrobial agents (Otto et al., 2016). Certain cations need special chemical environments to be released from clay minerals (i.e. Fe^{3+} needs acid environment) (Cunningham et al., 2010). Additionally, a combination of multiple factors could also be the reason for clay to have antimicrobial activity. For instance, clay minerals can affect microbial metabolism indirectly due to alterations of the growth medium (Haydel et al., 2007). Antibacterial effects of natural clays

from hydrothermal deposits have been evaluated (Morrison et al., 2014). Mineral composition of the deposit consisted of illite-smectite and quartz as major phases, while chlorite, feldspar, gypsum, pyrite and kaolinite were also present depending on the hydrothermal zone analysed. *Escherichia coli* and *Staphylococcus aureus* strains were incubated with samples from different alteration zones of the hydrothermal deposit. Authors found that clays from reduced mineral zones possessed bactericidal activity while clays from oxidized zones had variable antibacterial effects. The antibacterial effectiveness was correlated with elevated concentrations of Fe^{2+} , Fe^{3+} and Al^{3+} in the aqueous leachates. The authors hypothesized that “extracellular adsorption of Fe^{2+} , Fe^{3+} , and Al^{3+} may result in lipid and protein oxidation, increasing cellular membrane permeability and allowing the influx of toxic metals. Therefore, it may be a combination of cell wall attack and intracellular reactions that result in cell death or significant viability loss within the experimental time frames” (Morrison et al., 2014).

Synergic effects appear by combining the physical properties of clay minerals with other active substances. For instance, pustules, papules, cysts and comedones produced by mild *Acne vulgaris* were reduced in patients which applied clay jojoba oil mask 2/3 times a week. Jojoba oil reported anti-inflammatory and antibacterial effects which were improved by high adsorption capacity of the clay mineral (Meier et al., 2012).

1.3.1.2. Haemostatic Effect

The clotting process, or haemostasis, is a physiological process that prevents blood loss through the formation of a stable haemostatic clot at the site of bleeding. It can be divided into two basic pathways that finally lead to coagulation and clot forming: intrinsic pathway (contact activation) and extrinsic pathway (tissue factor).

Negatively charged surfaces can promote the intrinsic coagulation pathway via contact activation. It is a general surface phenomenon, not a biological recognition of certain functional groups, and has been recognized as an important cause for poor haemocompatibility of cardiovascular biomaterials since it is triggered by contacting blood with artificial materials. Another important characteristic of substances able to activate contact

coagulation cascade is their wettability (the inorganic ingredient water contact angle being close to 0°) (Vogler and Siedlecki, 2009; Smith et al., 2015). These two characteristics (negative net charge surface and hydrophilicity) can be found in clay minerals (such as kaolin) and other inorganic ingredients such as zeolites, thus explaining their use as blood clotting agents (Baker et al., 2008; Pourshahrestani et al., 2016). The underlying mechanisms of action of some inorganic ingredients are represented: adsorption of water molecules into zeolite cages is promoted by cation-water interaction, concentrating blood cells and clotting factors and promoting haemostasis (Figure 1.10); the negative surface charge of kaolin particles leads to the activation of intrinsic coagulation cascade (Figure 1.11).

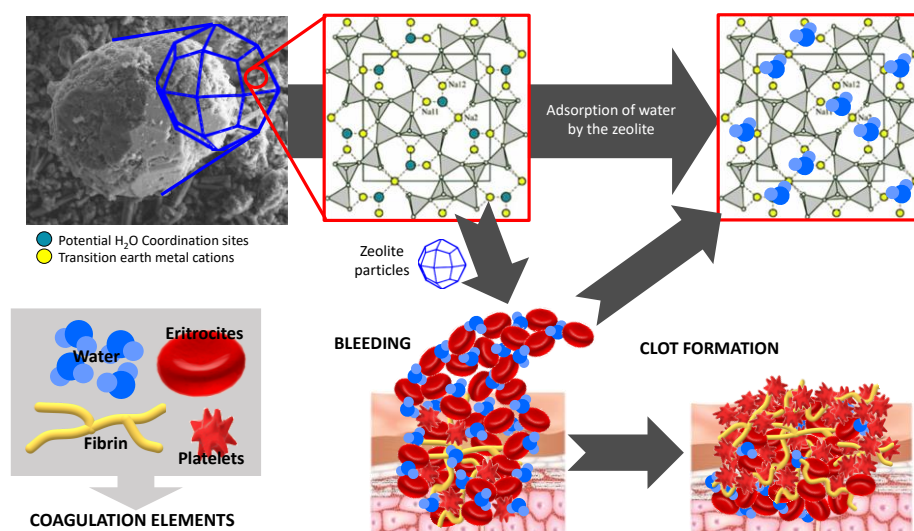


Figure 1.10. Mechanism of action of zeolites on blood coagulation: absorption of water molecules into zeolite cages promoted by cation-water interactions. This interaction produces concentration of blood cells and clotting factors, thus promoting haemostasis

1.3.2. Clay Minerals for Wound Healing

Natural clays show interesting properties for wound healing (Table 1.6) that can be improved due to synergic effects when formulated with polymers (Table 1.7).

1.3.2.1. Clay Minerals

Clay minerals are the minerals that are present in clay. Clay is defined as “a naturally occurring material composed primarily of fine-grained minerals, which is generally plastic at appropriate water contents and will harden when dried or fired” (BP, 2018). Clay minerals are mainly phyllosilicates (a group of silicates), but may also include other minerals that impart plasticity and harden when dried or fired. The health uses of clays result from their ubiquity in earth's crust and their physical (particle size and shape, specific surface area, texture, colour and brightness) and chemical (surface chemistry and charge) features. Particularly, clay materials mainly constituted by some special clays (kaolinite and halloysite; smectites (montmorillonite, saponite and hectorite); as well as fibrous clays (palygorskite and sepiolite)) are used. They act as excipients, to facilitate the administration of the active agents, improve their efficiency and ensure stability until the expiration date for use by the patient, or as actives (mainly as absorbent, antimicrobial and antiinflammatory agents) (Alberto López-Galindo and Viseras, 2004).

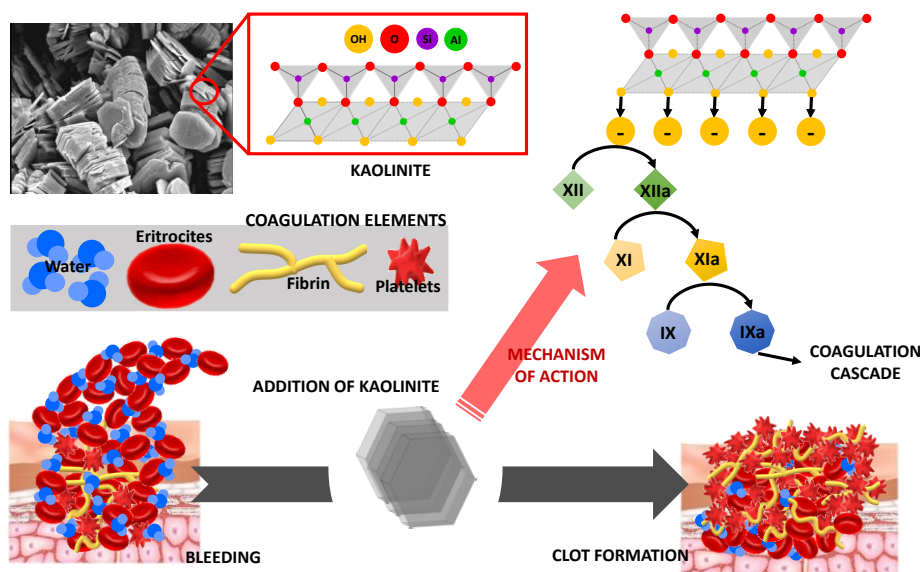


Figure 1.11. Effects of kaolin on the activation of intrinsic coagulation pathway through its negative surface charge, leading to activation of the coagulation cascade. XII, XIIa, XI, XIa, IX and IXa are intrinsic pathway clotting factors activating the coagulation cascade. The addition of “a” to the roman numbers indicates an “activated state” of each clotting factor

Table 1.6. Wound healing effects of clay minerals

Clay	Form	Effect	Ref
Oregon Mineral Technologies clay	Powder	Antimicrobial effect	(Morrison et al., 2014)
Palygorskite, modified palygorskite		Better collagen organization, angiogenesis, re-epithelialization and hair follicles formation	(Silva et al., 2013)
		Adequate wound healing with dermal papilla and hair follicles only with natural palygorskite	(de Gois da Silva et al., 2014)
Sepiolite and palygorskite		Fast edema inhibition	(Cervini-Silva et al., 2015b)
		Reduced lipid peroxidation	(Cervini-Silva et al., 2015a)
Mg-rich smectite		Promoted collagen formation and angiogenesis	(Sasaki et al., 2017)
Silica mud (Blue Lagoon) Volcanic deposit Black mud (Dead sea) Hectorite, montmorillonite, palygorskite	Suspension	Induction of skin barrier proteins genetic expression	(Grether-Beck et al., 2008)
		Formation of new granulation tissue, edema reduction	(Nasirov et al., 2009)
		Enhanced granulation, wound contraction, epithelialization, angiogenesis and collagen deposition	(Abu-al-Basal, 2012)
		Chronic wounds treatment (diabetic, venous and pressure ulcers)	(Belenky and Collins, 2011; Wallace and Wang, 2015; Davinelli et al., 2019)
		Improvement of cellular adhesion	(Abduljawwad and Ahmed, 2019)

Wound healing properties of a natural Brazilian palygorskite were evaluated by Silva and co-workers (Silva et al., 2013). They compared the natural clay sample with two organophilic samples of the same clay mineral (alkyl-dimethyl-benylammonium chloride-palygorskite and cetyl-trimethyl-ammonium chloride-palygorskite). Treatment of Wistar rats revealed that better wound healing was obtained when natural palygorskite was used, in comparison with the organophilized samples, which were considered toxic since they produced vascular congestion in the wounded area. The diameter of the lesion treated with Piauí palygorskite increased within the first week (bigger than control groups), but then reduced within the second one (same diameter than control groups). Despite the slower wound healing, histological

1.3. Natural Inorganic Ingredients in Wound Healing

cuts showed a better reorganization of collagen and angiogenesis within the first 7 days, followed by re-epithelialization, dermic papillae and pillous follicles in the 14th day. The same kind of study was performed by comparing organophilized palygorskite with cetyltrimethyl ammonium chloride and chloride alkyl dimethyl benzyl ammonium with a natural sample. These compounds were subsequently tested against wounded rats *in vivo* (de Gois da Silva et al., 2014). Histological cuts revealed that rats treated with organophilized palygorskite showed mild and moderate dermal papilla formation after 14 days, without hair follicles formation. On the other hand, rats treated with natural palygorskite developed dermal papilla with hair follicles after 14 days of treatment, thus revealing once again that natural clay sample performed better wound healing results.

Table 1.6. (Continued, part II)

Clay	Form	Effects	Ref
Illite-smectite, montmorillonite, kaolinite	Poultices, leachates	Antibacterial effect	(Adusumilli and Haydel, 2016)
Clay deposit (Ocara lake)	Emulsion	Thick collagen fibres deposition, deep dermis regeneration	(Dário et al., 2014)
Montmorillonite, halloysite		Total wound healing with vs. control group (gauze without clay mineral)	(Alavi et al., 2014)
Laponite	Drug combinations	Clay combined with Arginine, lisine, leucine, glutamic acid. Improved cell proliferation.	(Ghadiri et al., 2014b)
Montmorillonite		Clay and EFG. System did not compromise EFG effect, normal wound healing process	(Vaiana et al., 2011)
		Clay and AgNPs. Antibacterial effect, reduced silver cytotoxicity, less scar tissue, cleaner wound surface.	(Chu et al., 2012)
		Clay and AgNPs. Antibacterial, analgesic for burns	(Rangappa et al., 2018)
		Fentanyl AgNPs. Analgesic for burns.	(Han et al., 2017)

Sasaki and co-authors have recently reported that Mg²⁺ and Si⁴⁺ ions released by a synthetic Mg-rich smectite clay mineral can promote collagen formation and angiogenesis on skin wounds (Sasaki et al., 2017). Fibrous clay minerals (sepiolite and palygorskite) were evaluated in terms of wound healing properties by Cervini-Silva and co-workers (Cervini-Silva et al.,

2015b). These natural inorganic materials demonstrated to possess an anti-inflammatory *in vivo* effect (inhibiting edema shortly after exposure). Moreover, these very same palygorskite and sepiolite demonstrated to reduce lipid peroxidation, though their effect being lower when compared with other inorganic ingredients such as halloysite (Cervini-Silva et al., 2015a).

A recent and interesting study published by Abduljawad and Ahmed evaluated the modulation of different clay minerals toward cancer cell adhesion (Abduljawad and Ahmed, 2019). Kaolinite, montmorillonite, hectorite and palygorskite were evaluated. Results showed that kaolinite established van Der Waals interactions with cells, while hectorite, montmorillonite and palygorskite were the most effective clay minerals improving cell adhesion due to electrostatic forces. The establishment of medium-strong interactions between clays and cells made that, during wound healing scratch-assay, gap closure was found slower with respect to the control group. On the other hand, kaolinite showed no adhesion enhancement since the main mechanism of interaction occurred through van Deer Walls forces (Abduljawad and Ahmed, 2019). Author suggested these findings to be very useful for cancer treatments, since clays favouring cellular adhesion would potentially prevent metastasis to occur. Apart from this, these results would allow the design of highly specific systems and devices for wound healing (clays favouring proliferation and migration) and tissue regeneration (clays favouring cellular adhesion).

1.3.2.2. Clay Mineral Semisolid Formulations

Most of the times, clay minerals are formulated with other ingredients to obtain semisolid dosage forms in which the clay is an active or inactive ingredient.

Therapeutic muds are a classical topical dosage form of clay/water semisolid suspensions resulting from an inorganic and/or organic phase suspended in mineral medicinal water (Mefteh et al., 2014; García-Villén et al., 2018; Khiari et al., 2019). Suspended solids are most of the time clay materials that may be natural sediments of spring waters (natural muds) or, frequently, incorporated to the spring water as formulation additives to obtain “artificial muds” that should be fully characterized before using (Rebelo et al., 2011a,

1.3. Natural Inorganic Ingredients in Wound Healing

2011b; Sánchez-Espejo et al., 2014a). Both natural and artificial muds are used in spa centres for the treatment and control of musculoskeletal disorders and skin pathologies such as vitiligo, acne, contact dermatitis, seborrheic dermatitis, chronic wounds among others (Fraiole et al., 2011; Güngen et al., 2012; Ciprian et al., 2013; Tenti et al., 2015; Huang et al., 2018; Davinelli et al., 2019).

Table 1.7. Clay/polymer hybrids in wound healing

Clay	Polymer and Actives	Effects	Ref
MMT	Polyurethane, sodium alginate, bovine serum albumin	Controlled bovine serum albumin release	(Oh et al., 2011)
	PVA, CS	Faster wound healing process, higher skin flexibility	(Sirousazar et al., 2011)
	CS	Improved thermal stability, biocompatible, optimal water uptake, accelerated wound healing	(Salcedo et al., 2012; Aguzzi et al., 2014b)
	Bacterial cellulose	Antibacterial effects	(Ul-Islam et al., 2013)
	CS, silver sulfadiazine	Bactericidal, bacteriostatic against <i>P. aeruginosa</i> , reduction of drug toxicity	(Sandri et al., 2014)
	Methyl cellulose, sodium alginate	Antibacterial against <i>P. aeruginosa</i> and <i>E. faecium</i>	(Mishra et al., 2014)
	Hyperbranched epoxy resin, silver	Prevented wound infections and accelerated wound healing, biocompatible against cardiac and liver cells	(Barua et al., 2015)
	PVA, egg white	Faster wound healing process, higher skin flexibility	(Rangappa et al., 2017)
	CS and chlorhexidine	Antimicrobial	(Shanmugapriya et al., 2018)
	CS, PVP	Faster wound healing, less scar formation, abundant collagen deposition	(Sirousazar et al., 2016)
PVA, CS, honey	Biocompatibility, antibacterial and wound healing improvement	(Perioli et al., 2019)	
MMT, hydroxyapatite	PVA	Reinforcement of wound dressings and joint replacement devices (water vapour transmission rate, swelling, compressive and tensile properties)	(Fu et al., 2010)
Un/modified MMT, Cloisite 15A	Gellan gum	Biocompatibility, adequate swelling capacity and water vapour transmission	(Mohd et al., 2016)

Table 1.7. (Continued, part II)

Clay	Polymer and Actives	Effects	Ref.
Halloysite	poly(L-lactide), polymyxin B, dexamethasone	Antibacterial	(Shi et al., 2018)
	Poly(lactic-co-glycolic) acid	Controlled release of amoxicillin	(Fox et al., 2010)
	CS, amoxicillin	Early re-epithelization, haemostasis and angiogenesis	(Sandri et al., 2017)
	Hyaluronic acid	Low haemolysis (high biocompatibility) and high blood clotting formation	(Demirci et al., 2017)
	Poly(lactic acid), poly-dopamine	Three-dimensional scaffold with improved hydrophilicity, cellular adhesion and proliferation	(Wu et al., 2019)
Palygorskite	Poly(lactic-co-glycolic) acid	Clay improved cytocompatibility, induction osteoblast differentiation	(Wang et al., 2015)
	Chitosan, PVA, PVP, carvacrol	Improved healing of infected chronic ulcers	(Tenci et al., 2017)
Li, Mg silicate	N-isopropylacrylamide polymer (sericin)	Faster wound healing	(Yang et al., 2017)
Hectorite	poly(sulfobetaine acrylamide), AgNPS	Antibacterial, fast wound healing, non-stickiness to the wounded area	(Huang et al., 2017b)
Unspecified clay	Polydopamin, polyacrylamide, Epidermal Growth Factor.	Good adhesion, favoured cell attachment and proliferation	(Noori et al., 2018)
Rectorite	CS	Haemostatic with reduced thrombosis side effects due to effective retention of clay particles	(Li et al., 2018b)
Hydrotalcite	Carboxymethyl cellulose	Improved mechanical properties and skin adhesion, potential drug carrier	(Caramella et al., 2016)

Dead Sea water and mud are extremely high in salinity and contain sulphides, microorganisms, algae, and other bioactive materials that may contribute to the therapeutic effect of Dead Sea water and mud (Huang et al., 2018). The natural Dead Sea black mineral mud demonstrated wound healing properties against problematic and chronic wounds such as diabetic, venous and pressure ulcers (Belenky and Collins, 2011; Wallace and Wang, 2015; Davinelli et al., 2019). Dead Sea black mud and their salts accelerated wound healing in mice by enhancing granulation, wound contraction, epithelialization, angiogenesis and collagen deposition. Wound healing

1.3. Natural Inorganic Ingredients in Wound Healing

process of mice treated with Dead Sea mud was even faster than those treated with nitrofurazone (Abu-al-Basal, 2012).

The Blue Lagoon is a geothermal spa located in a volcanic lava field on the Reykjanes Peninsula (Iceland). Silica mud of this lake was evaluated against keratinocytes and fibroblasts cultures. The study revealed that silica mud was able to induce the gene expression of the skin barrier-associated proteins, a promising effect during wound healing treatments (Grether-Beck et al., 2008).

Pelotherapy with volcanic deposits from Azerbaijan allowed diabetic patients to recover from low-extremities gangrenous wounds in a more effective manner. Particularly, 86% of the patients reached complete wound healing by the end of the treatment (which accounted for 12-15 pelotherapy sessions of 20-30 min each). By this time, fresh granulation tissue began to develop and signs of edema to disappear (Nasirov et al., 2009).

Clay poultices and leachates have been used as ulcer treatment. Natural clay-rich mineral sample containing illite-smectite, montmorillonite, kaolinite, quartz, pyrite and jarosite was evaluated in terms of antibacterial activity (Adusumilli and Haydel, 2016). *In vivo* tests were performed on mice tails infected with *Mycobacterium ulcerans*. This microorganism causes a skin disease called "Buruli ulcer", which, untreated, could lead to severe skin necrosis. Results showed that clay poultices were more effective against *Mycobacterium ulcerans* than leachates, leading authors to the conclusion that natural inorganic ingredients were adsorbing both nutrients, cells and toxins (such as mycolactone) from the wound.

Double-blind, randomized study involving 60 patients was performed to evaluate the properties of a shampoo-clay (with montmorillonite clay) on diaper rash treatment, in comparison with *Calendula officinalis*. The study revealed that the clay formulation was more effective in controlling mild to moderate diaper rash than *Calendula officinalis* (Adib-Hajbaghery et al., 2014).

Talc, glycerin and polawax cream were mixed with a natural black clay (Ocara lake, Brazil) in order to form an emulsion aiming to treat *in vivo* wounds (Dário et al., 2014). Even if clay sample quality would need to be

improved, the formulations did not compromise wound healing process in rats. Moreover, the histological evaluation demonstrated a better deep dermis recovery (due to a greater formation of collagen fibers) in comparison with samples without Ocara clay.

1.3.2.3. Clay/polymer Composites and Nanocomposites

Polymer/clay mineral composite scaffolds are used in tissue engineering due to their enhanced wound healing properties (Ninan et al., 2015b). In most of the cases, clay minerals have demonstrated to play neutral or synergetic wound healing effects, most of the time demonstrating biocompatibility. Moreover, the combination of polymers and clay helps to resolve many stability problems of polymers themselves such as thermal stability.

Polyurethane foam was proposed by Oh and co-workers (Oh et al., 2011) as a support material to carry a polymer-clay composite loaded with active substances. In particular, montmorillonite-sodium alginate nanocomposite was loaded with bovine serum albumin protein and was subsequently added to polyurethane foam. Under vacuum conditions, the foam was able to absorb the nanocomposite (Figure 1.12). This system was proposed as a potential wound dressing material able to control drug release in a pH-dependent manner due to crosslinked alginate sensitivity to pH conditions. In this system, the presence of clay mineral was able to modify both physical properties and BSA drug release: as higher the ratio of montmorillonite added, the slower the BSA's drug release profile.

Sodium montmorillonite was proposed as an epidermal growth factor (EFG) carrier. This compound is one of the major growth factors that stimulate cell proliferation and motility during wound healing. The interaction between clay mineral and EFG did not cause any modification on EFG function and did not alter clay mineral. Scratch assay demonstrated that the composite stimulated *in vitro* keratinocyte growth and migration in a very similar manner with respect to EFG alone (Vaiana et al., 2011).

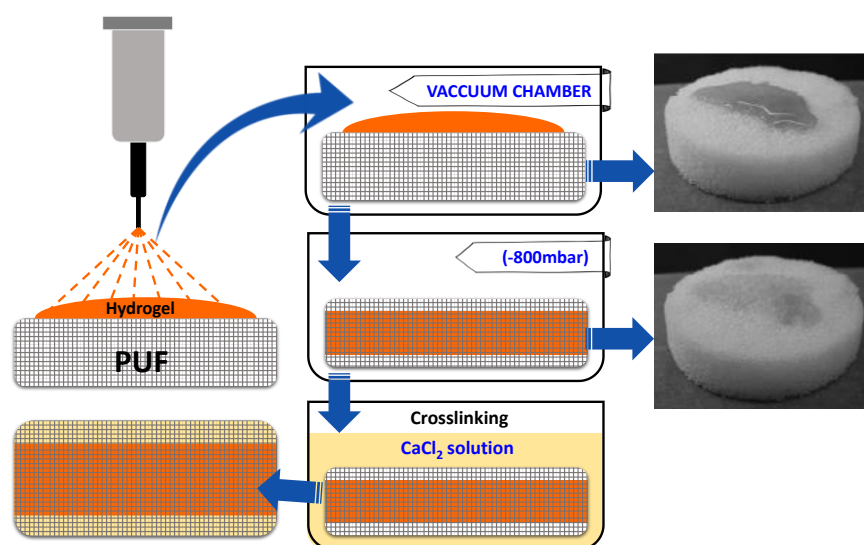


Figure 1.12. Polyurethane foam hydrogels (PUF) with montmorillonite and alginate, prepared by vacuum process. Schematic procedure and real aspect of the hydrogels (modified from Oh et al. (2011)). Under vacuum conditions the hydrogel was incorporated into PUF foam and then the crosslinking was produced in CaCl_2 solution

Nanoscale silica platelets obtained by the exfoliation of montmorillonite were combined with silver nanoparticles and studied as antibacterial dressings (Chu et al., 2012). The aforementioned composite in suspension was used to soak normal gauze and applied over mice infected wounds. In comparison with the rest of the systems evaluated (Aquacel®, silver sulfadiazine, silver nanoparticles and polymer, silver nanoparticles alone and nanoscale silica platelets alone), the nanoscale silica platelets with silver performed the best *in vivo* wound healing activity. It produced a cleaner wound surface, with better appearance and less scar tissue. Authors ascribed the better performance to a reduction on silver nanoparticles cytotoxicity, since cytokine expression was similar to Aquacel® and silver sulfadiazine.

Salcedo and co-authors evaluated water uptake, mucoadhesive properties, cell viability and wound healing properties of a montmorillonite-chitosan nanocomposite prepared by simple solid-liquid interaction (Salcedo et al., 2012). As expected, montmorillonite alone produced a slight decrease in the gap closure rate during *in vitro* wound healing, due to the previously reported cellular adhesion improvement produced by montmorillonite

(Abduljawwad and Ahmed, 2019). Nonetheless, the combination with chitosan accelerated gap closure when compared with the control group. Due to the promising results, montmorillonite-chitosan composites were employed to develop drug delivery systems with improved characteristics. The presence of montmorillonite allowed better thermal stability of chitosan and silver sulfadiazine antibacterial drug (Aguzzi et al., 2014b). It performed significant bacteriostatic and bactericidal properties against *Pseudomonas aeruginosa* (Sandri et al., 2014). Moreover, montmorillonite-chitosan combination was able to reduce the cytotoxicity of silver sulfadiazine against fibroblasts, making it a promising wound healing formulation with reduced skin side effects.

Montmorillonite-methyl cellulose-sodium alginate bionanocomposite was tested for antibacterial and wound healing activities (Mishra et al., 2014). Useful antibacterial properties were found against *Enterococcus faecium* and *Pseudomonas aeruginosa*. The incorporation of montmorillonite did not improve antibacterial properties in a significant manner. Nonetheless, the incorporation of the clay increased tensile strength and improved the physicochemical properties of the system.

Antibacterial hyperbranched epoxy resin was prepared in combination with octadecylamine-modified montmorillonite and silver nanoparticles (Barua et al., 2015). The slower release rate of silver from the nanocomposite produced a slight decrease in the minimum inhibitory concentration against *S. aureus*, *E. coli* and *Candida albicans*. The presence of the clay neither reduced cardiac nor liver cellular viability. Moreover, used as tissue scaffold over injured rats, this silver nanocomposite prevented wounds from infections (contrary to the control group) and significantly increased wound healing rates.

The hydrogel containing sodium montmorillonite revealed to be biocompatible against fibroblasts cultures, whereas a commercial sample (Cloisite 15A) and an N-hexadecyltrimethyl ammonium bromide montmorillonite were not. This revealed that sodium montmorillonite resulted more useful as a wound healing candidate in combination with gellan gum, both due to its physicochemical and biological properties (Mohd et al., 2016).

1.3. Natural Inorganic Ingredients in Wound Healing

The addition of palygorskite clay mineral into poly(lactic-co-glycolic acid) nanofibers has demonstrated to increase cytocompatibility and to induce osteoblastic differentiation (Wang et al., 2015).

Halloysite-chitosan nanocomposites were subjected to *in vitro* and *in vivo* tests. Both kinds of assay demonstrated the system to be biocompatible and to induce re-epithelialization, haemostasis and angiogenesis (Sandri et al., 2017). Cryogels of halloysite and hyaluronic acid were obtained and characterized. In terms of wound healing properties, the *in vitro* haemostatic assays revealed the gel containing the clay mineral produced low haemolysis and high blood clotting indices (Demirci et al., 2017).

Polymer/clay scaffolds have also been proposed for tissue engineering purposes, in which cellular orientation and interaction with the scaffold play an important role. Three-dimensional scaffolds formed of polylactic acid functionalized with polydopamine and halloysite nanotubes have been recently evaluated in terms of cellular adhesion, proliferation and orientation (Wu et al., 2019). The addition of polydopamine and halloysite nanotubes occurred simply by a coating process of the already prepared 3D polylactic acid scaffold. The authors concluded that the halloysite nanotubes effectively improved the surface roughness and the hydrophilicity of the scaffold as well as better cellular adhesion and proliferation.

A lithium magnesium silicate hydrate was crosslinked with N-isopropylacrylamide polymer and combined with sericin in order to create temperature-sensitive wound dressings with improved properties and antimicrobial activity (Yang et al., 2017). Sericin, a natural macromolecular protein derived from *Bombyx mori* (silkworm) and formed by 18 different aminoacids (mainly serine). Antimicrobial activity of the resultant hydrogel has been related to the interaction between sericin and bacteria: bacteria would be sorbed by sericin by charge interaction and adsorption of anion materials inside cells, once the protein passes the cellular membrane. These novel wound dressings were able to retain and effectively carry sericin, allowing faster *in vivo* wound healing process with respect to the control group. Moreover, antimicrobial properties would prevent secondary wound infections.

Laponite was combined with different aminoacids in order to test their effect during fibroblasts proliferation (Ghadiri et al., 2014a). Authors found that either laponite clay or the combination of arginine, lysine or leucine with the clay were able to improve cell proliferation.

Laponite combined with gellan gum methacrylate polymer has also been studied (Pacelli et al., 2016). Though no wound healing tests were performed, authors claimed that the presence of laponite gave the systems enough thermal stability to resist thermal sterilization. Moreover, laponite-gellan gum methacrylate was considered biocompatible according to the international guidelines on the biological evaluation of cytotoxicity.

Silver nanoparticles have also been proposed in combination with poly(sulfobetaine acrylamide)-hectorite hydrogels. The system has been evaluated as wound dressings aiming to treat chronic wounds (Huang et al., 2017b). Hydrogel's mechanical properties were reinforced by the presence of hectorite while silver nanoparticles allowed effective antimicrobial activity against *Pseudomonas aeruginosa* and *Staphylococcus epidermidis*. Wound healing test demonstrated that poly(sulfobetaine acrylamide)-hectorite hydrogels were effective for *in vivo* wound healing, having significant improvements with respect to Aquacel®Ag commercial dressings. At the end of the treatment, rats had full re-epithelialization and new-formed connective tissue. Another advantage of this system was its non-sticky property, allowing dressing changes without further injures in the wounded area, as it happens sometimes with traditional dressings. Therefore, it offers antibacterial, fast wound healing as well as less pain during wound treatments, which renders them as a perfect candidate in the treatment of burns.

Clay minerals, as well as their formulations and clay-polymer composites can be part of specific medical devices destined to treat wounds and denominated "wound dressings".

1.3.2.4. Clay Minerals in Wound Dressings

Dressings are a type of medical device used to cover wounds in order to promote wound healing and protection from further harm. Wound dressings are the main strategy for wound healing treatments and they are

1.3. Natural Inorganic Ingredients in Wound Healing

designed to control the environment during the healing process. Since they are intended to be in direct contact with the wounded area, they should accomplish certain characteristics and requirements (Jones et al., 2006; AAWC, 2020):

- should be able to maintain an adequate degree of humidity at the wound site and to control the excess of exudate, if it exists,
- must be free of toxic components and/or wound contaminants,
- non-toxic and non-allergenic,
- protect wound for further trauma,
- could be removed without causing trauma,
- impermeable to microorganisms,
- must provide thermal insulation,
- allow adequate water vapour transmission.

Other requirements such as comfort, conformability, long shelf life and cost-effectiveness are additional properties crucial for the acceptance of patients and the commercialization of the wound dressing. Currently it is possible to find different types of wound dressings that are able to address different kind of conditions: high, medium or low degree of wound exudation, infected wounds, necrosis, open/close wounds, place of the body in which the wound is located, etc (Jones et al., 2006; AAWC, 2020).

In recent years, different clay-based dressings have been proposed, in which clay minerals play different roles:

- Carriers of additional active substance, such as antimicrobial, anti-inflammatory, analgesic drugs, growth factors.
- As active substances themselves (adsorbents of bacteria, toxins and/or debris present in the wound, intrinsic anti-microbial properties, haemostatic agents, enhancers of loaded drugs activity, wound healing stimulators, physical support for cell growth) (Otto and Haydel, 2013a; Sandri et al., 2016).
- As additional ingredients improving mechanical and/or physical properties of the synthesized dressings such as tensile properties (including breaking stress and elongation at break), compressive properties, water vapour transmission rate (Figure 1.13) and swelling ratio.

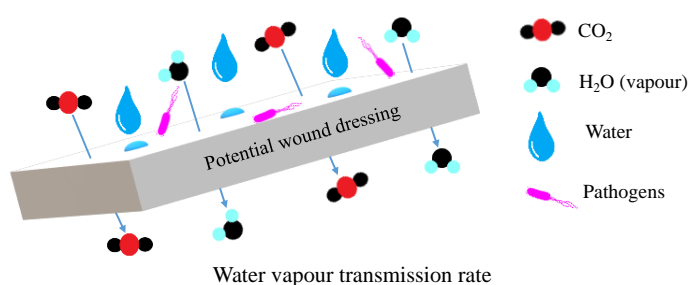


Figure 1.13. Ideal wound dressing should allow gas exchange and simultaneously protect the wound against external humidity and pathogens. In this schematic representation, carbon dioxide, water vapour and oxygen are able to cross the wound dressing, while water (liquid) and pathogens are retained in the surface

Laponite-mafenide wound dressing (synthetic smectite-antimicrobial agent) demonstrated to be effective against Gram-positive and Gram-negative bacteria (Ghadiri et al., 2014b). This device was proposed as burn wounds treatment, since it would not require to be spread over the skin, thus reducing pain during the treatment. The activity of mafenide was not compromised and, additionally, Mg²⁺ release from laponite structure favoured cell growth rate and decreased cytotoxicity of mafenide molecule.

Polymeric hydrogels are frequently used in wound dressing design, specifically in dry wounds, according to the Association for the Advancement of Wound Care (AAWC, 2020). The addition of clay minerals to the polymeric matrix allowed both materials to establish interactions leading to improvements on the mechanical properties (strength and elasticity) and absorptivity of the nanocomposite hydrogels. Unlike wound dressings without polymeric matrix, these kind of pads can keep the wound moist and prevent secondary infections (Zhao et al., 2015), which could also be useful in some cases.

Dressings of poly(vinyl alcohol) and organically-modified montmorillonite (cetyltrimethylammonium bromide) were prepared by using freezing-thawing method. Biocompatibility was tested against lymphoblasts and *in vivo* wound healing assays were performed with mice. The system was found biocompatible and was able to accelerate wound healing process in comparison with sterile normal gauze. Little scar formation was found and

the tensile properties of the re-epithelized skin were better for the group treated with poly(vinyl alcohol)-montmorillonite dressings (Sirousazar et al., 2011).

Bacterial cellulose dressings were impregnated with different cation-exchanged montmorillonites (sodium, calcium and copper). All nanocomposites were evaluated as antibacterial wound dressings aiming to reduce wound infection risks during healing. The study revealed that composites containing calcium and copper montmorillonite (together with cellulose) were the most effective against *Escherichia coli* and *Staphylococcus aureus* cultures. Antibacterial activity of dressings containing montmorillonite was more effective than bacterial cellulose alone (Ul-Islam et al., 2013). A similar study evaluated the effectiveness of gauzes impregnated with montmorillonite and halloysite on haemostasis and wound healing (Alavi et al., 2014). These impregnated sterile gauze pads absorbed water in the wound, thus concentrating the cellular and protein components of blood and consequently enhancing the formation of a clot. The evaluated system also played a significant role in accelerating the wound healing rate *in vivo* (Wistar rats). Additionally, authors did not report exothermic reactions during the clot formation, as happened with zeolitic-based gauze (QuikClot®) already commercialized (Baker et al., 2008).

One of the main problems of these inorganic based devices inducing clot formation is their risk of thrombosis. The entrance of mineral particles in the bloodstream could cause thrombosis, jeopardizing their safety. Current challenges imply the retention of mineral particles in a support material that prevents their release and entrance in the bloodstream. This was one of the main scopes of Li and co-workers (Li et al., 2018b) when they proposed the crosslinking of quaternized carboxymethyl chitosan and rectorite clay mineral. Rectorite is an interstratified dioctahedral natural phyllosilicate. The result was a viscous biomimetic mucus with effective haemostatic activity. The crosslinked polymer/clay network allowed high surface and reduced clay particle release. Moreover, this product was able to be injected, thus opening the possibility to be applied to irregular, severe wounds.

The presence of a negative net charge surface on clotting materials has been recently confirmed by Long and co-workers (Long et al., 2018). They

studied the platelet aggregation of kaolin particles charged with iron oxide and confirmed that as higher the negative net charge, the better the coagulation activity. Synergic activity between kaolin and iron oxide was found during the coagulation process. Moreover, *in vivo* wound healing demonstrated that the composite kaolin-iron oxide favoured wound healing and had lower haemolytic activity than raw kaolin. Despite natural inorganic ingredients effectiveness inducing clot formation and their effective commercialization, it is a study field still on its peak since toxicological studies are still necessary in order to optimize and reduce side effects such as vascular thrombosis. In fact, when used as haemostatic agents, montmorillonite and WoundStat® showed higher toxicity against endothelial cells and macrophages than zeolite and kaolin after direct contact (Bowman et al., 2011).

Montmorillonite-chitosan films loaded with chlorhexidine were proposed as wound dressings to prevent both wound infections and to reduce cytotoxicity of the active substance against human fibroblasts and keratinocytes (Ambrogi et al., 2017). Additionally, prolonged and localized chlorhexidine release was obtained. Montmorillonite and chitosan were also used by Shanmugapriya and co-workers in combination with polyvinylpyrrolidone to obtain films (Shanmugapriya et al., 2018). Full solid-state characterization was performed as well as cytotoxicity and wound healing studies. The authors concluded that *in vivo* wound healing occurred faster with these films, reaching full healing after 16 days. Less scar formation and abundant deposition of collagen were also demonstrated.

Egg white/polyvinyl alcohol/montmorillonite polymeric hydrogel dressings were developed by Sirousazar and co-workers. Rapid wound healing was obtained, the system protecting the wound from secondary infections. Authors ascribed the better tensile properties of healed skin to the moist environment created by the polymeric dressings as well as to the presence of egg white, thus collagen formation being improved (Sirousazar et al., 2016).

Montmorillonite dermal patches have been loaded with silver nanoparticles, lidocaine and fentanyl drugs in two different studies (Rangappa et al., 2017, 2018). In both cases, patches were intended for burns

1.3. Natural Inorganic Ingredients in Wound Healing

wound healing purposes due to the antimicrobial (silver) and antinociceptive (lidocaine and fentanyl) activities. Montmorillonite acted as a skin smothering agent and drug release controller, leading to effective drug doses since antibacterial and analgesic properties have been demonstrated *in vitro* and *in vivo*.

Han and co-workers elaborated wound dressings with good and reproducible adhesiveness. They combined polydopamine and polyacrylamide polymers with an unknown clay (not specified in the study) (Han et al., 2017). Apart from the characterization and evaluation of mechanical properties, cell adhesion and *in vivo* wound healing tests were also performed. Biocompatibility was confirmed since fibroblasts adhered to the hydrogel maintaining their normal phenotype. Moreover, the wound healing process was improved due to better cell migration and proliferation.

Poly (vinyl alcohol)/chitosan/honey/montmorillonite nanocomposite has been recently evaluated as wound dressing (Noori et al., 2018). This formulation showed *in vitro* and *in vivo* biocompatibility, antibacterial and wound healing activities. Cytotoxicity test results demonstrated no cytotoxicity in nanocomposite hydrogel system.

Hybrid films designed with palygorskite loaded with Carvacrol, a monoterpene phenolic compound with an antioxidant, antifungal and antimicrobial properties and different polymers (polyvinylalcohol, polyvinylpyrrolidone and chitosan) demonstrated a significant improvement of infected ulcers healing, compared to commercial dressings (Tenci et al., 2017).

Hydrotalcite is a layered double hydroxide clay (anionic clays) with interlayer anions easily exchanged for other inorganic or organic species. This mineral has been synthesized and proposed as polymeric wound dressing reinforcement by (Perioli et al., 2019). The addition of small amounts of hydrotalcite to carboxymethyl cellulose showed improvement in mechanical properties and skin adhesion properties. Moreover, the presence of a layered mineral gives the system the possibility to act as a potential drug carrier.

Electrospinning is one of the most versatile current techniques to produce polymeric nanosized fibers with advantageous properties such as wide range pore sizes, high specific surface and area/volume ratios. It consists

of the combination of electrical forces to produce polymer fibers with different diameters (from 2 nm to several micrometers). Natural and synthetic polymers have been electrospun starting from polymeric solutions. The way in which electrospun fibers assemble allows their use in a wide range of applications such as wound-dressing materials, drug delivery systems and tissue-engineering scaffolds (Caramella et al., 2016). Electrospun materials meet most of the requirements outlined for wound dressing devices (such as appropriate water-vapour transmission rate and gaseous exchange ability, adhesion and/or biocompatibility) due to their microfibrillar and nanofibrillar structure (Bhardwaj and Kundu, 2010).

Electrospun poly(L-lactide)/halloysite nanotubes mats were evaluated as dual drug carriers of polymyxin B sulphate (hydrophilic drug) and dexamethasone or ciprofloxacin (hydrophobic drugs). Due to its widely demonstrated biocompatibility, halloysite was chosen as a drug carrier, providing synergic controlled release of the drug together with the polymer matrix. Moreover, tensile strength and thermal stability of the electrospun dressings were also improved by the presence of the clay mineral. Additionally, systems performed considerable antibacterial activity and provided effective protection against secondary wound infections. *In vivo* studies revealed that, after 14 days, wounds treated with electrospun polymer/clay mats were completely healed with respect to the control group (Zhang et al., 2015; Shi et al., 2018). Similar results were obtained by Tohidi and co-workers (Tohidi et al., 2016) when halloysite was added to electrospun poly(lactic-co-glycolic acid) and loaded with amoxicillin. The authors proposed this system as potential wound dressing, in which halloysite allowed controlled release of amoxicillin, reducing burst release. Moreover, physical properties were improved by the presence of the clay.

1.3.3. Other Inorganic Materials for Wound Healing

1.3.3.1. Zeolites

Zeolites are hydrated tectosilicates, a type of microporous crystalline aluminosilicates formed of tetrahedra in which the nucleus is Si or Al covalently bonded to O atoms. These basic units combine to generate different

1.3. Natural Inorganic Ingredients in Wound Healing

frameworks with pore sizes ranging from 4-12Å. In the zeolite structure, the differences in Si and Al valence (Si tetravalent and Al trivalent) originate an excess of negative net charge, compensated by extra-framework cations (typically alkali and alkali earth metals). Zeolites are similar to clay minerals, since both materials are able to exchange cations and have high specific surface areas. Zeolites have multiple industrial uses and they have also been proposed as wound healing agents (Table 1.8). Particularly, zeolites are used as gas storage materials due to their large specific surface area. Exchangeable cations of zeolites have a high affinity for gases such as nitric oxide. Nitric oxide is important for the regulation of a number of diverse biological processes such as vascular tone, neurotransmission, inflammation, wound healing and barrier for pathogens. Topical delivery of nitric oxide through a wound dressing has the potential to reduce wound infections and improve the healing of acute and chronic wounds. In fact, zeolite A loaded with nitric oxide demonstrated to be effective against common wound pathogens with relatively low concentrations (Fox et al., 2010; Neidrauer et al., 2014). Zeolites have also the ability to deliver other gases, such as oxygen, to injured cells (Seifu et al., 2011).

Zeolites have potential for soft tissue engineering and regeneration. Scaffolds made of pectin, gelatine or gelatine/hyaluronan matrix with copper-activated faujasite (a natural zeolite) were used for skin tissue engineering. Skin regeneration of wounded rats was improved by these scaffolds due to the delivery of oxygen from faujasite particles. Additionally, antimicrobial properties were provided by copper particles (Ninan et al., 2013, 2014, 2015a). Zeolite Y (a synthetic zeolite) demonstrated to favour fibroblast migration when added to *in vitro* wound healing cultures (scratch-assay): control group needed 20 h to close, while zeolite Y samples closed the gap faster (Asraf et al., 2019). In this very same study, the functionalization of zeolite Y with (3-aminopropyl) triethoxysilane gave the system antibacterial activity. Nonetheless, the presence of the amine compromised the biocompatibility of the system, as demonstrated by the slower *in vitro* gap closure and necrosis of cells (Asraf et al., 2019).

Different wound dressings were evaluated in an *in vivo* study with rats. Traumadex®, clinoptilolite, alginate, hydrogel and Biobrane® dressings

were compared, clinoptilolite demonstrated to provide better wound healing rate and healing quality (Uraloğlu et al., 2014). Recently, zeolites have been proposed as part of wound dressings with control drug delivery properties. Natural zeolite clinoptilolite and a type-A zeolite have been loaded with silver ions and incorporated into chitosan films in order to be used as wound dressings for chronic wounds (Barbosa et al., 2016). In this study, researchers investigated the physical properties of the final composite films, comparing the synthetic zeolite (type A zeolite) with the natural one (clinoptilolite). Type-A zeolite film was more hydrophilic than clinoptilolite, although clinoptilolite/chitosan films demonstrated to have greater thermal resistance (Barbosa et al., 2016).

Salehi and co-workers tested the biocompatibility and wound dressing properties of starch-based nanocomposite hydrogel scaffolds reinforced with zeolite nanoparticles as wound dressings (Salehi et al., 2017). Chamomile extract was added to the system in order to accelerate wound healing, since the system was intended to treat chronic refractory ulcers. Wound dressings with all three components showed significant wound size contraction with respect to control groups. *In vitro*, and *in vivo* analyses were carried out in order to assess the safety of the system before being applied to real patients. The ulcers of all patients healed without hypersensitivity reaction.

More recently, sodium and zinc zeolite A particles were combined with low-methoxyl pectin to form hydrogel-based wound dressing. Theophylline was used as a model drug and loaded onto zeolites (Salehi et al., 2017). The system was biocompatible to human dermal fibroblasts and did not hinder cellular migration during *in vitro* wound healing. Moreover, swelling capacities and oxygen transmission rates were also optimal.

1.3. Natural Inorganic Ingredients in Wound Healing

Table 1.8. Use of zeolites in wound healing formulations

Zeolite	Formulation	Effects	Ref
Clinoptilolite	Cotton and polyester fabrics impregnated with micronized clinoptilolite	UV and antimicrobial protection, improved wound healing	(Ninan et al., 2013)
Clinoptilolite	Wound dressing	Better <i>in vivo</i> wound healing rate	(Barbosa et al., 2016)
Clinoptilolite, mordenite	Gauze	Haemostasis without exothermic reaction	(Paydar et al., 2016)
Fluorinated Zeolite Y	Polyurethane 3D scaffolds for vascular replacement	Oxygen supply by the zeolite increased proliferation activity of human coronary artery smooth muscle	(Grancarić et al., 2009)
Zeolite Y	Non specified	Faster <i>in vitro</i> wound closure with respect to control group. Antibacterial activity by cytotoxic to fibroblasts if combined with (3-aminopropyl) triethoxysilane	(Uraloğlu et al., 2014)
Faujasite	Polymeric porous scaffold of hyaluronic acid and gelatine	Increased oxygen supply accelerated re-epithelialization and collagen deposition	(Ninan et al., 2014)
	Composite scaffold of gelatine and copper	Increased oxygen supply promoted cell proliferation, antimicrobial activity	(Ninan et al., 2015a)
	Hybrid membrane with pectin, faujasite and copper	Antibacterial activity, improved wound healing and re-epithelialization	(Ninan et al., 2015b)
Zeolite A	Pectin hydrogel	Biocompatible, not hindering wound healing process	(Ostomel et al., 2006)
Zeolite, montmorillonite	Powder	Haemostasis	(Yu et al., 2019a)
Nanozeolite	Wound dressing with starch and chamomile	Biocompatible, improved wound healing, absence of hypersensitivity reactions	(Salehi et al., 2017)
Chabazite	Cotton wound dressing	Haemostasis without exothermic reaction	(Long et al., 2018)

Zeolites have demonstrated to be very useful for haemostatic procedures (Ostomel et al., 2006). QuikClot® is the most famous zeolite-based haemostatic product. It is composed of a synthetic zeolite that adsorbs water and promotes clot formation (Alam et al., 2003, 2004). Nonetheless, the haemostatic reaction was exothermic, which limited its use. This discovery opened a field of study to search for new natural inorganic, haemostatic

ingredients. Natural zeolite from Jinyun, China, composed of clinoptilolite and mordenite, was proposed to form a clotting gauze. This system was compared with Quikclot® *in vivo* and the results were very promising. Both systems achieved 100% blood clotting formation, but the natural zeolite system produced lower mortality and no exothermic reaction (Li et al., 2012). The combination of zeolite-montmorillonite as haemostatic ingredient and its wound healing interference was also tested through *in vitro* tests (Paydar et al., 2016). The wound healing process of rats after the application of zeolite-montmorillonite powder might negatively affect the healing process due to the vasoconstriction and inhibition of angiogenesis. That is, the system was effective during bleeding, but appeared to compromise the rest of the healing process. Another zeolite-cotton patch has been synthesized and evaluated by Yu and co-workers (Yu et al., 2019a). They synthesized chabazite particles onto the surface of cotton fibers, aiming to be used as an effective haemostatic material. The authors claimed that chabazite particles were tightly bound to cotton. *In vitro* and *in vivo* coagulation assays showed effective clot formation in short times with respect to the control (kaolin Combat Gauze). Moreover, no exothermic reaction was found for chabazite-cotton dressings, thus overcoming the initial problem of zeolite-based wound dressings.

1.3.3.2. Silica and Other Silicates

Polyethylene-silica particles were loaded with viable keratinocytes by Bayram and co-workers (Bayram et al., 2005). The aim of the study was to use the polymeric-mineral base to deliver cells into diabetic foot ulcers (40 patients, grade ulcers II and III). Results showed that these keratinocytes-loaded microcarriers were able to shorten and improve ulcer healing.

Fumed silica is an inorganic material (SiO₂) obtained by a pyrolysis method in which silicon tetrachloride reacts with oxygen in a flame, and the SiO₂ seed grows in size or aggregates. Fumed silica shows low bulk density and high surface area, being used in several medicinal applications. Electrospun-wound dressings containing chitosan-polyethylene oxide nanofibrous mats with fumed silica particles and cefazolin were produced (Fazli and Shariatnia, 2017). Cefazolin release occurred in a sustained manner and possessed remarkable antibacterial activities against *Staphylococcus aureus*

1.3. Natural Inorganic Ingredients in Wound Healing

and *Escherichia coli*. Wound healing process observed on Wistar rats allowed authors to confirm the usefulness of the proposed dressings.

Synthetic mesocellular foams are mesoporous silica materials, with a large surface area and open framework structure. The silica framework structure is made up of cages connected by windows, both of which are monodispersed in size. This inorganic material has been suggested as an accelerator of blood clotting formation, critical first step during healing process. Yao and co-workers (Li et al., 2013) synthesized MCF-26 and evaluated cytotoxicity over umbilical endothelial cells and keratinocytes, demonstrating better biocompatibility with other inorganic materials such as kaolin. Moreover, results showed that MCF-26 had a very similar role during coagulation with respect to other layered clay minerals.

Tourmaline is a boron-based ring silicate mineral group belonging to the trigonal system. In terms of wound healing and skin therapy, this material has demonstrated to improve cell growth (Jin et al., 2003; Xia et al., 2003). Recently, tourmaline films combined with chitosan were tested *in vitro* and *in vivo*. The study demonstrated that the nanocomposite improved cell adhesion and proliferation. Moreover, newly formed and mature blood vessels and faster dermis regeneration have been obtained (Zou et al., 2017).

A porous nanocrystalline mullite (a nesosilicate) composite was loaded with copper and silver nanoparticles by a simple adsorption process. Both copper and silver nanocomposites showed effective antibacterial activity, copper being the most active. *In vitro* wound healing scratch assay (fibroblasts) showed none of the nanocomposites hindered artificial gap closure with respect to the control group (Kar et al., 2014). Regarding mullite, there is also a patent in which mullite takes part of a product able to promote haemostasis, wound healing and antimicrobial properties, among others (Wuollett and Wuollett, 2013).

1.3.3.3. Other Minerals

Poly(vinyl alcohol) was combined with hydroxyapatite and bentonite to create hydrogel nanocomposites useful in joint replacement and as wound dressings, respectively (Gonzalez et al., 2012). Water vapour transmission rate, swelling, compression and tensile tests were performed, showing the

addition of minerals of great use since they reinforced specific properties of each nanocomposite. In particular, poly(vinyl alcohol) and bentonite composite possessed remarkable antibacterial activity against *Escherichia coli* and *Listeria monocytogens* as well as proper water vapour transmission rate values.

Mg/Al hydroxycarbonate was loaded with diclofenac sodium and combined with poly(ϵ -caprolactone) to synthesize suture fibers with analgesic effect (Catanzano et al., 2014). Fibers were prepared by melt-spinning process implying extrusion since this method produces fibers with better mechanical properties than electrospinning. Particularly, authors found that the addition of hydroxycarbonate loaded with diclofenac performed better tensile properties than poly(ϵ -caprolactone) loaded with diclofenac. Moreover, hydroxycarbonate loaded with diclofenac prolonged drug release for up to 55 days. Regarding *in vivo* studies, mice sutured with poly(ϵ -caprolactone)/hydroxycarbonate/diclofenac sodium were the only ones showing granulation tissues. The authors ascribed the presence of granulation tissue to a more effective and earlier wound healing process.

Borate bioactive glass is an inorganic, degradable, biocompatible material. Borate glass possesses a microstructure similar to that of dry human trabecular bone with remarkable applications in bone tissue engineering and wound healing (Fu et al., 2010). Copped-doped borate bioactive glass was combined with poly(lactic-co-glycolic acid) to form wound dressings loaded with vitamin E. Angiogenesis, migration, tubule formation and wound closure were improved by the use of the borate/polymer dressing (Hu et al., 2018a).

1.3.3.4. Transition Metals

Transition metals such as Cu, Zn, Mn, Fe, Ag, Co and Au are essential microelements with various biological functions in tissue regeneration (Yang et al., 2018). These metals play different roles in living organisms (i.e. cofactors of different essential enzymes) apart from antibacterial activity and wound healing (Table 1.9) (Mouriño et al., 2012; Olaiya and Fadason, 2017). A recent study has evaluated the effects of iron, copper, zinc and magnesium in wound healing process (Coger et al., 2019). Supplementation of Zn, Fe and Mg would

1.3. Natural Inorganic Ingredients in Wound Healing

be advisable from the late inflammation step until the mid-proliferation phase, while Cu may be more useful during the early stage of the wound healing. Authors claimed these results “help to optimize compositions of metal ion-based ointments and wound coverage’s to enhance the wound healing process”. On the other hand, iron concentration in the site of wound increases monocyte recruitment from blood circulation and senescent fibroblasts. Iron-dependent regulation of macrophages and fibroblasts and related pathologies linked to non-healing chronic wounds has been recently reviewed (Wlaschek et al., 2019). Iron-dependent oxidative stress affects distinct cells and initiates and maintains the pathology of non-healing wounds. Therefore, a proper equilibrium is required, thus reinforcing the idea of a proper supplementation of the element in different wound stages (Coger et al., 2019).

Silver has been used for centuries to prevent and treat a variety of diseases including pleurodesis, cauterisation, and healing of skin wounds (Klasen, 2000; Hanif et al., 2003; Antonangelo et al., 2006). Silver remains the most studied metal for medical purposes, especially due to its antibacterial activity. Classical formulations included silver as nitrate or other salts. Nanotechnology has provided a way of producing colloidal silver nanoparticles (AgNPs) with a wide variety of properties and high potential of new applications (Verma and Maheshwari, 2019).

In health science, one of the most important roles of AgNPs is their antimicrobial activity. AgNPs can play an important role during infected wound healing treatments, both as antimicrobial and as prophylactic agent (prevention of wound infection). They are effective against *Acinetobacter sp.*, *Escherichia sp.*, *Pseudomonas sp.*, *Salmonella sp.*, *Bacillus sp.*, *Enterococcus sp.*, *Listeria sp.*, *Staphylococcus sp.* and *Streptococcus sp.*, also being potentially active against fungi and virus.

Silver-based dressings are excellent candidates in the composition of wound dressing, in which AgNPs have shown antimicrobial activity, but also able to regulate the deposition of collagen (Kwan et al., 2011). Spongy composites with chitosan, glutamic and hyaluronic acid and AgNPs, synthesized by freeze-drying, showed activity against *Escherichia coli* and

Staphylococcus aureus and complementarily, promoted *in vivo* wound healing (Lu et al., 2017).

Table 1.9. Functions of transition metals in wound healing

Metal	Form	Effects	Ref
AgNPs	Grafted dressings	Overall decrease in the inflammatory response, modulation of local and systemic inflammatory response by cytokine modulation, no scar formation and faster wound healing	(Tian et al., 2007)
	Nanocrystalline silver dispersion in PVA	Suppression of inflammatory cytokines and metalloproteinase-9 help to heal ulcerative colitis	(Bhol and Schechter, 2007)
	Non specified	Suppression of endothelial cell migration mediated by vascular endothelial growth factor	(Kalishwaralal et al., 2009)
	Dressings moist with aqueous AgNPs	Interaction of AgNPs with dermal cells induced IL-4 release with antiinflammatory response of the surrounding tissue	(Nadworny et al., 2010)
	Non specified	Decrease of cytokines production, maintaining low level after UVB irradiation and Pre-administration of AgNPs reduced level of cytokines and presented long-term protective effect	(David et al., 2014)
	Spongy composites of silver nitrate, chitosan, glutamic and hyaluronic acid	Antibacterial activity	(Lu et al., 2017)
	Non specified	Anti-inflammatory and antimicrobial effect, amelioration of wound repair in diabetic mice	(Krishnan et al., 2018)
	Tannic acid-modified AgNPs	Antibacterial, anti-inflammatory, accelerated wound healing	(Orlowski et al., 2018)
	Gelatin/chitosan/AgNPs sponge dressings	Good biocompatibility, shorten wound healing time	(Ye et al., 2019)
	Chitosan dressing	Antibacterial, wound healing improvement, good biocompatibility	(Ran et al., 2019)
Ag, Zn	Electrospun fibers polycaprolactone and PVP	Synergic antibacterial effect, reduced cytotoxicity with excellent physicochemical properties	(Hu et al., 2018b)
Zn	Gelatin cryogel doped with Zn	Reduced leucocyte infiltration, improved dermis components generation and accelerated wound healing	(Luong et al., 2019)
Ti	Zein protein and polydopamine nanofibrous scaffolds	Higher wound healing closures both <i>in vitro</i> and <i>in vivo</i>	(Babitha and Korrapati, 2017)

1.3. Natural Inorganic Ingredients in Wound Healing

The importance of particle size in silver antibacterial activity has been demonstrated by Orłowski and co-workers (Orłowski et al., 2018). They synthesized different tannic acid-modified AgNPs. Particularly, silver nanoparticles higher than 26 nm showed good biocompatibility, effective antibacterial and anti-inflammatory properties, which translate into accelerated wound healing.

Table 1.9. (Continued, part II)

Metal	Form	Effects	Ref
Cu	Electrospun membranes of poly(ϵ -caprolactone), poly(lactic acid) and chitosan	Skin cancer treatment, cell adhesion support, cellular proliferation, migration and angiogenesis	(Wang et al., 2017)
Au	Gold nanoparticles and keratinocytes growth factor	Faster <i>in vivo</i> wound healing with respect to both components alone	(Pan et al., 2018)
	Gold nanoparticles and LL37 peptide	Synergic effect between gold and LL37 peptide, allowing faster wound closure, re-epithelialization and granulation tissue	(Wang et al., 2018)
	N-glucosamine gold nanoparticles	Remarkable biocompatibility, less inflammatory cells, better reepithelialisation and less bacteria	(Yang et al., 2019)
Fe	Chitosan/silk fibroin/tannic acid cryogel	Antibacterial, haemostatic agent (clot formation), wound healing acceleration	(Yu et al., 2019b)

Another important role of AgNPs during wound healing is their anti-inflammatory activity. Wound healing properties of AgNPs were evaluated by Tian and co-workers (Tian et al., 2007) in a rat model. They found that these particles were able to exert rapid healing in a dose-dependent manner with lower scar tissue formation. Authors related these effects to a local modulation of the inflammatory response.

Nanocrystalline silver particles were used to treat ulcerative colitis in an *in vivo* study by oral or intracolonic administration (Bhol and Schechter, 2007). Authors claimed that the suppression of inflammatory cytokines and metalloproteinase-9 (or gelatinase B) by nanocrystalline silver particles may be the mechanism of action responsible for the anti-inflammatory activity. The anti-inflammatory effects of AgNPs were related to a direct interaction between the nanoparticles and some skin cells (keratinocytes, fibroblasts and antigen-presenting cells) (Nadworny et al., 2010). These interactions released

biochemical signals such as IL-4, which resulted in anti-inflammatory response of the remote tissue. “Nanocrystalline silver placed on uninjured tissues, or portions of an injury, could potentially reduce inflammation throughout an injured area” (Nadworny et al., 2010). AgNPs obtained by a green method (using European black elderberry extract as reducer) also demonstrated anti-inflammatory and wound healing properties (David et al., 2014). Both *in vitro* and *in vivo* tests were performed and demonstrated a decrease in cytokine production. Moreover, the authors demonstrated the possible use of synthesized AgNPs for the treatment of psoriasis. The scarce biocompatibility of silver-ion compounds has opened a new research line. Biogenic silver nanoparticles were obtained by *Brevibacillus brevis* and its activity evaluated over wound diabetic mice (Krishnan et al., 2018). Authors reported that these AgNPs exerted antiinflammatory and antimicrobial activities since it decreases the expression of metalloproteinases 2 and 9. Also naturally *in situ* AgNPs obtained by *Sanghuangporus sanghuang* polysaccharides were combined with chitosan to prepare a composite sponge wound dressing material (Ran et al., 2019). Due to the presence of silver, the system possesses good antibacterial effects, thus providing the wound with a sterile, moist environment. The material also promoted *in vivo* wound healing of wounds with excellent biocompatibility.

Chitosan sponge dressings with AgNPs were synthesized by reducing silver with gelatine and crosslinking chitosan with tannic acid (Ye et al., 2019). Compared with the corresponding dressing without silver nanoparticles, *in vivo* tests showed the formation of new thin, uniform skin that completely covered the wound without inflammatory cells. The rest of the control systems did not show the growth of new skin. Wound contraction was very similar to that of Aquacel®Ag, but the authors claimed the epithelial tissue formed was thinner than chitosan/gelatin/AgNPs sponge dressings.

Angiogenesis is a crucial factor for the development of diabetic retinopathy, which is still one of the most common causes of blindness worldwide. Vascular endothelial growth factor (VEGF) as the primary mediator of retinal neovascularization. The *in vitro* interaction between silver nanoparticles and VEGF was assessed by Kalishwaralal and co-workers (Kalishwaralal et al., 2009). *In vitro* scratch assay demonstrated that silver

nanoparticles inhibited bovine retinal endothelial cell migration mediated by VEGF, thus proving silver nanoparticles as a promising treatment of diabetic retinopathy and other treatments such as chronic wounds.

Wound dressings including zinc and silver were obtained by electrospinning (Hu et al., 2018b). The two metal nanoparticles were included in polyvinylpyrrolidone and polycaprolactone and the corresponding antibacterial activity was assessed. Resulting electrospun fibers showed higher antibacterial effect against *Escherichia coli* and *Staphylococcus aureus* than the corresponding nanoparticles alone. At the same time, the cytotoxicity of silver and zinc was reduced towards fibroblasts if they were applied in the form of an electrospun dressing.

Silver and cobalt were used as antibacterial and angiogenic ingredients of poly(ϵ -caprolactone) fibers produced by electrospinning (Moura et al., 2017).

It has also been demonstrated the synergic effects that can be obtained in systems designed with polymer, clay mineral and AgNPs. This multicomponent formulation showed a controlled release of Ag which allowed increased antimicrobial activity and tissue repairing improvement (Depan and Misra, 2015).

Titanium oxide also showed antimicrobial activity. The study of Babitha and Korrapati (Babitha and Korrapati, 2017) included TiO₂ nanoparticles in combination with zein protein and polydopamine was used to produce tissue engineering nanoparticles by electrospinning. *In vitro* scratch assay was performed with keratinocyte cells and Wistar rats were used for the *in vivo* wound healing experiments. Authors compared different preparations and observed that those including titanium nanoparticles, experimented higher wound closures *in vitro*, which was also observed during *in vivo* tests. That is, the wound healing process was improved when TiO₂ was used to reinforce membranes.

Copper ions, incorporated into electrospun membranes made of poly(ϵ -caprolactone), poly(lactic acid) and chitosan, were proposed to treat skin tumours by photothermal therapies. The authors claimed that skin tumour cells were effectively killed *in vitro*, whereas it inhibited cancer cell

growth *in vivo*. More particularly, the membranes were able to support cell adhesion, proliferation and migration of normal skin cells. Angiogenesis and healing skin effects were also detected *in vivo* (Wang et al., 2017).

Gold nanoparticles have been used in photothermal therapy including hydroxyapatite and polydopamine (Xu et al., 2018). The photothermal therapy is based on the conversion of light into heat to exert antimicrobial activity. Gold nanoparticles here acted as catalytic material during the photothermal reaction. The system stimulated “tissue repairing-related gene expression to facilitate the formation of granulation tissue and collagen synthesis”.

Wang and co-workers (Wang et al., 2018) used gold to optimize a novel gene delivery system. Gold nanoparticles were used to graft the antimicrobial peptide LL37, which exerts immunomodulation such as cell proliferation and differentiation effects. Gold nanoparticles and LL37 produced a synergic effect promoting angiogenesis and antibacterial infection. These properties were very useful for the treatment of diabetic ulcers wound healing since it allowed accelerated wound closure rates, faster re-epithelialization and improved granulation tissue. N-glucosamine gold nanoparticles were evaluated as antibacterial against multidrug-resistant bacteria (Yang et al., 2019). The system performed remarkable biocompatibility. Moreover, less inflammatory cells (neutrophils or lymphocytes) were found in the group of mice treated with gold nanoparticles with respect to control together with better re-epithelialization and less bacteria.

In another study, gold nanoparticles were crosslinked with keratinocyte growth factor in order to reduce its degradation (Pan et al., 2018). Therefore, gold nanoparticles acted as biocompatible support for the growth factor. This combination demonstrated to be a potential clinical therapeutic agent for wound healing. Wound healing occurred faster with gold-growth factor combination than for keratinocyte growth factor alone.

Gelatine cryogels, loaded with Zn by a crosslinking method and including pectin as metal binding mediator, demonstrated enhancement on wound healing *in vivo* (rat excisional model). Moreover, the addition of Zn accelerated cryogel biodegradation and skin regeneration. Additionally, the

1.3. Natural Inorganic Ingredients in Wound Healing

gels reduced leucocyte infiltration and improved generation of other dermis components (Luong et al., 2019).

Ferric ion (Fe^{3+}) was incorporated together with tannic acid, into a chitosan/silk fibroin cryogel as a stimuli-responsive wound dressing for photothermal therapy. The cryogel showed excellent antibacterial activity against Gram-negative and Gram-positive bacteria and promoted *in vitro* cell proliferation, thus accelerating *in vivo* wound healing. Moreover, due to its strong hygroscopicity, the hydrogel absorbed blood from injury, thus showing haemostatic activity (Yu et al., 2019b).

1.3.4. Conclusions

The biological properties of therapeutic dressings are related not only to the drugs used, but to the presence of nanomaterials, which can improve tissue repair, reducing the local inflammatory process more efficiently. Natural inorganic ingredients are smart materials for wound healing. These natural materials greatly benefit the requisites of wound treatment: antimicrobial activity, antiinflammatory, and pro-angiogenic actions. They may also be included in wound dressings to control, target, or modify the b

As reviewed, several studies have revealed the versatility and potential utility of some clays, zeolites and transition metals in the development of advanced pharmaceutical systems for wound treatments.

1.4. Abbreviations

AgNP	silver nanoparticles
AMP clay	3-aminopropyl functionalized magnesium phyllosilicate
APTES	3-aminopropyltriethoxysilane
APMES	amino-propyldimethylethoxysilane
ALG	Alginate
AZPES	3-azidopropyltrimethoxysilane
CMC	carboxymethylcellulose
CS	chitosan
CTAB	n-cetyl-N,N,N-trimethylammonium bromide
DTG	Derivative thermogravimetry
EAN	Elemental analysis
EFG	epidermal growth factor
FGF2	fibroblast growth factor 2
Fmoc-F	fluoromethoxycarbonyl-L-phenylalanine
5-FU	5-fluorouracil
HPMCAS	hydroxypropyl methylcellulose acetate succinate
HNT	halloysite nanotubes
LDH	layered double hydroxides
LIP	soybean phospholipid
MAA	methacrylic acid
MC	methylcellulose
MMT	montmorillonite
Na ⁺ -MMT	sodium montmorillonite
PAA	poly-acrylic-acid
P(AAm-MA)	poly(acrylamide-co-maleic acid)
PAH	poly(allylamine) hydrochloride
PC	pectin
PCL	poly(ϵ -caprolactone)
PCLA	poly(ϵ -caprolactone-co-lactide)

1.4. Abbreviations

PEG	poly(ethylene glycol)
PEGdm	poly(ethylene glycol) dimethacrylate
PMMM	poly(methyl methacrylate-co-methacrylic acid)
PEG750/5000-PE	1,2-distearoyl-sn-glycero-3-phosphoethanolamine-N-[methoxy (polyethylene glycol)-750/5000] (ammonium salt)
PEI	polyethyleneimine
PLA	poly(D,L-lactide)
PLGA	poly(lactic-co-glycolic acid)
PLLA	poly (L-lactide)
PLL	poly-L-lysine
PSS	poly(sodium styrene) sulfonate
Poly(HEMA)	poly(hydroxyethyl methacrylate)
PPy	polypyrrole
PUF	Polyurethane foam hydrogels
PVA	polyvinyl alcohol
PVP	polyvinylpyrrolidone
rhBMP-2	bone morphogenetic protein-2
SBMP	commercial dental resin Scotchbond Multi-Purpose
SC	stratum corneum
TPT	oligo(trimethylene carbonate)-poly(ethylene glycol)-oligo (trimethylene carbonate) diacrylate
UVA, UVB	ultraviolet A and B radiations
VDC	vertical diffusion cell system
VEGF	vascular endothelial growth factor



References

- AAWC, 2020. Association for the Advancement of Wound Care [WWW Document]. URL <https://aawconline.memberclicks.net/board-of-directors> (accessed 7.17.19).
- Abduljawwad, S.N., Ahmed, H.-R., 2019. Enhancing cancer cell adhesion with clay nanoparticles for countering metastasis. *Sci. Rep.* 9, 5935. <https://doi.org/10.1038/s41598-019-42498-y>
- Abu-al-Basal, M.A., 2012. Histological evaluation of the healing properties of Dead Sea black mud on full-thickness excision cutaneous wounds in BALB/c mice. *Pakistan J. Biol. Sci.* 15, 306–315.
- Adib-Hajbaghery, M., Mahmoudi, M., Mashaieki, M., 2014. Shampoo-clay heals diaper rash faster than calendula officinalis - PubMed. *Nurs. Midwifery Stud.* 3, 14180.
- Adusumilli, S., Haydel, S.E., 2016. In vitro antibacterial activity and in vivo efficacy of hydrated clays on Mycobacterium ulcerans growth. *BMC Complement. Altern. Med.* 16. <https://doi.org/10.1186/s12906-016-1020-5>
- Aguzzi, C., Capra, P., Bonferoni, C., Cerezo, P., Salcedo, I., Sánchez, R., Caramella, C., Viseras, C., 2010. Chitosan–silicate biocomposites to be used in modified drug release of 5-aminosalicylic acid (5-ASA). *Appl. Clay Sci.* 50, 106–111. <https://doi.org/10.1016/J.CLAY.2010.07.011>
- Aguzzi, C., Cerezo, P., Sandri, G., Ferrari, F., Rossi, S., Bonferoni, C., Caramella, C., Viseras, C., 2014a. Intercalation of tetracycline into layered clay mineral material for drug delivery purposes. *Mater. Technol.* 29, B96–B99. <https://doi.org/10.1179/1753555714Y.0000000133>
- Aguzzi, C., Cerezo, P., Viseras, C., Caramella, C., 2007. Use of clays as drug delivery systems: Possibilities and limitations. *Appl. Clay Sci.* 36, 22–36. <https://doi.org/10.1016/j.clay.2006.06.015>
- Aguzzi, C., Sánchez-Espejo, R., Cerezo, P., Machado, J., Bonferoni, C., Rossi, S., Salcedo, I., Viseras, C., 2013a. Networking and rheology of concentrated clay suspensions “matured” in mineral medicinal water. *Int. J. Pharm.* 453, 473–479. <https://doi.org/10.1016/j.ijpharm.2013.06.002>
- Aguzzi, C., Sandri, G., Bonferoni, C., Cerezo, P., Rossi, S., Ferrari, F., Caramella, C., Viseras, C., 2014b. Solid state characterisation of silver sulfadiazine loaded on montmorillonite/chitosan nanocomposite for wound healing. *Colloids Surfaces B Biointerfaces* 113, 152–157. <https://doi.org/10.1016/J.COLSURFB.2013.08.043>
- Aguzzi, C., Sandri, G., Cerezo, P., Carazo, E., Viseras, C., 2016. Health and medical applications of tubular clay minerals, in: *Developments in Clay Science*. Elsevier, pp. 708–725. <https://doi.org/10.1016/B978-0-08-100293-3.00026-1>
- Aguzzi, C., Viseras, C., Cerezo, P., Salcedo, I., Sánchez-Espejo, R., Valenzuela, C., 2013b. Release kinetics of 5-aminosalicylic acid from halloysite. *Colloids Surfaces B Biointerfaces* 105, 75–80.

1.4. Abbreviations

- <https://doi.org/10.1016/J.COLSURFB.2012.12.041>
- Alam, H.B., Chen, Z., Jaskille, A., Querol, R.I.L.C., Koustova, E., Inocencio, R., Conran, R., Seufert, A., Ariaban, N., Toruno, K., Rhee, P., 2004. Application of a zeolite hemostatic agent achieves 100% survival in a lethal model of complex groin injury in swine. *J. Trauma - Inj. Infect. Crit. Care* 56, 974–983. <https://doi.org/10.1097/01.TA.0000127763.90890.31>
- Alam, H.B., Uy, G.B., Miller, D., Koustova, E., Hancock, T., Inocencio, R., Anderson, D., Llorente, O., Rhee, P., 2003. Comparative analysis of hemostatic agents in a swine model of lethal groin injury. *J. Trauma* 54, 1077–1082. <https://doi.org/10.1097/01.TA.0000068258.99048.70>
- Alavi, M., Totonchi, A., Okhovat, M.A., Motazedian, M., Rezaei, P., Atefi, M., 2014. The effect of a new impregnated gauze containing bentonite and halloysite minerals on blood coagulation and wound healing. *Blood Coagul. Fibrinolysis* 25, 856–859. <https://doi.org/10.1097/MBC.0000000000000172>
- Alexander, P., 1973. Sunscreen, Suntan and Sunburn Preparations, in: Harry, R.G. (Ed.), *Harry's Cosmeticology. The Principles and Practice of Modern Cosmetics*. Leonard Hill Books, London, p. 328.
- Ambrogi, V., Nocchetti, M., Latterini, L., 2014. Promethazine–montmorillonite inclusion complex to enhance drug photostability. *Langmuir* 30, 14612–14620. <https://doi.org/10.1021/la5033898>
- Ambrogi, V., Pietrella, D., Nocchetti, M., Casagrande, S., Moretti, V., De Marco, S., Ricci, M., 2017. Montmorillonite–chitosan–chlorhexidine composite films with antibiofilm activity and improved cytotoxicity for wound dressing. *J. Colloid Interface Sci.* 491, 265–272. <https://doi.org/10.1016/j.jcis.2016.12.058>
- Antonangelo, L., Vargas, F.S., Teixeira, L.R., Acencio, M.M.P., Vaz, M.A.C., Filho, M.T., Marchi, E., 2006. Pleurodesis Induced by Talc or Silver Nitrate: Evaluation of Collagen and Elastic Fibers in Pleural Remodeling. *Lung* 184, 105–111. <https://doi.org/10.1007/s00408-005-2569-9>
- Ariga, K., Abe, H., Ji, Q., Lvov, Y.M., 2017. Halloysite and related mesoporous carriers for advanced catalysis and drug delivery, in: Lvov, Y., Guo, B., Fakhrullin, R. (Eds.), *Functional Polymer Composites With Nanoclays*. ROYAL SOC CHEMISTRY, Cambridge, pp. 207–222.
- Asraf, M.H., Malek, N.A.N.N., Jemon, K., Sani, N.S., Muhammad, M.S., 2019. Antibacterial, cytotoxicity and wound healing assessments of amine-functionalised zeolite Y. *Particuology* 45, 116–123. <https://doi.org/10.1016/j.partic.2018.09.006>
- Aulton, M.E., Taylor, K.M.G. (Eds.), 2013. *Aulton's Pharmaceutics: The Design and Manufacture of Medicines*, 4th ed. Elsevier Health Sciences, Amsterdam.
- Awad, M.E., López-Galindo, A., El-Rahmany, M.M., El-Desoky, H.M., Viseras, C., 2017. Characterization of Egyptian kaolins for health-care uses. *Appl. Clay Sci.* 135, 176–189. <https://doi.org/10.1016/j.clay.2016.09.018>
- Babitha, S., Korrapati, P.S., 2017. Biodegradable zein–polydopamine polymeric scaffold impregnated with TiO₂ nanoparticles for skin tissue engineering.

- Biomed. Mater. 12, 055008. <https://doi.org/10.1088/1748-605X/aa7d5a>
- Baker, S., Sawvel, A., Stucky, G.D., 2008. Hemostatic Compositions and Methods of Use. WO2008127497.
- Bakre, L.G., Sarvaiya, J.I., Agrawal, Y.K., 2016. Synthesis, characterization, and study of drug release properties of curcumin from polycaprolactone/organomodified montmorillonite nanocomposite. *J. Pharm. Innov.* 11, 300–307. <https://doi.org/10.1007/s12247-016-9253-x>
- Barbosa, G.P., Debone, H.S., Severino, P., Souto, E.B., da Silva, C.F., 2016. Design and characterization of chitosan/zeolite composite films – Effect of zeolite type and zeolite dose on the film properties. *Mater. Sci. Eng. C* 60, 246–254. <https://doi.org/10.1016/j.msec.2015.11.034>
- Barry, B.W., 1983. *Dermatological Formulations - Percutaneous Absorption*. Taylor & Francis, Madison Avenue, New York.
- Barua, S., Chattopadhyay, P., Aidew, L., Buragohain, A.K., Karak, N., 2015. Infection-resistant hyperbranched epoxy nanocomposite as a scaffold for skin tissue regeneration. *Polym. Int.* 64, 303–311. <https://doi.org/10.1002/pi.4790>
- Baschini, M.T., Pettinari, G.R., Vallés, J.M., Aguzzi, C., Cerezo, P., López-Galindo, A., Setti, M., Viseras, C., 2010. Suitability of natural sulphur-rich muds from Copahue (Argentina) for use as semisolid health care products. *Appl. Clay Sci.* 49, 205–212. <https://doi.org/10.1016/j.clay.2010.05.008>
- Bayaomy, F.E.A., Darwish, A.S., 2016. Exfoliated Egyptian kaolin immobilized heteropolyoxotungstate nanocomposite as an innovative antischistosomal agent: In vivo and in vitro bioactive studies. *Mater. Sci. Eng. C* 59, 717–730. <https://doi.org/10.1016/j.msec.2015.10.074>
- Bayram, Y., Deveci, M., Imirzalioglu, N., Soysal, Y., Sengezer, M., 2005. The cell based dressing with living allogenic keratinocytes in the treatment of foot ulcers: a case study. *Br. J. Plast. Surg.* 58, 988–996. <https://doi.org/10.1016/J.BJPS.2005.04.031>
- Bazmi Zeynabad, F., Salehi, R., Alizadeh, E., Kafil, H.S., Hassanzadeh, A.M., Mahkam, M., 2015. pH-Controlled multiple-drug delivery by a novel antibacterial nanocomposite for combination therapy. *R. Soc. Chem. Adv.* 5, 105678–105691. <https://doi.org/10.1039/C5RA22784D>
- BCC, 2016. Annual Economic Report.
- Belenky, P., Collins, J.J., 2011. Antioxidant Strategies to Tolerate Antibiotics. *Sci.* 334.
- Beringhs, A.O.R., Rosa, J.M., Stulzer, H.K., Budal, R.M., Sonaglio, D., 2013. Green clay and aloe vera peel-off facial masks: Response surface methodology applied to the formulation design. *AAPS PharmSciTech* 14, 445–455. <https://doi.org/10.1208/s12249-013-9930-8>
- Bhardwaj, N., Kundu, S.C., 2010. Electrospinning: A fascinating fiber fabrication technique. *Biotechnol. Adv.* 28, 325–347. <https://doi.org/10.1016/J.BIOTECHADV.2010.01.004>
- Bhol, K.C., Schechter, P.J., 2007. Effects of Nanocrystalline Silver (NPI 32101) in a Rat Model of Ulcerative Colitis. *Dig. Dis. Sci.* 52, 2732–2742.

1.4. Abbreviations

- <https://doi.org/10.1007/s10620-006-9738-4>
- Biggs, R.D., 2013. Medicine, Surgery, and Public Health in Ancient Mesopotamia - History of the Ancient World. *J. Assyrian Acad. Stud.* 19, 1–19.
- Bindschadler, M., McGrath, J.L., 2007. Sheet migration by wounded monolayers as an emergent property of single-cell dynamics. *J. Cell Sci.* 120, 876–884. <https://doi.org/10.1242/jcs.03395>
- Bonferoni, M.C., Cerri, G., de' Gennaro, M., Juliano, C., Caramella, C., 2007. Zn²⁺-exchanged clinoptilolite-rich rock as active carrier for antibiotics in anti-acne topical therapy: In-vitro characterization and preliminary formulation studies. *Appl. Clay Sci.* 36, 95–102. <https://doi.org/10.1016/j.clay.2006.04.014>
- Bonifacio, M.A., Gentile, P., Ferreira, A.M., Cometa, S., De Giglio, E., 2017. Insight into halloysite nanotubes-loaded gellan gum hydrogels for soft tissue engineering applications. *Carbohydr. Polym.* 163, 280–291. <https://doi.org/10.1016/j.carbpol.2017.01.064>
- Borrego-Sánchez, A., Carazo, E., Aguzzi, C., Viseras, C., Sainz-Díaz, C.I., 2017. Biopharmaceutical improvement of praziquantel by interaction with montmorillonite and sepiolite. *Appl. Clay Sci.* <https://doi.org/10.1016/J.CLAY.2017.12.024>
- Bothiraja, C., Thorat, U.H., Pawar, A.P., Shaikh, K.S., 2014. Chitosan coated layered clay montmorillonite nanocomposites modulate oral delivery of paclitaxel in colonic cancer. *Mater. Technol.* 29, 120–126. <https://doi.org/10.1179/1753555714Y.0000000174>
- Bounabi, L., Mokhnachi, N.B., Haddadine, N., Ouazib, F., Barille, R., 2016. Development of poly(2-hydroxyethyl methacrylate)/clay composites as drug delivery systems of paracetamol. *J. Drug Deliv. Sci. Technol.* 33, 58–65. <https://doi.org/10.1016/j.jddst.2016.03.010>
- Bowman, P.D., Wang, X., Meledeo, M.A., Dubick, M.A., Kheirabadi, B.S., 2011. Toxicity of aluminum silicates used in hemostatic dressings toward human umbilical veins endothelial cells, HeLa cells, and RAW267.4 mouse macrophages. *J. Trauma - Inj. Infect. Crit. Care* 71, 727–732. <https://doi.org/10.1097/TA.0b013e3182033579>
- BP - British Pharmacopoeia, 2018. . British Pharmacopoeia Commission, London.
- Brigatti, M.F., Galan, E., Theng, B.K.G., 2006. Structures and mineralogy of clay minerals, in: Bergaya, F., Theng, B.K., Lagaly, G. (Eds.), *Handbook of Clay Science*. Elsevier, pp. 19–86. [https://doi.org/10.1016/S1572-4352\(05\)01002-0](https://doi.org/10.1016/S1572-4352(05)01002-0)
- Burns, J.L., Mancoll, J.S., Phillips, L.G., 2003. Impairments to wound healing. *Clin. Plast. Surg.* 30, 47–56. [https://doi.org/10.1016/S0094-1298\(02\)00074-3](https://doi.org/10.1016/S0094-1298(02)00074-3)
- Byrd, A.L., Belkaid, Y., Segre, J.A., 2018. The human skin microbiome. *Nat. Rev. Microbiol.* 16, 143–155. <https://doi.org/10.1038/nrmicro.2017.157>
- Cafilisch, K.M., Schmidt-Malan, S.M., Mandrekar, J.N., Karau, M.J., Nicklas, J.P., Williams, L.B., Patel, R., 2018. Antibacterial activity of reduced iron clay against pathogenic bacteria associated with wound infections. *Int. J. Antimicrob. Agents* 52, 692–696. <https://doi.org/10.1016/j.ijantimicag.2018.07.018>

- Caramella, C., Conti, B., Modena, T., Ferrari, F., Bonferoni, M.C., Genta, I., Rossi, S., Torre, M.L., Sandri, G., Sorrenti, M., Catenacci, L., Dorati, R., Tripodo, G., 2016. Controlled delivery systems for tissue repair and regeneration. *J. Drug Deliv. Sci. Technol.* 32, 206–228. <https://doi.org/10.1016/j.jddst.2015.05.015>
- Carazo, E., Borrego-Sánchez, A., Aguzzi, C., Cerezo, P., Viseras, C., 2017a. Use of clays as nanocarriers of first-line tuberculostatic drugs. *Curr. Drug Deliv.* 14, 902–903. <https://doi.org/10.2174/1567201813666160714160727>
- Carazo, E., Borrego-Sánchez, A., García-Villén, F., Sánchez-Espejo, R., Aguzzi, C., Viseras, C., Sainz-Díaz, C.I., Cerezo, P., 2017b. Assessment of halloysite nanotubes as vehicles of isoniazid. *Colloids Surfaces B Biointerfaces* 160, 337–344. <https://doi.org/10.1016/J.COLSURFB.2017.09.036>
- Carazo, E., Borrego-Sánchez, A., García-Villén, F., Sánchez-Espejo, R., Cerezo, P., Aguzzi, C., Viseras, C., 2018a. Advanced Inorganic Nanosystems for Skin Drug Delivery. *Chem. Rec.* 18, 891–899. <https://doi.org/10.1002/tcr.201700061>
- Carazo, E., Borrego-Sánchez, A., García-Villén, F., Sánchez-Espejo, R., Viseras, C., Cerezo, P., Aguzzi, C., 2018b. Adsorption and characterization of palygorskite-isoniazid nanohybrids. *Appl. Clay Sci.* 160. <https://doi.org/10.1016/j.clay.2017.12.027>
- Carretero, M.I., 2002. Clay minerals and their beneficial effects upon human health. A review. *Appl. Clay Sci.* 21, 155–163. [https://doi.org/10.1016/S0169-1317\(01\)00085-0](https://doi.org/10.1016/S0169-1317(01)00085-0)
- Carretero, M.I., Gomes, C.S.F., Tateo, F., 2006. Clays and Human Health, in: Bergaya, F., Theng, B.K., Lagaly, G. (Eds.), *Handbook of Clay Science*. Elsevier Ltd., pp. 717–742.
- Carter, H.M., 1940. Fingernail cleaning composition. U.S. Patent No. 2,197,630.
- Catanzano, O., Acierno, S., Russo, P., Cervasio, M., Del Basso De Caro, M., Bolognese, A., Sammartino, G., Califano, L., Marenzi, G., Calignano, A., Acierno, D., Quaglia, F., 2014. Melt-spun bioactive sutures containing nanohybrids for local delivery of anti-inflammatory drugs. *Mater. Sci. Eng. C* 43, 300–309. <https://doi.org/10.1016/J.MSEC.2014.07.012>
- Cerri, G., de Gennaro, M., Bonferoni, M.C., Caramella, C., 2004. Zeolites in biomedical application: Zn-exchanged clinoptilolite-rich rock as active carrier for antibiotics in anti-acne topical therapy. *Appl. Clay Sci.* 27, 141–150. <https://doi.org/10.1016/j.clay.2004.04.004>
- Cervini-Silva, J., Nieto-Camacho, A., Gómez-Vidales, V., 2015a. Oxidative stress inhibition and oxidant activity by fibrous clays. *Colloids Surfaces B Biointerfaces* 133, 32–35. <https://doi.org/10.1016/j.colsurfb.2015.05.042>
- Cervini-Silva, J., Nieto-Camacho, A., Ramírez-Apan, M.T., Gómez-Vidales, V., Palacios, E., Montoya, A., Ronquillo de Jesús, E., 2015b. Anti-inflammatory, anti-bacterial, and cytotoxic activity of fibrous clays. *Colloids Surfaces B Biointerfaces* 129, 1–6. <https://doi.org/10.1016/j.colsurfb.2015.03.019>
- Chen, H., Ye, Z., Sun, L., Li, X., Shi, S., Hu, J., Jin, Y., Xu, Q., Wang, B., 2018. Synthesis of chitosan-based micelles for pH responsive drug release and antibacterial

1.4. Abbreviations

- application. Carbohydr. Polym. 189, 65–71.
<https://doi.org/10.1016/j.carbpol.2018.02.022>
- Chu, C.-Y., Peng, F.-C., Chiu, Y.-F., Lee, H.-C., Chen, C.-W., Wei, J.-C., Lin, J.-J., 2012. Nanohybrids of Silver Particles Immobilized on Silicate Platelet for Infected Wound Healing. PLoS One 7, e38360.
<https://doi.org/10.1371/journal.pone.0038360>
- Ciprian, L., Lo Nigro, A., Rizzo, M., Gava, A., Ramonda, R., Punzi, L., Cozzi, F., 2013. The effects of combined spa therapy and rehabilitation on patients with ankylosing spondylitis being treated with TNF inhibitors. Rheumatol. Int. 33, 241–245. <https://doi.org/10.1007/s00296-011-2147-9>
- Coger, V., Million, N., Rehbock, C., Sures, B., Nachev, M., Barcikowski, S., Wistuba, N., Strauß, S., Vogt, P.M., 2019. Tissue Concentrations of Zinc, Iron, Copper, and Magnesium During the Phases of Full Thickness Wound Healing in a Rodent Model. Biol. Trace Elem. Res. 191, 167–176. <https://doi.org/10.1007/s12011-018-1600-y>
- Committee, C.N. (Ed.), 2018. The Clay Minerals Society Glossary of Clay Science. Part 1. The Clay Minerals Society, Chantilly, VA, USA.
- Cornejo, J., 1990. Las Arcillas en Formulaciones Farmacéuticas, in: Galán, E., Ortega, M. (Eds.), Conferencias de IX y X Reuniones de La Sociedad Española de Arcillas. SEA, Madrid, pp. 51–68.
- Couto, A., Fernandes, R., Cordeiro, M.N.S., Reis, S.S., Ribeiro, R.T., Pessoa, A.M., 2014. Dermic diffusion and stratum corneum: A state of the art review of mathematical models. J. Control. Release 177, 74–83.
<https://doi.org/10.1016/j.jconrel.2013.12.005>
- Cunningham, T.M., Koehl, J.L., Summers, J.S., Haydel, S.E., 2010. pH-dependent metal ion toxicity influences the antibacterial activity of two natural mineral mixtures. PLoS One 5. <https://doi.org/10.1371/journal.pone.0009456>
- Da Silva, G.R., Silva-Cunha, A. Da, Vieira, L.C., Silva, L.M., Ayres, E., Oréfice, R.L., Fialho, S.L., Saliba, J.B., Behar-Cohen, F., 2013. Montmorillonite clay based polyurethane nanocomposite as substrate for retinal pigment epithelial cell growth. J. Mater. Sci. Mater. Med. 24, 1309–1317. <https://doi.org/10.1007/s10856-013-4885-6>
- Dadkhah, D., Navarchian, A.H., Aref, L., Tavakoli, N., 2014. Application of Taguchi Method to investigate the drug release behavior of poly(acrylamide-co-maleic acid)/montmorillonite nanocomposite hydrogels. Adv. Polym. Technol. 33, n/a-n/a. <https://doi.org/10.1002/adv.21426>
- Dário, G.M.I., Da Silva, G.G., Gonçalves, D.L., Silveira, P., Junior, A.T., Angioletto, E., Bernardin, A.M., 2014. Evaluation of the healing activity of therapeutic clay in rat skin wounds. Mater. Sci. Eng. C 43, 109–116.
<https://doi.org/10.1016/j.msec.2014.06.024>
- Das, G., Kalita, R.D., Gogoi, P., Buragohain, A.K., Karak, N., 2014. Antibacterial activities of copper nanoparticle-decorated organically modified montmorillonite/epoxy nanocomposites. Appl. Clay Sci. 90, 18–26.

<https://doi.org/10.1016/J.CLAY.2014.01.002>

- David, L., Moldovan, B., Vulcu, A., Olenic, L., Perde-Schrepler, M., Fischer-Fodor, E., Florea, A., Crisan, M., Chiorean, I., Clichici, S., Filip, G.A., 2014. Green synthesis, characterization and anti-inflammatory activity of silver nanoparticles using European black elderberry fruits extract. *Colloids Surfaces B Biointerfaces* 122, 767–777. <https://doi.org/10.1016/J.COLSURFB.2014.08.018>
- Davinelli, S., Bassetto, F., Vitale, M., Scapagnini, G., 2019. Thermal Waters and the hormetic effects of hydrogen sulfide on inflammatory arthritis and wound healing. *Sci. Hormesis Heal. Longev.* 121–126. <https://doi.org/10.1016/B978-0-12-814253-0.00010-3>
- de Almeida Borges, V.R., da Silva, J.H., Barbosa, S.S., Nasciutti, L.E., Cabral, L.M., de Sousa, V.P., 2016. Development and pharmacological evaluation of in vitro nanocarriers composed of lamellar silicates containing copaiba oil-resin for treatment of endometriosis. *Mater. Sci. Eng. C* 64, 310–317. <https://doi.org/10.1016/J.MSEC.2016.03.094>
- de Gois da Silva, M.L., Fortes, A.C., Oliveira, M.E.R., de Freitas, R.M., da Silva Filho, E.C., de La Roca Soares, M.F., Soares-Sobrinho, J.L., da Silva Leite, C.M., 2014. Palygorskite organophilic for dermopharmaceutical application. *J. Therm. Anal. Calorim.* 115, 2287–2294. <https://doi.org/10.1007/s10973-012-2891-4>
- De Vos, P., 2010. European materia medica in historical texts: Longevity of a tradition and implications for future use. *J. Ethnopharmacol.* 132, 28–47. <https://doi.org/10.1016/j.jep.2010.05.035>
- Demidova-Rice, T.N., Hamblin, M.R., Herman, I.M., 2012. Acute and impaired wound healing: Pathophysiology and current methods for drug delivery, part 1: Normal and chronic wounds: Biology, causes, and approaches to care. *Adv. Ski. Wound Care* 25, 304–314. <https://doi.org/10.1097/01.ASW.0000416006.55218.d0>
- Demir, A.K., Elçin, A.E., Elçin, Y.M., 2018. Strontium-modified chitosan/montmorillonite composites as bone tissue engineering scaffold. *Mater. Sci. Eng. C* 89, 8–14. <https://doi.org/10.1016/j.msec.2018.03.021>
- Demirci, S., Suner, S.S., Sahiner, M., Sahiner, N., 2017. Superporous hyaluronic acid cryogel composites embedding synthetic polyethyleneimine microgels and Halloysite Nanotubes as natural clay. *Eur. Polym. J.* 93, 775–784. <https://doi.org/10.1016/j.eurpolymj.2017.04.022>
- Demling, R.H., 2001. The Role of Silver in Wound Healing. Part 1: Effects of Silver on Wound Management | Request PDF. *Wounds a Compend. Clin. Res. Pract.* 13, 4–15.
- Depan, D., Misra, R.D.K., 2015. Hybrid nanoscale architecture of wound dressing with super hydrophilic, antimicrobial, and ultralow fouling attributes. *J. Biomed. Nanotechnol.* 11, 306–318. <https://doi.org/10.1166/jbn.2015.1908>
- Dionisi, C., Hanafy, N., Nobile, C., Luisa De Giorgi, M., Rinaldi, R., Casciaro, S., Lvov, Y.M., Leporatti, S., 2016. Halloysite clay nanotubes as carriers for curcumin: Characterization and application. *IEEE Trans. Nanotechnol.* 15, 720–724. <https://doi.org/10.1109/TNANO.2016.2524072>

1.4. Abbreviations

- Dunn, K., Edwards-Jones, V., 2004. The role of Acticoat™ with nanocrystalline silver in the management of burns. *Burns* 30, S1–S9. [https://doi.org/10.1016/S0305-4179\(04\)90000-9](https://doi.org/10.1016/S0305-4179(04)90000-9)
- Dziadkowiec, J., Mansa, R., Quintela, A., Rocha, F., Detellier, C., 2017. Preparation, characterization and application in controlled release of ibuprofen-loaded guar gum/montmorillonite bionanocomposites. *Appl. Clay Sci.* 135, 52–63. <https://doi.org/10.1016/j.clay.2016.09.003>
- Eming, S.A., Krieg, T., Davidson, J.M., 2007. Inflammation in Wound Repair: Molecular and Cellular Mechanisms. *J. Invest. Dermatol.* 127, 514–525. <https://doi.org/10.1038/SJ.JID.5700701>
- Fakhrullin, R.F., Lvov, Y.M., 2016. Halloysite clay nanotubes for tissue engineering. *Nanomedicine* 11, 2243–2246. <https://doi.org/10.2217/nnm-2016-0250>
- Fakhrullina, G.I., Akhatova, F.S., Lvov, Y.M., Fakhrullin, R.F., 2015. Toxicity of halloysite clay nanotubes in vivo: a *Caenorhabditis elegans* study. *Environ. Sci. Nano* 2, 54–59. <https://doi.org/10.1039/C4EN00135D>
- Falkinham, J.O., Wall, T.E., Tanner, J.R., Tawaha, K., Alali, F.Q., Li, C., Oberlies, N.H., 2009. Proliferation of antibiotic-producing bacteria and concomitant antibiotic production as the basis for the antibiotic activity of Jordan's red soils. *Appl. Environ. Microbiol.* 75, 2735–2741. <https://doi.org/10.1128/AEM.00104-09>
- Fazli, Y., Shariatnia, Z., 2017. Controlled release of cefazolin sodium antibiotic drug from electrospun chitosan-polyethylene oxide nanofibrous Mats. *Mater. Sci. Eng. C* 71, 641–652. <https://doi.org/10.1016/J.MSEC.2016.10.048>
- Feitosa, S.A., Palasuk, J., Kamocki, K., Geraldeli, S., Gregory, R.L., Platt, J.A., Windsor, L.J., Bottino, M.C., 2014. Doxycycline-encapsulated nanotube-modified dentin adhesives. *J. Dent. Res.* 93, 1270–1276. <https://doi.org/10.1177/0022034514549997>
- Fernandes, A.C., Pinto, M.L., Antunes, F., Pires, J., 2013. Clay based materials for storage and therapeutic release of nitric oxide. *J. Mater. Chem. B* 1, 3287–3294. <https://doi.org/10.1039/c3tb20535e>
- Fernández-González, M.V., Martín-García, J.M., Delgado, G., Párraga, J., Carretero, M.I., Delgado, R., 2017. Physical properties of peloids prepared with medicinal mineral waters from Lanjarón Spa (Granada, Spain). *Appl. Clay Sci.* 135, 465–474. <https://doi.org/10.1016/j.clay.2016.10.034>
- Ferrell, R.E., 2008. Medicinal clay and spiritual healing. *Clays Clay Miner.* 56, 751–760. <https://doi.org/10.1346/CCMN.2008.0560613>
- Fong, J., 2005. The Use of Silver Products in the Management of Burn Wounds: Change in Practice for the Burn Unit at Royal Perth Hospital. *Medicine (Baltimore)*.
- Fox, S., Wilkinson, T.S., Wheatley, P.S., Xiao, B., Morris, R.E., Sutherland, A., Simpson, A.J., Barlow, P.G., Butler, A.R., Megson, I.L., Rossi, A.G., 2010. NO-loaded Zn²⁺-exchanged zeolite materials: A potential bifunctional anti-bacterial strategy. *Acta Biomater.* 6, 1515–1521. <https://doi.org/http://dx.doi.org/10.1016/j.actbio.2009.10.038>
- Fraioli, A., Serio, A., Mennuni, G., Ceccarelli, F., Petracchia, L., Fontana, M., Grassi, M., Valesini, G., 2011. A study on the efficacy of treatment with mud packs and baths

- with Sillene mineral water (Chianciano Spa Italy) in patients suffering from knee osteoarthritis. *Rheumatol. Int.* 31, 1333–1340. <https://doi.org/10.1007/s00296-010-1475-5>
- Friedlander, L.R., Puri, N., Schoonen, M.A.A., Karzai, A.W., 2015. The effect of pyrite on *Escherichia coli* in water: Proof-of-concept for the elimination of waterborne bacteria by reactive minerals. *J. Water Health* 13, 42–53. <https://doi.org/10.2166/wh.2014.013>
- Fu, Q., Rahaman, M.N., Fu, H., Liu, X., 2010. Silicate, borosilicate, and borate bioactive glass scaffolds with controllable degradation rate for bone tissue engineering applications. I. Preparation and in vitro degradation. *J. Biomed. Mater. Res. - Part A* 95, 164–171. <https://doi.org/10.1002/jbm.a.32824>
- Gabriel, D.M., 1973. Vanishing and Foundation Creams, in: *Harry's Cosmeticology. The Principles and Practice of Modern Cosmetics*. Leonard Hill Books, London, p. 83.
- Ganguli-Indra, G., 2014. Protocol for Cutaneous Wound Healing Assay in a Murine Model. Humana Press, New York, NY, pp. 151–159. https://doi.org/10.1007/978-1-4939-1435-7_12
- Gao, M., Lu, L., Wang, X., Lin, H., Zhou, Q., 2017. Preparation of a novel breviscapine-loaded halloysite nanotubes complex for controlled release of breviscapine. *Mater. Sci. Eng.* 265, 1–8. <https://doi.org/10.1088/1757-899X/265/1/012011>
- García-Villén, F., Carazo, E., Borrego-Sánchez, A., Sánchez-Espejo, R., Cerezo, P., Viseras, C., Aguzzi, C., 2019a. Clay minerals in drug delivery systems, in: Mercurio, M., Sarkar, B., Langella, A. (Eds.), *Modified Clay and Zeolite Nanocomposite Materials*. Elsevier Inc. <https://doi.org/https://doi.org/10.1016/B978-0-12-814617-0.00010-4>
- García-Villén, F., Faccendini, A., Aguzzi, C., Cerezo, P., Bonferoni, M.C., Rossi, S., Grisoli, P., Ruggeri, M., Ferrari, F., Sandri, G., Viseras, C., 2019b. Montmorillonite-norfloxacin nanocomposite intended for healing of infected wounds. *Int. J. Nanomedicine* 14, 5051–5060. <https://doi.org/https://doi.org/10.2147/IJN.S208713>
- García-Villén, F., Sánchez-Espejo, R., Carazo, E., Borrego-Sánchez, A., Aguzzi, C., Cerezo, P., Viseras, C., 2018. Characterisation of Andalusian peats for skin health care formulations. *Appl. Clay Sci.* 160, 201–205. <https://doi.org/10.1016/j.clay.2017.12.017>
- Ghadiri, M., Chrzanowski, W., Lee, W.H., Rohanizadeh, R., 2014a. Layered silicate clay functionalized with amino acids: Wound healing application. *RSC Adv.* 4, 35332–35343. <https://doi.org/10.1039/c4ra05216a>
- Ghadiri, M., Chrzanowski, W., Rohanizadeh, R., 2015. Biomedical applications of cationic clay minerals. *RSC Adv.* 5, 29467–29481. <https://doi.org/10.1039/c4ra16945j>
- Ghadiri, M., Chrzanowski, W., Rohanizadeh, R., 2014b. Antibiotic eluting clay mineral

1.4. Abbreviations

- (Laponite®) for wound healing application: an in vitro study. *J. Mater. Sci. Mater. Med.* 25, 2513–26. <https://doi.org/10.1007/s10856-014-5272-7>
- Ghebaour, A., Balanuca, B., Garea, S.A., Iovu, H., 2016. pH-sensitive clays as drug delivery carriers for controlled release of hydrocortisone. *Mater. Plast.* 53, 419–423.
- Gomes, C., Carretero, M.I., Pozo, M., Maraver, F., Cantista, P., Armijo, F., Legido, J.L., Teixeira, F., Rautureau, M., Delgado, R., 2013. Peloids and pelotherapy: Historical evolution, classification and glossary. *Appl. Clay Sci.* 75–76, 28–38. <https://doi.org/10.1016/j.clay.2013.02.008>
- Gomes, C. de S.F., Silva, J.B.P., 2007. Minerals and clay minerals in medical geology. *Appl. Clay Sci.* 36, 4–21. <https://doi.org/10.1016/j.clay.2006.08.006>
- Gonzalez, J.S., Maiolo, A.S., Hoppe, C.E., Alvarez, V.A., 2012. Composite Gels Based on Poly (Vinyl alcohol) for Biomedical Uses. *Procedia Mater. Sci.* 1, 483–490. <https://doi.org/10.1016/j.mspro.2012.06.065>
- Gorrasi, G., 2015. Dispersion of halloysite loaded with natural antimicrobials into pectins: characterization and controlled release analysis. *Carbohydr. Polym.* 127, 47–53. <https://doi.org/10.1016/J.CARBPOL.2015.03.050>
- Grancarić, A.M., Tarbuk, A., Kovaček, I., 2009. Nanoparticles of activated natural zeolite on textiles for protection and therapy. *Chem. Ind. Chem. Eng. Q.* 15, 203–210. <https://doi.org/10.2298/CICEQ0904203G>
- Grether-Beck, S., Mühlberg, K., Brenden, H., Felsner, I., Bryjólfssdóttir, Á., Einarsson, S., Krutmann, J., 2008. Bioactive molecules from the Blue Lagoon: In vitro and in vivo assessment of silica mud and microalgae extracts for their effects on skin barrier function and prevention of skin ageing. *Exp. Dermatol.* 17, 771–779. <https://doi.org/10.1111/j.1600-0625.2007.00693.x>
- Guggenheim, S., Krekeler, M.P.S., 2011. The structures and microtextures of the palygorskite–sepiolite group minerals, in: Galán, E., Singer, A. (Eds.), *Developments in Clay Science*. Elsevier, pp. 3–32. <https://doi.org/10.1016/B978-0-444-53607-5.00001-3>
- Güngen, G., Ardic, F., Fundikoğlu, G., Rota, S., 2012. The effect of mud pack therapy on serum YKL-40 and hsCRP levels in patients with knee osteoarthritis. *Rheumatol. Int.* 32, 1235–1244. <https://doi.org/10.1007/s00296-010-1727-4>
- Gür, E., Altinisik, A., Yurdakoc, K., 2015. Preparation and characterization of chitosan/sepiolite bionanocomposites for tetracycline release. *Polym. Polym. Compos.* 38, 1810–1818. <https://doi.org/10.1002/pc>
- Hamilton, A.R., Hutcheon, G.A., Roberts, M., Gaskell, E.E., 2014. Formulation and antibacterial profiles of clay-ciprofloxacin composites. *Appl. Clay Sci.* 87, 129–135. <https://doi.org/10.1016/j.clay.2013.10.020>
- Han, L., Lu, X., Liu, K., Wang, K., Fang, L., Weng, L.-T., Zhang, H., Tang, Y., Ren, F., Zhao, C., Sun, G., Liang, R., Li, Z., 2017. Mussel-Inspired Adhesive and Tough Hydrogel Based on Nanoclay Confined Dopamine Polymerization. *ACS Nano* 11, 2561–2574. <https://doi.org/10.1021/acs.nano.6b05318>
- Hanif, J., Tasca, R.A., Frosh, A., Ghufoor, K., Stirling, R., 2003. Silver nitrate:

- histological effects of cautery on epithelial surfaces with varying contact times. *Clin. Otolaryngol. Allied Sci.* 28, 368–370. <https://doi.org/10.1046/j.1365-2273.2003.00727.x>
- Haraguchi, K., Takehisa, T., Ebato, M., 2006. Control of cell cultivation and cell sheet detachment on the surface of polymer/clay nanocomposite hydrogels. *Biomacromolecules* 7, 3267–3275. <https://doi.org/10.1021/bm060549b>
- Haydel, S.E., Remenih, C.M., Williams, L.B., 2007. Broad-spectrum in vitro antibacterial activities of clay minerals against antibiotic-susceptible and antibiotic-resistant bacterial pathogens. *J. Antimicrob. Chemother.* 61, 353–361. <https://doi.org/10.1093/jac/dkm468>
- Holešová, S., Valášková, M., Hlaváč, D., Madejová, J., Samlíková, M., Tokarský, J., Pazdziora, E., 2014. Antibacterial kaolinite/urea/chlorhexidine nanocomposites: experiment and molecular modelling. *Appl. Surf. Sci.* 305, 783–791. <https://doi.org/10.1016/J.APSUSC.2014.04.008>
- Hong, H.J., Kim, J., Suh, Y.J., Kim, D., Roh, K.M., Kang, I., 2017. pH-sensitive mesalazine carrier for colon-targeted drug delivery: A two-fold composition of mesalazine with a clay and alginate. *Macromol. Res.* 25, 1145–1152. <https://doi.org/10.1007/s13233-017-5150-5>
- Hu, H., Tang, Y., Pang, L., Lin, C., Huang, W., Wang, D., Jia, W., 2018a. Angiogenesis and full-thickness wound healing efficiency of a copper-doped borate bioactive glass/poly(lactic-co-glycolic acid) dressing loaded with vitamin E in vivo and in vitro. *ACS Appl. Mater. Interfaces* 10, 22939–22950. <https://doi.org/10.1021/acsami.8b04903>
- Hu, M., Li, C., Li, X., Zhou, M., Sun, J., Sheng, F., Shi, S., Lu, L., 2018b. Zinc oxide/silver bimetallic nanoencapsulated in PVP/PCL nanofibres for improved antibacterial activity. *Artif. Cells, Nanomedicine, Biotechnol.* 46, 1248–1257. <https://doi.org/10.1080/21691401.2017.1366339>
- Huang, A., Seité, S., Adar, T., 2018. The use of balneotherapy in dermatology. *Clin. Dermatol.* 36, 363–368. <https://doi.org/10.1016/J.CLINDERMATOL.2018.03.010>
- Huang, B., Liu, M., Zhou, C., 2017. Cellulose–halloysite nanotube composite hydrogels for curcumin delivery. *Cellulose* 24, 2861–2875. <https://doi.org/10.1007/s10570-017-1316-8>
- Huang, K.T., Fang, Y.L., Hsieh, P.S., Li, C.C., Dai, N.T., Huang, C.J., 2017. Non-sticky and antimicrobial zwitterionic nanocomposite dressings for infected chronic wounds. *Biomater. Sci.* 5, 1072–1081. <https://doi.org/10.1039/c7bm00039a>
- Iannuccelli, V., Maretti, E., Bellini, A., Malferrari, D., Ori, G., Montorsi, M., Bondi, M., Truzzi, E., Leo, E., 2018. Organo-modified bentonite for gentamicin topical application: Interlayer structure and in vivo skin permeation. *Appl. Clay Sci.* 158, 158–168. <https://doi.org/10.1016/j.clay.2018.03.029>
- ICH, 2000. ICH Topic Q6A Specifications: Test Procedures and Acceptance Criteria for New Drug Substances and New Drug Products: Chemical Substances. EMEA, European Union.
- Ijiri, H., Sato, K., Suzuki, M., Hasegawa, Y., 2015. No Title. U.S. Patent No. 9,114,266.

1.4. Abbreviations

- Jafarbeglou, Maryam, Abdouss, M., Shoushtari, A.M., Jafarbeglou, Majid, 2016. Clay nanocomposites as engineered drug delivery systems. *RSC Adv.* 6, 50002–50016. <https://doi.org/10.1039/C6RA03942A>
- Jain, S., Datta, M., 2016. Montmorillonite-alginate microspheres as a delivery vehicle for oral extended release of Venlafaxine hydrochloride. *J. Drug Deliv. Sci. Technol.* 33, 149–156. <https://doi.org/10.1016/J.JDDST.2016.04.002>
- Jain, S., Datta, M., 2015. Oral extended release of dexamethasone: Montmorillonite–PLGA nanocomposites as a delivery vehicle. *Appl. Clay Sci.* 104, 182–188. <https://doi.org/10.1016/J.CLAY.2014.11.028>
- Jana, S., Kondakova, A. V., Shevchenko, S.N., Sheval, E. V, Gonchar, K.A., Yu, V., Vasiliev, A.N., 2017. Halloysite nanotubes with immobilized silver nanoparticles for anti-bacterial application. *Colloids Surfaces B Biointerfaces* 151, 249–254. <https://doi.org/10.1016/j.colsurfb.2016.12.017>
- Jiang, W.-T., Chang, P.-H., Tsai, Y., Li, Z., 2016. Halloysite nanotubes as a carrier for the uptake of selected pharmaceuticals. *Microporous Mesoporous Mater.* 220, 298–307. <https://doi.org/10.1016/J.MICROMESO.2015.09.011>
- Jin, H., Liang, G., Zhang, G., 2003. Effects of tourmaline on the proliferation of human endothelial cells using millicell membrane culture dish. *J. Chinese Microcirc.*
- Jones, V., Grey, J.E., Harding, K.G., 2006. Wound dressings. *BMJ* 332, 777–80. <https://doi.org/10.1136/bmj.332.7544.777>
- Jonkman, J.E.N., Cathcart, J.A., Xu, F., Bartolini, M.E., Amon, J.E., Stevens, K.M., Colarusso, P., 2014. An introduction to the wound healing assay using live-cell microscopy. *Cell Adh. Migr.* 8, 440–51. <https://doi.org/10.4161/cam.36224>
- Kalishwaralal, K., Banumathi, E., Pandian, S.R.K., Deepak, V., Muniyandi, J., Eom, S.H., Gurunathan, S., 2009. Silver nanoparticles inhibit VEGF induced cell proliferation and migration in bovine retinal endothelial cells. *Colloids Surfaces B Biointerfaces* 73, 51–57. <https://doi.org/10.1016/J.COLSURFB.2009.04.025>
- Kar, S., Bagchi, B., Kundu, B., Bhandary, S., Basu, R., Nandy, P., Das, S., 2014. Synthesis and characterization of Cu/Ag nanoparticle loaded mullite nanocomposite system: A potential candidate for antimicrobial and therapeutic applications. *Biochim. Biophys. Acta - Gen. Subj.* 1840, 3264–3276. <https://doi.org/10.1016/J.BBAGEN.2014.05.012>
- Katti, K.S., Katti, D.R., Dash, R., 2008. Synthesis and characterization of a novel chitosan/montmorillonite/hydroxyapatite nanocomposite for bone tissue engineering. *Biomed. Mater.* 3. <https://doi.org/10.1088/1748-6041/3/3/034122>
- Kaur, M., Datta, M., 2014. Diclofenac Sodium Adsorption onto Montmorillonite: Adsorption Equilibrium Studies and Drug Release Kinetics. *Adsorpt. Sci. Technol.* 32, 365–387. <https://doi.org/10.1260/0263-6174.32.5.365>
- Kevadiya, B.D., Chettiar, S.S., Rajkumar, S., Bajaj, H.C., Gosai, K.A., Brahmabhatt, H., 2013. Evaluation of clay/poly (L-lactide) microcomposites as anticancer drug, 6-mercaptopurine reservoir through in vitro cytotoxicity, oxidative stress markers and in vivo pharmacokinetics. *Colloids Surfaces B Biointerfaces* 112, 400–407. <https://doi.org/10.1016/J.COLSURFB.2013.07.008>

- Khiari, I., Mefteh, S., Sánchez-Espejo, R., Cerezo, P., Aguzzi, C., López-Galindo, A., Jamoussi, F., Viseras Iborra, C., 2014. Study of traditional Tunisian medina clays used in therapeutic and cosmetic mud-packs. *Appl. Clay Sci.* 101, 141–148. <https://doi.org/10.1016/J.CLAY.2014.07.029>
- Khiari, I., Sánchez-Espejo, R., García-Villén, F., Cerezo, P., Aguzzi, C., López-Galindo, A., Jamoussi, F., Viseras, C., 2019. Rheology and cation release of tunisian medina mud-packs intended for topical applications. *Appl. Clay Sci.* 171, 110–117. <https://doi.org/10.1016/J.CLAY.2019.01.018>
- Khodzhaeva, V., Makeeva, A., Ulyanova, V., Zelenikhin, P., Evtugyn, V., Hardt, M., Rozhina, E., Lvov, Y., Fakhruллин, R., Ilinskaya, O., 2017. Binase immobilized on halloysite nanotubes exerts enhanced cytotoxicity toward human colon adenocarcinoma cells. *Front. Pharmacol.* 8, 1–10. <https://doi.org/10.3389/fphar.2017.00631>
- Klasen, H.J., 2000. A historical review of the use of silver in the treatment of burns. II. Renewed interest for silver. *Burns* 26, 131–138. [https://doi.org/10.1016/S0305-4179\(99\)00116-3](https://doi.org/10.1016/S0305-4179(99)00116-3)
- Kohay, H., Sarisozen, C., Sawant, R., Jhaveri, A., Torchilin, V.P., Mishael, Y.G., 2017. PEG-PE/clay composite carriers for doxorubicin: Effect of composite structure on release, cell interaction and cytotoxicity. *Acta Biomater.* 55, 443–454. <https://doi.org/10.1016/j.actbio.2017.04.008>
- Kommireddy, D.S., Ichinose, I., Lvov, Y.M., Mills, D.K., 2006. Nanoparticle multilayers: surface modification for cell attachment and growth. *J. Biomed. Nanotechnol.* 1, 286–290. <https://doi.org/10.1166/jbn.2005.046>
- Kong, Y., Ge, H., Xiong, J., Zuo, S., Wei, Y., Yao, C., Deng, L., 2014. Palygorskite polypyrrole nanocomposite: a new platform for electrically tunable drug delivery. *Appl. Clay Sci.* 99, 119–124. <https://doi.org/10.1016/J.CLAY.2014.06.020>
- Krishnan, B., Mahalingam, S., 2017. Ag/TiO₂/bentonite nanocomposite for biological applications: Synthesis, characterization, antibacterial and cytotoxic investigations. *Adv. Powder Technol.* 28, 2265–2280. <https://doi.org/10.1016/j.apt.2017.06.007>
- Krishnan, N., Velramar, B., Ramatchandirin, B., Abraham, G.C., Duraisamy, N., Pandiyan, R., Velu, R.K., 2018. Effect of biogenic silver nanocubes on matrix metalloproteinases 2 and 9 expressions in hyperglycemic skin injury and its impact in early wound healing in streptozotocin-induced diabetic mice. *Mater. Sci. Eng. C* 91, 146–152. <https://doi.org/10.1016/J.MSEC.2018.05.020>
- Kurczewska, J., Pecyna, P., Ratajczak, M., Gajęcka, M., Schroeder, G., 2017. Halloysite nanotubes as carriers of vancomycin in alginate-based wound dressing. *Saudi Pharm. J.* 25, 911–920. <https://doi.org/10.1016/j.jsps.2017.02.007>
- Kwan, K.H.L., Liu, X., To, M.K.T., Yeung, K.W.K., Ho, C., Wong, K.K.Y., 2011. Modulation of collagen alignment by silver nanoparticles results in better mechanical properties in wound healing. *Nanomedicine Nanotechnology, Biol. Med.* 7, 497–504. <https://doi.org/10.1016/j.nano.2011.01.003>
- Lal, S., Datta, M., 2015. In vitro prolonged gastric residence and sustained release of

1.4. Abbreviations

- atenolol using novel clay polymer nanocomposite. *Appl. Clay Sci.* 114, 412–421. <https://doi.org/10.1016/J.CLAY.2015.06.017>
- Lal, S., Perwez, A., Rizvi, M.A., Datta, M., 2017. Design and development of a biocompatible montmorillonite PLGA nanocomposites to evaluate in vitro oral delivery of insulin. *Appl. Clay Sci.* 147, 69–79. <https://doi.org/10.1016/j.clay.2017.06.031>
- Lam, P.L., Lee, K.K.H., Wong, R.S.M., Cheng, G.Y.M., Bian, Z.X., Chui, C.H., Gambari, R., 2018. Recent advances on topical antimicrobials for skin and soft tissue infections and their safety concerns. *Crit. Rev. Microbiol.* 44, 40–78. <https://doi.org/10.1080/1040841X.2017.1313811>
- Lee, I.W., Li, J., Chen, X., Park, H.J., 2016. Electrospun poly(vinyl alcohol) composite nanofibers with halloysite nanotubes for the sustained release of sodium D-pantothenate. *J. Appl. Polym. Sci.* 133, n/a-n/a. <https://doi.org/10.1002/app.42900>
- Li, H., Zhu, X., Xu, J., Peng, W., Zhong, S., Wang, Y., 2016. The combination of adsorption by functionalized halloysite nanotubes and encapsulation by polyelectrolyte coatings for sustained drug delivery. *RSC Adv.* 6, 54463–54470. <https://doi.org/10.1039/C6RA09599B>
- Li, K., Zhang, Y., Chen, M., Hu, Y., Jiang, W., Zhou, L., Li, S., Xu, M., Zhao, Q., Wan, R., 2018. Enhanced antitumor efficacy of doxorubicin- encapsulated halloysite nanotubes. *Int. J. Nanomedicine* 13, 19–30. <https://doi.org/10.2147/IJN.S143928>
- Li, W., Liu, D., Zhang, H., Correia, A., Mäkilä, E., Salonen, J., Hirvonen, J., Santos, H.A., 2017. Microfluidic assembly of a nano-in-micro dual drug delivery platform composed of halloysite nanotubes and a pH-responsive polyurethane for colon cancer therapy. *Acta Biomater.* 48, 238–246. <https://doi.org/10.1016/J.ACTBIO.2016.10.042>
- Li, X., Li, Y.-C., Chen, M., Shi, Q., Sun, R., Wang, X., 2018. Chitosan/rectorite nanocomposite with injectable functionality for skin hemostasis. *J. Mater. Chem. B* 6, 6544–6549. <https://doi.org/10.1039/C8TB01085D>
- Li, X., Qian, Y., Ouyang, J., Yang, H., Chang, S., 2016. Chitosan modified halloysite nanotubes as emerging porous microspheres for drug carrier. *Appl. Clay Sci.* 126, 306–312. <https://doi.org/10.1016/J.CLAY.2016.03.035>
- Li, Y., Li, H., Xiao, L., Zhou, L., Shentu, J., Zhang, X., Fan, J., 2012. Hemostatic efficiency and wound healing properties of natural zeolite granules in a lethal rabbit model of complex groin injury. *Materials (Basel)*. 5, 2586–2596. <https://doi.org/10.3390/ma5122586>
- Li, Y., Sawvel, A.M., Jun, Y.-S., Nownes, S., Ni, M., Kudela, D., Stucky, G.D., Zink, D., 2013. Cytotoxicity and potency of mesocellular foam-26 in comparison to layered clays used as hemostatic agents. *Toxicol. Res.* 2, 136–144. <https://doi.org/10.1039/C2TX20065A>
- Liang, C.-C., Park, A.Y., Guan, J.-L., 2007. In vitro scratch assay: a convenient and inexpensive method for analysis of cell migration in vitro. *Nat. Protoc.* 2, 329–333. <https://doi.org/10.1038/nprot.2007.30>
- Liu, M., Chang, Y., Yang, J., You, Y., He, R., Chen, T., Zhou, C., 2016. Functionalized

- halloysite nanotube by chitosan grafting for drug delivery of curcumin to achieve enhanced anticancer efficacy. *J. Mater. Chem. B* 4, 2253–2263. <https://doi.org/10.1039/C5TB02725J>
- Liu, M., Dai, L., Shi, H., Xiong, S., Zhou, C., 2015. In vitro evaluation of alginate/halloysite nanotube composite scaffolds for tissue engineering. *Mater. Sci. Eng. C, Mater. Biol. Appl.* 49, 700–712. <https://doi.org/10.1016/j.msec.2015.01.037>
- Liu, M., Jia, Z., Jia, D., Zhou, C., 2014. Recent advance in research on halloysite nanotubes-polymer nanocomposite. *Prog. Polym. Sci.* 39, 1498–1525. <https://doi.org/10.1016/J.PROGPOLYMSCI.2014.04.004>
- Liu, M., Zhang, Y., Wu, C., Xiong, S., Zhou, C., 2012. Chitosan/halloysite nanotubes bionanocomposites: Structure, mechanical properties and biocompatibility. *Int. J. Biol. Macromol.* 51, 566–575. <https://doi.org/10.1016/j.ijbiomac.2012.06.022>
- Lizarbe, M.A., Olmo, N., Gavilanes, J.G., 1987. Outgrowth of fibroblasts on sepiolite-collagen complex. *Biomaterials* 8, 35–37. [https://doi.org/10.1016/0142-9612\(87\)90025-1](https://doi.org/10.1016/0142-9612(87)90025-1)
- Long, M., Zhang, Y., Huang, P., Chang, S., Hu, Y., Yang, Q., Mao, L., Yang, H., 2018. Emerging Nanoclay Composite for Effective Hemostasis. *Adv. Funct. Mater.* 28, 1704452. <https://doi.org/10.1002/adfm.201704452>
- Long, Z., Zhang, J., Shen, Y., Zhou, C., Liu, M., 2017. Polyethyleneimine grafted short halloysite nanotubes for gene delivery. *Mater. Sci. Eng. C* 81, 224–235. <https://doi.org/10.1016/j.msec.2017.07.035>
- López-Galindo, A., Viseras, C., 2004. Pharmaceutical and cosmetic application of clays, in: Wypyc, F., Satyanarayana, K.G. (Eds.), *Clay Surfaces: Fundamentals and Applications*. Elsevier Ltd, pp. 267–289.
- López-Galindo, Alberto, Viseras, C., 2004. Pharmaceutical and Cosmetic Applications of Clays, in: Wypych, F., Satyanarayana, K.G. (Eds.), *Clay Surfaces: Fundamentals and Applications, Interface Science and Technology*. Elsevier, Ireland, pp. 267–289. [https://doi.org/10.1016/S1573-4285\(04\)80044-9](https://doi.org/10.1016/S1573-4285(04)80044-9)
- López-Galindo, A., Viseras, C., Aguzzi, C., Cerezo, P., 2011. Pharmaceutical and cosmetic uses of fibrous clays, in: Galán, E., Singer, A. (Eds.), *Developments in Clay Science*. Elsevier, pp. 299–324. <https://doi.org/10.1016/B978-0-444-53607-5.00013-X>
- López-Galindo, A., Viseras, C., Cerezo, P., 2007. Compositional, technical and safety specifications of clays to be used as pharmaceutical and cosmetic products. *Appl. Clay Sci.* 36, 51–63. <https://doi.org/10.1016/J.CLAY.2006.06.016>
- Lu, B., Lu, F., Zou, Y., Liu, J., Rong, B., Li, Z., Dai, F., Wu, D., Lan, G., 2017. In situ reduction of silver nanoparticles by chitosan-l-glutamic acid/hyaluronic acid: Enhancing antimicrobial and wound-healing activity. *Carbohydr. Polym.* 173, 556–565. <https://doi.org/10.1016/J.CARBPOL.2017.06.035>
- Luong, D., Yergeshov, A.A., Zoughaib, M., Sadykova, F.R., Gareev, B.I., Savina, I.N., Abdullin, T.I., 2019. Transition metal-doped cryogels as bioactive materials for wound healing applications. *Mater. Sci. Eng. C* 103, 109759.

1.4. Abbreviations

- <https://doi.org/10.1016/J.MSEC.2019.109759>
- Lvov, Y., Aerov, A., Fakhrullin, R., 2014. Clay nanotube encapsulation for functional biocomposites. *Adv. Colloid Interface Sci.* 207, 189–198. <https://doi.org/10.1016/J.CIS.2013.10.006>
- Lvov, Y., DeVilliers, M.M., Fakhrullin, R.F., 2016a. The application of halloysite tubule nanoclay in drug delivery. *Expert Opin. Drug Deliv.* 13, 977–986. <https://doi.org/10.1517/17425247.2016.1169271>
- Lvov, Y., Wang, W., Zhang, L., Fakhrullin, R., 2016b. Halloysite clay nanotubes for loading and sustained release of functional compounds. *Adv. Mater.* 28, 1227–1250. <https://doi.org/10.1002/adma.201502341>
- Macgregor, A., 2013. Medicinal terra sigillata: A historical, geographical and typological review, in: Duffin, C.J., Moody R. T. J., Gardner-Thorpe, C. (Eds.), *A History Of geology and Medicine*. Geological Society, London, pp. 113–136. <https://doi.org/10.1144/SP375.1>
- Madusanka, N., de Silva, K.M.N., Amaratunga, G., 2015. A curcumin activated carboxymethyl cellulose–montmorillonite clay nanocomposite having enhanced curcumin release in aqueous media. *Carbohydr. Polym.* 134, 695–699. <https://doi.org/10.1016/J.CARBPOL.2015.08.030>
- Mahdavinia, G.R., Hosseini, R., Darvishi, F., Sabzi, M., 2016. The release of cefazolin from chitosan/polyvinyl alcohol/sepiolite nanocomposite hydrogel films. *Iran. Polym. J.* 25, 933–943. <https://doi.org/10.1007/s13726-016-0480-2>
- Mahkam, M., Latifpour, A., Rafi, A.A., Gheshlaghi, L.M., Takfallah, A., 2015. Preparation of Montmorillonite-pH-Sensitive Positive Charges Nanocomposites as a Drug Delivery System. *Int. J. Polym. Mater. Polym. Biomater.* 64, 32–37. <https://doi.org/10.1080/00914037.2014.886241>
- Mantle, D., Gok, M.A., Lennard, T.W.J., 2001. Adverse and beneficial effects of plant extracts on skin and skin disorders. *Adverse Drug React. Toxicol. Rev.* 20, 89–103.
- Mao, H., Liu, X., Yang, J., Li, B., Chen, Q., Zhong, J., 2014. Fabrication of magnetic silica-pillared clay (SPC) nanocomposites with ordered interlayer mesoporous structure for controlled drug release. *Microporous Mesoporous Mater.* 184, 169–176. <https://doi.org/10.1016/J.MICROMESO.2013.10.020>
- Mao, H., Zhu, K., Liu, X., Yao, C., Kobayashi, M., 2016. Facile synthetic route to Fe₃O₄/silica nanocomposites pillared clay through cationic surfactant-aliphatic acid mixed system and application for magnetically controlled drug release. *Microporous Mesoporous Mater.* 225, 216–223. <https://doi.org/10.1016/J.MICROMESO.2015.11.045>
- Massaro, M., Amorati, R., Cavallaro, G., Guernelli, S., Lazzara, G., Milioto, S., Noto, R., Poma, P., Riela, S., 2016a. Direct chemical grafted curcumin on halloysite nanotubes as dual-responsive prodrug for pharmacological applications. *Colloids Surfaces B Biointerfaces* 140, 505–513. <https://doi.org/10.1016/J.COLSURFB.2016.01.025>
- Massaro, M., Riela, S., Baiamonte, C., Blanco, J.L.J., Giordano, C., Lo Meo, P., Milioto,

- S., Noto, R., Parisi, F., Pizzolanti, G., Lazzara, G., 2016b. Dual drug-loaded halloysite hybrid-based glycocluster for sustained release of hydrophobic molecules. *RSC Adv.* 6, 87935–87944. <https://doi.org/10.1039/C6RA14657K>
- Massaro, M., Riela, S., Guernelli, S., Parisi, F., Lazzara, G., Baschieri, A., Valgimigli, L., Amorati, R., 2016. A synergic nanoantioxidant based on covalently modified halloysite–trolox nanotubes with intra-lumen loaded quercetin. *J. Mater. Chem. B* 4, 2229–2241. <https://doi.org/10.1039/C6TB00126B>
- Mattioli, M., Giardini, L., Roselli, C., Desideri, D., 2016. Mineralogical characterization of commercial clays used in cosmetics and possible risk for health. *Appl. Clay Sci.* 119, 449–454. <https://doi.org/10.1016/j.clay.2015.10.023>
- Mauro, N., Chiellini, F., Bartoli, C., Gazzarri, M., Laus, M., Antonioli, D., Griffiths, P., Manfredi, A., Ranucci, E., Ferruti, P., 2017. RGD-mimic polyamidoamine–montmorillonite composites with tunable stiffness as scaffolds for bone tissue-engineering applications. *J. Tissue Eng. Regen. Med.* 11, 2164–2175. <https://doi.org/10.1002/term.2115>
- Medicamentarius, C., 1866. *Pharmacopoea Française*. Paris.
- Mefteh, S., Khiari, I., Sánchez-Espejo, R., Aguzzi, C., López-Galindo, A., Jamoussi, F., Viseras, C., 2014. Characterisation of Tunisian layered clay materials to be used in semisolid health care products. *Mater. Technol.* 29, B88–B95. <https://doi.org/10.1179/1753555714Y.0000000152>
- Meier, L., Stange, R., Michalsen, A., Uehleke, B., 2012. Clay Jojoba Oil Facial Mask for Lesioned Skin and Mild Acne – Results of a Prospective, Observational Pilot Study. *Forschende Komplementärmedizin / Res. Complement. Med.* 19, 75–79. <https://doi.org/10.1159/000338076>
- Meirelles, L.M.A., Raffin, F.N., 2017. Clay and polymer-based composites applied to drug release: A scientific and technological prospection. *J Pharm Pharm Sci* 115–134.
- Mieszawska, A.J., Llamas, J.G., Vaiana, C.A., Kadakia, M.P., Naik, R.R., Kaplan, D.L., 2011. Clay enriched silk biomaterials for bone formation. *Acta Biomater.* 7, 3036–3041. <https://doi.org/10.1016/j.actbio.2011.04.016>
- Minullina, R., Tully, J., Yendluri, R., Lvov, Yuri, 2017. Halloysite clay nanotubes for long acting controlled release of drugs and proteins, in: Lvov, Y, Guo, B., Fakhruddin, R.F. (Eds.), *Functional Polymer Composites With Nanoclays*. Royal Society of Chemistry, Cambridge, pp. 354–378.
- Mishra, R.K., Ramasamy, K., Lim, S.M., Ismail, M.F., Majeed, A.B.A., 2014. Antimicrobial and in vitro wound healing properties of novel clay based bionanocomposite films. *J. Mater. Sci. Mater. Med.* 25, 1925–1939. <https://doi.org/10.1007/s10856-014-5228-y>
- Mohd, S.S., Abdullah, M.A.A., Mat Amin, K.A., 2016. Gellan gum/clay hydrogels for tissue engineering application: Mechanical, thermal behavior, cell viability, and antibacterial properties. *J. Bioact. Compat. Polym.* 31, 648–666. <https://doi.org/10.1177/0883911516643106>
- Moraes, J.D.D., Bertolino, S.R.A., Cuffini, S.L., Ducart, D.F., Bretzke, P.E., Leonardi,

1.4. Abbreviations

- G.R., 2017. Clay minerals: Properties and applications to dermocosmetic products and perspectives of natural raw materials for therapeutic purposes – A review. *Int. J. Pharm.* 534, 213–219. <https://doi.org/10.1016/j.ijpharm.2017.10.031>
- Morrison, K.D., Misra, R., Williams, L.B., 2016. Unearthing the Antibacterial Mechanism of Medicinal Clay: A Geochemical Approach to Combating Antibiotic Resistance. *Sci. Rep.* 6, 1–13. <https://doi.org/10.1038/srep19043>
- Morrison, K.D., Underwood, J.C., Metge, D.W., Eberl, D.D., Williams, L.B., 2014. Mineralogical variables that control the antibacterial effectiveness of a natural clay deposit. *Environ. Geochem. Health* 36, 613–631. <https://doi.org/10.1007/s10653-013-9585-0>
- Moura, D., Souza, M.T., Liverani, L., Rella, G., Luz, G.M., Mano, J.F., Boccaccini, A.R., 2017. Development of a bioactive glass-polymer composite for wound healing applications. *Mater. Sci. Eng. C* 76, 224–232. <https://doi.org/10.1016/J.MSEC.2017.03.037>
- Mouriño, V., Cattalini, J.P., Boccaccini, A.R., 2012. Metallic ions as therapeutic agents in tissue engineering scaffolds: An overview of their biological applications and strategies for new developments. *J. R. Soc. Interface* 9, 401–419. <https://doi.org/10.1098/rsif.2011.0611>
- Mousa, M., Evans, N.D., Oreffo, R.O.C., Dawson, J.I., 2018. Clay nanoparticles for regenerative medicine and biomaterial design: A review of clay bioactivity. *Biomaterials* 159, 204–214. <https://doi.org/10.1016/J.BIOMATERIALS.2017.12.024>
- Mura, P., Maestrelli, F., Aguzzi, C., Viseras, C., 2016. Hybrid systems based on “drug – in cyclodextrin – in nanoclays” for improving oxaprozin dissolution properties. *Int. J. Pharm.* 509, 8–15. <https://doi.org/10.1016/J.IJPHARM.2016.05.028>
- Nadworny, P.L., Landry, B.K., Wang, J., Tredget, E.E., Burrell, R.E., 2010. Does nanocrystalline silver have a transferable effect? *Wound Repair Regen.* 18, 254–265. <https://doi.org/10.1111/j.1524-475X.2010.00579.x>
- Nasirov, M.I., Efendieva, F.M., İsmailova, D.A., 2009. The influence of peloids from volcanic deposits in Azerbaijan on the dynamics of sugar content in blood and urine and the wound healing in patients at the early stages of diabetic gangrene of the lower extremities. *Vopr. Kurortol. Fizioter. Lech. Fiz. Kult.* 42–3.
- Naumenko, E.A., Guryanov, I.D., Yendluri, R., Lvov, Y.M., Fakhrullin, R.F., 2016. Clay nanotube-biopolymer composite scaffolds for tissue engineering. *Nanoscale* 8, 7257–7271. <https://doi.org/10.1039/c6nr00641h>
- Nazir, M.S., Mohamad Kassim, M.H., Mohapatra, L., Gilani, M.A., Raza, M.R., Majeed, K., 2016. Characteristic properties of nanoclays and characterization of nanoparticulates and nanocomposites, in: *Jawaid, M., Qaiss, A., Bouhfid, R. (Eds.), Nanoclay Reinforced Polymer Composites*. Springer, Singapore, pp. 35–55.
- Neidrauer, M., Ercan, U.K., Bhattacharyya, A., Samuels, J., Sedlak, J., Trikha, R.,

- Barbee, K.A., Weingarten, M.S., Joshi, S.G., 2014. Antimicrobial efficacy and wound-healing property of a topical ointment containing nitric-oxide-loaded zeolites. *J. Med. Microbiol.* 63, 203–209. <https://doi.org/10.1099/jmm.0.067322-0>
- Ng, K.W., Lau, W.M., 2015. Skin deep: The basics of human skin structure and drug penetration, in: *Percutaneous Penetration Enhancers Chemical Methods in Penetration Enhancement: Drug Manipulation Strategies and Vehicle Effects*. Springer Berlin Heidelberg, pp. 3–11. https://doi.org/10.1007/978-3-662-45013-0_1
- Ninan, N., Muthiah, M., Nur, N.A., Park, I.K., Elain, A., Wong, T.W., Thomas, S., Grohens, Y., 2014. Antibacterial and wound healing analysis of gelatin/zeolite scaffolds. *Colloids Surfaces B Biointerfaces* 115, 244–252. <https://doi.org/10.1016/j.colsurfb.2013.11.048>
- Ninan, N., Muthiah, M., Park, I.K., Elain, A., Wong, T.W., Thomas, S., Grohens, Y., 2015a. In vitro and in vivo evaluation of pectin/copper exchanged faujasite composite membranes. *J. Biomed. Nanotechnol.* 11, 1550–1567. <https://doi.org/10.1166/jbn.2015.2098>
- Ninan, N., Muthiah, M., Park, I.K., Elain, A., Wong, T.W., Thomas, S., Grohens, Y., 2013. Faujasites incorporated tissue engineering scaffolds for wound healing: In vitro and in vivo analysis. *ACS Appl. Mater. Interfaces* 5, 11194–11206. <https://doi.org/10.1021/am403436y>
- Ninan, N., Muthiah, M., Park, I.K., Wong, T.W., Thomas, S., Grohens, Y., 2015b. Natural polymer/inorganic material based hybrid scaffolds for skin wound healing. *Polym. Rev.* 55, 453–490. <https://doi.org/10.1080/15583724.2015.1019135>
- Noori, S., Kokabi, M., Hassan, Z.M., 2018. Poly(vinyl alcohol)/chitosan/honey/clay responsive nanocomposite hydrogel wound dressing. *J. Appl. Polym. Sci.* 135, 46311. <https://doi.org/10.1002/app.46311>
- Nussbaum, S.R., Carter, M.J., Fife, C.E., DaVanzo, J., Haught, R., Nusgart, M., Cartwright, D., 2018. An Economic Evaluation of the Impact, Cost, and Medicare Policy Implications of Chronic Nonhealing Wounds. *Value Heal.* 21, 27–32. <https://doi.org/10.1016/j.jval.2017.07.007>
- Oh, S.T., Kim, W.R., Kim, S.H., Chung, Y.C., Park, J.S., 2011. The preparation of polyurethane foam combined with pH-sensitive alginate/bentonite hydrogel for wound dressings. *Fibers Polym.* 12, 159–165. <https://doi.org/10.1007/s12221-011-0159-4>
- Olad, A., Farshi-Azhar, F., 2014. The synergetic effect of bioactive ceramic and nanoclay on the properties of chitosan–gelatin/nanohydroxyapatite–montmorillonite scaffold for bone tissue engineering. *Ceram. Int.* 40, 10061–10072. <https://doi.org/10.1016/j.CERAMINT.2014.04.010>
- Olaiya, A.K., Fadason, S.T., 2017. Studies on Zinc and Copper Ion in Relation to Wound Healing in Male and Female West African Dwarf Goats. *Niger. J. Physiol. Sci.* 31, 171–176.
- Oliveira, A.S., Alcântara, A.C.S., Pergher, S.B.C., 2017. Bionanocomposite systems based on montmorillonite and biopolymers for the controlled release of

1.4. Abbreviations

- olanzapine. *Mater. Sci. Eng. C* 75, 1250–1258. <https://doi.org/10.1016/j.msec.2017.03.044>
- Olmo, N., Lizarbe, M.A., Gavilanes, J.G., 1987. Biocompatibility and degradability of sepiolite-collagen complex. *Biomaterials* 8, 67–9. [https://doi.org/10.1016/0142-9612\(87\)90033-0](https://doi.org/10.1016/0142-9612(87)90033-0)
- Olsson, M., Järbrink, K., Ni, G., Sönnergren, H., Schmidtchen, A., Pang, C., Bajpai, R., Car, J., 2017. The humanistic and economic burden of chronic wounds: A protocol for a systematic review. *Syst. Rev.* 6. <https://doi.org/10.1186/s13643-016-0400-8>
- Orlowski, P., Zmigrodzka, M., Tomaszewska, E., Ranoszek-Soliwoda, K., Czupryn, M., Antos-Bielska, M., Szemraj, J., Celichowski, G., Grobelny, J., Krzyzowska, M., 2018. Tannic acid-modified silver nanoparticles for wound healing: The importance of size. *Int. J. Nanomedicine* 13, 991–1007. <https://doi.org/10.2147/IJN.S154797>
- Ostomel, T.A., Stoimenov, P.K., Holden, P.A., Alam, H.B., Stucky, G.D., 2006. Host-guest composites for induced hemostasis and therapeutic healing in traumatic injuries. *J. Thromb. Thrombolysis* 22, 55–67. <https://doi.org/10.1007/s11239-006-7658-y>
- Othman, R., Vladisavljević, G.T., Thomas, N.L., Nagy, Z.K., 2016. Fabrication of composite poly(D,L-lactide)/montmorillonite nanoparticles for controlled delivery of acetaminophen by solvent-displacement method using glass capillary microfluidics. *Colloids Surfaces B Biointerfaces* 141, 187–195. <https://doi.org/10.1016/j.colsurfb.2016.01.042>
- Otto, C.C., Haydel, S.E., 2013a. Microbicidal clays: composition, activity, mechanism of action, and therapeutic applications., in: Méndez-Vilas, A. (Ed.), *Microbial Pathogens and Strategies for Combating Them: Science, Technology and Education*. Formatex Research Center, Badajoz, pp. 1169–1180.
- Otto, C.C., Haydel, S.E., 2013b. Exchangeable Ions Are Responsible for the In Vitro Antibacterial Properties of Natural Clay Mixtures. *PLoS One* 8, e64068. <https://doi.org/10.1371/journal.pone.0064068>
- Otto, C.C., Kilbourne, J., Haydel, S.E., 2016. Natural and ion-exchanged illite clays reduce bacterial burden and inflammation in cutaneous meticillin-resistant *Staphylococcus aureus* infections in mice. *J. Med. Microbiol.* 65, 19–27. <https://doi.org/10.1099/jmm.0.000195>
- Otto, C.C., Koehl, J.L., Solanky, D., Haydel, S.E., 2014. Metal ions, not metal-catalyzed oxidative stress, cause clay leachate antibacterial activity. *PLoS One* 9. <https://doi.org/10.1371/journal.pone.0115172>
- Pacelli, S., Paolicelli, P., Moretti, G., Petralito, S., Di Giacomo, S., Vitalone, A., Casadei, M.A., 2016. Gellan gum methacrylate and laponite as an innovative nanocomposite hydrogel for biomedical applications. *Eur. Polym. J.* 77, 114–123. <https://doi.org/10.1016/j.eurpolymj.2016.02.007>
- Palasuk, J., Windsor, L.J., Platt, J.A., Lvov, Y., Geraldelli, S., Bottino, M.C., 2017. Doxycycline-loaded nanotube-modified adhesives inhibit MMP in a dose-

- dependent fashion. *Clin. Oral Investig.* 1–10. <https://doi.org/10.1007/s00784-017-2215-y>
- Pan, A., Zhong, M., Wu, H., Peng, Y., Xia, H., Tang, Q., Huang, Q., Wei, L., Xiao, L., Peng, C., 2018. Topical application of keratinocyte growth factor conjugated gold nanoparticles accelerate wound healing. *Nanomedicine Nanotechnology, Biol. Med.* 14, 1619–1628. <https://doi.org/10.1016/J.NANO.2018.04.007>
- Pan, Q., Li, N., Hong, Y., Tang, H., Zheng, Z., Weng, S., Zheng, Y., Huang, L., 2017. Halloysite clay nanotubes as effective nanocarriers for the adsorption and loading of vancomycin for sustained release. *RSC Adv.* 7, 21352–21359. <https://doi.org/10.1039/C7RA00376E>
- Park, J.H., Shin, H.J., Kim, M.H., Kim, J.S., Kang, N., Lee, J.Y., Kim, K.T., Lee, J.I., Kim, D.D., 2016. Application of montmorillonite in bentonite as a pharmaceutical excipient in drug delivery systems. *J. Pharm. Investig.* 46, 363–375. <https://doi.org/10.1007/s40005-016-0258-8>
- Paydar, S., Noorafshan, A., Dalfardi, B., Jahanabadi, S., Mortazavi, S.M.J., Yahyavi, S.-S., Khoshmohabat, H., 2016. Structural alteration in dermal vessels and collagen bundles following exposure of skin wound to zeolite–bentonite compound. *J. Pharm.* 2016, 1–5. <https://doi.org/10.1155/2016/5843459>
- Perfitt, R.J., Carimbocas, C.A.R., 2017. No Title. U.S. Patent No. 9,801,793.
- Perioli, L., Dorigato, A., Pagano, C., Leoni, M., Pegoretti, A., 2019. Thermo-mechanical and adhesive properties of polymeric films based on ZnAl-hydrotalcite composites for active wound dressings. *Polym. Eng. Sci.* 59, E112–E119. <https://doi.org/10.1002/pen.24877>
- Pesciaroli, C., Viseras, C., Aguzzi, C., Rodelas, B., González-López, J., 2016. Study of bacterial community structure and diversity during the maturation process of a therapeutic peloid. *Appl. Clay Sci.* 132–133, 59–67. <https://doi.org/10.1016/j.clay.2016.05.015>
- Petkewich, R., 2008. Healing Clays. *Chem. Eng. News* 86.
- Ph.Eur.9th., 2017. Council of Europe & Convention on the Elaboration of a European Pharmacopoeia, ninth. ed. Maisonneuve, Sainte-Ruffine, France.
- Phan, V.H.G., Lee, E., Maeng, J.H., Thambi, T., Kim, B.S., Lee, D., Lee, D.S., 2016. Pancreatic cancer therapy using an injectable nanobiohybrid hydrogel. *RSC Adv.* 6, 41644–41655. <https://doi.org/10.1039/C6RA07934B>
- Phukan, A., Bhattacharjee, R.P., Dutta, D.K., 2017. Stabilization of SnO₂ nanoparticles into the nanopores of modified Montmorillonite and their antibacterial activity. *Adv. Powder Technol.* 28, 139–145. <https://doi.org/10.1016/j.apt.2016.09.005>
- Pongjanyakul, T., Khunawattanakul, W., Strachan, C.J., Gordon, K.C., Puttipipatkachorn, S., Rades, T., 2013. Characterization of chitosan–magnesium aluminum silicate nanocomposite films for buccal delivery of nicotine. *Int. J. Biol. Macromol.* 55, 24–31. <https://doi.org/10.1016/J.IJBIOMAC.2012.12.043>
- Popriadukhin, P.V., Dobrovol'skaia, I.P., Iudin, V.E., Ivan'kova, E.M., Smolianinov, A.B., Smirnova, N.V., 2011. Composite materials based on chitosan and

1.4. Abbreviations

- montmorillonite: prospects for use as a matrix for stem and regenerative cell cultivation. *Tsitologiya* 53, 952–958.
- Popryadukhin, P. V., Dobrovolskaya, I.P., Yudin, V.E., Ivan'kova, E.M., Smolyaninov, A.B., Smirnova, N. V., 2012. Composite materials based on chitosan and montmorillonite: Prospects for use as a matrix for cultivation of stem and regenerative cells. *Cell tissue biol.* 6, 82–88. <https://doi.org/10.1134/S1990519X12010099>
- Pourshahrestani, S., Zeimaran, E., Djordjevic, I., Kadri, N.A., Towler, M.R., 2016. Inorganic hemostats: The state-of-the-art and recent advances. *Mater. Sci. Eng. C* 58, 1255–1268. <https://doi.org/10.1016/j.msec.2015.09.008>
- Prow, T.W., Grice, J.E., Lin, L.L., Faye, R., Butler, M., Becker, W., Wurm, E.M.T., Yoong, C., Robertson, T.A., Soyer, H.P., Roberts, M.S., 2011. Nanoparticles and microparticles for skin drug delivery. *Adv. Drug Deliv. Rev.* 63, 470–491. <https://doi.org/10.1016/j.addr.2011.01.012>
- Qi, R., Guo, R., Shen, M., Cao, X., Zhang, L., Xu, J., Yu, J., Shi, X., 2010. Electrospun poly(lactic-co-glycolic acid)/halloysite nanotube composite nanofibers for drug encapsulation and sustained release. *J. Mater. Chem.* 20, 10622. <https://doi.org/10.1039/c0jm01328e>
- Qi, R., Guo, R., Zheng, F., Liu, H., Yu, J., Shi, X., 2013. Controlled release and antibacterial activity of antibiotic-loaded electrospun halloysite/poly(lactic-co-glycolic acid) composite nanofibers. *Colloids Surfaces B Biointerfaces* 110, 148–155. <https://doi.org/10.1016/J.COLSURFB.2013.04.036>
- Quintela, A., Terroso, D., Ferreira da Silva, E., Rocha, F., 2012. Certification and quality criteria of peloids used for therapeutic purposes. *Clay Miner.* 47, 441–451. <https://doi.org/10.1180/claymin.2012.047.4.04>
- Rabiei, M., Sabahi, H., Rezayan, A.H., 2016. Gallic acid-loaded montmorillonite nanostructure as a new controlled release system. *Appl. Clay Sci.* 119, 236–242. <https://doi.org/10.1016/J.CLAY.2015.10.020>
- Ran, L., Zou, Y., Cheng, J., Lu, F., 2019. Silver nanoparticles in situ synthesized by polysaccharides from *Sanghuangporus sanghuang* and composites with chitosan to prepare scaffolds for the regeneration of infected full-thickness skin defects. *Int. J. Biol. Macromol.* 125, 392–403. <https://doi.org/10.1016/J.IJBIOMAC.2018.12.052>
- Rangappa, S., Rangan, K.K., Sudarshan, T.S., Murthy, S.N., 2018. Antiallodynic and Antihyperalgesic Activities of Fentanyl-Loaded Dermal Clay Dressings in Rat Model of Second-Degree Burn Injury. *J. Pharm. Sci.* 107, 2628–2634. <https://doi.org/10.1016/j.xphs.2018.06.005>
- Rangappa, S., Rangan, K.K., Sudarshan, T.S., Murthy, S.N., 2017. Evaluation of lidocaine loaded clay based dermal patch systems. *J. Drug Deliv. Sci. Technol.* 39, 450–454. <https://doi.org/10.1016/j.jddst.2017.03.026>
- Rao, K.M., Nagappan, S., Seo, D.J., Ha, C.-S., 2014. pH sensitive halloysite-sodium hyaluronate/poly(hydroxyethyl methacrylate) nanocomposites for colon cancer drug delivery. *Appl. Clay Sci.* 97–98, 33–42.

- <https://doi.org/10.1016/J.CLAY.2014.06.002>
- Rapacz-Kmita, A., Bu, M.M., Stodolak-Zych, E., Miko, M., Dudek, P., Trybus, M., 2017a. Characterisation, in vitro release study, and antibacterial activity of montmorillonite-gentamicin complex material. *Mater. Sci. Eng. C* 70, 471–478. <https://doi.org/10.1016/j.msec.2016.09.031>
- Rapacz-Kmita, A., Stodolak-Zych, E., Dudek, M., Gajek, M., Ziabka, M., 2017b. Magnesium aluminium silicate–gentamicin complex for drug delivery systems: Preparation, physicochemical characterisation and release profiles of the drug. *J. Therm. Anal. Calorim.* 127, 871–880. <https://doi.org/10.1007/s10973-016-5918-4>
- Rebelo, M., Viseras, C., López-Galindo, A., Rocha, F., da Silva, E.F., 2011a. Rheological and thermal characterization of peloids made of selected Portuguese geological materials. *Appl. Clay Sci.* 52, 219–227. <https://doi.org/10.1016/j.clay.2011.02.018>
- Rebelo, M., Viseras, C., López-Galindo, A., Rocha, F., da Silva, E.F., 2011b. Characterization of Portuguese geological materials to be used in medical hydrology. *Appl. Clay Sci.* 51, 258–266. <https://doi.org/10.1016/j.clay.2010.11.029>
- Rebitski, E.P., Aranda, P., Darder, M., Carraro, R., Ruiz-Hitzky, E., 2018. Intercalation of metformin into montmorillonite. *Dalt. Trans.* <https://doi.org/10.1039/c7dt04197g>
- Reddy, A.B., Manjula, B., Jayaramudu, T., Sadiku, E.R., Anand Babu, P., Periyar Selvam, S., 2016. 5-Fluorouracil loaded chitosan–PVA/Na+MMT nanocomposite films for drug release and antimicrobial activity. *Nano-Micro Lett.* 8, 260–269. <https://doi.org/10.1007/s40820-016-0086-4>
- Riela, S., Massaro, M., Colletti, C.G., Bommarito, A., Giordano, C., Milioto, S., Noto, R., Poma, P., Lazzara, G., 2014. Development and characterization of co-loaded curcumin/triazole-halloysite systems and evaluation of their potential anticancer activity. *Int. J. Pharm.* 475, 613–623. <https://doi.org/10.1016/J.IJPHARM.2014.09.019>
- Rizzo, C., Arrigo, R., D’Anna, F., Di Blasi, F., Dintcheva, N.T., Lazzara, G., Parisi, F., Riela, S., Spinelli, G., Massaro, M., 2017. Hybrid supramolecular gels of Fmoc-F/halloysite nanotubes: systems for sustained release of camptothecin. *J. Mater. Chem. B* 5, 3217–3229. <https://doi.org/10.1039/C7TB00297A>
- Rochette, S., Doyon, S., Elkurdi, M., 2017. No Title. U.S. Patent Application No. 15/293,733.
- Rodrigues, L.A. de S., Figueiras, A., Veiga, F., de Freitas, R.M., Nunes, L.C.C., da Silva Filho, E.C., da Silva Leite, C.M., 2013. The systems containing clays and clay minerals from modified drug release: A review. *Colloids Surfaces B Biointerfaces* 103, 642–651. <https://doi.org/10.1016/j.colsurfb.2012.10.068>
- Roy, A., Butola, B.S., Joshi, M., 2017. Synthesis, characterization and antibacterial properties of novel nano-silver loaded acid activated montmorillonite. *Appl. Clay Sci.* 146, 278–285. <https://doi.org/10.1016/j.clay.2017.05.043>
- Saha, K., Butola, B.S., Joshi, M., 2014a. Drug release behavior of polyurethane/clay nanocomposite: film vs. nanofibrous web. *J. Appl. Polym. Sci.* 131. <https://doi.org/10.1002/app.40824>

1.4. Abbreviations

- Saha, K., Butola, B.S., Joshi, M., 2014b. Synthesis and characterization of chlorhexidine acetate drug-montmorillonite intercalates for antibacterial applications. *Appl. Clay Sci.* 101, 477–483. <https://doi.org/10.1016/j.clay.2014.09.010>
- Saha, N.R., Sarkar, G., Roy, I., Rana, D., Bhattacharyya, A., Adhikari, A., Mukhopadhyay, A., Chattopadhyay, D., 2016. Studies on methylcellulose/pectin/montmorillonite nanocomposite films and their application possibilities. *Carbohydr. Polym.* 136, 1218–1227. <https://doi.org/10.1016/J.CARBPOL.2015.10.046>
- Salahuddin, N., Elbarbary, A., Allam, N.G., Hashim, A.F., 2014. Polyamide-montmorillonite nanocomposites as a drug delivery system: Preparation, release of 1,3,4-oxa(thia)diazoles, and antimicrobial activity. *J. Appl. Polym. Sci.* 131, n/a-n/a. <https://doi.org/10.1002/app.41177>
- Salcedo, I., Aguzzi, C., Sandri, G., Bonferoni, M.C., Mori, M., Cerezo, P., Sánchez, R., Viseras, C., Caramella, C., 2012. In vitro biocompatibility and mucoadhesion of montmorillonite chitosan nanocomposite: A new drug delivery. *Appl. Clay Sci.* 55, 131–137. <https://doi.org/10.1016/j.clay.2011.11.006>
- Salcedo, I., Sandri, G., Aguzzi, C., Bonferoni, C., Cerezo, P., Sánchez-Espejo, R., Viseras, C., 2014. Intestinal permeability of oxytetracycline from chitosan-montmorillonite nanocomposites. *Colloids Surfaces B Biointerfaces* 117, 441–448. <https://doi.org/10.1016/J.COLSURFB.2013.11.009>
- Salehi, H., Mehrasa, M., Nasri-Nasrabadi, B., Doostmohammadi, M., Seyedebrahimi, R., Davari, N., Rafenia, M., Ebrahimian-Hosseiniabadi, M., Agheb, M., Siavash, M., 2017. Effects of nanozeolite/starch thermoplastic hydrogels on wound healing. *J. Res. Med. Sci.* 22. https://doi.org/10.4103/jrms.JRMS_1037_16
- Sánchez-Espejo, R., Aguzzi, C., Cerezo, P., Salcedo, I., López-Galindo, A., Viseras, C., 2014a. Folk pharmaceutical formulations in western Mediterranean: Identification and safety of clays used in pelotherapy. *J. Ethnopharmacol.* 155, 810–814. <https://doi.org/10.1016/j.jep.2014.06.031>
- Sánchez-Espejo, R., Aguzzi, C., Salcedo, I., Cerezo, P., Viseras, C., 2014b. Clays in complementary and alternative medicine. *Mater. Technol.* 29, B78–B81. <https://doi.org/10.1179/1753555714Y.0000000173>
- Sánchez-Espejo, R., Cerezo, P., Aguzzi, C., López-Galindo, A., Machado, J., Viseras, C., 2015. Physicochemical and in vitro cation release relevance of therapeutic muds “maturation”. *Appl. Clay Sci.* 116–117, 1–7. <https://doi.org/10.1016/j.clay.2015.08.007>
- Sánchez-Espejo, R., García-Villén, F., Aguzzi, C., Cerezo, P., Viseras, C., 2017. Medicinal Use of Clays from Antiquity to the Twenty-First Century, in: López-Galindo, A. (Ed.), *Scientific Research Abstracts. XVI International Clay Conference*. Digilabs, Bari, Italy.
- Sánchez-Fernández, A., Peña-Parás, L., Vidaltamayo, R., Cué-Sampedro, R., Mendoza-Martínez, A., Zomosa-Signoret, V., Rivas-Estilla, A., Riojas, P., 2014. Synthesis, characterization, and in vitro evaluation of cytotoxicity of biomaterials based on halloysite nanotubes. *Materials (Basel)*. 7, 7770–7780.

- <https://doi.org/10.3390/ma7127770>
- Sandri, G., Aguzzi, C., Rossi, S., Bonferoni, M.C., Bruni, G., Boselli, C., Cornaglia, A.I., Riva, F., Viseras, C., Caramella, C., Ferrari, F., 2017. Halloysite and chitosan oligosaccharide nanocomposite for wound healing. *Acta Biomater.* 57, 216–224. <https://doi.org/10.1016/j.ACTBIO.2017.05.032>
- Sandri, G., Bonferoni, M.C., Ferrari, F., Rossi, S., Aguzzi, C., Mori, M., Grisoli, P., Cerezo, P., Tenci, M., Viseras, C., Caramella, C., 2014. Montmorillonite-chitosan-silver sulfadiazine nanocomposites for topical treatment of chronic skin lesions: in vitro biocompatibility, antibacterial efficacy and gap closure cell motility properties. *Carbohydr. Polym.* 102, 970–977. <https://doi.org/10.1016/j.carbpol.2013.10.029>
- Sandri, G., Bonferoni, M.C., Rossi, S., Ferrari, F., Aguzzi, C., Viseras, C., Caramella, C., 2016. Clay minerals for tissue regeneration, repair, and engineering, in: Ågren, M.S. (Ed.), *Wound Healing Biomaterials*. Elsevier, pp. 385–402. <https://doi.org/10.1016/B978-1-78242-456-7.00019-2>
- Santana, A.C.S.G.V., Soares Sobrinho, J.L., da Silva Filho, E.C., Nunes, L.C.C., 2017. Preparation and physicochemical characterization of binary composites palygorskite–chitosan for drug delivery. *J. Therm. Anal. Calorim.* 128, 1327–1334. <https://doi.org/10.1007/s10973-016-6075-5>
- Saporito, F., Sandri, G., Bonferoni, M.C., Rossi, S., Boselli, C., Icaro Cornaglia, A., Mannucci, B., Grisoli, P., Vigani, B., Ferrari, F., 2017. Essential oil-loaded lipid nanoparticles for wound healing. *Int. J. Nanomedicine* 13, 175–186. <https://doi.org/10.2147/IJN.S152529>
- Sarfaraz, N.K., 2004. *Handbook of Pharmaceutical Manufacturing Formulations. Semisolid Products*. CRC Press, Boca Raton.
- Sasaki, Y., Sathi, G.A., Yamamoto, O., 2017. Wound healing effect of bioactive ion released from Mg-smectite. *Mater. Sci. Eng. C. Mater. Biol. Appl.* 77, 52–57. <https://doi.org/10.1016/j.msec.2017.03.236>
- Sastry, S.V., Nyshadham, J.R., Fix, J.A., 2000. Recent technological advances in oral drug delivery – a review. *Pharm. Sci. Technol. Today* 3, 138–145. [https://doi.org/10.1016/S1461-5347\(00\)00247-9](https://doi.org/10.1016/S1461-5347(00)00247-9)
- Schoonheydt, R.A., Jonhston, C.T., 2006. Surface and interface chemistry of clay minerals, in: Bergaya, F., Lagaly, G. (Eds.), *Handbook of Clay Science*. Elsevier, pp. 87–113.
- Seifu, D.G., Isimjan, T.T., Mequanint, K., 2011. Tissue engineering scaffolds containing embedded fluorinated-zeolite oxygen vectors. *Acta Biomater.* 7, 3670–3678. <https://doi.org/10.1016/j.actbio.2011.06.010>
- Sen, C.K., Gordillo, G.M., Roy, S., Kirsner, R., Lambert, L., Hunt, T.K., Gottrup, F., Gurtner, G.C., Longaker, M.T., 2009. Human skin wounds: A major and snowballing threat to public health and the economy: PERSPECTIVE ARTICLE. *Wound Repair Regen.* 17, 763–771. <https://doi.org/10.1111/j.1524-475X.2009.00543.x>
- Shanmugapriya, K., Kim, H., Saravana, P.S., Chun, B.S., Kang, H.W., 2018. Fabrication

1.4. Abbreviations

- of multifunctional chitosan-based nanocomposite film with rapid healing and antibacterial effect for wound management. *Int. J. Biol. Macromol.* 118, 1713–1725. <https://doi.org/10.1016/j.ijbiomac.2018.07.018>
- Shi, R., Niu, Y., Gong, M., Ye, J., Tian, W., Zhang, L., 2018. Antimicrobial gelatin-based elastomer nanocomposite membrane loaded with ciprofloxacin and polymyxin B sulfate in halloysite nanotubes for wound dressing. *Mater. Sci. Eng. C* 87, 128–138. <https://doi.org/10.1016/J.MSEC.2018.02.025>
- Silva, M.L. de G. da, Fortes, A.C., Tomé, A. da R., Silva Filho, E.C. da, Freitas, R.M. de, Soares-Sobrinho, J.L., Leite, C.M. da S., Soares, M.F. de L.R., 2013. The effect of natural and organophilic palygorskite on skin wound healing in rats. *Brazilian J. Pharm. Sci.* 49, 729–736. <https://doi.org/10.1590/S1984-82502013000400012>
- Sirousazar, M., Jahani-Javanmardi, A., Kheiri, F., Hassan, Z.M., 2016. In vitro and in vivo assays on egg white/polyvinyl alcohol/clay nanocomposite hydrogel wound dressings. *J. Biomater. Sci. Polym. Ed.* 27, 1569–1583. <https://doi.org/10.1080/09205063.2016.1218210>
- Sirousazar, M., Kokabi, M., Hassan, Z.M., 2011. In vivo and cytotoxic assays of a poly(vinyl alcohol)/clay nanocomposite hydrogel wound dressing. *J. Biomater. Sci. Polym. Ed.* 22, 1023–1033. <https://doi.org/10.1163/092050610X497881>
- Smith, S.A., Travers, R.J., Morrissey, J.H., 2015. How it all starts: Initiation of the clotting cascade. *Crit. Rev. Biochem. Mol. Biol.* 50, 326–36. <https://doi.org/10.3109/10409238.2015.1050550>
- Tan, D., Yuan, P., Annabi-Bergaya, F., Liu, D., Wang, L., Liu, H., He, H., 2014. Loading and in vitro release of ibuprofen in tubular halloysite. *Appl. Clay Sci.* 96, 50–55. <https://doi.org/10.1016/J.CLAY.2014.01.018>
- Tao, L., Zhonglong, L., Ming, X., Zezheng, Y., Zhiyuan, L., Xiaojun, Z., Jinwu, W., 2017. In vitro and in vivo studies of a gelatin/carboxymethyl chitosan/LAPONITE® composite scaffold for bone tissue engineering. *RSC Adv.* 7, 54100–54110. <https://doi.org/10.1039/c7ra06913h>
- Tenci, M., Rossi, S., Aguzzi, C., Carazo, E., Sandri, G., Bonferoni, M.C., Grisoli, P., Viseras, C., Caramella, C.M., Ferrari, F., 2017. Carvacrol/clay hybrids loaded into in situ gelling films. *Int. J. Pharm.* 531, 676–688. <https://doi.org/10.1016/J.IJPHARM.2017.06.024>
- Tenti, S., Cheleschi, S., Galeazzi, M., Fioravanti, A., 2015. Spa therapy: can be a valid option for treating knee osteoarthritis? *Int. J. Biometeorol.* 59, 1133–1143. <https://doi.org/10.1007/s00484-014-0913-6>
- Thakur, A., Wanchoo, R.K., Singh, P., 2012. Hydrogels of poly(acrylamide-co-acrylic acid): In-vitro study on release of gentamicin sulfate. *Chem. Biochem. Eng. Q.* 25, 471–482.
- Tian, J., Wong, K.K.Y., Ho, C.M., Lok, C.N., Yu, W.Y., Che, C.M., Chiu, J.F., Tam, P.K.H., 2007. Topical delivery of silver nanoparticles promotes wound healing. *ChemMedChem* 2, 129–136. <https://doi.org/10.1002/cmdc.200600171>
- Timothy, G.R.A.Y., Cziryak, P., Kljuic, A., 2015. No Title. U.S. Patent No., 9, 034,302.
- Tohidi, S., Ghaee, A., Barzin, J., 2016. Preparation and characterization of poly(lactic-

- co-glycolic acid)/chitosan electrospun membrane containing amoxicillin-loaded halloysite nanoclay. *Polym. Adv. Technol.* 27, 1020–1028. <https://doi.org/10.1002/pat.3764>
- Trivedi, V., Nandi, U., Maniruzzaman, M., Coleman, N.J., 2018. Intercalated theophylline-smectite hybrid for pH-mediated delivery. *Drug Deliv. Transl. Reserach* 1–9.
- Tu, J., Cao, Z., Jing, Y., Fan, C., Zhang, C., Liao, L., Liu, L., 2013. Halloysite nanotube nanocomposite hydrogels with tunable mechanical properties and drug release behavior. *Compos. Sci. Technol.* 85, 126–130. <https://doi.org/10.1016/J.COMPSCITECH.2013.06.011>
- Tuba, T., 2018. Antibacterial Clay Compositions for Use as a Topical Ointment. 15/216940.
- Ul-Islam, M., Khan, T., Khattak, W.A., Park, J.K., 2013. Bacterial cellulose-MMTs nanoreinforced composite films: Novel wound dressing material with antibacterial properties. *Cellulose* 20, 589–596. <https://doi.org/10.1007/s10570-012-9849-3>
- Uraloğlu, M., Livaoğlu, M., Agdoğan, Ö., Mungan, S., Alhan, E., Karaçal, N., 2014. An evaluation of five different dressing materials on split-thickness skin graft donor site and full-thickness cutaneous wounds: An experimental study. *Int. Wound J.* 11, 85–92. <https://doi.org/10.1111/j.1742-481X.2012.01071.x>
- USP, 2018. 1724 - Semisolid Drug Products. Performance Tests, in: USP 42 - NF 37 - United States Pharmacopeia and National Formulary. United States Pharmacopeial Convention, Rockville, pp. 1273–84.
- USP42-NF37, 2019. United States Pharmacopeia and National Formulary. United States Pharmacopeial Convention, Rockville, MD.
- Vaiana, C.A., Leonard, M.K., Drummy, L.F., Singh, K.M., Bubulya, A., Vaia, R.A., Naik, R.R., Kadakia, M.P., 2011. Epidermal growth factor: Layered silicate nanocomposites for tissue regeneration. *Biomacromolecules* 12, 3139–3146. <https://doi.org/10.1021/bm200616v>
- Veniale, F., Bettero, A., Jobstainbizer, P., Setti, M., 2007. Thermal muds: Perspectives of innovations. *Appl. Clay Sci.* 36, 141–147. <https://doi.org/10.1016/j.clay.2006.04.013>
- Verma, P., Maheshwari, S., 2019. Applications of silver nanoparticles in diverse sectors. *Int. J. Nanodimensions* 10, 18–36.
- Viseras, C., Aguzzi, C., Cerezo, P., 2015. Medical and health applications of natural mineral nanotubes, in: Pasbakhsh, P., Churchman, G.J. (Eds.), *Natural Mineral Nanotubes: Properties and Applications*. Apple Academic Press, Inc., Oakville, pp. 437–448.
- Viseras, C., Aguzzi, C., Cerezo, P., Bedmar, M.C., 2008. Biopolymer–clay nanocomposites for controlled drug delivery. *Mater. Sci. Technol.* 24, 1020–1026. <https://doi.org/10.1179/174328408X341708>
- Viseras, C., Aguzzi, C., Cerezo, P., López-Galindo, A., 2007. Uses of clay minerals in semisolid health care and therapeutic products. *Appl. Clay Sci.* 36, 37–50.

1.4. Abbreviations

- <https://doi.org/10.1016/j.clay.2006.07.006>
- Viseras, C., Carazo, E., Borrego-Sánchez, A., García-Villén, F., Sánchez-Espejo, R., Cerezo, P., Aguzzi, C., 2019. Clay minerals in skin drug delivery. *Clays Clay Miner.* 67, 59–71. <https://doi.org/10.1007/s42860-018-0003-7>
- Viseras, C., Cerezo, P., Sanchez, R., Salcedo, I., Aguzzi, C., 2010. Current challenges in clay minerals for drug delivery. *Appl. Clay Sci.* 48, 291–295. <https://doi.org/10.1016/j.clay.2010.01.007>
- Viseras, M.-T., Aguzzi, C., Cerezo, P., Cultrone, G., Viseras, C., 2009. Supramolecular structure of 5-aminosalicylic acid/halloysite composites. *J. Microencapsul.* 26, 279–286. <https://doi.org/10.1080/02652040802312499>
- Vogler, E.A., Siedlecki, C.A., 2009. Contact activation of blood-plasma coagulation. *Biomaterials* 30, 1857–69. <https://doi.org/10.1016/j.biomaterials.2008.12.041>
- Wallace, J.L., Wang, R., 2015. Hydrogen sulfide-based therapeutics: Exploiting a unique but ubiquitous gasotransmitter. *Nat. Rev. Drug Discov.* 14, 329–345. <https://doi.org/10.1038/nrd4433>
- Wang, Q., Zhang, J., Wang, A., 2014a. Freeze-drying: A versatile method to overcome re-aggregation and improve dispersion stability of palygorskite for sustained release of ofloxacin. *Appl. Clay Sci.* 87, 7–13. <https://doi.org/10.1016/J.CLAY.2013.11.017>
- Wang, Q., Zhang, J., Zheng, Y., Wang, A., 2014b. Adsorption and release of ofloxacin from acid- and heat-treated halloysite. *Colloids Surfaces B Biointerfaces* 113, 51–58. <https://doi.org/10.1016/J.COLSURFB.2013.08.036>
- Wang, S., Castro, R., An, X., Song, C., Luo, Y., Shen, M., Tomás, H., Zhu, M., Shi, X., 2012. Electrospun laponite-doped poly(lactic-co-glycolic acid) nanofibers for osteogenic differentiation of human mesenchymal stem cells. *J. Mater. Chem.* 22, 23357–23367. <https://doi.org/10.1039/c2jm34249a>
- Wang, S., Yan, C., Zhang, X., Shi, D., Chi, L., Luo, G., Deng, J., 2018. Antimicrobial peptide modification enhances the gene delivery and bactericidal efficiency of gold nanoparticles for accelerating diabetic wound healing. *Biomater. Sci.* 6, 2757–2772. <https://doi.org/10.1039/C8BM00807H>
- Wang, X., Lv, F., Li, T., Han, Y., Yi, Z., Liu, M., Chang, J., Wu, C., 2017. Electrospun Micropatterned Nanocomposites Incorporated with Cu₂S Nanoflowers for Skin Tumor Therapy and Wound Healing. *ACS Nano* 11, 11337–11349. <https://doi.org/10.1021/acsnano.7b05858>
- Wang, Z., Zhao, Y., Luo, Y., Wang, S., Shen, M., Tomás, H., Zhu, M., Shi, X., 2015. Attapulgite-doped electrospun poly(lactic-co-glycolic acid) nanofibers enable enhanced osteogenic differentiation of human mesenchymal stem cells. *RSC Adv.* 5, 2383–2391. <https://doi.org/10.1039/c4ra09839k>
- Williams, L.B., 2017. Geomimicry: harnessing the antibacterial action of clays. *Clay Miner.* 52, 1–24. <https://doi.org/10.1180/claymin.2017.052.1.01>
- Williams, L.B., Haydel, S.E., Giese, R.F., Eberl, D.D., Eberl, D.D., 2008. Chemical and mineralogical characteristics of frenal green clays used for healing. *Clays Clay Miner.* 56, 437–452. <https://doi.org/10.1346/CCMN.2008.0560405>

- Williams, L.B., Holland, M., Eberl, D.D., Brunet, T., Courrsou, L.B. De, 2004. Killer clays! Natural antibacterial clay minerals. *Mineral. Soc. Bull.* 3–8.
- Williams, L.B., Metge, D.W., Eberl, D.D., Harvey, R.W., Turner, A.G., Prapaipong, P., Poret-Peterson, A.T., 2011. What Makes a Natural Clay Antibacterial? *Environ. Sci. Technol.* 45, 3768–3773. <https://doi.org/10.1021/es1040688>
- Wlaschek, M., Singh, K., Sindrilaru, A., Crisan, D., Scharffetter-Kochanek, K., 2019. Iron and iron-dependent reactive oxygen species in the regulation of macrophages and fibroblasts in non-healing chronic wounds. *Free Radic. Biol. Med.* 133, 262–275. <https://doi.org/10.1016/j.FREERADBIOMED.2018.09.036>
- Wu, F., Zheng, J., Li, Z., Liu, M., 2019. Halloysite nanotubes coated 3D printed PLA pattern for guiding human mesenchymal stem cells (hMSCs) orientation. *Chem. Eng. J.* 359, 672–683. <https://doi.org/10.1016/j.CEJ.2018.11.145>
- Wu, J., Ding, S., Chen, J., Zhou, S., Ding, H., 2014. Preparation and drug release properties of chitosan/organomodified palygorskite microspheres. *Int. J. Biol. Macromol.* 68, 107–112. <https://doi.org/10.1016/j.ijbiomac.2014.04.030>
- Wu, L., Lv, G., Liu, M., Wang, D., 2017. Drug release material hosted by natural montmorillonite with proper modification. *Appl. Clay Sci.* 148, 123–130. <https://doi.org/10.1016/j.clay.2017.07.034>
- Wuollett, M., Wuollett, S., 2013. Composition and dressing for wound treatment. CA2848351A1.
- Xia, M., Hu, C., Zhang, H., Xiong, L., Xu, Z., 2003. Effects of tourmaline-treated-water on the growth and the activity of alkaline phosphatase of Caco-2 cell. *Chinese J. Cell Biol.* 27, 222–225.
- Xu, X., Liu, X., Tan, L., Cui, Z., Yang, X., Zhu, S., Li, Z., Yuan, X., Zheng, Y., Yeung, K.W.K., Chu, P.K., Wu, S., 2018. Controlled-temperature photothermal and oxidative bacteria killing and acceleration of wound healing by polydopamine-assisted Au-hydroxyapatite nanorods. *Acta Biomater.* 77, 352–364. <https://doi.org/10.1016/j.ACTBIO.2018.07.030>
- Xue, J., Niu, Y., Gong, M., Shi, R., Chen, D., Zhang, L., Lvov, Y., 2015. Electrospun microfiber membranes embedded with drug-loaded clay nanotubes for sustained antimicrobial protection. *ACS Nano* 9, 1600–1612. <https://doi.org/10.1021/nn506255e>
- Yang, C., Xue, R., Zhang, Q., Yang, S., Liu, P., Chen, L., Wang, K., Zhang, X., Wei, Y., 2017. Nanoclay cross-linked semi-IPN silk sericin/poly(NIPAm/LMSH) nanocomposite hydrogel: An outstanding antibacterial wound dressing. *Mater. Sci. Eng. C* 81, 303–313. <https://doi.org/10.1016/j.MSEC.2017.08.008>
- Yang, G., Zhang, M., Qi, B., Zhu, Z., Yao, J., Yuan, X., Sun, D., 2018. Nanoparticle-Based Strategies and Approaches for the Treatment of Chronic Wounds. *J. Biomater. Tissue Eng.* 8, 455–464. <https://doi.org/10.1166/jbt.2018.1776>
- Yang, J., Wu, Y., Shen, Y., Zhou, C., Li, Y.F., He, R.R., Liu, M., 2016a. Enhanced therapeutic efficacy of doxorubicin for breast cancer using chitosan oligosaccharide-modified halloysite nanotubes. *ACS Appl. Mater. Interfaces* 8, 26578–26590. <https://doi.org/10.1021/acsami.6b09074>

1.4. Abbreviations

- Yang, J.H., Lee, J.H., Ryu, H.J., Elzatahry, A.A., Alothman, Z.A., Choy, J.H., 2016b. Drug-clay nanohybrids as sustained delivery systems. *Appl. Clay Sci.* 130, 20–32. <https://doi.org/10.1016/j.clay.2016.01.021>
- Yang, X., Wei, Q., Shao, H., Jiang, X., 2019. Multivalent aminosaccharide-based gold nanoparticles as narrow-spectrum antibiotics in vivo. *ACS Appl. Mater. Interfaces* 11, 7725–7730. <https://doi.org/10.1021/acsami.8b19658>
- Ye, H., Cheng, J., Yu, K., 2019. In situ reduction of silver nanoparticles by gelatin to obtain porous silver nanoparticle/chitosan composites with enhanced antimicrobial and wound-healing activity. *Int. J. Biol. Macromol.* 121, 633–642. <https://doi.org/10.1016/J.IJBIOMAC.2018.10.056>
- Yendluri, R., Lvov, Y., de Villiers, M.M., Vinokurov, V., Naumenko, E., Tarasova, E., Fakhrullin, R., 2017a. Paclitaxel encapsulated in halloysite clay nanotubes for intestinal and intracellular delivery. *J. Pharm. Sci.* 106, 3131–3139. <https://doi.org/10.1016/J.XPHS.2017.05.034>
- Yendluri, R., Otto, D.P., De Villiers, M.M., Vinokurov, V., Lvov, Y.M., 2017b. Application of halloysite clay nanotubes as a pharmaceutical excipient. *Int. J. Pharm.* 521, 267–273. <https://doi.org/10.1016/j.ijpharm.2017.02.055>
- Yu, L., Shang, X., Chen, H., Xiao, L., Zhu, Y., Fan, J., 2019a. A tightly-bonded and flexible mesoporous zeolite-cotton hybrid hemostat. *Nat. Commun.* 10, 1–9. <https://doi.org/10.1038/s41467-019-09849-9>
- Yu, Y., Li, P., Zhu, C., Ning, N., Zhang, S., Vancso, G.J., 2019b. Multifunctional and Recyclable Photothermally Responsive Cryogels as Efficient Platforms for Wound Healing. *Adv. Funct. Mater.* 1904402. <https://doi.org/10.1002/adfm.201904402>
- Zhang, J.A., Zhang, Z., Zhang, W., 2018. Burn Ointment for Promoting Tissue Regeneration and Skin Growth, and Preparation of Method Therefor. 20180021343.
- Zhang, X., Guo, R., Xu, J., Lan, Y., Jiao, Y., Zhou, C., Zhao, Y., 2015. Poly(l - lactide)/halloysite nanotube electrospun mats as dual-drug delivery systems and their therapeutic efficacy in infected full-thickness burns. *J. Biomater. Appl.* 30, 512–525. <https://doi.org/10.1177/0885328215593837>
- Zhang, Y., Chen, Y., Zhang, H., Zhang, B., Liu, J., 2013. Potent antibacterial activity of a novel silver nanoparticle-halloysite nanotube nanocomposite powder. *J. Inorg. Biochem.* 118, 59–64. <https://doi.org/10.1016/J.JINORGBIO.2012.07.025>
- Zhang, Y., Long, M., Huang, P., Yang, H., Chang, S., Hu, Y., Tang, A., Mao, L., 2017. Intercalated 2D nanoclay for emerging drug delivery in cancer therapy. *Nano Res.* 10, 2633–2643. <https://doi.org/10.1007/s12274-017-1466-x>
- Zhao, L.Z., Zhou, C.H., Wang, J., Tong, D.S., Yu, W.H., Wang, H., 2015. Recent advances in clay mineral-containing nanocomposite hydrogels. *Soft Matter* 11, 9229–9246. <https://doi.org/10.1039/C5SM01277E>
- Zou, Q., Cai, B., Li, Junfeng, Li, Jidong, Li, Y., 2017. In vitro and in vivo evaluation of the chitosan/Tur composite film for wound healing applications. *J. Biomater. Sci. Polym. Ed.* 28, 601–615. <https://doi.org/10.1080/09205063.2017.1289036>



Chapter 2

Layered Clay Minerals in Wound
Healing

2.1. Characterisation of Andalusian Peats for Skin Health Care Formulations

Prólogo

El segundo capítulo de esta tesis se abre con dos trabajos que sentaron las bases de conocimiento experimental aplicado en estudios posteriores de la tesis doctoral e incluye un artículo en el que se caracterizan muestras complejas naturales con arcillas y materia orgánica de interés terapéutico (sección 2.1). A continuación, se incluye un trabajo experimental en el que se desarrolló un sistema de liberación modificada de fármacos basado en el uso de montmorillonita, una arcilla esmectita de tipo laminar, como transportadora de un fármaco de tipo antibiótico, el norfloxacino (sección 2.2). El objetivo fue elaborar un nanocomposite capaz de favorecer la curación de heridas, por lo que tanto la carga como la liberación del fármaco junto con la biocompatibilidad dérmica del sistema fueron evaluadas.

Siguiendo la normativa establecida por la Escuela de Doctorado en Farmacia, se indican los indicios de calidad de las publicaciones científicas que conforman el presente capítulo:

Sección 2.1.

García-Villén, F., Sánchez-Espejo, R., Carazo, E., Borrego-Sánchez, A., Aguzzi, C., Cerezo, P., Viseras, C. **Characterisation of Andalusian peats for skin health care formulations.** Applied Clay Science, 2018, 160, 201–205.

DOI: 10.1016/j.clay.2017.12.017

Indicios de calidad de la publicación:

- Artículo científico
- Indexada en JCR: [APPL CLAY SCI](#)
- Factor de impacto 2019: 4.605
- Ranking: Q1 (mineralogy).

Sección 2.2.

García-Villén, F., Faccendini, A., Aguzzi, C., Cerezo, P., Bonferoni, M.C., Rossi, S., Grisoli, P., Ruggeri, M., Ferrari, F., Sandri, G.; et al. **Montmorillonite-norfloxacin nanocomposite intended for healing of infected wounds.** International Journal of Nanomedicine, 2019, 14, 5051–5060. DOI: 10.2147/IJN.S208713

Indicios de calidad de la publicación:

- Artículo científico
- Indexada en JCR: [INT J NANOMED](#)
- Factor de impacto 2019: 5.115
- Ranking: Q1 (pharmacology & pharmacy).



2.1. Characterisation of Andalusian Peats for Skin Health Care Formulations

Peat pastes are semisolid systems used in medical hydrology and cosmetic treatments on the basis of chemical and physical mechanisms derived from their composition (Dudare and Klavins, 2013; Gomes de Melo et al., 2015). Typical peat pastes applications imply temperatures between 42 and 44 °C for 15–30 min (Flaig, 1992). Peats have demonstrated adsorptive, estrogenic, astringency, antioxidant and revulsive actions (Beer et al., 2000, 2001, 2002, 2003; Suárez et al., 2011). Fungicidal, antibacterial and antiviral properties, UV absorption as well as influences on smooth muscles and prostaglandin synthesis are also been reported (Klöcking and Helbig, 2005; Fioravanti et al., 2007; Sławinska et al., 2007; Khil'ko et al., 2011; Gomes de Melo et al., 2015).

Peats are complex mixtures of organic and inorganic components. Organic fraction comes from vegetable wastes transformed under anaerobic and waterlogged conditions for extended periods and includes humic acids, humin and fulvic acids as principal compounds. Organic compounds have demonstrated biologic activities, which make them potentially useful in topical health care and cosmetology (Summa and Tateo, 1999; Beer et al., 2003). Mineral fraction of peats is composed of clay minerals such as illite and chlorite as well as gypsum, muscovite and quartz (Summa and Tateo, 1999; Romão et al., 2007; Orru et al., 2011). The presence and the type of minerals in peats hugely depend on the deposit location (Summa and Tateo, 1999). Inorganic components, and in particular clay minerals, may greatly influence the technological and biopharmaceutical properties of peats, as for example, stability and rheology of the solid/water systems or bioavailability of the organic actives (Aguzzi et al., 2007; Viseras et al., 2007). Consequently, detailed identification of the mineral phases associated with organic substances in peat deposits must be considered in the design of semisolid health care formulations with these materials.

With these premises, the aims of the present study were i) to characterise three different peat strata from a deposit located in El Padul (Granada), ii) to prepare dispersed systems with the aforementioned strata in

order to determine the technological properties and iii) to study dispersed systems feasibility as potential semisolid health care formulations.

2.1.1. Materials and Methods

2.1.1.1. Materials

Peat samples were extracted from the peatbog “Turbera del Agia” located in El Padul (Granada, Spain). Peat is currently extracted from an area of approximately 20,000m² (Figure 2.1). The actually exploited peat (P2), mainly commercialized as fertilizer, is characterized by deep black chrome and appears as a stratum of approximately 5m thickness, delimited by two other non-commercialized peat strata (P1 and P3). Details of sample position and depth are included in Figure 2.1. Each stratum was separately extracted and hermetically sealed to prevent loss of natural moisture and preserved at room temperature.

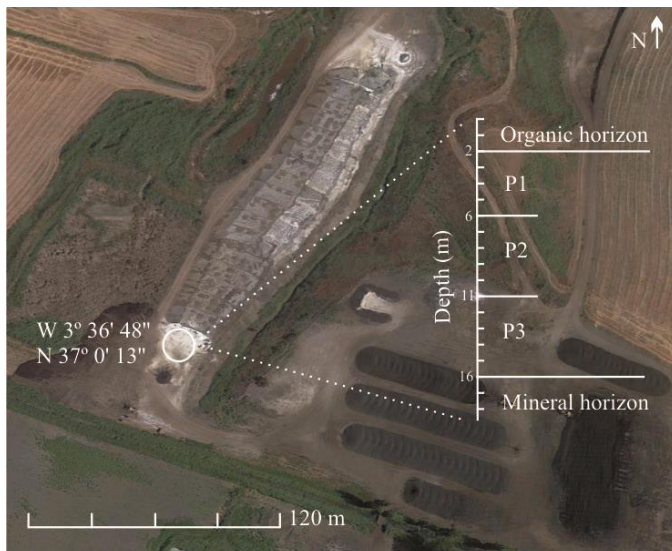


Figure 2.1. Location of sampling position in “Turbera del Agia” and vertical-cross section of the samples (Photo from Google®2017)

2.1.1.2. Methods

X-ray Powder Diffraction

Peat samples were dried at 40 °C for 24 h and grounded previous X-ray powder diffraction analysis (XRPD). Mineralogical study was carried out using a PANalytical X'Pert Pro diffractometer equipped with an X'Celerator solid-state detector and a sample holder spinning. X-ray powder diffraction patterns were recorded using random oriented mounts with CuK α radiation, at 45 kV, 40 mA, in the range 3 to 50 °2 θ . The estimation of the solid composition in crystalline phases was obtained by X'Pert HighScore Plus (PANalytical, 2005). Chemical analysis by X-Ray fluorescence (XRF) was performed using a Bruker® S4 Pioneer equipment working at 60 kV and 150 mA.

Elemental Analysis

Elemental analyses (EAN) were performed in order to determine the content of carbon, hydrogen, nitrogen and sulphur in P1, P2 and P3. These determinations were carried out once samples were dried after 24 h at 40 °C. Elemental analyser used was Thermo Scientific, Flash 2000 model, equipped with a thermal conductivity detector and a precision microbalance (precision 0.01).

Thermal Analysis

Thermogravimetric Analysis (TGA and DTG) of peat samples was carried out by using a Mettler Toledo mod. TGA/DSC1 with FRS5 sensor and a microbalance (precision 0.1 μ g) (Mettler-Toledo GMBH). Samples were heated in air atmosphere at 10 °C/min, in the range of temperature 30–950 °C. All the experiments were run in triplicate.

Preparation of Peat Dispersed Systems

Raw peats and their mixtures in different w/w ratios were dispersed in purified water to obtain a final solid concentration of 60% (w/w) (Table 2.1). The systems were manually homogenized until the disappearance of heavy lumps and then by a high speed agitation of 3000 rpm for 10 min by using a Silverson® L4RT (Silverson Machines, UK). All systems were packed inside hermetic containers and preserved at room temperature.

Table 2.1. Composition of dispersed systems

Dispersed system	S1	S2	S3	S4	S5	S6	S7
Solid phase (60% w/w)	P1	P2	P3	P1:P2 (20:80)	P1:P2 (30:70)	P2:P3 (80:20)	P2:P3 (70:30)

Determination of pH

Values of pH for each peat strata and the aforementioned dispersed systems were determined by using a Crison 25+ pH-meter, equipped with a solid electrode (code 5053T), with a pH tolerance range between 2 and 11.

Rheological Properties

Rheological analysis was carried out by means a viscometer (Thermo Scientific HAAKE, RotoVisco 1; HAAKE RheoWin software) with a plate/plate combination (Plate Ø 20 mm serrated PP20/S sensor) as measuring system. Measurements were carried out at 25 °C (TCP/P, HAAKE unit control temperature system), 90 s of rest time and 0–800 s⁻¹ of shear rate. Six replicates were performed on each sample.

Cooling Kinetics

Cooling curves were obtained following the procedure described by Sánchez-Espejo and co-workers (Sánchez-Espejo et al., 2015). Experimental cooling data were fitted by using the Newton law, describing thermal exchange between two bodies in contact at different temperatures (Eq. 2.1),

$$(T - T_{min}) = (T_{max} - T_{min})e^{-kt} \quad \text{Eq. 2.1}$$

where T_{min} was the room temperature (25 °C), T_{max} was the initial temperature (50 °C), t was the time in minutes and k was a constant that depends on the material and apparatus, given by Eq. 2.2,

$$k = \frac{P}{C} = \frac{P}{mC_p} \quad \text{Eq. 2.2}$$

where P is the instrumental constant of the apparatus, C the heat capacity of the heated material, m the heated mass and C_p the specific heat. The apparatus constant was obtained by fitting of cooling data obtained with a known amount of a reference water dispersion of TiO₂. Experimental thermal parameters of the studied samples were then obtained by using the aforementioned equations.

2.1. Characterisation of Andalusian Peats for Skin Health Care Formulations

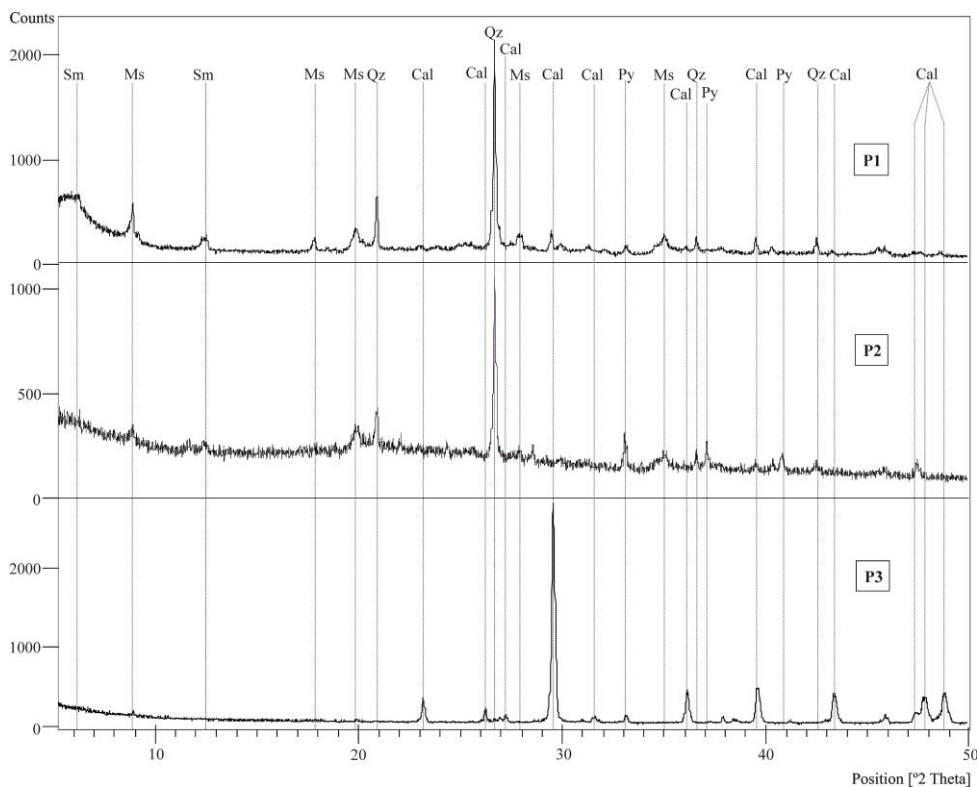


Figure 2.2. X-ray powder diffraction patterns for peat strata. Sm: smectite; Ms: muscovite; Qz: quartz; Cal: calcite; Arg: aragonite; Py: pyrite

2.1.2. Results and Discussion

2.1.2.1. X-ray Powder Diffraction

X-powder diffractograms and X-ray fluorescence results were used to identify the mineral composition of the samples. Main mineral phases in sample P1 were smectites, quartz and mica (Figure 2.2). Other minerals presented were calcium carbonates (calcite and aragonite) as well as pyrite in minor proportion. The studied samples came from a sedimentary basin and the minor presence of pyrite was ascribed to microbial sulphate reduction. The presence of smectites is positive in terms of technological properties due to their swelling and rheological properties in water dispersions (Viseras et al., 2007). Presence of calcium carbonate must be considered in the interpretation of EAN results. Sample P2 contained high amounts of amorphous organic matter, causing a lower crystallinity pattern.

Nevertheless, presence of quartz, mica and pyrite was clearly stated. The presence of pyrite (FeS_2) in higher amount than P1 confirmed its biogenic origin. Sample P3 was mainly constituted by calcium carbonates with absence of quartz, smectites and organic matter.

2.1.2.2. Elemental Analysis

P2 presented high amounts of carbon and nitrogen, clear indicators of its organic composition (Table 2.2). Sulphur content was in agreement with the pyrite presence discussed previously. The C/N ratio is used to measure the degree of decomposition of the organic matter in peat. During the evolution of peat, the organic matter suffers a mineralization process marked by a nitrogen enrichment relative to carbon (Kuhry and Vitt, 1996; Gandois et al., 2013; Biester et al., 2014).

Nitrogen in samples P1 and P3 revealed the presence of minor amounts of organic matter. Sample P3 showed a carbon content higher than expected, in view of its low organic matter content. Microbes responsible for peat decay are more active in more oxygenated and dryer conditions (Scott et al., 2001; Biester et al., 2014). Depth of P2 is higher than P1, causing that the organic matter of P2 suffered higher anoxic and watery conditions, which favoured a slower rate of decay with increasing depths. In sample P3, the high content in carbonates is responsible for the measured C value that distorted the C/N ratio.

Table 2.2. Elemental analysis results for each sample

Stratum	N	C	H	S	C/N
P1	0.12	1.85	1.08	-	15.42
P2	1.01	36.90	4.96	3.72	36.53
P3	0.12	12.95	0.41	-	107.92

2.1.2.3. Thermal Analysis

Figure 2.3 shows TGA results of peat strata studied. Total average weight losses were 46, 92 and 61% (w/w) for P1, P2 and P3, respectively. In P1, loss of hydration and interlayer water (~40% w/w) was mainly ascribed to organic matter and smectite hydration water and occurred at temperatures lower than 130 °C. Dehydroxylation of biotite and organic carbon

2.1. Characterisation of Andalusian Peats for Skin Health Care Formulations

decarboxylation occurred at ~ 500 °C (6% w/w). Final $\sim 1\%$ w/w of weight loss at ~ 885 °C was ascribed to the trioctahedral smectites (the smectite content of this sample based on dehydroxylation was $\sim 20\%$ w/w). P2 showed intense weight loss due to hydration of the organic matter (75% w/w). Then, oxidative pyrolysis and subsequent carbonization in the interval 260–340 °C accounted for a 17% w/w of the total weight loss. This second interval included thermal degradation of organic compounds typically present in peats, including hemicellulose, cellulose and lignine derivatives such as humic and fulvic acids (Schnitzer and Hoffman, 1965; Aho et al., 1989; Romão et al., 2007). P3 presented a first weight loss corresponding to hydration water (the samples were assayed without any previous drying). Once dried, the TGA curve of P3 solely corresponded to typical thermal decomposition of carbonates ($\sim 20\%$ w/w; ~ 800 °C).

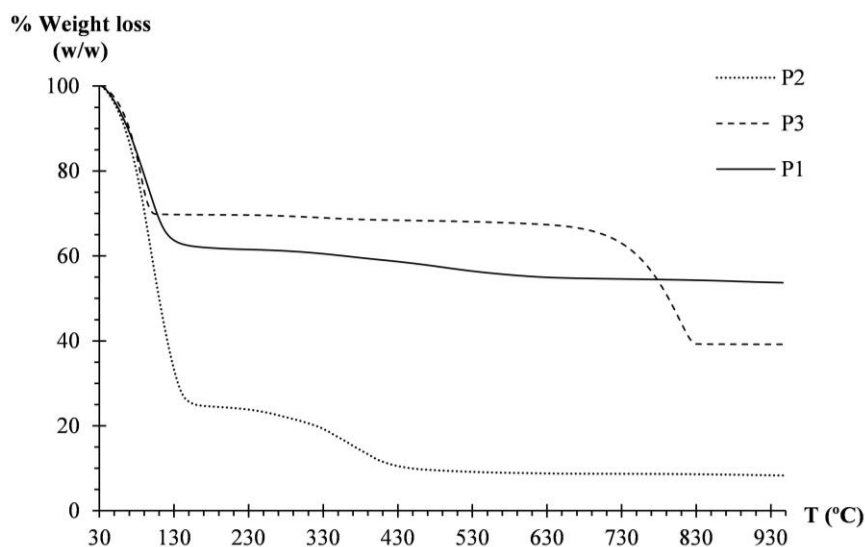


Figure 2.3. Thermogravimetric curves of the peats

2.1.2.4. pH

Values of pH of the raw samples and the dispersed systems in purified water are shown in Table 2.3. The measured pH of distilled water was 5.50 (± 0.012). pHs of the pure samples (P1–P3) were not physiologically adequate, as none of them were in the optimal tolerated interval (4.5–6.0)

required for skin formulations (Pons Gimier and Parra Juez, 1995; Sánchez-Espejo et al., 2014). P1 and P3 showed very similar pH values, proximal to neutrality. On the other hand, stratum P2 presented acidic character due to the presence of humic substances. Particularly, the basic nature of P3 stratum is justified by the presence of carbonate minerals, previously identified by XRPD and TGA analyses.

Table 2.3. pH values of natural peat strata (P1-P3) and dispersed systems (S1-S7)

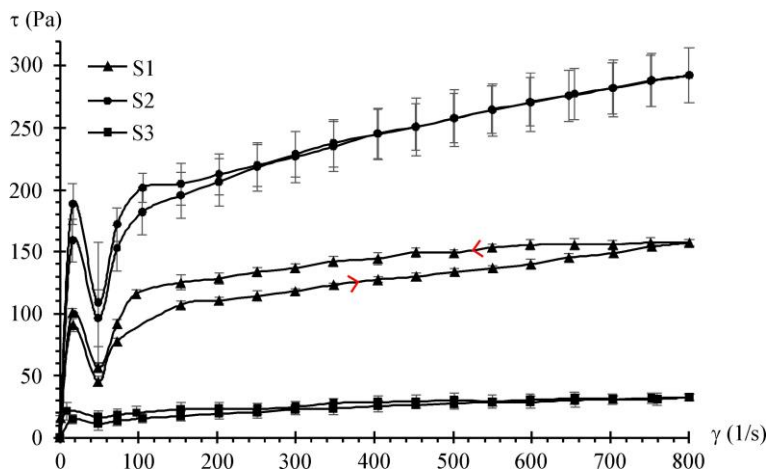
	pH \pm s.e.; n=8
P1	7.29 \pm 0.053
P2	3.10 \pm 0.114
P3	7.82 \pm 0.059
S1	7.62 \pm 0.030
S2	5.03 \pm 0.023
S3	7.76 \pm 0.017
S4	5.62 \pm 0.013
S5	5.23 \pm 0.061
S6	6.22 \pm 0.017
S7	5.91 \pm 0.038

Dispersed systems S1 and S3 showed non-significant changes in pH values compared to the pH of the corresponding peat strata used for their preparation (P1 and P3), probably due to the presence of carbonates acting as buffers. On the other hand, S2 experimented an increase of two units in the pH value compared to that of P2 stratum. Suspensions from S4 to S7 showed acidic pH values since in all of them, stratum P2 prevailed as the main ingredient. Dispersed systems S4 and S5, which contain strata P1 and P2, showed pH values between those of S1 and S2 due to the mixture of the strata. The presence of P3 stratum in systems S6 and S7 could be noted by a slight increase on pH values (\sim 6) ascribable to the amphoteric nature of carbonate minerals.

S1, S3 and S6 showed pH values which were above the tolerance range of the skin (4.5–6). Dispersions S2, S4, S5 and S7 possessed pH values that could allow their topical application in terms of pH tolerability. In particular, pH of S2 and S5 were closer to the most healthy human skin pH (approximately 4.7) which favours the skin microflora (Lambers et al., 2006) and prevents the growth of pathogenic bacteria (Fluhr and Elias, 2002).

2.1.2.5. Rheological Properties

The studied dispersed systems showed non-Newtonian viscoplastic flow curves with spur points at low shear stress values (S2 showed very high viscosity and yield stress values, as a result of the interconnections between the lignin and other organic fibres (Hendry et al., 2012). These values could make difficult spreading of S2 suspension over the skin surface. On the other hand, S3 did not show suitable viscosity and yield values to ensure the permanence of the product during application. Intermediate behaviour was observed in the case of S1. In comparison with S2, viscosity and yield stress values decreased by mixing P1 and P2 strata (samples S4 and S5). In the case of S5, containing higher amount of P1, values were very similar to those observed for S1. Dispersed systems S6 and S7 (composed of P2 and P3 stratum) presented the lowest viscosities and yield points due to the influence of P3 stratum.



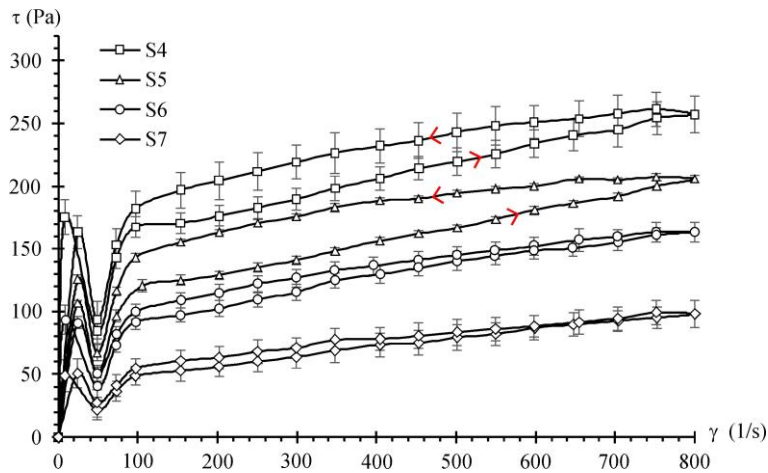


Figure 2.4). This behaviour has been described for high concentrated suspensions used in pelotherapy (Aguzzi et al., 2013). S1 exhibited rheopectic behaviour, ascribable to the smectitic content of P1 stratum. Smectite suspensions are often thixotropic (shear thinning), although rare cases of rheopectic (shear thickening) behaviour have also been reported (Abu-Jdayil, 2011). S2 and S3 did not show any hysteresis areas, according to the absence of clay minerals in their compositions.

The influence exerted by stratum P1 was noticeable in systems S4 and S5, showing rheopectic behaviour. In these dispersions, although P2 was the main ingredient, clear hysteresis areas were observed.

Apparent viscosities and the yield values of the systems are shown in Table 2.4. Viscosity was calculated at a shear value (250s^{-1}) representative of the stress produced by skin spreading during application (Schott, 1995). Yield stresses were obtained according to the experimental spur points (Barry, 1974) and represent the shear stress necessary to break particle attractions in the dispersed systems.

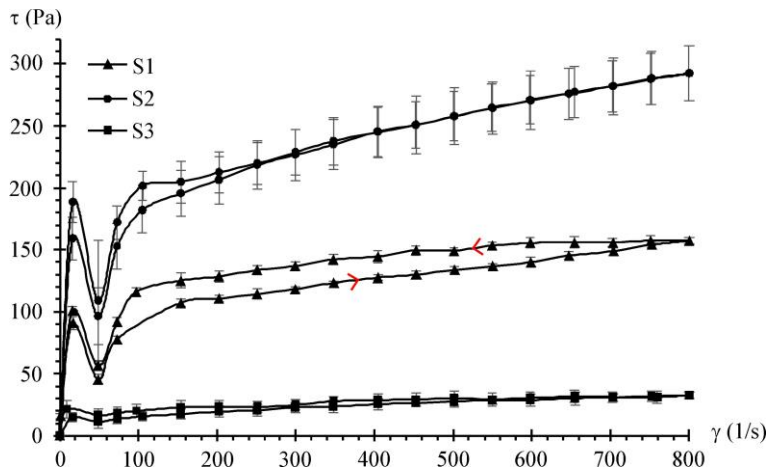
Table 2.4. Apparent viscosities (250 s^{-1} ; $25\text{ }^{\circ}\text{C}$) and yield values of the samples (mean values \pm s.d.; $n = 6$)

	Viscosity (Pa·s)	Yield value (Pa)
S1	0.46 ± 0.016	90.83 ± 5.000
S2	0.88 ± 0.068	188.50 ± 14.164
S3	0.09 ± 0.020	14.79 ± 3.809
S4	0.74 ± 0.013	175.18 ± 13.907

2.1. Characterisation of Andalusian Peats for Skin Health Care Formulations

S5	0.54 ± 0.017	106.77 ± 2.600
S6	0.44 ± 0.022	93.59 ± 11.816
S7	0.24 ± 0.034	46.00 ± 11.599

S2 showed very high viscosity and yield stress values, as a result of the interconnections between the lignin and other organic fibres (Hendry et al., 2012). These values could make difficult spreading of S2 suspension over the skin surface. On the other hand, S3 did not show suitable viscosity and yield values to ensure the permanence of the product during application. Intermediate behaviour was observed in the case of S1. In comparison with S2, viscosity and yield stress values decreased by mixing P1 and P2 strata (samples S4 and S5). In the case of S5, containing higher amount of P1, values were very similar to those observed for S1. Dispersed systems S6 and S7 (composed of P2 and P3 stratum) presented the lowest viscosities and yield points due to the influence of P3 stratum.



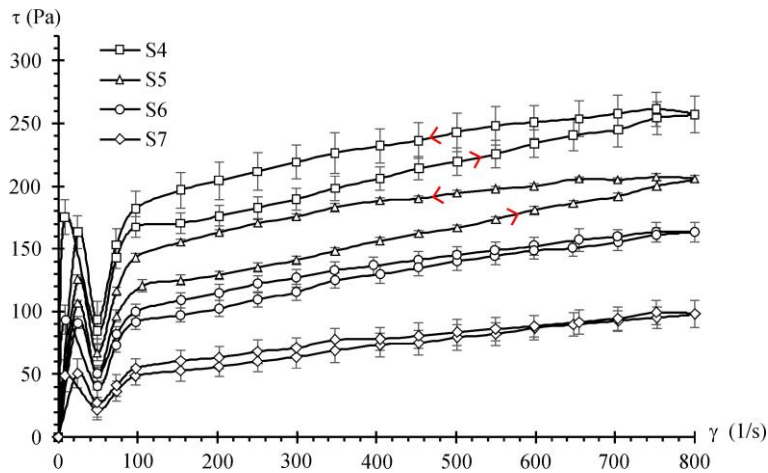


Figure 2.4. Flow curves (shear stress (τ) versus shear flow (γ)) of the dispersed systems (mean values \pm s.d.; $n = 6$)

2.1.2.6. Cooling Kinetics

Results of cooling kinetic studies are shown in Table 2.5. Linear regression of Eq. 2.1 was used to calculate the time required for each dispersed system to achieve 32 °C (t_{32}) and the temperature after 20 min (T_{20}), which is within the time range for traditional peat pastes application. Experimental specific heats (C_p) are homogeneous and similar to other systems used in pelotherapy (Sánchez-Espejo et al., 2014). In all samples, the temperature after 20 min (T_{20}), were around 36 °C and t_{32} values were around 30 min. These values assured heat transfer during the normal application of peat pastes, which corresponds to treatments of 15–30 min with a paste temperature around 42–44 °C. The homogeneity of the values in Table 2.5, despite the compositional differences of samples, confirmed that thermal behaviour of peat pastes mainly depends on water content, as previously observed (Sánchez-Espejo et al., 2015).

Table 2.5. Thermal studies: experimental specific heats (C_p), temperature after 20 min (T_{20}) and time until reaching 32 °C (t_{32})

	$C_p(\text{J/g}\cdot\text{K}) \pm \text{s.d. (n=3)}$	$T_{20}(\text{°C}) \pm \text{s.d. (n=3)}$	$t_{32}(\text{min}) \pm \text{s.d. (n=3)}$
S1	3.05 ± 0.048	35 ± 1.0	29 ± 1.3
S2	3.26 ± 0.087	36 ± 1.2	30 ± 1.2
S3	3.04 ± 0.065	35 ± 1.0	28 ± 1.1
S4	3.12 ± 0.029	36 ± 1.2	30 ± 1.3

2.1. Characterisation of Andalusian Peats for Skin Health Care Formulations

S5	3.31 ± 0.023	36 ± 0.9	31 ± 1.1
S6	3.86 ± 0.045	36 ± 0.8	32 ± 0.9
S7	3.81 ± 0.075	36 ± 1.1	33 ± 0.9

2.1.3. Conclusions

Composition and properties of three different peat strata from “El Padul” peatbog greatly vary, making necessary their combination to formulate health care peat pastes with adequate features. Stratum P2 should always be present in the systems since it possessed the highest amount of organic matter, which are responsible for therapeutic effects of peat pastes. The addition of P1 allowed to control final pH and to modify rheological properties, although the addition of P3 stratum produced an undesirable decrease in viscosity. On the other hand, dispersed systems S2 and S4 possessed proper viscosities for topical applications, similar to pelotherapy formulations previously studied (Aguzzi et al., 2013). Thermal behaviours of dispersed systems greatly depended on water content and, in all cases, the results showed that heat transfer during peat paste treatment was assured.

2.2. Montmorillonite-Norfloxacin Nanocomposite Intended for Healing of Infected Wounds

Wound repair is a complex and tightly regulated physiological process: different cell types, including immune cells, are involved. Wound healing includes homeostasis stage (clotting and immune activation), inflammation (recruitment of neutrophils and macrophages, production of cytokine and growth factor), proliferation phase, tissue neoformation (re-epithelialization, angiogenesis and granulation) and subsequent remodelling of neoformed-tissue (Mofazzal Jahromi et al., 2018). Considering the crucial barrier role of the skin, non-healing wounds (such as venous leg ulcers, diabetic foot ulcers, arterial insufficiency and pressure ulcers) and burns impose substantial morbidity and mortality, deeply affecting the quality of life with high economic burden (Stejskalová and Almquist, 2017). Severe cutaneous wounds represent a major issue in medical care, with approximately 300 million chronic and 100 million traumatic wound patients worldwide. Moreover, chronic wounds affect roughly 37 million of patients globally. Only in the USA in 2017 (Lim et al., 2017), the skin wounds led to an estimated direct health care cost of \$75 billion and an indirect cost of \$11 billion. The population aging is likely to dramatically increase the incidence of chronic wounds due to the rising prevalence of type 2 diabetes, peripheral vascular disease and metabolic syndrome. In addition, surgery, more common in the elder population, could cause risk of wound complication, especially in patients affected by diabetes. While acute wounds generally heal without significant interventions, chronic wounds are challenging and are characterized by an intrinsic inability to heal. The presence of microbial contamination occurring at wound bed significantly and deeply alter the normal recovery phases, leading to a possible impairment of the healing path and finally to non-healing wounds. Moreover, among skin wounds, burns require special attention because they are often prone to infections and to abnormal scarring (Mofazzal Jahromi et al., 2018).

The employment of antimicrobial agents, particularly antibiotics, in the treatment of non-healing wounds is particularly controversial due to the possible rising of resistance. However, the nanoparticle-based approach, creating anti-microbial nanotherapeutics, seems a valid option to eliminate

bacterial infections, avoiding antimicrobial resistance. In fact, it is reported that nanomaterials interact with bacteria and microorganisms upon multiple interactions such as electrostatic attraction, hydrophobic and Van der Waals forces through surface interactions. Moreover, the physicochemical properties of nanomaterials allow multiple pathways to interact with microorganisms, and this makes them promising candidates to achieve enhanced therapeutic efficacy against multidrug-resistant infections (Gupta et al., 2019). In literature, different therapeutic approaches based on nanostructures and several types of nanomaterials (including electrospun nanofibers, hydrogel, showed improved antibacterial properties) are reported (Han et al., 2017; Ding et al., 2018; Gao et al., 2019; Lv et al., 2019; Sun et al., 2019). These systems are generally polymer-based and prepared with high energy and sophisticated processes.

Recently, the studies focused on nanocomposites based on clay minerals and drugs and/or biopolymers evidence the capability of these to interact with biological structures and open opportunities for tissue engineering and in particular for wound healing. Nanocomposites are prepared with simple procedures (spontaneous absorption of organic moieties into/onto clay following the mixture of the components in solution) easy to scale up. Moreover, the various characteristics of clay minerals in terms of the composition may offer a range of possibilities to develop systems able to facilitate both antimicrobial activity of loaded antibacterial drugs, mainly due to the capability to decrease water activity (Sandri et al., 2014; Naumenko et al., 2016; Bramhill et al., 2017) and cell adhesion, proliferation and neotissue formation (Sandri et al., 2016, 2017).

Given this premise, the aim of this study is to design and develop nanocomposite based on montmorillonite (VHS, clay mineral) and norfloxacin (NF, antimicrobial drug) as a powder for cutaneous application intended for the treatment of infected wounds to enhance their healing. NF is a synthetic antibacterial fluoroquinolone, active against a broad spectrum of Gram-positive and Gram-negative aerobic bacteria. Its mechanism of action consists in the inhibition of DNA gyrase enzyme causing an interruption of deoxyribonucleic acid synthesis (Wiles et al., 2010). In the literature, it is proposed as a prophylactic drug in wound healing, sometimes as a

component of scaffolds and wound dressings (Nakamura et al., 1993; Malipeddi et al., 2006; Mpharm et al., 2010; Wiles et al., 2010). A NF-montmorillonite nanocomposite was prepared by means of intercalation technique in order to obtain a powder characterized by means of adsorption isotherm and solid-state, drug loading capacity and release and antimicrobial properties (Nakamura et al., 1993; Malipeddi et al., 2006; Mpharm et al., 2010; Tian et al., 2013; Galperin et al., 2015; Mahmoud and Salama, 2016; Rusanu et al., 2017).

2.2.1. Materials and Methods

2.2.1.1. Materials

NF (Sigma Aldrich-Merck, Italy) and a pharmaceutical grade montmorillonite (VHS) (Veegum[®] HS, Vanderbilt, USA) were used. VHS was dried in oven (approximately 40 °C) for at least 48h prior to be used.

2.2.1.2. Methods

Clay-Drug Adsorption Isotherm

The intercalation solution technique has been chosen as the methodology to study the adsorption of NF onto VHS. Firstly, a fixed amount of clay mineral (100 mg) was dispersed into 5 mL of a glacial acetic acid/water (1:1) to achieve the dissolution of NF (initial concentrations of drug (C_0) ranging from $5 \cdot 10^{-5}$ to $1 \cdot 10^{-2}$ M). These dispersions were protected from light, stirred (150 rpm) in a thermostatic bath (25 ± 1 °C) for 24h and subsequently centrifuged (9000 rpm, 45 min) in order to separate the solid phase, containing the nanocomposite (VHS-NF). At this point, the equilibrium concentration of NF in the supernatant (C_e) was determined at 273 nm by UV spectroscopy (UV-Vis spectrophotometer Lambda 25, Perkin Elmer, Italy). It was assumed that the difference between C_0 and C_e corresponded to the amount of NF adsorbed onto VHS and the amount of drug retained per gram of clay was calculated. The obtained results were mathematically fitted (TableCurve 2D, Systat Software Inc., UK) to obtain the monolayer adsorption capacity of the clay and the adsorption rate constant, according to a mechanist model able to describe the adsorption of drug molecules onto solid inorganic surfaces

(Nakamura et al., 1993; Malipeddi et al., 2006; Viseras et al., 2008a; Wiles et al., 2010; Mpharm et al., 2010; Tian et al., 2013; Galperin et al., 2015; Sandri et al., 2017; Mahmoud and Salama, 2016; Sandri et al., 2016; Carazo et al., 2017, 2018; Rusanu et al., 2017).

Solid State Characterization

X-ray powder diffraction (XRPD) analysis was carried out using a diffractometer (X'Pert Pro model, Malvern Panalytical) equipped with a solid-state detector (X'Celerator) and a spinning sample holder. The diffractogram patterns were recorded using random oriented mounts with $\text{CuK}\alpha$ radiation, operating at 45 kV and 40 mA, in the range $4\text{--}60^\circ 2\theta$. Fourier-transform infrared spectroscopy (FT-IR) spectra of the powdery samples were obtained with a JASCO 6200 apparatus equipped with a Ge ATR. All analyses were performed from 400 to $4,000\text{ cm}^{-1}$ with a resolution of 2 cm^{-1} , and results processed with Spectra Manager v2 software.

Thermogravimetric analysis (TGA) (mod. TGA-50H, Shimadzu) was performed using a vertical oven and a precision of 0.001 mg. Approximately 40 mg of each sample were weighted in aluminium sample pans. The experiments were performed in $30\text{--}950^\circ\text{C}$ range, atmospheric air and a heating rate of $10^\circ\text{C}/\text{min}$. Additionally, differential scanning calorimetry (DSC) analyses were done in a Mettler Toledo and using aluminium crucibles. The temperature range was defined between 30°C and 400°C at a heating rate of $10^\circ\text{C}/\text{min}$. All the analyses were done in atmospheric air.

Measurements of zeta potential (ζ) of both the clay and the nanocomposite were performed in an aqueous solution with a concentration 0.05% w/V by using a Zetasizer Nano ZS90 apparatus (Malvern Panalytical, USA). High-Resolution Transmission Electron Microscopy (HRTEM) was performed by means of a FEI Titan G2 60–300 high-resolution transmission electron microscope coupled with analytical electron microscopy (AEM) performed with a SUPER-X silicon-drift windowless energy-dispersive X-ray spectroscopy detector. AEM spectra were saved in mode scanning transmission electron microscopy with a high-angle annular dark field detector. X-ray chemical element maps were also collected. The samples were

directly deposited onto copper grids (300 mesh coated by formvar/carbon film, Agar Scientific).

Drug Release

NF released from nanocomposite and NF-free drug dissolution were assessed by means of HPLC-UV/DAD apparatus (PerkinElmer Series 200) using as stationary phase Zorbax Eclipse XDB-C8 column (4.6 mm x 150 mm, silica particle size 5 μm) at 25 °C, as mobile phase 7:15:78 (% v/v) acetonitrile/methanol/citric acid (0.4 M), fluxed at 1 mL/min (time of analysis 15 min). The quantification was assessed at 275 nm, as maximum absorption wavelength (Mahmoud and Salama, 2016). The method was linear in the range of 200–1 $\mu\text{g/mL}$ with R^2 higher than 0.995.

An exact amount of nanocomposite or free drug was dispersed in 3 mL of saline solution (NaCl 0.9% w/v). At prefixed times, 500 μL of dissolution medium was collected and the total volume replaced. Each sample was filtered (HA 0.22 μm , Millipore) before HPLC analysis.

Antibacterial Activity Measurements

The antimicrobial activity of nanocomposite compared to NF as a free drug was evaluated against the bacteria strains *Staphylococcus aureus* ATCC 6538 and *Pseudomonas aeruginosa* ATCC 15442. In particular, killing time was determined as the exposure time required to kill a standardized microbial inoculum (Samanidou et al., 2003). Bacteria used for killing time evaluation were grown overnight in Tryptone Soya Broth (Oxoid; Basingstoke) at 37 °C. The bacteria cultures were centrifuged at 2,000 rpm for 20 min to separate cells from broth and then suspended in PBS (pH 7.3). The suspension was diluted to adjust the number of cells to $1 \cdot 10^7$ – $1 \cdot 10^8$ CFU/mL.

An exact amount of nanocomposite VHS-NF or NF was added to the microorganism suspensions to obtain 5 $\mu\text{g/mL}$ NF concentrations. For each microorganism, a suspension was prepared in PBS without drug and used as control. Bacterial suspensions were incubated at 37 °C. Viable microbial counts were evaluated after contact for 0.5 and 24 h with the samples and microorganism suspensions grown in the same conditions and used as control. The bacterial colonies were enumerated in Tryptone Soya Agar (Oxoid; Basingstoke) after incubation at 37 °C for 24 h. The microbiocidal

effect value was calculated for each test organisms and contact times according to the following equation (Rossi et al., 2007),

$$ME = \log N_c - \log N_d \quad \text{Eq. 2.3}$$

where N_c is the number of CFU of the control microbial suspension and N_d is the number of CFU of the microbial suspension in presence of drug.

In Vitro Biocompatibility: Fibroblasts

Biocompatibility (cytotoxicity) was evaluated using fibroblasts (normal human dermal fibroblasts, from juvenile foreskin from 2 to 5 passages, PromoCell, WVR, Italy).

Fibroblasts were grown in DMEM (Lonza, I), 10% v/v (FBS (EuroClone, Italy) and penicillin/streptomycin solution (pen/strep, 100 UI/100 $\mu\text{m}/\text{mL}$, Sigma Aldrich-Merck, Italy).

VHS (1.2 mg/mL), NF (0.1 mg/mL) and VHS-NF (VHS: 1.2 mg/mL and NF 0.1 mg/mL) were suspended/ solubilized in cell culture medium and put in contact with the cells in suspension just after cell seeding in 96-well plate at seeding density of 35,000 cells/well. Fibroblasts were grown for 2 days. Fibroblast growth on tissue culture plastic was considered as standard growth (control).

At prefixed end point, cell growth was assessed by means of MTT test. Briefly, the medium was removed and 50 μL of MTT solution (Sigma Aldrich, Italy) at 2.5 mg/mL concentration in Hank's Buffered Salt Solution pH 7.4 was added to cover each scaffold for 3 h. Subsequently, MTT solution was removed from each well, and the substrates were washed with 200 μL of PBS. After the removal of PBS, 100 μL of DMSO was put in each well, and the absorbance was assayed at 570 nm by means of an ELISA plate reader (Imark Absorbance Reader, Biorad, Italy), with a reference wavelength of 690 nm. Cell viability was expressed as optical density (OD).

Statistical Analysis

Statistical differences were evaluated by means of Mann-Whitney (Wilcoxon) W test (Statgraphics Centurion XV, Statistical Graphics Corporation, MD, USA). Differences were considered significant at $p < 0.05$, and each significant p-value is reported in the captions.

2.2.2. Results and Discussion

2.2.2.1. Clay-Drug Adsorption Isotherm

Equilibrium adsorption isotherm is shown in Figure 2.5, where experimental points are plotted as n^s (moles of NF retained per gram of VHS) versus C_e (mol/L). The kinetic model used to fit the adsorption data is expressed by Eq. 2.4 (Table 2.6), which describes drug adsorption as one single process. Montmorillonite is a phyllosilicate based on two tetrahedral sheets of silica sandwiching a central octahedral sheet of alumina spaced out interlayer spaces (galleries). On this basis, protonated NF molecules interact to the active sites of VHS located at edges and within interlayer space of montmorillonite, thus forming a drug monolayer onto the clay mineral interlayer surface (Viseras et al., 2008b). Figure 2.5 shows that the obtained theoretical curve satisfactorily described the experimental points, as confirmed by the calculated correlation coefficient ($R^2 > 0.99$, Table 2.6). Additionally, the relatively high value of kinetic equilibrium constant (k) (Table 2.6) can be ascribed to great stability of the resultant VHS-NF system.

Table 2.6. Fitting equation and parameters for the adsorption of NF onto VHS. n^s : mol of NF per gram of VHS (mol/g); n^s_m : monolayer retention capacity (mol/g); C : equilibrium concentration (mol/L); k : kinetic equilibrium constant (mean values \pm s.d.; $n=3$)

Eq. 2.4	R^2	n^s_m	k
$n^s = \frac{k \cdot n^s_m \cdot C}{k \cdot C + 1}$	0.9959	0.0007 ± 0.00002	130.4 ± 0.43

2.2.2.2. Solid State Characterization

X-ray diffractogram patterns of the nanohybrid and pristine components are plotted in Figure 2.6. VHS diffractogram shows reflections ascribable to a highly pure homoionic Na montmorillonite, as previously described. (Nakamura et al., 1993; Aguzzi et al., 2014; Borrego-Sánchez et al., 2017; Carazo et al., 2018).

2.2. Montmorillonite-Norfloxacin Nanocomposite Intended for Healing of Infected Wounds

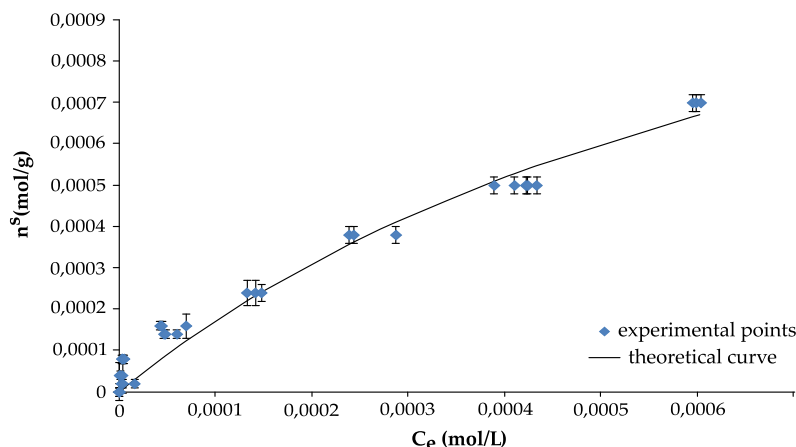


Figure 2.5. Equilibrium adsorption isotherm of NF and VHS (mean values \pm s.d.; $n=3$)

In particular, VHS shows d001 basal reflection at $7.5^\circ 2\theta$, which indicates an interlayer space of 12 \AA according to Bragg's law. These results are consistent with the literature (Tunç and Duman, 2010; Carazo et al., 2018). Diffractogram of VHS-NF also shows typical reflections of montmorillonite with the exception of the basal reflection d001, which shifts to lower 2θ values ($5.94^\circ 2\theta$) in comparison with the pristine clay mineral. The corresponding interlayer space is expanded ($\approx 15 \text{ \AA}$), indicating the presence of NF molecules adsorbed into clay mineral structure. Moreover, this new basal reflection turns to be sharper and more intense in comparison with VHS basal reflection, which is an indicator of a highly ordered VHS-NF nanohybrid structure. Diffractogram of NF has been found to be a combination of both anhydrous and sesquihydrate forms (Figure 2.6) (Katdare et al., 1986; Mazuel, 1991; Puigjaner et al., 2010). Nonetheless, any of these reflections are observed in VHS-NF diffraction pattern, indicating the absence of crystalline drug on the nanohybrid surface. The XRPD analysis suggests that the nanocomposite is characterized by NF intercalation into the VHS galleries.

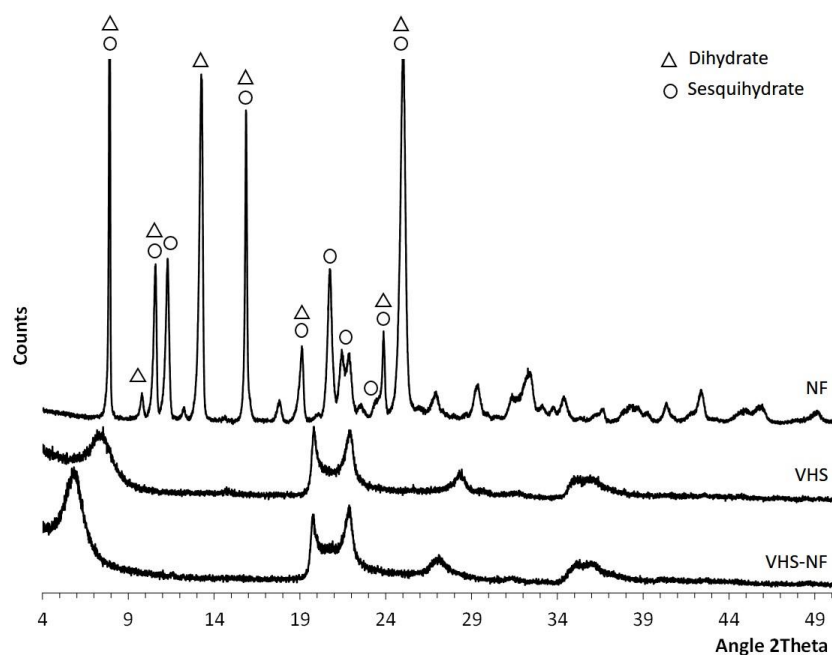


Figure 2.6. XRPD diffraction patterns of NF, VHS and VHS-NF

Figure 2.7 reports the FT-IR spectra of VHS-NF in comparison to NF and VHS. The infrared spectrum of NF shows typical bands of a hydrated form of NF. In particular, the broad bands between $3,600$ and $3,250$ cm^{-1} belong to hydration water stretching (O-H stretching vibration, at about 3404 cm^{-1}) together with N-H vibrations of the piperazine ring. The vibration of methyl group, methylene of ethyl side chain and piperazine groups determine multiple and more defined bands in $3,070$ – $2,500$ cm^{-1} . A shoulder at $2,500$ cm^{-1} is attributable to hydrogen bonded O-H groups, and this also confirms the hydrate state of NF. Band detected at $1,728$ cm^{-1} belongs to the C=O stretch of the carboxylic acid (Barry et al., 1984; Mazuel, 1991; Földvári, 2011). The first and intense band in the fingerprint region belongs to NF quinolone ring vibration located between $1,600$ and $1,650$ cm^{-1} (Mazuel, 1991). The vibrations of C=C of the aromatic ring are also located in this area ($1,400$ – $1,600$ cm^{-1}). Moreover, the band at $1,030$ cm^{-1} is attributable to C-F vibration (Földvári, 2011). Regarding VHS, vibrational band at $3,622$ cm^{-1} belongs to octahedral layer-OH groups (Al-OH-Al, Al-OH-Mg and Mg-OH-Mg vibrations) typical of clay minerals. Moreover, the broad band around $3,400$ cm^{-1} are due to the stretching of OH from hydration H_2O molecules located in the interlayer

space of VHS. Moreover, H₂O molecules coordinated to the VHS exchangeable cations create a band at 1,632 cm⁻¹. The most intense band of the VHS spectrum, located at 985 cm⁻¹, is due to Si-O-Si in-plane vibration for layered silicates. Out-of-plane Si-O-Si stretching is responsible for the shoulder appearing at 1,100 cm⁻¹. On the other hand, the overlapped band at 914 cm⁻¹ is related to Si-O-Al stretching mode, while bending vibration of Si-O-Al occurs at 512 cm⁻¹ (Aguzzi et al., 2014; Borrego-Sánchez et al., 2017; Baptista et al., 2018; Carazo et al., 2018).

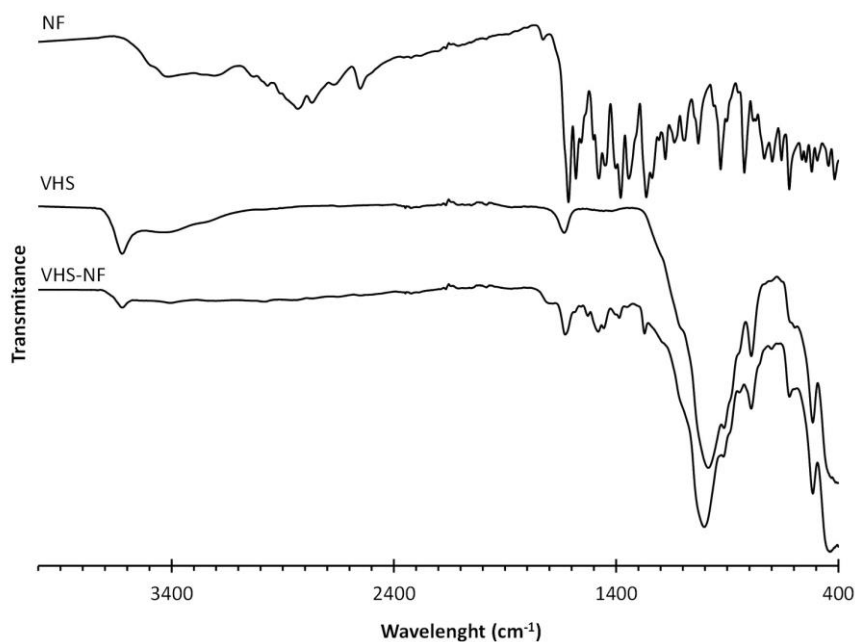


Figure 2.7. FT-IR spectra of NF, VHS and VHS-NF

Vibrational bands of the octahedral Al-OH-Al, Al-OH-Mg and Mg-OH-Mg are also present in the VHS-NF. The adsorption of NF in the VHS interlayer space produces a displacement of the hydrated exchangeable cations, thus reducing the intensity of the H₂O band around 3,400 cm⁻¹ (Földvári, 2011). Moreover, the presence of the drug in the nanohybrid can be identified by its typical vibrational bands located between 1,760 and 1,200 cm⁻¹, all of them coinciding with the NF spectrum. Particularly, the band at 1,702 cm⁻¹ belongs to C=O of the carboxylic acid of NF. From 1,200 cm⁻¹ onwards, the intense vibrations of the clay mineral obscure the NF bands in

the same region. Nonetheless, the bands in 3,070–2,500 cm^{-1} range, which correspond to N-H and CH_2 of the drug, are not visible in the VHS-NF spectrum. This disappearance can be related to the stiffening of the corresponding functional group due to the position of adsorbed NF molecules in the interlayer space of VHS.

The TGA analysis of NF showed total drug decomposition before 630 °C (Figure 2.8 – high panel). The first weight loss gradually occurs in the temperature range from 30 to 196 °C, with an inflection point at 100 °C. This step is due to the evaporation of water and corresponds to the first endothermic event of the corresponding DSC curve (Figure 2.8 – low panel). Nonetheless, the presence of an inflection point could be related to different types of crystallization water. In fact, different hydrated forms of NF have been reported in literature, such as dihydrate and sesquihydrate, among others (Kumar et al., 2018). In particular, water evaporation of NF dihydrate form is described as a two different step process although this is not visible in DSC profile and on the contrary it is evident in TGA profile (Kumar et al., 2018). These results are related to the presence of both dihydrate and sesquihydrate forms (as confirmed by XRPD diffraction peaks) having overlapped steps of H_2O molecule evaporation in DSC. The sharp and intense endothermic peak located at 227 °C (T onset 218 °C) corresponds to NF melting point, confirmed by the absence of weight loss in the TGA curve of NF. Decomposition of the drug starts at 300 °C according to TGA profile and three overlapped steps (inflection point at ~370 °C and ~500 °C) are attributable to the loss of different functional groups of the NF molecule ($6\text{C}_2\text{H}_2+3\text{NO}+\text{HF}+1/2\text{H}_2$) (Kumar et al., 2018) and/or gaseous products (Norrby and Jonsson, 1983). By the same token, DSC thermogram (low panel) shows an exothermic event at 370 °C, and this is in coincidence of the first inflection point of the TGA corresponding to NF decomposition.

TGA thermogram of VHS (Figure 2.8 – high panel) shows a first slight weight loss of 2% (w/w), which corresponds to a small amount of hydration water. Moreover, a typical clay mineral dehydroxylation step (Wang et al., 2012) is present with an onset at about 600 °C and an offset at 720 °C, accounting 3% (w/w) weight loss. From 800 °C onwards, there is no signal that could be related to VHS impurity decomposition (such as quartz, mullite,

corderite, cristobalite) (Wang et al., 2012), to confirm its high purity. DSC thermogram of VHS confirms its stability in the temperature range evaluated (Figure 2.8 – low panel).

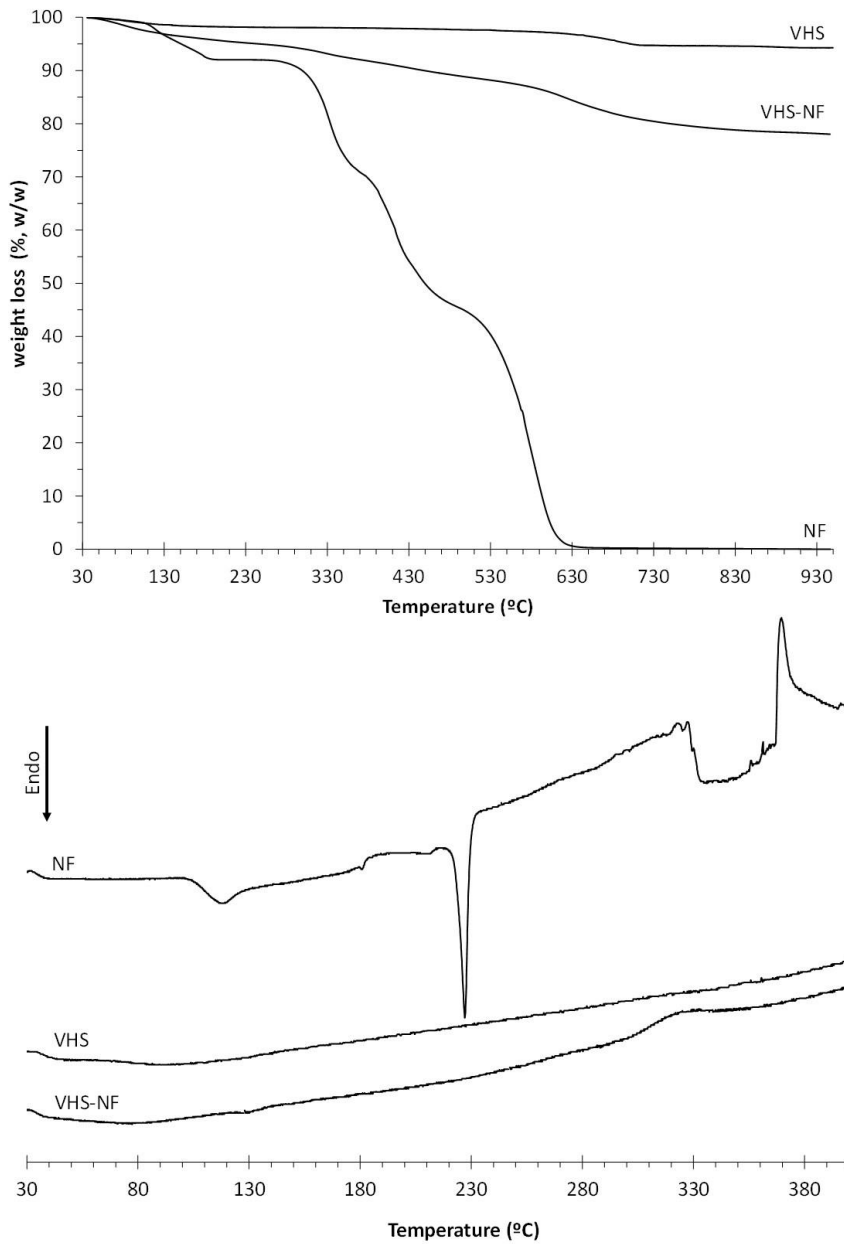


Figure 2.8. Thermal analysis (TGA – high panel curves- and DSC – low panel curves) of NF, VHS and VHS-NF samples

VHS-NF nanocomposite shows TGA thermogram characterized by overlapped events (Figure 2.8 – high panel). In particular, it is evident that water loss is followed by the decomposition of NF and dehydroxylation of clay. Considering that NF fully decomposes before 630 °C, the difference in weight loss between VHS and VHS-NF reveals that VHS-NF is characterized by 16% (w/w) NF loading. Moreover, NF is present in an amorphous state in VHS-NF since melting event is not evident in VHS-NF DSC thermogram (Figure 2.8 – low panel) while the actual NF loading can be justified by the exothermic phenomenon observable at 300–345 °C.

A 0.05% w/v VHS aqueous suspension is characterized by zeta potential of -43.5 ± 0.9 mV, thus confirming the negative net charge of the clay. A 0.05% w/v VHS-NF nanocomposite aqueous suspension shows a zeta potential of -15.9 ± 0.3 mV. VHS and NF probably interact via electrostatic bonds partially shielding the negative charges located into VHS galleries. The dissolution of NF in acetic acid during the nanocomposite preparation causes the protonation of its nitrogen atom in the piperazine ring. In this condition, NF in solution, positively charged, can interact with the negatively charges in the interlayer space of VHS, normally compensated by exchangeable cations increasing the zeta potential. Similar results were reported for clay–cationic moieties interaction products (Norrby and Jonsson, 1983; Wang et al., 2012).

High-resolution TEM microphotographs of VHS sample (Figure 2.9A) show the typical layered morphology of montmorillonite. The EDX analysis performed in the marked zone (red square) confirms the nature of VHS, thanks to the presence of Si, Al and O, together with Mg and Fe and the typical exchangeable cations (Na, K and Ca).

NF (Figure 2.9B) microphotographs confirm NF crystallinity and agree with XRD results. Moreover, the EDX analysis evidences the presence of C, O and N (typical of organic compounds) and that of F peculiar of NF molecule.

2.2. Montmorillonite-Norfloxacin Nanocomposite Intended for Healing of Infected Wounds

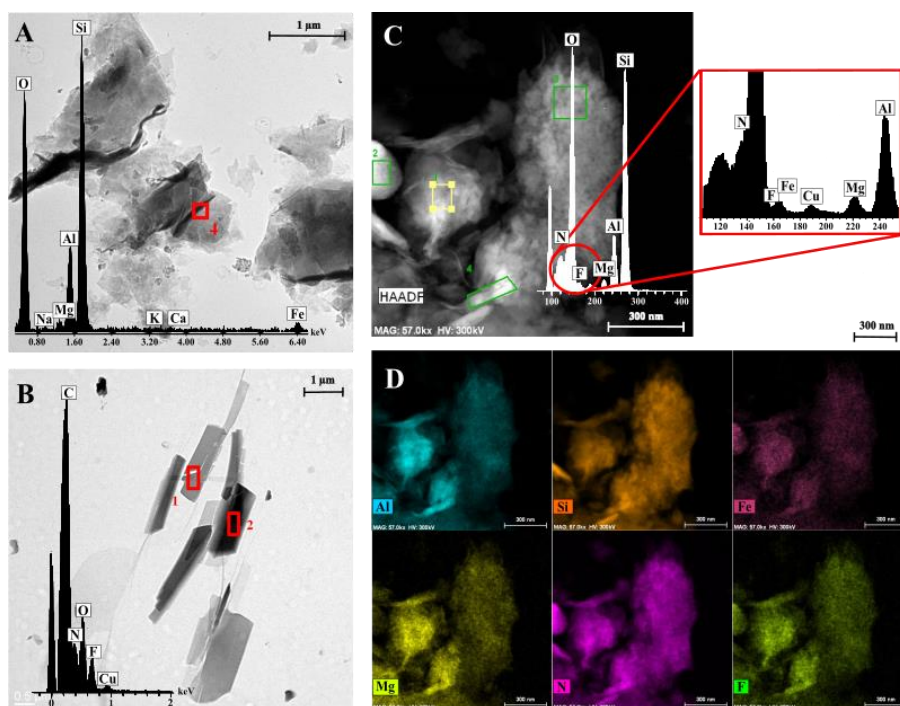


Figure 2.9. TEM microphotographs and EDX analysis of VHS (A), NF (B) and VHS (C) together with EDX mapping of VHS-NF (D)

VHS-NF nanocomposite (Figure 2.9C) shows a morphology similar to that of VHS. The NF crystals are not detectable in this sample, in agreement with XRPD results (no peak of NF diffraction in VHS-NF sample, Figure 2.6) although the NF presence in nanocomposite is confirmed by means of the EDX analysis. The elemental composition evidences the characteristic components of montmorillonite (Si, Al, Mg) and those of organic compounds (C, N, O); moreover, F is also detectable as NF indicator. Additionally, EDX maps (Figure 2.9D) corroborate not only the presence of VHS and NF in nanocomposite but also the homogeneous distribution of NF into montmorillonite, confirming the presence of NF monolayer adsorbed onto the interlayer spaces, as resulted from adsorption studies.

2.2.2.3. Drug Release

Figure 2.10 reports the NF release profiles (%) evaluated for NF and VHS-NF nanocomposite. The dissolution of NF from free drug is very rapid

and reaches 80% within the first hour and the plateau value in 2 h at 100% of NF release.

VHS-NF shows a significantly lower NF release profile and the whole dose is released in 48 h evidencing a controlled release. Considering the application (skin lesions), the capability of the system to control drug release should decrease the number of applications over time. This is an important aspect to allow the healing of lesion since the frequent medical treatment could impair the granulation tissue and new tissue formation. Moreover, the slower release profile of NF could allow to control microbial growth over time.

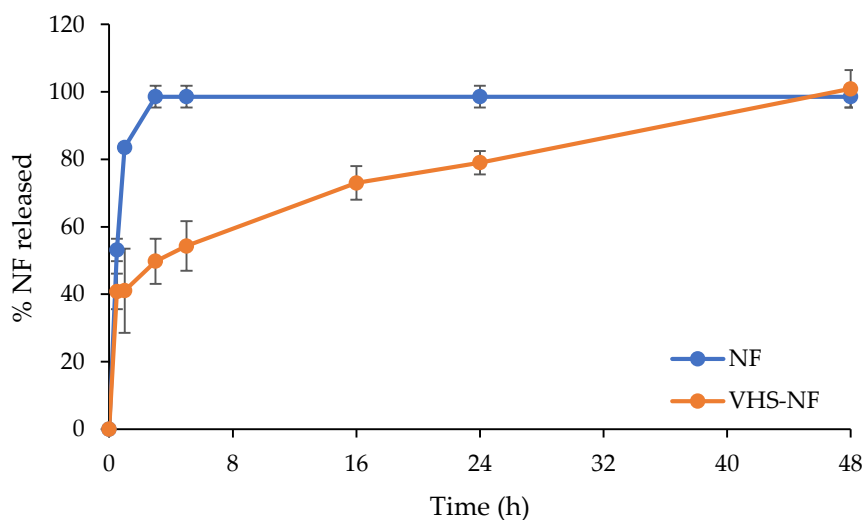


Figure 2.10. % of norfloxacin (NF) released from NF and VHS-NF (mean values \pm s.d.; $n=3$). Abbreviations: NF, norfloxacin; VHS-NF, montmorillonite/norfloxacin nanocomposite

2.2.2.4. Antimicrobial Properties

Figure 2.11 reports microbicidal effect versus time profiles of NF released from NF and VHS-NF against a) *Pseudomonas aeruginosa* and b) *Staphylococcus aureus*.

Pseudomonas aeruginosa is a common Gram-negative, rod-shaped bacterium, facultative anaerobe, of considerable medical importance. It is recognized as a multidrug-resistant pathogen for its ubiquity, its intrinsically advanced antibiotic resistance mechanisms and its association with hospital-

2.2. Montmorillonite-Norfloxacin Nanocomposite Intended for Healing of Infected Wounds

acquired infections such as various sepsis syndromes. *P. aeruginosa* is considered opportunistic insofar as serious infection often occurs during existing diseases or conditions, most notably traumatic burns.

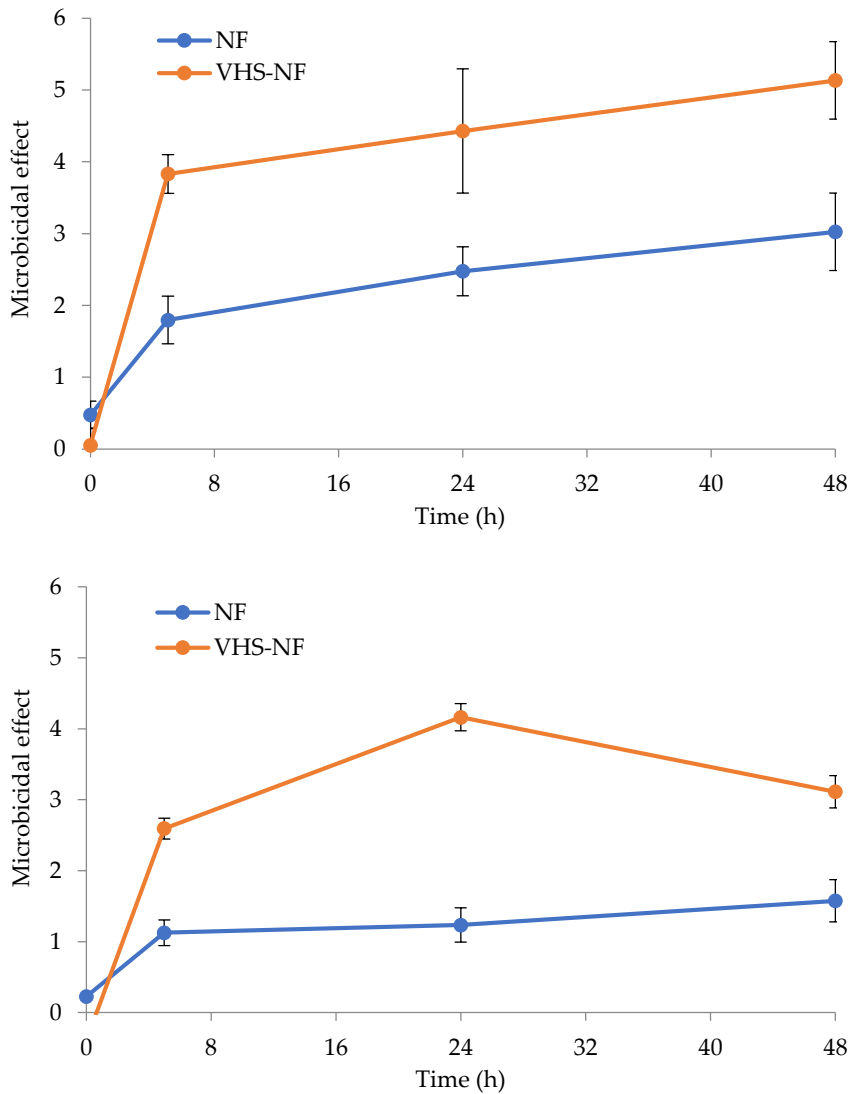


Figure 2.11. Microbicidal effect versus time profiles of norfloxacin (NF) released from NF and VHS-NF against (UP) *Pseudomonas aeruginosa* and (DOWN) *Staphylococcus aureus* (mean values \pm s.d.; $n=3$). Abbreviations: NF, norfloxacin; VHS-NF, montmorillonite / norfloxacin nanocomposite.

Staphylococcus aureus is a Gram-positive, round-shaped bacterium and, as *P. aeruginosa*, it is a facultative anaerobe. It is a usual member of the microbiota of the body, frequently found on the skin, usually acting as a commensal. However, it can also become an opportunistic pathogen, being a common cause of skin infections. The onset of *S. aureus* strains antibiotic-resistant (such as methicillin-resistant *S. aureus*) is a worldwide emergence in clinical medicine.

NF is reported in the literature as effective against both *P. aeruginosa* and *S. aureus* having a MIC of 2 µg/mL in both cases (Norrby and Jonsson, 1983). However, the microbicidal effect is slightly higher against *P. aeruginosa* than that against *S. aureus*. The loading of NF in montmorillonite in VHS-NF nanocomposite significantly increases NF microbicidal effect. The increase of NF potency due to the nanocomposite is probably due to high surface area to volume ratio, which increases the contact area with target organisms (Wang et al., 2012).

2.2.2.5. Fibroblasts *In Vitro* Biocompatibility

Figure 2.12 reports bioavailability (OD, optical density) evaluated for VHS (1.2 mg/mL), NF (0.1 mg/mL) and VHS-NF (VHS: 1.2 mg/mL and NF 0.1 mg/mL). VHS and NF are characterized by OD values not significantly different from the control (growth medium, standard growth conditions). The nanocomposite, VHS-NF, is characterized by OD significantly lower than that of the control although it is higher than 80% and this is normally considered as the lower limit for the cytocompatibility.

VHS, NF and VHS-NF are characterized by no significantly different OD to suggest similar behaviour. Anyhow, it should be considered that the cytocompatibility is assayed to a 20-fold concentration higher than that considered for antimicrobial assay. This evidences that nanocomposite does not impair fibroblast growth also at concentrations higher than those effective against *P. aeruginosa* and *S. aureus* as assessed in the antimicrobial assay.

2.2. Montmorillonite-Norfloxacin Nanocomposite Intended for Healing of Infected Wounds

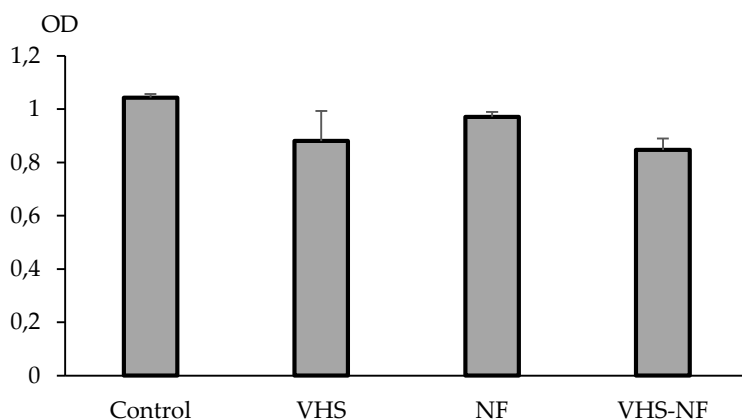


Figure 2.12. Bioavailability (OD) evaluated for VHS (1.2 mg/mL), NF (0.1 mg/mL) and VHS-NF (VHS: 1.2 mg/mL and NF 0.1 mg/mL) compared to the control (growth medium, standard growth conditions) (mean values \pm s.d.; $n=8$) (Statistical analysis W test: control vs VHS-NF: $p=0.030$). Abbreviations: NF, norfloxacin; VHS, montmorillonite; VHS-NF, montmorillonite/norfloxacin nanocomposite

2.2.3. Conclusions

NF is loaded into montmorillonite to have a nanocomposite by means of adsorption mechanism, as one single process. In particular, protonated NF molecules interact with the active sites of montmorillonite located at edges and within its interlayer space, thus forming a drug monolayer onto the clay mineral interlayer surface. NF in the nanocomposites is in an amorphous state, and its loading is homogeneous and causes an expansion of montmorillonite interlayer spaces. Moreover, the nanocomposite causes a prolonged NF release over time. The nanocomposite is characterized by good biocompatibility *in vitro* toward fibroblasts, and it is able to increase antimicrobial potency of the free drug against *P. aeruginosa* and *S. aureus*, Gram-negative and Gram-positive bacteria, respectively, that are often a concurrent cause of wound chronicization, leading to a possible impairment of the healing path and finally to non-healing wounds. NF-montmorillonite nanocomposite demonstrates to possess suitable properties as a tool to enhance wound healing in infected wounds: the possibility to use a flexible dosage, as a powder for cutaneous application, should also allow easy administration, depending on lesion dimensions.

2.3. Abbreviations

AEM	Analytical Electron Microscopy
CFU	Colony forming unit
DMEM	Dulbecco's Modified Eagle Medium
DMSO	dimethyl sulfoxide
DSC	Differential Scanning Calorimetry
FBS	Fetal Bovine Serum
FT-IR	Fourier-Transform Infrared Spectroscopy
HRTEM	High-Resolution Transmission Electron Microscopy
MIC	Minimum Inhibitory Concentration
MTT	3-(4,5-Dimethylthiazol-2-yl)-2,5-Diphenyltetrazolium bromide
NF	Norfloxacin
OD	Optical density
P1, P2 and P3	Peat strata from top to bottom
TGA	Thermogravimetric Analysis
TGA	Thermogravimetric analysis
VHS	Montmorillonite (Veegum [®] HS)
VHS-NF	Montmorillonite-norfloxacin nanocomposite
XRPD	X-Ray Powder Diffraction

References

- Abu-Jdayil, B., 2011. Rheology of sodium and calcium bentonite-water dispersions: Effect of electrolytes and aging time. *Int. J. Miner. Process.* 98, 208–213. <https://doi.org/10.1016/j.minpro.2011.01.001>
- Aguzzi, C., Cerezo, P., Viseras, C., Caramella, C., 2007. Use of clays as drug delivery systems: Possibilities and limitations. *Appl. Clay Sci.* 36, 22–36. <https://doi.org/10.1016/j.clay.2006.06.015>
- Aguzzi, C., Sánchez-Espejo, R., Cerezo, P., Machado, J., Bonferoni, C., Rossi, S., Salcedo, I., Viseras, C., 2013. Networking and rheology of concentrated clay suspensions “matured” in mineral medicinal water. *Int. J. Pharm.* 453, 473–479. <https://doi.org/10.1016/j.ijpharm.2013.06.002>
- Aguzzi, C., Sandri, G., Bonferoni, C., Cerezo, P., Rossi, S., Ferrari, F., Caramella, C., Viseras, C., 2014. Solid state characterisation of silver sulfadiazine loaded on montmorillonite/chitosan nanocomposite for wound healing. *Colloids Surfaces B Biointerfaces* 113, 152–157. <https://doi.org/10.1016/J.COLSURFB.2013.08.043>
- Aho, M.J., Tummavuori, J.L., Hämäläinen, J.P., Saastamoinen, J.J., 1989. Determination of heats of pyrolysis and thermal reactivity of peats. *Fuel* 68, 1107–1111. [https://doi.org/10.1016/0016-2361\(89\)90179-8](https://doi.org/10.1016/0016-2361(89)90179-8)
- Baptista, P. V., McCusker, M.P., Carvalho, A., Ferreira, D.A., Mohan, N.M., Martins, M., Fernandes, A.R., 2018. Nano-strategies to fight multidrug resistant bacteria- "A Battle of the Titans". *Front. Microbiol.* 9, 1441. <https://doi.org/10.3389/fmicb.2018.01441>
- Barry, A.L., Jones, R.N., Thornsberry, C., Ayers, L.W., Gerlach, E.H., Sommers, H.M., 1984. Antibacterial activities of ciprofloxacin, norfloxacin, oxolinic acid, cinoxacin, and nalidixic acid. *Antimicrob. Agents Chemother.* 25, 633–637. <https://doi.org/10.1128/AAC.25.5.633>
- Barry, B.W., 1974. Rheology of pharmaceutical and cosmetic semisolids., in: Bean, H.S., Beckett, A.H., Carless J. E. (Eds.), *Advances in Pharmaceutical Sciences*. Academic Press Inc. , London, pp. 1–72.
- Beer, a M., Sagorchev, P., Lukanov, J., 2002. Isolation of biologically active fractions from the water soluble components of fulvic and ulmic acids from peat. *Phytomedicine* 9, 659–66. <https://doi.org/10.1078/094471102321616490>
- Beer, A.M., Fey, S., Walch, S., Lüthgens, K., Ostermann, T., Lukanov, J., 2001. The effect of peat components on endocrine and immunological parameters and on trace elements--results of two pilot studies. *Clin. Lab.* 47, 161–167.
- Beer, A.M., Grozeva, A., Sagorchev, P., Lukanov, J., 2003. Comparative study of the thermal properties of mud and peat solutions applied in clinical practice. *Biomed. Tech. (Berl)*. 48, 301–305.

- Beer, A.M., Lukanov, J., Sagorchev, P., 2000. The influence of fulvic and humic acids from peat, on the spontaneous contractile activity of smooth muscles. *Phytomedicine* 7, 407–415. [https://doi.org/10.1016/S0944-7113\(00\)80062-8](https://doi.org/10.1016/S0944-7113(00)80062-8)
- Biester, H., Knorr, K.H., Schellekens, J., Basler, A., Hermanns, Y.M., 2014. Comparison of different methods to determine the degree of peat decomposition in peat bogs. *Biogeosciences* 11, 2691–2707. <https://doi.org/10.5194/bg-11-2691-2014>
- Borrego-Sánchez, A., Carazo, E., Aguzzi, C., Viseras, C., Sainz-Díaz, C.I., 2017. Biopharmaceutical improvement of praziquantel by interaction with montmorillonite and sepiolite. *Appl. Clay Sci.* <https://doi.org/10.1016/J.CLAY.2017.12.024>
- Bramhill, J., Ross, S., Ross, G., 2017. Bioactive nanocomposites for tissue repair and regeneration: a review. *Int. J. Environ. Res. Public Health* 14, 66. <https://doi.org/10.3390/ijerph14010066>
- Carazo, E., Borrego-Sánchez, A., García-Villén, F., Sánchez-Espejo, R., Aguzzi, C., Viseras, C., Sainz-Díaz, C.I., Cerezo, P., 2017. Assessment of halloysite nanotubes as vehicles of isoniazid. *Colloids Surfaces B Biointerfaces* 160, 337–344. <https://doi.org/10.1016/J.COLSURFB.2017.09.036>
- Carazo, E., Borrego-Sánchez, A., García-Villén, F., Sánchez-Espejo, R., Viseras, C., Cerezo, P., Aguzzi, C., 2018. Adsorption and characterization of palygorskite-isoniazid nanohybrids. *Appl. Clay Sci.* 160. <https://doi.org/10.1016/j.clay.2017.12.027>
- Ding, Q., Xu, X., Yue, Y., Mei, C., Huang, C., Jiang, S., Wu, Q., Han, J., 2018. Nanocellulose-mediated electroconductive self-healing hydrogels with high strength, plasticity, viscoelasticity, stretchability, and biocompatibility toward multifunctional applications. *ACS Appl. Mater. Interfaces* 10, 27987–28002. <https://doi.org/10.1021/acsami.8b09656>
- Dudare, D., Klavins, M., 2013. Complex-forming properties of peat humic acids from a raised bog profiles. *J. Geochemical Explor.* 129, 18–22. <https://doi.org/10.1016/j.gexplo.2012.12.001>
- Fioravanti, A., Perpignano, G., Tirri, G., Cardinale, G., Gianniti, C., Lanza, C.E., Loi, A., Tirri, E., Sfriso, P., Cozzi, F., 2007. Effects of mud-bath treatment on fibromyalgia patients: A randomized clinical trial. *Rheumatol. Int.* 27, 1157–1161. <https://doi.org/10.1007/s00296-007-0358-x>
- Flaig, W., 1992. Humic substances and associated small molecules from peats in balneology. *Sci. Total Environ.* 117/118, 561–567.
- Fluhr, J.W., Elias, P.M., 2002. Stratum corneum pH: Formation and Function of the ‘Acid Mantle.’ *Exog. Dermatology* 1, 163–175. <https://doi.org/10.1159/000066140>
- Földvári, M., 2011. Handbook of thermogravimetric system of minerals and its use in geological practice. Innova-Print Kft., Budapest.
- Galperin, A., Smith, K., Geisler, N.S., Bryers, J.D., Ratner, B.D., 2015. Precision-Porous PolyHEMA-Based Scaffold as an Antibiotic-Releasing Insert for a Scleral Bandage. *ACS Biomater. Sci. Eng.* 1, 593–600. <https://doi.org/10.1021/acsbiomaterials.5b00133>

2.3. Abbreviations

- Gandois, L., Cobb, A.R., Hei, I.C., Lim, L.B.L., Salim, K.A., Harvey, C.F., 2013. Impact of deforestation on solid and dissolved organic matter characteristics of tropical peat forests: implications for carbon release. *Biogeochemistry* 114, 183–199. <https://doi.org/10.1007/s10533-012-9799-8>
- Gao, S., Tang, G., Hua, D., Xiong, R., Han, J., Jiang, S., Zhang, Q., Huang, C., 2019. Stimuli-responsive bio-based polymeric systems and their applications. *J. Mater. Chem. B* 7, 709–729. <https://doi.org/10.1039/c8tb02491j>
- Gomes de Melo, B.A., Lopes Motta, F., Andrade Santana, M.H., 2015. Humic acids: Structural properties and multiple functionalities for novel technological developments. *Mater. Sci. Eng. C* 62, 967–974. <https://doi.org/10.1016/j.msec.2015.12.001>
- Gupta, A., Mumtaz, S., Li, C.H., Hussain, I., Rotello, V.M., 2019. Combatting antibiotic-resistant bacteria using nanomaterials. *Chem. Soc. Rev.* 48, 415–427. <https://doi.org/10.1039/c7cs00748e>
- Han, J., Yue, Y., Wu, Q., Huang, C., Pan, H., Zhan, X., Mei, C., Xu, X., 2017. Effects of nanocellulose on the structure and properties of poly(vinyl alcohol)-borax hybrid foams. *Cellulose* 24, 4433–4448. <https://doi.org/10.1007/s10570-017-1409-4>
- Hendry, M.T., Sharma, J.S., Martin, C.D., Barbour, S.L., 2012. Effect of fibre content and structure on anisotropic elastic stiffness and shear strength of peat. *Can. Geotech. J.* 49, 403–415.
- Katdare, A. V., Ryan, J.A., Bavitz, J.F., Erb, D.M., Guillory, J.K., 1986. Characterization of hydrates of norfloxacin. *Mikrochim. Acta* 3, 1–12. <https://doi.org/10.1007/BF01196816>
- Khil'ko, S.L., Efimova, I. V., Smirnova, O. V., 2011. Antioxidant properties of humic acids from brown coal. *Solid Fuel Chem.* 45, 367–371. <https://doi.org/10.3103/S036152191106005X>
- Klößing, R., Helbig, B., 2005. Medical aspects and applications of humic substances, in: Steinbüchel, A., Marchessault, R.H. (Eds.), *Biopolymers for Medical and Pharmaceutical Applications*. WILEY-VCH Verlag GmbH & Co. KGaA, Weinheim.
- Kuhry, P., Vitt, D.H., 1996. Fossil Carbon/Nitrogen Ratios as a Measure of Peat Decomposition. *Source Ecol.* 77, 271–275.
- Kumar, M., Curtis, A., Hoskins, C., 2018. Application of nanoparticle technologies in the combat against anti-microbial resistance. *Pharmaceutics* 10. <https://doi.org/10.3390/pharmaceutics10010011>
- Lambers, H., Piessens, S., Bloem, A., Pronk, H., Finkel, P., 2006. Natural skin surface pH is on average below 5, which is beneficial for its resident flora. *Int. J. Cosmet. Sci.* 28, 359–370. <https://doi.org/10.1111/j.1467-2494.2006.00344.x>
- Lim, H.W., Collins, S.A.B., Resneck, J.S., Bolognia, J.L., Hodge, J.A., Rohrer, T.A., Van Beek, M.J., Margolis, D.J., Sober, A.J., Weinstock, M.A., Nerenz, D.R., Smith Begolka, W., Moyano, J. V., 2017. The burden of skin disease in the United States. *J. Am. Acad. Dermatol.* 76, 958–972.e2. <https://doi.org/10.1016/j.jaad.2016.12.043>

- Lv, D., Wang, R., Tang, G., Mou, Z., Lei, J., Han, J., De Smedt, S., Xiong, R., Huang, C., 2019. Ecofriendly electrospun membranes loaded with visible-light-responding nanoparticles for multifunctional usages: highly efficient air filtration, dye scavenging, and bactericidal activity. *ACS Appl. Mater. Interfaces* 11, 12880–12889. <https://doi.org/10.1021/acscami.9b01508>
- Mahmoud, A.A., Salama, A.H., 2016. Norfloxacin-loaded collagen/chitosan scaffolds for skin reconstruction: Preparation, evaluation and in-vivo wound healing assessment. *Eur. J. Pharm. Sci.* 83, 155–165. <https://doi.org/10.1016/J.EJPS.2015.12.026>
- Malipeddi, V.R., Dua, K., Sara, U.V.S., Malipeddi, H., Agrawal, A., 2006. Comparative evaluation of transdermal formulations of norfloxacin with silver sulfadiazine cream, USP, for burn wound healing property. *J. Burns Wounds* 5, e4.
- Mazuel, C., 1991. Norfloxacin, in: Florey, K., Brittain, H., Mazzo, D., Wozniak, T., Brenner, G., Forcier, G., Al-Bad, A. (Eds.), *Analytical Profiles of Drug Substances and Excipients*. Academic Press Inc., pp. 557–600.
- Mofazzal Jahromi, M.A., Sahandi Zangabad, P., Moosavi Basri, S.M., Sahandi Zangabad, K., Ghamarypour, A., Aref, A.R., Karimi, M., Hamblin, M.R., 2018. Nanomedicine and advanced technologies for burns: Preventing infection and facilitating wound healing. *Adv. Drug Deliv. Rev.* 123, 33–64. <https://doi.org/10.1016/j.addr.2017.08.001>
- Mpharm, K.D., Ramana, M. V., Sara, U.V.S., Agrawal, D.K., Mpharm, K.P., Chakravarthi, S., 2010. Preparation and evaluation of transdermal plasters containing norfloxacin: a novel treatment for burn wound healing. *Eplasty* 10, e44.
- Nakamura, M., Nishida, T., Mishima, H., Otori, T., 1993. Effects of antimicrobials on corneal epithelial migration. *Curr. Eye Res.* 12, 733–740. <https://doi.org/10.3109/02713689308995769>
- Naumenko, E.A., Guryanov, I.D., Yendluri, R., Lvov, Y.M., Fakhrullin, R.F., 2016. Clay nanotube-biopolymer composite scaffolds for tissue engineering. *Nanoscale* 8, 7257–7271. <https://doi.org/10.1039/c6nr00641h>
- Norrby, S.R., Jonsson, M., 1983. Antibacterial activity of norfloxacin. *Antimicrob. Agents Chemother.* 23, 15–18. <https://doi.org/10.1128/AAC.23.1.15>
- Orru, M., Übner, M., Orru, H., 2011. Chemical properties of peat in three peatlands with balneological potential in Estonia. *Est. J. Earth Sci.* 60, 43–49. <https://doi.org/10.3176/earth.2011.1.04>
- Pons Gimier, L., Parra Juez, J.L., 1995. *Ciencia cosmética. Bases fisiológicas y criterios prácticos*, First. ed. Heliotipia Artística S.L., Madridf.
- Puigjaner, C., Barbas, R., Portell, A., Font-Bardia, M., Alcobé, X., Prohens, R., 2010. Revisiting the solid state of Norfloxacin. *Cryst. Growth Des.* 10, 2948–2953. <https://doi.org/10.1021/cg9014898>
- Romão, L.P.C., Lead, J.R., Rocha, J.C., Oliveira, L.C. de, Rosa, A.H., Mendonça, A.G.R., Ribeiro, A. de S., 2007. Structure and properties of brazilian peat: analysis by spectroscopy and microscopy. *J. Braz. Chem. Soc.* 18, 714–720.

2.3. Abbreviations

- <https://doi.org/10.1590/S0103-50532007000400008>
- Rossi, S., Marciello, M., Sandri, G., Ferrari, F., Bonferoni, M.C., Papetti, A., Caramella, C., Dacarro, C., Grisoli, P., 2007. Wound dressings based on chitosans and hyaluronic acid for the release of chlorhexidine diacetate in skin ulcer therapy. *Pharm. Dev. Technol.* 12, 415–422. <https://doi.org/10.1080/10837450701366903>
- Rusanu, A., Tamaş, A.I., Vulpe, R., Rusu, A., Butnaru, M., Vereştiuc, L., 2017. Biocompatible and Biodegradable Hydrogels Based on Chitosan and Gelatin with Potential Applications as Wound Dressings. *J. Nanosci. Nanotechnol.* 17, 4584–4591. <https://doi.org/10.1166/jnn.2017.14298>
- Samanidou, V.F., Demetriou, C.E., Papadoyannis, I.N., 2003. Direct determination of four fluoroquinolones, enoxacin, norfloxacin, ofloxacin, and ciprofloxacin, in pharmaceuticals and blood serum by HPLC. *Anal. Bioanal. Chem.* 375, 623–629. <https://doi.org/10.1007/s00216-003-1749-9>
- Sánchez-Espejo, R., Aguzzi, C., Cerezo, P., Salcedo, I., López-Galindo, A., Viseras, C., 2014. Folk pharmaceutical formulations in western Mediterranean: Identification and safety of clays used in pelotherapy. *J. Ethnopharmacol.* 155, 810–814. <https://doi.org/10.1016/j.jep.2014.06.031>
- Sánchez-Espejo, R., Cerezo, P., Aguzzi, C., López-Galindo, A., Machado, J., Viseras, C., 2015. Physicochemical and in vitro cation release relevance of therapeutic muds “maturation”. *Appl. Clay Sci.* 116–117, 1–7. <https://doi.org/10.1016/j.clay.2015.08.007>
- Sandri, G., Aguzzi, C., Rossi, S., Bonferoni, M.C., Bruni, G., Boselli, C., Cornaglia, A.I., Riva, F., Viseras, C., Caramella, C., Ferrari, F., 2017. Halloysite and chitosan oligosaccharide nanocomposite for wound healing. *Acta Biomater.* 57, 216–224. <https://doi.org/10.1016/j.ACTBIO.2017.05.032>
- Sandri, G., Bonferoni, M.C., Ferrari, F., Rossi, S., Aguzzi, C., Mori, M., Grisoli, P., Cerezo, P., Tenci, M., Viseras, C., Caramella, C., 2014. Montmorillonite-chitosan-silver sulfadiazine nanocomposites for topical treatment of chronic skin lesions: in vitro biocompatibility, antibacterial efficacy and gap closure cell motility properties. *Carbohydr. Polym.* 102, 970–977. <https://doi.org/10.1016/j.carbpol.2013.10.029>
- Sandri, G., Bonferoni, M.C., Rossi, S., Ferrari, F., Aguzzi, C., Viseras, C., Caramella, C., 2016. Clay minerals for tissue regeneration, repair, and engineering, in: Ågren, M.S. (Ed.), *Wound Healing Biomaterials*. Elsevier, pp. 385–402. <https://doi.org/10.1016/B978-1-78242-456-7.00019-2>
- Schnitzer, M., Hoffman, I., 1965. Thermogravimetry of soil humic compounds. *Geochim. Cosmochim. Acta* 29, 859–870. [https://doi.org/10.1016/0016-7037\(65\)90083-9](https://doi.org/10.1016/0016-7037(65)90083-9)
- Schott, H., 1995. *Reologia*, Remington Farmacia. Medica Panamericana, Buenos Aires.
- Scott, M.J., Jones, M.N., Woof, C., Simon, B., Tipping, E., 2001. The molecular properties of humic substances isolated from a UK upland peat system: A temporal investigation. *Environ. Int.* 27, 449–462. [https://doi.org/10.1016/S0160-4120\(01\)00100-3](https://doi.org/10.1016/S0160-4120(01)00100-3)

- Sławinska, D., Polewski, K., Rolewski, P., Sławiński, J., 2007. Synthesis and properties of model humic substances derived from gallic acid 21, 199–208.
- Stejskalová, A., Almquist, B.D., 2017. Using biomaterials to rewire the process of wound repair. *Biomater. Sci.* 5, 1421–1434. <https://doi.org/10.1039/c7bm00295e>
- Suárez, M., González, P., Domínguez, R., Bravo, A., Melián, C., Pérez, M., Herrera, I., Blanco, D., Hernández, R., Fagundo, J.R., 2011. Identification of Organic Compounds in San Diego de los Baños Peloid (Pinar del Río, Cuba). *J. Altern. Complement. Med.* 17, 155–165. <https://doi.org/10.1089/acm.2009.0587>
- Summa, V., Tateo, F., 1999. Geochemistry of two peats suitable for medical uses and their behaviour during leaching. *Appl. Clay Sci.* 15, 477–489. [https://doi.org/10.1016/S0169-1317\(99\)00036-8](https://doi.org/10.1016/S0169-1317(99)00036-8)
- Sun, L., Li, A., Hu, Y., Li, Y., Shang, L., Zhang, L., 2019. Self-assembled fluorescent and antibacterial GHK-Cu nanoparticles for wound healing applications. *Part. Part. Syst. Charact.* 36, 1800420. <https://doi.org/10.1002/ppsc.201800420>
- Tian, Z., Zhang, Y., Liu, X., Chen, C., Guiltinan, M.J., Allcock, H.R., 2013. Biodegradable polyphosphazenes containing antibiotics: synthesis, characterization, and hydrolytic release behavior. *Polym. Chem.* 4, 1826. <https://doi.org/10.1039/c2py21064a>
- Tunç, S., Duman, O., 2010. Preparation and characterization of biodegradable methyl cellulose/montmorillonite nanocomposite films. *Appl. Clay Sci.* 48, 414–424. <https://doi.org/10.1016/j.clay.2010.01.016>
- Viseras, C., Aguzzi, C., Cerezo, P., Bedmar, M.C., 2008a. Biopolymer–clay nanocomposites for controlled drug delivery. *Mater. Sci. Technol.* 24, 1020–1026. <https://doi.org/10.1179/174328408X341708>
- Viseras, C., Aguzzi, C., Cerezo, P., López-Galindo, A., 2007. Uses of clay minerals in semisolid health care and therapeutic products. *Appl. Clay Sci.* 36, 37–50. <https://doi.org/10.1016/j.clay.2006.07.006>
- Viseras, M.T., Aguzzi, C., Cerezo, P., Viseras, C., Valenzuela, C., 2008b. Equilibrium and kinetics of 5-aminosalicylic acid adsorption by halloysite. *Microporous Mesoporous Mater.* 108, 112–116. <https://doi.org/10.1016/j.micromeso.2007.03.033>
- Wang, Y., Zhu, L., Dong, Z., Xie, S., Chen, X., Lu, M., Wang, X., Li, X., Zhou, W.Z., 2012. Preparation and stability study of norfloxacin-loaded solid lipid nanoparticle suspensions. *Colloids Surfaces B Biointerfaces* 98, 105–111. <https://doi.org/10.1016/j.colsurfb.2012.05.006>
- Wiles, J.A., Bradbury, B.J., Pucci, M.J., 2010. New quinolone antibiotics: A survey of the literature from 2005 to 2010. *Expert Opin. Ther. Pat.* 20, 1295–1319. <https://doi.org/10.1517/13543776.2010.505922>

Chapter 3

Objetivos y Plan de Trabajo

3.1. Objetivos de la Tesis

3.1. Objetivos de la Tesis

Los aluminosilicatos son un amplio grupo de materiales en los que se incluyen tanto sustancias naturales como sintéticas y que presentan numerosas aplicaciones, muchas de ellas derivadas de sus características superficiales, y en particular de su porosidad y presencia de poros de distintas dimensiones y elevada superficie específica. Entre estos materiales, ocupan un lugar relevante los de origen natural, incluyendo, entre otros, las zeolitas naturales y algunos minerales de la arcilla. En nuestro caso, los aluminosilicatos centro de estudio pertenecen a las denominadas “arcillas especiales”, concretamente a las arcillas fibrosas, que pueden ser usadas en salud y debido a sus propiedades como sustancias auxiliares (excipientes) o a su actividad farmacológica (López-Galindo and Viseras, 2004; Viseras et al., 2007). España alberga uno de los mayores depósitos de sepiolita del mundo (más de 67 Mt, de los cuales 52 Mt se encuentran en la provincia de Madrid (Vicálvaro) y tiene unas reservas superiores a los 30 Mt de palygorskita, mineral presente también en otros países en cantidades que permiten su explotación por el líder mundial en extracción de este mineral (Tolsa, Madrid), con la que colabora desde hace años el grupo investigador que avala el proyecto de tesis. En concreto, estas arcillas fibrosas pueden emplearse en el desarrollo de geles de administración tópica con aguas mineromedicinales como fase externa con efectos terapéuticos y cosméticos (Viseras et al., 2015), siendo este el centro de estudio de este proyecto de tesis.

Los fangos terapéuticos son “productos medicinales de consistencia semisólida, resultado de la interposición de sólidos orgánicos y/o inorgánicos en agua mineromedicinal” (Viseras et al., 2007). Los fangos terapéuticos se administran tópicamente en aplicaciones locales o baños y debido a una serie de acciones biofísicas y/o bioquímicas, se emplean terapéuticamente en el tratamiento o prevención de patologías tanto sistémicas como locales (de la piel). El uso de arcillas en la elaboración de fangos termales requiere que los productos se elaboren siguiendo protocolos que tengan en cuenta la concentración óptima de arcilla, energía de interposición, tiempo de contacto, temperatura, fuerza iónica del medio, entre otros, de manera que se garantice el desarrollo de sistemas estructurados (Viseras and López-Galindo, 1999; Viseras et al., 2001; Aguzzi et al., 2013b). Los fangos son susceptibles de

mejoras en su comportamiento (Viseras et al., 2006a; Rebelo et al., 2011a, 2011b) y requieren el cumplimiento de distintos requisitos (Cerezo et al., 2013). En particular la composición química elemental tanto de los materiales de partida como de los productos una vez elaborados debe ser controlada, dado que muchos de los efectos beneficiosos, pero también perjudiciales, derivados de su empleo dependerán de mecanismos químicos (Cultrone et al., 2003; Viseras et al., 2006b, 2006a).

Las acciones bioquímicas de los fangos terapéuticos son debidas al quimismo de las aguas y de los fangos, de forma que sus efectos dependerán de la posible penetración y/o permeación dérmica de estos componentes. Los estudios centrados en la presencia de iones metálicos susceptibles de tener efectos biológicos (positivos o negativos) cuando los fangos son aplicados son escasos y hasta la fecha poco concluyentes (Summa and Tateo, 1998; Tateo and Summa, 2007; Tateo et al., 2009). No está claro qué elementos son esenciales y cuál es la concentración ideal de cada elemento para conseguir una respuesta óptima al tratamiento. Además, la presencia de un determinado elemento en el fango no implica necesariamente su biodisponibilidad en el organismo. No se conoce la permeabilidad de iones desde fangos y aguas mineromedicinales, y tan sólo se estima que es variable y mayor para los gases que para las sustancias disueltas en el agua. Algunos estudios han determinado la permeación desde suspensiones de metales pesados a través de la piel para evaluar sus efectos tóxicos (Van Lierde et al., 2006; Larese et al., 2007). Conviene señalar la importancia del control en el contenido de determinados elementos traza potencialmente tóxicos y de su movilidad y estado durante el proceso de elaboración de los fangos, como As, Sc, Tl, Pb, Cd, Cu, Zn, Hg, Se y Sb, con objeto de evitar posibles intoxicaciones durante el tratamiento (Mascolo et al., 1999; Summa and Tateo, 1999; Sánchez-Espejo et al., 2015). La posible interacción entre los componentes del fango termal debe ser evaluada mediante pruebas específicas (Aguzzi et al., 2013a). De especial importancia resulta el hecho de que, dependiendo de los metales pesados en cuestión y su especiación, la toxicidad puede ocurrir justo por encima de los niveles de detección de muchas técnicas analíticas. El plomo (Pb), cadmio (Cd), arsénico (As) y mercurio (Hg) son los metales y metaloides con el potencial tóxico más alto entre los presentes en las muestras de arcilla. Otros metales o metaloides

como el cobre (Cu), antimonio (Sb), molibdeno (Mo) y cromo (Cr) también pueden ser la fuente de riesgos tóxicos. Por lo general, las concentraciones de estos metales en las arcillas varían ampliamente, pero pueden encontrarse en rangos que van desde partes por billón (ppb) hasta partes por trillón (ppt), por lo que su medida necesita de técnicas instrumentales de alta precisión tales como la espectrometría de masas cuadrupolar con fuente de plasma acoplada inductivamente (ICP-MS). El ICP-MS se ha convertido en una herramienta vital en el análisis de metales pesados, ya que proporciona un análisis rápido y fiable a lo largo de un amplio rango de concentración y se ha incorporado como la técnica referente en normativas de control de estos metales en Europa y EE.UU.

3.1.1. Objetivos específicos

- **Objetivo 1.** Caracterizar fangos naturales de elevada riqueza en azufre.
- **Objetivo 2.** Evaluar la composición mineral y química de muestras de arcillas fibrosas susceptibles de empleo en la elaboración de fangos sintéticos, incluyendo la puesta a punto de metodologías novedosas para la determinación de metales pesados.
- **Objetivo 3.** Elaborar fangos sintéticos con muestras seleccionadas en virtud de su composición, correlacionando las características de las arcillas fibrosas seleccionadas, y sus modificaciones como resultado de la maduración, con las propiedades técnicas de los productos.
- **Objetivo 4.** Evaluar la biocompatibilidad *in vitro* de los ingredientes por separado y de las correspondientes formulaciones para su uso en el tratamiento de la curación de heridas.
- **Objetivo 5.** Establecer las propiedades fisicoquímicas, geodisponibilidad y contenido inorgánico relacionado con los efectos terapéuticos o perjudiciales del fango, a partir de la composición y geoquímica original de los componentes.
- **Objetivo 6.** Evaluar la seguridad de los excipientes y las formulaciones en lo que a impurezas elementales se refiere, aplicando las regulaciones y/o guías disponibles y susceptibles de ser aplicadas

3.1. Objetivos de la Tesis

a formulaciones tópicas tipo “hidrogel” preparados con ingredientes naturales.

- **Objetivo 7.** Determinar la liberación y la movilidad (penetración y permeabilidad) *in vitro* de los elementos con interés terapéutico presentes en el fango, susceptibles de inducir efectos biológicos útiles, especialmente relacionados con la curación de heridas.

3.1.2. Plan de Trabajo

De acuerdo con los objetivos citados con anterioridad, el plan de trabajo de la tesis doctoral se organizó en los siguientes apartados, correspondientes a diferentes secciones del capítulo 4 de esta memoria de tesis.

Sección 4.1. Las arcillas especiales son materias primas empleadas en farmacia y cuyas características y propiedades aparecen claramente especificadas en las correspondientes farmacopeas. No obstante, estos mismos materiales arcillosos son usados en la obtención de preparados empleados en balneoterapia, los cuales aún no son reconocidos como cosméticos ni medicamentos. En un primer trabajo se estudiaron hidrogeles preparados con dos aguas mineromedicinales y dos arcillas fibrosas. Tanto los excipientes como los hidrogeles fueron totalmente caracterizados y estudiados en este estudio. En esta sección se da cumplimiento a los objetivos 1, 2 y 3 de la tesis.

García-Villén, F., Sánchez-Espejo, R., López-Galindo, A., Cerezo, P., Viseras, C. (2020). Design and characterization of spring water hydrogels with natural inorganic excipients. *Applied Clay Science*, 197, 105772.

Sección 4.2. En este capítulo se aborda principalmente los objetivos 4 y 5, ya que se el estudio se centra en la biocompatibilidad *in vitro* de los ingredientes utilizados en la preparación de hidrogeles abordados en el estudio anteriormente mencionado. Así mismo, tras confirmar la biocompatibilidad de los hidrogeles, se realiza un estudio más específico para evaluar la actividad *in vitro* de los hidrogeles en la curación de heridas.

García-Villén, F., Faccendini, A., Miele, D., Ruggeri, M., Sánchez-Espejo, R., Borrego-Sánchez, A., Cerezo, P., Rossi, S., Viseras, C., Sandri, G. (2020). **Wound healing activity of nanoclay/spring water hydrogels.** *Pharmaceutics*, 12(467), 1-24.

Sección 4.3. En esta sección el foco se centra exclusivamente en el objetivo 6, ya que se realizaron estudios de liberación de impurezas elementales *in vitro* (celdas de Franz), evaluando de esta manera la posible toxicidad o efectos adversos asociados al uso de los hidrogeles.

García-Villén, F., Sánchez-Espejo, R., Borrego-Sánchez, A., Cerezo, P., Perioli, L., Viseras, César (2020). **Safety of nanoclay/spring water hydrogels: assessment and mobility of hazardous elements.** *Pharmaceutics*, 12(764), 1-17.

Sección 4.4. En la sección final de este proyecto de tesis, se abordan los objetivos 4, 5 y, especialmente, el objetivo 7. Se evalúa la liberación *in vitro* de elementos con potencial actividad terapéutica sobre la piel, y más concretamente sobre la curación de heridas.

García-Villén, F., Sánchez-Espejo, R., Borrego-Sánchez, A., Cerezo, P., Cucca, L., Giuseppina S., Viseras, C. (2020). **Correlation between elemental composition/mobility and skin cell proliferation of fibrous nanoclay/spring water hydrogels.** *Pharmaceutics*, 12(891), 1-20.

Referencias

- Aguzzi, C., Cerezo, P., Sandri, G., Viseras, C., 2013a. Aspectos farmacéuticos de peloides de empleo cosmético y dermatológico, in: Agencia Estatal de Tecnologías Sanitarias, A. (Ed.), *Peloterapia: Aplicaciones Médicas y Cosméticas de Fangos Termales*. BOE, Madrid, pp. 135–144.
- Aguzzi, C., Sánchez-Espejo, R., Cerezo, P., Machado, J., Bonferoni, C., Rossi, S., Salcedo, I., Viseras, C., 2013b. Networking and rheology of concentrated clay suspensions “matured” in mineral medicinal water. *Int. J. Pharm.* 453, 473–479. <https://doi.org/10.1016/j.ijpharm.2013.06.002>
- Cerezo, P., Aguzzi, C., Viseras, C., 2013. Desarrollo galénico de peloides terapéuticos, in: Agencia Estatal de Tecnologías Sanitarias, A. (Ed.), *Peloterapia: Aplicaciones Médicas y Cosméticas de Fangos Termales*. BOE, Madrid, pp. 129–134.
- Cultrone, G., Linares, L., Cerezo, P., Aguzzi, C., Sebastián, E., Viseras, C., 2003. Estudio de filosilicatos naturales para su uso en farmacia. I. Caracterización mineralógica y textural, in: *IV Congreso SEFIG*.
- Larese, F., Gianpietro, A., Venier, M., Maina, G., Renzi, N., 2007. In vitro percutaneous absorption of metal compounds. *Toxicol. Lett.* 170, 49–56. <https://doi.org/10.1016/j.toxlet.2007.02.009>
- López-Galindo, A., Viseras, C., 2004. Pharmaceutical and cosmetic application of clays, in: Wypyc, F., Satyanarayana, K.G. (Eds.), *Clay Surfaces: Fundamentals and Applications*. Elsevier Ltd, pp. 267–289.
- Mascolo, N., Summa, V., Tateo, F., 1999. Characterization of toxic elements in clays for human healing use. *Appl. Clay Sci.* 15, 491–500. [https://doi.org/10.1016/S0169-1317\(99\)00037-X](https://doi.org/10.1016/S0169-1317(99)00037-X)
- Rebelo, M., Viseras, C., López-Galindo, A., Rocha, F., da Silva, E.F., 2011a. Rheological and thermal characterization of peloids made of selected Portuguese geological materials. *Appl. Clay Sci.* 52, 219–227. <https://doi.org/10.1016/j.clay.2011.02.018>
- Rebelo, M., Viseras, C., López-Galindo, A., Rocha, F., da Silva, E.F., 2011b. Characterization of Portuguese geological materials to be used in medical hydrology. *Appl. Clay Sci.* 51, 258–266. <https://doi.org/10.1016/j.clay.2010.11.029>
- Sánchez-Espejo, R., Cerezo, P., Aguzzi, C., López-Galindo, A., Machado, J., Viseras, C., 2015. Physicochemical and in vitro cation release relevance of therapeutic muds “maturation”. *Appl. Clay Sci.* 116–117, 1–7. <https://doi.org/10.1016/j.clay.2015.08.007>
- Summa, V., Tateo, F., 1999. Geochemistry of two peats suitable for medical uses and their behaviour during leaching. *Appl. Clay Sci.* 15, 477–489. [https://doi.org/10.1016/S0169-1317\(99\)00036-8](https://doi.org/10.1016/S0169-1317(99)00036-8)
- Summa, V., Tateo, F., 1998. The use of pelitic raw materials in thermal centres: Mineralogy, geochemistry, grain size and leaching tests. Examples from the Lucania area (southern Italy). *Appl. Clay Sci.* 12, 403–417.

- [https://doi.org/10.1016/S0169-1317\(97\)00024-0](https://doi.org/10.1016/S0169-1317(97)00024-0)
- Tateo, F., Ravaglioli, A., Andreoli, C., Bonina, F., Coiro, V., Degetto, S., Giaretta, A., Menconi Orsini, A., Puglia, C., Summa, V., 2009. The in-vitro percutaneous migration of chemical elements from a thermal mud for healing use. *Appl. Clay Sci.* 44, 83–94. <https://doi.org/10.1016/j.clay.2009.02.004>
- Tateo, F., Summa, V., 2007. Element mobility in clays for healing use. *Appl. Clay Sci.* 36, 64–76. <https://doi.org/10.1016/j.clay.2006.05.011>
- Van Lierde, V., Chéry, C.C., Roche, N., Monstrey, S., Moens, L., Vanhaecke, F., 2006. In vitro permeation of chromium species through porcine and human skin as determined by capillary electrophoresis–inductively coupled plasma–sector field mass spectrometry. *Anal. Bioanal. Chem.* 384, 378–384. <https://doi.org/10.1007/s00216-005-0226-z>
- Viseras, C., Aguzzi, C., Cerezo, P., 2015. Medical and health applications of natural mineral nanotubes, in: Pasbakhsh, P., Churchman, G.J. (Eds.), *Natural Mineral Nanotubes: Properties and Applications*. Apple Academic Press, Inc., Oakville, pp. 437–448.
- Viseras, C., Aguzzi, C., Cerezo, P., López-Galindo, A., 2007. Uses of clay minerals in semisolid health care and therapeutic products. *Appl. Clay Sci.* 36, 37–50. <https://doi.org/10.1016/j.clay.2006.07.006>
- Viseras, C., Cerezo, P., Meeten, G., Lopez-Galindo, A., 2001. One-dimensional filtration of pharmaceutical grade phyllosilicate dispersions. *Int. J. Pharm.* 217, 201–213. [https://doi.org/10.1016/S0378-5173\(01\)00606-8](https://doi.org/10.1016/S0378-5173(01)00606-8)
- Viseras, C., Cerezo, P., Mirchandani, J.N., Aguzzi, C., López-Galindo, A., 2006a. Efecto de la maduración en las propiedades reológicas de hidrogeles empleados en balnearios españoles e influencia en la mineralogía y textura del componente arcilloso., in: Suárez, M., Vicente, M.A., Ribes, V., Sánchez, M.J. (Eds.), *Materiales Arcillosos: De La Geología a Las Nuevas Aplicaciones*. University of Salamanca, Salamanca, pp. 279–290.
- Viseras, C., Cultrone, G., Cerezo, P., Aguzzi, C., Baschini, M.T., Vallés, J., López-Galindo, A., 2006b. Characterisation of northern Patagonian bentonites for pharmaceutical uses. *Appl. Clay Sci.* 31, 272–281. <https://doi.org/10.1016/j.clay.2005.11.002>
- Viseras, C., López-Galindo, A., 1999. Pharmaceutical applications of some spanish clays (sepiolite, palygorskite, bentonite): some preformulation studies. *Appl. Clay Sci.* 14, 69–82. [https://doi.org/10.1016/S0169-1317\(98\)00050-7](https://doi.org/10.1016/S0169-1317(98)00050-7)

3.1. Objetivos de la Tesis

Chapter 4

Fibrous Clays in Wound Healing

4.1. Design and Characterization of Spring Water Hydrogels with Natural Inorganic Excipients

Prólogo

Este capítulo se corresponde con el corazón del presente proyecto de tesis, en el que se abordan los resultados y discusión de los estudios realizados sobre arcillas fibrosas (sepiolita y palygorskita) como ingredientes en la preparación de formulaciones semisólidas con aguas mineromedicinales naturales.

El primer paso fue la caracterización al estado sólido de las muestras de arcilla en estudio junto con las formulaciones semisólidas preparadas. Especial atención se presta a la pureza de las arcillas y al comportamiento reológico y estabilidad de las formulaciones semisólidas.

En la siguiente fase del estudio se evalúa la biocompatibilidad y la actividad terapéutica en la curación de heridas de las formulaciones previamente caracterizadas.

Por último, las dos últimas secciones están centradas en la composición y el intercambio de elementos químicos presentes en las formulaciones. En primer lugar la atención se centró en las impurezas elementales, entendidas éstas como la presencia de elementos tóxicos o potencialmente tóxicos, metales pesados, etc. En segundo lugar, y como broche de este proyecto de tesis, se estudió la liberación del resto de elementos químicos con potencial actividad terapéutica en la curación de heridas.

Cumpliendo con la normativa de formato de Tesis Doctoral especificado por la Escuela de Doctorado en Farmacia, los indicios de calidad de las publicaciones que conforman el siguiente capítulo son:

Sección 4.1.

García-Villén, F., Sánchez-Espejo, R., López-Galindo, A., Cerezo, P., Viseras, C. (2020). **Design and characterization of spring water hydrogels with natural inorganic excipients.** Applied Clay Science, 197, 105772. DOI: 10.1016/j.clay.2020.105772

Indicios de calidad de la publicación:

- Artículo científico
- Indexada en JCR: [APPL CLAY SCI](#)

4.1. Design and Characterization of Spring Water Hydrogels with Natural Inorganic Excipients

- Factor de impacto 2019: 4.605
- Ranking: Q1 (mineralogy).

Sección 4.2.

García-Villén, F., Faccendini, A., Miele, D., Ruggeri, M., Sánchez-Espejo, R., Borrego-Sánchez, A., Cerezo, P., Rossi, S., Viseras, C., Sandri, G. (2020).

Wound healing activity of nanoclay/spring water hydrogels. *Pharmaceutics*, 12(467), 1-24. DOI: 10.3390/pharmaceutics12050467

Indicios de calidad de la publicación:

- Artículo científico
- Indexada en JCR: [PHARMACEUTICS](#)
- Factor de impacto 2019: 4.421
- Ranking: Q1 (pharmacology & pharmacy).

Sección 4.3.

García-Villén, F., Sánchez-Espejo, R., Borrego-Sánchez, A., Cerezo, P., Perioli, L., Viseras, César (2020).

Safety of nanoclay/spring water hydrogels: assessment and mobility of hazardous elements. *Pharmaceutics*, 12(764), 1-17. DOI: 10.3390/pharmaceutics12080764

Indicios de calidad de la publicación:

- Artículo científico
- Indexada en JCR: [PHARMACEUTICS](#)
- Factor de impacto 2019: 4.421
- Ranking: Q1 (pharmacology & pharmacy).

Sección 4.4.

García-Villén, F., Sánchez-Espejo, R., Borrego-Sánchez, A., Cerezo, P., Cucca, L., Giuseppina S., Viseras, C. (2020).

Correlation between elemental composition/mobility and skin cell proliferation of fibrous nanoclay/spring water hydrogels. *Pharmaceutics*, 12(891), 1-20. DOI: 10.3390/pharmaceutics12090891

Indicios de calidad de la publicación:

- Artículo científico
- Indexada en JCR: [PHARMACEUTICS](#)
- Factor de impacto 2019: 4.421
- Ranking: Q1 (pharmacology & pharmacy).

Chapter 4. Fibrous Clays in Wound Healing



4.1. Design and Characterization of Spring Water Hydrogels with Natural Inorganic Excipients

The medicinal use of minerals by human cultures is as old as medicine itself and continues to be part of nature-derived medicines as well as western industrial medicinal products. In particular, the use of natural inorganic ingredients, such as clay minerals, in skin therapy goes back to prehistoric times. Clays are used as excipients in skin dosage forms such as pastes, poultices, liniments, lotions, suspensions, etc. For example, kaolin and bentonite are included in “titanium dioxide paste” and “calamine lotion”, respectively (USP42-NF37, 2019). Clay minerals act as abrasive, adsorbent, anticaking, opacifying agents, stabilizers, etc. Most recently, clays have also demonstrated crucial activities in the treatment of problematic skin pathologies (Sandri et al., 2016) and giving rise to the novel design of advanced skin-addressed drug delivery systems (Viseras et al., 2019).

Therapeutic muds are semisolid dosage forms composed of an inorganic and/or organic phase suspended in spring water (Mefteh et al., 2014; Khiari et al., 2019). Suspended solids of thermal muds can be natural sediments present in the spring water (natural muds) or, more frequently, solid ingredients incorporated to the spring water as formulation additives to obtain “artificial muds” (Rebelo et al., 2011a; Gomes et al., 2015). Both natural and artificial muds are used in spa centres for the treatment and control of musculoskeletal disorders and skin pathologies (Fioravanti et al., 2011, 2017; Fraioli et al., 2011; Forestier et al., 2016; Huang et al., 2018; Kiełczawa, 2018; Davinelli et al., 2019).

Although the mechanisms of action are not yet fully understood (Veniale et al., 2007), the effects are believed to be the result of a combination of mechanical, thermal and chemical factors (Fioravanti et al., 2011). Mechanical and thermal activities are mainly related to the structure and inorganic composition of the hydrogel and/or to the conditions of application (temperature, amount and time) (Sánchez-Espejo et al., 2014a; Drobnik and Stebel, 2020). Chemical effects have been ascribed to inorganic soluble complexes and ions (Tateo et al., 2009) together with organic components associated to the presence and growth of microorganisms (Quintela et al.,

2010; Pesciaroli et al., 2016; Drobniak and Stebel, 2020). The composition of the spring water is crucial for the therapeutic activity of thermal muds. Sulphurous spring waters have demonstrated to improve wound healing, due to their ability to reduce inflammation and to promote angiogenesis, particularly by increasing proliferation, migration and tube formation of the endothelial cells (Liu et al., 2014).

The preparation of artificial thermal muds also allow studying and comparing the performances of different solid phases. Traditionally, smectites such as montmorillonite and kaolinite have been used as the main inorganic phases of artificial muds. Nonetheless, fibrous clay minerals such as sepiolite and palygorskite have played a secondary role in balneotherapy, as shown by the scarce scientific literature. Recently, Pozo and co-workers (Pozo et al., 2018, 2019) have compared sepiolite with montmorillonite, finding a better performance of the fibrous clay mineral over the layered one in balneotherapy. The high specific surface area of fibrous clay minerals makes them able to adsorb and retain high amounts of water. This has a valuable economic impact in balneotherapy, since low amount of solid phase is able to carrier a large amount of spring water in form of a semisolid system. Moreover, fibrous clay minerals have demonstrated to adsorb and retain a wide variety of substances, which make them potential active ingredients intended to treat the skin (elimination of skin impurities) and infected wounds (by adsorption of microorganisms and toxins), among others.

Thermal muds formulations currently fail to be designed and produced following quality standards that assure a consistency of their composition and effects, partly because of the absence of specific regulation or guidelines. In recent years, some attempts have been done to establish the optimal properties of these therapeutic muds (Baschini et al., 2010; Karakaya et al., 2010; Sánchez-Espejo et al., 2014a; Modabberi et al., 2015; Khiari et al., 2019; Carretero, 2020). It is advisable that artificial muds should be designed, prepared and controlled by spa centres following normalized protocols (Gomes and de Sousa, 2018).

With these premises, the aim of this paper was to design and characterize hydrogels with sulphurous water and selected clay minerals under a “pharmaceutics” perspective; i.e., with reproducible product quality

that results in a safe and efficacious dosage form (Moraes et al., 2017). To comply with the scientific and technological aspects of the design and manufacture of semisolid clay/mineral water products, two commercial fibrous clay minerals (sepiolite and palygorskite) were fully solid-state characterized and then used to manufacture hydrogels with two spring waters. The resultant semisolid compounds were characterized and controlled by means of rheology, cooling rate, pH and water content.

4.1.1. Materials and Methods

4.1.1.1. Materials

Pangel S9 (PS9) and Cimsil G30 (G30) were kindly gifted by TOLSA (Madrid, Spain). PS9 and G30 were mainly composed by sepiolite and palygorskite, respectively. Their corresponding pharmacopoeial denominations are “Magnesium trisilicate” (PS9) and “Attapulgit” (G30) (Ph.Eur.9th, 2018a,b; USP42-NF37, 2019). Both excipients were dried in oven at 40 °C for at least 48 h prior to be used.

Spring waters from Graena spa (GR) and Alicún spa (ALI), Granada (Spain) were used. According to their properties, these spring waters are classified as hypothermal (ALI) and hyperthermal (GR), both of them having a strong mineralization (Maraver Eyzaguirre and Armijo de Castro, 2010).

4.1.1.2. Characterization of Solids

X-ray powder diffraction analysis (XRPD) of PS9 and G30 were carried out using a PANalytical diffractometer, X'Pert Pro model, equipped with an X'Celerator solid-state detector and a spinning sample holder. The diffractogram patterns were recorded using random oriented mounts with CuK α radiation, operating at 45 kV and 40 mA, in the range 4–70 °2 θ (0.008 °2 θ step size, 9.73 s as scan step time). Oriented aggregates were also performed with PANalytical diffractometer in the very same operating conditions previously mentioned (45 kV, 40 mA, step size: 0.008 °2 θ ; scan step time: 9.73 s). Particularly, glycolated oriented aggregates were analysed from 3 to 30 °2 θ , while air dried and 550 °C-heated oriented aggregates were obtained from 4 to 50 °2 θ . Compositional study of PS9 and G30 was complemented by chemical X-Ray fluorescence analysis (XRF). XRF of clay

minerals were performed using a Bruker® S4 Pioneer equipment, with an Rh anode X-ray tube operating at 60 kV and 150 mA.

Fourier-Transform Infrared spectroscopy (FT-IR) spectra of PS9 and G30 were obtained with a JASCO 6200 apparatus equipped with an ATR accessory. All analyses were performed from 400 to 4000 cm^{-1} with a resolution of 2 cm^{-1} and results processed with Spectra Manager v2 software in transmittance units.

Shimadzu (mod. TGA-50H) calorimeter was used to perform thermogravimetric analysis (TGA), equipped with a vertical oven and a precision of 0.001 mg. Approximately 40 mg of each sample were weighted in aluminium sample crucibles (capacity 70 μL). The experiments were performed in 30–950 $^{\circ}\text{C}$ range, atmospheric air (50 mL/ min) and a heating rate of 10 $^{\circ}\text{C}/\text{min}$. Differential Scanning Calorimetry (DSC) was performed with a Mettler Toledo (DSC1) apparatus equipped with a FRS5 sensor. In this case, approximately 7 mg of clay mineral samples were weighted in aluminium sample crucibles (40 μL). They were evaluated from 26 $^{\circ}\text{C}$ to 400 $^{\circ}\text{C}$ at 10 $^{\circ}\text{C}/\text{min}$ in atmospheric air (50 mL/min).

Scanning electron microscopy (SEM) of particles textures and their aggregates were performed with a GEMINI (FESEM) CARL Zeiss coupled to an EDX microanalyser (Oxford Instruments). Samples were dried at 40 $^{\circ}\text{C}$ for a minimum of 48 h. Then, powdery samples were mounted over standard aluminium stubs and coated with carbon. Textural microphotographs were obtained at 3 kV, while EDX were acquired at 15 kV. In both cases, immersion lens detector was used (InLens, Zeiss).

4.1.1.3. Characterization of Liquids

Values of pH and conductivity of GR and ALI were controlled at room temperature. pH was studied by a Crison BASIC 20 pH-meter equipped with an electrode intended for dissolutions and at 20 ± 0.5 $^{\circ}\text{C}$. Conductivity was determined at 28 ± 0.15 $^{\circ}\text{C}$ by using a Mettler Toledo (FiveGo F3). Six replicates were collected for both pH and conductivity.

Major cations (Na, Ca, K and Mg) of ALI and GR were determined by ICP-OES (Perkin Elmer ICP-OES 3300DV). More particularly, prior to any

ICP-OES determination, calibration curves were obtained for each element by using standardized patterns (concentration 1000 ppm for all of them).

The presence of trace elements (As, Ba, B, Cd, Cu, Cr, Fe, Mn, Pb, Sb, Hg, Ni, Se, I, Li, Rb, Zn, Co and U) in ALI and GR were determined by a PerkinElmer ELAN DRCe inductively coupled plasma mass spectrometer (ICP-MS). These analytes were measured by using both standard and dynamic reaction cell (DRC). Quantification was carried out with an external calibration method. Standard reference calibration solutions were obtained by dilution of certified multielement stock solutions with ultra-purified water (Milli-Q® water) 1, 5, 10, 100 µg/L for ICP-MS.

4.1.1.4. Preparation of Inorganic Hydrogels

The effect of solid concentration and agitation was studied in a preliminary experiment. Four solid/water concentrations (5, 10, 15 and 20% w/w), three agitation times (1, 5 and 10 min) and three rotor speeds (1000, 5000 and 8000 rpm) provided by a turbine high-speed agitator (Silverson LT, United Kingdom) were tested. Rheological measurements were performed onto the resultant suspensions by a controlled rate viscometer (Thermo Scientific HAAKE, RotoVisco 1) equipped with a plate/plate combination (Ø 20 mm serrated PP20S sensor system). Temperature was maintained constant during the whole experiment at 25 °C (± 0.5 °C) by means of a Peltier temperature controller. Rheological properties of hydrogel samples were measured within the shear rate range of 70–800 s⁻¹. Apparent viscosities of the suspensions were taken at 250 s⁻¹. The results were used to select the best optimal solid concentration and agitation energy that would allow comparisons among the two inorganic excipients. Apparent viscosities and agitation energies were correlated following a previous work (Viseras et al., 1999). The solid concentration and agitation conditions allowing measurable, reproducible and comparable viscosity values were selected for the subsequent studies (10% w/w, 8000 rpm, 10 min).

The selected concentrations were prepared by suspension of 25 g of solids (PS9 or G30) in 225 mL of liquid (GR or ALI), obtaining a final concentration of 10% (w/w) (Table 4.1).

Table 4.1. Composition of prepared hydrogels with a final concentration of 10% (w/w)

Clay mineral	Spring water	Hydrogel code
PS9	ALI	PS9ALI
	GR	PS9GR
G30	ALI	G30ALI
	GR	G30GR

The dispersions were firstly homogenized by a glass rod in order to disaggregate solid lumps. Then, hydrogels were prepared with a turbine high-speed agitator (Silverson LT, United Kingdom). The agitator was equipped with a high-traction stirrer head of square mesh performing at 8000 rpm for 10 min. Polyethylene containers were used to preserve the aforementioned hydrogels in static conditions at room temperature.

4.1.1.5. Characterization of Hydrogels

Thermal Properties

Experimental and theoretical thermal parameters of the prepared hydrogels were obtained by the following procedure, previously described and used by Sánchez-Espejo and co-workers (Sánchez-Espejo et al., 2015). Known amounts of each hydrogel was weighed and conditioned at 50 °C inside polyethylene terephthalate cells and subsequently immersed in a thermostatic bath at 25 °C. While inside the bath, the temperature of the sample was monitored by a thermometric probe located in the middle of the cell until it reached approximately 32 °C (normal skin temperature). The resultant experimental data were fitted by using the Newton law (Eq. 4.1, already mentioned in chapter 1) which described the transmission of temperature between two bodies in contact. In this equation, T_{min} represents the room temperature (25 °C), T_{max} is the initial temperature (50 °C), t is the time in minutes the constant k depends on the material and apparatus used, given by Eq. (4.2).

$$(T - T_{min}) = (T_{max} - T_{min})e^{-kt} \quad \text{Eq. 4.1}$$

$$k = \frac{P}{C} = \frac{P}{mC_p} \quad \text{Eq. 4.2}$$

As a reminder, in Eq. 4.2, P is the instrumental constant of the apparatus, C the heat capacity of the heated material, m the heated mass and

C_p the specific heat. The apparatus constant (P) was obtained by fitting the cooling data obtained with a known amount of a reference water dispersion of TiO_2 . Experimental and calculated T_{20min} and $t_{32^\circ\text{C}}$ results were used to study hydrogels thermal properties. T_{20min} indicates the actual temperature of the analysed hydrogel after 20 min (usually the duration of treatments) and $t_{32^\circ\text{C}}$ indicates the time that takes the hydrogel to equal the temperature of the skin. These analyses were performed over the prepared hydrogels at different times, including time after 48 h, 6 and 12 months.

Rheological Studies

Rheological measurements were performed by a controlled rate viscometer (Thermo Scientific HAAKE, RotoVisco 1) equipped with a plate/plate combination (\varnothing 20 mm serrated PP20S sensor system). Temperature was maintained constant during the whole experiment at 25°C ($\pm 0.5^\circ\text{C}$) by means of a Peltier temperature controller. Rheological properties of hydrogel samples were measured within the shear rate range of $70\text{--}800\text{ s}^{-1}$. The measurement interval was chosen to simulate typical stresses that may suffer these systems when used: $70\text{--}200\text{ s}^{-1}$ (skin spreading), $100\text{--}200\text{ s}^{-1}$ (manual mixing) and $400\text{--}2000\text{ s}^{-1}$ (container removal) (Schott, 1995). Rheological characterization was performed just after their preparation (time 0) and after 48 h. Characterization was also done after 1, 2, 6 and 12 months. Data were collected and processed by the HAAKE RheoWin software. Six replicates were obtained for each sample. Rheological characterization included flow curves, apparent viscosity taken at 250 s^{-1} , hysteresis area and yield stress. Hysteresis area was obtained by calculating the inner space between the upper and lower flow curves. Yield stress values were obtained by modelling upper flow curves according to Bingham, Casson and Herschel–Bulkley models (dynamic yield stress) or, if possible, by experimental spur points (if presents). Fitting of models was performed by using Excel's Solver tool. The goodness-of-fit of the data to each model was evaluated and described by correlation coefficient R^2_{adjusted} (Eq. 4.3 and Eq. 4.4), which is used when models with different number of parameters are being compared. In these equations, z are the predicted values, y_i are the experimental data, n accounted for the number of data points (sample size) and p is the number of parameters determined on each model.

$$R^2 = \frac{\sum_{i=1}^n (z - \bar{y}_i)^2}{\sum_{i=1}^n (y_i - \bar{y}_i)^2} \quad \text{Eq. 4.3}$$

$$R_{adjusted}^2 = 1 - \frac{(n-1)}{(n-p)} (1 - R^2) \quad \text{Eq. 4.4}$$

pH and Water Content Measurements

All hydrogels prepared were monitored in terms of pH and water content in order to detect possible changes associated with their stability. Both water content and pH were controlled at time 0, after 48 h and after 1, 2, 6 and 12 months. Particularly, pH was studied by a pH-meter Crison pH 25+ equipped with a semisolid electrode (5053T). Eight replicates were collected for each sample. The water content of the hydrogels was controlled by a gravimetric method consisting of weighting a known amount of hydrogel (approximately 1 g). Then the weighted amount was dried in an oven at 40 °C until the dry weight was found stable. Three replicates were performed for each sample.

4.1.1.6. Statistical Analysis

One-way analysis of variance (ANOVA) with post-hoc Scheffé and Bonferroni tests for multiple comparisons were used by means of SPSS Statistic software (USA). Differences between groups were considered significant when p -value were ≤ 0.05 .

4.1.2. Results and Discussion

4.1.2.1. Characterization of Solids

Identity, Purity and Richness

X-ray powder diffraction pattern of PS9 showed the typical diffraction pattern of the mineral sepiolite. No other crystalline mineral phases were detectable with this analysis, thus demonstrating this sample to be highly pure (Figure 4.1, up). On the other hand, diffraction pattern of G30 sample corresponded majorly with palygorskite, although in this case other mineral phases were also detected, such as quartz, fluorapatite, calcite and sepiolite. The presence of impurities in natural excipients must be controlled and quantified as they may bring potential concerns.

4.1. Design and Characterization of Spring Water Hydrogels with Natural Inorganic Excipients

XRF results complemented XRPD results. The typical composition of sepiolite does not include Al_2O_3 nor K_2O . Nonetheless, these oxides were detected by XRF analysis of PS9 sample. These elements were also detected by other studies in which PS9 was characterized, though no further explanations were given (Carmona et al., 2018). The presence of muscovite impurities in the sample could explain aluminium and potassium oxide results produced by PS9's XRF. Furthermore, diffraction pattern of muscovite allowed the total explanation of PS9 diffraction peaks, such as the intensity of the reflections at 19.75 and 34.32 $^{\circ}2\theta$ (Figure 4.1, up).

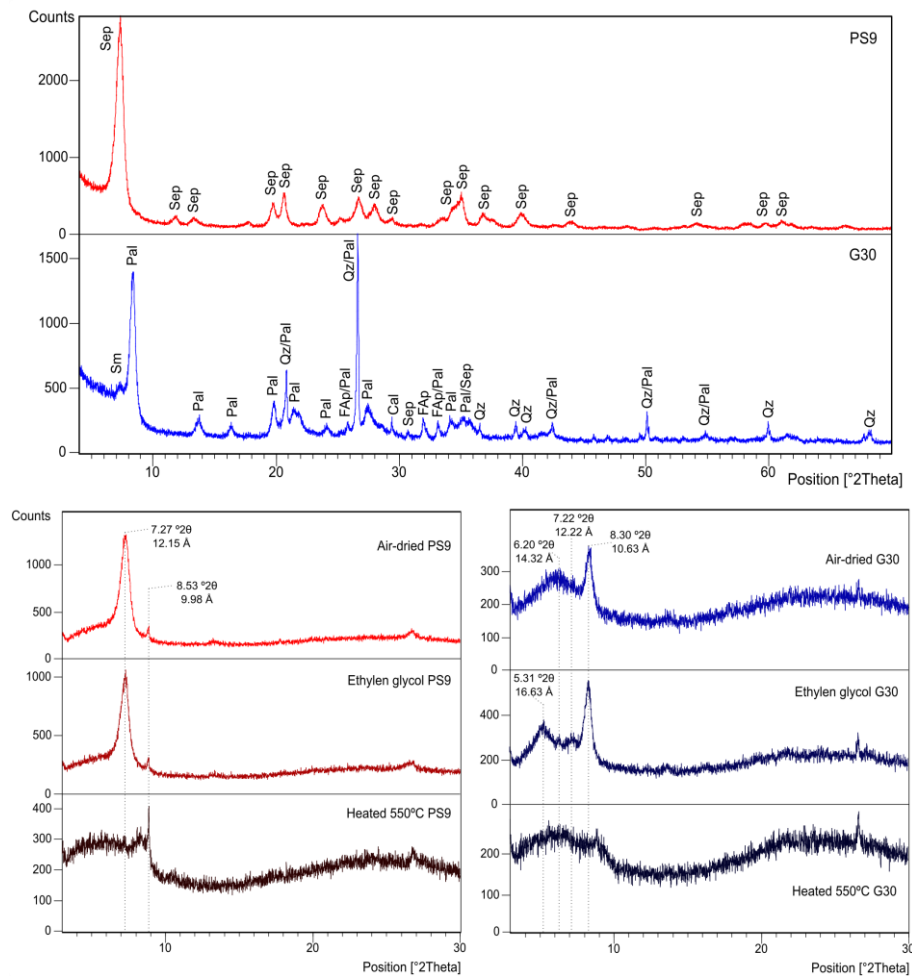


Figure 4.1. XRPD patterns and oriented mounts X-ray patterns of PS9 and G30. Sep: sepiolite; Pal: palygorskite; Qz: quartz; FAp: fluorapatite; Sm: smectite

The presence of fluorapatite in G30 can be supported by a ~3% of P₂O₅ detected in XRF results of G30 (Table 4.2). In the same way, the presence of CaO detected in G30's XRF allowed to confirm calcite presence. Both solids showed LOI values around 10%. FT-IR and thermal analysis were used to discern the nature (water and/or organic components) of this mass loss.

Oriented mounts of PS9 are plotted in Figure 4.1, down. Diffraction peak at 7.27 °2θ (12.15 Å) was present both in air dried and glycolated oriented mounts, the intensity being higher for the former one, meaning the evaluated sample did not possess smectite mineral phases (which would have swelled in presence of ethylene glycol). When the aforementioned oriented mount was heated at 550 °C, the diffraction peak at 7.27 °2θ was destroyed, evolution which coincided to sepiolite clay mineral presence. An additional reflection was found at 8.53 °2θ (9.98 Å), which maintained constant in the three oriented mounts analyzed (air dried, glycolated and heated at 550 °C). This evolution was in agreement with illite (and/or mica), muscovitic mineral phases. Although glauconite, celadonite and biotite could also be related with this diffraction peak, the characterization previously done (XRPD of randomly oriented powder and XRF) allowed to identify it as muscovite. Consequently, PS9 was composed of sepiolite (~91.5% w/w) and muscovite (~8.5% w/w) and corresponds to "Magnesium silicate" (USP42-NF37, 2019) or "Magnesium trisilicate" monographs (Ph.Eur.9th., 2018b; USP42-NF37, 2019).

Table 4.2. XRF results of PS9 and G30

Oxide	PS9	G30
SiO ₂ (%)	59.645	59.578
Al ₂ O ₃ (%)	3.435	8.324
Fe ₂ O ₃ (%)	1.054	4.024
MnO (%)	0.022	0.027
MgO (%)	22.435	8.411
CaO (%)	0.56	5.279
Na ₂ O (%)	0.139	0.176
K ₂ O (%)	0.952	0.356
TiO ₂ (%)	0.148	0.382
P ₂ O ₅ (%)	0.057	2.868
LOI (%)	10.7	9.94

G30 X-ray oriented mounts (Figure 4.1, down) confirmed the presence of palygorskite as the main mineral phase, since the diffraction at 8.37 °2θ

maintained symmetrical until the application of temperature (550 °C), which produced its collapse. At first sight, the diffraction peak at 7.32 °2θ in G30's randomly oriented mount (Figure 4.1, down), could be related to sepiolite. Nevertheless, oriented mounts showed a swelling process typical of laminar clay minerals. More particularly, there is a small diffraction with a maximum detected at 6.20 °2θ. This diffraction expanded to 5.31 °2θ in the glycolated oriented mount, collapsing when heated at 550 °C. Nonetheless, the presence of sepiolite cannot be discarded due to a small diffraction at 7.22 °2θ present in air-dried and glycolated sample. In G30 sample, quantitative calculations according to XRF and oriented mounts results showed that fluorapatite accounted for ~7.0% (w/w) and calcite was present in a ~3.0% w/w. Quartz reported to be a 26.0% (w/w), smectites and sepiolite accounted for ~6.0% (w/w) and the rest of G30 sample was identified as palygorskite ~58.0% (w/w). Pharmaceutical grade "Attapulgites" shows palygorskite amounts around 60% w/w, in agreement with previous studies (Viseras et al., 1999) and the aforementioned results. G30 is, therefore, a usual "Attapulgite" excipient as included in USP 42-37, 2019 and Ph. Eur. 9th (2018a,b). On the other hand, as regarding the use in medical hydrology, quartz and carbonate minerals have been traditionally used in some thermal centres (Mihelčić et al., 2012) and the world-famous Dead Sea "black mud" is composed by > 60% of carbonate minerals (Nissenbaum et al., 2002).

FT-IR spectra (Figure 4.2) showed vibrational bands of sepiolite (PS9) and palygorskite (G30), respectively (McKeown et al., 2002; Chukanov and Chervonnyi, 2016). The two most intense bands for both samples (1003, 969 cm⁻¹ for PS9 and 1012 and 974 cm⁻¹ for G30) are due to Si-O stretching vibrations. A band at about 1200 cm⁻¹ due to Si-O-Si bonds between alternative ribbons (periodical inversion of apical oxygen in tetrahedral happening in fibrous clay minerals which is not present in other clay minerals) (Mendelovici, 1973; Alkan et al., 2005). Additionally, fingerprint region of both samples (1200–400 cm⁻¹) coincided with those of sepiolite and palygorskite (Chukanov and Chervonnyi, 2016). Calcite presence in G30 was confirmed by the small band at 1431 cm⁻¹ (the most intense one of calcite infrared spectrum) (Suárez and García-Romero, 2006). Fluorapatite, quartz and sepiolite were not detected in infrared results due to their low amount

overlapping of vibrational bands with those of palygorskite. Al–Al–OH deformation appears in G30 at 912 cm^{-1} due to the dioctahedral character of palygorskite. The intensity of this vibrational band varies between palygorskites since it is directly related to aluminium content (Madejová and Komadel, 2001).

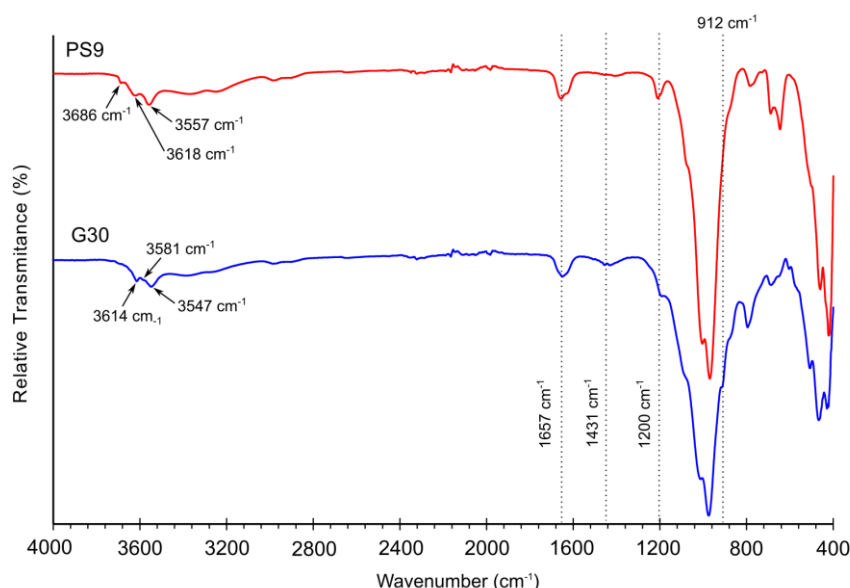


Figure 4.2. FT-IR transmittance spectra of clay mineral samples PS9 and G30

XRF results showed LOI values whose nature (water and/or organic components) needed to be clarified. FT-IR spectra (Figure 4.2) showed lack of vibrational bands in the region of C–C vibrations, confirming the absence of organic matter. O–H bending modes produced by adsorbed and zeolitic water create two bands at 1657 and 1625 cm^{-1} in sepiolite (PS9), while for palygorskite (G30) the aforementioned bands are unresolved, showing just a single band at 1650 cm^{-1} . Bands located between 3700 and 3200 cm^{-1} can be assigned to water OH groups stretching, including Al₂–OH and Fe/Al–OH, Al/Mg–OH, Fe/Mg–OH and Fe₂–OH (Frost and Ding, 2003; Mora et al., 2010). The small shoulder at 3581 cm^{-1} , present in G30 and absent in PS9, has been ascribed to coordinated water present within fibrous clay mineral channels (Augsburger et al., 1998). Nonetheless, some studies revealed a possible correlation between the detection and intensity of this band and the presence of Fe (Al–Fe–OH stretching) in palygorskite structure (Chahi et al., 2002;

4.1. Design and Characterization of Spring Water Hydrogels with Natural Inorganic Excipients

Suárez and García-Romero, 2006). The latter statement was in agreement with G30 chemical composition (Table 4.2), since Fe was detected in higher amount in comparison with PS9. The band at 3680 cm^{-1} in PS9 can be ascribed to 3 Mg-OH due to hydroxyls in the octahedral sheet (Alkan et al., 2005).

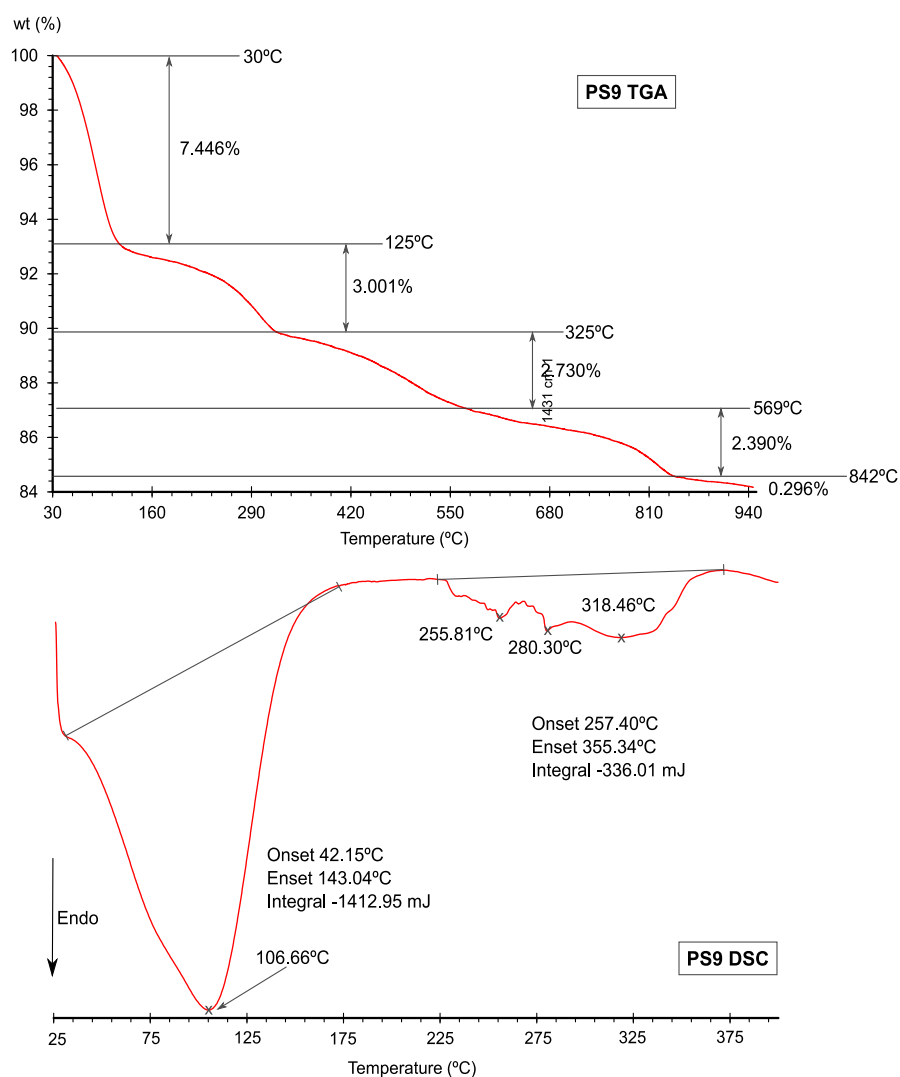


Figure 4.3. Thermogravimetric analyses of PS9. Corresponding TGA (up) and DSC curve (down)

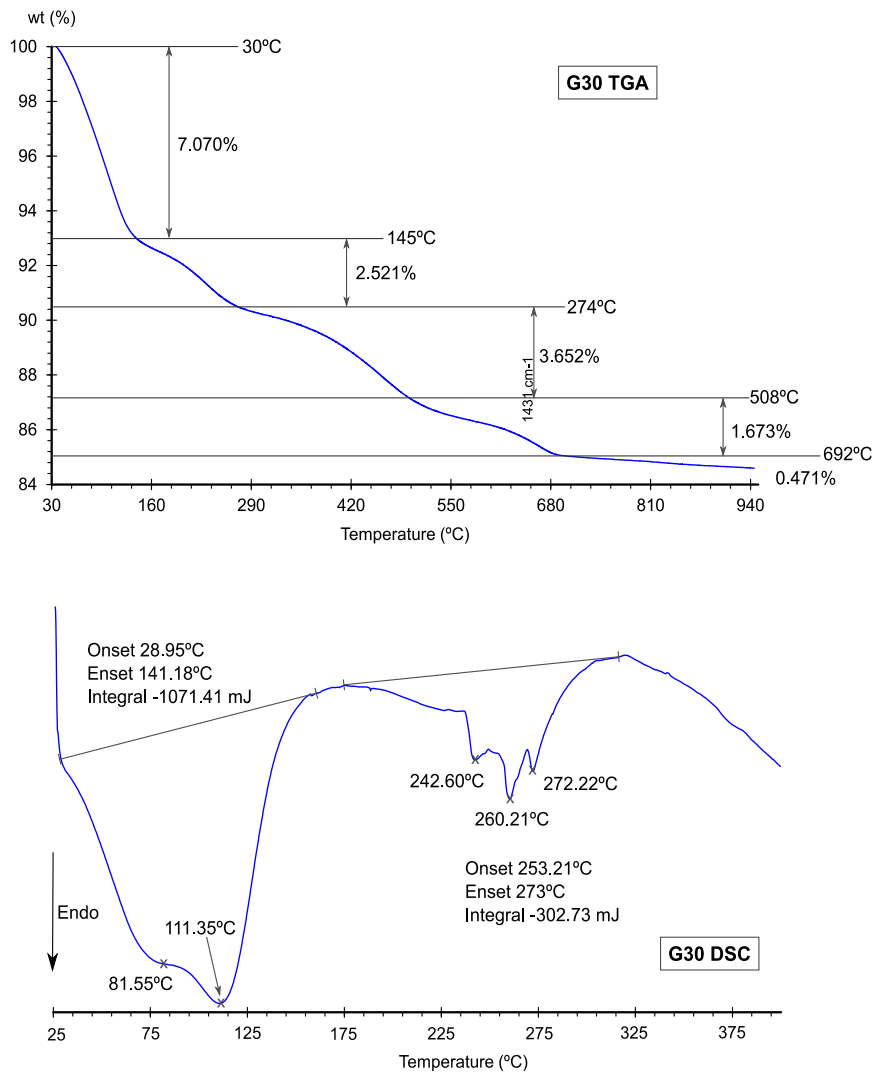


Figure 4.4. Thermogravimetric analyses of G30. Corresponding TGA (up) and DSC curve (down)

4.1. Design and Characterization of Spring Water Hydrogels with Natural Inorganic Excipients

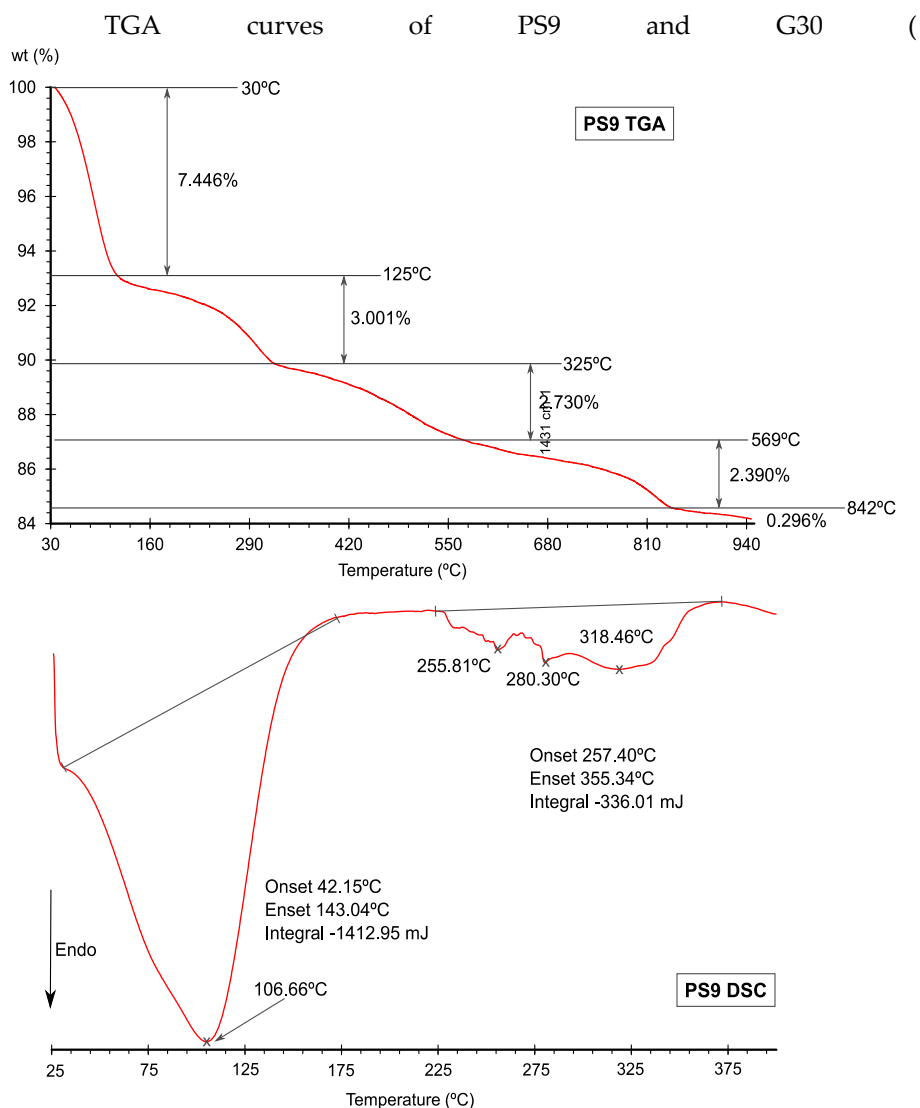


Figure 4.3 and 4.4) showed mass losses coinciding with those of typical of fibrous clay minerals (Földvári, 2011). The first weight loss corresponded to adsorbed water molecules and zeolitic water, usually called “free water”. Second and third steps corresponded to bound water weight losses (bound water I and II), also typical of fibrous clay minerals. Differential activation energies of water molecules present in unfolded open channels with those in folded ones, together with differential rates between separation and water diffusion processes explains why bound water evaporation occurs in two steps (Kiyohiro and Otsuka, 1989). Dehydroxylation and destruction of clay

mineral framework occurred from 500 °C to 950 °C (

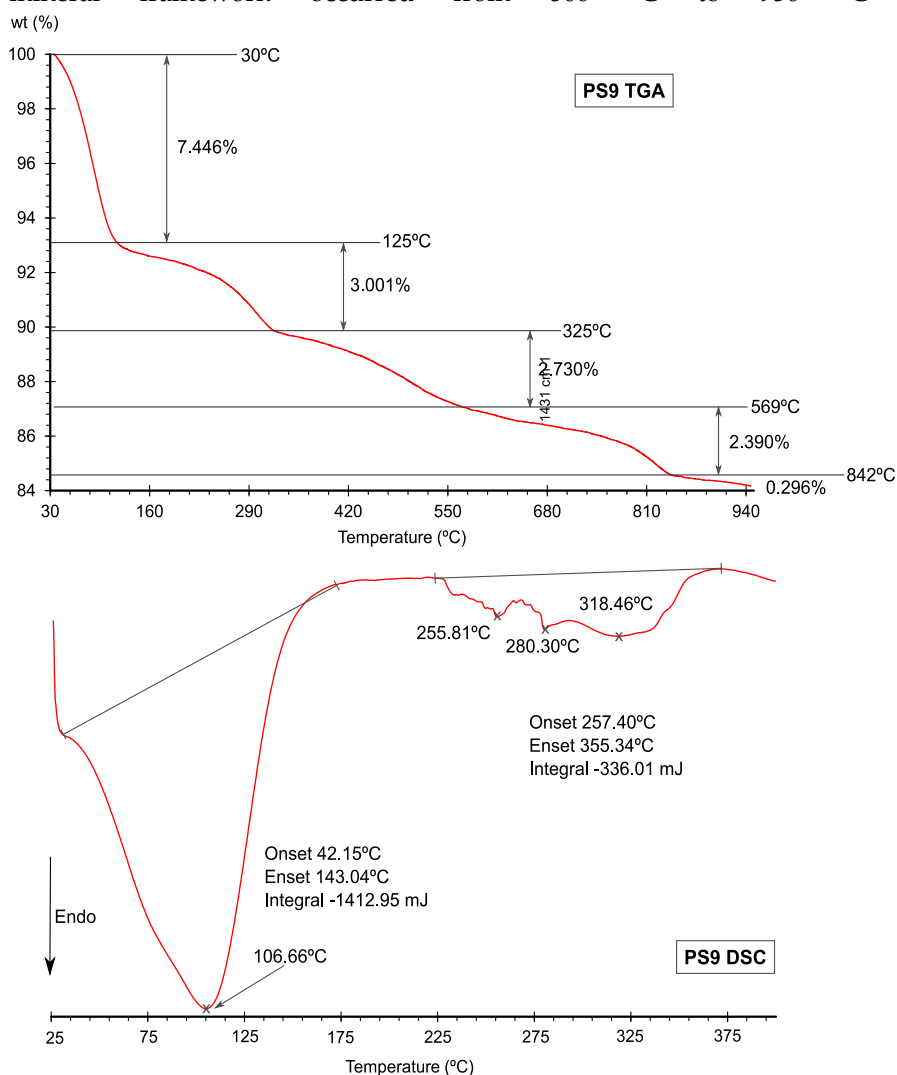


Figure 4.3 and 4.4) for both sepiolite and palygorskite. Dehydroxylation of PS9 occurred at higher temperature than for G30, due to higher amounts of magnesium in sepiolite structure (Shuali et al., 1988).

Regarding the presence of impurities in G30, quartz suffers a structural transition, from trigonal to hexagonal, which is detectable during thermogravimetric analyses. It occurs around 500 °C and it is accompanied by a slight weight loss. Minor amount of these impurities detected in G30, as well as the overlap of this step with palygorskite dehydroxylation made

impossible to discern its presence by thermal analysis. Calcite possesses a weight loss from 800 °C, maximum exothermic peak around 930 °C (Földvári, 2011), visible in the last part of the G30's TGA curve Figure 4.4. Fluorapatite thermal alterations happen at temperatures higher than 1000 °C and were not detected in the performed analyses (Tõnsuaadu et al., 2012).

Regarding DSC analyses, PS9 showed a first endotherm between 25 and 143 °C (

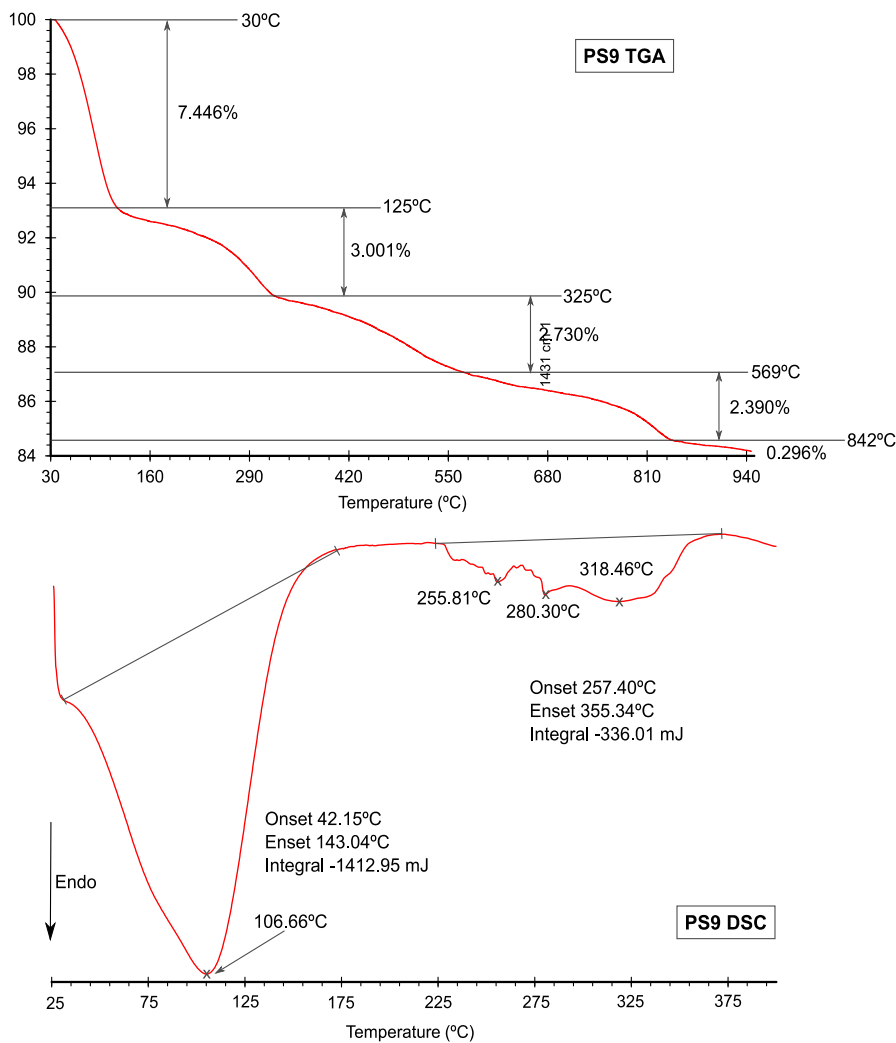


Figure 4.3). This step corresponds with evaporation of free water. The same profile was found for G30, with water loss step starting at 28 °C and finishing

at 141 °C (Figure 4.4). In both cases these endotherms coincided with the first weight loss in TGA, though it seemed to be formed of two overlapped endotherms, more marked in the case of G30 than in PS9. Since palygorskite and sepiolite lose these two types of water in this temperature range, the difference between them could explain the existence of two overlapped endotherms (Frost and Ding, 2003). The enthalpy of the aforementioned processes accounted for -1071.41 mJ for G30 and -1412.95 mJ. These results were in agreement with TGA results, in which the amount of weight loss is higher in PS9 (7.45% w/w) than in G30 (7.07% w/w). Second part of DSC in both PS9 and G30 also coincided with second weight loss in TGA analysis, though they are formed of different small endothermic steps (Földvári, 2011). Once again, the resultant calculated enthalpies were in agreement with weight losses indicated by TGA: -336.01 mJ (3.00% w/w) for PS9 and 302.73 mJ for G30 (2.52% w/w). As observed in previous studies with untreated sepiolites and palygorskites, temperatures for the removal of water for palygorskites are, in general, lower than for sepiolites.

According to thermal analysis results, sample PS9 comply with pharmacopoeial requirements for “Magnesium silicate” monograph (loss on drying 7.44% and loss on ignition 15.8% ≤ 17-34% required in the USP (USP42-NF37, 2019) and sample G30 with those requirements for “Attapulgit” monograph (loss on drying 7.07% ≤ 17.0% and loss on ignition 15.4% ≤ 15.0–27.0%) (Table 4.3).

Table 4.3. Thermal analyses for PS9 and G30 and normative limits (USP42-NF37 and/or Ph.Eur.9th 2018a,b)

	Thermal event	Interval (°C)	Weight loss (% w/w)	Pharmacopoeia Limits (% w/w)
PS9	Free water	30-125	7.4	Loss on drying ≤ 15
	Bound Water I	125-325	3.0	Loss on ignition ≤ 17.0-34
	Bound Water II	325-569	2.7	
	Dehydroxylation	569-940	2.7	
G30	Free water	30-145	7.1	Loss on drying ≤ 17.0
	Bound Water I	145-274	2.5	Loss on ignition ≤ 15.0-27.0
	Bound Water II	274-508	3.7	
	Dehydroxylation	508-940	2.1	

SEM microphotographs showed aggregates of particles in both samples (Figure 4.5), with PS9 aggregates mean sizes smaller than those of

G30. PS9 aggregates were formed of acicular particles (Figure 4.5B, D) composed by sepiolite (EDX analysis, Figure 4.5B). No other crystal habits were observed in this sample. G30 was a more heterogeneous sample. In Figure 4.5F fluorapatite particles were mixed with palygorskite acicular crystals (EDX spectra 2 and 3, respectively). The presence of carbonate minerals was also confirmed (Figure 4.5G). In particular, the rhombohedral particle seemed to correspond to dolomite in view of the high proportion of Ca and Mg (spectrum 4), even if calcite was the main carbonate detected in the mineralogical identification. Palygorskite fibers covering the crystal explained the detection of Si. Lastly, microphotograph 4H and spectrum 5 corresponded to quartz impurities, also detectable.

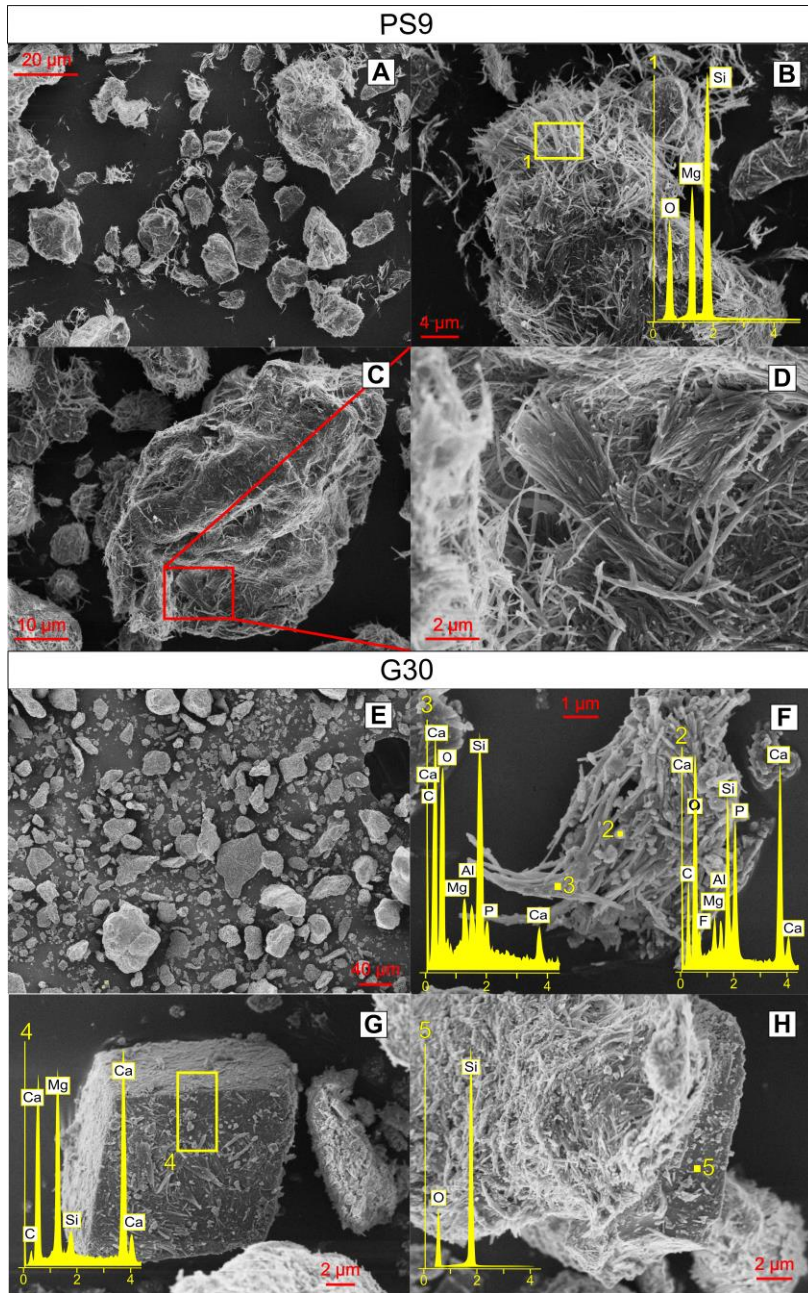


Figure 4.5. Microphotographs of PS9 and G30 with corresponding EDX analyses. A) General view of PS9; B) Sepiolite fibers; C) and D) Detail of aggregation of sepiolite fibers; E) General view of G30; F) Palygorskite fibers mixed with fluorapatite particles; G) Calcite crystals covered by palygorskite fibers; H) Quartz crystals covered by palygorskite fibers

4.1.2.2. Characterization of Spring Waters

pH and Conductivity

GR and ALI water samples presented pH and conductivity values summarized in Table 4.4. In terms of pH, both waters were very similar, being slightly alkaline. Regarding conductivity, GR showed to have higher conductivity than ALI (Table 4.4). The measured values were within the range of previous studies. It has been reported the conductivity of GR to be 1729.75 $\mu\text{S}/\text{cm}$ (20 °C) (Aguzzi et al., 2013), 3452 $\mu\text{S}/\text{cm}$ (25 °C) (Maraver Eyzaguirre and Armijo de Castro, 2010) and 2650 $\mu\text{S}/\text{cm}$. Regarding ALI, it has been reported to possess 3008 $\mu\text{S}/\text{cm}$ (25 °C) (Maraver Eyzaguirre and Armijo de Castro, 2010). Differences are due to the natural variability of spring waters and influence of temperature of measure.

Table 4.4. pH and conductivity results of spring waters employed in the study (mean values \pm s.d.; n=6)

	ALI	GR
pH \pm s.d.	7.90 \pm 0.047	8.02 \pm 0.082
Conductivity ($\mu\text{S}/\text{cm}$) \pm s.d.	2251.5 \pm 6.74	2465.5 \pm 8.89

Elemental Composition of Spring Waters

Main elements present in ALI and GR spring waters were Ca, Mg, Na and K (Table 4.5). Among minor/trace elements Zn and Li content highlighted for both of them (Table 4.5). It was also remarkable the difference in Mn content between ALI and GR (< 1 and 109 $\mu\text{g}/\text{L}$, respectively), though Rb, B, Ba, Sb, Ni, Se were also detected.

Ca, Mg, Na and K content of both ALI and GR waters were in agreement with previous studies (Maraver Eyzaguirre and Armijo de Castro, 2010; Prado-Pérez and Pérez del Villar, 2011). Since Alicún thermal system depends on two main hydrogeochemical processes, dedolomitization and CO₂ leakage (the former one involving Mg, Ca cations) (Prado-Pérez and Pérez del Villar, 2011), it was expectable to detect remarkable concentrations of these two elements in ALI spring water.

Table 4.5. Elemental composition of spring waters ALI and GR determined by ICP-OES and ICP-MS. (*) symbol indicates elements which presence in cosmetic products is limited according to European Regulation (EC 1223/2009)

	ALI	GR
Ca (mg/L)	348.00	460.00
Mg (mg/L)	109.0	88.00
Na (mg/L)	57.00	27.40
K (mg/L)	4.60	6.80
I (µg/L) *	<1	<1
Rb (µg/L)	5.0	18.0
Co (µg/L) *	<1	<1
Tl (µg/L) *	<1	<1
Al (µg/L) *	<1	<1
As (µg/L) *	<1	4.32
B (µg/L)	25.00	12.00
Ba (µg/L) *	18.80	13.00
Cd (µg/L) *	<1	<1
Cu (µg/L) *	<1	<1
Hg (µg/L) *	<0.5	<0.5
Mn (µg/L)	<1	108.66
Pb (µg/L) *	<1	<1
Li (µg/L) *	244.2	65.00
Sb (µg/L) *	<1	0.90
U (µg/L)	1.8	<1
Cr (µg/L) *	4.3	<1
Ni (µg/L) *	9.4	5.20
Fe (µg/L)	6.00	21.00
Se (µg/L) *	2.3	1.00

Elements considered essential or possibly essential for the human body, such as B, Li, Ni, Zn, Mn, Fe and Se, were present in both waters (Table 4.5). These elements particular concentration would determine a possible higher or lower absorption through the skin during thermal treatments. The presence of the elements marked in the table with (*) symbol are limited in cosmetic products according to the (EC 1223/2009). Nonetheless, in the very same regulation, traces of these elements would be allow if they are inevitable (because they are naturally present) and they do not compromise stability nor safety of the product. Further studies are needed in order to discern if these elements could be potentially absorbed through the skin, and their potential bioavailability.

4.1.2.3. Characterization of Hydrogels

Thermal Properties

Clay hydrogels are usually heated prior to their topical application to obtain thermotherapeutic effects, since the typical high specific heat values and low thermal conductivity of clays. Specific heats C_p together with T_{20min} and $t_{32^\circ C}$ values of the studied gels are summarized in Figure 4.6. These data were obtained by a linear regression of Eq. 4.2 ($R^2 > 0.99$, in all cases).

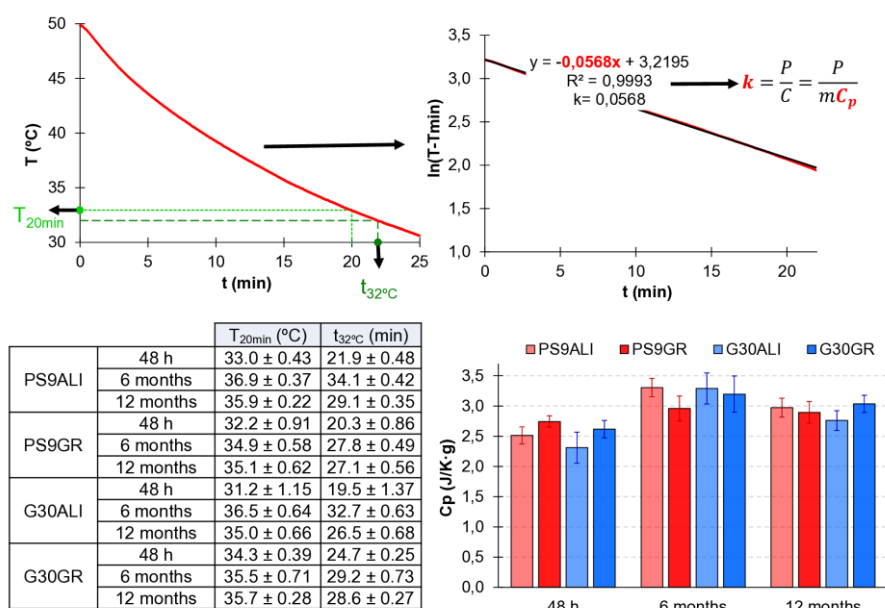


Figure 4.6. Thermal properties of hydrogels. Right: T_{20} (°C) and t_{32min} ; left: histogram of C_p (J/K·g) obtained from linear fitting (mean values \pm s.d.; $n=3$)

All studied hydrogels showed adequate thermal performances for topical application as thermotherapeutic agents, regardless of composition and time. In other words, all hydrogels had $t_{32^\circ C}$ values higher than 20 min and T_{20} values higher than 32 °C.

The thermal parameters obtained in this work were smaller than those measured with smectite-rich hydrogels (Sánchez-Espejo et al., 2015). The differences are ascribed to solid concentrations (50% w/w of smectite in Sánchez-Espejo and co-workers vs. 10% w/w of sepiolite or palygorskite in the present study). In fact, smectites performed lower cooling rates than

fibrous clay minerals suspensions when compared at similar solid/liquid ratios (Legido et al., 2007; Baschini et al., 2010; Karakaya et al., 2010; Glavaš et al., 2017).

Differences between hydrogels thermal performances at different times were found. C_p values slightly increased with time (48 h vs. 6 and 12 months; histogram, Figure 4.6). The changes did not affect the usefulness of the gels, as both T_{20min} and $t_{32^\circ C}$ were in all cases adequate for their use in thermotherapy.

Rheological Measurements

Flow curves (shear rate vs. shear stress) of hydrogels PS9ALI, PS9GR, G30ALI and G30GR are plotted in Figures 4.7 to 4.9. All the hydrogels behave as non-Newtonian, pseudoplastic materials. Rheological profiles of hydrogels prepared with the same solid were almost identical, with minor differences due to the liquid phases, in agreement with previous studies that concluded that the solid phase of clay/spring water suspensions was the major factor determining their rheological properties (Aguzzi et al., 2013). PS9 hydrogels (Figure 4.7 and 4.8) showed apparent viscosities ten times higher than the corresponding G30 hydrogels (Figure 4.9 and Figure 4.10). The difference could be explained as a result of multiple factors. The ability of low sepiolite concentrations to give high viscosity suspensions has been demonstrated in previous studies (Simonton et al., 1988; Viseras et al., 1999; Çınar et al., 2009). Previous comparative studies have revealed that sepiolite produced more viscous and easy-to-obtain hydrogels than palygorskite or bentonite (Simonton et al., 1988; Viseras et al., 1999). The presence of impurities in G30 modify rheological properties, in agreement with previous studies with palygorskite suspensions (Neaman and Singer, 2000a; Bailey et al., 2015; Khiari et al., 2019). Additionally, textural particularities of G30 fibers, appearing as more compact aggregates than PS9 (Figure 4.5), also help to explain the rheological differences and the higher surface of PS9 fibers allowed higher water adsorption capacities, leading to more viscous systems. Xu and Wang stated that bundles of particles disaggregate during high-speed agitation, thus increasing the specific surface area, favouring the migration and attaching of water cation species over the negatively charged clay

4.1. Design and Characterization of Spring Water Hydrogels with Natural Inorganic Excipients

surfaces (Xu and Wang, 2012). It is feasible that more compact aggregates of G30 will offer a higher resistance to be disaggregated than PS9.

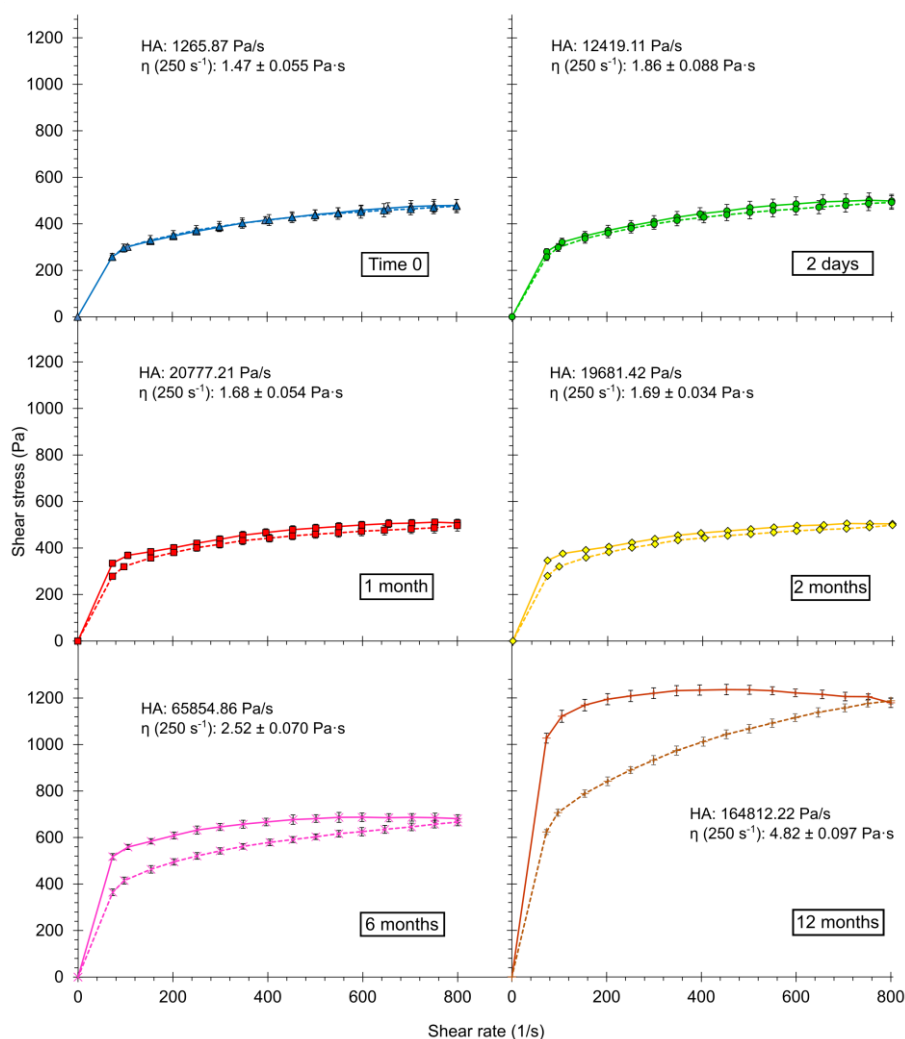


Figure 4.7. Flow curves, apparent viscosities (Pa·s; 250 s⁻¹; 25 °C) and hysteresis areas (HA; Pa/s) of PS9ALI hydrogels through time

The elongated and asymmetric particles of palygorskite and sepiolite hinder settling and allow suspensions to be highly viscous and to maintain stable through time (Simonton et al., 1988; Álvarez et al., 2011). Visual observations of the hydrogels discarded any syneresis phenomenon during the full time lapse of study. The rheological curves profiles remained similar

within the first 60 days and showed major changes after 6 months (Figures 4.7 to 4.10). During the first 60 days all gel-like suspensions showed no or almost negligible hysteresis areas. That is, the hydrogels did not perform time-dependent rheological properties, meaning that the internal structure of these suspensions recovers immediately once the stress removed. The stability of gels during first 60 days was expected regarding the crystal habit and structure of the solid phase, since fibrous clays do not suffer from osmotic swelling as happens with layered clays (Simonton et al., 1988; Viseras et al., 1999).

The studied hydrogels showed significant increase in apparent viscosity at 6 and 12 months (ANOVA, post-hoc Scheffé) as well as thixotropic behaviour with high and positive hysteresis area values. Thixotropy of palygorskite and sepiolite hydrogels has been correlated with a coagulated (agglomerated) state of the clay (Harvey and Lagaly, 2006; Viseras et al., 2007; Çınar et al., 2009; Carmona et al., 2018) due to factors such as high concentration of electrolytes and/or moderately attractive particle-particle interactions. This time-dependent behaviour implies that, in practical use, under stresses like rubbing or agitation, the gels easily flow and become less viscous, thus facilitating their application over the skin (Lee et al., 2009). Thixotropy does not only favours skin spreading ($70\text{--}200\text{ s}^{-1}$) but also manual mixing ($100\text{--}200\text{ s}^{-1}$) and container filling and removal operations ($400\text{--}2000\text{ s}^{-1}$) (Scott, 1995; Neaman and Singer, 2000b). However, it is preferable that thixotropy or other rheological features were controllable and foreseeable, to achieve a quality control of the products. The measured changes in rheological properties after long periods of time could be related to water losses and resultant increasing in solid/ liquid ratios. These changes could be difficult both to control and predict in clinical practice.

Dynamic yield stress values were calculated after model fitting of the flow curves due to the absence of experimental spur points. Three models were used (Bingham, Casson and Herschel–Bulkley).

Bingham model is the simplest and frequently used to describe the rheological behaviour of concentrated suspensions of solid particles. It is described by Eq. 4.5, where σ_0 is the yield stress and η_B is the Bingham

viscosity or plastic viscosity, which describes the slope of the Newtonian portion of the curve, thus not being a real value of viscosity.

$$\sigma = \sigma_0 + \eta_B \dot{\gamma} \quad \text{Eq. 4.5}$$

Casson model is a structured-based model that has all components in the Bingham model raised to the power of 0.5, which produces a more gradual transition between the yield and Newtonian regions (Eq. 4.6). It is very useful to fit materials such as inks, food dispersions or slurries. Once again, σ_0 describe the yield stress, whereas η_C is the Casson viscosity.

$$\sqrt{\sigma} = \sqrt{\sigma_0} + \sqrt{\eta_C \dot{\gamma}} \quad \text{Eq. 4.6}$$

Unlike the previous models, Herschel–Bulkley equation describes non-Newtonian behaviour once the yield stress overcome. Basically, it is a powder-law model with a yield stress term (Eq. 4.7). In this model, K is the consistency value ($Pa \cdot s^n$) and n is a value that describes if the material is shear-thinning ($n < 1$) or shear-thickening ($n > 1$).

$$\sigma = \sigma_0 + K \dot{\gamma}^n \quad \text{Eq. 4.7}$$

Herschel–Bulkley equation was selected to model the flow curves and to obtain the corresponding yield values (Table 4.6). This model gave the highest R^2_{adjusted} coefficients compared to Bingham and Casson equations.

PS9 hydrogels showed higher yield stresses than those with G30. High yield stresses in suspensions have been related to higher time- stability in terms of sedimentation/precipitation events (Marins et al., 2019). Rheological features of the PS9 hydrogels were in the same order of magnitude of those measured with hydrogels used in different Italian spa centres (Sánchez-Espejo et al., 2014a; Sánchez-Espejo et al., 2015). Moreover, the Italian spa gels showed lower yield stress and apparent viscosities despite their high solid concentration (50% w/w). Both apparent viscosity and yield values demonstrate the efficacy of PS9 to form gel-like systems. As well as thixotropy, topical formulations are preferred to have high yield values since in these conditions they can maintain themselves over the skin for longer times without sliding (Lee et al., 2009). The type of spring water was not exerting significant differences in the stability of the hydrogels.

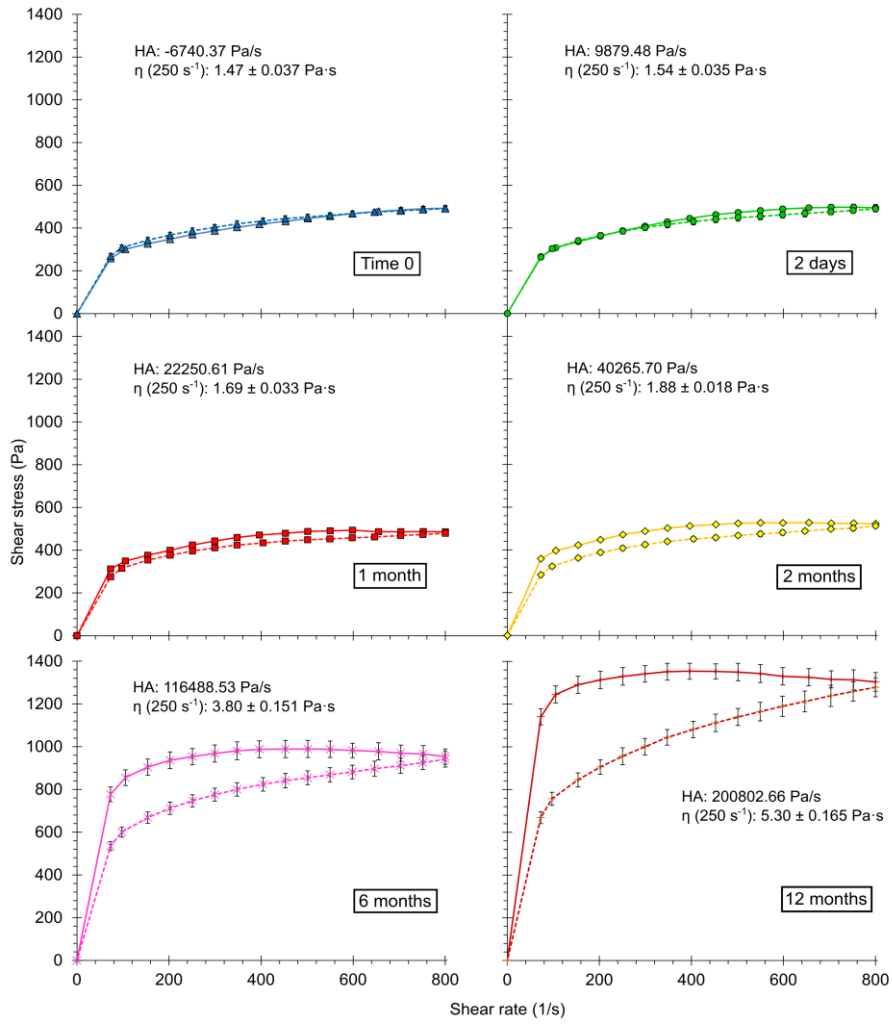


Figure 4.8. Flow curves, apparent viscosities ($\text{Pa}\cdot\text{s}$; 250 s^{-1} ; $25 \text{ }^\circ\text{C}$) and hysteresis areas (HA; Pa/s) of PS9GR hydrogels through time

4.1. Design and Characterization of Spring Water Hydrogels with Natural Inorganic Excipients

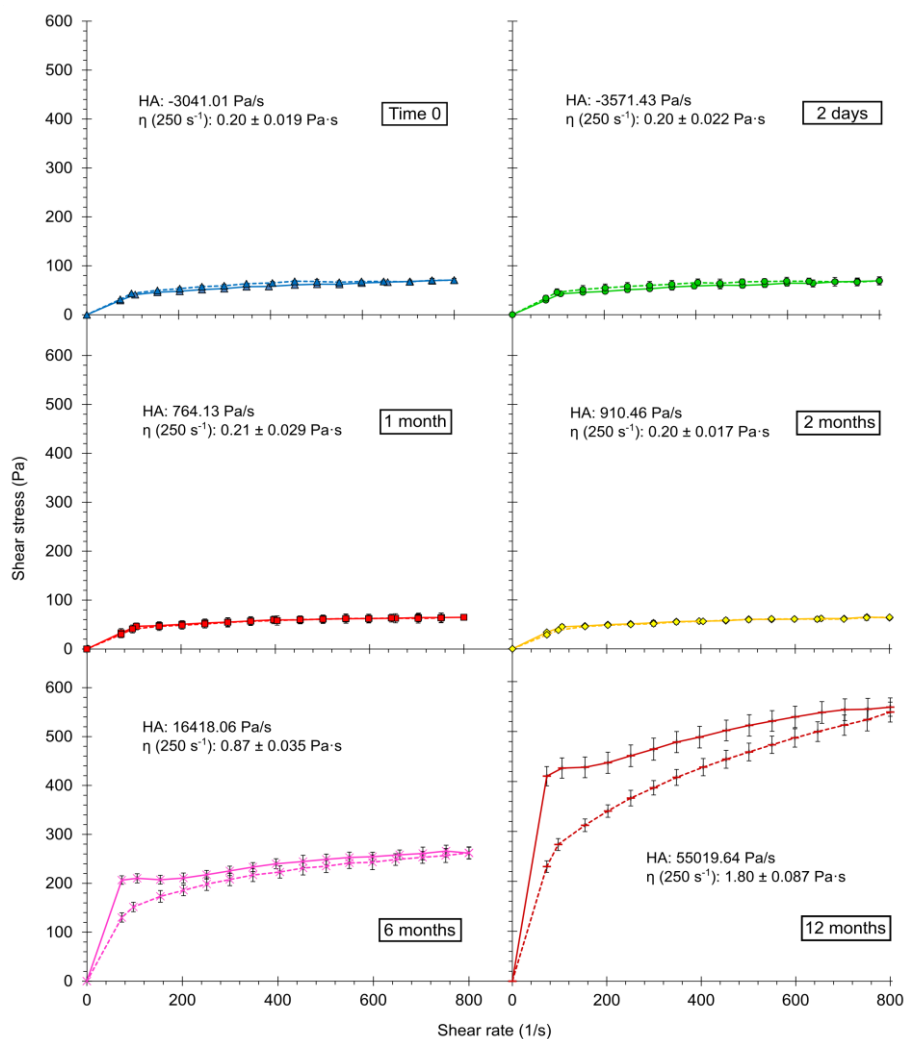


Figure 4.9. Flow curves, apparent viscosities (Pa·s; 250 s⁻¹; 25 °C) and hysteresis areas (HA; Pa/s) of G30ALI hydrogels through time

The exact mechanism of gel formation in fibrous clay mineral systems is still under discussion since both electrostatic and physical interactions have been proposed (Viseras et al., 1999; Xu and Wang, 2012). Even if electrostatic properties influence the gel formation of fibrous clays up to an extent, other mechanisms would also dominate the remarked rheological differences of PS9 and G30 hydrogels. These mechanisms probably involve physical interactions regarding fibers morphology, surface and/or dimension. It has been demonstrated that higher specific surfaces lead to higher physical interaction

between palygorskite fibers in suspension and therefore, higher viscosities and yield stresses. SEM analyses performed shown PS9 particles to be less compact than those of G30 (Figure 4.5). This fact imply a potentially higher specific surface area and, therefore, higher physical interactions between particles. The more intimate association of particles could explain the higher viscosity and yield values of PS9 hydrogels. Moreover, the higher specific surface area would allow potentially higher water adsorption capacity, thus generating more viscous suspensions.

Control of pH and Water Content

pH evolution of hydrogels is plotted in Table 4.7. Values of pH maintained between 7 and 8 during the whole studied time lapse. The reported pH values were in agreement with ALI and GR pHs (Table 4.4) and with the expected pH of sepiolite and palygorskite water suspensions. Pharmacopeial specifications (USP42-NF37, 2019; Ph. Eur. 9th, 2018a,b) indicate a pH ranging from 9 and 10.5 for smectites included in pharmaceutical products but, for common clays, the pH range is not regulated. Glavaš and co-workers stated that a hydrogel pH range between 4 and 8 should be guaranteed to avoid skin irritation (Glavaš et al., 2017). Numerous are the literature references in which natural thermal-mud used showed alkaline pH values, thus demonstrating this feature not to limit their usefulness (Mihelčić et al., 2012; Aguzzi et al., 2013; Modabberi et al., 2015; Rebelo et al., 2015; Sánchez-Espejo et al., 2015; Khiari et al., 2019). Additionally, it has been reported that as higher the pH of a hydrogel, the less its bacterial activity, allowing a higher stability and microbiological preservation (Veniale et al., 2007). Natural skin pH tends to be slightly acidic, particularly between 4.5 and 6.0 (Fluhr and Elias, 2002; Lambers et al., 2006). Nonetheless, a healthy skin is able to revert any alteration in normal pH value produced by cosmetic products within 90 min to 8 h (Moldovan and Nanu, 2010).

4.1. Design and Characterization of Spring Water Hydrogels with Natural Inorganic Excipients

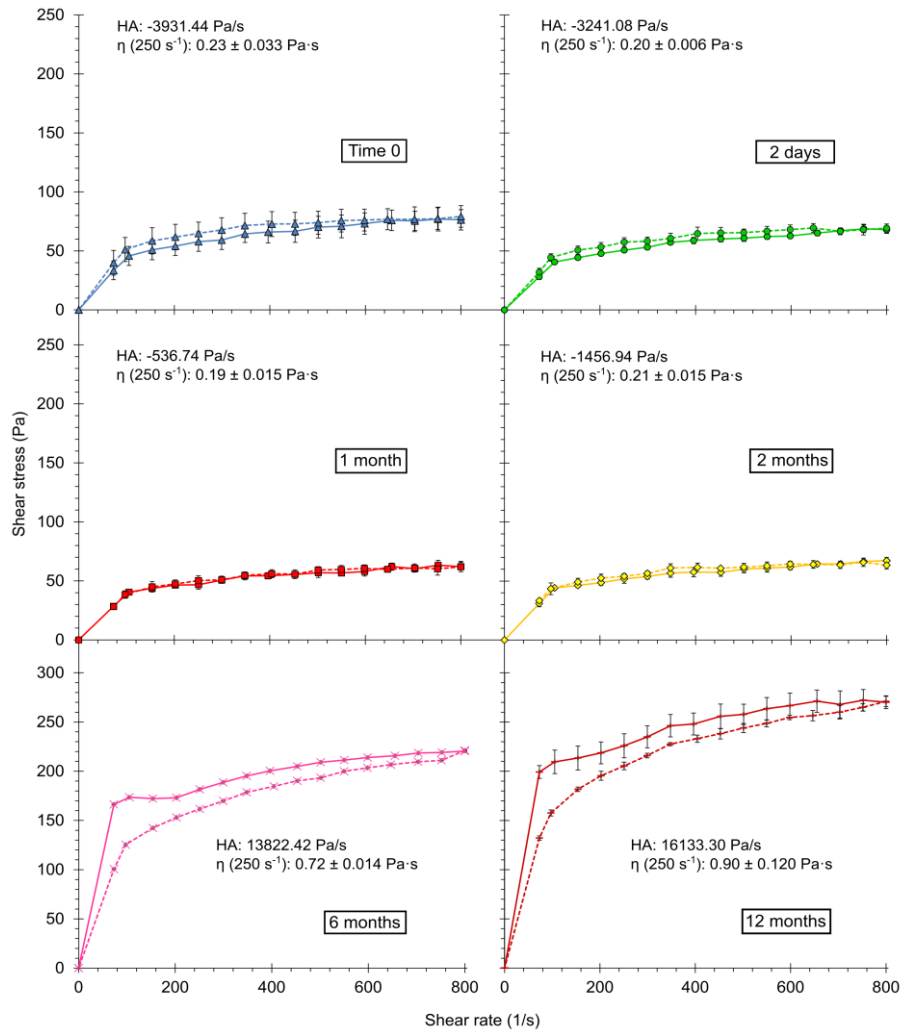


Figure 4.10. Flow curves, apparent viscosities (Pa·s; 250 s⁻¹; 25 °C) and hysteresis areas (HA; Pa/s) of G30ALI hydrogels through time

Table 4.6. Herschel–Bulkley model fitting of hydrogels

		Herschel-Bulkley				Herschel-Bulkley	
PS9ALI	t0	σ_0	163.3	G30ALI	t0	σ_0	9.5
		K	14.62			K	5.84
		n	0.47			n	0.35
		$R^2_{adjusted}$	0.9873			$R^2_{adjusted}$	0.9760
	48 h	σ_0	220.1		48 h	σ_0	16.5
		K	6.15			K	3.93
		n	0.60			n	0.39
		$R^2_{adjusted}$	0.9874			$R^2_{adjusted}$	0.9616
	1m	σ_0	287.8		1m	σ_0	21.8
		K	4.87			K	3.03
		n	0.60			n	0.42
		$R^2_{adjusted}$	0.9738			$R^2_{adjusted}$	0.9504
	2m	σ_0	331.1		2m	σ_0	32.3
		K	1.64			K	0.59
		n	0.73			n	0.62
		$R^2_{adjusted}$	0.9689			$R^2_{adjusted}$	0.9442
	6m	σ_0	483.5		6m	σ_0	192.7
		K	5.24			K	0.23
		n	0.59			n	0.85
		$R^2_{adjusted}$	0.9050			$R^2_{adjusted}$	0.9692
12m	σ_0	934.7	12m	σ_0	408.1		
	K	33.0		K	0.09		
	n	0.37		n	1.13		
	$R^2_{adjusted}$	0.6919		$R^2_{adjusted}$	0.9793		

4.1. Design and Characterization of Spring Water Hydrogels with Natural Inorganic Excipients

Table 4.6. Continued (part II)

		Herschel-Bulkey				Herschel-Bulkey	
PS9GR	t0	σ_0	176.2	G30GR	t0	σ_0	9.4
		K	9.99			K	6.97
		n	0.53			n	0.35
		R ² _{adjusted}	0.9919			R ² _{adjusted}	0.9800
	48h	σ_0	195.8		48h	σ_0	20.7
		K	5.93			K	2.25
		n	0.62			n	0.47
		R ² _{adjusted}	0.9899			R ² _{adjusted}	0.9915
	1m	σ_0	280.6		1m	σ_0	22.3
		K	2.39			K	1.81
		n	0.73			n	0.48
		R ² _{adjusted}	0.9664			R ² _{adjusted}	0.9352
	2m	σ_0	281.9		2m	σ_0	25.9
		K	11.32			K	1.77
		n	0.50			n	0.48
		R ² _{adjusted}	0.9592			R ² _{adjusted}	0.9500
	6m	σ_0	565.8		6m	σ_0	147.7
		K	101.18			K	1.10
		n	0.23			n	0.64
		R ² _{adjusted}	0.8402			R ² _{adjusted}	0.9649
12m	σ_0	999.8	12m	σ_0	193.0		
	K	67.5		K	0.29		
	n	0.27		n	0.87		
	R ² _{adjusted}	0.7098		R ² _{adjusted}	0.9725		

Table 4.7. Control of hydrogel pH

	t0	48h	1m	2m	6m	12m
PS9ALI	7.60 ± 0.037	7.74 ± 0.018	7.52 ± 0.047	7.24 ± 0.028	7.53 ± 0.063	7.90 ± 0.078
PS9GR	7.93 ± 0.037	7.87 ± 0.036	7.54 ± 0.026	7.38 ± 0.076	7.63 ± 0.015	7.95 ± 0.049
G30ALI	7.69 ± 0.063	7.89 ± 0.022	7.47 ± 0.039	7.50 ± 0.024	7.78 ± 0.111	7.94 ± 0.024
G30GR	7.75 ± 0.037	7.67 ± 0.072	7.56 ± 0.052	7.49 ± 0.076	7.51 ± 0.143	7.89 ± 0.008

Hydrogels are sensitive to water losses due to manipulation, particularly when they are subjected to filling and removal operations. The

influence of water loss in hydrogel properties must be determined. In this study, hydrogels were preserved in static conditions and room temperature, meaning they were only manipulated during the sampling at the studied intervals resulting in minor water content changes (Table 4.8). Apparently, water loss values maintained until 2 months without significant differences (p -value > 0.05). At 6 months, the decrease in water content was significant (p -values ≤ 0.05 for PS9GR, G30GR and G30ALI) but not for PS9ALI (results with high standard deviation). At 12 months, all hydrogels showed significant changes (p -values ≤ 0.05). As previously stated in this paper, the type of spring water (ALI or GR) did not influence hydrogels rheological performances. With this premise, water loss and yield stress results of PS9ALI-PS9GR and G30ALI-G30GR were grouped (PS9 and G30, respectively). Interestingly, a direct and linear relation between water loss and yield stress was found (Figure 4.11), which confirmed water loss as one of the main factors influencing rheological changes of hydrogels. The higher slope of PS9 linear relationship with respect to G30 demonstrated a higher sensibility to concentration variations.

Table 4.8. Control of water content control of hydrogels

	t0	48h	1m	2m	6m	12m
PS9ALI	89.50 ± 0.0495	90.53 ± 0.7027	89.59 ± 0.3276	88.99 ± 0.1005	88.20 ± 5.0152	85.48 ± 0.1631
PS9GR	89.15 ± 0.0291	89.35 ± 0.2357	89.19 ± 0.1356	88.94 ± 0.1806	87.78 ± 0.8138	84.48 ± 0.2651
G30ALI	89.63 ± 0.0149	89.77 ± 0.0187	88.71 ± 0.4905	89.81 ± 0.1464	84.33 ± 0.6049	82.17 ± 0.0277
G30GR	89.49 ± 0.0439	89.61 ± 0.0847	89.48 ± 0.2467	89.52 ± 0.1448	87.65 ± 0.2531	84.94 ± 0.0895

Different studies have revealed the changes that occur during time in similar gels (clay/spring water suspensions) (Veniale et al., 2004; Carretero et al., 2007; Viseras et al., 2007; Fernández-González et al., 2013; Glavaš et al., 2017). Particularly, changes in water-retention, absorption capacity, cooling kinetics, grain size modifications or microorganism growth have been pointed out (Carretero et al., 2007; Aguzzi et al., 2013; Fernández-González et al., 2013; Rebelo et al., 2015; Pesciaroli et al., 2016). These changes affect the properties and, unless they are necessary for the therapeutic effect (Marcolongo et al., 2006; Haydel et al., 2007; Williams et al., 2008), they should be controlled

and/or avoided. These unforeseeable alterations could jeopardize the resultant quality properties. Moreover, they could also entail health risks for the patients due to the possibilities of uncontrollable microbial content and growth.

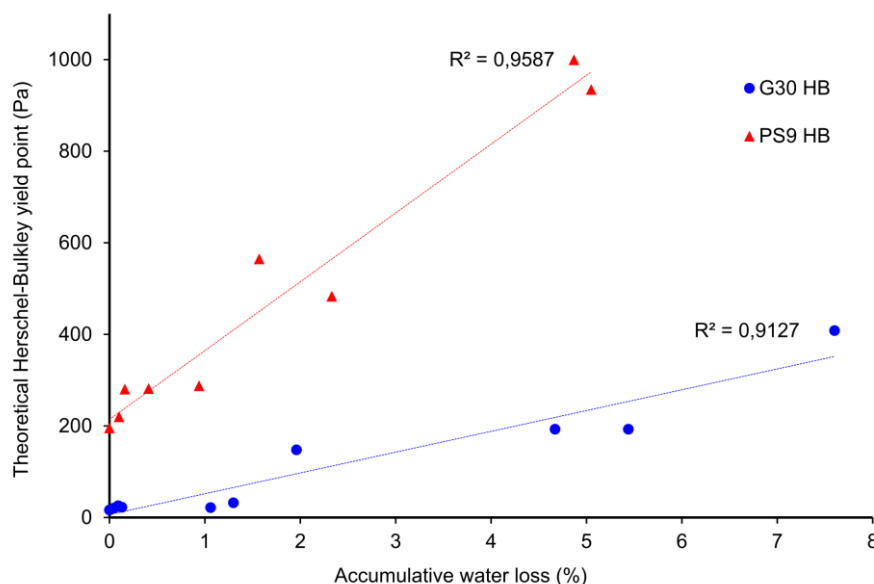


Figure 4.11. Relationship of dynamic yield values (Pa) versus water loss (% w/w) of hydrogels prepared with each type of clay (PS9 and G30)

4.1.3. Conclusions

Both clay minerals employed in this study PS9 and G30 showed high pureness in sepiolite and palygorskite, respectively. PS9 corresponds to “Magnesium silicate” or “Magnesium trisilicate” monographs (USP 42-37, 2019; Ph. Eur. 9th, 2018b). G30, despite the impurities detected, corresponds to “Attapulgit” (USP42-NF37, 2019; Ph. Eur. 9th, 2018a). FT-IR and XRF corroborate the absence of organic matter in both excipients. Loss of drying and loss on ignition pharmacopoeial limits (USP 42-N37, 2019) were also accomplished by PS9 (“Magnesium Silicate” monograph) and G30 (“Attapulgit” monograph).

Cooling rates of 10% w/w hydrogels prepared with PS9 and G30 and two different spring waters were adequate for topical application as thermotherapeutic agents. Rheology measurements showed that PS9 was more

effective in the formation of gel-like systems than G30 and, consequently, higher concentrations of G30 would be necessary to obtain hydrogels with apparent viscosities and yield values similar to those of PS9 hydrogels.

Hydrogels prepared with the two studied excipients and two natural spring waters showed adequate properties to be used in thermotherapy, showing remarkable stability within 60 days. It is advisable not to use them at longer times. After 6 months, unpredictable changes in rheology and water content have been reported. According to the unpredictability and uncontrollable nature of these modifications, it is estimated that, in order to guaranty predictable quality of the studied hydrogels, they should be used within the first 2 months from their preparation (preliminary estimated expiration date).

4.2. Wound Healing Activity of Nanoclay/Spring Water Hydrogels

Chronic wounds are a current health problem with devastating consequences for patients and contribute to major costs to healthcare systems and societies. This type of wounds result from an impaired wound healing process and are usually characterized by prolonged or excessive inflammation, persistent infections and inability of the dermal and/or epidermal cells to respond to repair stimuli (Fonder et al., 2008; Olsson et al., 2017; Nussbaum et al., 2018). The USA total Medicare spending for all wound types has been estimated to range from \$28.1 to \$96.8 billion. Diabetic foot ulcers (one of the main chronic wounds) accounted for \$6.1 to \$18.7 billion (Nussbaum et al., 2018), the main cost burden attributed to amputations (Olsson et al., 2017). The development and implementation of new wound healing management strategies and healthcare products is, therefore, imperative. In recent years, different technological strategies have been proposed, including clays, metals, polymer and lipid based systems among others, as reviewed by Bernal-Chávez, García-Villén and co-workers (Bernal-Chávez et al., 2019; García-Villén et al., 2020d). Particularly, clay based dressings have been proved to be useful in wound healing (Tenci et al., 2017; García-Villén et al., 2019, 2020d). Among the different clay-based formulations, those composed of a clay suspended in mineral medicinal water, known as therapeutic muds, are widely used in clinical medical hydrology (Mefteh et al., 2014; García-Villén et al., 2018; Khiari et al., 2019). The solid phase of these systems is frequently incorporated into the spring water to obtain a semisolid formulation known as “artificial thermal mud” (Viseras and Cerezo, 2006; Rebelo et al., 2011a, 2011b; Sánchez-Espejo et al., 2014a). Thermal muds have demonstrated their clinical effectiveness against dermatological affections such as psoriasis (Elkayam et al., 2000; Delfino et al., 2003; Harari, 2012; Cozzi et al., 2015), atopic dermatitis, vitiligo, (Riyaz and Arakkal, 2011; Huang et al., 2018), seborrhoeic dermatitis, fungal infections, eczema (Comacchi and Hercogova, 2004; Williams et al., 2008; López-Galindo et al., 2011; Harari, 2012), or acne (Argenziano et al., 2004). These clinical effects have been traditionally associated to the liquid phase. Avène and La Roche-Posay spring waters increase the fluidity of plasma membranes on

cultured human skin fibroblasts (Cézanne et al., 1993; Mahé et al., 2006; Castex-Rizzi et al., 2011; Mahe et al., 2013) and have been useful in the management of chronic inflammatory skin diseases. La Roche-Posay spring water protected cultured human skin fibroblasts against lipid peroxidation induced by ultraviolet A and B radiation (Moysan et al., 1995). Boron and manganese-rich thermal waters are used for the treatment of ulcers and chronic wounds (Chebassier et al., 2004b; Chiarini et al., 2006; Faga et al., 2012; Liang et al., 2015; Nicoletti et al., 2017a).

The influence of the thermal mud's solid phase in the resulting clinical efficacy has not been studied in depth. The inorganic solid phase of thermal muds is mainly composed of clay minerals (Khiari et al., 2014, 2019; Meftteh et al., 2014; Sánchez-Espejo et al., 2014b, 2015). The clay mineral presence in wound healing formulations is supported by their already demonstrated biocompatibility with different types of skin cells (Lizarbe et al., 1987; Olmo et al., 1987; Kommireddy et al., 2006). The combination of clay minerals with other ingredients, such as polymers, allows the formation of scaffolding materials. In these occasions, clay minerals did not only improved mechanical strength and functionality of the polymers, but also acted as synergistic ingredients for wound healing (Ishikawa et al., 2010a; Dawson and Oreffo, 2013; Aguzzi et al., 2016; Sandri et al., 2016). Biocompatibility of clay minerals such as halloysite, montmorillonite, palygorskite, sepiolite, imogolite, have been widely studied (Ishikawa et al., 2010b; Li et al., 2010; Vergaro et al., 2010; Salcedo et al., 2012; Lai et al., 2013; Rotoli et al., 2014; Sandri et al., 2014, 2017; Wang et al., 2015; Maisanaba et al., 2015; Shanmugapriya et al., 2018). Sasaki and co-workers have reported that Mg^{2+} and Si^{4+} ions released by a synthetic Mg-rich smectite clay mineral can promote collagen formation and angiogenesis on skin wounds (Sasaki et al., 2017).

Moreover, palygorskite ("attapulgate") has been used as scaffolding material when included in poly(lactic-co-glycolic acid) nanofibers being crucial for mesenchymal cell adhesion and proliferation (Wang et al., 2015). Sepiolite and palygorskite inhibit lipid peroxidation and possess anti-inflammatory properties by reducing neutrophil migration and edema (Cervini-Silva et al., 2015a, 2015b). Pharmaceutical grade palygorskite

4.2. Wound Healing Activity of Nanoclay/Spring Water Hydrogels

(Pharmasorb® colloidal) did not only demonstrate to be biocompatible but also to protect fibroblasts from carvacrol cytotoxicity (Tenci et al., 2017).

As discussed, both spring waters and clay minerals have been separately studied as potential wound healing ingredients. Synergistic effects would be expectable when both ingredients are formulated as spring-water/clay hydrogels. The role of these systems in wound healing studies have been scarcely addressed. The existing studies include a clinic study of diabetic gangrenous wounds treated with volcanic deposits muds (Nasirov et al., 2009), black-mud Dead Sea effects in wounded mice (Abu-al-Basal, 2012) and wound healing activity of emulsions prepared with a Brazilian clay (Dário et al., 2014).

With these premises, spring water hydrogels have been recently formulated and characterized, including mineralogical and chemical composition, textural and thermal properties as a first step in the design of pharmaceutical grade systems (García-Villén et al., 2020c). The second step would involve the study and evaluation of their biocompatibility. In this regard, the simplest starting point would include *in vitro* biocompatibility studies over skin cells like fibroblasts and *in vitro* wound healing studies.

Particularly, the *in vitro* biocompatibility and cell gap motility (wound healing) properties of two selected Spanish medicinal waters (obtained from Graena and Alicún de las Torres thermal stations), two clay minerals (palygorskite and sepiolite) and their corresponding hydrogels were studied. Additionally, particle size distribution and zeta potential measures as well as cation exchange capacities of the solid phases were carried out. *In vitro* wound healing tests were also evaluated by analysing fibroblasts F-actin microfilament organization by means of phalloidin staining. To the best of author's knowledge, this is the first time that nanoclay/spring water mineral medicinal hydrogels are evaluated in terms of *in vitro* cytotoxicity and wound healing.

4.2.1. Materials and Methods

4.2.1.1. Materials

Two pharmaceutical grade clays granted by TOLSA Company (Madrid, Spain); magnesium aluminium silicate (PS9) and attapulgite (G30), with mineralogical identification previously evaluated Table 4.9, were used (García-Villén et al., 2020c).

Table 4.9. Fibrous clay minerals (PS9 and G30) mineralogical composition (modified from (García-Villén et al., 2020c))

Mineralogical composition	PS9		G30	
		Sepiolite	92%	Palygorskite
	Muscovite	8%	Quartz	26%
			Fluorapatite	7%
			Smectites and sepiolite	6%
			Calcite/dolomite	3%

Table 4.10. Spring water characteristics and elemental composition determined by means of ICP-OES and ICP-MS (modified from (García-Villén et al., 2020c))

	ALI	GR	
	pH \pm s.d.	7.90 \pm 0.0472	8.02 \pm 0.0823
Conductivity (μ S/cm) \pm s.d.	2251.5 \pm 6.74537	2465.5 \pm 8.89482	
Elemental composition	Ca (mg/L)	348.00	460.00
	Mg (mg/L)	109.0	88.00
	Na (mg/L)	57.00	27.40
	K (mg/L)	4.60	6.80
	B (μ g/L)	25.00	12.00
	Ba (μ g/L)	18.80	13.00
	Cr (μ g/L)	4.3	1
	Zn (μ g/L)	464.99	301.08
	Mn (μ g/L)	<1	108.66
	Li (μ g/L)	244.2	65.00
	Ni (μ g/L)	9.4	5.20
	Fe (μ g/L)	6.00	21.00
	Se (μ g/L)	2.3	1.00

According to previous studies and characterizations (García-Villén et al., 2020c), hydrogels were prepared mixing 10% w/w of each clay mineral with the corresponding spring water by means of a turbine-high speed agitator (Silverson LT, United Kingdom) at 8000 rpm for 10 minutes. The obtained hydrogels are summarized in Table 4.11.

4.2. Wound Healing Activity of Nanoclay/Spring Water Hydrogels

Table 4.11. Hydrogels tested, identification codes and composition

Identification code	Composition
PS9ALI	10% w/w PS9, 90% w/w ALI
PS9GR	10% w/w PS9, 90% w/w GR
G30ALI	10% w/w G30, 90% w/w ALI
G30GR	10% w/w G30, 90% w/w GR

4.2.1.2. Characterization of Inorganic Ingredients

Particle Size

Particle size distribution was determined by a Malvern Mastersizer 2000 LF granulometer (Malvern Instruments™). Measurements were performed in purified water after dispersing the solids by midst sonication for 30 seconds. The amount of sample added in each experiment was determined by the real-time laser obscuration degree indicated by Mastersizer 2000 software. The optimal laser obscuration was delimited between 10-20%. Three replicates were performed for each sample and statistical particle diameters (d_{10} , d_{50} , d_{90}) were calculated together with the SPAN factor as an index of the amplitude of particle size distribution calculated according to Eq. 4.8.

$$\text{SPAN} = \frac{d_{90} - d_{10}}{d_{50}} \quad \text{Eq. 4.8}$$

Cation Exchange Capacity

Cation exchange capacity (CEC) of PS9 and G30 was determined by dispersing 1g of dry powder in 25mL of tetramethyl ammonium bromide (TMAB) aqueous solution (1M). The resultant dispersions were shaken in a Roller Mixer for 24 h and subsequently centrifuged (8000 rpm, 30 min) and filtered (0.45 μm pore size, HAWP-Millipore filter). Three replicates were performed for each sample together with two blanks of pure TMAB (1M). The CEC determination is based on the exchange between bromine (in the TMAB solution) and cations present in the clay. The main exchangeable cations released from the clay mineral, once the Br exchanged, are K^+ , Na^+ , Mg^{2+} , Ca^{2+} . Cations released, present in the resultant solution, were determined by ICP-OES (Optima 8300 ICP-OES Spectrometer, Perkin Elmer, USA) and CEC was calculated as the sum of exchangeable cations, expressed in mEq/100g of clay mineral.

Zeta Potential

Zeta-potential (ζ -potential) measurements determine the electrical potential difference between the stationary layer of fluid surrounding the solid particles and the bulk (electric double layer). Zeta potential of different concentrations of PS9 and G30, suspended in Dulbecco's modified Eagle medium (DMEM), supplemented with 10% fetal bovine serum and 200 IU/mL penicillin 0.2 mg/mL streptomycin, were also measured. Afterwards, ζ -potential of the aforementioned suspensions were determined by using an electrophoretic light scattering (ELS) Zetasizer Nano-ZTM (Malvern Instruments). Samples were placed inside a folded capillary zeta potential cell (DTS1061, Malvern Instruments). Three replicates were obtained for each sample, analyses done at 25 ± 0.5 °C. During the analyses, 20 points were collected for each replicate and results expressed in mV.

4.2.1.3. *In Vitro* Tests of Inorganic Ingredients, Spring Waters and Hydrogels

Biocompatibility Tests

Normal human dermal fibroblasts (NHDF) from juvenile foreskin (PromoCell GmbH, G) were used. All cells were between 10th and 13rd passages. NHDF were grown in Dulbecco's modified Eagle medium (DMEM, Sigma Aldrich®-Merck, Italy), supplemented with 10% fetal bovine serum (FBS, Euroclone, I) and 200 IU/mL penicillin 0.2 mg/mL streptomycin (PBI International, I), kept at 37 °C in a 5% CO₂ atmosphere with 95% relative humidity (RH). Fibroblasts were seeded in 96-well plates (area 0.34 cm²/well) at a density of 10⁵ cells/cm². Cells were grown 24 h to obtain sub-confluence. Then cell substrates were washed with saline solution and the cell substrates were put in contact with the samples. Biocompatibility of all samples were assessed after 24 h contact between samples and NHDF cultures. Powdered PS9 and G30 clay minerals were used in concentrations of 1000, 500, 50 and 5 μ g/mL. ALI and GR medicinal waters were used in concentrations 0.25, 2.5, 25 and 50% v/v. Regarding PS9ALI, PS9GR, G30ALI and G30GR, cell-contact concentrations were prepared in order to have equal amounts of clay mineral with respect to powdery samples, bearing in mind that hydrogels were prepared with 10% w/w of the corresponding clay. Since the final amount of

4.2. Wound Healing Activity of Nanoclay/Spring Water Hydrogels

clay fibroblasts were put in contact with was the same as in the experiments with pristine clays, same concentration codes (1000, 500, 50 and 5 $\mu\text{g}/\text{mL}$) were used. Briefly, clay and hydrogels samples were dispersed in sterile Hanks' Balanced Salt Solution (Sigma-Aldrich) and mixed with Ultra-Turrax® (S 25N,-18G, IKA stirring-probe) for 5 min, 150000 rpm. These initial suspensions were subsequently diluted in order to obtain samples having concentration in the range previously mentioned. Eight replicates were assessed for all samples and for the control (NHDF cultures in pure DMEM phenol red).

After the 24 hours of contact, growth medium and samples were withdrawn from each well and MTT (3-(4,5-dimethylthiazol-2-yl)-2,5-diphenyltetrazolium bromide) test was performed. This test is based on the activity of mitochondrial dehydrogenases of vital cells that convert MTT in formazan crystals. DMEM phenol red-free and 50 μL of MTT dissolution were added in each well, final MTT concentration being 2.5 mg/mL . The MTT-NHDF contact was maintained for 3h before the whole supernatant was withdrawn and substituted by 100 μL of dimethyl sulfoxide solution (DMSO, Sigma-Aldrich) to dissolve formazan purple-salts. The absorbance was assayed at 570 nm by means of an ELISA plate reader (Imark Absorbance Reader, Biorad, I), with a reference wavelength set at 655 nm. Cell viability was calculated as % ratio of the absorbance of each sample and the absorbance of the cells kept in contact with the growth medium (control).

Cell Motility Assay for Wound Healing

The gap closure cell motility assay is based on the employment of Petri $\mu\text{-Dish}^{35\text{mm, low}}$ (Ibidi, Giardini, I) in which a silicone insert is enclosed. The insert is constituted of 2 chambers with a growth area of 0.22 cm^2 divided by a septum with a width of cell-free gap of $500 \pm 50 \mu\text{m}$. NHDF were seeded in each chamber at 10^5 cells/ cm^2 concentration and were grown until confluence in the same conditions described in the previous section. After 24 h fibroblasts reached confluence, the silicone inserts subsequently removed with sterile tweezers, displaying two areas of cell substrates divided by the 500 μm (± 50) gap.

Cell substrates were washed with sterile phosphate buffer solution PBS (10% v/v) to eliminate debris. Then, they were put in contact with a final volume of 700 μL of phenol red DMEM in which samples were included at determined concentrations. These concentrations were selected according to MTT results. Particularly, PS9, G30, PS9ALI, PS9GR, G30ALI and G30GR were used at 50 $\mu\text{g}/\text{mL}$ and spring waters were used in concentrations 2.5% v/v. Cells kept in contact with pure growth medium (GM) were used as control.

Microphotographs were taken at prefixed time intervals (0, 24, 48 h) to evaluate cell growth inside the gap. A Leica optical microscope (DMI3000-B model) equipped with LAS EZ software was used. In order to analyze results in a more objective way, the full-area of the wound healing space was photographed in all samples. Then, the wound closure was monitored by measuring the remaining gap with ImageJ software. The percentage of wound closure was calculated according to Eq. 4.9, where WS_0 stands for “wound space at time 0” and WS_{24} is “wound space after 24h”, both of them measured as an area (μm^2).

$$\% \text{ Wound Closed after 24 h} = 100 \cdot \frac{WS_{24}(\mu\text{m}^2) \cdot 100}{WS_0(\mu\text{m}^2)} \quad \text{Eq. 4.9}$$

4.2.1.4. Confocal-Laser Scanning Microscopy

An additional sequence of wound healing experiments was stopped at 24 h of growth in order to study the morphology of fibroblasts during the wound closure procedure. NDHF were washed three times with PSB (10% v/v) and fixed with glutaraldehyde solution in PBS (3% v/v, 800 μL ; Sigma-Aldrich). The contact with glutaraldehyde was maintained for 2 h (4-8 $^{\circ}\text{C}$), all samples protected from light. Three PBS washes were once again performed prior to fibroblast permeabilisation. Permeabilisation was performed by adding Triton X-10 (0.1% w/v) for 10 minutes at room temperature. Triple PBS wash was again performed. Fluorescein isothiocyanate (FITC, $\lambda_{\text{ex}}=495 \text{ nm}$; $\lambda_{\text{em}}=513 \text{ nm}$) labeled phalloidin (Phalloidin-FITC, Sigma-Aldrich) was used to mark polymerized F-actin in the cytoplasm of NHDF (50 $\mu\text{g}/\text{mL}$, darkness, 40 min at room temperature). Procedure was defined according to fabricant indications. After several PBS washings aiming to eliminate unbound phalloidin-FITC, fibroblast nuclei staining was done. Blue fluorescence

nucleic acid stain 4',6-Diamidino-2-phenylindole (DAPI, Sigma-Aldrich) was used. This molecule binds to double-stranded DNA, thus labelling nuclei ($\lambda_{\text{ex}}=485$ nm; $\lambda_{\text{em}}=552$ nm). Contact between DAPI and cells was maintained for 10 min at room temperature, in darkness. Finally, samples were washed and preserved in PBS (10% v/v) to avoid dryness. Confocal-Laser Scanning Microscopy (CLSM) microphotographs were obtained by a Leica TCS SP2 (Leica Microsystems, Milan, Italy). Images were processed with ImageJ software.

4.2.1.5. Statistical Analysis

The statistical differences were determined by means of non-parametric Mann-Whitney (Wilcoxon) *W* test. In all cases, SPSS Statistic software was used and differences were considered significant at *p*-values ≤ 0.05 . Only significant differences are reported.

4.2.2. Results and Discussion

4.2.2.1. Characterization of Inorganic Ingredients

Particle size

The granulometric distribution of PS9 and G30 is plotted in Figure 4.12. Both samples were mainly unimodal and, therefore, homogeneous. PS9 showed to be finer than G30 (Table 4.12), the latter one slightly asymmetric. Calculated SPAN factors showed that the amplitude of particle size distribution for both samples had no significant difference (Table 4.12).

In terms of hydrogels, the finer the particles of the solid phase, the higher the stability of the resultant semisolid system (no phase separation) and better textural properties (smoothness). Mineralogical composition of G30 (Table 4.9) included 26% w/w of quartz. The presence of this mineral could influence rheology and textural properties of hydrogels. Particularly, it infers an abrasive texture to the preparation if quartz particle sizes are big. Particle sizes higher than 150 μm could be abrasive, particularly when they have remarkable hardness, such in the case of quartz (Quintela et al., 2014). Despite the presence of 26% of quartz mineral in G30, its particles were smaller than 100 μm (Figure 4.12), which means that resultant hydrogels

possessed smooth textures, which are crucial for the acceptance of the patients (Ganfoud et al., 2015).

Table 4.12. Statistical particles diameters, SPAN factor (average \pm s.d.; $n=3$) and main modes of PS9 and G30 clay minerals

	PS9	G30
d_{10} (μm)	4.0 ± 0.07	4.8 ± 0.03
d_{50} (μm)	9.9 ± 0.15	20.2 ± 0.03
d_{90} (μm)	23.9 ± 0.2	49.3 ± 0.10
SPAN factor	2.0 ± 0.02	2.2 ± 0.01
Main mode (μm)	8.9	28.3

Cation Exchange Capacity

The individual exchangeable elements and total CEC of PS9 and G30 are summarized in Table 4.13. Total CEC values were inside the expected CEC limits for sepiolite (9.18 mEq/100g) and palygorskite (16.29 mEq/100g) (Álvarez et al., 2011; Santos and Boaventura, 2016). Sepiolite and palygorskite CEC are usually < 25 mEq/100g (McLean et al., 1972) with higher values usually related to impurities (Galan, 1996; Paolisso and Barbagallo, 1997; Shariatmadari, 1999; Rytwo et al., 2000; Lemić et al., 2005; Shirvani et al., 2006b; Al-Futaisi et al., 2007; Chang et al., 2009; Rhouta et al., 2013; Zeng et al., 2017; Lobato-Aguilar et al., 2018). The higher CEC showed by G30 with respect to PS9 could be explained by the presence of 6% w/w of smectites and/or sepiolite in G30, as previously described.

The main exchangeable cations for both clays were Mg^{2+} and Ca^{2+} , which was in agreement with the chemical composition of PS9 and G30 showed by XRF (García-Villén et al., 2020c), though Na^+ and K^+ were also detected in small amounts. Na^+ , K^+ , Mg^{2+} and Ca^{2+} are essential elements since they are widely found inside and outside human cells (Lansdown et al., 1999; Gomes and Silva, 2007; Tateo et al., 2009). The presence of suitable levels of ions such as calcium, magnesium, sodium and potassium in the wound bed are important to enhance the healing process. They allow the activity of the enzymes involved in the healing process, leading to the cascade of the repairing and regenerative processes.

4.2. Wound Healing Activity of Nanoclay/Spring Water Hydrogels

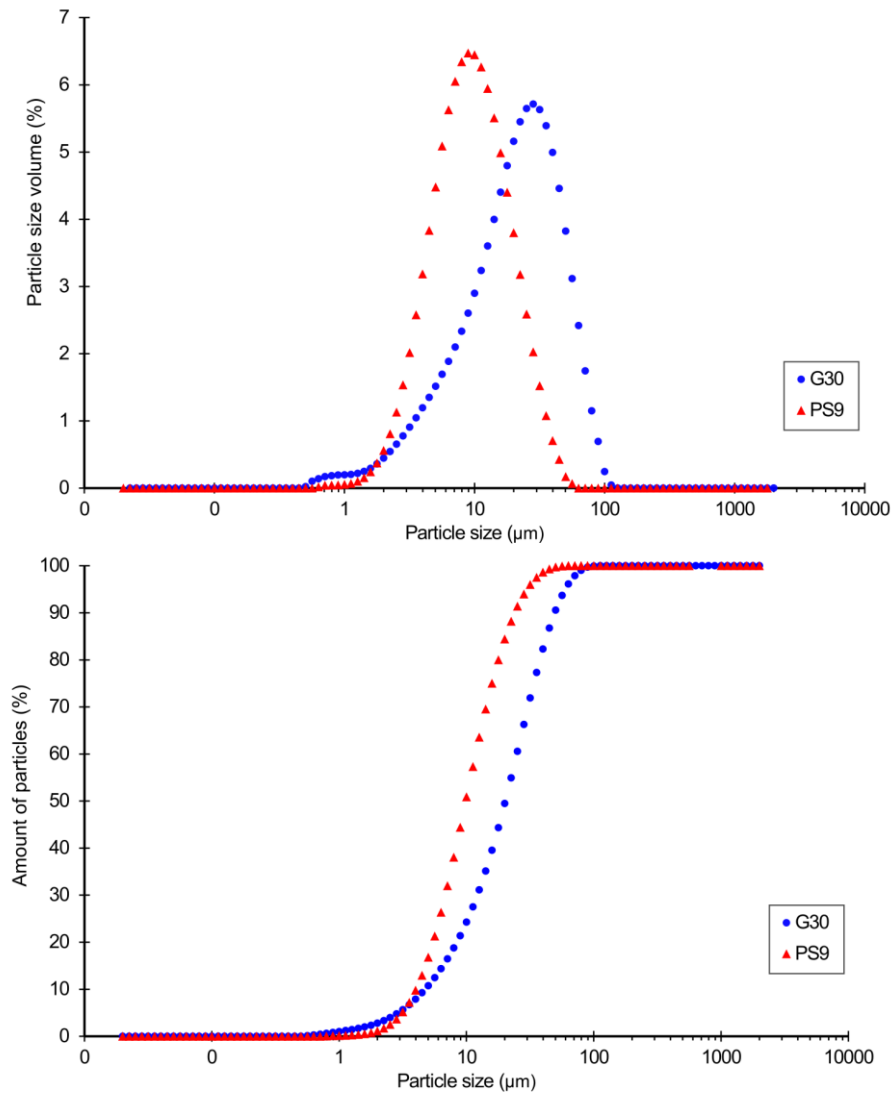


Figure 4.12. Particle size analysis of PS9 and G30. Differential analysis (up) and cumulative percentage of particles (down)

Specifically, calcium and magnesium levels should raise during the first 5 days of wound healing in order to promote granulation tissue formation and epidermal cell proliferation (Dubé et al., 2010). Moreover, during the restoration of the trans-epithelial potential of cells in the damaged tissue, Na^+ , K^+ and/or Ca^{2+} play a crucial role (Ma et al., 2016). The bioavailability of these

cations in the wound site should promote the healing process and contribute to fasten the damaged area reparation.

Table 4.13. CEC results of PS9 and G30 (average mEq/100g \pm s.d.; n=3)

mEq/100g	PS9	G30
Na ⁺	0.70 \pm 0.045	1.68 \pm 0.071
K ⁺	0.33 \pm 0.023	0.13 \pm 0.032
Mg ²⁺	3.62 \pm 0.341	7.61 \pm 0.326
Ca ²⁺	4.53 \pm 0.123	6.87 \pm 0.186
Total	9.18	16.29

Mg²⁺ cations, ALI and GR are rich of, demonstrated to possess remarkable properties for tissue regeneration and repair, particularly, promoting collagen formation and angiogenesis on skin wounds (Lansdown, 2002; Sasaki et al., 2017). For this reason, it is conceivable that ALI and GR should perform wound healing effects, as previously remarked. The maximum exchangeable amount of Mg²⁺ from PS9 and G30 corresponded to 17.67 and 37.14 mg/L, respectively (Table 4.13). Magnesium concentration due to the spring water was 5-12 mg/L and this proved to be effective during wound healing by Sasaki and co-workers (Sasaki et al., 2017). Consequently, both PS9 and G30 were considered as potentially effective minerals due to their exchangeable Mg²⁺ content.

Normal homeostasis of mammalian skin is also maintained by elements such as calcium, modulating keratinocyte and fibroblasts proliferation and differentiation (Fairley et al., 1985). Certain skin disorders, such as psoriasis, have been related to Ca²⁺ disorders in keratinocytes (Karvonen et al., 2000; Gao and Jin, 2019). Extracellular calcium is a determinant factor in the differentiation and maturation of fibroblasts and its effectiveness is dose-dependent (Fairley et al., 1985). Another recent study on wound healing demonstrated that calcium cations released from a calcium alginate wound dressing promoted endothelial cell growth and proliferation (Hotta et al., 2018).

Zinc is also important during wound healing steps (Fairley et al., 1985; Dubé et al., 2010), though it was not detected as an exchangeable cation of PS9 nor G30 through the ICP-OES measurements performed. However both ALI and GR waters contained Zn (Table 4.10).

Potassium has also demonstrated to favour wound healing (fibroblast differentiation, re-epithelialization, migration and proliferation of dermal cells), so its presence both in spring waters and hydrogels is considered as a positive feature (Shim et al., 2015; Hotta et al., 2018).

Zeta Potential

Zeta-potential results of PS9 and G30 at different concentrations are presented in Figure 4.13. Regarding ζ potential of minerals in pH 7 buffer, PS9 and G30 results were in agreement with other sepiolite and palygorskite samples previously studied (Berg et al., 2009; Middea et al., 2015; Li et al., 2018; Di Credico et al., 2019). In particular, PS9 zeta potential in aqueous pH 7 solution were more negative (higher) than G30's.

It has been demonstrated that surface charge of nanoparticles has the potential to influence cell viability (Berg et al., 2009). The importance of clay particles zeta potential during biocompatibility and wound healing tests lies in the fact that cells possess a negative surface zeta potential. Negative zeta potential is one of the most decisive factors of biocompatible materials, showing higher cell viability (Honary and Zahir, 2013; Spriano et al., 2017). It is known that particles with positive zeta potential interact and/or penetrate cells easily due to their opposite charge, thus being one of the main strategies to improve transfection efficiency (Takeuchi et al., 1996; Bengali et al., 2005). Negatively charged particles have also proved to interact with cells up to a certain extent and even be able to enter by endocytosis-mediated mechanisms (Wang et al., 2008; Zhang et al., 2008), although this happens with higher difficulty for negative particles than for positive ones. The uncontrolled entrance of certain substances into the cells could jeopardize their viability, thus inferring that positively charged materials are more likely to put the cell viability at risk.

Another factor by which nanoparticles surface charge demonstrated to influence cell viability is due to their agglomeration state (Takeuchi et al., 1996). Berg and co-workers revealed that hepatocytes showed less viability when exposed to metal nanoparticles with zeta potentials close to their isoelectric point (Spriano et al., 2017). This change in zeta potential was also strongly related to the agglomeration state of the very same particles. That is,

as more neutral are the nanoparticles, the more easily they aggregate and, subsequently, the faster their precipitation over the cell tapestry and/or their interaction with the negatively charged cell membranes.

Cell medium such as DMEM have demonstrated to significantly modify zeta potential of different suspended particles (Su et al., 2010; de Souza e Silva et al., 2016; da Silva et al., 2019). These changes are ascribed to the presence of a wide variety of charged molecules such as amino acids and vitamins, among others. The interaction of clay particles with these molecules changes zeta potential of the former ones. In fact, PS9 and G30 suffered a significant change of zeta potential when added to full DMEM culture medium (Figure 4.13). In this occasion, no significant differences were found between PS9 and G30 values, thus confirming that the resultant surface charges of the particles is governed by the culture medium. Therefore, during biocompatibility and wound healing tests, clay particles should maintain a -10 mV zeta potential. The reduction of zeta potential strength would reduce the stability of the clay suspensions, turning them into less flocculated and consequently, more prone to precipitation phenomena. Precipitation of clay particles could hinder cell viability by cell suffocation. Nonetheless, the fact that they still showed a negative surface charge would difficult the entrance of clay particles inside cells. These results will be confirmed by MTT analysis.

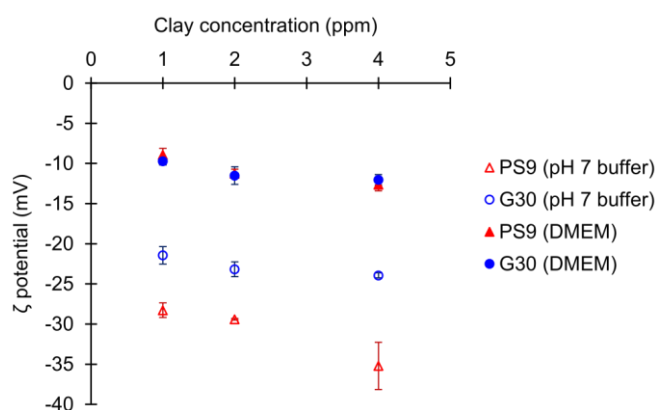


Figure 4.13. Zeta potential variations of PS9 and G30 (mean values \pm s.d.; $n=3$) in pH 7 buffer and complete DMEM culture medium at different concentrations

4.2.2.2. *In Vitro* Tests of Inorganic Ingredients, Spring Waters and Hydrogels

Biocompatibility Tests

Biocompatibility results on NHDF treated with medicinal ALI and GR waters for 24h are plotted in Figure 4.14. No significant differences were found, even when multiple comparisons were performed. In fact, ALI and GR viability results were around 100% for all water dilutions. Therefore, mineral medicinal waters studied in this work did not hinder dermal fibroblasts viability, thus determining their biocompatibility. Internal comparisons between ALI and GR concentrations were also performed. Mann-Whitney marked differences in ALI viability results, between 50% vs. 0.25% and 25% vs. 0.25% (Figure 4.14). Su and co-workers detected an optimal dilution of a concentrated underground mineral spring water that made skin cells to grow better in comparison with other dilutions (Fukushima et al., 2013). By the same token, ALI concentrations higher than 25% (v/v) could allow slightly better NHDF growth performances with respect to more diluted samples.

PS9 clay mineral and corresponding peloids PS9ALI and PS9GR are plotted in Figure 4.15 (left) as well as G30 and its corresponding peloids G30ALI and G30GR Figure 4.15 (right). In a general view, as lower the sample concentration (either clay or thermal mud), the higher the cell viability. None of the samples nor their concentrations presented a cellular viability below 80%. This fact indicated the absence of drastic cellular cytotoxicity within 24 h. With respect to PS9 and G30 clays, it was possible to observe a slight reduction of the cellular viability (with respect to GM) as the clay concentration increased. In fact, when clay mineral concentration corresponded to 1 mg/mL, cellular viability was closed to 80% (for both pristine clays and thermal muds). Nonetheless, statistical analyses indicated no significant differences between PS9 and G30 1000 µg/mL concentrations vs. GM, which confirmed that PS9 and G30 were highly biocompatible against NHDF cells. G30 5 µg/mL concentration showed significant differences vs. GM.

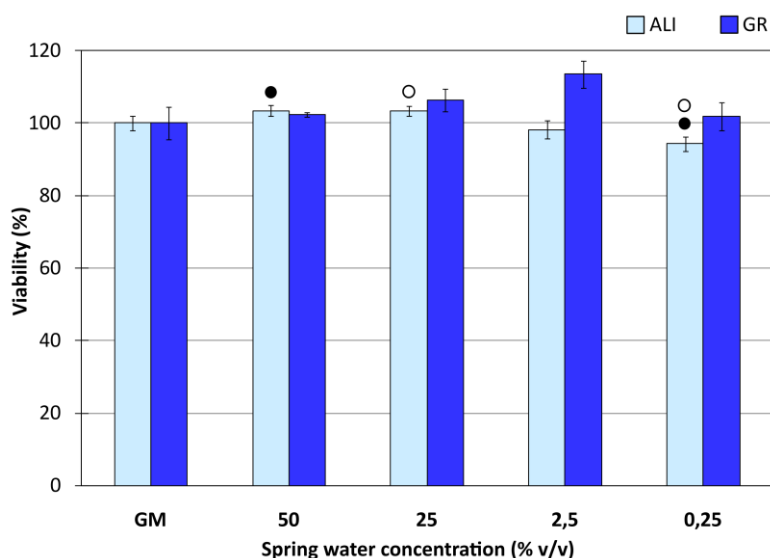


Figure 4.14. Biocompatibility tests (contact time 24h) of medicinal waters ALI and GR. Viability (%) vs. medicinal water concentration (% v/v) toward NHDF. GM stands for “growth medium” and referred to control test. Mean values \pm s.d.; $n=8$. Significant differences are marked as (●) ALI 50% (v/v) vs. ALI 0.25% (v/v); (○) ALI 25% (v/v) vs. ALI 0.25% (v/v). Mann-Whitney (Wilcoxon) W tests, p values ≤ 0.05

Apparently, the lower the concentration of the clay, the better the cellular proliferation. It has been suggested by some studies that the precipitation of clay minerals could hinder cell viability by some sort of physical effect (Wang et al., 2008; Salcedo et al., 2012). The biocompatibility of Veegum® HS (Bentonite clay) was evaluated by Salcedo et al. finding that at 167 $\mu\text{g}/\text{mL}$ of Veegum® HS concentration, the viability of Caco-2 cells reduced approximately to 50% (Salcedo et al., 2012). This effect was ascribed to the precipitation of clay particles, which blocked cell membrane channels. According to the authors, montmorillonite had a particle size ranging from 45-75 μm (Salcedo et al., 2012), which is a particle size range very similar to that of PS9 and G30. In these conditions, it was argued that if the precipitation of clay particles occurred, cell viability could be compromised at concentrations ≥ 160 $\mu\text{g}/\text{mL}$. On the contrary, neither PS9 nor G30 showed fibroblasts viabilities lower than 50% even at the highest concentration tested, thus demonstrating to possess a remarkable biocompatibility.

4.2. Wound Healing Activity of Nanoclay/Spring Water Hydrogels

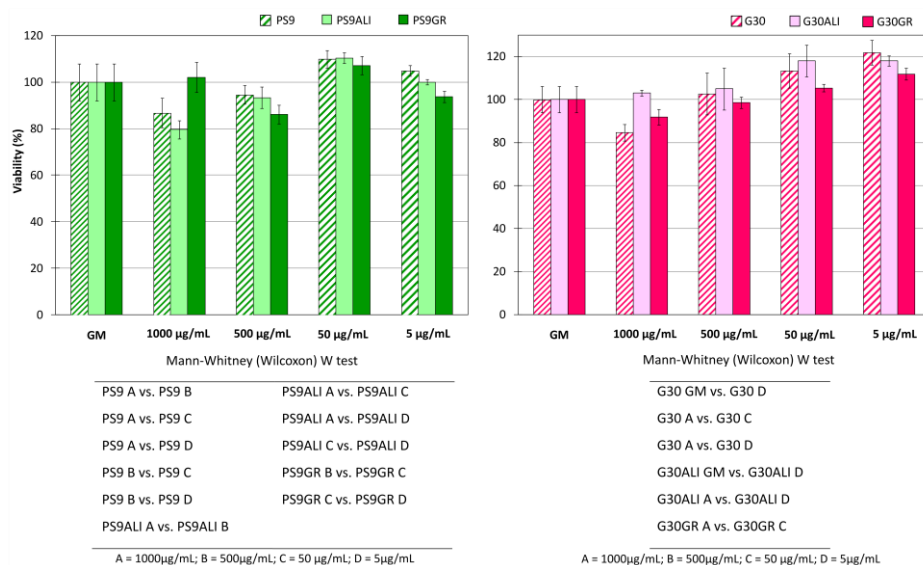


Figure 4.15. Biocompatibility tests (contact time 24h) of PS9, PS9ALI and PS9GR (left) and G30, G30ALI and G30GR (right). Viability (%) vs. clay concentrations toward NHDF. GM stands for "growth medium" and referred to control test. Mean values \pm s.d.; $n=8$. Significant differences were reported within the figure (down) as "sig" which refers to "p-values"

Internal statistical studies for PS9 and G30 results detected significant differences in G30 1000 $\mu\text{g/mL}$ vs. 50 $\mu\text{g/mL}$ and 5 $\mu\text{g/mL}$. For PS9, concentrations of PS9 1000 and 500 $\mu\text{g/mL}$ differed both between them as well as with 50 and 5 $\mu\text{g/mL}$ (Figure 4.15). These findings mean that, for both clays, smaller clay amounts in contact with fibroblasts were characterized by a higher degree of fibroblast biocompatibility. The biocompatibility results obtained for both clays were in agreement with the existing literature. Sepiolite clay mineral (Pangel S9) has been previously tested by Fukushima et al. towards fibroblasts and osteoblasts (Fukushima et al., 2013). In this case, authors combined 10% of sepiolite with poly(butylene adipate-co-terephthalate) reporting no cytotoxicity. A Tolsa's Group sepiolite clay was also employed by Fernandes et al. (Fernandes et al., 2013). In this case, they reported a reduction of HeLa cell viability of 50% when sepiolite was present in 1000 $\mu\text{g/mL}$ concentration. No such a reduction was found in this work when PS9 was used at the same concentration. Nonetheless, these differences could be ascribed to differences in the type of cell culture (Toledano-Magaña et al., 2015). Apart from anti-inflammatory, antibacterial and anti-oxidant

properties of a natural Spanish palygorskite, its cytotoxicity against murine macrophages has been reported to start from 300 $\mu\text{g}/\text{mL}$ onwards (Cervini-Silva et al., 2015a, 2015b). Particularly, authors reported a reduction of 20% viability at the aforementioned concentration. Once again, in the present study, G30 showed higher biocompatibility (at least against fibroblasts) because, even at 500 $\mu\text{g}/\text{mL}$ concentration, fibroblasts did not show a viability reduction. In more recent studies, pharmaceutical grade palygorskite (Pharmasorb® colloidal) was able to protect human dermal fibroblasts against carvacrol cytotoxicity at clay concentrations ranging from 8 to 12 $\mu\text{g}/\text{mL}$ (Tenci et al., 2017).

Neither PS9ALI nor PS9GR showed significant differences between GM and tested concentrations thus demonstrating the total biocompatibility of these hydrogels. Statistically, PS9ALI and PS9GR thermal mud showed similar significant differences between concentrations, following the same trend previously described for PS9. In fact, 50 and 5 $\mu\text{g}/\text{mL}$ clay concentrations apparently favored cellular viability (Figure 4.15, left). The agreement among PS9ALI, PS9GR and PS9 biocompatibility results allowed the confirmation of their reproducibility. Both PS9ALI and PS9GR, as well as PS9, shared significant differences of concentration 50 $\mu\text{g}/\text{mL}$ due to the higher viability results obtained at this concentration (Figure 4.15, left).

Regarding G30ALI and G30GR peloids, Mann-Whitney statistical analysis pointed out significant discrepancy in activity between G30ALI GM and 1000 $\mu\text{g}/\text{mL}$ concentration vs. 5 $\mu\text{g}/\text{mL}$ and between G30GR 1000 $\mu\text{g}/\text{mL}$ vs. 50 $\mu\text{g}/\text{mL}$ (as specified in Figure 4.15, right). Since same trend has been reported for G30 samples, once again it was possible to confirm the reproducibility of the results.

Despite the complexity generated by the statistical analysis, all solid samples (Figure 4.15) showed a better result for 50 $\mu\text{g}/\text{mL}$ concentration, always with cellular viabilities higher than 100%. According to these findings, 50 $\mu\text{g}/\text{mL}$ clay concentration was the safest/most ideal one for fibroblast cultures, regardless of the type (PS9 or G30) or the origin of the clay (powder or thermal mud). It is also important not to forget the fact that all the tested concentrations were biocompatible for fibroblasts within 24 h of contact. Due to the conclusions reached with MTT test 50 $\mu\text{g}/\text{mL}$ was the clay concentration

4.2. Wound Healing Activity of Nanoclay/Spring Water Hydrogels

selected for further studies including cell motility assay (wound healing) and proliferation CLSM tests. For spring waters, 50% v/v concentration was used.

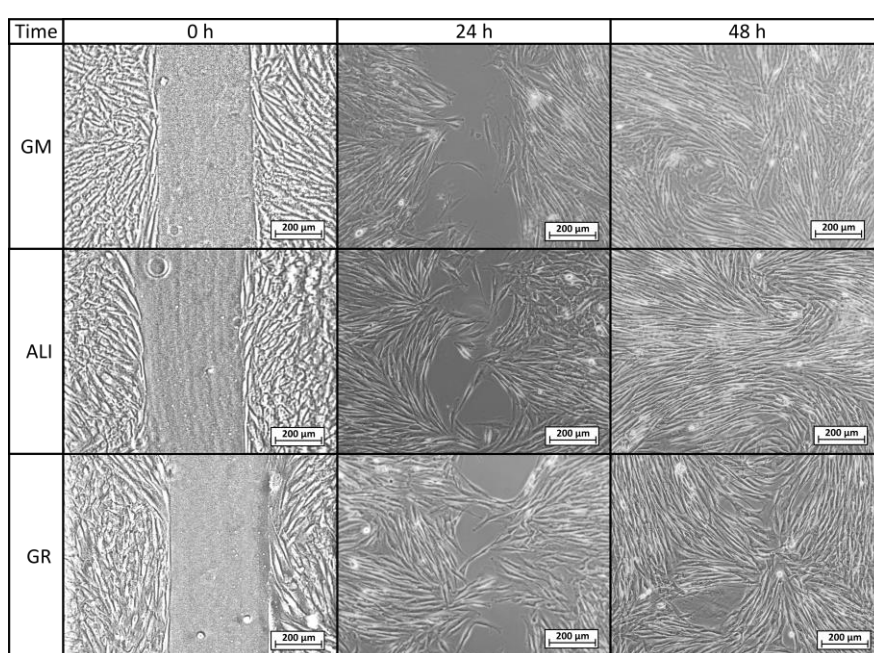


Figure 4.16. Optical microscopy of wound healing tests for control group (GM) and spring waters (ALI and GR) at 50% (v/v) culture concentration

Cell Motility Assay for Wound Healing

Microscopy images of gap closure results are reported in Figure 4.16 to 4.18. Samples ALI and GR were tested for 50% (v/v) concentration, while PS9, G30, PS9ALI, PS9GR, G30ALI and G30GR were tested at 50 $\mu\text{g}/\text{mL}$ of clay mineral. The microphotographs taken at zero time (0 h) showed for all the samples the presence of defined gaps mimicking wounds. Normal fibroblasts grown at confluence are clearly visible in each side of the wound. The time 0 gaps were reported to measure approximately 500 μm , which was in agreement with the variability of the silicone inserts of the Petri μ -Dishes used ($500 \pm 50 \mu\text{m}$). Insoluble clay particles are visible in the cultures treated with PS9, G30 and hydrogels PS9ALI, PS9GR, G30ALI and G30GR, unlike GM, ALI and GR. In all cases, after 24 h, fibroblasts started to invade the gap and even established contact with the cells of the opposite side in certain points of some samples. NHDF cells also maintained their typical fusiform

morphology during the whole experiment. These facts confirmed that the presence of spring waters, clay or hydrogels did not impair cell growth. This was in line with the biocompatibility results previously discussed. In all cases, fibroblasts crossed the empty zone after 48 h, thus forming anastomosis.

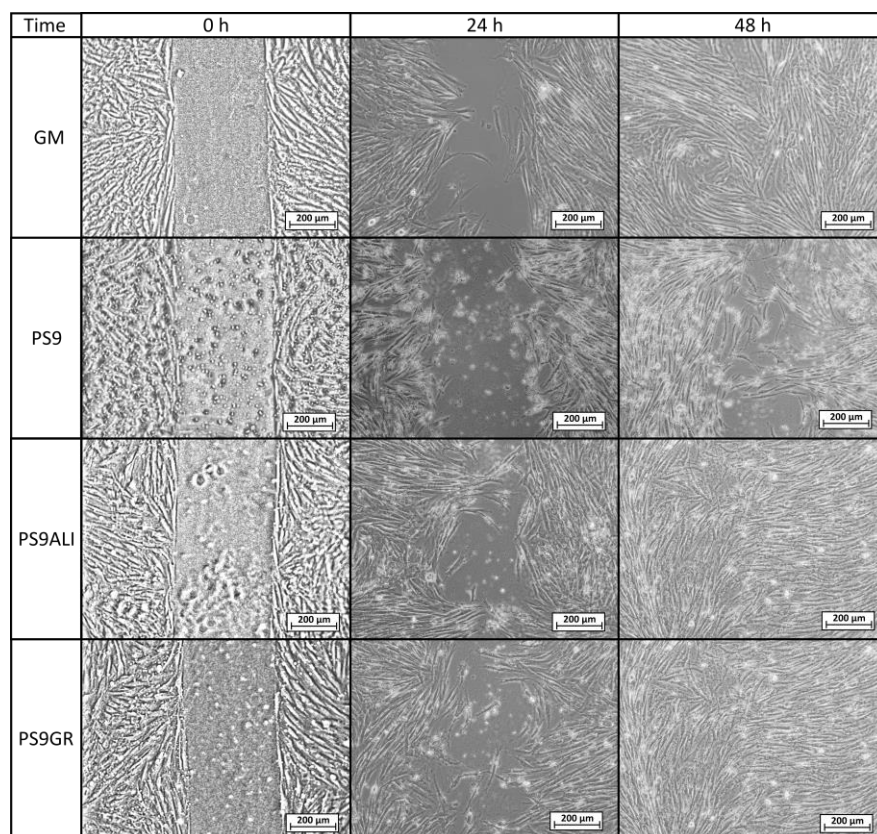


Figure 4.17. Optical microscopy of wound healing tests for control group (GM), PS9 clay mineral and corresponding peloids PS9ALI and PS9GR, all of them with a clay concentration of 50 $\mu\text{g/mL}$

In spring waters ALI and GR samples, fibroblasts of both sides of the wound established contact within 24 h (Figure 4.16). In comparison with the control (GM), it was clear that the addition of ALI and GR favored wound closure, since the contact points between fibroblasts were more numerous. According to the measurements of the wounded area performed by image analysis, ALI and GR samples covered, respectively, 62.9 and 59.1% of the initial wounded area, whereas GM covered about 31.8% of the wound (Figure

4.2. Wound Healing Activity of Nanoclay/Spring Water Hydrogels

4.19). After 48 h all the cell substrates reached the confluence, and this further supports the biocompatibility of the hydrogels and their components *in vitro*.

Previous works have claimed that the presence of elements such as B^{3+} and Mn^{+2} in keratinocytes culture mediums induced the migration of these cells (Chebassier et al., 2004b). They tested boron and manganese at different concentrations (500-1000 $\mu\text{g/L}$ and 100-1500 $\mu\text{g/L}$, respectively). In fact, keratinocytes in contact with these elements were able to cover the artificial gap (scratch-assay method) with 20% more efficiency with respect to the control group (without B^{3+} and Mn^{+2}) in 24 h. ALI and GR chemical composition has been previously reported by Aguzzi and co-workers (Aguzzi et al., 2013) and García-Villén et al. (García-Villén et al., 2020c) (Table 4.10). The absence of significant differences between GR, ALI and GM groups further confirmed the biocompatibility of both mineral medicinal waters since they did not hinder wound closure. The presence of B^{3+} and Mn^{+2} in both GR and ALI could explain why they did not interfere with cell motility during wound healing in a significant manner. Other elements such as As^{3+} and Fe^{2+} (both presents in ALI and GR waters) have also demonstrated to improve wound healing, particularly of the nasal mucosa (Staffieri et al., 2008). General skin regenerative properties of spring waters have been reported in the literature (Chiarini et al., 2006; Faga et al., 2012; Nicoletti et al., 2017b; Davinelli et al., 2019). The study of Liang et al. demonstrated that skin regenerative properties of Nagano spring water were related to the spring water chemical composition, with no influence of microorganisms (Liang et al., 2015). Another beneficial effect that could be ascribed to ALI and GR according to their chemical composition is the protective effect against oxidative stress due to the presence of sulfur (Guzmán et al., 2015).

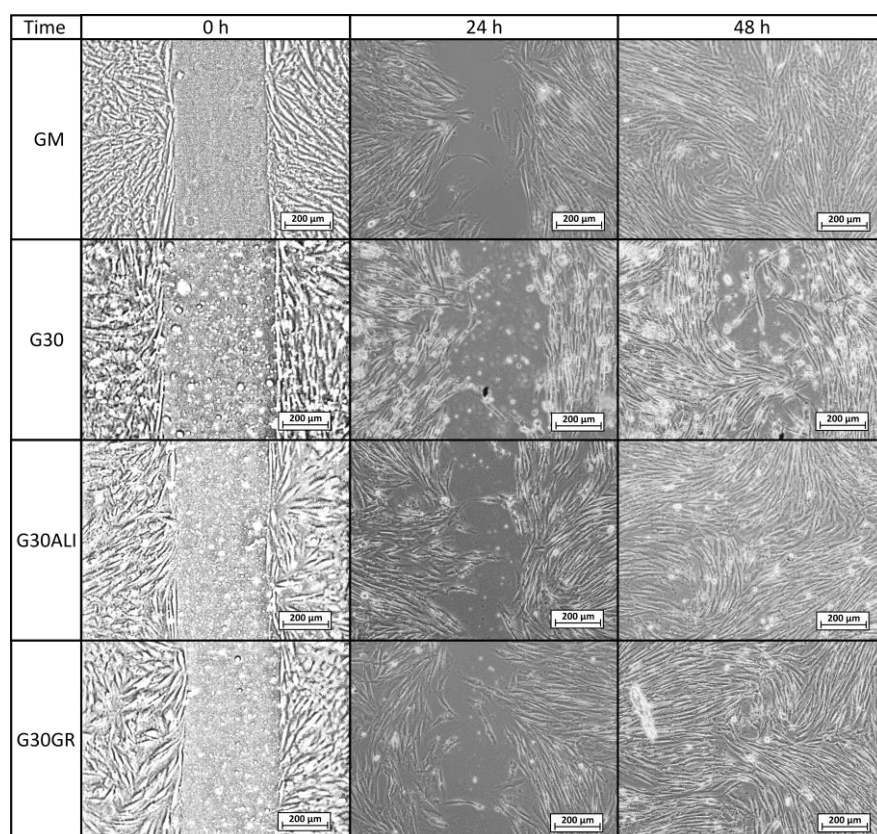


Figure 4.18. Optical microscopy of wound healing tests for control group (GM), G30 clay mineral and corresponding peloids G30ALI and G30GR, all of them with a clay concentration of 50 $\mu\text{g}/\text{mL}$

Regarding clay samples PS9 and G30 (Figure 4.17 and Figure 4.18) it was not possible to find zones with full fibroblast confluence after 48 h, though both sides of the wound were able to establish contact at this time. Fibroblast contacts of PS9 and G30 samples in the culture medium, were slower with respect to GM. According to MTT results, which were also performed for 24 h, pristine clays did not hinder cell viability. However, their presence seems to impede fibroblasts mobility during wound healing assay, slowing down the total gap closure with respect to GM and studied peloids. In fact, the uncovered gap width after 24 h was significantly higher for PS9 and G30 with respect to the rest of the samples (Figure 4.19), thus indicating a slower coverage of the wounded area. For these similar samples, the majority of insoluble particles visible within the cell substrate were

concentrated beside or over/inside fibroblasts. It is well-known that cell membranes are negatively charged and can be penetrated by positive substances. Negatively charged particles can also interact and event penetrate cells by endocytosis mediated mechanisms (Lin et al., 2006; Wang et al., 2008; Zhang et al., 2008). According to the zeta potential results previously reported (Figure 4.13), PS9 and G30 had a negative net charge in the major part of the pH range tested. These clay particles could interact between them (thus forming bigger aggregates) and with cells by establishing interactions such as Van der Waals forces. This hypothesis was the starting point of Abduljawad and Ahmed, who proposed that the interaction between clay minerals and cells would hinder cell migration (Abduljawad and Ahmed, 2019). They evaluated the role of montmorillonite, hectorite and palygorskite particles in cancer cell migration and demonstrated these materials could prevent cellular metastasis. Results of scratch-induced wound healing assays reported by these authors demonstrated that clay mineral particles significantly delayed the gap closure in comparison with control experiments. For instance, while the control showed full gap closure within 24 h, palygorskite showed a mean gap closure of $59\% \pm 3\%$ after 24 h. Polymeric composite films containing montmorillonite were evaluated by Salcedo and co-workers (Salcedo et al., 2012) and Mishra et al. (Mishra et al., 2014). The scratch assay showed, in both cases, that the presence of montmorillonite particles alone was able to alter cell behaviour (Caco-2 and fibroblasts, respectively for each study), slowing down the gap closure. Similar results were reported by Vaiana and co on montmorillonite and keratinocytes (Vaiana et al., 2011). These results were in agreement with PS9 and G30 performances during wound healing: though clays were not cytotoxic, more time would be necessary to obtain complete cell confluence within the artificial wound (gap) in their presence. The biocompatibility and safety of natural clay minerals such as palygorskite during wound healing is also supported by *in vivo* studies. A natural Brazilian palygorskite was tested for *in vivo* wound healing of rats (de Gois da Silva et al., 2014). In comparison with functionalized clay minerals, the natural one provided more advanced and safer wound healing, since histological cuts demonstrated the presence of dermal papilla and hair follicles after 14 days of treatment (de Gois da Silva et al., 2014).

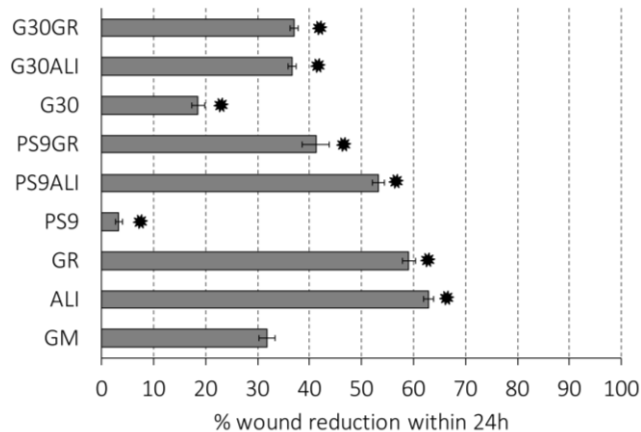


Figure 4.19. Histogram of % wound reduction after 24 h, calculated according to Eq. 2. Mean values \pm s.d. ($n=6$). Significant differences between samples and GM are marked with *

The presence of hydrogels promoted *in vitro* fibroblasts mobility during wound healing processes. In fact, the coverage of the artificial gap was faster for PS9ALI, PS9GR, G30ALI and G30GR with respect to GM and pristine clays (Figure 4.19). It is worth to notice that all therapeutic muds were used in concentrations equal to the powdered clay samples. That is, the amount of peloid within the culture medium was higher in order to compensate that they only possessed a 10% w/w of clay mineral. Whatsoever the nature of the interaction between clay particles and fibroblasts, responsible for the gap closure deceleration (observed in PS9 and G30 tests), was reduced to the minimum when it comes to thermal mud formulations. In fact, significant differences were found between gap closures of peloids vs. GM, demonstrating that the evaluated hydrogels induced a positive effect during wound healing.

These results are supported by previous studies in which clay minerals have reported to exert neutral or positive wound healing effects when combined with other substances (Ninan et al., 2015; Sandri et al., 2016). For instance, no significant changes have been found during *in vitro* wound healing studies of montmorillonite-chitosan-silver sulfadiazine nanocomposites with respect to the control. That is, the presence of the clay mineral did not hinder gap-closure procedure and did not affect fibroblasts phenotypes (Sandri et al., 2014). On the other hand, better skin re-

4.2. Wound Healing Activity of Nanoclay/Spring Water Hydrogels

epithelialization and reorganization have been found when halloysite and chitosan were combined to form a nanocomposite with respect to the use of both materials independently (Sandri et al., 2017). *In vivo* infected-wound treatment with silver nanoparticles was improved by the use of montmorillonite as a carrier, which reduced the drug cytotoxicity (Chu et al., 2012). Montmorillonite also demonstrated to exert wound-healing effect when combined with chitosan and polyvinyl-pyrrolidone polymers (Shanmugapriya et al., 2018). The nanocomposites films containing bentonite increased *in vivo* wound healing processes in mice when compared with the formulations without the clay. For instance, wound closure after 16 days was 92-93% for samples without clay and 95-97% for those with montmorillonite and all of them higher than the negative control at the same time (84%) (Shanmugapriya et al., 2018).

Despite the scarce literature regarding the use of therapeutic muds in skin regenerative properties, the existing studies were also in agreement with the present observations. Thermal mud treatments with volcanic deposits of Azerbaijan facilitated the healing of chronic gangrenous wounds of diabetic patients (Nasirov et al., 2009). The major part of the patients subjected to pelotherapy reached total wound recovery by the end of the treatment. Two natural Dead Sea black mud samples were evaluated by Abu-al-Basal for their *in vivo* wound healing properties (Abu-al-Basal, 2012). One of them was used in its pristine state, while the other was formulated in form of facial mask by adding plant extracts and vitamin E. Both samples accelerated wound healing process by enhancing granulation, wound contraction, epithelialization, angiogenesis and collagen deposition. Another *in vivo* wound healing study was performed by Dário and co-workers (Dário et al., 2014). They evaluated a natural peloid extracted from the Ocara lake (northeast of Brazil), which was sieved, solid-state characterized and sterilized. The solid fraction was mainly composed of quartz, illite and kaolinite and it was formulated as an emulsion. The emulsion was put in contact with injured Wistar rats. The formulation including the Ocara lake solid fraction induced histological changes in the deep dermis that allowed an effective healing with respect to control groups. On the other hand, there is evidence in literature about the anti-inflammatory properties of peloids (Carretero, 2020). Moreover, recently a study focused on

the fibrous clays suggests that sepiolite and palygorskite, the main components of PS9 and G30, respectively, did not influence the *in vitro* NO (inflammation signal) production of murine macrophages (RAW 264.7). Furthermore both clays decreased the leucocyte infiltration shortly after exposure *in vivo* on mouse ear edema (12-O-tetradecanoylphorbol-13-acetate as inflammatory agent). In particular, sepiolite and palygorskite caused decreases on the number of infiltrated cells per field (Cervini-Silva et al., 2015b). Analogously, other clay minerals, as halloysite and montmorillonite, proved macrophage cytocompatibility and negligible secretion of TNF α , as pro-inflammatory cytokine (Sandri et al., 2020). The anti-inflammatory properties of clays could control the inflammatory phase in the healing process shortening healing time and avoiding the wound chronicity.

4.2.2.3. Confocal-Laser Scanning Microscopy

CLSM microphotographs results (Figure 4.20) showed fluorescence of fibroblasts nucleus and cytoplasm. Green fluorescence is due to the binding of phalloidin specifically with F-actin and the blue one is due to DAPI, bounded to DNA. Morphology of fibroblasts during wound healing is very important, since it gives information about migration and adhesion of cells. F-actin filaments facilitate cell-cell interaction and tissue regeneration (Lehtimaki et al., 2017). In all samples, regardless of the type of sample with which fibroblasts were put in contact with, NHDF showed typical fusiform morphology. Moreover, fibroblasts located in the wounded area, possessed typical morphology of migrating cells. Therefore, it was possible to identify retraction/protrusion parts of fibroblasts due to the position of F-actin. Typical actin filament structures were detectable in all samples: lamellipodia, filopodia and stress fibers (dorsal stress fibers and transverse arcs). Moreover, fibroblasts in mitosis were also visible in some points.

4.2. Wound Healing Activity of Nanoclay/Spring Water Hydrogels

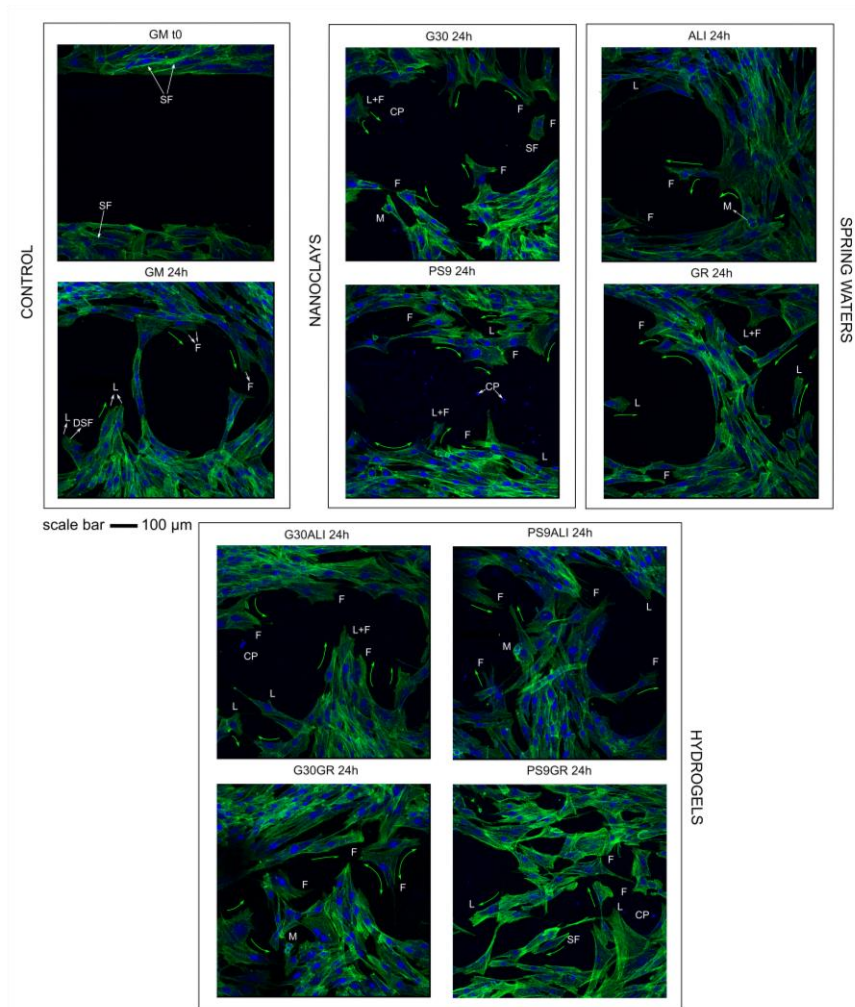


Figure 4.20. CLSM microphotographs during wound healing. NHDM were stained with phalloidin-FITC (green, F-actin filaments) and DAPI (blue, nucleus). Green arrows indicate the migration direction; different F-actin structures have been identified by L (lamellipodia), F (filopodia), SF (stress fibres), DSF (dorsal stress fibres). Additionally, M stands for (mitosis) and CP stands for (clay particles)

Regarding the speed of wound closure, the CLSM results were in agreement with those obtained by optical microscopy. GM control after 24 h demonstrated that NHDF are able to make contact and start to close the gap, though yet some empty zones are clearly visible. The number of cells inside the wound gap in ALI and GR samples was more numerous than in GM. PS9 and G30 showed the worst result in terms of “gap closure”, which confirmed

the previous results. Once again, it was possible to observe that the “slowing down” effect of PS9 and G30 did not happen when both clays were formulated in form of nanoclay/spring water hydrogels. Particularly, hydrogels G30ALI, G30GR, PS9ALI and PS9GR induced a faster wound healing with respect to the rest of the samples.

4.2.3. Conclusions

Fibroblast biocompatibility and wound healing efficacy of inorganic hydrogels formulated with two nanoclays in two natural spring waters have been studied. Both spring waters were fully biocompatible and favoured wound healing, inducing faster gap-closure with respect to control. The studied nanoclays did not interfere with cell viability to a great extent ($\geq 80\%$ of cell viability), thus not being cytotoxic at the studied concentrations. Nonetheless, they interfered with *in vitro* wound healing processes, slightly delaying gap-closure when used as powders. This effect could be ascribed to the presence of non-flocculated nanoclay particles in the culture medium. Hydrogels formulated with the aforementioned ingredients did not hindered gap-closure and reported a higher percentage of wound closure after 24 h with respect to the control.

In conclusion, this study has demonstrated the usefulness and potential of PS9 and G30 clay minerals as excipients in the preparation of hydrogels intended for wound healing and other therapeutic uses. Maximum *in vitro* wound healing effects were achieved by using PS9 in the formulation of the hydrogels. These promising results encourage the use of clay minerals as wound healing ingredients. Thermal centre's treatments are mostly focused in the physical effects of thermal muds, which are very effective against musculoskeletal disorders. Nonetheless, the findings of this study have opened new perspectives, since the addressed nanoclay/spring water hydrogels could also be used to treat chronic wounds.

4.3. Safety of Nanoclay/Spring Water Hydrogels: Assessment and Mobility of Hazardous Elements

The concentration and bioavailability of impurities such as hazardous elements in both health products and medicines is a main preformulation concern during their development. Different health care products must comply with specific normatives and guidelines, depending on the administration route, and most of the times, on the region or country in which they are written and applied. It is generally accepted that levels of elemental impurities below toxicity thresholds could be considered as safe, with diverse limits depending on the consulted normative. In Canada, natural health products that do not require a medical prescription, are included in a guide in which heavy metals (Pb, As, Cd, Hg, and Sb, among others) are banned or limited to a maximum amount, in accordance with the administration route (Government of Canada, 2012). In the USA, similar health products fall into FDA legislation, which only considers Hg as a forbidden element and limits the Pb concentration (FDA, 2017). On the other hand, European cosmetic legislation is much more detailed and restrictive regarding the presence of elemental impurities (EU, 2009).

Similar health products may also be considered into different categories depending on the country. The boundaries between medicinal products, natural health care products, cosmetics, and others, are not internationally normalized, even if generally accepted definitions have been achieved. In fact, the absence of clear boundaries made it necessary to address some products on a case-by-case basis. Particularly interesting is the cosmetic category, in which the presence of some ingredients, their origin, the administration route, and the scope of the product could raise doubts about their classification. A manual on the scope of the application of the cosmetics regulation EC 1223/2009 has been published by the working group on cosmetic products in order to shed some light on this matter (EU, 2017). The global cosmetics market have grown by an estimated 5.25% in 2019 (L'Oréal, 2019), and, due to this continuous growth, the attention is being increasingly focused on the quality and safety of these products. Cosmetics are, according to the European Council Directive 2003/15/EC and the US Food Drug and Cosmetic Act, those products or mixtures of substances prepared and

destined to be applied in different parts of the human body in order to clean, protect, maintain them in good conditions, improve their aspect, or relieve/eliminate body odours (EU, 2003; United States Code, 2006). It has been recognized and demonstrated that, although cosmetics are intended to be applied on the surface of the body or mucous membranes, they may not remain there exclusively, since some topically applied substances may penetrate through the skin (Hostynek, 2003; Tateo et al., 2009; Borowska and Brzóska, 2015). This fact is more pronounced for those cosmetics which are intended to remain at their application site for several hours or days, without subsequent rinse or wash. The European Union established a Regulation on Cosmetic Products (1223/2009) where it states that “cosmetic products should be safe under normal or reasonably foreseeable conditions of use. In particular, a risk-benefit reasoning should not justify a risk to human health” (EU, 2009). According to the European legislation, all cosmetic products should be subjected to safety assessments, taking into consideration the toxicology of all the ingredients used, as well as their chemical structure and their potential to produce local and systemic side effects.

The use of clay minerals in health care comes from prehistoric times, as reviewed in various paperwork and databases (Viseras and López-Galindo, 1999; Viseras et al., 2000; López-Galindo and Viseras, 2004; Sánchez-Espejo et al., 2014b; Health Canada, 2019). Some properties of these minerals have made them one of the most frequently used materials in pharmaceutical formulations and cosmetics, due to both their potential therapeutic activities and their useful properties as excipients. These features depend on colloidal dimensions and high surface areas of clay minerals, which give rise to optimal rheological and sorption capacities (López-Galindo and Viseras, 2004; López-Galindo et al., 2007, 2011). Kaolin, talc, smectites (montmorillonite and saponite), and fibrous clays (palygorskite and sepiolite) are some of the clay minerals most used in pharmacy. Hydrotherapy, and more particularly, balneotherapy, is one of the most frequent uses of clay minerals from a traditional and natural point of view. Clay minerals are used to prepare semisolid suspensions (frequently known as thermal muds or peloids) after the interposition of clays with spring waters, thus forming a nanoclay/spring water hydrogel. That is, thermal muds are semisolid, topical, natural

medicinal hydrogels prepared by the interposition of organic and inorganic solids in mineral–medicinal water (Sánchez-Espejo et al., 2014b).

On the view of the uses and properties of these clay-based hydrogels, they could be considered as cosmetics with skin-care functions such as cleansing, degreasing, exfoliating, hydrating, invigorating, and firming activities (Potpara and Duborija-Kovacevic, 2012; Centini et al., 2015; Khiari et al., 2019). These clay-based products could also be considered as medicinal products, as they have demonstrated activities against dermatological affections such as psoriasis (Elkayam et al., 2000; Delfino et al., 2003; Cozzi et al., 2015), atopic dermatitis, vitiligo, eczemas, seborrhoeic dermatitis, fungal infections, or acne have also been treated by clay/spring water hydrogels (Argenziano et al., 2004; Comacchi and Hercogova, 2004; Williams et al., 2008; Riyaz and Arakkal, 2011; Harari, 2012). Moreover, in view of the current Covid-19 worldwide state of emergency, Masiero and co-authors (Masiero et al., 2020) have pointed out the already demonstrated positive effects of balneotherapy and thermal muds over the human immune system. Therefore, according to the guidelines of the borderline products manual (EU, 2017), these formulations could fall either in the cosmetic or in the medicine category. Nonetheless, they are usually prepared in thermal stations, without a deep characterization of their therapeutical functions, activities, safety, or quality control. This unclear boundary between cosmetic and medical products showed by thermal muds, justifies the necessity of a harmonized regulation that compel for a full characterization of these products. Either way, since clay-based hydrogel formulations are intended to be applied over the skin (either health, ill, or injured skin), safety assessments should be one of the main milestones to be accomplished.

A remarkable feature of materials such as clays is the wide spectrum of mineralogical and chemical composition they have, something that is inevitable when it comes to natural products, most of the time accompanied by other naturally-associated mineral phases. Even if nanoclay/spring water hydrogels (thermal muds) are not legally considered as cosmetics or medicines and, therefore, they are not subjected to any kind of compulsory regulation; their accomplishment would highlight their quality constancy attributes and safety. The use of pharmaceutical-grade minerals in the

preparation of thermal muds would guarantee the compositional safety of the gel-like system. In this regard, the chemical composition of the substances present in the formulation is crucial, since hazardous elements such as heavy metals and other elements are prohibited or limited in cosmetic products by different regulations. For instance, the ICH Harmonized Guideline for elemental impurities Q3D(R1) (ICH, 2019) published by the European Medicines Agency and Regulation No 1223/2009, European Parliament (EU, 2009) are some of the regulations in which the discussion of this paperwork will be based. The safety assessment of the elements, such as heavy metals in cosmetics should start from the knowledge of the type and concentration of ingredients contained in the product in order to evaluate their potential intrinsic hazard (Bocca et al., 2014). The next step would include the analysis and studies of the mobility of those elements, either beneficial or harmful, in order to understand the potential biological and therapeutical effects of the formulation. This is especially important when it comes to “technically unavoidable” elements.

Recently, sepiolite and palygorskite (two inorganic excipients mainly composed of clay minerals) were mixed with natural spring water to prepare hydrogels intended for topical application. In previous studies, these excipients have demonstrated remarkable purity in terms of mineralogical composition (> 92% and > 58% of sepiolite and palygorskite richness, respectively) and quality performance (García-Villén et al., 2020c). Moreover, these very same hydrogels have also proved to possess wound healing effects.

The aim of this paper was to prepare, characterize, and address the elemental composition of nanoclay/spring water hydrogels made of sepiolite and palygorskite clay minerals and natural spring water. Since the present hydrogels are intended to be applied over potentially damaged or wounded skin, the mobility of their elements was also characterized. The final objective of this study was to assess the safety attributes of these formulations on the basis of the content and bioavailability of the elemental impurities.

4.3.1. Materials and Methods

4.3.1.1. Materials

Pangel S9 (PS9) and Cimsil G30 (G30) were kindly gifted by the TOLSA Group (Madrid, Spain). PS9 (d_{90} 23.9 μm) and G30 (d_{90} 49.3 μm) were mainly composed by sepiolite and palygorskite, respectively. According to their composition and properties, previously characterized by García-Villén et al., they could be classified as “pharmaceutical-grade” excipients (García-Villén et al., 2020c). Their corresponding pharmacopoeial denominations are “magnesium trisilicate” (PS9) and “Attapulgit” (G30) (Ph. Eur. 9th, 2018a, b; USP42-NF37, 2019). Sepiolite was present in PS9 in >92%, muscovite being the main mineralogical impurity detected. Palygorskite was present in G30 in 58%, accompanied by quartz (26%), fluorapatite (7%), smectites, and sepiolite (6%) and carbonates (3%) as associated minerals. Both PS9 and G30 excipients were dried in an oven at 40 °C for at least 48 h prior to being used in the preparation of the hydrogels. Spring water from Alicún thermal station (ALI), located in Granada (Spain) was used. ALI water is classified as hypothermal with strong mineralization (Maraver Eyzaguirre and Armijo de Castro, 2010).

Nanoclay/spring water hydrogels were prepared according to a process previously studied and optimized (García-Villén et al., 2020c). Briefly, clay minerals were mixed with ALI by means of a turbine high-speed agitator (Silverson LT, Chesham, UK), equipped with a high-traction stirrer head of square mesh, at 8000 rpm for 5 min. Samples were preserved in closed polyethylene containers, from which aliquots were sampled in order to monitor further analysis. Nanoclay/spring water hydrogels prepared had a 10% w/w of PS9 concentration (ALIPS9) and 20% w/w of G30 nanoclay (ALIG30). Both of them were preserved and characterized in the same way.

4.3.1.2. Methods

Elemental Composition of Pristine Ingredients

Elements present in PS9 and G30 as well as ALI water has been addressed by Inductively Coupled Plasma mass spectrometry (ICP-MS) measurements. Solid samples were prepared by acid digestion in strong acids (HNO_3 and HF at a 3:5 ratio) inside a Teflon reactor, thus the samples were

subjected to high pressure and temperature by heating in a microwave oven (Milestone ETHOS ONE, Sorisole, Italy). The quantification of the elements was done by a NexION-300 ICP-MS spectrometer (Perkin Elmer, MS, U.S.) equipped with a triple cone interface and a quadrupole ion deflector using argon for plasma formation. Standard solutions of 100 and 1000 ppb were prepared for each element (Multi-Element standards, Perkin Elmer, MS, U.S.), and Rh was employed as an internal standard. All standards were prepared from ICP single-element standard solutions (Merck, Darmstadt, Germany) after dilution with 10% HNO₃. Ultra-purified water (Milli-Q® grade, 18MΩ·cm) was used during the whole experiment. The accuracy of the ICP-MS equipment used ranges between ± 2 and ± 5% for analyte concentrations between 50 and 5 ppm, respectively. The detection limits were < 0.1 ppt for Ir and Ta; < 1 ppt for Ba, Li, Cu, Mo, Sb, Sn, Ag, Au, Co, Ni, V, As, Cd, Pb, Zr, Be and Nd; < 10 ppt for Cr, Hg and Te; < 1 ppb for P.

In Vitro Release of Elemental Impurities from Hydrogels

The element mobility from nanoclay/spring water hydrogels (ALIPS9, ALIG30) was assessed by *in vitro* cation release studies performed in a Franz diffusion cell system FDC40020FF (BioScientific Inc., Phoenix, US) (COLIPA, 1997). This system is designed to recreate conditions of formulations placed over the skin and mucosa membranes. Particularly, the selected Franz diffusion cells possessed a contact area of 0.64 cm² and an approximate total volume of 6.4 mL in the receptor chamber. In this study, the aim is to explore the potential number of elements that would be released by the formulation and that are potentially able to establish contact with the skin. To do so, dialysis membranes (cut-off 12–14 kDa (31.7 mm), Medicell International, London, UK) were placed and used to separate the donor and receptor chambers, just acting as physical support for the hydrogel and not as a permeation barrier. The membranes were boiled in ultra-purified water (milli-Q® water) for 10 min in order to hydrate them. Over the membrane, in the donator chamber, 0.025 g of each hydrogel was placed. The receptor chamber of the Franz diffusion cells was filled with degassed, ultra-purified water, which was maintained at a constant temperature of 32 ± 0.5 °C (to reproduce human skin temperature) through a thermostatic bath circulation. The experiment lasted for 30 min, this being the typical time of topical

nanoclay/spring water hydrogels application. At the end of the experiments, the receptor aqueous phase was withdrawn and filtered through 0.45 μm single-use, sterile filters. Then, the elemental composition on each sample was assessed by ICP-MS, following the same protocol previously described for the pristine materials. All samples (six replicates) were subjected to *in vitro* release experiments 48 h after the preparation and after one month. During the experiment, the manipulation of different materials and instruments could contaminate the ultra-purified water of the Franz cell receptor chamber. To eliminate this error, blanks were also analysed in order to monitor the elements coming from the materials and the ultra-purified water itself. Briefly, it consisted of analysing the ultra-purified water that was placed in the receptor chamber of the Franz cell device. The concentration of the elements detected in the milli-Q[®] water (which was considered the blank, data not shown) were subtracted from the concentration detected in the receptor chamber. This way, it will be possible to discern the real number of elements exchanged/released from the semisolid formulation and, thus, able to establish contact with the patient skin.

4.3.1.3. Results Discussion and Interpretation Bases and Criteria

Different regulations could be used for the interpretation of the obtained results. In this paperwork, the discussion and interpretation of the results will be centred on the documents summarized in Table 4.14.

The HC-SC guideline is focused on heavy metals (As, Pb, Cd, Hg, and Sb). Other metal elements such as Se, Ba, and Cr are considered less significant in terms of toxicity; therefore, no impurity limits are found for these elements in this document (Government of Canada, 2012). The Natural and Non-prescription Health Products Directorate (NNPHD) (Health Canada, 2015) is a guidance document intended to give support to stakeholders “in assuring that natural health products are produced in a high-quality manner”. NNPHD is focused on natural and non-prescription health products, which is the case of PS9, G30, and ALI ingredients and resultant hydrogels. Acceptable limits for As, Cd, Pb, Hg, Cr, and Sb elemental impurities are defined in this guide, including the limits for topical administration (Figure 4.21).

Table 4.14. Documents used during the interpretation and discussion of the obtained results

Type of Document	Region	Year	References
Regulation of the European Parliament and Council of the European Union on cosmetic products (EC 1223/2009)	EU	2009	(EU, 2009)
Guidance on Heavy Metal Impurities in Cosmetics (HC-SC)	Canada	2012	(Government of Canada, 2012)
Quality of Natural Health Products Guide - Natural and Non-prescription Health Products Directorate (NNPHD)	Canada	2015	(HealthCanada, 2015)
Guideline for Elemental Impurities Q3D(R1)	EU	2019	(ICH, 2019)

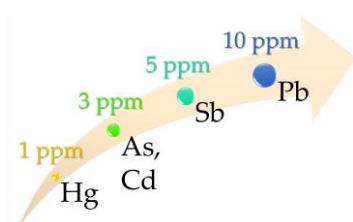


Figure 4.21. Acceptable limits for heavy metals in topical products (HealthCanada, 2015)

The ICH guideline for Elemental Impurities Q3D(R1) refers to medicinal products and classifies elements into four groups based on their toxicity and likelihood of occurrence in these products (Figure 4.22). The fourth group called “other elements” includes elements for which Permitted Daily Exposure (PDE) limits have not been established. As a result of this, these elements have not been included in this manuscript. Regarding the most toxic elements, the Q3D(R1) guideline also reports the PDE limits by oral, parenteral, and inhalation administration routes (ICH, 2019). PDE is the maximum acceptable intake of the elemental impurity per day. Although this guideline is not specific for cosmetics, the fact that it deals with elemental impurities of drugs (which are intended to reach the bloodstream) makes it useful to also ensure the safety of cosmetics.

4.3. Safety of Nanoclay/Spring Water Hydrogels: Assessment and Mobility of Hazardous Elements

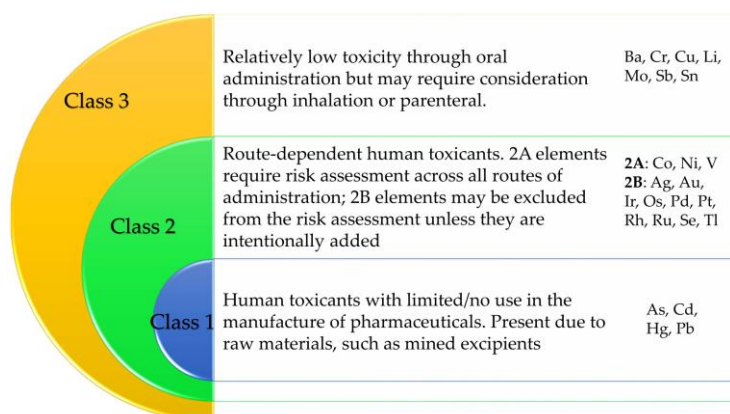


Figure 4.22. Element classification of the ICH Q3D(R1) guideline. Based on ICH Q3D(R1) (ICH, 2019)

Finally, the European Regulation EC 1223/2009, from all the documents and guidelines included in this study, is the most restricting one in terms of impurities present in cosmetics (EU, 2009). Only those elements considered safe and innocuous for the human being are allowed in cosmetics, while the rest of them are banned without any limit or maximum dose established. Furthermore, according to article 17 of this regulation, “the presence of traces of banned substances will only be allowed if they are technically inevitable and do not impair the safety of the cosmetic product”. In this regard, *in vitro* studies such as Franz cells could help to discern and discuss this point since they allow the study of the mobility of the elements present in the ingredients.

Dose of Nanoclay/Natural Spring Water Hydrogels

The toxicity of elemental impurities obviously depends on the administration route of the dosage form. Nanoclay hydrogels prepared in this study are intended to be topically applied over either the healthy or wounded skin of patients subjected to balneotherapy treatments. In thermal stations, natural or artificial clay-based/spring water formulations could be applied in different forms. The most common one includes the administration of semisolid systems at 45–50 °C on restricted body regions (mainly isolated joints) with 210 cm of thickness or in the form of total/partial baths. Most of these treatments usually last for 15 to 30 min (Meijide Faílde et al., 2013; Sánchez-Espejo, 2014; Gomes et al., 2015). The density of the hydrogels was

obtained by the Minimum Square Method applied to experimental volume, and mass hydrogels measurements (R^2 were > 0.998 in both cases): $\rho_{ALIP9} = 1.0606$ g/mL; $\rho_{ALIG30} = 1.0992$ g/mL. These data would be used to calculate safe doses of hydrogels in order to not exceed the PDE limits defined in the Guideline for Elemental Impurities (ICH, 2019) for each element. Moreover, despite the bioavailability of topically administered dosage forms hardly reaching 100%, in the discussion, we will systematically consider the maximum potential bioavailability in order to guarantee safe doses.

4.3.2. Results

4.3.2.1. Elemental Composition of Pristine Ingredients

The elemental composition of PS9, G30 nanoclays, and natural spring water (ALI) is summarized in Table 4.15. Below, the results will be discussed from the most innocuous to the most dangerous elements, as well as by the amount in which they were detected.

Regarding PS9 and G30, Ba, Cr, and Li (Class 3) and V (class 2A), were detected in remarkable amounts. The presence of Zr and Nd was also reported. Except for Li, the amount of the aforementioned elements was higher in G30 than in PS9, thus highlighting the presence of more impurities in G30. This statement is in agreement with the solid-state characterization of G30 made by García-Villén et al. (García-Villén et al., 2020c). The presence of hazardous elements such as Pb, As, and Cd in fibrous clay minerals have been reported as a common feature of natural deposits, though the present values are minimal with respect to previously reported levels (Post and Crawford, 2007).

With respect to the ALI spring water, the main hazardous impurities detected were Li and Ba, followed by Cr (class 3 elements in all cases). Therefore, the major elements detected (Table 4.15) belong to class 3 or class 2A (ICH, 2019), which indicates that they are elements whose presence in the raw materials should be borne in mind, though with relatively low toxicity. Additionally, the presence of Cr, Zr, and Nd is not allowed in cosmetics, according to the EC 1223/2009 (EU, 2009). From class 2B, only the presence of Se and Tl is banned in cosmetics, though the three of them were detected as

4.3. Safety of Nanoclay/Spring Water Hydrogels: Assessment and Mobility of Hazardous Elements

traces (Table 4.15). Ni, which belongs to class 2A and its not allowed in cosmetics, was detected in significant amounts in G30, unlike PS9 and ALI.

Table 4.15. Elemental composition of pristine ingredients (PS9 and G30 nanoclays and ALI spring water) determined by ICP-MS. The elements are classified depending on regulations (EU, 2009; ICH, 2019). "ND" stands for "Not detected"

Element	PS9 (ppm)	G30 (ppm)	ALI (ppb)	Comments
Ba	56.2	144.8	18.8	Class 3 in Q3D(R1); Not listed as element in EC 1223/2009
Cr	14.0	391.8	4.3	Class 3 in Q3D(R1); Not allowed in EC 1223/2009
Cu	8.1	11.3	2.5	Class 3 in Q3D(R1); Allowed in EC 1223/2009
Li	149.0	30.4	244.2	Class 3 in Q3D(R1); Not listed in EC 1223/2009
Mo	0.2	0.2	3.8	
Sb	0.3	2.1	0.1	Class 3 in Q3D(R1); Not allowed in EC 1223/2009
Sn	10.8	3.3	ND	Class 3 in Q3D(R1); Not listed in EC 1223/2009
Ag	0.04	0.2	0.1	Class 2B in Q3D(R1); Allowed in EC 1223/2009
Au		ND		
Ir	0.2	0.9	ND	Class 2B in Q3D(R1); Not listed in EC 1223/2009
Se	0.9	1.5	2.3	Class 2B in Q3D(R1); Not allowed in EC 1223/2009
Tl	0.2	0.1	0.1	
Co	2.3	7.4	0.4	Class 2A in Q3D(R1); Not listed in EC 1223/2009
Ni	3.7	50.7	9.4	Class 2A in Q3D(R1); Not allowed in EC 1223/2009
V	24.9	249.1	ND	Class 2A in Q3D(R1); Not listed in EC 1223/2009
As	2.0	1.3	0.2	Class 1 in Q3D(R1); Not allowed in EC 1223/2009
Cd	0.02	1.5	ND	
Hg		ND		
Pb	3.2	4.1	ND	
P	0.3	8.5	0.1	Not allowed in EC 1223/2009
Be	1.8	3.6	0.01	
Zr	21.5	50.3	0.2	
Te		ND		
Nd	8.0	30.2	ND	
Ta	0.9	0.7	0.005	

Class 1 element group is formed by hazardous elements As, Cd, Hg, Nd, Pb (Figure 4.21), all of them prohibited according to EC 1223/2009. As,

Cd, and Pb were similar to the ones reported for natural products used in cosmetics (Borowska and Brzóška, 2015). Unlike class 1 and EC 1223/2009, the NNHPD (Health Canada, 2015) specifies the acceptable limits for heavy metals in topical products (Figure 1), including Sb (class 3). All the aforementioned elements were below the limits established by the NNHPD.

The rest of the elements (from P onwards, Table 4.15 are not classified in Q3D(R1), thus not belonging to any specific group previously mentioned. Among them, Zr highlights due to the high amount present both in PS9 and G30 in comparison with the rest of the non-allowed elements.

4.3.2.2. *In Vitro* Release of Hazardous Elements from Hydrogels

The results obtained after the Franz cell studies regarding the release of the elements from nanoclay hydrogels at 48 h and after one month are summarized in Table 4.16.

Ba release was very variable between ALIPS9 and ALIG30, though the higher values detected in ALIG30 could be ascribed to higher Ba presence in the pristine material G30 in comparison with PS9 (Table 4.15). Cu mobility, which was higher in ALIG30 due to a higher amount in G30, significantly decreased after one month for both ALIG30 and ALIPS9.

The Li release was higher in ALIPS9 due to the higher Li levels in PS9 and maintained constant with time (no significant differences between 48 h and 1 month). On the other hand, ALIG30 hydrogels showed a reduction in Li release as time passed. The highest Mo was found in ALIG30—48 h and significantly decreased after one month. On the other hand, ALIPS9 demonstrated a constant release of Mo through time. Sn, V, and Cd released from both hydrogels came from clay minerals since none of these elements were detected in ALI (Table 4.15). The V release increased with time, while Sn showed the opposite trend.

Heavy metals Hg, Pb, and Sb, though present in the pristine materials, were not released. Other not-allowed elements, such as Cr, Se, Tl, Ni, P, Be, Zr, Te, Nd, and Ta were neither release elements, which means that they do not pose any problem in terms of safety. On the other hand, Cd and As were slightly released, with higher results in the case of ALIG30 hydrogels. The

4.3. Safety of Nanoclay/Spring Water Hydrogels: Assessment and Mobility of Hazardous Elements

absence of Cd in ALIPS9 is due to the extremely low amounts detected in PS9 and its absence in ALI. On the contrary, G30 possessed a higher amount of Cd (Table 4.15), which explains the release results (Table 4.16). In conclusion, Cd and As are the most crucial elements determining the safety of the hydrogels. It is worth mentioning that with respect to the As and Cd amounts and release, ALIPS9 hydrogel is considered the safest formulation.

Table 4.16. Release of hazardous elements after Franz diffusion cell tests. The concentrations are expressed in $\mu\text{g}/100\text{ g}$ of hydrogel. Mean values \pm s.e. ($n = 6$). "ND" stands for "not detected"

Elements	ALIPS9		ALIG30	
	48h	1 month	48h	1 month
Ba	5.6 ± 1.55	1.8 ± 0.934	8.3 ± 0.944	1.2 ± 0.360
Cr	ND		ND	
Cu	10.8 ± 3.293	3.6 ± 2.17	20.6 ± 3.725	0.91 ± 0.608
Li	20.5 ± 3.293	17.7 ± 3.214	4.3 ± 0.362	1.7 ± 0.379
Mo	0.7 ± 0.095	0.61 ± 0.125	1.8 ± 0.0572	0.21 ± 0.123
Sb	ND		ND	
Sn	28.7 ± 8.232	10.4 ± 2.138	50.4 ± 4.866	6.5 ± 1.945
Ag, Au, Ir, Se, Tl	ND		ND	
Co	0.26 ± 0.206	0.6 ± 0.093	1.1 ± 0.660	0.58 ± 0.237
Ni	ND		ND	
V	1.7 ± 0.310	1.8 ± 0.492	5.9 ± 0.306	7.5 ± 0.315
As	0.1 ± 0.010	0.4 ± 0.039	0.08 ± 0.050	0.1 ± 0.063
Cd	ND		0.1 ± 0.064	0.2 ± 0.0087
Hg, Pb	ND		ND	
P, Be, Zr, Te, Nd, Ta	ND		ND	

4.3.3. Discussion

4.3.3.1. In Vitro Release of Elements: Safety Concerns and Doses

The toxicity of elemental impurities obviously depends on the administration route of the dosage form. The studied hydrogels are topically administered, and the bioavailability of a certain element hardly reached 100%. Tateo and co-workers, in previous studies regarding elemental percutaneous mobility, stated that the major part of the elements could cross the skin (Tateo et al., 2009). Nonetheless, they reported that "none of these elements reaches concentrations so high as to represent hazardous conditions". In the discussion, we systematically will consider a theoretical 100% bioavailability in order to guarantee safe doses in any case.

According to the results, the maximum amount of Ba released came from ALIG30, 48 h, and it counted for 8.3 $\mu\text{g}/100\text{ g}$ of hydrogel. The oral PDE of barium was established as 730 $\mu\text{g}/\text{day}$ (ICH, 2019). If we consider the maximum mobility and a 100% bioavailability of Ba through the skin, the administration of ALIG30 and ALIPS9 hydrogels would be considered safe if doses are less than 8.79 kg hydrogel/day (Table 4.16). In view of the high amounts of hydrogels needed to pose a risk regarding Ba, it is possible to state that both ALIPS9 and ALIG30 are safe with respect to this element.

Among the possible adverse effects associated with Cu, allergic dermatitis is the most commonly experienced (Ababneh et al., 2013). Safe amounts of hydrogels regarding Cu release (Table 4.16) have been calculated according to parenteral PDE (Table 4.17). In view of the results, hydrogels aged for one month could be considered safe in terms of allergenic copper effects, since its mobility practically disappears. Moreover, ALIPS9 would be more advisable than ALIG30; the amount of Cu being lower in the former one. The amount of Cu released from extemporaneous formulated hydrogels could limit their use in general baths, as the calculated safe dose (Table 4.17) should be lesser than two kilograms of hydrogel.

Table 4.17. Theoretical safe doses of ALIPS9 and ALIG30 hydrogels based on elements with defined parenteral Permitted Daily Exposure (PDE) levels. Calculations have been made by using the higher mobility value reported by Franz cells (either ALIPS9 or ALIG30). Additionally, safety doses are calculated assuming a theoretical dermal bioavailability of 100%

Element	PDE _{parent} Limits	Maximum release detected	Hydrogel safe dose/day
Ba	730 $\mu\text{g}/\text{day}$	8.3 $\mu\text{g}/100\text{g}$ (ALIPS9 – 1month)	$\leq 8.79\text{ kg}$
Cu	340 $\mu\text{g}/\text{day}$	20.6 $\mu\text{g}/100\text{g}$ (ALIG30 – 48h)	$\leq 1.65\text{ kg}$
Li	280 $\mu\text{g}/\text{day}$	20.5 $\mu\text{g}/100\text{g}$ (ALIPS9 – 48h)	$\leq 1.37\text{ kg}$
Mo	1700 $\mu\text{g}/\text{day}$	1.8 $\mu\text{g}/100\text{g}$ (ALIG30 – 48h)	$\leq 94.4\text{ kg}$
Sn	640 $\mu\text{g}/\text{day}$	50.4 $\mu\text{g}/100\text{g}$ (ALIG30 – 48h)	$\leq 1.27\text{ kg}$
Co	5 $\mu\text{g}/\text{day}$	1.1 $\mu\text{g}/100\text{g}$ (ALIG30 – 48h)	$\leq 454\text{ g}$
V	12 $\mu\text{g}/\text{day}$	7.5 $\mu\text{g}/100\text{g}$ (ALIG30 – 1 month)	$\leq 160\text{ g}$
As	15 $\mu\text{g}/\text{day}$	0.4 $\mu\text{g}/100\text{g}$ (ALIPS9 – 1 month)	$\leq 3.75\text{ kg}$
Cd	1.7 $\mu\text{g}/\text{day}$	0.2 $\mu\text{g}/100\text{g}$ (ALIG30 – 1 month)	$\leq 850\text{ g}$

Li is of relatively low toxicity by the oral route. Is a common metal present in animal tissues and is used in certain kinds of treatments, such as bipolar disorder or depression, among others. Recently, Yuan and co-workers (Yuan et al., 2019) prepared a sponge scaffold with LiCl and evaluated wound

healing activity *in vitro*. The presence of Li reduced inflammation and improved angiogenesis, re-epithelialization, and expression of β -catenin. Seborrhoea dermatitis is another skin disorder that has been addressed by Li as an active lithium gluconate/succinate, with successful results (Leeming, 1993; Dreno and Moyse, 2002; Dreno et al., 2003; Gupta and Versteeg, 2017). The main problem of Li is the narrow therapeutic margin it possesses (Grandjean and Aubry, 2009; McKnight et al., 2012). Parenteral Li PDE was established to be 280 $\mu\text{g}/\text{day}$ (ICH, 2019). Considering that all the released Li would be able to reach the bloodstream once the hydrogel is applied, the administration of ≤ 1.37 kg hydrogel/day would guarantee safe doses of Li (below the parenteral PDE, Table 4.17).

Mo could be considered as an essential element since its deficiencies have been related to night-blindness, nausea, disorientation, coma, tachycardia, tachypnea, and other biochemical abnormalities (ICH, 2019). Nonetheless, excessive accumulation of Mo could also produce toxicity, so its limits need to be controlled. In particular, Mo could be accumulated in the skin, bound to dermal collagen. The amount of Mo released from ALIPS9 was constant with time, while it significantly reduced after one month in ALIG30 (Table 4.16). Parenteral PDE levels of Mo are 1700 $\mu\text{g}/\text{day}$. Considering the highest released amount of Mo (ALIG30—48 h), and supposing 100% of bioavailability, 94 kg/day of hydrogels would be necessary to reach PDE limits (Table 4.17). In view of these calculations, it is possible to guarantee that ALIPS9 and ALIG30 are safe with respect to Mo levels.

Tin is an element widely used nowadays (Granjeiro et al., 2020). The PDE limits of Sn have been established since it has been reported to increase *in vitro* oxidative stress or DNA breakage (Bai et al., 2018). In view of tin's released amounts in ALIPS9 and ALIG30, its toxicity and PDE limits should be borne in mind. In particular, this element showed lower release from both hydrogels after one month of preparation. The inhalation and oral consumption of Sn are the main routes for Sn intoxication (Boogaard et al., 2003; Roopan et al., 2014; Tabei et al., 2015), thus meaning that the topical application of these hydrogels would be a safe administration route. In fact, *in vitro* cytotoxicity studies of these hydrogels were not shown to hinder

normal dermal human fibroblast growth nor cell motility during *in vitro* wound healing (García-Villén et al., 2020a).

Ni has been widely detected in cosmetic products, together with Co and Cr, among others (Hepp et al., 2014; Borowska and Brzóška, 2015). The attention paid to Ni, Co, and Cr is based mainly on skin conditions, such as contact allergic dermatitis, itching, and edema, among others (Schaumlöffel, 2012; Zulaikha et al., 2015; Chou et al., 2016; Al Hossain et al., 2019; Pathania and Budania, 2019; Román-Razo et al., 2019). What is more, these elements can be solubilized by sweat during prolonged contact (Larese Filon et al., 2004; Schaumlöffel, 2012). Pristine materials possessed higher amounts of Ni than Co. Nonetheless, no Ni and Cr mobility was detected in Franz cell tests, thus reducing the risk of contact skin alterations produced by ALIPS9 and ALIG30 hydrogels. The Co mobility in ALIPS9 increased with time, while in ALIG30, it maintained constant (Table 4.16). The application of young hydrogels (ALIPS9) would entail the lowest risk of skin allergies related to cobalt. Co is an integral component of vitamin B₁₂, which means that it is essential for the human body. It is estimated that the average person receives about 11 µg Co/day with normal diet, and the parenteral PDE is established to be 5 µg/day (EU, 2009). Additionally, it has been demonstrated that Co is able to pass the skin (Larese Filon et al., 2004; Filon et al., 2009), though its percutaneous absorption was found to be very low (0.0123 µg·cm⁻²·h⁻¹). Time of hydrogels application in thermal stations takes at about 20–30 min, which is not enough time for all the mobile Co (Table 4.16) to cross the human skin, thus making the “hydrogel safe dose/day” (calculated assuming a 100% of bioavailability, Table 4.17) to be remarkably higher in real conditions.

V is a ubiquitous element in the human body, though no essential role has been found yet for this element. Although systemic toxicity of V has already been accepted, its deficiency has also proved to be problematic since it is associated to thyroid, glucose, and lipid metabolism malfunctions. It also participates in the regulation of several genes and has been demonstrated to influence cancer development, including skin cancers such as malignant melanoma (Mukherjee et al., 2004; Pisano et al., 2019). V was a mobile element in both hydrogels prepared. No V was detected in the ALI, Franz cells results ascribable to pristine clay minerals composition (Table 4.15). In ALIG30, the

release of V was higher due to the higher amount of this element in G30 in comparison with ALIPS9 (Table 4.16). Although antiproliferative properties of V ions have been found (Pisano et al., 2019), neither ALIPS9 nor ALIG30 hydrogels impaired normal human fibroblasts *in vitro* proliferation, according to previous studies (García-Villén et al., 2020a).

As is a forbidden element in cosmetics (EU, 2009). Arsenic mobility is reported to be very low in both hydrogels. It maintains constant through time in ALIG30, while it increases in ALIPS9 after one month. This element is very ubiquitous in the environment, so it is expected to be present in natural ingredients such as clay minerals. This element is classified in the category 1A in view of its carcinogenicity, as reported in the European Regulation EC 1272/2008 (EU, 2008). For greater clarity, substances belonging to the 1A category are known to have carcinogenic potential to humans. It possesses a pronounced affinity for skin and keratinizing structures, although it does not act as a sensitizer due to poor skin penetrating ability. According to article 1 of the EC 1223/2009, “prohibited substances should be acceptable at trace levels only if they are technologically inevitable with correct manufacturing processes and provided that the product is safe”. Assuming 100% bioavailability and using parenteral PDE levels, the maximum dose of hydrogels that could be used without exceeding these levels is 3.75 kg·day⁻¹ (Table 4.17) (ICH, 2019). Moreover, the maximum mobility of As is far less than the maximum permissible concentration of inorganic As in drinking water (10 µg/L (US EPA, 2001; WHO, 2017) vs. 4.24 µg/L in ALIPS9 one month).

Cd is another element whose presence in cosmetics is forbidden. Cd did not show mobility from ALIPS9. Higher amounts of Cd in G30 justified the higher mobility of this element in ALIG30. The low release of Cd from fibrous clay minerals is in agreement with previous studies, which reported irreversible interaction between Cd and the solid phase, thus hindering the mobility of this element (Shirvani et al., 2006a). Regarding toxicity, Cd is classified in the category 2 (suspected human carcinogen). It can accumulate in the skin, having deleterious effects on this organ, as recently demonstrated by an *in vivo* study (Tucovic et al., 2018). Nonetheless, the *in vitro* percutaneous bioavailability of cadmium chloride salt tested through human

skin was determined to be among 0.07% (from water) and 0.01% (from soil) (Wester et al., 1992).

Other heavy metals such as Pb and Sb, though present in the pristine materials (Table 4.15), were not mobile (Table 4.16). Hg and Au were not detected in the pristine materials, and their absence after Franz cell diffusion guaranteed the absence of contamination during preparation, conservation, packaging, and manipulation of the hydrogels (art. 17 of the EC 1223/2009 (EU, 2009)). Additionally, the cytotoxicity of these hydrogels has been previously tested *in vitro* (García-Villén et al., 2020a), obtaining very positive results, which supports the hypothesis of product safety.

4.3.3.2. Mobility of Hazardous Elements

The presence in a product of an elemental impurity will have safety concerns only once released, with different mechanisms underlying the release of each particular element, mainly depending on its position in the structure of the hydrogel components. Nevertheless, it is possible to calculate a parameter of general comparative interest; mobility of the elements from the dosage form. The mobility of an element could be calculated as the ratio between the element content/element released.

In view of the previously shown results, the mobility of hazardous elements from ALIPS9 and ALIG30 hydrogels was minimal in the major part of the cases (Figure 4.23). These results could be explained by the high adsorption capacity of palygorskite and sepiolite clay minerals, their low cation exchange capacity, and the gel network of hydrogels. The mobility of tracers has been explained due to the formation of inner-sphere complexes with clay and other associated mineral surfaces (Bradbury et al., 2005; Elzinga et al., 2006; Altmann et al., 2012). It also seems clear that different ionic equilibriums are established through time in both hydrogels (Figure 4.24). For instance, Co, Ba, and Sn reduce their mobility while As and Cd increase it, thus demonstrating that elements established different equilibriums within the hydrogel.

4.3. Safety of Nanoclay/Spring Water Hydrogels: Assessment and Mobility of Hazardous Elements

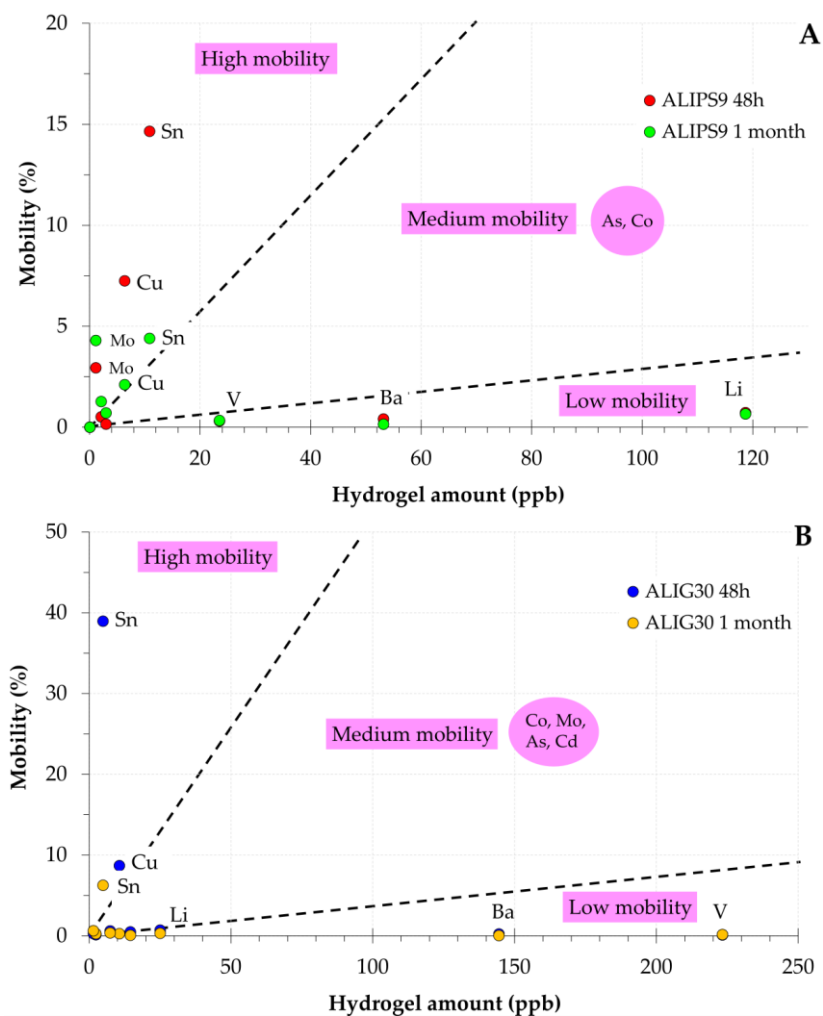


Figure 4.23. Element mobility (%) versus the total amount of element in ALIPS9 (A) and ALIG30 (B). Only mobile elements are shown

Sn showed to be the most mobile element, followed by Cu (Figure 4.23). Sn was not detected in ALI, which indicates that the release of this element came from PS9 and G30. On the other hand, Cu was detected in the three ingredients. In ALIPS9, the third element with significant mobility was Mo (Figure 4.23, A). Molybdenum was also detected as an element with remarkable mobility in ALIPS9, while the mobility in ALIG30 was significantly smaller. The differences in Mo amounts released (Table 4.16) could be ascribed to the differential solid-liquid equilibrium established within both hydrogels since both PS9 and G30 presented the same amount of

this element (Table 4.15). The reduction of Mo mobility in ALIG30 indicates that the G30 clay mineral has a better ability to retain the Mo in ALI.

Li, Ba, V, and Cd were the elements with the smaller mobility. V was not detected in ALI, which means that the released amount was due to the clay minerals. V and Li did not participate in the solid-liquid equilibrium established between solid and liquid phases since their mobility was constant with time. Although Ba was an element with minimal mobility, it reduced with time in both hydrogels. The fact that G30 showed higher Ba amount than PS9 together with the fact that Ba mobility in this hydrogel was smaller than in ALIPS9 indicates that it is a structural element of G30. Moreover, the similar release of Ba from ALIPS9 and ALIG30 means that, probably, the major part of the Ba released came from ALI instead of PS9 and G30.

Cd and As were slightly mobile, with higher results in the case of ALIG30 hydrogels. The absence of Cd mobility in ALIPS9 was due to the extremely low amounts detected in PS9 and its absence in ALI. On the contrary, G30 possessed higher amounts of Cd (Table 4.15), which explains the mobility results (Table 4.16). Cd and As were the most crucial elements determining the safety of the hydrogels. It is worth to mention that, with respect to the As and Cd amounts and mobility, ALIPS9 hydrogels could be considered the safest formulation.

The mobility of Sn, Cu, Mo, and Ba from hydrogels reduced as time passed. The mobility reduction could be explained by the irreversible adsorption of the elements by PS9 and G30. In fact, fibrous clay minerals have been proposed as environmental remediation ingredients and wastewater treatments aiming to eliminate heavy metals with promising results (Wang and Wang, 2010; Zhang et al., 2011; Guo et al., 2014; Cheng and Ye, 2015).

The spider diagram (Figure 4.24) clearly shows that, as a general trend, palygorskite hydrogels reduced the mobility of hazardous elements with time (with a reduction in area), whereas this was not obvious for sepiolite hydrogels.

4.3. Safety of Nanoclay/Spring Water Hydrogels: Assessment and Mobility of Hazardous Elements

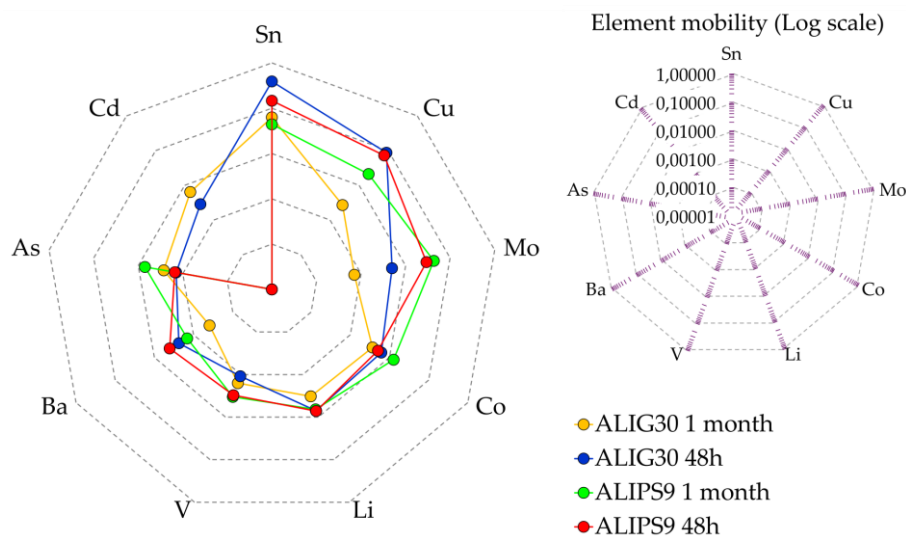


Figure 4.24. Spider diagram of element mobility. Only mobile elements are shown. The logarithmic scale was used, though not include in the spider diagram for simplicity and clarity

At this point of the study, and looking at the safe dose calculations (Table 4.17), the way to guarantee the absence of any intoxication risk would be to apply the hydrogels locally (over restricted areas of the skin, wounds, joints, etc.). That is, hydrogel bath treatment should be avoided if potentially toxic doses of the elemental impurities want to be minimized. Nonetheless, bioavailability and percutaneous permeation studies would be highly useful and valuable to establish safe usage guidelines for these formulations.

4.3.4. Conclusions

Elemental impurities in medicinal products have to be controlled within safety limits with different guidelines and normatives being useful from a pharmaceutical quality perspective. The essential role of clay minerals in drug products and cosmetics is widely known. Nanoclay/natural spring water hydrogels have been prepared by mixing a sepiolite and a palygorskite with local spring water (Alicún de las Torres, Granada, Spain). Clay hydrogels are traditionally used in balneotherapy or as natural cosmetics (masks, shampoos, etc.). Since these formulations are intended to establish an intimate contact with the skin (either healthy, sensitive, or damaged skin) their composition is of high importance in terms of safety. In this study, special attention has been paid to the presence of heavy metals and other hazardous

elements. As expected, pristine materials possessed a wide variety of hazardous elements such as Cd, Pb, or P, among others. Since these elements are specifically forbidden in cosmetics according to the European Regulation (EC 1223/2009), pristine materials do not accomplish cosmetic regulations on their own. Nonetheless, the presence of certain substances in a cosmetic does not imply that they are able to be absorbed or enter in contact with the skin. In order to discern the potential bioavailability of these elements, their mobility was evaluated by using Franz cells *in vitro* tests. Among all the specifically forbidden elements in cosmetics, only As and Cd were detected as mobile, though in very low amounts. Their mobility was so low that, taking into account the corresponding PDE for the parenteral route and assuming 100% of bioavailability through the skin, the calculated safe doses were approximately 1 kg of hydrogel per day. In conclusion, the present study demonstrates that the composition and nature of the solid phases of the hydrogel determine the mobility of the elements. Legally speaking, the mobility of As and Cd could hinder the authorization of ALIPS9 and ALIG30 hydrogels as cosmetic products. Nonetheless, there is no sufficient evidence to confirm that the presence of these elements is detrimental to their safety and, though further studies are still necessary, ALIPS9 and ALIG30 hydrogels could be used in practice. Finally, it is worth to mention that, despite that ALIG30 showed higher ability to reduce the elements mobility, the ALIPS9 hydrogel would be easier to authorize as a medicine or cosmetic, since the mobility of As and Cd in this hydrogel was minimum or absent. Future perspectives of this particular study include the assessment of the percutaneous mobility of the elements (bioavailability) both *in vitro* and *in vivo*. These kinds of studies would help to better define the best techniques to apply fibrous clay-based hydrogels to maximize benefits by minimizing the risks.

4.4. Correlation between Elemental Composition/Mobility and Skin Cell Proliferation of Fibrous Nanoclay/Spring Water Hydrogels

Inorganic hydrogels formulated with spring waters and nanoclays are successfully used in the treatment of musculoskeletal disorders and skin affections. There is a general agreement that their therapeutic activity against musculoskeletal disorders is achieved through physical mechanisms such as thermic activity, osmotic pressure and electric conductivity (Fioravanti et al., 2007, 2011, 2017; Tateo et al., 2009; Cozzi et al., 2015). On the other hand, the underlying mechanism of action responsible for the therapeutic skin effects are usually ascribed to the chemical composition of the formulation (Andreoli and Rascio, 1975; Sukenik et al., 1999; Tateo et al., 2009; Quintela et al., 2010; Pesciaroli et al., 2016; Drobnik and Stebel, 2020), although the exact therapeutic activities and mechanisms of action are still unknown.

Several dermatological affections have been successfully treated by formulations that include clay minerals (Elkayam et al., 2000; Delfino et al., 2003; Argenziano et al., 2004; Fioravanti et al., 2007; Harari, 2012). Currently, special attention is being paid to wound healing treatments, in which clay minerals have been demonstrated to be very useful (Sandri et al., 2016; García-Villén et al., 2019, 2020a, 2020d). During the administration of the formulation, elements from the hydrogel could permeate and/or penetrate across the skin barrier. In a previous study, hydrogels prepared with two different fibrous nanoclays were shown to be fully biocompatible and to exert in vitro wound healing activity (García-Villén et al., 2020a). More particularly, it was demonstrated that the fibrous nanoclay hydrogels promoted in vitro fibroblast mobility during wound healing processes.

It is well known that adequate concentrations of certain elements, including Ca, Mg, Na and K, in the wound bed are important for enhancing the healing process (Fairley et al., 1985; Lansdown et al., 1999; Karvonen et al., 2000; Lansdown, 2002; Dubé et al., 2010; Shim et al., 2015; Sasaki et al., 2017; Hotta et al., 2018; Gao and Jin, 2019). Transition metals such as Cu, Zn, Mn, Fe, Ag, and Au (among others) have also been demonstrated to play different biological functions in tissue regeneration, as reviewed by Yang and co-

authors (Yang et al., 2018). It has also been demonstrated that Zn:Ca ratios reach their maximum during the proliferative stage of wound healing and then decline during the remodelling stage (Lansdown, 2002). Moreover, manganese-rich spring waters have been demonstrated to possess wound healing activity (Chebassier et al., 2004b), and changes in Mg:Ca ratios are essential for a proper wound healing cascade. Consequently, formulations providing adequate bioavailability of elements with wound healing activity will promote the healing process and speed up restoration of the damaged area.

Based on these premises, the aim of this study was to assess the *in vitro* release and mobility of elements with potential wound healing effects from hydrogels formulated with spring waters and nanoclays that have recently been demonstrated to enhance fibroblast mobility (García-Villén et al., 2020a). *In vitro* Franz cell studies were performed in order to reproduce the topical administration of the formulations and elemental concentration was measured by inductively coupled plasma techniques. The results will be discussed on the basis of both the legal status of elements present in the formulation and their potential therapeutic effects.

4.4.1. Materials and Methods

4.4.1.1. Materials

Nanoclay/spring water hydrogels were prepared by mixing Alicún thermal station spring water (ALI, Granada, Spain) with two commercial fibrous nanoclays; sepiolite (PS9) and palygorskite (G30). Nanoclays were kindly gifted by the TOLSA group (Madrid, Spain).

Sepiolite hydrogel included in this study was prepared with a concentration of 10% (*w/w*) of PS9 dispersed in ALI spring water (ALIPS9, 250 g in total). Additionally, two palygorskite hydrogels (250 g each), ALIG30@10 and ALIG30@20, were also obtained and their final concentration was 10% *w/w* and 20% *w/w* of G30, respectively. The three formulations were prepared by means of a turbine high-speed agitator (Silverson LT, Chesham, UK) equipped with a high-traction stirrer head of square mesh and working at 8000 rpm for 5 min.

4.4.1.2. Methods

Elemental Characterization of Pristine Materials

The elemental composition of ALI, PS9 and G30 was obtained by two Inductively Coupled Plasma techniques: ICP-OES (Optima 8300 ICP-OES Spectrometer, Perkin Elmer, Waltham, Massachusetts, USA) and ICP-MS (NexION-300d ICP mass spectrometer, Perkin Elmer), equipped with a triple cone interface and a quadrupole ion deflector using argon for plasma formation. PS9 and G30 were subjected to acid digestion in strong acids (HNO₃ and HF at a 3:5 ratio, Sigma-Aldrich, Missouri, U.S) inside a Teflon reactor, placed in a microwave oven (Milestone ETHOS ONE, Sorisole, Italy). Calibration curves for ICP-OES were obtained by means of standards solution of 1000 ppm for each element. For ICP-MS, single-element standard solutions (Merck, Darmstadt, Germany) were prepared after dilution with 10% HNO₃. Ultra-purified water (Milli-Q® grade) was used in both techniques.

In vitro Release of Elements

Element mobility from ALIPS9, ALIG30@10 and ALIG30@20 was studied by in vitro release studies performed in Franz diffusion cells system (FDC40020FF, BioScientific Inc., Phoenix, U.S) (COLIPA, 1997). This system is purposely designed to reproduce dermal and/or mucosal administration conditions. The Franz diffusion cells possessed a contact area of 0.64 cm² and a total volume of 6.4 mL. Dialysis membranes (cut-off 12–14 kDa, 31.7 mm, Medicell International, London) were used to separate the donor and receptor chambers. The membranes were boiled in ultra-purified water (Milli-Q® water, ISO 3696) for 10 min in order to hydrate them. Over the membrane, in the donator chamber, known amounts of each hydrogel (approximately 0.025 g) were placed. The receptor chamber was filled with degassed, ultra-purified water. The whole system was maintained at a constant temperature of 32 ± 0.5 °C through thermostatic bath circulation. The experiment lasted for 30 min, which is the typical time of topical nanoclay/spring water hydrogels application. Experiments were performed in sextuplicate. At the end of the experiments, the aqueous content of the receptor chamber was carefully withdrawn and filtered through 0.45 µm single-use, syringe filters (Merck Millipore, Madrid, Spain). Finally, the elemental composition on each sample

was assessed by ICP-OES. Element release tests were performed after 48 h and 1 month after hydrogel preparation, in order to study the evolution of the elemental mobility. Hydrogel batches were preserved in static conditions inside closed polyethylene containers, which were placed inside a drawer with an average mean temperature of 20 ± 5 °C. Blanks were also analysed in order to monitor the elements coming from the materials and the ultra-purified water.

Biocompatibility of ALIG30@20

ALIPS9 and ALIG30@10 hydrogels (both with a solid concentration of 10%) have been demonstrated to be biocompatible against fibroblasts (García-Villén et al., 2020a). Moreover, in the very same study, the *in vitro* scratch assay proved that the hydrogels were able to accelerate wound closure by favouring fibroblast migration. Nonetheless, the ALIG30@10 hydrogel showed insufficient viscosity, as proven in another study that included a full rheological characterization of ALIPS9 and ALIG30@10 hydrogels (García-Villén et al., 2020c). The low consistency of a hydrogel could hinder its topical administration due to excessive fluidity of the formulation. Consequently, the ALIG30@20 hydrogel was prepared and its biocompatibility was evaluated. To do so, the methodology described by García-Villén and co-workers (García-Villén et al., 2020a) was used. Normal human dermal fibroblasts (NHDFs, PromoCell GmbH, Heidelberg, Germany) were seeded and cultured in Dulbecco's modified Eagle medium (DMEM, Sigma Aldrich®-Merck, Milan, Italy), supplemented with 10% fetal bovine serum (FBS, Euroclone, Milan, Italy), 200 IU/mL penicillin and 0.2 mg/mL streptomycin (PBI International, I). Once cellular confluence was obtained (area 0.34 cm²/well, density 10⁵ cells/cm²), ALIG30@20 was added to the cell culture in concentrations ranging from 1000 to 5 µg/mL and kept in contact with cells for 24 h. Then, the MTT test (3-(4,5-dimethylthiazol-2-yl)-2,5-diphenyltetrazolium bromide) was performed. DMEM phenol red-free and 50 µL of MTT dissolution were added in each well, the final MTT concentration being 2.5 mg/mL. MTT-NHDF contact was maintained for 3 h before the whole supernatant was withdrawn and substituted by 100 µL of dimethyl sulfoxide solution (DMSO, Sigma-Aldrich®-Merck, Milan, Italy) to dissolve formazan. The absorbance of each well was measured at 570 nm with

4.4. Correlation between Elemental Composition/Mobility and Skin Cell Proliferation of Fibrous Nanoclay/Spring Water Hydrogels

an ELISA plate reader (Imark Absorbance Reader, Bio-rad, Hercules, CA, USA), with the reference wavelength set at 655 nm. Fibroblast viability was calculated with respect to the viability of the corresponding control (fibroblasts cultured in fresh DMEM, abbreviated as GM). MTT tests over ALIPS9, ALIG30@10 and ALIG30@20 were performed after 1 month of hydrogel preparation.

Selection of Elements under Study

A wide variety of elements were analysed in this study. In order to organize and facilitate the interpretation of the results, the discussion will be centred on two main aspects: the potential wound healing activity of the elements and their legal situation regarding cosmetics and medicines regulations. The importance of the latter point lies in the fact that, depending on the final therapeutic activity of the present hydrogels, they could be considered as cosmetics or as medicines (EU, 2017). Elements will be classified and addressed according to the European regulations and guidelines summarized in Figure 4.25. The present study is focused on those elements that are considered “safe” or “non-hazardous”. Additionally, elements without toxicity limits (most of the time not mentioned in the aforementioned regulations) were also included in this study.

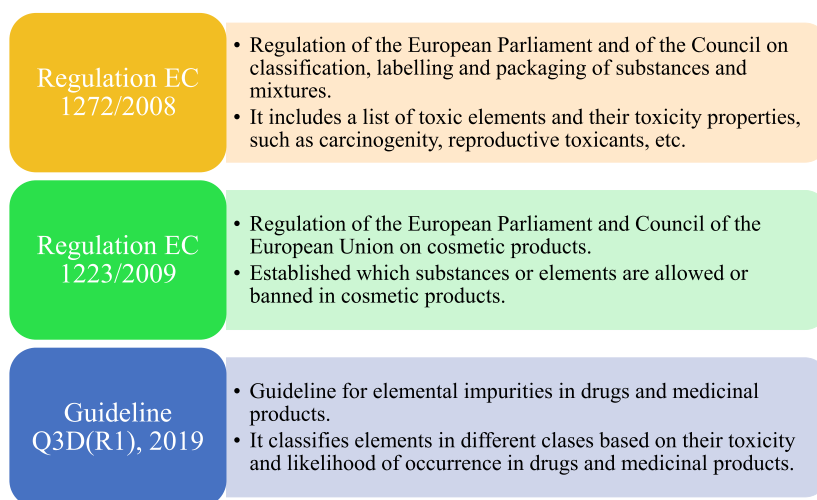


Figure 4.25. Main regulations and guidelines used for the selection of elements, interpretation and discussion of results, ordered by year of publication or latest update.

The guideline for elemental impurities Q3D(R1) (ICH, 2019) of the European Medicines Agency is focused on toxic elements and classifies them in three groups. In view of their limitations and toxicity, all of them with well-defined “permitted daily exposure” (PDE) limits, these elements are not addressed in this manuscript. Nonetheless, there is also a non-defined fourth group that includes elements with low inherent toxicity, without PDE limits. In conclusion, elements in this group should be controlled more for the quality of the final product than for high toxicity and safety considerations. Examples of these elements are Al, B, Ca, Fe, K, Mg, Mn, Na, W and Zn, which are the subject of study of this research. For simplicity throughout the manuscript, these elements are referred to as “class 4”. The European Regulation EC 1223/2009 (EU, 2009) was used to determine those elements whose presence is either allowed or not mentioned in cosmetic products.

Statistical Analysis

Statistical analysis were determined by means of non-parametric Mann–Whitney (Wilcoxon) W test. In all cases, SPSS Statistic software (IBM, version 21, 2012, New York, U.S) was used and differences were considered significant at p -values ≤ 0.05 .

4.4.2. Results

4.4.2.1. Elemental Characterization of Pristine Materials

Elemental composition of pristine components (PS9, G30 and ALI) is reported in Table 4.18. According to the EC 1272/2008, any of the detected elements are not considered as carcinogens.

Major elements in the pristine water (ALI) were Sr, S, Ca, Mg and Na (from higher to lower concentrations). The high presence of S, Ca and Mg are in agreement with the nature of the spring water source (Prado Pérez, 2011; Prado-Pérez and Pérez del Villar, 2011). Ti, Mn, Mg, Sr, Zn and Al are the major elements present in PS9 and G30. In particular, Zn, Mn, Mg and Al belong to class 4 in the Q3D(R1) guideline (ICH, 2019). Regarding the cosmetic regulation EC 1223/2009 (EU, 2009), aluminium is the only one specifically allowed in cosmetics, the rest of them are not mentioned in this regulation. Cu and Ag are elements present in the pristine ingredients that have a “special

situation” as far as regulation is concerned, since their presence is allowed in cosmetics (mainly due to their role as colorants) but they are classified as class 3 and 2B by the Q3D(R1).

4.4.2.2. *In Vitro* Release of Elements

Elements released from ALIPS9, ALIG30@10 and ALIG30@20 are summarized in

Table 4.19. As expected from the nature and composition of the pristine ingredients, the release of major elements (Ca, K, S, Mg, Na) was not only confirmed but desirable due to their physiologic activities, which will be discussed later. In particular, Ca showed significant release levels in all hydrogels, which is in agreement with the high levels of this element in pristine materials (Table 4.18). Moreover, S is the major element in ALI, which explains the high release levels of this element from the formulations.

The release levels of Mg were very similar for the three hydrogels. The release of Al increased with time in all cases, not being detected in any of the young hydrogels. On the other hand, the amount of B released after 1 month was lower. The most remarkable release regarding trace elements was shown by Zn and Sr, followed by Cu. Cu release significantly decreased after 1 month in the three hydrogels. As previously reported, the amount of Cu detected in G30 was higher than PS9 (

Table 4.19). This was in agreement with the lower release of both elements in ALIPS9 versus ALIG30@10 and ALIG30@20. Mn release increased with time in ALIPS9 and ALIPS9@20, while it was under the detection limit of the technique for ALIG30@10 experiments. Levels of Mn were the same for both PS9 and G30 (and absent in ALI, Table 4.18) but ALIG30@20 showed a remarkably higher release of this element.

The rest of the elements were not released or released in very low amounts. Except for Au, Cu and Ag, the rest of the trace elements are not included/mentioned in the EC 1223/2009 regulation. This means that their safety has not been thoroughly assessed or their toxicity is considered non-significant. It is worth mentioning that In and Re were not present in the pristine materials and that they were also not detected during the *in vitro*

release tests. This fact confirmed the absence of contamination with these elements during ALIPS9, ALIG30@10 and ALIG30@20 formulation processes and preservation.

Table 4.18. Elemental composition of PS9, G30 and ALI determined by ICP-OES and ICP-MS. "ND" = "Not Detected". Values marked as (*) were obtained from (García-Villén et al., 2020b).

	PS9 (ppm)	G30 (ppm)	ALI (ppb)	Comments
Al	15.9	31.9	37	Class 4 Q3D(R1); Allowed in EC 1223/2009
B	0.3	0.3	395	Class 4 Q3D(R1); Not listed in EC 1223/2009
Ca	2.8	33.3	312,700	Class 4 Q3D(R1); Not listed as element in EC 1223/2009
Fe	5.2	24.2	58	
K	6.0	1.9	6836	
Mg	122.0	41.8	114,267	
Na	0.1	0.1	49,150	
S	0.1	0.4	388,367	Not listed as element in EC 1223/2009
Mn	177.0	178.5	ND	Class 4 Q3D(R1); Not listed in EC 1223/2009
W	0.9	0.4	ND	
Zn	81.2	96.1	3.3	Class 4 Q3D(R1); Not listed as element in EC 1223/2009
Cu*	8.1	11.3	2.5	Class 3 Q3D(R1); Allowed in EC 1223/2009
Ag*	0.04	0.2	0.1	Class 2B Q3D(R1); Allowed in EC 1223/2009.
Au*	ND	ND	ND	
Sc	2.7	7.9	1.8	Not listed in EC 1223/2009
Ti	689.6	1820.5	0.2	Not listed as element in EC 1223/2009
Ga	8.2	16.1	0.8	Not listed in EC 1223/2009
Ge	3.2	0.8	0.1	
Tb	43.2	17.9	7.2	
Sr	24.4	106.0	10,049	Not listed as element in EC 1223/2009
Y	6.2	39.9	0.04	Not listed in EC 1223/2009
Nb	3.8	6.1	0.002	
In	ND	0.002	ND	
La	7.7	36.3	ND	
Ce	17.1	48.9	ND	
Pr	2.0	7.5	0.003	
Sm	1.7	5.5	0.001	
Eu	0.2	1.2	0.001	
Gd	1.5	5.6	0.003	
Dy	1.2	4.7	0.002	
Ho	0.2	1.0	0.002	
Er	0.6	2.9	0.002	
Tm	0.1	0.4	0.002	
Yb	0.5	2.4	ND	
Lu	0.1	0.4	0.002	
Hf	44.7	13.9	2.3	
Re	ND	ND	0.01	
Bi	0.1	ND	ND	Not listed as element in EC 1223/2009
Th	4.6	5.6	0.1	Not listed in EC 1223/2009

4.4.2.3. Biocompatibility of ALIG30@20

Biocompatibility results of ALIPS9@20 are reported in Figure 4.26. As previously mentioned, G30 and ALIG30@10 results have already been assessed by García-Villén and co-authors (García-Villén et al., 2020a). The reduction in viability produced by the pristine G30 alone at 1 mg/mL was not found in any of the hydrogels. In fact, the viability results of ALIG30@20 demonstrated, once again, that the type of formulation exerts a significant role in the results. That is, despite all tests subjected to the same amount of clay mineral in the culture, the hydrogels increased the biocompatibility. In particular, ALIG30@20 showed cellular viabilities higher than 100% at every concentration ($p > 0.05$ with respect to GM, Figure 4.26). In view of the experimental results and the statistical analysis, it is possible to state that ALIG30@20 exerts proliferative effects over fibroblasts at the tested concentrations. No other internal statistical differences were found between ALIG30@20 concentrations.

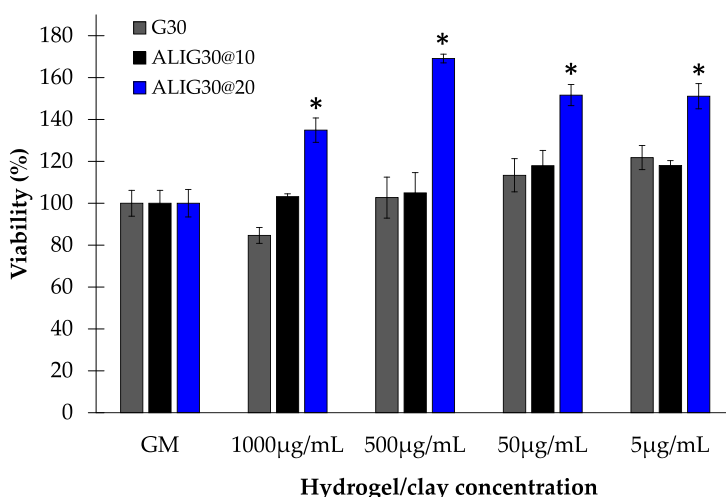


Figure 4.26. Biocompatibility tests of ALIG30@20 (blue). Viability (%) vs. hydrogel or clay concentration (% w/w). GM (growth medium) indicates the control. G30 and ALIG30@10 results (taken from García-Villén et al., 2020b) were included to compare viability results of hydrogels with different concentrations. Mean values \pm s.e.; $n = 8$. Significant differences, compared to GM, are marked with (*). Mann–Whitney (Wilcoxon) W tests, p values ≤ 0.05 .

Table 4.19. Mobility of elements after Franz cell diffusion tests. Major elements are expressed in mg/100 g of hydrogel, while the rest of the elements are expressed as µg/100 g of hydrogel. Mean values ± s.e. (n=6). "ND" stands for "Not Detected". Elements marked with * were obtained from (García-Villén et al., 2020b).

	Element	ALIPS9		ALIG30@10		ALIG30@20	
		48h	1m	48h	1m	48h	1m
mg / 100 g	Ca	11.7±2.91	8.1 ± 1.30	14.9 ± 1.758	30.4 ± 7.379	17.5 ± 3.51	7.0 ± 1.25
	K	1.8 ± 0.843	2.8 ± 0.628	2.7 ± 1.183	1.9 ± 0.491	3.4 ± 1.004	2.6 ± 1.09
	Mg	2.7 ± 0.48	3.7 ± 0.52	2.5 ± 0.237	5.2 ± 1.433	4.9 ± 0.23	3.0 ± 0.48
	Na	5.4 ± 1.40	6.3 ± 1.65	8.8 ± 2.727	10.5 ± 3.185	12.4 ± 1.136	6.43 ± 0.469
	S	14.8 ± 3.80	5.5 ± 2.81	23.3 ± 2.063	11.7 ± 2.162	10.4 ± 2.34	6.7 ± 2.29
	B	0.2 ± 0.016	0.04 ± 0.020	0.1 ± 0.021	ND	0.3 ± 0.062	ND
	Fe	0.06 ± 0.036	0.07 ± 0.028	ND	0.02 ± 0.018	0.1 ± 0.054	0.01 ± 0.009
	Al	ND	0.1 ± 0.056	ND	0.58 ± 0.452	ND	0.67 ± 0.100
µg / 100 g	Mn	ND	0.7 ± 0.39	ND	ND	4.9 ± 2.64	7.4 ± 3.69
	W	ND	ND	ND	ND	ND	ND
	Zn	25.9 ± 16.07	165.9 ± 68.51	132.1 ± 38.17	181.4 ± 99.18	164.8 ± 53.09	175.1 ± 80.91
	Cu*	10.8 ± 3.29	3.6 ± 2.17	32.6 ± 11.59	1.5 ± 1.01	20.6 ± 3.725	0.9 ± 0.61
	Ag*, Au*, Sc, Ti, Ge, Tb	ND	ND	ND	ND	ND	ND
	Ga	ND	0.08 ± 0.050	ND	ND	0.2 ± 0.019	0.04 ± 0.001
	Sr	176.5 ± 15.89	148.7 ± 20.37	90.4 ± 18.67	65.9 ± 10.39	82.8 ± 15.64	68.5 ± 7.93
	Y, Nb, In, La, Ce, Pr, Sm, Eu, Gd, Dy, Ho, Er, Tm, Yb, Lu, Hf, Re, Bi, Th	ND	ND	ND	ND	ND	ND

4.4.3. Discussion

4.4.3.1. Release of Elements and Potentially Useful Therapeutic Activities

According to the ICH Q3D(R1) guideline, no PDE limits have been established for class 4 elements (ICH, 2019). The presence of Al in cosmetics is allowed according to EC 1223/2009 since it specifies that “natural hydrated aluminum silicates ($\text{Al}_2\text{O}_3 \cdot 2\text{SiO}_2 \cdot 2\text{H}_2\text{O}$) containing calcium, magnesium or iron carbonates, ferric hydroxides, quartz-sand, mica, etc. as impurities” are allowed. Aluminum has shown to be released from 1-month-old hydrogels (

Table 4.19). The WHO has established a tolerable weekly intake of 7 mg/kg of body weight for aluminum (WHO, 1996). In view of the low bioavailability of aluminum from cosmetic products ($\leq 0.07\%$) (Flarend et al., 2001; Pineau et al., 2012; de Ligt et al., 2018), applications with more than 213 kg of hydrogel would be necessary to subject patients to potentially dangerous Al doses. Therefore, it is possible to guarantee that ALIPS9, ALIG30@10 and ALIG30@20 are totally safe regarding aluminum release. Additionally, some Al^{3+} “misfolds cell membrane proteins”, which gives it antibacterial activity (Morrison et al., 2016).

Ca, Fe, Mn, Zn and S are not listed in this regulation (EU, 2009), which means that, legally speaking, the presence of these elements does not limit the use of the present hydrogels as cosmetics from a legal point of view. Major elements such Mg, Ca, Na and K are considered as “essential” for both animals and human beings, and their presence in the pristine materials is considered totally safe and, sometimes, even favorable in certain cases. The usefulness of metals during wound healing has also been pointed out by some studies. For instance, it has been demonstrated that wound supplementation of Zn, Cu and Mg would be advisable during the healing process (Wlaschek et al., 2019).

The amount of K in solids was higher than Na and Ca, though its release from hydrogels was remarkably lower than that of Ca and Na. This result is in agreement with the cation exchange capacity (CEC) of PS9 and G30 reported in previous studies (García-Villén et al., 2020a), which showed calcium as one of the main exchangeable cations. Additionally, Ca is the

second most abundant element in ALI. It has been reported that low concentrations of extracellular potassium may accelerate and favour fibroblast differentiation, thus forming scar tissue (Grasman et al., 2019). Low intracellular K^+ concentrations favour interleukin-8 expression, which plays an important role in stimulating re-epithelialization, migration and proliferation of dermal cells during wound healing (Hotta et al., 2018). Therefore, a limited potassium release from both hydrogels would be beneficial during wound healing treatments.

Sodium is the second/third element with higher *in vitro* release levels (Table 4.19) and the third/fourth element in terms of abundance in the pristine materials (Table 4.18). Moreover, Na was one of the minor exchanged cations of PS9 and G30. This apparently contradictory result has previously been observed for other clay-based hydrogels subjected to the very same *in vitro* release methodology (Khiari et al., 2019). This result could be related to the hydrophilicity of the exchangeable cations of the clay, that follow the order $Ca^{2+} > Na^+ > K^+$ (Bish, 2006). The higher the hydrophilicity of the element, the higher the ability of water to enter the interlayer space and the higher the exchange capacity. The very same trend has been found for Ca, Na and K release (Table 4.19) and CEC (García-Villén et al., 2020a), despite this not being the same exact order of abundance in the pristine materials (Table 4.18).

Mg release increased with time in ALIPS9 and ALIG30@10, whereas it reduced in ALIG30@20 (Table 4.19). This element has been shown to easily permeate the skin (Kass et al., 2017) and possess anti-inflammatory activity, and is thus able to treat skin disorders such as psoriasis and atopic dermatitis (Schempp et al., 2000; Chandrasekaran et al., 2016). The combination of Mg and Ca has been reported to accelerate skin barrier repair, as well as skin hydration by synergic effects (Denda et al., 1999). Moreover, apart from the beneficial effects of Mg in the skin, this element, along with Ca, is also essential for good bone and muscle health. Therefore, if any of these elements are able to reach the bloodstream during the hydrogel treatment, they could also help treat other systemic musculoskeletal disorders, such as fibromyalgia (Engen et al., 2015).

Boron compounds have been demonstrated to be beneficial for wound healing of burned skin and in diabetic wound healing processes, both

in vitro and *in vivo* (Demirci et al., 2015, 2016). B has proved useful in several metabolic pathways as well as in the increase of the wound healing rate (Benderdour et al., 2000; Chebassier et al., 2004a). Release of B decreased with time in the three hydrogels until it reached undetectable levels. Consequently, if any benefit should be obtained from B, those benefits would be at its maximum in young hydrogels.

ALI composition also played an important role in the levels of elements released during the *in vitro* tests. In fact, the release of S can be totally ascribed to the natural spring water composition (ALI) (Table 4.18). The release of sulphur reduced with time in all cases (Table 4.19). Higher S release was reported for ALIG30@10 48 h. For ALIPS9 and ALIG30@20, the release amounts of S were very similar. Differences in ALIG30@10 and ALIG30@20 can be ascribed to the clay mineral concentration. Balneotherapy with sulphurous waters and peloids has been proven to help with several disorders and diseases (Sieghart et al., 2015; Carbajo and Maraver, 2017). Specifically, keratolytic, anti-inflammatory, keratoplastic and antipruritic effects have been related to S (Rodrigues et al., 2017). Sulphurous mineral waters may be absorbed through the skin causing vasodilation, analgesia, immune response inhibition, and keratolytic effects that reduce skin desquamation (Nasermoaddel and Kagamimori, 2005). Moreover, S could potentiate angiogenesis (endothelial cell proliferation) and regulate skin immunity. Consequently, the mobility of this element would be positive, since it can ameliorate several skin disorders. In this particular case, to obtain the maximum beneficial effects from sulphur, young hydrogels should be used, when the mobility of this element is maximum.

Mn works as a coenzyme in several biological processes, such as the transition between quiescent and proliferative phases of fibroblasts (Sarsour et al., 2008). Nonetheless, Mn levels contained in healthcare formulations should be controlled due to possible toxic brain accumulation (Horning et al., 2015; Lucchini et al., 2018; Erikson and Aschner, 2019). Levels of Mn were the same for pristine PS9 and G30 (while absent in ALI, Table 4.18). Consequently, it is possible to state that the release of this element is solely due to the clay mineral. Mn release increased with time in ALIG30@20, while it was not measurable in ALIG30@10, probably due to the lower concentration of G30 in

this formulation. A study on the bioavailability of manganese from soils revealed that in acid soils, Mn bioavailability grows (Dinić et al., 2019). Previously it has been shown that G30 and PS9 hydrogels prepared with ALI water suffer from a reduction in pH values during the first 6 months (García-Villén et al., 2020c). This modification of the pH could be the explanation for a higher release of Mn after 1 month in ALIPS9 and ALIG30@20. In terms of safety, ALIG30@10 would be the safest formulation, since Mn release was not detectable during Franz cells study.

Zinc is a class 4 element, but it is not listed in EC 1223/2009. The ALIPS9 hydrogel showed an increase in Zn release with time, while ALIG30@20 showed stable levels (Table 4.19). The increase in Zn release in ALIPS9 and ALIG30@10 could also be related to pH changes in the formulation with time, although the literature results are contradictory (Dinić et al., 2019). Regarding safety and regulations, Zn did possess a defined PDE level in the Q3D(R1) (ICH, 2019) (13,000 µg/day for both oral and parenteral routes). Moreover, the WHO defined a provisional maximum tolerable daily intake amount of 18–60 mg/day for an adult of 60 kg. As previously mentioned, it has been reported that this element could compromise renal and hepatic functions when high doses reach the bloodstream. Nonetheless, Zn has also been demonstrated to be essential for keratinocyte and fibroblast proliferation, differentiation and survival. Its deficiency has been related to different disorders such as acquired acrodermatitis enteropathica, biotic deficiency, alopecia and delayed wound healing. Moreover, Zn concentration is usually higher in the epidermis than in the dermis (Ogawa et al., 2016, 2018). Consequently, the mobility of Zn from the studied hydrogels is seen as a positive and potentially useful feature for wound healing. Moreover, the released amount of Zn in Franz cells can be considered safe, since it was below the WHO and PDE limits previously mentioned and they are intended to be topically administered.

Together with Zn, Cu is a useful element in terms of wound healing (Ogen-Shtern et al., 2019) and its presence is allowed in cosmetics by EC 1223/2009. This element has been demonstrated to increase the expression of TGF-β1 in *ex vivo* skin models, thus leading to higher pro-collagen 1 and elastin production by fibroblasts (Ogen-Shtern et al., 2019). Moreover, Cu has

been demonstrated to enhance skin cell migration (keratinocytes and fibroblasts), which is crucial for wound healing (Tenaud et al., 2000; Qiao et al., 2019). ALIPS9 and ALIG30@10 were shown to favour fibroblast migration in a previous study (García-Villén et al., 2020a), which could be related to copper release. Additionally, copper possesses an antimicrobial effect and has been proposed as an ingredient for wound dressings (Ul-Islam et al., 2013). In fact, some clay minerals with Cu were demonstrated to be the most effective against *Escherichia coli* and *Staphylococcus aureus*. Release levels of Cu revealed that, to obtain the aforementioned effects, extemporaneous hydrogels should be used (Table 4.19).

Ga showed minimum mobility in both hydrogels (Table 4.19) and significantly reduced mobility in ALIG30@20 after 1 month. Higher release levels in ALIG30@20 versus ALIPS9 can be ascribed to a higher concentration of this element in G30 pristine material (Table 4.18). This element is not addressed in any of the aforementioned regulations (EU, 2009; Health Canada, 2015, 2019; ICH, 2019) since it is currently considered a relatively non-toxic element for humans. Antimicrobial activity of Ga has been reported (Goss et al., 2018; Young et al., 2019), which could be of use for the treatment of infected wounds. A biocompatible, gallium-loaded, antimicrobial, artificial dermal scaffold has been recently proposed (Xu et al., 2019). Other biomedical uses of Ga have also been previously reported due to its low toxicity (Chitambar, 2010; Jalali et al., 2019; Kimura et al., 2019; Melnikov et al., 2019; Nguyen et al., 2019; Song et al., 2019). In view of the existing bibliography and the present results, extemporaneous ALIG30@20 hydrogels would be a proper choice to obtain antimicrobial activity.

Strontium mobility was one of the most remarkable among the trace elements, mainly because of its presence in ALI. The presence of this element in cosmetics is not considered determinant in terms of safety, maybe because symptoms of Sr overdose are not yet clear in humans. What is more, despite the *in vivo* studies performed in animals, no Sr limits have been established for humans (since dietary intake variations did not induced acute toxicity symptoms) (Bartley and Reber, 1961; Kirrane et al., 2006). Wound healing effects of strontium chloride hexahydrate has been evaluated *in vivo*. This strontium salt was shown to reduce TNF- α expression in the wound site and,

therefore, reduce inflammation (Berksoy Hayta et al., 2018), which is of special use in chronic inflammatory disorders. The antioxidant effect is also related to Sr, according to previous studies (Jebahi et al., 2013) that used strontium-substituted bioglass for tissue engineering purposes. Strontium has also been included in wound dressings as a wound healing promoter (Li et al., 2017) and has been demonstrated to exert useful systemic effects when it reaches the bloodstream (Cabrera et al., 1999; Buehler et al., 2001; Gunawardana et al., 2004; Nielsen, 2004). In conclusion, the release of Sr release is desirable, ALIPS9 being the formulation providing the highest levels of this element.

4.4.3.2. Mobility of Elements

The sole presence of an element or chemical compound in a formulation does not mean that it would exert its therapeutic effect: it also needs to be released and be able to reach the active site. Moreover, the release process can be determined by different factors, one of them being its location in the formulation (clay structure or the spring water) or the age of the system (Sánchez-Espejo et al., 2015; García-Villén et al., 2020b). Element mobility is a normalized parameter that allows comparisons between released levels of different elements. It can be calculated as the ratio between total concentration in the formulation and the released concentration. Mobility values of elements in ALIPS9 and ALIG30@20 hydrogels are plotted in Figure 4.27. In this figure, the delimited areas within the graphic were defined in a speculative manner. As can be seen from the dispersion (Figure 4.27), the majority of the elements showed a mobility lower than 2%.

Even if Ca, S and Mg were present in remarkable amounts in the studied formulations, their released levels were very low in proportion, thus giving rise to low element mobility. This result demonstrates that, despite the spring water having remarkable amounts of these elements, their mobility is probably limited by the presence of the solid phase. Consequently, the solid and the liquid phases of the formulations establish a very close interaction that affects the final performance of the system, something that highlights the necessity to fully characterize this kind of formulation. Another visible result is the higher mobility of elements in ALIG30@10 with respect to ALIG30@20 and ALIPS9, which also demonstrates that the type and the concentration of

4.4. Correlation between Elemental Composition/Mobility and Skin Cell Proliferation of Fibrous Nanoclay/Spring Water Hydrogels

the clay mineral exert a remarkable influence. Elements in the “medium mobility” area (Figure 4.27) were located in this section since they have low mobility (<1%) together with low concentration (<150 ppm) in the final formulation.

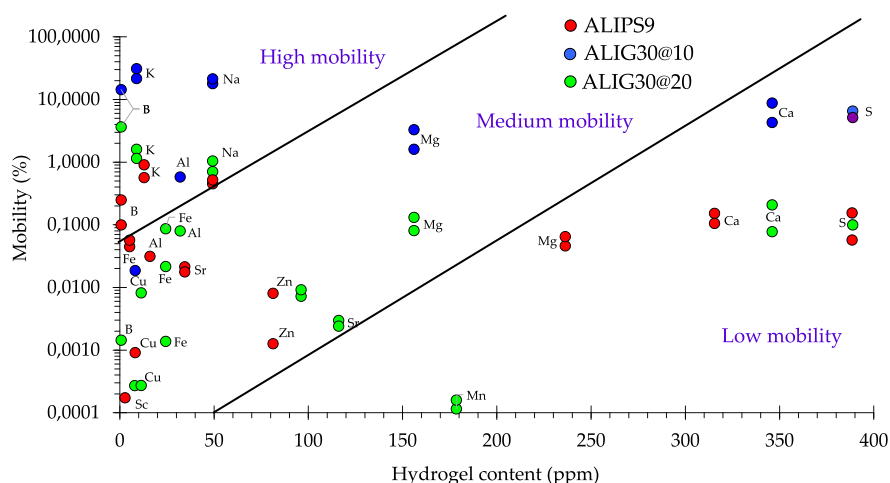


Figure 4.27. Percentage of mobility (logarithmic scale) versus total content of the element in ALIPS9, ALIG30@10 and ALIG30@20 hydrogels (ppm). “High”, “Medium” and “Low mobility” areas are hypothetical. Non-detected elements (mobility = 0%) do not appear in the logarithmic scale.

In view of the mobility results, K, Na, B and Al are the elements with the highest mobility. They showed relatively low amounts in the hydrogels but their mobility was clearly significantly higher with respect to the rest of the elements. We hypothesized that the high mobility of the aforementioned elements could be related to both the hydrophilicity of cations (previously mentioned in section 4.4.3.1) and to a small/absent interaction between the pristine ingredients and, therefore, the released levels ascribed to the influence of the liquid phase (ALI) more than to the solid phase. That is, even if K, Na and B were not the main major elements in the pristine ingredients, the low interaction between K, Na and B (coming from ALI) with fibrous clay structure let these elements be relatively “free” within the system and, therefore, more prone to move. This hypothesis is confirmed by the fact that the mobility of elements in ALIG30@10 is higher than in ALIG30@20, due to the lower amount of G30 in the former. In this formulation, the reduced

amount of clay mineral implies less retention of the elements and, therefore, higher mobility.

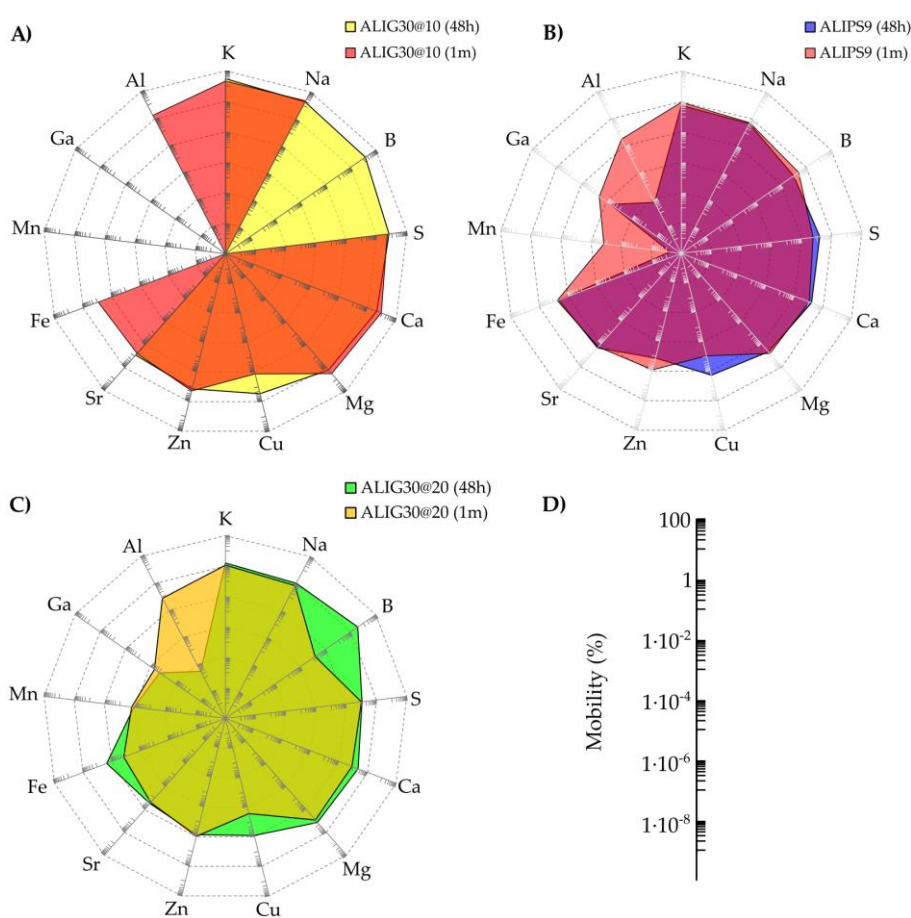


Figure 4.28. Spider diagrams of element mobility. (A) ALIG30@10; (B) ALIPS9 (C) ALIG30@20. For simplicity, the scale of the diagrams has been represented independently in (D).

Spider diagrams represent more clearly the different mobility of elements between the same hydrogels at 48 h and 1 month (Figure 4.28). This comparison reveals that nanoclay/spring water hydrogels are “living formulations” since their ingredients constantly interact with each other, changing the final properties of the system. The area of ALIG30@10 (48 h and 1 month) is higher than the area of ALIPS9 and ALIG30@20, which is in agreement with the previous mobility results (Figure 4.28). The “liveliness” of

the hydrogels can be ascribed to the different elemental equilibriums established between the solid and liquid phases in the formulation (adsorption and desorption equilibriums). Upholding this hypothesis, the solid phase mainly influenced the time-mobility of Cu, Mn, Ga, Al, B, and Fe, either increasing or reducing the corresponding mobility, depending on each particular case.

The reduction of some elements' mobility with time (for instance B, Mg, Al, Zn, Mn, and Na) could also be explained by the stabilization of the system, and the clay better adsorbing/retaining these elements as time passes. In fact, clay minerals have been widely used for decontamination purposes due to their remarkable adsorptive properties (Adeleye et al., 1994; Vengris et al., 2001; Missana et al., 2008; Sun and Selim, 2018). Moreover, rheological changes have also been detected in these samples. A different structure of the system network could modify the mobility of certain elements and vice versa (Sánchez-Espejo et al., 2015). As can be seen in Appendix (Figure A1), both ALIG30@20 and ALIPS9 suffered rheological changes within one month. Moreover, it is also possible from these results to hypothesize that the rheological performance of the system could also be influencing the element mobility. ALIPS9 and ALIG30@20, having a much more structured internal network (Figure A1), could hinder the mobility of elements that will find a more intricate path to travel towards the exterior. On the other hand, ALIG30@10 was shown to have a less structured gel network (see García-Villén et al., 2020c) for information on the rheology of ALIG30@10).

4.4.3.3. Biocompatibility of ALIG30@20

In vitro biocompatibility of clay minerals has been widely studied (Salcedo et al., 2012, 2014; Sandri et al., 2016; Tenci et al., 2017; Mousa et al., 2018). Some clay minerals have already been shown to have proliferating activity in cellular cultures, such as montmorillonite and halloysite (Cervini-Silva et al., 2016; Carazo et al., 2017). Nonetheless, the induction of cellular proliferation by palygorskite clay mineral is a rare result (Wang et al., 2015). This result leads us to hypothesize that if ALIG30@10 was biocompatible and able to induce fibroblast motility during *in vitro* wound healing (García-Villén et al., 2020a), ALIG30@20, with proliferative activity, is also a promising

formulation for wound healing treatments, especially during the proliferative stage. The different performance between these two hydrogels could be due to physicochemical differences of the systems. That is, different rheological behaviours as well as different chemical performances of both hydrogels could be the factors governing the biocompatibility results. Moreover, the present results could also be due to the combination of both physical and chemical performances of the formulations. Table A1 shows the theoretical amount of mobile element released in the fibroblast culture during MTT tests. These calculations have been made in order to correlate Franz cells results with those of MTT.

Mn has been reported as an active ingredient of spring waters with wound healing activity (Chebassier et al., 2004b). This, together with the Mn released results in ALIG30@10 and ALIG30@20 (Table 4.19), leads us to propose manganese as one of the possible factors explaining the proliferative effect of ALIG30@20 versus ALIG30@10 (Figure 4.26).

Calcium and zinc have been demonstrated to actively participate in cellular growth, in particular the Zn:Ca ratio, which was demonstrated to increase Zn:Ca during cell proliferation and the decline Zn:Ca during the remodelling phase (Lansdown et al., 1999; Lansdown, 2002; Zhang et al., 2018). This is due to a redistribution of calcium within dermal cells during the wound healing cascade (Lansdown, 1995), which is dependent on certain trace elements such as zinc. In fact, extracellular calcium has been shown to stimulate DNA synthesis in cultured fibroblasts in the presence of Zn (Huang et al., 1999). This has been mainly ascribed to the cofactor role of Zn in different enzymes involved in fibroblast growth. Moreover, Zn also plays an important role as a structural component of essential proteins. Some in vitro studies demonstrated that, even if proper growth factors and nutrients are present in the fibroblast culture medium, deficiencies of Zn translate to insufficient intracellular calcium and, ultimately, to impaired fibroblast proliferation (O'Dell and Browning, 2011, 2013). From the release values of these elements, the Zn:Ca ratio of ALIG30@10 was 0.00465 and 0.01060 for ALIG30@20 (obtained from Table A1), which could be a significant factor inducing the proliferation of fibroblasts in ALIG30@20. It is also worth pointing out the fact that G30 showed a remarkable amount of Zn, thus being

the ingredient providing this element. On the other hand, the major amount of Ca is provided by ALI. Any of the formulation ingredients on their own have been shown to induce cellular proliferation (see MTT results in García-Villén et al., 2020a and Figure 4.26). This indicates that both ALI and G30, properly combined in a certain concentration, are necessary to induce fibroblast proliferation. Consequently, the proliferative effect is ascribed to the formulation itself, proving once again the major importance of formulative studies. By the same token, the Ca:Mg ratio also changes along the wound healing cascade. In fact, an increase in Mg levels is observed to favour cellular migration. Grzesiak and Pierschbacher stated that the Mg:Ca ratio was close to 1 during the migratory phase, and it reversed during the rest of the process (Grzesiak and Pierschbacher, 1995). ALIPS9 and ALIG30@10 hydrogels (aged for 1 month) showed Mg:Ca ratios (Table 4.19) closest to 1, which is in agreement with the induction of fibroblast migration already demonstrated for these formulations (García-Villén et al., 2020a). Nonetheless, the ALIG30@20 Mg:Ca ratio was significantly distant from this value, which happens during the proliferative phase.

The present results ultimately lead us to think that, apart from the amount of elements released from each hydrogel, their ratio and specific identity highly influence the final therapeutic performance of the formulation. Notwithstanding the fact that further studies are needed, it is noteworthy that the present formulations have the potential to be combined and administered at different times of the wound treatment by virtue of their chemical performance.

4.4.3.4. Conclusions

The present study dealt with the *in vitro* release and mobility of potentially bioactive elements present in semisolid gel-like formulations obtained by mixing sepiolite and palygorskite with a natural spring water. Hydrogels were subjected to *in vitro* Franz cell tests and the elements released were analysed by inductively coupled plasma techniques. Then, the element release and mobility were compared with *in vitro* biocompatibility tests of the very same formulation. The results demonstrated that, unlike other

formulations, the potential therapeutic activity of nanoclay/spring water hydrogels should be studied in depth and characterized.

Clay/spring water hydrogels are “living formulations” since their ingredients constantly interact with each other, changing the properties of the system. For instance, the presence of an element in high concentration does not mean it would be released in high amounts. Moreover, the high release of bioactive elements is not a *sine qua non* to obtain maximum therapeutic effect. In fact, the ALIG30@20 hydrogel, with lower elemental mobility, not only proved to be biocompatible, but to exert potential proliferative effects over fibroblast cultures. According to the present *in vitro* release studies, it is possible to state that the ratios of the elements released play a significant role in the final therapeutic activity of the formulation. Moreover, the importance of formulative studies is again highlighted, since it is the optimal combination of the correct ingredients that makes a formulation effective.

As a general conclusion, the present study demonstrates that synergistic effects can be achieved from the formulation of the liquid phase in a semisolid system, in which elemental composition of the solid phase and structure of the system will determine elements’ mobility and, ultimately, the therapeutic effects.

4.5. Abbreviations

12m	12 months
1m	1 month
2m	2 months
6m	6 months
ALI	Alicún de las Torres' spring water
ALIG30@20	Hydrogel of G30 and ALI water at 20% w/w
CEC	Cation Exchange Capacity
CLSM	Confocal-Laser Scanning Microscopy
CP	Clay particles
DAPI	4',6-Diamidino-2-phenylindole
DMEM	Dulbecco's modified Eagle medium
DMSO	Dimethyl sulfoxide
DSC	Differential Scanning Calorimetry
DSF	Dorsal stress fibres
EDX	Energy-dispersive X-ray spectroscopy
ELS	Electrophoretic Light Scattering
F	Filopodia
FBS	Fetal Bovine Serum
FESEM	Field Emission Scanning Electron Microscope
FITC	Fluorescein isothiocyanate
FT-IR	Fourier-Transform Infrared spectroscopy
G30	Attapulgit (palygorskite)
G30ALI and ALIG30@10	Hydrogel of G30 and ALI water at 10% w/w
G30GR	Hydrogel of G30 and GR water at 10% w/w
GM	Pure fibroblasts' growth medium (control)
GR	Graena's spring water
HC-SC	Guidance on Heavy Metal Impurities in Cosmetics
ICH	International Council for Harmonisation

ICP-MS	Inductively Coupled Plasma Mass spectrometer
ICP-OES	Inductively Coupled Plasma Optical Emission Spectroscopy
L	Lamellipodia
M	Mitosis
MTT	3-(4,5-dimethylthiazol-2-yl)-2,5-diphenyltetrazolium bromide
ND	Not detected
NHDF	Normal Human Dermal Fibroblasts
NNPHD	Natural and Non-prescription Health Products Directorate
PBS	Phosphate-Buffered Saline
PDE	Permitted Daily Exposure
PS9	magnesium aluminium silicate (sepiolite)
PS9ALI and ALIPS9	Hydrogel of PS9 and ALI water at 10% w/w
PS9GR	Hydrogel of PS9 and GR water at 10% w/w
Q3D(R1)	Guideline for Elemental Impurities
RAW 264.7	Murine macrophages
SEM	Scanning Electron Microscopy
SF	Stress fibres
TGA	Thermogravimetric Analysis
TMBA	Tetramethyl ammonium bromide
XRF	X-ray Fluorescence
XRPD	X-ray Powder Diffraction

References

- Ababneh, F.A., Abu-Sbeih, K.A., Al-Momani, I.F., 2013. Evaluation of allergenic metals and other trace elements in personal care products. *Jordan J. Chem.* 8, 179–190. <https://doi.org/10.12816/0001527>
- Abduljawwad, S.N., Ahmed, H.-R., 2019. Enhancing cancer cell adhesion with clay nanoparticles for countering metastasis. *Sci. Rep.* 9, 5935. <https://doi.org/10.1038/s41598-019-42498-y>
- Abu-al-Basal, M.A., 2012. Histological evaluation of the healing properties of Dead Sea black mud on full-thickness excision cutaneous wounds in BALB/c mice. *Pakistan J. Biol. Sci.* 15, 306–315.
- Adeleye, S.A., Clay, P.G., Oladipo, M.O.A., 1994. Sorption of caesium, strontium and europium ions on clay minerals. *J. Mater. Sci.* 29, 954–958. <https://doi.org/10.1007/BF00351416>
- Aguzzi, C., Sánchez-Espejo, R., Cerezo, P., Machado, J., Bonferoni, C., Rossi, S., Salcedo, I., Viseras, C., 2013. Networking and rheology of concentrated clay suspensions “matured” in mineral medicinal water. *Int. J. Pharm.* 453, 473–479. <https://doi.org/10.1016/j.ijpharm.2013.06.002>
- Aguzzi, C., Sandri, G., Cerezo, P., Carazo, E., Viseras, C., 2016. Health and medical applications of tubular clay minerals, in: *Developments in Clay Science*. Elsevier, pp. 708–725. <https://doi.org/10.1016/B978-0-08-100293-3.00026-1>
- Al-Futaisi, A., Jamrah, A., Al-Rawas, A., Al-Hanai, S., 2007. Adsorption capacity and mineralogical and physico-chemical characteristics of Shuwaymiyah palygorskite (Oman). *Environ. Geol.* 51, 1317–1327. <https://doi.org/10.1007/s00254-006-0430-y>
- Al Hossain, M.M.A., Yajima, I., Tazaki, A., Xu, H., Saheduzzaman, M., Ohgami, N., Ahsan, N., Akhand, A.A., Kato, M., 2019. Chromium-mediated hyperpigmentation of skin in male tannery workers in Bangladesh. *Chemosphere* 229, 611–617. <https://doi.org/10.1016/j.chemosphere.2019.04.112>
- Alkan, M., Hopa, Ç., Yilmaz, Z., Güler, H., 2005. The effect of alkali concentration and solid/liquid ratio on the hydrothermal synthesis of zeolite NaA from natural kaolinite. *Microporous Mesoporous Mater.* 86, 176–184. <https://doi.org/10.1016/j.micromeso.2005.07.008>
- Altmann, S., Tournassat, C., Goutelard, F., Parneix, J.C., Gimmi, T., Maes, N., 2012. Diffusion-driven transport in clayrock formations. *Appl. Geochemistry* 27, 463–478. <https://doi.org/10.1016/j.apgeochem.2011.09.015>
- Álvarez, A., Santarén, J., Esteban-Cubillo, A., Aparicio, P., 2011. Current Industrial Applications of Palygorskite and Sepiolite, in: Galán, E., Singer, A. (Eds.), *Developments in Palygorskite-Sepiolite Research. A New Outlook of These Nanomaterials*. Elsevier B.V, Oxford, pp. 281–298.
- Andreoli, C., Rascio, N., 1975. The algal flora in the Thermal Baths of Montegrotto

- Terme (Padua). Its distribution over one-year period. *Int. Rev. der gesamten Hydrobiol. und Hydrogr.* 60, 857–871. <https://doi.org/10.1002/iroh.19750600606>
- Argenziano, G., Delfino, M., Russo, N., 2004. Mud and baththerapy in the acne cure. *Clin. Ter.* 155, 125.
- Atlas Hidrogeológico de la Provincia de Granada [WWW Document], 1990. . Diput. Prov. Granada, Inst. Tecnológico Geomin. España. URL http://aguas.igme.es/igme/publica/libro75/lib_75.htm (accessed 9.10.18).
- Augsburger, M.S., Strasser, E., Perino, E., Mercader, R.C., Pedregosa, J.C., 1998. Ftr and mössbauer investigation of a substituted palygorskite: Silicate with a channel structure. *J. Phys. Chem. Solids* 59, 175–180. [https://doi.org/10.1016/S0022-3697\(97\)00166-2](https://doi.org/10.1016/S0022-3697(97)00166-2)
- Bai, D., Li, Q., Xiong, Y., Zhao, J., Bai, L., Shen, P., Yuan, L., 2018. Editor’s Highlight: Effects of Intraperitoneal Injection of SnS₂ Flowers on Mouse Testicle . *Toxicol. Sci.* 161, 388–400. <https://doi.org/10.1093/TOXSCI>
- Bailey, L., Lekkerkerker, H.N.W., Maitland, G.C., 2015. Smectite clay-inorganic nanoparticle mixed suspensions: Phase behaviour and rheology. *Soft Matter* 11, 222–236. <https://doi.org/10.1039/c4sm01717j>
- Bartley, J., Reber, E., 1961. Toxic effects of stable strontium in young pigs. *J. Nutr.* 75, 21–28.
- Baschini, M.T., Pettinari, G.R., Vallés, J.M., Aguzzi, C., Cerezo, P., López-Galindo, A., Setti, M., Viseras, C., 2010. Suitability of natural sulphur-rich muds from Copahue (Argentina) for use as semisolid health care products. *Appl. Clay Sci.* 49, 205–212. <https://doi.org/10.1016/j.clay.2010.05.008>
- Benderdour, M., Van Bui, T., Hess, K., Dicko, A., Belleville, F., Dousset, B., 2000. Effects of boron derivatives on extracellular matrix formation. *J. Trace Elem. Med. Biol.* 14, 168–173. [https://doi.org/10.1016/S0946-672X\(00\)80006-1](https://doi.org/10.1016/S0946-672X(00)80006-1)
- Bengali, Z., Pannier, A.K., Segura, T., Anderson, B.C., Jang, J.-H., Mustoe, T.A., Shea, L.D., 2005. Gene delivery through cell culture substrate adsorbed DNA complexes. *Biotechnol. Bioeng.* 90, 290–302. <https://doi.org/10.1002/bit.20393>
- Berg, J.M., Romoser, A., Banerjee, N., Zebda, R., Sayes, C.M., 2009. The relationship between pH and zeta potential of ~30 nm metal oxide nanoparticle suspensions relevant to in vitro toxicological evaluations. *Nanotoxicology* 3, 276–283. <https://doi.org/10.3109/17435390903276941>
- Berksoy Hayta, S., Durmuş, K., Altuntaş, E.E., Yildiz, E., Hisarciklio, M., Akyol, M., 2018. The reduction in inflammation and impairment in wound healing by using strontium chloride hexahydrate. *Cutan. Ocul. Toxicol.* 37, 24–28. <https://doi.org/10.1080/15569527.2017.1326497>
- Bernal-Chávez, S., Nava-Arzaluz, M.G., Quiroz-Segoviano, R.I.Y., Ganem-Rondero, A., 2019. Nanocarrier-based systems for wound healing. *Drug Dev. Ind. Pharm.* 45, 1389–1402. <https://doi.org/10.1080/03639045.2019.1620270>
- Bish, D.L., 2006. Parallels and distinctions between clay minerals and zeolites, in: Bergaya, F., Theng, B.K.G., Lagaly, G. (Eds.), *Handbook of Clay Science*. Elsevier Ltd., pp. 1097–1112.

4.5. Abbreviations

- Bocca, B., Pino, A., Alimonti, A., Forte, G., 2014. Toxic metals contained in cosmetics: A status report. *Regul. Toxicol. Pharmacol.* 68, 447–467. <https://doi.org/10.1016/j.yrtph.2014.02.003>
- Boogaard, P.J., Boisset, M., Blunden, S., Davies, S., Ong, T.J., Taverne, J.P., 2003. Comparative assessment of gastrointestinal irritant potency in man of tin(II) chloride and tin migrated from packaging. *Food Chem. Toxicol.* 41, 1663–1670. [https://doi.org/10.1016/S0278-6915\(03\)00216-3](https://doi.org/10.1016/S0278-6915(03)00216-3)
- Borowska, S., Brzóska, M.M., 2015. Metals in cosmetics: implications for human health. *J. Appl. Toxicol.* 35, 551–572. <https://doi.org/10.1002/jat.3129>
- Bradbury, M.H., Baeyens, B., Geckeis, H., Rabung, T., 2005. Sorption of Eu(III)/Cm(III) on Ca-montmorillonite and Na-illite. Part 2: Surface complexation modelling. *Geochim. Cosmochim. Acta* 69, 5403–5412. <https://doi.org/10.1016/j.gca.2005.06.031>
- Buehler, J., Chappuis, P., Saffar, J.L., Tsouderos, Y., Vignery, A., 2001. Strontium ranelate inhibits bone resorption while maintaining bone formation in alveolar bone in monkeys (*Macaca fascicularis*). *Bone* 29, 176–179. [https://doi.org/10.1016/S8756-3282\(01\)00484-7](https://doi.org/10.1016/S8756-3282(01)00484-7)
- Cabrera, W.E., Schrooten, I., De Broe, M.E., D'Haese, P.C., 1999. Strontium and Bone. *J. Bone Miner. Res.* 14, 661–668. <https://doi.org/10.1359/jbmr.1999.14.5.661>
- Carazo, E., Borrego-Sánchez, A., García-Villén, F., Sánchez-Espejo, R., Aguzzi, C., Viseras, C., Sainz-Díaz, C.I., Cerezo, P., 2017. Assessment of halloysite nanotubes as vehicles of isoniazid. *Colloids Surfaces B Biointerfaces* 160, 337–344. <https://doi.org/10.1016/J.COLSURFB.2017.09.036>
- Carbajo, J.M., Maraver, F., 2017. Sulphurous Mineral Waters: New Applications for Health. *Evidence-Based Complement. Altern. Med.* 2017, 1–11. <https://doi.org/10.1155/2017/8034084>
- Carmona, J.A., Ramírez, P., Trujillo-Cayado, L.A., Caro, A., Muñoz, J., 2018. Rheological and microstructural properties of sepiolite gels. Influence of the addition of ionic surfactants. *J. Ind. Eng. Chem.* 59, 1–7. <https://doi.org/10.1016/J.JIEC.2017.09.030>
- Carretero, M.I., 2020. Clays in pelotherapy. A review. Part II: Organic compounds, microbiology and medical applications. *Appl. Clay Sci.* 189, 105531. <https://doi.org/10.1016/j.clay.2020.105531>
- Carretero, M.I., Pozo, M., Sánchez, C., García, F.J., Medina, J.A., Bernabé, J.M., 2007. Comparison of saponite and montmorillonite behaviour during static and stirring maturation with seawater for pelotherapy. *Appl. Clay Sci.* 36, 161–173. <https://doi.org/10.1016/J.CLAY.2006.05.010>
- Castex-Rizzi, N., Charveron, M., Merial-Kieny, C., 2011. Inhibition of TNF-alpha induced-adhesion molecules by Avène Thermal Spring Water in human endothelial cells. *J. Eur. Acad. Dermatology Venereol.* 25, 6–11. <https://doi.org/10.1111/j.1468-3083.2010.03893.x>
- Centini, M., Tredici, M.R., Biondi, N., Buonocore, A., Maffei Facino, R., Anselmi, C., 2015. Thermal mud maturation: organic matter and biological activity. *Int. J.*

- Cosmet. Sci. 37, 339–347. <https://doi.org/10.1111/ics.12204>
- Cervini-Silva, J., Nieto-Camacho, A., Gómez-Vidales, V., 2015a. Oxidative stress inhibition and oxidant activity by fibrous clays. *Colloids Surfaces B Biointerfaces* 133, 32–35. <https://doi.org/10.1016/j.colsurfb.2015.05.042>
- Cervini-Silva, J., Nieto-Camacho, A., Ramírez-Apan, M.T., Gómez-Vidales, V., Palacios, E., Montoya, A., Ronquillo de Jesús, E., 2015b. Anti-inflammatory, anti-bacterial, and cytotoxic activity of fibrous clays. *Colloids Surfaces B Biointerfaces* 129, 1–6. <https://doi.org/10.1016/j.colsurfb.2015.03.019>
- Cervini-Silva, J., Ramírez-Apan, M.T., Kaufhold, S., Ufer, K., Palacios, E., Montoya, A., 2016. Role of bentonite clays on cell growth. *Chemosphere* 149, 57–61. <https://doi.org/10.1016/j.chemosphere.2016.01.077>
- Cézanne, L., Gaboriau, F., Charveron, M., Morlière, P., Tocanne, J.F., Dubertret, L., 1993. Effects of the Avène spring water on the dynamics of lipids in the membranes of cultured fibroblasts. *Skin Pharmacol.* 6, 231–40.
- Chahi, A., Petit, S., Decarreau, A., 2002. Infrared evidence of dioctahedral-trioctahedral site occupancy in palygorskite. *Clays Clay Miner.* 50, 306–313. <https://doi.org/10.1346/00098600260358067>
- Chandrasekaran, N.C., Sanchez, W.Y., Mohammed, Y.H., Grice, J.E., Roberts, M.S., Barnard, R.T., 2016. Permeation of topically applied Magnesium ions through human skin is facilitated by hair follicles. *Magnes. Res.* 29, 35–42. <https://doi.org/10.1684/mrh.2016.0402>
- Chang, P.-H., Li, Z., Yu, T.-L., Munkhbayer, S., Kuo, T.-H., Hung, Y.-C., Jean, J.-S., Lin, K.-H., 2009. Sorptive removal of tetracycline from water by palygorskite. *J. Hazard. Mater.* 165, 148–155. <https://doi.org/10.1016/J.JHAZMAT.2008.09.113>
- Chebassier, N., El Houssein, O., Viegas, I., Dreno, B., 2004a. In vitro induction of matrix metalloproteinase-2 and matrix metalloproteinase-9 expression in keratinocytes by boron and manganese. *Exp. Dermatol.* 13, 484–490. <https://doi.org/10.1111/j.0906-6705.2004.00197.x>
- Chebassier, N., Oujija, E.H., Viegas, I., Dreno, B., 2004b. Stimulatory effect of boron and manganese salts on keratinocyte migration. *Acta Derm. Venereol.* 84, 191–194. <https://doi.org/10.1080/00015550410025273>
- Cheng, Q., Ye, R., 2015. A kind of hydrogel expanded material for handling heavy metal containing sewage and preparation method thereof. CN105542095B.
- Chiarini, A., Dal Pra, I., Pacchiana, R., Zumiani, G., Zanoni, M., Armato, U., 2006. Comano's (Trentino) thermal water interferes with interleukin-6 production and secretion and with cytokeratin-16 expression by cultured human psoriatic keratinocytes: further potential mechanisms of its anti-psoriatic action. *Int. J. Mol. Med.* 18, 1073–9.
- Chitambar, C.R., 2010. Medical applications and toxicities of gallium compounds. *Int. J. Environ. Res. Public Health* 7, 2337–2361. <https://doi.org/10.3390/ijerph7052337>
- Chou, T.C., Wang, P.C., Wu, J. De, Sheu, S.C., 2016. Chromium-induced skin damage among Taiwanese cement workers. *Toxicol. Ind. Health* 32, 1745–1751.

4.5. Abbreviations

- <https://doi.org/10.1177/0748233715584699>
- Chu, C.-Y., Peng, F.-C., Chiu, Y.-F., Lee, H.-C., Chen, C.-W., Wei, J.-C., Lin, J.-J., 2012. Nanohybrids of Silver Particles Immobilized on Silicate Platelet for Infected Wound Healing. *PLoS One* 7, e38360. <https://doi.org/10.1371/journal.pone.0038360>
- Chukanov, N. V., Chervonnyi, A.D., 2016. *Infrared Spectroscopy of Minerals and Related Compounds*. Springer Mineralogy.
- Çınar, M., Can, M.F., Sabah, E., Karagüzel, C., Çelik, M.S., 2009. Rheological properties of sepiolite ground in acid and alkaline media. *Appl. Clay Sci.* 42, 422–426. <https://doi.org/10.1016/J.CLAY.2008.04.010>
- COLIPA, 1997. Guidelines for percutaneous absorption/penetration.
- Comacchi, C., Hercogova, J., 2004. A single mud treatment induces normalization of stratum corneum hydration, transepidermal water loss, skin surface pH and sebum content in patients with seborrhoeic dermatitis. *J. Eur. Acad. Dermatology Venereol.* 18, 372–4. <https://doi.org/10.1111/j.1468-3083.2004.00484.x>
- Cozzi, F., Raffeiner, B., Beltrame, V., Ciprian, L., Coran, A., Botsios, C., Perissinotto, E., Grisan, E., Ramonda, R., Oliviero, F., Stramare, R., Punzi, L., 2015. Effects of mud-bath therapy in psoriatic arthritis patients treated with TNF inhibitors. Clinical evaluation and assessment of synovial inflammation by contrast-enhanced ultrasound (CEUS). *Joint. Bone. Spine* 82, 104–8. <https://doi.org/10.1016/j.jbspin.2014.11.002>
- da Silva, J., Jesus, S., Bernardi, N., Colaço, M., Borges, O., 2019. Poly(D, L-lactic Acid) nanoparticle size reduction increases its immunotoxicity. *Front. Bioeng. Biotechnol.* 7, 1–10. <https://doi.org/10.3389/fbioe.2019.00137>
- Dário, G.M.I., Da Silva, G.G., Gonçalves, D.L., Silveira, P., Junior, A.T., Angioletto, E., Bernardin, A.M., 2014. Evaluation of the healing activity of therapeutic clay in rat skin wounds. *Mater. Sci. Eng. C* 43, 109–116. <https://doi.org/10.1016/j.msec.2014.06.024>
- Davinelli, S., Bassetto, F., Vitale, M., Scapagnini, G., 2019. Thermal Waters and the hormetic effects of hydrogen sulfide on inflammatory arthritis and wound healing. *Sci. Hormesis Heal. Longev.* 121–126. <https://doi.org/10.1016/B978-0-12-814253-0.00010-3>
- Dawson, J.I., Oreffo, R.O.C., 2013. Clay: New opportunities for tissue regeneration and biomaterial design. *Adv. Mater.* 25, 4069–4086. <https://doi.org/10.1002/adma.201301034>
- de Gois da Silva, M.L., Fortes, A.C., Oliveira, M.E.R., de Freitas, R.M., da Silva Filho, E.C., de La Roca Soares, M.F., Soares-Sobrinho, J.L., da Silva Leite, C.M., 2014. Palygorskite organophilic for dermopharmaceutical application. *J. Therm. Anal. Calorim.* 115, 2287–2294. <https://doi.org/10.1007/s10973-012-2891-4>
- de Ligt, R., van Duijn, E., Grossouw, D., Bosgra, S., Burggraaf, J., Windhorst, A., Peeters, P.A.M., van der Luijt, G.A., Alexander-White, C., Vaes, W.H.J., 2018. Assessment of Dermal Absorption of Aluminum from a Representative

- Antiperspirant Formulation Using a ²⁶Al Microtracer Approach. *Clin. Transl. Sci.* 11, 573–581. <https://doi.org/10.1111/cts.12579>
- de Souza e Silva, J.M., Hanchuk, T.D.M., Santos, M.I., Kobarg, J., Bajgelman, M.C., Cardoso, M.B., 2016. Viral inhibition mechanism mediated by surface-modified silica nanoparticles. *ACS Appl. Mater. Interfaces* 8, 16564–16572. <https://doi.org/10.1021/acsami.6b03342>
- Delfino, M., Russo, N., Migliaccio, G., Carraturo, N., 2003. Experimental study on efficacy of thermal muds of Ischia Island combined with balneotherapy in the treatment of psoriasis vulgaris with plaques. *Clin. Ter.* 154, 167–71.
- Demirci, S., Doğan, A., Aydın, S., Dülger, E.Ç., Şahin, F., 2016. Boron promotes streptozotocin-induced diabetic wound healing: roles in cell proliferation and migration, growth factor expression, and inflammation. *Mol. Cell. Biochem.* 417, 119–133. <https://doi.org/10.1007/s11010-016-2719-9>
- Demirci, S., Doğan, A., Karakuş, E., Halıcı, Z., Topçu, A., Demirci, E., Şahin, F., 2015. Boron and Poloxamer (F68 and F127) Containing Hydrogel Formulation for Burn Wound Healing. *Biol. Trace Elem. Res.* 168, 169–180. <https://doi.org/10.1007/s12011-015-0338-z>
- Denda, M., Katagiri, C., Hiraio, T., Maruyama, N., Takahashi, M., 1999. Some magnesium salts and a mixture of magnesium and calcium salts accelerate skin barrier recovery. *Arch. Dermatol. Res.* 291, 560–563. <https://doi.org/10.1007/s004030050454>
- Di Credico, B., Tagliaro, I., Cobani, E., Conzatti, L., D'Arienzo, M., Giannini, L., Mascotto, S., Scotti, R., Stagnaro, P., Tadiello, L., 2019. A green Approach for preparing high-loaded sepiolite/polymer biocomposites. *Nanomaterials* 9. <https://doi.org/10.3390/nano9010046>
- Dinić, Z., Maksimović, J., Stanojković-Sebić, A., Pivić, R., 2019. Prediction models for bioavailability of Mn, Cu, Zn, Ni and Pb in soils of Republic of Serbia. *Agronomy* 9, 1–14. <https://doi.org/10.3390/agronomy9120856>
- Dreno, B., Chosidow, O., Revuz, J., Moyses, D., 2003. Lithium gluconate 8% vs. ketoconazole 2% in the treatment of seborrheic dermatitis: A multicentre, randomized study. *Br. J. Dermatol.* 148, 1230–1236. <https://doi.org/10.1046/j.1365-2133.2003.05328.x>
- Dreno, B., Moyses, D., 2002. Lithium gluconate in the treatment of seborrheic dermatitis: A multicenter, randomised, double-blind study versus placebo. *Eur. J. Dermatology* 12, 549–552.
- Drobnik, J., Stebel, A., 2020. Central European ethnomedical and officinal uses of peat, with special emphasis on the Tolpa peat preparation (TPP): An historical review. *J. Ethnopharmacol.* 246, 112248. <https://doi.org/10.1016/j.jep.2019.112248>
- Dubé, J., Rochette-Drouin, O., Lévesque, P., Gauvin, R., Roberge, C.J., Auger, F.A., Goulet, D., Bourdages, M., Plante, M., Germain, L., Moulin, V.J., 2010. Restoration of the transepithelial potential within tissue-engineered human skin in vitro and during the wound healing process in vivo. *Tissue Eng. Part A* 16, 3055–3063. <https://doi.org/10.1089/ten.tea.2010.0030>

4.5. Abbreviations

- Elkayam, O., Ophir, J., Brener, S., Paran, D., Wigler, I., Efron, D., Even-Paz, Z., Politi, Y., Yaron, M., 2000. Immediate and delayed effects of treatment at the Dead Sea in patients with psoriatic arthritis. *Rheumatol. Int.* 19, 77–82.
- Elzinga, E.J., Rouff, A.A., Reeder, R.J., 2006. The long-term fate of Cu²⁺, Zn²⁺, and Pb²⁺ adsorption complexes at the calcite surface: An X-ray absorption spectroscopy study. *Geochim. Cosmochim. Acta* 70, 2715–2725. <https://doi.org/10.1016/j.gca.2006.02.026>
- Engen, D.J., McAllister, S.J., Whipple, M.O., Cha, S.S., Dion, L.J., Vincent, A., Bauer, B.A., Wahner-Roedler, D.L., 2015. Effects of transdermal magnesium chloride on quality of life for patients with fibromyalgia: a feasibility study. *J. Integr. Med.* 13, 306–313. [https://doi.org/10.1016/S2095-4964\(15\)60195-9](https://doi.org/10.1016/S2095-4964(15)60195-9)
- Erikson, K.M., Aschner, M., 2019. Manganese: Its Role in Disease and Health. *Met. Ions Life Sci.* 19. <https://doi.org/10.1515/9783110527872-016>
- EU, 2017. Manual of the working group on cosmetic products (sub-group on borderline products) on the scope of application of the cosmetics regulation (EC) No 1223/2009 (Art. 2(1)(A)). Brussels, Belgium.
- EU, 2009. Regulation (EC) No 1223/2009 on Cosmetic Products, Official Journal of the European Union. Brussels, Belgium.
- EU, 2008. Regulation (EC) No 1272/2008 on classification, labelling and packaging of substances and mixtures, amending and repealing Directives 67/548/EEC and 1999/45/EC, and amending Regulation (EC) No 1907/2006. European Union.
- EU, 2003. Directive 2003/15/EC of the European Parliament and of the Council amending Council Directive 76/768/EEC on the approximation of the laws of the Member States relating to cosmetic products. Brussels, Belgium.
- Faga, A., Nicoletti, G., Gregotti, C., Finotti, V., Nitto, A., Gioglio, L., 2012. Effects of thermal water on skin regeneration. *Int. J. Mol. Med.* 29, 732–740. <https://doi.org/10.3892/ijmm.2012.917>
- Fairley, J.A., Marcelo, C.L., Hogan, V.A., Voorhees, J.J., 1985. Increased calmodulin levels in psoriasis and low Ca⁺⁺ regulated mouse epidermal keratinocyte cultures. *J. Invest. Dermatol.* 84, 195–198. <https://doi.org/10.1111/1523-1747.ep12264823>
- FDA, 2017. Prohibited & Restricted Ingredients in Cosmetics [WWW Document]. U.S. Food Drug Adm. URL <https://www.fda.gov/cosmetics/cosmetics-laws-regulations/prohibited-restricted-ingredients-cosmetics> (accessed 12.12.19).
- Fernandes, A.C., Antunes, F., Pires, J., 2013. Sepiolite based materials for storage and slow release of nitric oxide. *New J. Chem.* 37, 4052–4060. <https://doi.org/10.1039/c3nj00452j>
- Fernández-González, M.V., Martín-García, J.M., Delgado, G., Párraga, J., Delgado, R., 2013. A study of the chemical, mineralogical and physicochemical properties of peloids prepared with two medicinal mineral waters from Lanjarón Spa (Granada, Spain). *Appl. Clay Sci.* 80–81, 107–116. <https://doi.org/10.1016/j.clay.2013.06.011>
- Filon, F.L., D'Agostin, F., Crosera, M., Adami, G., Bovenzi, M., Maina, G., 2009. In vitro

- absorption of metal powders through intact and damaged human skin. *Toxicol. Vitr.* 23, 574–579. <https://doi.org/10.1016/J.TIV.2009.01.015>
- Fioravanti, A., Cantarini, L., Guidelli, G.M., Galeazzi, M., 2011. Mechanisms of action of spa therapies in rheumatic diseases: what scientific evidence is there? *Rheumatol. Int.* 31, 1–8. <https://doi.org/10.1007/s00296-010-1628-6>
- Fioravanti, A., Karagülle, M., Bender, T., Karagülle, M.Z., 2017. Balneotherapy in osteoarthritis: Facts, fiction and gaps in knowledge. *Eur. J. Integr. Med.* 9, 148–150. <https://doi.org/10.1016/J.EUJIM.2017.01.001>
- Fioravanti, A., Perpignano, G., Tirri, G., Cardinale, G., Gianniti, C., Lanza, C.E., Loi, A., Tirri, E., Sfriso, P., Cozzi, F., 2007. Effects of mud-bath treatment on fibromyalgia patients: A randomized clinical trial. *Rheumatol. Int.* 27, 1157–1161. <https://doi.org/10.1007/s00296-007-0358-x>
- Flarend, R., Bin, T., Elmore, D., Hem, S.L., 2001. A preliminary study of the dermal absorption of aluminium from antiperspirants using aluminium-26. *Food Chem. Toxicol.* 39, 163–168. [https://doi.org/10.1016/S0278-6915\(00\)00118-6](https://doi.org/10.1016/S0278-6915(00)00118-6)
- Fluhr, J.W., Elias, P.M., 2002. Stratum corneum pH: Formation and Function of the ‘Acid Mantle.’ *Exog. Dermatology* 1, 163–175. <https://doi.org/10.1159/000066140>
- Földvári, M., 2011. Handbook of thermogravimetric system of minerals and its use in geological practice. Innova-Print Kft., Budapest.
- Fonder, M.A., Lazarus, G.S., Cowan, D.A., Aronson-Cook, B., Kohli, A.R., Mamelak, A.J., 2008. Treating the chronic wound: A practical approach to the care of nonhealing wounds and wound care dressings. *J. Am. Acad. Dermatol.* <https://doi.org/10.1016/j.jaad.2007.08.048>
- Forestier, R., Erol Forestier, F.B., Francon, A., 2016. Spa therapy and knee osteoarthritis: A systematic review. *Ann. Phys. Rehabil. Med.* 59, 216–226. <https://doi.org/10.1016/J.REHAB.2016.01.010>
- Fraioli, A., Serio, A., Mennuni, G., Ceccarelli, F., Petracchia, L., Fontana, M., Grassi, M., Valesini, G., 2011. A study on the efficacy of treatment with mud packs and baths with Sillene mineral water (Chianciano Spa Italy) in patients suffering from knee osteoarthritis. *Rheumatol. Int.* 31, 1333–1340. <https://doi.org/10.1007/s00296-010-1475-5>
- Frost, R.L., Ding, Z., 2003. Controlled rate thermal analysis and differential scanning calorimetry of sepiolites and palygorskites. *Thermochim. Acta* 397, 119–128. [https://doi.org/10.1016/S0040-6031\(02\)00228-9](https://doi.org/10.1016/S0040-6031(02)00228-9)
- Fukushima, K., Rasyida, A., Yang, M.C., 2013. Characterization, degradation and biocompatibility of PBAT based nanocomposites. *Appl. Clay Sci.* 80–81, 291–298. <https://doi.org/10.1016/j.clay.2013.04.015>
- Galan, E., 1996. Properties and applications of palygorskite-sepiolite clays. *Clay Miner.* 31, 443–453. <https://doi.org/10.1180/claymin.1996.031.4.01>
- Ganfoud, R., Puchot, L., Fouquet, T., Verge, P., 2015. H-bonding supramolecular interactions driving the dispersion of kaolin into benzoxazine: A tool for the reinforcement of polybenzoxazines thermal and thermo-mechanical properties. *Compos. Sci. Technol.* 110, 1–7.

4.5. Abbreviations

- <https://doi.org/10.1016/J.COMPSCITECH.2015.01.014>
- Gao, Y., Jin, X., 2019. Needle-punched three-dimensional nonwoven wound dressings with density gradient from biocompatible calcium alginate fiber. *Text. Res. J.* 89, 2776–2788. <https://doi.org/10.1177/0040517518801198>
- García-Villén, F., Faccendini, A., Aguzzi, C., Cerezo, P., Bonferoni, M.C., Rossi, S., Grisoli, P., Ruggeri, M., Ferrari, F., Sandri, G., Viseras, C., 2019. Montmorillonite-norfloxacin nanocomposite intended for healing of infected wounds. *Int. J. Nanomedicine* 14, 5051–5060. <https://doi.org/https://doi.org/10.2147/IJN.S208713>
- García-Villén, F., Faccendini, A., Miele, D., Ruggeri, M., Sánchez-Espejo, R., Borrego-Sánchez, A., Cerezo, P., Rossi, S., Viseras, C., Sandri, G., 2020a. Wound healing activity of nanoclay/spring water hydrogels. *Pharmaceutics* 12, 1–24. <https://doi.org/doi:10.3390/pharmaceutics12050467>
- García-Villén, F., Sánchez-Espejo, R., Borrego-Sánchez, A., Cerezo, P., Perioli, L., Viseras, C., 2020b. Safety of nanoclay/spring water hydrogels: assessment and mobility of hazardous elements. *Pharmaceutics* 12, 1–17. <https://doi.org/doi:10.3390/pharmaceutics12080764>
- García-Villén, F., Sánchez-Espejo, R., Carazo, E., Borrego-Sánchez, A., Aguzzi, C., Cerezo, P., Viseras, C., 2018. Characterisation of Andalusian peats for skin health care formulations. *Appl. Clay Sci.* 160, 201–205. <https://doi.org/10.1016/j.clay.2017.12.017>
- García-Villén, F., Sánchez-Espejo, R., López-Galindo, A., Cerezo, P., Viseras, C., 2020c. Design and characterization of spring water hydrogels with natural inorganic excipients. *Appl. Clay Sci.* 197, 105772.
- García-Villén, F., Souza, I.M.S., de Melo Barbosa, R., Borrego-Sánchez, A., Sánchez-Espejo, R., Ojeda-Riascos, S., Viseras, C., 2020d. Natural inorganic ingredients in wound healing. *Curr. Pharm. Des.* 26. <https://doi.org/10.2174/1381612826666200113162114>
- Glavaš, N., Mourelle, M.L., Gómez, C.P., Legido, J.L., Rogan Šmuc, N., Dolenc, M., Kovač, N., 2017. The mineralogical, geochemical, and thermophysical characterization of healing saline mud for use in pelotherapy. *Appl. Clay Sci.* 135, 119–128. <https://doi.org/10.1016/j.clay.2016.09.013>
- Gomes, C. de S.F., Silva, J.B.P., 2007. Minerals and clay minerals in medical geology. *Appl. Clay Sci.* 36, 4–21. <https://doi.org/10.1016/j.clay.2006.08.006>
- Gomes, C., de Sousa, F., 2018. Healing and edible clays: a review of basic concepts, benefits and risks. *Environ. Geochem. Health* 40, 1739–1765. <https://doi.org/10.1007/s10653-016-9903-4>
- Gomes, C., Silva, J., Gomes, J., 2015. Natural peloids versus designed and engineered peloids. *Bol. Soc. Española Hidrol. Medica* 30, 15–36. <https://doi.org/10.23853/bsehm.2017.0377>
- Goss, C.H., Kaneko, Y., Khuu, L., Anderson, G.D., Ravishankar, S., Aitken, M.L., Lechtzin, N., Zhou, G., Czyz, D.M., McLean, K., Olakanmi, O., Shuman, H.A., Teresi, M., Wilhelm, E., Caldwell, E., Salipante, S.J., Hornick, D.B., Siehnel, R.J.,

- Becker, L., Britigan, B.E., Singh, P.K., 2018. Gallium disrupts bacterial iron metabolism and has therapeutic effects in mice and humans with lung infections. *Sci. Transl. Med.* 10. <https://doi.org/10.1126/scitranslmed.aat7520>
- Government of Canada, 2012. Guidance on Heavy Metal Impurities in Cosmetics.
- Grandjean, E., Aubry, J., 2009. Lithium: updated human knowledge using an evidence-based approach. Part II: clinical pharmacology and therapeutic monitoring. *CNS Drugs* 23, 331–349.
- Granjeiro, J.M., Cruz, R., Leite, P.E., Gemini-Piperni, S., Boldrini, L.C., Ribeiro, A.R., 2020. Health and environment perspective of tin nanocompounds: A safety approach, in: Ornaghi-Orlandi, M. (Ed.), *Tin Oxide Materials. Synthesis, Properties, and Applications*. Elsevier, Berlin, pp. 133–162. <https://doi.org/10.1016/b978-0-12-815924-8.00006-2>
- Grasman, J.M., Williams, M.D., Razis, C.G., Bonzanni, M., Golding, A.S., Cairns, D.M., Levin, M., Kaplan, D.L., 2019. Hyperosmolar Potassium Inhibits Myofibroblast Conversion and Reduces Scar Tissue Formation. *ACS Biomater. Sci. Eng.* 5, 5327–5336. <https://doi.org/10.1021/acsbiomaterials.9b00810>
- Grzesiak, J.J., Pierschbacher, M.D., 1995. Shifts in the concentrations of magnesium and calcium in early porcine and rat wound fluids activate the cell migratory response. *J. Clin. Invest.* 95, 227–233. <https://doi.org/10.1172/JCI117644>
- Gunawardana, D.H., Lichtenstein, M., Better, N., Rosenthal, M., 2004. Results of Strontium-89 Therapy in Patients With Prostate Cancer Resistant to Chemotherapy. *Clin. Nucl. Med.* 29, 81–85. <https://doi.org/10.1097/01.rlu.0000109721.58471.44>
- Guo, N., Wang, J.S., Li, J., Teng, Y.G., Zhai, Y.Z., 2014. Dynamic adsorption of Cd²⁺ onto acid-modified attapulgite from aqueous solution. *Clays Clay Miner.* 62, 415–424. <https://doi.org/10.1346/CCMN.2014.0620505>
- Gupta, A.K., Versteeg, S.G., 2017. Topical Treatment of Facial Seborrheic Dermatitis: A Systematic Review. *Am. J. Clin. Dermatol.* <https://doi.org/10.1007/s40257-016-0232-2>
- Guzmán, R., Campos, C., Yuguero, R., Masegù, C., Gil, P., Moragón, Á.C., 2015. Protective effect of sulfurous water in peripheral blood mononuclear cells of Alzheimer's disease patients. *Life Sci.* 132, 61–67. <https://doi.org/10.1016/J.LFS.2015.04.006>
- Harari, M., 2012. Beauty is not only skin deep: the Dead Sea features and cosmetics 5, 75–88. https://doi.org/10.5209/rev_ANHM.2012.v5.n1.39171
- Harvey, C.C., Lagaly, G., 2006. Conventional applications, in: Bergaya, F., Theng, B., Lagaly, G. (Eds.), *Handbook of Clay Science*. Elsevier Ltd, pp. 501–540.
- Haydel, S.E., Remenih, C.M., Williams, L.B., 2007. Broad-spectrum in vitro antibacterial activities of clay minerals against antibiotic-susceptible and antibiotic-resistant bacterial pathogens. *J. Antimicrob. Chemother.* 61, 353–361. <https://doi.org/10.1093/jac/dkm468>
- HealthCanada, 2019. Natural Health Products Ingredients Database [WWW Document]. Gov. Canada, Nat. Heal. Prod. Dir. URL <http://webprod.hc->

4.5. Abbreviations

- sc.gc.ca/nhp/ndp/bdipsn/search-rechercheReq.do (accessed 12.18.19).
- HealthCanada, 2015. Quality of Natural Health Products Guide - Natural and Non-Prescription Health Products Directorate.
- Hepp, N.M., Mindak, W.R., Gasper, J.W., Thompson, C.B., Barrows, J.N., 2014. Survey of cosmetics for arsenic, cadmium, chromium, cobalt, lead, mercury, and nickel content. *J. Cosmet. Sci.* 65, 125–145.
- Honary, S., Zahir, F., 2013. Effect of zeta potential on the properties of nano-drug delivery systems - A review (Part 2). *Trop. J. Pharm. Res.* 12, 265–273. <https://doi.org/10.4314/tjpr.v12i2.20>
- Horning, K.J., Caito, S.W., Tipps, K.G., Bowman, A.B., Aschner, M., 2015. Manganese Is Essential for Neuronal Health. *Annu. Rev. Nutr.* 35, 71–108. <https://doi.org/10.1146/annurev-nutr-071714-034419>
- Hostynek, J.J., 2003. Factors determining percutaneous metal absorption. *Food Chem. Toxicol.* 41, 327–345. [https://doi.org/10.1016/S0278-6915\(02\)00257-0](https://doi.org/10.1016/S0278-6915(02)00257-0)
- Hotta, E., Hara, H., Kamiya, T., Adachi, T., 2018. Non-thermal atmospheric pressure plasma-induced IL-8 expression is regulated via intracellular K⁺ loss and subsequent ERK activation in human keratinocyte HaCaT cells. *Arch. Biochem. Biophys.* 644, 64–71. <https://doi.org/10.1016/j.abb.2018.03.005>
- Huang, A., Seité, S., Adar, T., 2018. The use of balneotherapy in dermatology. *Clin. Dermatol.* 36, 363–368. <https://doi.org/10.1016/J.CLINDERMATOL.2018.03.010>
- Huang, J.S., Mukherjee, J.J., Chung, T., Crilly, K.S., Kiss, Z., 1999. Extracellular calcium stimulates DNA synthesis in synergism with zinc, insulin and insulin-like growth factor I in fibroblasts. *Eur. J. Biochem.* 266, 943–951. <https://doi.org/10.1046/j.1432-1327.1999.00932.x>
- ICH, 2019. Guideline for Elemental Impurities Q3D(R1).
- Ishikawa, K., Akasaka, T., Abe, S., Yawaka, Y., Suzuki, M., Watari, F., 2010a. Application of imogolite, alumino-silicate nanotube, as scaffold for the mineralization of osteoblasts. *Bioceram. Dev. Appl.* 1, 1–3.
- Ishikawa, K., Akasaka, T., Yawaka, Y., Watari, F., 2010b. High functional expression of osteoblasts on imogolite, aluminosilicate nanotubes. *J. Biomed. Nanotechnol.* 6, 59–65. <https://doi.org/10.1166/jbn.2010.1092>
- Jalali, A., Zahmatkesh, M.H., Jalilian, A.R., Borujeni, A.T., Alirezapour, B., 2019. Preparation and Biological Evaluation of ⁶⁷Gallium- Labeled Iranian Hemiscorpius Lepturus Scorpion Venom. *Curr. Radiopharm.* 12. <https://doi.org/10.2174/1874471012666190828155227>
- Jebahi, S., Oudadesse, H., Jardak, N., Khayat, I., Keskes, H., Khabir, A., Rebai, T., El Feki, H., El Feki, A., 2013. Biological therapy of strontium-substituted bioglass for soft tissue wound-healing: Responses to oxidative stress in ovariectomised rats. *Ann. Pharm. Fr.* 71, 234–242. <https://doi.org/10.1016/j.pharma.2013.05.003>
- Karakaya, M.Ç., Karakaya, N., Sarioğlan, Ş., Koral, M., 2010. Some properties of thermal muds of some spas in Turkey. *Appl. Clay Sci.* 48, 531–537. <https://doi.org/10.1016/J.CLAY.2010.02.005>

- Karvonen, S.L., Korkiamäki, T., Ylä-Outinen, H., Nissinen, M., Teerikangas, H., Pummi, K., Karvonen, J., Peltonen, J., 2000. Psoriasis and altered calcium metabolism: Downregulated capacitative calcium influx and defective calcium-mediated cell signaling in cultured psoriatic keratinocytes. *J. Invest. Dermatol.* 114, 693–700. <https://doi.org/10.1046/j.1523-1747.2000.00926.x>
- Kass, L., Rosanoff, A., Tanner, A., Sullivan, K., McAuley, W., Plesset, M., 2017. Effect of transdermal magnesium cream on serum and urinary magnesium levels in humans: A pilot study. *PLoS One* 12. <https://doi.org/10.1371/journal.pone.0174817>
- Khiari, I., Meftah, S., Sánchez-Espejo, R., Cerezo, P., Aguzzi, C., López-Galindo, A., Jamoussi, F., Viseras Iborra, C., 2014. Study of traditional Tunisian medina clays used in therapeutic and cosmetic mud-packs. *Appl. Clay Sci.* 101, 141–148. <https://doi.org/10.1016/J.CLAY.2014.07.029>
- Khiari, I., Sánchez-Espejo, R., García-Villén, F., Cerezo, P., Aguzzi, C., López-Galindo, A., Jamoussi, F., Viseras, C., 2019. Rheology and cation release of tunisian medina mud-packs intended for topical applications. *Appl. Clay Sci.* 171, 110–117. <https://doi.org/10.1016/J.CLAY.2019.01.018>
- Kielczawa, B., 2018. Balneological use of geothermal springs in selected regions of the world, in: *Geothermal Water Management*. CRC Press, pp. 319–364. <https://doi.org/10.1201/9781315734972-13>
- Kimura, Y., Seguchi, O., Mochizuki, H., Iwasaki, K., Toda, K., Kumai, Y., Kuroda, K., Nakajima, S., Tateishi, E., Watanabe, T., Matsumoto, Y., Fukushima, S., Kiso, K., Yanase, M., Fujita, T., Kobayashi, J., Fukushima, N., 2019. Role of Gallium-SPECT-CT in the Management of Patients With Ventricular Assist Device-Specific Percutaneous Driveline Infection. *J. Card. Fail.* 25, 795–802. <https://doi.org/10.1016/j.cardfail.2019.08.009>
- Kirrane, B.M., Nelson, L.S., Hoffman, R.S., 2006. Massive strontium ferrite ingestion without acute toxicity. *Toxicology* 99.
- Kiyohiro, T., Otsuka, R., 1989. Dehydration mechanism of bound water in sepiolite. *Thermochim. Acta* 147, 127–138. [https://doi.org/10.1016/0040-6031\(89\)85169-X](https://doi.org/10.1016/0040-6031(89)85169-X)
- Kommireddy, D.S., Ichinose, I., Lvov, Y.M., Mills, D.K., 2006. Nanoparticle multilayers: surface modification for cell attachment and growth. *J. Biomed. Nanotechnol.* 1, 286–290. <https://doi.org/10.1166/jbn.2005.046>
- L'Oréal, 2019. Annual growth of the global cosmetics market from 2004 to 2018.
- Lai, X., Agarwal, M., Lvov, Y.M., Pachpande, C., Varahramyan, K., Witzmann, F.A., 2013. Proteomic profiling of halloysite clay nanotube exposure in intestinal cell co-culture. *J. Appl. Toxicol.* 33, 1316–29. <https://doi.org/10.1002/jat.2858>
- Lambers, H., Piessens, S., Bloem, A., Pronk, H., Finkel, P., 2006. Natural skin surface pH is on average below 5, which is beneficial for its resident flora. *Int. J. Cosmet. Sci.* 28, 359–370. <https://doi.org/10.1111/j.1467-2494.2006.00344.x>
- Lansdown, A.B.G., 2002. Calcium: a potential central regulator in wound healing in the skin. *Wound Repair Regen.* 10, 271–285. <https://doi.org/10.1046/j.1524-475X.2002.10502.x>

4.5. Abbreviations

- Lansdown, A.B.G., 1995. Physiological and toxicological changes in the skin resulting from the action and interaction of metal ions. *Crit. Rev. Toxicol.* 25, 397–462. <https://doi.org/10.3109/10408449509049339>
- Lansdown, A.B.G., Sampson, B., Rowe, A., 1999. Sequential changes in trace metal, metallothionein and calmodulin concentrations in healing skin wounds. *J. Anat.* 195, 375–386.
- Larese Filon, F., Maina, G., Adami, G., Venier, M., Coceani, N., Bussani, R., Massiccio, M., Barbieri, P., Spinelli, P., 2004. In vitro percutaneous absorption of cobalt. *Int. Arch. Occup. Environ. Health* 77, 85–89. <https://doi.org/10.1007/s00420-003-0455-4>
- Lee, C.H., Moturi, V., Lee, Y., 2009. Thixotropic property in pharmaceutical formulations. *J. Control. Release* 136, 88–98. <https://doi.org/10.1016/j.jconrel.2009.02.013>
- Leeming, J.P., 1993. Use of topical lithium succinate in the treatment of seborrhoeic dermatitis. *Dermatology*. <https://doi.org/10.1159/000247228>
- Legido, J.L., Medina, C., Lourdes Mourelle, M., Carretero, M.I., Pozo, M., 2007. Comparative study of the cooling rates of bentonite, sepiolite and common clays for their use in pelotherapy. *Appl. Clay Sci.* 36, 148–160. <https://doi.org/10.1016/J.CLAY.2006.06.014>
- Lehtimäki, J., Hakala, M., Lappalainen, P., 2017. Actin filament structures in migrating cells. *Handb. Exp. Pharmacol.* 235, 1–30. https://doi.org/10.1007/164_2016_28
- Lemić, J., Tomašević-Čanović, M., Djuričić, M., Stanić, T., 2005. Surface modification of sepiolite with quaternary amines. *J. Colloid Interface Sci.* 292, 11–19. <https://doi.org/10.1016/j.jcis.2005.05.080>
- Li, P.-R., Wei, J.-C., Chiu, Y.-F., Su, H.-L., Peng, F.-C., Lin, J.-J., 2010. Evaluation on cytotoxicity and genotoxicity of the exfoliated silicate nanoclay. *ACS Appl. Mater. Interfaces* 2, 1608–13. <https://doi.org/10.1021/am1001162>
- Li, S., Li, L., Guo, C., Qin, H., Yu, X., 2017. A promising wound dressing material with excellent cytocompatibility and proangiogenesis action for wound healing: Strontium loaded Silk fibroin/Sodium alginate (SF/SA) blend films. *Int. J. Biol. Macromol.* 104, 969–978. <https://doi.org/10.1016/j.ijbiomac.2017.07.020>
- Li, Yunfei, Wang, M., Sun, D., Li, Yujiang, Wu, T., 2018. Effective removal of emulsified oil from oily wastewater using surfactant-modified sepiolite. *Appl. Clay Sci.* 157, 227–236. <https://doi.org/10.1016/J.CLAY.2018.02.014>
- Liang, J., Kang, D., Wang, Y., Yu, Y., Fan, J., Takashi, E., 2015. Carbonate ion-enriched hot spring water promotes skin wound healing in nude rats. *PLoS One* 10. <https://doi.org/10.1371/journal.pone.0117106>
- Lin, F.H., Chen, C.H., Cheng, W.T.K., Kuo, T.F., 2006. Modified montmorillonite as vector for gene delivery. *Biomaterials* 27, 3333–3338. <https://doi.org/10.1016/j.biomaterials.2005.12.029>
- Liu, F., Chen, D.-D., Sun, X., Xie, H.-H., Yuan, H., Jia, W., Chen, A.F., Chen, A.F., 2014. Hydrogen sulfide improves wound healing via restoration of endothelial progenitor cell functions and activation of angiopoietin-1 in Type 2 diabetes.

- Diabetes 63, 1763–1778. <https://doi.org/10.2337/db13-0483>
- Lizarbe, M.A., Olmo, N., Gavilanes, J.G., 1987. Outgrowth of fibroblasts on sepiolite-collagen complex. *Biomaterials* 8, 35–37. [https://doi.org/10.1016/0142-9612\(87\)90025-1](https://doi.org/10.1016/0142-9612(87)90025-1)
- Lobato-Aguilar, H., Uribe-Calderón, J.A., Herrera-Kao, W., Duarte-Aranda, S., Baas-López, J.M., Escobar-Morales, B., Cauich-Rodríguez, J.V., Cervantes-Uc, J.M., 2018. Synthesis, characterization and chlorhexidine release from either montmorillonite or palygorskite modified organoclays for antibacterial applications. *J. Drug Deliv. Sci. Technol.* 46, 452–460. <https://doi.org/10.1016/J.JDDST.2018.06.007>
- López-Galindo, A., Viseras, C., 2004. Pharmaceutical and cosmetic application of clays, in: Wypyc, F., Satyanarayana, K.G. (Eds.), *Clay Surfaces: Fundamentals and Applications*. Elsevier Ltd, pp. 267–289.
- López-Galindo, A., Viseras, C., Aguzzi, C., Cerezo, P., 2011. Pharmaceutical and cosmetic uses of fibrous clays, in: Galán, E., Singer, A. (Eds.), *Developments in Clay Science*. Elsevier, pp. 299–324. <https://doi.org/10.1016/B978-0-444-53607-5.00013-X>
- López-Galindo, A., Viseras, C., Cerezo, P., 2007. Compositional, technical and safety specifications of clays to be used as pharmaceutical and cosmetic products. *Appl. Clay Sci.* 36, 51–63. <https://doi.org/10.1016/J.CLAY.2006.06.016>
- Lucchini, R.G., Aschner, M., Landrigan, P.J., Cranmer, J.M., 2018. Neurotoxicity of manganese: Indications for future research and public health intervention from the Manganese 2016 conference, in: *NeuroToxicology*. Elsevier B.V., pp. 1–4. <https://doi.org/10.1016/j.neuro.2018.01.002>
- Ma, J., Zhao, N., Zhu, D., 2016. Biphasic responses of human vascular smooth muscle cells to magnesium ion. *J. Biomed. Mater. Res. Part A* 104, 347–356. <https://doi.org/10.1002/jbm.a.35570>
- Madejová, J., Komadel, P., 2001. Baseline Studies of the Clay Minerals Society Source Clays: Infrared Methods. *Clays Clay Miner.* 49, 410–432.
- Mahé, Y.F., Martin, R., Aubert, L., Billoni, N., Collin, C., Pruche, F., Bastien, P., Drost, S.S., Lane, A.T., Meybeck, A., 2006. Induction of the skin endogenous protective mitochondrial MnSOD by *Vitreoscilla filiformis* extract. *Int. J. Cosmet. Sci.* 28, 277–287. <https://doi.org/10.1111/j.1467-2494.2006.00333.x>
- Mahe, Y.F., Perez, M.J., Tacheau, C., Fanchon, C., Martin, R., Rousset, F., Seite, S., 2013. A new *Vitreoscilla filiformis* extract grown on spa water-enriched medium activates endogenous cutaneous antioxidant and antimicrobial defenses through a potential Toll-like receptor 2/protein kinase C, zeta transduction pathway. *Clin. Cosmet. Investig. Dermatol.* 6, 191–196. <https://doi.org/10.2147/CCID.S47324>
- Maisanaba, S., Pichardo, S., Puerto, M., Gutiérrez-Praena, D., Cameán, A.M., Jos, A., 2015. Toxicological evaluation of clay minerals and derived nanocomposites: A review. *Environ. Res.* 138, 233–254. <https://doi.org/10.1016/J.ENVRES.2014.12.024>

4.5. Abbreviations

- Maraver Eyzaguirre, F., Armijo de Castro, F., 2010. *Vademécum II de aguas mineromedicinales españolas*. Editorial Complutense, Madrid.
- Marcolongo, G., De Appolonia, F., Venzo, A., Berrie, C.P., Carofiglio, T., Ceschi Berrini, C., 2006. Diacylglycerolipids isolated from a thermophile cyanobacterium from the Euganean hot springs. *Nat. Prod. Res.* 20, 766–774. <https://doi.org/10.1080/14786410500176393>
- Marins, J.A., Plachý, T., Kuzhir, P., 2019. Iron–sepiolite magnetorheological fluids with improved performances. *J. Rheol. (N. Y. N. Y.)*. 63, 125–139. <https://doi.org/10.1122/1.5048051>
- Masiero, S., Maccarone, M.C., Magro, G., 2020. Balneotherapy and human immune function in the era of COVID-19. *Int. J. Biometeorol.* 1, 1–2. <https://doi.org/10.1007/s00484-020-01914-z>
- McKeown, D.A., Post, J.E., Etz, E.S., 2002. Vibrational analysis of palygorskite and sepiolite. *Clays Clay Miner.* 50, 667–680.
- McKnight, R., Adida, M., Budge, K., Stockton, S., Goodwin, G., Geddes, J., 2012. Lithium toxicity profile: a systematic review and meta-analysis. *Lancet* 379, 721–728.
- McLean, S.A., Allen, B.L., Craig, J.R., 1972. The occurrence of sepiolite and attapulgite on the southern High Plains. *Clays Clay Miner.* 20, 143–149. <https://doi.org/10.1346/CCMN.1972.0200305>
- Mefteh, S., Khiari, I., Sánchez-Espejo, R., Aguzzi, C., López-Galindo, A., Jamoussi, F., Viseras, C., 2014. Characterisation of Tunisian layered clay materials to be used in semisolid health care products. *Mater. Technol.* 29, B88–B95. <https://doi.org/10.1179/1753555714Y.0000000152>
- Mejide Faílde, R., Mourelle Mosqueira, L., Vela Anero, Á., Muñíos López, E., Fernández Burguera, E., Gómez Pérez, C.P., 2013. Aplicación a pacientes: peloterapia en patologías dermatológicas, in: *Peloterapia: Aplicaciones Médicas y Cosméticas de Fangos Termales*. Fundación BILBILIS para la Investigación e Innovación en Hidrología Médica y Balneoterapia, Madrid, pp. 169–183.
- Melnikov, P., de Fatima Cepa Matos, M., Malzac, A., Rainho Teixeira, A., de Albuquerque, D.M., 2019. Evaluation of in vitro toxicity of hydroxyapatite doped with gallium. *Mater. Lett.* 253, 343–345. <https://doi.org/10.1016/j.matlet.2019.06.095>
- Mendelovici, E., 1973. Infrared study of attapulgite and HCl treated attapulgite. *Clays Clay Miner.* 21, 115–119.
- Middea, A., Spinelli, L.S., Souza, F.G., Neumann, R., Gomes, O. da F.M., Fernandes, T.L.A.P., de Lima, L.C., Barthem, V.M.T.S., de Carvalho, F. V., 2015. Synthesis and characterization of magnetic palygorskite nanoparticles and their application on methylene blue remotion from water. *Appl. Surf. Sci.* 346, 232–239. <https://doi.org/10.1016/j.apsusc.2015.03.080>
- Mihelčić, G., Kniewald, G., Ivanišević, G., Čepelak, R., Mihelčić, V., Vdović, N., 2012. Physico-chemical characteristics of the peloid mud from Morinje Bay (eastern Adriatic coast, Croatia): suitability for use in balneotherapy. *Environ. Geochem.*

- Health 34, 191–198. <https://doi.org/10.1007/s10653-011-9434-y>
- Mishra, R.K., Ramasamy, K., Lim, S.M., Ismail, M.F., Majeed, A.B.A., 2014. Antimicrobial and in vitro wound healing properties of novel clay based bionanocomposite films. *J. Mater. Sci. Mater. Med.* 25, 1925–1939. <https://doi.org/10.1007/s10856-014-5228-y>
- Missana, T., Garcia-Gutierrez, M., Alonso, U., 2008. Sorption of strontium onto illite/smectite mixed clays. *Phys. Chem. Earth* 33, S156–S162. <https://doi.org/10.1016/j.pce.2008.10.020>
- Modabberi, S., Namayandeh, A., López-Galindo, A., Viseras, C., Setti, M., Ranjbaran, M., 2015. Characterization of Iranian bentonites to be used as pharmaceutical materials. *Appl. Clay Sci.* 116–117, 193–201. <https://doi.org/10.1016/J.CLAY.2015.03.013>
- Moldovan, M., Nanu, A., 2010. Influence of cleansing product type on several skin parameters after single use. *Farm.* 58, 29–37.
- Mora, M., Isabel López, M., Ángeles Carmona, M., Jiménez-Sanchidrián, C., Rafael Ruiz, J., 2010. Study of the thermal decomposition of a sepiolite by mid- and near-infrared spectroscopies. *Polyhedron* 29, 3046–3051. <https://doi.org/10.1016/J.POLY.2010.08.009>
- Moraes, J.D.D., Bertolino, S.R.A., Cuffini, S.L., Ducart, D.F., Bretzke, P.E., Leonardi, G.R., 2017. Clay minerals: Properties and applications to dermocosmetic products and perspectives of natural raw materials for therapeutic purposes— A review. *Int. J. Pharm.* 534, 213–219. <https://doi.org/10.1016/j.ijpharm.2017.10.031>
- Morrison, K.D., Misra, R., Williams, L.B., 2016. Unearthing the Antibacterial Mechanism of Medicinal Clay: A Geochemical Approach to Combating Antibiotic Resistance. *Sci. Rep.* 6, 1–13. <https://doi.org/10.1038/srep19043>
- Mousa, M., Evans, N.D., Oreffo, R.O.C., Dawson, J.I., 2018. Clay nanoparticles for regenerative medicine and biomaterial design: A review of clay bioactivity. *Biomaterials* 159, 204–214. <https://doi.org/10.1016/J.BIOMATERIALS.2017.12.024>
- Moysan, A., Morlière, P., Marquis, I., Richard, A., Dubertret, L., 1995. Effects of selenium on UVA-Induced lipid peroxidation in cultured human skin fibroblasts. *Skin Pharmacol. Physiol.* 8, 139–148. <https://doi.org/10.1159/000211337>
- Mukherjee, B., Patra, B., Mahapatra, S., Banerjee, P., Tiwari, A., Chatterjee, M., 2004. Vanadium - An element of atypical biological significance. *Toxicol. Lett.* 150, 135–143. <https://doi.org/10.1016/j.toxlet.2004.01.009>
- Nasermoaddel, A., Kagamimori, S., 2005. Balneotherapy in medicine: A review. *Environ. Health Prev. Med.* 10, 171–179. <https://doi.org/10.1007/BF02897707>
- Nasirov, M.I., Efendieva, F.M., Ismailova, D.A., 2009. The influence of peloids from volcanic deposits in Azerbaijan on the dynamics of sugar content in blood and urine and the wound healing in patients at the early stages of diabetic gangrene of the lower extremities. *Vopr. Kurortol. Fizioter. Lech. Fiz. Kult.* 42–3.

4.5. Abbreviations

- Neaman, A., Singer, A., 2000a. Rheology of mixed palygorskite-montmorillonite suspensions. *Clays Clay Miner.* 48, 713–715.
- Neaman, A., Singer, A., 2000b. Rheological properties of aqueous suspensions of palygorskite. *Soil Sci. Soc. Am.* 64, 427–436.
- Nguyen, P., Knapp-Wachsner, A., Hsieh, C.G., Kamangar, N., 2019. Pulmonary Kaposi Sarcoma without Mucocutaneous Involvement: The Role of Sequential Thallium and Gallium Scintigraphy. *J. Clin. Imaging Sci.* 9, 12. https://doi.org/10.25259/JCIS_76_18
- Nicoletti, G., Saler, M., Pellegatta, T., Tresoldi, M.M., Bonfanti, V., Malovini, A., Faga, A., Riva, F., 2017a. Ex vivo regenerative effects of a spring water. *Biomed. Reports* 7, 508–514. <https://doi.org/10.3892/br.2017.1002>
- Nicoletti, G., Saler, M., Pellegatta, T., Tresoldi, M.M., Bonfanti, V., Malovini, A., Faga, A., Riva, F., 2017b. Ex vivo regenerative effects of a spring water. *Biomed. Reports* 7, 508–514. <https://doi.org/10.3892/br.2017.1002>
- Nielsen, S.P., 2004. The biological role of strontium. *Bone.* <https://doi.org/10.1016/j.bone.2004.04.026>
- Ninan, N., Muthiah, M., Park, I.K., Wong, T.W., Thomas, S., Grohens, Y., 2015. Natural polymer/inorganic material based hybrid scaffolds for skin wound healing. *Polym. Rev.* 55, 453–490. <https://doi.org/10.1080/15583724.2015.1019135>
- Nissenbaum, A., Rullkötter, J., Yechieli, Y., 2002. Are the curative properties of ‘black mud’ from the dead sea due to the presence of bitumen (asphalt) or other types of organic matter? *Environ. Geochem. Health* 24, 327–335. <https://doi.org/10.1023/A:1020559717754>
- Nussbaum, S.R., Carter, M.J., Fife, C.E., DaVanzo, J., Haught, R., Nussgart, M., Cartwright, D., 2018. An Economic Evaluation of the Impact, Cost, and Medicare Policy Implications of Chronic Nonhealing Wounds. *Value Heal.* 21, 27–32. <https://doi.org/10.1016/j.jval.2017.07.007>
- O’Dell, B.L., Browning, J.D., 2013. Impaired calcium entry into cells is associated with pathological signs of zinc deficiency. *Adv. Nutr.* 4, 287–293. <https://doi.org/10.3945/an.112.003624>
- O’Dell, B.L., Browning, J.D., 2011. Zinc deprivation impairs growth factor-stimulated calcium influx into murine 3T3 cells associated with decreased cell proliferation. *J. Nutr.* 141, 1036–1040. <https://doi.org/10.3945/jn.110.137042>
- Ogawa, Y., Kawamura, T., Shimada, S., 2016. Zinc and skin biology. *Arch. Biochem. Biophys.* 611, 113–119. <https://doi.org/10.1016/j.abb.2016.06.003>
- Ogawa, Y., Kinoshita, M., Shimada, S., Kawamura, T., 2018. Zinc and skin disorders. *Nutrients* 10. <https://doi.org/10.3390/nu10020199>
- Ogen-Shtern, N., Chumin, K., Cohen, G., Borkow, G., 2019. Increased pro-collagen 1, elastin, and TGF- β 1 expression by copper ions in an ex-vivo human skin model. *J. Cosmet. Dermatol.* [jocd.13186. https://doi.org/10.1111/jocd.13186](https://doi.org/10.1111/jocd.13186)
- Olmo, N., Lizarbe, M.A., Gavilanes, J.G., 1987. Biocompatibility and degradability of sepiolite-collagen complex. *Biomaterials* 8, 67–9. <https://doi.org/10.1016/0142->

9612(87)90033-0

- Olsson, M., Järbrink, K., Ni, G., Sönnergren, H., Schmidtchen, A., Pang, C., Bajpai, R., Car, J., 2017. The humanistic and economic burden of chronic wounds: A protocol for a systematic review. *Syst. Rev.* 6. <https://doi.org/10.1186/s13643-016-0400-8>
- Paolisso, G., Barbagallo, M., 1997. Hypertension, diabetes mellitus, and insulin resistance. The role of intracellular magnesium. *Am. J. Hypertens.* [https://doi.org/10.1016/S0895-7061\(96\)00342-1](https://doi.org/10.1016/S0895-7061(96)00342-1)
- Pathania, Y.S., Budania, A., 2019. Chrome Ulcers: An occupational hazard. *J. Eur. Acad. Dermatology Venereol.* *jd.v.16141.* <https://doi.org/10.1111/jdv.16141>
- Pesciaroli, C., Viseras, C., Aguzzi, C., Rodelas, B., González-López, J., 2016. Study of bacterial community structure and diversity during the maturation process of a therapeutic peloid. *Appl. Clay Sci.* 132–133, 59–67. <https://doi.org/10.1016/j.clay.2016.05.015>
- Ph.Eur.9th., 2018a. Magnesium Trisilicate monograph, in: Council of Europe & Convention on the Elaboration of a European Pharmacopoeia. Council of Europe, Strasbourg.
- Ph.Eur.9th, 2018b. Magnesium Aluminium Silicate monograph, in: Council of Europe & Convention on the Elaboration of a European Pharmacopoeia. Council of Europe, Strasbourg.
- Pineau, A., Guillard, O., Fauconneau, B., Favreau, F., Marty, M.H., Gaudin, A., Vincent, C.M., Marraud, A., Marty, J.P., 2012. In vitro study of percutaneous absorption of aluminum from antiperspirants through human skin in the Franz™ diffusion cell. *J. Inorg. Biochem.* 110, 21–26. <https://doi.org/10.1016/j.jinorgbio.2012.02.013>
- Pisano, M., Arru, C., Serra, M., Galleri, G., Sanna, D., Garribba, E., Palmieri, G., Rozzo, C., 2019. Antiproliferative activity of vanadium compounds: Effects on the major malignant melanoma molecular pathways. *Metallomics* 11, 1687–1699. <https://doi.org/10.1039/c9mt00174c>
- Post, J.L., Crawford, S., 2007. Varied forms of palygorskite and sepiolite from different geologic systems. *Appl. Clay Sci.* 36, 232–244. <https://doi.org/10.1016/j.clay.2006.10.003>
- Potpara, Z., Duborija-Kovacevic, N., 2012. Effects of the peloid cream from the Montenegrin Adriatic coast on skin humidity, transepidermal water loss and erythema index, examined with skin bioengineering in vivo methods. *Farmacia* 60, 524–534.
- Pozo, M., Armijo, F., Maraver, F., Ejeda, J.M., Corvillo, I., 2018. Texture profile analysis (TPA) of clay/seawater mixtures useful for peloid preparation: Effects of clay concentration, pH and salinity. *Appl. Clay Sci.* 165, 40–51.
- Pozo, M., Armijo, F., Maraver, F., Zuluaga, P., Ejeda, J.M., Corvillo, I., 2019. Variations in the Texture Profile Analysis (TPA) Properties of Clay/Mineral-Medicinal Water Mixtures for Pelotherapy: Effect of Anion Type. *Minerals* 9.
- Prado-Pérez, A.J., Pérez del Villar, L., 2011. Dedolomitization as an analogue process

4.5. Abbreviations

- for assessing the long-term behaviour of a CO₂ deep geological storage: The Alicún de las Torres thermal system (Betic Cordillera, Spain). *Chem. Geol.* 289, 98–113. <https://doi.org/10.1016/j.chemgeo.2011.07.017>
- Prado Pérez, A.J., 2011. El sistema termal de Alicún de las Torres (Granada) como análogo natural de escape de CO₂ en forma de DIC: Implicaciones paleoclimáticas y como sumidero de CO₂. Complutense University of Madrid. <https://doi.org/ISBN:978-84-693-1123-3>
- Qiao, Y., Ping, Y., Zhang, H., Zhou, B., Liu, F., Yu, Y., Xie, T., Li, W., Zhong, D., Zhang, Y., Yao, K., Santos, H.A., Zhou, M., 2019. Laser-activatable CuS nanodots to treat multidrug-resistant bacteria and release copper ion to accelerate healing of infected chronic nonhealing wounds. *ACS Appl. Mater. Interfaces* 11, 3809–3822. <https://doi.org/10.1021/acsami.8b21766>
- Quintela, A., Costa, C., Terroso, D., Rocha, F., 2014. Abrasiveness index of dispersions of Portuguese clays using the Einlehner method: influence of clay parameters. *Clay Miner.* 49, 27–34. <https://doi.org/10.1180/claymin.2014.049.1.03>
- Quintela, A., Terroso, D., Almeida, S., Reis, A., 2010. Geochemical and microbiological characterization of some Azorean volcanic muds after maturation. *Res. J. Chem. Environ.* 14, 66–74.
- Rebello, M., da Silva, E.F., Rocha, F., 2015. Characterization of Portuguese thermomineral waters to be applied in peloids maturation. *Environ. Earth Sci.* 73, 2843–2862. <https://doi.org/10.1007/s12665-014-3670-2>
- Rebello, M., Viseras, C., López-Galindo, A., Rocha, F., da Silva, E.F., 2011a. Rheological and thermal characterization of peloids made of selected Portuguese geological materials. *Appl. Clay Sci.* 52, 219–227. <https://doi.org/10.1016/j.clay.2011.02.018>
- Rebello, M., Viseras, C., López-Galindo, A., Rocha, F., da Silva, E.F., 2011b. Characterization of Portuguese geological materials to be used in medical hydrology. *Appl. Clay Sci.* 51, 258–266. <https://doi.org/10.1016/j.clay.2010.11.029>
- Rhouta, B., Zatile, E., Bouna, L., Lakbita, O., Maury, F., Daoudi, L., Lafont, M.C., Amjoud, M., Senocq, F., Jada, A., Aït Aghzzaf, A., 2013. Comprehensive physicochemical study of dioctahedral palygorskite-rich clay from Marrakech High Atlas (Morocco). *Phys. Chem. Miner.* 40, 411–424. <https://doi.org/10.1007/s00269-013-0579-3>
- Riyaz, N., Arakkal, F., 2011. Spa therapy in dermatology. *Indian J. Dermatology, Venereol. Leprol.* 77, 128. <https://doi.org/10.4103/0378-6323.77450>
- Rodrigues, L., Ekundi-Valentim, E., Florenzano, J., Cerqueira, A.R.A., Soares, A.G., Schmidt, T.P., Santos, K.T., Teixeira, S.A., Ribela, M.T.C.P., Rodrigues, S.F., de Carvalho, M.H., De Nucci, G., Wood, M., Whiteman, M., Muscará, M.N., Costa, S.K.P., 2017. Protective effects of exogenous and endogenous hydrogen sulfide in mast cell-mediated pruritus and cutaneous acute inflammation in mice. *Pharmacol. Res.* 115, 255–266. <https://doi.org/10.1016/j.phrs.2016.11.006>
- Román-Razo, E.A., O’Farrill, P.M., Cambray, C., Herrera, A., Mendoza-Revilla, D.A., Aguirre, D., 2019. Allergic contact dermatitis to cobalt and nickel in a metal industry worker. Case report and literature review. *Rev. Alerg. Mex.* 66, 371–

374. <https://doi.org/10.29262/ram.v66i3.537>
- Roopan, S.M., Kumar, S.H.S., Madhumitha, G., Suthindhiran, K., 2014. Biogenic-Production of SnO₂ Nanoparticles and Its Cytotoxic Effect Against Hepatocellular Carcinoma Cell Line (HepG2). *Appl. Biochem. Biotechnol.* 175, 1567–1575. <https://doi.org/10.1007/s12010-014-1381-5>
- Rotoli, B.M., Guidi, P., Bonelli, B., Bernardeschi, M., Bianchi, M.G., Esposito, S., Frenzilli, G., Lucchesi, P., Nigro, M., Scarcelli, V., Tomatis, M., Zanello, P.P., Fubini, B., Bussolati, O., Bergamaschi, E., 2014. Imogolite: an aluminosilicate nanotube endowed with low cytotoxicity and genotoxicity. *Chem. Res. Toxicol.* 27, 1142–54. <https://doi.org/10.1021/tx500002d>
- Rytwo, G., Nir, S., Crespin, M., Margulies, L., 2000. Adsorption and interactions of methyl green with montmorillonite and sepiolite. *J. Colloid Interface Sci.* 222, 12–19. <https://doi.org/10.1006/JCIS.1999.6595>
- Salcedo, I., Aguzzi, C., Sandri, G., Bonferoni, M.C., Mori, M., Cerezo, P., Sánchez, R., Viseras, C., Caramella, C., 2012. In vitro biocompatibility and mucoadhesion of montmorillonite chitosan nanocomposite: A new drug delivery. *Appl. Clay Sci.* 55, 131–137. <https://doi.org/10.1016/j.clay.2011.11.006>
- Salcedo, I., Sandri, G., Aguzzi, C., Bonferoni, C., Cerezo, P., Sánchez-Espejo, R., Viseras, C., 2014. Intestinal permeability of oxytetracycline from chitosan-montmorillonite nanocomposites. *Colloids Surfaces B Biointerfaces* 117, 441–448. <https://doi.org/10.1016/J.COLSURFB.2013.11.009>
- Sánchez-Espejo, R., Aguzzi, C., Cerezo, P., Salcedo, I., López-Galindo, A., Viseras, C., 2014a. Folk pharmaceutical formulations in western Mediterranean: Identification and safety of clays used in pelotherapy. *J. Ethnopharmacol.* 155, 810–814. <https://doi.org/10.1016/j.jep.2014.06.031>
- Sánchez-Espejo, R., Aguzzi, C., Salcedo, I., Cerezo, P., Viseras, C., 2014b. Clays in complementary and alternative medicine. *Mater. Technol.* 29, B78–B81. <https://doi.org/10.1179/1753555714Y.0000000173>
- Sánchez-Espejo, R., Cerezo, P., Aguzzi, C., López-Galindo, A., Machado, J., Viseras, C., 2015. Physicochemical and in vitro cation release relevance of therapeutic muds “maturation”. *Appl. Clay Sci.* 116–117, 1–7. <https://doi.org/10.1016/j.clay.2015.08.007>
- Sánchez-Espejo, R.M., 2014. Suspensions of special clays in mineromedicinal waters to be used in therapeutics. Andalusian Institute of Earth Science and University of Granada.
- Sandri, G., Aguzzi, C., Rossi, S., Bonferoni, M.C., Bruni, G., Boselli, C., Cornaglia, A.I., Riva, F., Viseras, C., Caramella, C., Ferrari, F., 2017. Halloysite and chitosan oligosaccharide nanocomposite for wound healing. *Acta Biomater.* 57, 216–224. <https://doi.org/10.1016/J.ACTBIO.2017.05.032>
- Sandri, G., Bonferoni, M.C., Ferrari, F., Rossi, S., Aguzzi, C., Mori, M., Grisoli, P., Cerezo, P., Tenci, M., Viseras, C., Caramella, C., 2014. Montmorillonite-chitosan-silver sulfadiazine nanocomposites for topical treatment of chronic skin lesions: in vitro biocompatibility, antibacterial efficacy and gap closure cell motility

4.5. Abbreviations

- properties. *Carbohydr. Polym.* 102, 970–977. <https://doi.org/10.1016/j.carbpol.2013.10.029>
- Sandri, G., Bonferoni, M.C., Rossi, S., Ferrari, F., Aguzzi, C., Viseras, C., Caramella, C., 2016. Clay minerals for tissue regeneration, repair, and engineering, in: Ågren, M.S. (Ed.), *Wound Healing Biomaterials*. Elsevier, pp. 385–402. <https://doi.org/10.1016/B978-1-78242-456-7.00019-2>
- Sandri, G., Faccendini, A., Longo, M., Ruggeri, M., Rossi, S., Bonferoni, M.C., Miele, D., Prina-Mello, A., Aguzzi, C., Viseras, C., Ferrari, F., 2020. Halloysite-and montmorillonite-loaded scaffolds as enhancers of chronic wound healing. *Pharmaceutics* 12. <https://doi.org/10.3390/pharmaceutics12020179>
- Santos, S.C.R., Boaventura, R.A.R., 2016. Adsorption of cationic and anionic azo dyes on sepiolite clay: Equilibrium and kinetic studies in batch mode. *J. Environ. Chem. Eng.* 4, 1473–1483. <https://doi.org/10.1016/J.JECE.2016.02.009>
- Sarsour, E.H., Venkataraman, S., Kalen, A.L., Oberley, L.W., Goswami, P.C., 2008. Manganese superoxide dismutase activity regulates transitions between quiescent and proliferative growth. *Aging Cell* 7, 405–417. <https://doi.org/10.1111/j.1474-9726.2008.00384.x>
- Sasaki, Y., Sathi, G.A., Yamamoto, O., 2017. Wound healing effect of bioactive ion released from Mg-smectite. *Mater. Sci. Eng. C. Mater. Biol. Appl.* 77, 52–57. <https://doi.org/10.1016/j.msec.2017.03.236>
- Schaumlöffel, D., 2012. Nickel species: Analysis and toxic effects. *J. Trace Elem. Med. Biol.* 26, 1–6. <https://doi.org/10.1016/j.jtemb.2012.01.002>
- Schempp, C.M., Dittmar, H.C., Hummler, D., Simon-Haarhaus, B., Schulte-Mönting, Jürgen, Schöpf, E., Simon, J.C., 2000. Magnesium ions inhibit the antigen-presenting function of human epidermal Langerhans cells in vivo and in vitro. Involvement of ATPase, HLA-DR, B7 molecules, and cytokines. *J. Invest. Dermatol.* 115, 680–686. <https://doi.org/10.1046/j.1523-1747.2000.00090.x>
- Schott, H., 1995. *Reologia*, Remington Farmacia. Medica Panamericana, Buenos Aires.
- Scott, H., 1995. *Reología*, in: Gennaro, A.R. (Ed.), Remington Farmacia. Medica Panamericana, Buenos Aires, pp. 426–455.
- Shanmugapriya, K., Kim, H., Saravana, P.S., Chun, B.S., Kang, H.W., 2018. Fabrication of multifunctional chitosan-based nanocomposite film with rapid healing and antibacterial effect for wound management. *Int. J. Biol. Macromol.* 118, 1713–1725. <https://doi.org/10.1016/j.ijbiomac.2018.07.018>
- Shariatmadari, H., 1999. Sorption of Selected Cationic and Neutral Organic Molecules on Palygorskite and Sepiolite. *Clays Clay Miner.* 47, 44–53. <https://doi.org/10.1346/CCMN.1999.0470105>
- Shim, J.H., Lim, J.W., Kim, B.K., Park, S.J., Kim, S.W., Choi, T.H., 2015. KCl mediates K⁺ channel-activated mitogen activated protein kinases signaling in wound healing. *Arch. Plast. Surg.* 42, 11–19. <https://doi.org/10.5999/aps.2015.42.1.11>
- Shirvani, M., Kalbasi, M., Shariatmadari, H., Nourbakhsh, F., Najafi, B., 2006a. Sorption-desorption of cadmium in aqueous palygorskite, sepiolite, and calcite suspensions: Isotherm hysteresis. *Chemosphere* 65, 2178–2184.

- <https://doi.org/10.1016/j.chemosphere.2006.06.002>
- Shirvani, M., Shariatmadari, H., Kalbasi, M., Nourbakhsh, F., Najafi, B., 2006b. Sorption of cadmium on palygorskite, sepiolite and calcite: Equilibria and organic ligand affected kinetics. *Colloids Surfaces A Physicochem. Eng. Asp.* 287, 182–190. <https://doi.org/10.1016/J.COLSURFA.2006.03.052>
- Shuali, U., Yariv, S., Steinberg, M., Vonmoos, M.M., Kahr, G., Rub, A., 1988. Thermal analysis study of the adsorption of D2O by sepiolite and palygorskite. *Thermochim. Acta* 135, 291–297. [https://doi.org/10.1016/0040-6031\(88\)87400-8](https://doi.org/10.1016/0040-6031(88)87400-8)
- Sieghart, D., Liszt, M., Wanivenhaus, A., Bröll, H., Kiener, H., Klösch, B., Steiner, G., 2015. Hydrogen sulphide decreases IL-1 β -induced activation of fibroblast-like synoviocytes from patients with osteoarthritis. *J. Cell. Mol. Med.* 19, 187–197. <https://doi.org/10.1111/jcmm.12405>
- Simonton, T.C., Komarneni, S., Roy, R., 1988. Gelling properties of sepiolite versus montmorillonite. *Appl. Clay Sci.* 3, 165–176. [https://doi.org/10.1016/0169-1317\(88\)90016-6](https://doi.org/10.1016/0169-1317(88)90016-6)
- Song, H., Kim, T., Kang, S., Jin, H., Lee, K., Yoon, H.J., 2019. Ga-Based Liquid Metal Micro/Nanoparticles: Recent Advances and Applications. *Small*. <https://doi.org/10.1002/sml.201903391>
- Spriano, S., Sarath Chandra, V., Cochis, A., Uberti, F., Rimondini, L., Bertone, E., Vitale, A., Scolaro, C., Ferrari, M., Cirisano, F., Gautier di Confienzo, G., Ferraris, S., 2017. How do wettability, zeta potential and hydroxylation degree affect the biological response of biomaterials? *Mater. Sci. Eng. C* 74, 542–555. <https://doi.org/10.1016/j.msec.2016.12.107>
- Staffieri, A., Marino, F., Staffieri, C., Giacomelli, L., D'Alessandro, E., Maria Ferraro, S., Fedrazzoni, U., Marioni, G., 2008. The effects of sulfurous-arsenical-ferruginous thermal water nasal irrigation in wound healing after functional endoscopic sinus surgery for chronic rhinosinusitis: a prospective randomized study. *Am. J. Otolaryngol.* 29, 223–229. <https://doi.org/10.1016/J.AMJOTO.2007.07.002>
- Su, Y., Liao, J.L., Wang, F., 2010. Effect of Orient House-Chuen, a concentrate of deep underground mineral spring water, on proliferation and tyrosinase activity of melanocytes. *Chinese J. Biol.* 23, 964–966.
- Suárez, M., García-Romero, E., 2006. FTIR spectroscopic study of palygorskite: Influence of the composition of the octahedral sheet. *Appl. Clay Sci.* 31, 154–163. <https://doi.org/10.1016/j.clay.2005.10.005>
- Sukenik, S., Flusser, D., Codish, S., Abu-Shakra, M., 1999. Balneotherapy at the Dead Sea area for knee osteoarthritis. *Isr. Med. Assoc. J.* 1, 83–5.
- Sun, W., Selim, H.M., 2018. Kinetics of Molybdenum Adsorption and Desorption in Soils. *J. Environ. Qual.* 47, 504–512. <https://doi.org/10.2134/jeq2018.01.0013>
- Tabei, Y., Sonoda, A., Nakajima, Y., Biju, V., Makita, Y., Yoshida, Y., Horie, M., 2015. In vitro evaluation of the cellular effect of indium tin oxide nanoparticles using the human lung adenocarcinoma A549 cells. *Metallomics* 7, 816–827. <https://doi.org/10.1039/c5mt00031a>

4.5. Abbreviations

- Takeuchi, K. ichiro, Ishihara, M., Kawaura, C., Noji, M., Furuno, T., Nakanishi, M., 1996. Effect of zeta potential of cationic liposomes containing cationic cholesterol derivatives on gene transfection. *FEBS Lett.* 397, 207–209. [https://doi.org/10.1016/S0014-5793\(96\)01136-2](https://doi.org/10.1016/S0014-5793(96)01136-2)
- Tateo, F., Ravaglioli, A., Andreoli, C., Bonina, F., Coiro, V., Degetto, S., Giaretta, A., Menconi Orsini, A., Puglia, C., Summa, V., 2009. The in-vitro percutaneous migration of chemical elements from a thermal mud for healing use. *Appl. Clay Sci.* 44, 83–94. <https://doi.org/10.1016/j.clay.2009.02.004>
- Tenaud, I., Leroy, S., Chebassier, N., Dreno, B., 2000. Zinc, copper and manganese enhanced keratinocyte migration through a functional modulation of keratinocyte integrins. *Exp. Dermatol.* 9, 407–416. <https://doi.org/10.1034/j.1600-0625.2000.009006407.x>
- Tenci, M., Rossi, S., Aguzzi, C., Carazo, E., Sandri, G., Bonferoni, M.C., Grisoli, P., Viseras, C., Caramella, C.M., Ferrari, F., 2017. Carvacrol/clay hybrids loaded into in situ gelling films. *Int. J. Pharm.* 531, 676–688. <https://doi.org/10.1016/J.IJPHARM.2017.06.024>
- Toledano-Magaña, Y., Flores-Santos, L., Montes de Oca, G., González-Montiel, A., Laclette, J.-P., Carrero, J.-C., 2015. Effect of Clinoptilolite and Sepiolite Nanoclays on Human and Parasitic Highly Phagocytic Cells. *Biomed Res. Int.* 2015. <https://doi.org/10.1155/2015/164980>
- Tõnsuaadu, K., Gross, K.A., Plüduma, L., Veiderma, M., 2012. A review on the thermal stability of calcium apatites. *J. Therm. Anal. Calorim.* 110, 647–659. <https://doi.org/10.1007/s10973-011-1877-y>
- Tucovic, D., Popov Aleksandrov, A., Mirkov, I., Ninkov, M., Kulas, J., Zolotarevski, L., Vukojevic, V., Mutic, J., Tatalovic, N., Kataranovski, M., 2018. Oral cadmium exposure affects skin immune reactivity in rats. *Ecotoxicol. Environ. Saf.* 164, 12–20. <https://doi.org/10.1016/J.ECOENV.2018.07.117>
- Ul-Islam, M., Khan, T., Khattak, W.A., Park, J.K., 2013. Bacterial cellulose-MMTs nanoreinforced composite films: Novel wound dressing material with antibacterial properties. *Cellulose* 20, 589–596. <https://doi.org/10.1007/s10570-012-9849-3>
- UnitedStatesCode, 2006. Federal Food, Drug, and Cosmetic Act [WWW Document]. URL <https://uscode.house.gov/browse/prelim@title21/chapter9/subchapter2&edition=prelim> (accessed 11.22.19).
- US EPA, O. of W., 2001. Technical Fact Sheet: Final Rule for Arsenic in Drinking Water. United States.
- USP42-NF37, 2019. United States Pharmacopeia and National Formulary. United States Pharmacopeial Convention, Rockville, MD.
- Vaiana, C.A., Leonard, M.K., Drummy, L.F., Singh, K.M., Bubulya, A., Vaia, R.A., Naik, R.R., Kadakia, M.P., 2011. Epidermal growth factor: Layered silicate nanocomposites for tissue regeneration. *Biomacromolecules* 12, 3139–3146. <https://doi.org/10.1021/bm200616v>

- Vengris, T., Binkiene, R., Sveikauskaite, A., 2001. Nickel, copper and zinc removal from waste water by a modified clay sorbent. *Appl. Clay Sci.* 18, 183–190. [https://doi.org/10.1016/S0169-1317\(00\)00036-3](https://doi.org/10.1016/S0169-1317(00)00036-3)
- Veniale, F., Barberis, E., Carcangiu, G., Morandi, N., Setti, M., Tamanini, M., Tessier, D., 2004. Formulation of muds for pelotherapy: Effects of “maturation” by different mineral waters. *Appl. Clay Sci.* 25, 135–148. <https://doi.org/10.1016/j.clay.2003.10.002>
- Veniale, F., Bettero, A., Jobstrainbizer, P., Setti, M., 2007. Thermal muds: Perspectives of innovations. *Appl. Clay Sci.* 36, 141–147. <https://doi.org/10.1016/j.clay.2006.04.013>
- Vergaro, V., Abdullayev, E., Lvov, Y.M., Zeitoun, A., Cingolani, R., Rinaldi, R., Leporatti, S., 2010. Cytocompatibility and uptake of halloysite clay nanotubes. *Biomacromolecules* 11, 820–826. <https://doi.org/10.1021/bm9014446>
- Viseras, C., Aguzzi, C., Cerezo, P., López-Galindo, A., 2007. Uses of clay minerals in semisolid health care and therapeutic products. *Appl. Clay Sci.* 36, 37–50. <https://doi.org/10.1016/j.clay.2006.07.006>
- Viseras, C., Carazo, E., Borrego-Sánchez, A., García-Villén, F., Sánchez-Espejo, R., Cerezo, P., Aguzzi, C., 2019. Clay minerals in skin drug delivery. *Clays Clay Miner.* 67, 59–71. <https://doi.org/10.1007/s42860-018-0003-7>
- Viseras, C., Cerezo, P., 2006. Aplicación de peloides y fangos termales, in: Hernández-Torres, A., Alcázar-Alcázar, R. (Eds.), *Técnicas y Tecnologías En Hidrología Médica e Hidroterapia*. Agencia de Evaluación de Tecnologías Sanitarias - Instituto de Salud Carlos III - Ministerio de Sanidad y Consumo, Madrid, pp. 141–146.
- Viseras, C., López-Galindo, A., 1999. Pharmaceutical applications of some spanish clays (sepiolite, palygorskite, bentonite): some preformulation studies. *Appl. Clay Sci.* 14, 69–82. [https://doi.org/10.1016/S0169-1317\(98\)00050-7](https://doi.org/10.1016/S0169-1317(98)00050-7)
- Viseras, C., Lopez-Galindo, A., Yebra, A., 2000. Characteristics of pharmaceutical grade phyllosilicate compacts. *Pharm Dev Technol* 5, 53–58.
- Viseras, C., Meeten, G.H., Lopez-Galindo, A., 1999. Pharmaceutical grade phyllosilicate dispersions: The influence of shear history on floc structure. *Int. J. Pharm.* 182, 7–20. [https://doi.org/10.1016/S0378-5173\(99\)00075-7](https://doi.org/10.1016/S0378-5173(99)00075-7)
- Wang, X., Du, Y., Luo, J., 2008. Biopolymer/montmorillonite nanocomposite: Preparation, drug-controlled release property and cytotoxicity. *Nanotechnology* 19. <https://doi.org/10.1088/0957-4484/19/6/065707>
- Wang, X., Wang, A., 2010. Removal of Cd(II) from aqueous solution by a composite hydrogel based on attapulgite. *Environ. Technol.* 31, 745–753. <https://doi.org/10.1080/09593330903514490>
- Wang, Z., Zhao, Y., Luo, Y., Wang, S., Shen, M., Tomás, H., Zhu, M., Shi, X., 2015. Attapulgite-doped electrospun poly(lactic-co-glycolic acid) nanofibers enable enhanced osteogenic differentiation of human mesenchymal stem cells. *RSC Adv.* 5, 2383–2391. <https://doi.org/10.1039/c4ra09839k>
- Wester, R.C., Maibach, H.I., Sedik, L., Melendres, J., DiZio, S., Wade, M., 1992. In vitro

4.5. Abbreviations

- percutaneous absorption of cadmium from water and soil into human skin. *Fundam. Appl. Toxicol.* 19, 1–5.
- WHO, 2017. *Guidelines for Drinking-water Quality*, 4th editio. ed.
- WHO, 1996. Trace elements in human nutrition and health World Health Organization. World Heal. Organ. Geneva 1-360. <https://doi.org/10.1586/14760584.2015.1081067>
- Williams, L.B., Haydel, S.E., Giese Jr., R.F., Eberl, D.D., 2008. Chemical and mineralogical characteristics of French Green clays used for healing. *Clays Clay Miner.* 56, 437–452. <https://doi.org/10.1346/CCMN.2008.0560405>
- Wlaschek, M., Singh, K., Sindrilaru, A., Crisan, D., Scharffetter-Kochanek, K., 2019. Iron and iron-dependent reactive oxygen species in the regulation of macrophages and fibroblasts in non-healing chronic wounds. *Free Radic. Biol. Med.* 133, 262–275. <https://doi.org/10.1016/J.FREERADBIOMED.2018.09.036>
- Xu, J., Wang, A., 2012. Electrokinetic and colloidal properties of homogenized and unhomogenized palygorskite in the presence of electrolytes. *J. Chem. Eng. Data* 57, 1586–1593. <https://doi.org/10.1021/je300213u>
- Xu, Z., Chen, X., Tan, R., She, Z., Chen, Z., Xia, Z., 2019. Preparation and characterization of a gallium-loaded antimicrobial artificial dermal scaffold. *Mater. Sci. Eng. C* 105, 110063. <https://doi.org/10.1016/j.msec.2019.110063>
- Yang, G., Zhang, M., Qi, B., Zhu, Z., Yao, J., Yuan, X., Sun, D., 2018. Nanoparticle-Based Strategies and Approaches for the Treatment of Chronic Wounds. *J. Biomater. Tissue Eng.* 8, 455–464. <https://doi.org/10.1166/jbt.2018.1776>
- Young, M., Ozcan, A., Lee, B., Maxwell, T., Andl, T., Rajasekaran, P., Beazley, M.J., Tetard, L., Santra, S., 2019. N-acetyl cysteine coated gallium particles demonstrate high potency against *Pseudomonas aeruginosa* PAO1. *Pathogens* 8. <https://doi.org/10.3390/pathogens8030120>
- Yuan, J., Hou, Q., Chen, D., Zhong, L., Dai, X., Zhu, Z., Li, M., Fu, X., 2019. Chitosan/LiCl composite scaffolds promote skin regeneration in full-thickness loss. *Sci. China Life Sci.* <https://doi.org/10.1007/s11427-018-9389-6>
- Zeng, H.F., Lin, L.J., Xi, Y.M., Han, Z.Y., 2017. Effects of raw and heated palygorskite on rumen fermentation in vitro. *Appl. Clay Sci.* 138, 125–130. <https://doi.org/10.1016/J.CLAY.2017.01.006>
- Zhang, J., Jin, Y., Wang, A., 2011. Rapid removal of Pb(II) from aqueous solution by chitosan-g-poly(acrylic acid)/attapulgit/sodium humate composite hydrogels. *Environ. Technol.* 32, 523–531. <https://doi.org/10.1080/09593330.2010.504748>
- Zhang, L.L., Du, J.B., Tang, C.S., Jin, H.F., Huang, Y.Q., 2018. Inhibitory effects of sulfur dioxide on rat myocardial fibroblast proliferation and migration. *Chin. Med. J. (Engl)*. 131, 1715–1723. <https://doi.org/10.4103/0366-6999.235875>
- Zhang, Y., Yang, M., Portney, N.G., Cui, D., Budak, G., Ozbay, E., Ozkan, M., Ozkan, C.S., 2008. Zeta potential: A surface electrical characteristic to probe the interaction of nanoparticles with normal and cancer human breast epithelial cells. *Biomed. Microdevices* 10, 321–328. <https://doi.org/10.1007/s10544-007-9139-2>

Chapter 4. References

Zulaikha, S., Syed Ismail, S.N., Praveena, S.M., 2015. Hazardous ingredients in cosmetics and personal care products and health concern: A review. *Public Heal. Res.* 5, 7–15. <https://doi.org/10.5923/j.phr.20150501.02>

Chapter 5

Conclusiones

La presente tesis doctoral planteaba como objetivo principal el diseño y desarrollo de hidrogeles inorgánicos de empleo en la curación de heridas. La fase sólida de las formulaciones eran filosilicatos fibrosos (sepiolita y palygorskita) y la fase líquida, agua mineromedicinal.

Para alcanzar dicho objetivo general se plantearon una lista de objetivos específicos que incluían:

- la puesta punto de métodos de caracterización de hidrogeles naturales similares a los que se pretendía formular.
- la puesta a punto de metodologías *in vitro* capaces de informar de la eficacia en la curación de heridas de un sistema.

El cumplimiento de estos dos primeros objetivos dio lugar a dos publicaciones en las que se sentaron las bases de conocimiento experimental aplicado en estudios posteriores de la tesis doctoral. Concretamente, un primer artículo en el que se caracterizaron muestras complejas naturales con arcillas y materia orgánica de interés terapéutico y un segundo artículo en el que se estudió un sistema de liberación modificada basado en una arcilla laminar. En estos dos trabajos se puso de manifiesto que:

- 1) Resulta imprescindible determinar de forma precisa la identidad, pureza y riqueza de los componentes empleados a efectos de asegurar la calidad de las formulaciones. En el caso de los materiales mesoporosos empleados en esta tesis, esta caracterización requiere metodologías específicas, incluyendo difracción y fluorescencia de rayos X.
- 2) Cuando los sistemas son termodinámicamente inestables, como es el caso de sistemas dispersos de tipo hidrogel, resulta necesario establecer la estabilidad física mediante estudios reológicos.
- 3) Los sistemas de empleo en la curación de heridas requieren de estudios específicos destinados a conocer su eficacia, asociada a la capacidad del excipiente inorgánico de modificar la liberación de los componentes activos y seguridad (biocompatibilidad dérmica).

Alcanzados estos dos objetivos transversales, se diseñaron hidrogeles con arcillas de elevada pureza y agua mineromedicinal. El estudio de estos sistemas permitió cumplir con el resto de objetivos de la tesis, incluyendo:

- El establecimiento de las propiedades fisicoquímicas, geodisponibilidad y contenido inorgánico relacionado con los efectos terapéuticos (eficacia) o perjudiciales (seguridad) de los hidrogeles, a partir de la composición y geoquímica original de los componentes.
- la determinación de la liberación y la movilidad (penetración y permeabilidad) *in vitro* de los elementos con interés terapéutico (eficacia) o perjudiciales (seguridad).
- la evaluación de la biocompatibilidad *in vitro* de los ingredientes por separado y de las correspondientes formulaciones para su uso en el tratamiento de la curación de heridas, incluyendo la evaluación de la eficacia terapéutica *in vitro*.

Los resultados obtenidos en esta fase del trabajo de tesis doctoral dieron lugar a cuatro artículos en los que se pudo concluir lo siguiente:

- 4) Los dos excipientes minerales usados (PS9 y G30) son de elevada pureza en el componente principal (sepiolita y palygorskita).
- 5) PS9 se corresponde con la monografía "Magnesium silicate" o "Magnesium trisilicate" (USP 42-37, 2019; Ph. Eur. 9th, 2018b).
- 6) G30 se corresponde con la monografía "Attapulgit" (USP42-NF37, 2019; Ph. Eur. 9th, 2018a).
- 7) Las velocidades de enfriamiento de los hidrogeles preparados con estos dos excipientes (10% m/m) eran adecuados para su empleo en terapéutica termal.
- 8) PS9 era más efectiva que G30 en la formación de sistemas hidrogel, alcanzando valores de los parámetros reológicos similares a concentraciones sensiblemente menores.
- 9) La estabilidad física de los hidrogeles permitía su empleo durante al menos dos meses desde su elaboración.

Conclusiones

- 10) Tanto los excipientes como los hidrogeles eran biocompatibles de acuerdo con los ensayos realizados con fibroblastos.
- 11) Los hidrogeles favorecían la curación *in vitro* de heridas sin interferir con la morfología de los fibroblastos.
- 12) Los excipientes sin formular retardan la curación de heridas, posiblemente debido a la presencia de partículas no floculadas en el medio.
- 13) Cuando los excipientes se dispersan formando un hidrogel la curación se ve favorecida.
- 14) La liberación y movilidad de los elementos presentes en los hidrogeles, estudiada empleando celdas de Franz y técnicas de espectroscopia de plasma inductivo demostró que los sistemas son seguros.
- 15) La presencia en el hidrogel de un determinado elemento en concentración elevada no implica necesariamente su liberación.
- 16) La liberación elevada de un elemento desde el hidrogel tampoco es necesariamente la razón de la eficacia terapéutica.
- 17) La eficacia en la curación de heridas esta relacionada con las proporciones relativas de ciertos elementos liberados desde los hidrogeles.
- 18) Las formulaciones de estos sistemas deben ajustarse para optimizar los efectos terapéuticos que serán resultado de la interacción y sinergia entre la fase líquida y sólida del hidrogel y de la movilidad relativa de determinados elementos.

Conclusiones



Anexo A

Material adicional del Capítulo 4

Figura

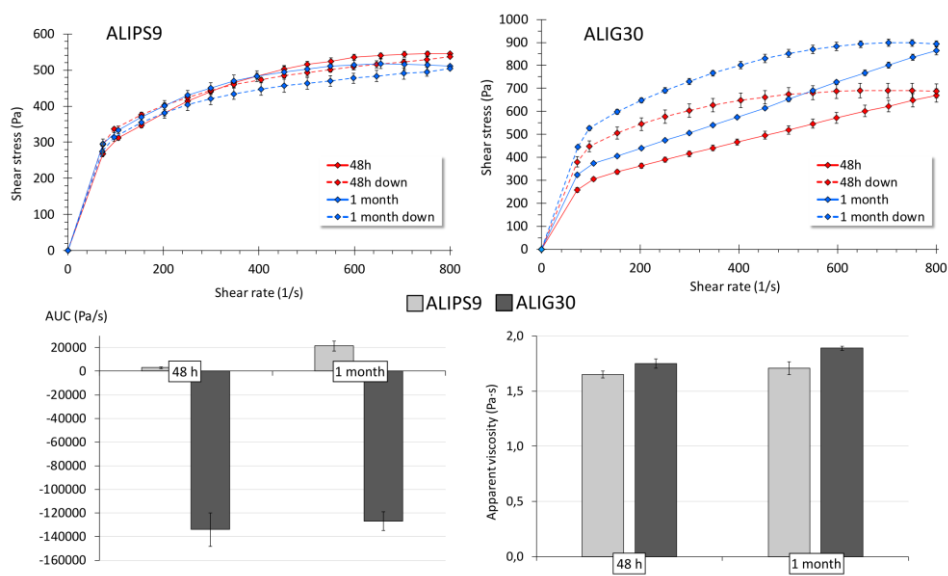


Figure A.1. Rheological characterization of ALIPS9 and ALIG30@20 hydrogels after 48 h and 1 month. Up: flow curves (from 70 to 800 s⁻¹, mean values ± s.d., n = 6). Down: hysteresis areas (mean values ± s.d., n = 6) and apparent viscosities (250 s⁻¹, mean values ± s.d., n = 6). Positive AUC values indicates thixotropic behaviour, while negative ones correspond to anti-thixotropic profile.

Tabla

Table A.1. Amount of mobile elements released from the corresponding hydrogels into fibroblast cultures (MTT well-plate). Results were calculated from Franz experiments at 1 month and expressed in nanograms. NM stands for “Not Released”.

Hydrogel	Element (ng)	Amount of hydrogel in cell wells during MTT test			
		1000 µg/mL	500 µg/mL	50 µg/mL	5 µg/mL
ALIPS9	Al	2.25	1.13	0.11	0.01
	B	0.79	0.39	0.04	0.004
	Ca	161.5	80.7	8.08	0.81
	K	55.3	27.6	2.76	0.28
	Mg	73.8	36.9	3.69	0.37
	Na	125.7	62.8	6.28	0.63
	S	109.4	54.7	5.47	0.55
	Fe	1.46	0.73	0.07	0.01
	Sr	2.97	1.49	0.15	0.01
	Zn	3.32	1.66	0.17	0.02
	Mn	0.01	0.01	0.0007	0.0001
Cu	0.07	0.04	0.0036	0.0004	
ALIG30@10	Al	11.6	5.78	0.58	0.06
	B	NR	NR	NR	NR
	Ca	608.3	304.1	30.41	3.04
	K	38.3	19.1	1.91	0.19
	Mg	103.1	51.6	5.16	0.52
	Na	210.7	105.3	10.53	1.05
	S	234.0	117.0	11.70	1.17
	Fe	0.42	0.21	0.02	0.002
	Sr	1.32	0.66	0.07	0.01
	Zn	2.83	1.41	0.14	0.01
	Mn	NR	NR	NR	NR
Cu	0.036	0.018	0.002	0.0002	
ALIG30@20	Al	6.72	3.36	0.34	0.03
	B	0.001	5·10 ⁴	5·10 ⁻⁵	5·10 ⁻⁶
	Ca	165.2	82.6	8.26	0.83
	K	25.9	12.9	1.29	0.13
	Mg	29.7	14.8	1.48	0.15
	Na	84.8	42.4	4.24	0.42
	S	79.4	39.7	3.97	0.4
	Fe	0.09	0.04	4.4·10 ⁻³	4.4·10 ⁻⁴
	Sr	0.69	0.34	0.03	0.003
	Zn	1.75	0.88	0.09	0.01
	Mn	0.07	0.04	0.0004	3.7·10 ⁻⁴
Cu	0.01	0.005	4.6·10 ⁻⁴	4.6·10 ⁻⁵	

Anexo B

Indicios de Calidad de las Publicaciones

B.1. Indicios de calidad de las publicaciones que componen el documento de Tesis Doctoral

B.1.1. Capítulo 1

García-Villén, F., Carazo, E., Borrego-Sánchez, A., Sánchez-Espejo, R., Cerezo, P., Viseras, C., Aguzzi, C. **Clay minerals in drug delivery systems**. In: Modified Clay and Zeolite Nanocomposite Materials; Mercurio, M., Sarkar, B., Langella, A., Eds.; Elsevier Inc., 2019 ISBN 978-0-12-814617-0.

Indicios de calidad de la publicación:

- Capítulo de libro - Elsevier
- Scholarly publishers indicators (general SPI): Q1. ICEE = 319 (2018).

Viseras, C., Carazo, E., Borrego-Sánchez, A., García-Villén, F., Sánchez-Espejo, R., Cerezo, P., Aguzzi, C. **Clay minerals in skin drug delivery**. Clays Clay Minerals, 2019, 67, 59–71.

Indicios de calidad de la publicación:

- Artículo científico
- Indexada en JCR: [CLAY CLAY MINER](#)
- Factor de impacto 2019: 1.507
- Ranking: Q3 (geosciences, multidisciplinary).

García-Villén, F., Souza, I.M.S., de Melo Barbosa, R., Borrego-Sánchez, A., Sánchez-Espejo, R., Ojeda-Riascos, S., Viseras, C. **Natural inorganic ingredients in wound healing**. Current Pharmaceutical Design, 2020, 26.

Indicios de calidad de la publicación:

- Artículo científico
- Indexada en JCR: [CURR PHARM DESIGN](#)
- Factor de impacto 2019: 2.208
- Ranking: Q3 (pharmacology & pharmacy).

B.1.2. Capítulo 2

García-Villén, F., Sánchez-Espejo, R., Carazo, E., Borrego-Sánchez, A., Aguzzi, C., Cerezo, P., Viseras, C. **Characterisation of Andalusian peats for skin health care formulations**. Applied Clay Science, 2018, 160, 201–205.

Indicios de calidad de la publicación:

- Artículo científico
- Indexada en JCR: [APPL CLAY SCI](#)
- Factor de impacto 2019: 4.605
- Ranking: Q1 (mineralogy).

García-Villén, F., Faccendini, A., Aguzzi, C., Cerezo, P., Bonferoni, M.C., Rossi, S., Grisoli, P., Ruggeri, M., Ferrari, F., Sandri, G.; et al. **Montmorillonite-norfloxacin nanocomposite intended for healing of infected wounds**. *International Journal of Nanomedicine*, 2019, 14, 5051–5060.

Indicios de calidad de la publicación:

- Artículo científico
- Indexada en JCR: [INT J NANOMED](#)
- Factor de impacto 2019: 5.115
- Ranking: Q1 (pharmacology & pharmacy).

B.1.3. Capítulo 4

García-Villén, F., Sánchez-Espejo, R., López-Galindo, A., Cerezo, P., Viseras, C. (2020). **Design and characterization of spring water hydrogels with natural inorganic excipients**. *Applied Clay Science*, 197, 105772.

Indicios de calidad de la publicación:

- Artículo científico
- Indexada en JCR: [APPL CLAY SCI](#)
- Factor de impacto 2019: 4.605
- Ranking: Q1 (mineralogy).

García-Villén, F., Faccendini, A., Miele, D., Ruggeri, M., Sánchez-Espejo, R., Borrego-Sánchez, A., Cerezo, P., Rossi, S., Viseras, C., Sandri, G. (2020). **Wound healing activity of nanoclay/spring water hydrogels**. *Pharmaceutics*, 12(467), 1-24.

Indicios de calidad de la publicación:

- Artículo científico
- Indexada en JCR: [PHARMACEUTICS](#)
- Factor de impacto 2019: 4.421

- Ranking: Q1 (pharmacology & pharmacy).

García-Villén, F., Sánchez-Espejo, R., Borrego-Sánchez, A., Cerezo, P., Perioli, L., Viseras, César (2020). **Safety of nanoclay/spring water hydrogels: assessment and mobility of hazardous elements.** *Pharmaceutics*, 12(764), 1-17.

Indicios de calidad de la publicación:

- Artículo científico
- Indexada en JCR: [PHARMACEUTICS](#)
- Factor de impacto 2019: 4.421
- Ranking: Q1 (pharmacology & pharmacy).

García-Villén, F., Sánchez-Espejo, R., Borrego-Sánchez, A., Cerezo, P., Cucca, L, Giuseppina S., Viseras, C. (2020). **Correlation between elemental composition/mobility and skin cell proliferation of fibrous nanoclay/spring water hydrogels.** *Pharmaceutics*, 12(891), 1-20.

Indicios de calidad de la publicación:

- Artículo científico
- Indexada en JCR: [PHARMACEUTICS](#)
- Factor de impacto 2019: 4.421
- Ranking: Q1 (pharmacology & pharmacy).

ACEPTACIONES Y RENUNCIAS TRABAJO 1



UNIVERSIDAD
DE GRANADA

Escuela
Internacional
de Posgrado

ACEPTACION Y RENUNCIA DE LOS COAUTORES DE LA PUBLICACION

Publicación: **Clay minerals in drug delivery systems**. En: Modified Clay and Zeolite Nanocomposite Materials: Environmental and Pharmaceutical Applications. 2018, 129-166. DOI: 10.1016/B978-0-12-814617-0.00010-4

Los coautores:

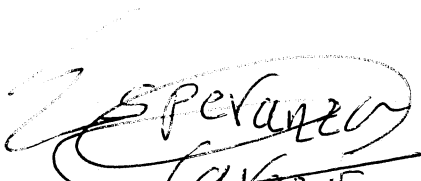
D/D ^a .	Esperanza Carazo
D/D ^a .	Ana Borrego Sánchez
D/D ^a .	Rita Sánchez Espejo
D/D ^a .	Pilar Cerezo González
D/D ^a .	César Viseras
D/D ^a .	Carola Aguzzi


declaran que:


ACEPTAN y AUTORIZAN la utilización de dicha publicación/artículo como parte de la documentación de depósito y defensa de la tesis doctoral de D./D^a. Fátima García Villén titulada **Aplicaciones Farmacéuticas de aluminosilicatos mesoporosos: estudio de arcillas fibrosas (sepiolita y palygorskita) en geles con agua mineromedicinal,**


NO HAN UTILIZADO dicha publicación/artículo como parte de la documentación de depósito y defensa de otra tesis doctoral y/ o RENUNCIAN a utilizarlo en una futura tesis doctoral.


En Granada, a 03 de noviembre de 2020


Fdo.: *Carazo*


Fdo.:


Fdo.:


Fdo.:


Fdo.: *César Viseras*


Fdo.:

ACEPTACIONES Y RENUNCIAS TRABAJO 2



UNIVERSIDAD
DE GRANADA

Escuela
Internacional
de Posgrado

ACEPTACION Y RENUNCIA DE LOS COAUTORES DE LA PUBLICACION

Publicación: **Clay minerals in skin drug delivery**. Clays and Clay Minerals, 67, 1, 59-71, 2019. DOI: 10.1007/s42860-018-0003-7

Los coautores:

D/D ^a .	César Viseras
D/D ^a .	Esperanza Carazo
D/D ^a .	Ana Borrego Sánchez
D/D ^a .	Rita Sánchez Espejo
D/D ^a .	Pilar Cerezo González
D/D ^a .	Carola Aguzzi

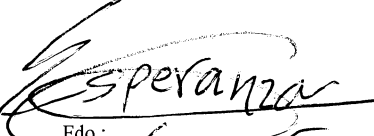
declaran que:

ACEPTAN y AUTORIZAN la utilización de dicha publicación/artículo como parte de la documentación de depósito y defensa de la tesis doctoral de D/D^a. Fátima García Villén titulada **Aplicaciones Farmacéuticas de aluminosilicatos mesoporosos: estudio de arcillas fibrosas (sepiolita y palygorskita) en geles con agua mineromedicinal,**

NO HAN UTILIZADO dicha publicación/artículo como parte de la documentación de depósito y defensa de otra tesis doctoral y/ o RENUNCIAN a utilizarlo en una futura tesis doctoral.


En Granada, a 03 de noviembre de 2020


Fdo.: César Viseras


Fdo.: Esperanza Carazo


Fdo.: Ana Borrego Sánchez


Fdo.: Rita Sánchez Espejo


Fdo.: Pilar Cerezo González


Fdo.: Carola Aguzzi

ACEPTACIONES Y RENUNCIAS TRABAJO 3



UNIVERSIDAD
DE GRANADA

Escuela
Internacional
de Posgrado

ACEPTACION Y RENUNCIA DE LOS COAUTORES DE LA PUBLICACION

Publicación: **Natural inorganic ingredients in wound healing**. Current Pharmaceutical Design 26, 6, 621-641, 2020. DOI: 10.2174/1381612826666200113162114

Los coautores:

D/D ^a .	Iane M.S. Souza
D/D ^a .	Raquel de Melo Barbosa
D/D ^a .	Ana Borrego Sánchez
D/D ^a .	Rita Sánchez Espejo
D/D ^a .	Santiago Ojeda Riascos
D/D ^a .	César Viseras

declaran que:

ACEPTAN y AUTORIZAN la utilización de dicha publicación/artículo como parte de la documentación de depósito y defensa de la tesis doctoral de D./D^a. Fátima García Villén titulada **Aplicaciones Farmacéuticas de aluminosilicatos mesoporosos: estudio de arcillas fibrosas (sepiolita y palygorskita) en geles con agua mineromedicinal,**

NO HAN UTILIZADO dicha publicación/artículo como parte de la documentación de depósito y defensa de otra tesis doctoral y/ o RENUNCIAN a utilizarlo en una futura tesis doctoral.

En Granada, a 03 de noviembre de 2020

Fdo.:

Fdo.:

Fdo.:

Fdo.:

Fdo.:

Fdo.:

ACEPTACIONES Y RENUNCIAS TRABAJO 4



UNIVERSIDAD
DE GRANADA

Escuela
Internacional
de Posgrado

ACEPTACION Y RENUNCIA DE LOS COAUTORES DE LA PUBLICACION

Publicación: **Characterisation of Andalusian peats for skin health care formulations**. Applied Clay Science, 160, 201-205, 2018. DOI: 10.1016/j.clay.2017.12.017

Los coautores:

D/D ^a .	Rita Sánchez Espejo
D/D ^a .	Esperanza Carazo
D/D ^a .	Ana Borrego Sánchez
D/D ^a .	Carola Aguzzi
D/D ^a .	Pilar Cerezo González
D/D ^a .	César Viseras

declaran que:

ACEPTAN y AUTORIZAN la utilización de dicha publicación/artículo como parte de la documentación de depósito y defensa de la tesis doctoral de D./D^a. Fátima García Villén titulada **Aplicaciones Farmacéuticas de aluminosilicatos mesoporosos: estudio de arcillas fibrosas (sepiolita y palygorskita) en geles con agua mineromedicinal,**

NO HAN UTILIZADO dicha publicación/artículo como parte de la documentación de depósito y defensa de otra tesis doctoral y/ o RENUNCIAN a utilizarlo en una futura tesis doctoral.

En Granada, a 03 de noviembre de 2020

Fdo.:

Fdo.:

Fdo.:

Fdo.:

Fdo.:

Fdo.:

ACEPTACIONES Y RENUNCIAS TRABAJO 5



UNIVERSIDAD
DE GRANADA

Escuela
Internacional
de Posgrado

ACEPTACION Y RENUNCIA DE LOS COAUTORES DE LA PUBLICACION

Publicación: **Montmorillonite-norfloxacina nanocomposite intended for healing of infected wounds.**
International Journal of Nanomedicine, 14, 5051-5060, 2019. DOI: 10.2147/IJN.S208713

Los coautores:

D/D ^a .	Carola Aguzzi
D/D ^a .	Pilar Cerezo González
D/D ^a .	César Viseras


declaran que:


ACEPTAN y AUTORIZAN la utilización de dicha publicación/artículo como parte de la documentación de depósito y defensa de la tesis doctoral de D./D^a. Fátima García Villén titulada **Aplicaciones Farmacéuticas de aluminosilicatos mesoporosos: estudio de arcillas fibrosas (sepiolita y palygorskita) en geles con agua mineromedicinal,**

NO HAN UTILIZADO dicha publicación/artículo como parte de la documentación de depósito y defensa de otra tesis doctoral y/ o RENUNCIAN a utilizarlo en una futura tesis doctoral.

Universidad

En Granada, a 03 de noviembre de 2020


Fdo.:


Fdo.:


Fdo.: César Viseras

Asunto: R: Artículo Montmorillonite norfloxacin...

De: <g.sandri@unipv.it>

Fecha: 04/11/2020 9:14

Para: 'César Viseras' <cviseras@ugr.es>

Prof. Giuseppina Sandri, PhD
Department of Drug Sciences,
University of Pavia,
Viale Taramelli 12,
27100 Pavia – Italy

Tel 00390382987728
e-mail giuseppina.sandri@unipv.it

AUTHORIZATION AND WITHDRAWAL FROM CO-AUTHORS OF A SCIENTIFIC PUBLICATION SUBMITTED AS PART OF A DOCTORAL THESIS

TO: International School for Postgraduate Studies, University of Granada

Regarding the deposit and defense of the Doctoral Thesis of Ms. Fátima García Villén entitled Aplicaciones Farmacéuticas de aluminosilicatos mesoporosos: estudio de arcillas fibrosas (sepiolita y palygorskita) en geles con agua mineromedicinal (**Pharmaceutical Applications of mesoporous aluminosilicates: study of fibrous clay minerals (sepiolite and palygorskite)** in spring water hydrogels) which contains the publication/article **Montmorillonite-norfloxacin nanocomposite intended for healing of infected wounds. International Journal of Nanomedicine, 14, 5051-5060, 2019. DOI: 10.2147/IJN.S208713**, I declare, as co-author that:

I ACCEPT and AUTHORIZE the use of this publication/article as part of the Doctoral Thesis.

Additionally, I declare that I have NEITHER ACCEPTED NOR AUTHORIZED NOR USED this publication/article as part of the documents of a different Doctoral Thesis at the University of Granada or at any other University. Furthermore, I RESIGN myself to accept/authorize/use it in a future Doctoral Thesis at the University of Granada and or any other University.

Giuseppina Sandri

Department of Drug Sciences, Faculty of Pharmacy, University of Pavia, Pavia, 27100, Italy

Asunto: Re: Artículo Montmorillonite norfloxacin...

De: Silvia Rossi <silviastefania.rossi@unipv.it>

Fecha: 04/11/2020 19:55

Para: César Viseras <cviseras@ugr.es>

AUTHORIZATION AND WITHDRAWAL FROM CO-AUTHORS OF A SCIENTIFIC PUBLICATION
SUBMITTED AS
PART OF A DOCTORAL THESIS

TO: International School for Postgraduate Studies, University of Granada

Regarding the deposit and defense of the Doctoral Thesis of Ms. Fátima García Villén entitled **Aplicaciones Farmacéuticas de aluminosilicatos mesoporosos: estudio de arcillas fibrosas (sepiolita y palygorskita) en geles con agua mineromedicinal (Pharmaceutical Applications of mesoporous aluminosilicates: study of fibrous clay minerals (sepiolite and palygorskite) in spring water hydrogels)** which contains the publication/article **Montmorillonite-norfloxacin nanocomposite intended for healing of infected wounds. International Journal of Nanomedicine, 14, 5051-5060, 2019. DOI: 10.2147/IJN.S208713**, I declare, as co-author that:

I ACCEPT and AUTHORIZE the use of this publication/article as part of the Doctoral Thesis.

Additionally, I declare that I have NEITHER ACCEPTED NOR AUTHORIZED NOR USED this publication/article as part of the documents of a different Doctoral Thesis at the University of Granada or at any other University. Furthermore, I RESIGN myself to accept/authorize/use it in a future Doctoral Thesis at the University of Granada and or any other University.

Silvia Rossi

Department of Drug Sciences, Faculty of Pharmacy, University of Pavia, Pavia, 27100, Italy

Asunto: Re: Artículo Montmorillonite norfloxacin...

De: Pietro Grisoli <pietro.grisoli@unipv.it>

Fecha: 04/11/2020 9:23

Para: César Viseras <cviseras@ugr.es>

AUTHORIZATION AND WITHDRAWAL FROM CO-AUTHORS OF A SCIENTIFIC PUBLICATION SUBMITTED AS PART OF A DOCTORAL THESIS

TO: International School for Postgraduate Studies, University of Granada

Regarding the deposit and defense of the Doctoral Thesis of Ms. Fátima García Villén entitled Aplicaciones Farmacéuticas de aluminosilicatos mesoporosos: estudio de arcillas fibrosas (sepiolita y palygorskita) en geles con agua mineromedicinal (**Pharmaceutical Applications of mesoporous aluminosilicates: study of fibrous clay minerals (sepiolite and palygorskite) in spring water hydrogels**) which contains the publication/article **Montmorillonite-norfloxacin nanocomposite intended for healing of infected wounds. International Journal of Nanomedicine, 14, 5051-5060, 2019. DOI: 10.2147/IJN.S208713**, I declare, as co-author that:

I ACCEPT and AUTHORIZE the use of this publication/article as part of the Doctoral Thesis.

Additionally, I declare that I have NEITHER ACCEPTED NOR AUTHORIZED NOR USED this publication/article as part of the documents of a different Doctoral Thesis at the University of Granada or at any other University. Furthermore, I RESIGN myself to accept/authorize/use it in a future Doctoral Thesis at the University of Granada and or any other University.

PIETRO GRISOLI

Department of Drug Sciences, Faculty of Pharmacy, University of Pavia, Pavia, 27100, Italy

Cordiali saluti
Pietro Grisoli

Professore Aggregato di Microbiologia
Dipartimento di Scienze del Farmaco
Viale Taramelli 14, 27100 Pavia

Asunto: Fwd: Artículo Montmorillonite norfloxacin...

De: MARCO RUGGERI <marco.ruggeri02@universitadipavia.it>

Fecha: 04/11/2020 17:08

Para: cviseras@ugr.es

Buonasera Cesar,

ecco la mia approvazione.

Buona serata, Marco

AUTHORIZATION AND WITHDRAWAL FROM CO-AUTHORS OF A SCIENTIFIC PUBLICATION SUBMITTED AS PART OF A DOCTORAL THESIS

TO: International School for Postgraduate Studies, University of Granada

Regarding the deposit and defense of the Doctoral Thesis of Ms. Fátima García Villén entitled Aplicaciones Farmacéuticas de aluminosilicatos mesoporosos: estudio de arcillas fibrosas (sepiolita y palygorskita) en geles con agua mineromedicinal (**Pharmaceutical Applications of mesoporous aluminosilicates: study of fibrous clay minerals (sepiolite and palygorskite)** in spring water hydrogels) which contains the publication/article **Montmorillonite-norfloxacin nanocomposite intended for healing of infected wounds. International Journal of Nanomedicine, 14, 5051-5060, 2019. DOI: 10.2147/IJN.S208713**, I declare, as co-author that:

I ACCEPT and AUTHORIZE the use of this publication/article as part of the Doctoral Thesis.

Additionally, I declare that I have NEITHER ACCEPTED NOR AUTHORIZED NOR USED this publication/article as part of the documents of a different Doctoral Thesis at the University of Granada or at any other University. Furthermore, I RESIGN myself to accept/authorize/use it in a future Doctoral Thesis at the University of Granada and or any other University.

MARCO RUGGERI

Department of Drug Sciences, Faculty of Pharmacy, University of Pavia, Pavia, 27100, Italy

--

Marco Ruggeri, Ph.D. student
Department of Drug Sciences,
University of Pavia,
V.le Taramelli 12,
27100 Pavia - Italy

Asunto: Re: Artículo Montmorillonite norfloxacin...

De: Ferrari Franca <franca.ferrari@unipv.it>

Fecha: 04/11/2020 15:14

Para: César Viseras <cviseras@ugr.es>

AUTHORIZATION AND WITHDRAWAL FROM CO-AUTHORS OF A SCIENTIFIC PUBLICATION SUBMITTED AS PART OF A DOCTORAL THESIS

TO: International School for Postgraduate Studies, University of Granada

Regarding the deposit and defense of the Doctoral Thesis of Ms. Fátima García Villén entitled Aplicaciones Farmacéuticas de aluminosilicatos mesoporosos: estudio de arcillas fibrosas (sepiolita y palygorskita) en geles con agua mineromedicinal (**Pharmaceutical Applications of mesoporous aluminosilicates: study of fibrous clay minerals (sepiolite and palygorskite)** in spring water hydrogels) which contains the publication/article **Montmorillonite-norfloxacin nanocomposite intended for healing of infected wounds. International Journal of Nanomedicine, 14, 5051-5060, 2019. DOI: 10.2147/IJN.S208713**, I declare, as co-author that:

I ACCEPT and AUTHORIZE the use of this publication/article as part of the Doctoral Thesis.

Additionally, I declare that I have NEITHER ACCEPTED NOR AUTHORIZED NOR USED this publication/article as part of the documents of a different Doctoral Thesis at the University of Granada or at any other University. Furthermore, I RESIGN myself to accept/authorize/use it in a future Doctoral Thesis at the University of Granada and or any other University.

Franca Ferrari

Department of Drug Sciences, Faculty of Pharmacy, University of Pavia, Pavia, 27100, Italy



Mail priva di virus. www.avast.com

Asunto: Fwd: Artículo Montmorillonite norfloxacin...

De: angela faccendini <angela.faccendini@gmail.com>

Fecha: 04/11/2020 9:20

Para: cviseras@ugr.es

AUTHORIZATION AND WITHDRAWAL FROM CO-AUTHORS OF A SCIENTIFIC PUBLICATION SUBMITTED AS PART OF A DOCTORAL THESIS

TO: International School for Postgraduate Studies, University of Granada

Regarding the deposit and defense of the Doctoral Thesis of Ms. Fátima García Villén entitled Aplicaciones Farmacéuticas de aluminosilicatos mesoporosos: estudio de arcillas fibrosas (sepiolita y palygorskita) en geles con agua mineromedicinal (**Pharmaceutical Applications of mesoporous aluminosilicates: study of fibrous clay minerals (sepiolite and palygorskite) in spring water hydrogels**) which contains the publication/article **Montmorillonite-norfloxacin nanocomposite intended for healing of infected wounds. International Journal of Nanomedicine, 14, 5051-5060, 2019. DOI: 10.2147/IJN.S208713**, I declare, as co-author that:

I ACCEPT and AUTHORIZE the use of this publication/article as part of the Doctoral Thesis.

Additionally, I declare that I have NEITHER ACCEPTED NOR AUTHORIZED NOR USED this publication/article as part of the documents of a different Doctoral Thesis at the University of Granada or at any other University. Furthermore, I RESIGN myself to accept/authorize/use it in a future Doctoral Thesis at the University of Granada and or any other University.

ANGELA FACCELDINI

Department of Drug Sciences, Faculty of Pharmacy, University of Pavia, Pavia, 27100, Italy

--

Angela Faccendini, Ph.D. student

Department of Drug Sciences,
University of Pavia,
V.le Taramelli 12,
27100 Pavia - Italy

Phone: +39 331 213 9389

Asunto: Re: Artículo Montmorillonite norfloxacin...

De: Maria Cristina Bonferoni <mariacristina.bonferoni@unipv.it>

Fecha: 04/11/2020 20:20

Para: César Viseras <cviseras@ugr.es>

AUTHORIZATION AND WITHDRAWAL FROM CO-AUTHORS OF A SCIENTIFIC PUBLICATION SUBMITTED AS PART OF A DOCTORAL THESIS

TO: International School for Postgraduate Studies, University of Granada

Regarding the deposit and defense of the Doctoral Thesis of Ms. Fátima García Villén entitled Aplicaciones Farmacéuticas de aluminosilicatos mesoporosos: estudio de arcillas fibrosas (sepiolita y palygorskita) en geles con agua mineromedicinal (**Pharmaceutical Applications of mesoporous aluminosilicates: study of fibrous clay minerals (sepiolite and palygorskite) in spring water hydrogels**) which contains the publication/article **Montmorillonite-norfloxacin nanocomposite intended for healing of infected wounds. International Journal of Nanomedicine, 14, 5051-5060, 2019. DOI: 10.2147/IJN.S208713**, I declare, as co-author that:

I ACCEPT and AUTHORIZE the use of this publication/article as part of the Doctoral Thesis.

Additionally, I declare that I have NEITHER ACCEPTED NOR AUTHORIZED NOR USED this publication/article as part of the documents of a different Doctoral Thesis at the University of Granada or at any other University. Furthermore, I RESIGN myself to accept/authorize/use it in a future Doctoral Thesis at the University of Granada and or any other University.

Cristina Bonferoni

ACEPTACIONES Y RENUNCIAS TRABAJO 6



UNIVERSIDAD
DE GRANADA



ACEPTACION Y RENUNCIA DE LOS COAUTORES DE LA PUBLICACION

Publicación: **Design and characterization of spring water hydrogels with natural inorganic excipients.** Applied Clay Science, 197, 105772, 2020. DOI: 10.1016/j.clay.2020.105772

Los coautores:

D/D ^a .	Rita Sánchez Espejo
D/D ^a .	Alberto López Galindo
D/D ^a .	Pilar Cerezo González
D/D ^a .	César Viseras

declaran que:

ACEPTAN y AUTORIZAN la utilización de dicha publicación/artículo como parte de la documentación de depósito y defensa de la tesis doctoral de D./D^a. Fátima García Villén titulada **Aplicaciones Farmacéuticas de aluminosilicatos mesoporosos: estudio de arcillas fibrosas (sepiolita y palygorskita) en geles con agua mineromedicinal,**

NO HAN UTILIZADO dicha publicación/artículo como parte de la documentación de depósito y defensa de otra tesis doctoral y/ o RENUNCIAN a utilizarlo en una futura tesis doctoral.

En Granada, a 03 de noviembre de 2020

Fdo.:

Fdo.:



Fdo.: Pilar Cerezo González

Fdo.:

César Viseras

Alberto López Galindo

ACEPTACIONES Y RENUNCIAS TRABAJO 7



UNIVERSIDAD
DE GRANADA

Escuela
Internacional
de Posgrado

ACEPTACION Y RENUNCIA DE LOS COAUTORES DE LA PUBLICACION

Publicación: **Wound healing activity of nanoclay/spring water hydrogels.** Pharmaceutics, 12, 5, 467, 2020. DOI: 10.3390/pharmaceutics12050467

Los coautores:

D/D ^a .	Rita Sánchez Espejo
D/D ^a .	Ana Borrego Sánchez
D/D ^a .	Pilar Cerezo González
D/D ^a .	César Viseras

declaran que:

ACEPTAN y AUTORIZAN la utilización de dicha publicación/artículo como parte de la documentación de depósito y defensa de la tesis doctoral de D./D^a. Fátima García Villén titulada **Aplicaciones Farmacéuticas de aluminosilicatos mesoporosos: estudio de arcillas fibrosas (sepiolita y palygorskita) en geles con agua mineromedicinal,**

NO HAN UTILIZADO dicha publicación/artículo como parte de la documentación de depósito y defensa de otra tesis doctoral y/o RENUNCIAN a utilizarlo en una futura tesis doctoral.

En Granada, a 03 de noviembre de 2020

Fdo.:

Fdo.:

Fdo.:

Fdo.:

Asunto: Re: Artículo Wound Healing activity... **De:**
Silvia Rossi <silviastefania.rossi@unipv.it> **Fecha:**
04/11/2020 19:56
Para: César Viseras <cviseras@ugr.es>

AUTHORIZATION AND WITHDRAWAL FROM CO-AUTHORS OF A SCIENTIFIC PUBLICATION
SUBMITTED AS
PART OF A DOCTORAL THESIS

TO: International School for Postgraduate Studies, University of Granada

Regarding the deposit and defense of the Doctoral Thesis of Ms. Fátima García Villén entitled Aplicaciones Farmacéuticas de aluminosilicatos mesoporosos: estudio de arcillas fibrosas (sepiolita y palygorskita) en geles con agua mineromedicinal (**Pharmaceutical Applications of mesoporous aluminosilicates: study of fibrous clay minerals (sepiolite and palygorskite)** in spring water hydrogels) which contains the publication/article **Wound healing activity of nanoclay/spring water hydrogels. Pharmaceutics, 12, 5, 467, 2020. DOI: 10.3390/pharmaceutics12050467**, I declare, as co-author that:

I ACCEPT and AUTHORIZE the use of this publication/article as part of the Doctoral Thesis.

Additionally, I declare that I have NEITHER ACCEPTED NOR AUTHORIZED NOR USED this publication/article as part of the documents of a different Doctoral Thesis at the University of Granada or at any other University. Furthermore, I RESIGN myself to accept/authorize/use it in a future Doctoral Thesis at the University of Granada and or any other University.

Silvia Rossi

Department of Drug Sciences, Faculty of Pharmacy, University of Pavia, Pavia, 27100, Italy

Asunto: Fwd: Articolo Wound healing activity....

De: marco.ruggeri02@universitadipavia.it

Fecha: 04/11/2020 19:51

Para: César Viseras <cviseras@ugr.es>

Ecco l'altra autorizzazione,

Buona serata,

Marco

AUTHORIZATION AND WITHDRAWAL FROM CO-AUTHORS OF A SCIENTIFIC PUBLICATION SUBMITTED AS PART OF A DOCTORAL THESIS

TO: International School for Postgraduate Studies, University of Granada

Regarding the deposit and defense of the Doctoral Thesis of Ms. Fátima García Villén entitled Aplicaciones Farmacéuticas de aluminosilicatos mesoporosos: estudio de arcillas fibrosas (sepiolita y palygorskita) en geles con agua mineromedicinal (**Pharmaceutical Applications of mesoporous aluminosilicates: study of fibrous clay minerals (sepiolite and palygorskite)** in spring water hydrogels) which contains the publication/article **Wound healing activity of nanoclay/spring water hydrogels. *Pharmaceutics*, 12, 5, 467, 2020. DOI: 10.3390/pharmaceutics12050467**, I declare, as co-author that:

I ACCEPT and AUTHORIZE the use of this publication/article as part of the Doctoral Thesis.

Additionally, I declare that I have NEITHER ACCEPTED NOR AUTHORIZED NOR USED this publication/article as part of the documents of a different Doctoral Thesis at the University of Granada or at any other University. Furthermore, I RESIGN myself to accept/authorize/use it in a future Doctoral Thesis at the University of Granada and or any other University.

MARCO RUGGERI

Department of Drug Sciences, Faculty of Pharmacy, University of Pavia, Pavia, 27100, Italy

Asunto: R: Artículo Wound healing activity....

De: <g.sandri@unipv.it>

Fecha: 04/11/2020 18:57

Para: 'César Viseras' <cviseras@ugr.es>

CC: 'Fátima García Villén' <fgarvillen@ugr.es>

Prof. Giuseppina Sandri, PhD
Department of Drug Sciences,
University of Pavia,
Viale Taramelli 12,
27100 Pavia – Italy

Tel 00390382987728
e-mail giuseppina.sandri@unipv.it

AUTHORIZATION AND WITHDRAWAL FROM CO-AUTHORS OF A SCIENTIFIC PUBLICATION SUBMITTED AS PART OF A DOCTORAL THESIS

TO: International School for Postgraduate Studies, University of Granada

Regarding the deposit and defense of the Doctoral Thesis of Ms. Fátima García Villén entitled Aplicaciones Farmacéuticas de aluminosilicatos mesoporosos: estudio de arcillas fibrosas (sepiolita y palygorskita) en geles con agua mineromedicinal (**Pharmaceutical Applications of mesoporous aluminosilicates: study of fibrous clay minerals (sepiolite and palygorskite) in spring water hydrogels**) which contains the publication/article **Wound healing activity of nanoclay/spring water hydrogels. *Pharmaceutics*, 12, 5, 467, 2020. DOI: 10.3390/pharmaceutics12050467**, I declare, as co-author that:

I ACCEPT and AUTHORIZE the use of this publication/article as part of the Doctoral Thesis.

Additionally, I declare that I have NEITHER ACCEPTED NOR AUTHORIZED NOR USED this publication/article as part of the documents of a different Doctoral Thesis at the University of Granada or at any other University. Furthermore, I RESIGN myself to accept/authorize/use it in a future Doctoral Thesis at the University of Granada and or any other University.

Giuseppina Sandri

Department of Drug Sciences, Faculty of Pharmacy, University of Pavia, Pavia, 27100, Italy

Asunto: Fwd: Articulo Wound healing activity...
De: angela faccendini <angela.faccendini@gmail.com>
Fecha: 04/11/2020 9:18
Para: cviseras@ugr.es

AUTHORIZATION AND WITHDRAWAL FROM CO-AUTHORS OF A SCIENTIFIC PUBLICATION SUBMITTED AS PART OF A DOCTORAL THESIS

TO: International ~~School for Postgraduate Studies~~, University of Granada

Regarding the deposit and defense of the Doctoral Thesis of Ms. Fátima García Villén entitled Aplicaciones Farmacéuticas de aluminosilicatos mesoporosos: estudio de arcillas fibrosas (sepiolita y palygorskita) en geles con agua mineromedicinal (**Pharmaceutical Applications of mesoporous aluminosilicates: study of fibrous clay minerals (sepiolite and palygorskite) in spring water hydrogels**) which contains the publication/article **Wound healing activity of nanoclay/spring water hydrogels. Pharmaceutics, 12, 5, 467, 2020. DOI: 10.3390/pharmaceutics12050467**, I declare, as co-author that:

I ACCEPT and AUTHORIZE the use of this publication/article as part of the Doctoral Thesis.

Additionally, I declare that I have NEITHER ACCEPTED NOR AUTHORIZED NOR USED this publication/article as part of the documents of a different Doctoral Thesis at the University of Granada or at any other University. Furthermore, I RESIGN myself to accept/authorize/use it in a future Doctoral Thesis at the University of Granada and or any other University.

ANGELA FACCENDINI

Department of Drug Sciences, Faculty of Pharmacy, University of Pavia, Pavia, 27100, Italy

Angela Faccendini, Ph.D. student
Department of Drug Sciences,
University of Pavia,
V.le Taramelli 12,
27100 Pavia - Italy

Phone: +39 331 213 9389

--

Asunto: Fwd: Articulo Wound healing activity...
De: DALILA MIELE <dalila.miele01@universitadipavia.it>
Fecha: 04/11/2020 22:38
Para: cviseras@ugr.es

Dalila Miele, PhD
Department of Drug Sciences
University of Pavia
Via Taramelli, 12
27100- Pavia, Italy
Tel +39-0382 987392

AUTHORIZATION AND WITHDRAWAL FROM CO-AUTHORS OF A SCIENTIFIC PUBLICATION SUBMITTED AS PART OF A DOCTORAL THESIS

TO: [International School for Postgraduate Studies, University of Granada](#)

Regarding the deposit and defense of the Doctoral Thesis of Ms. Fátima García Villén entitled Aplicaciones Farmacéuticas de aluminosilicatos mesoporosos: estudio de arcillas fibrosas (sepiolita y palygorskita) en geles con agua mineromedicinal (**Pharmaceutical Applications of mesoporous aluminosilicates: study of fibrous clay minerals (sepiolite and palygorskite) in spring water hydrogels**) which contains the publication/article **Wound healing activity of nanoclay/spring water hydrogels. *Pharmaceutics*, 12, 5, 467, 2020. DOI: 10.3390/pharmaceutics12050467**, I declare, as co-author that:

I ACCEPT and AUTHORIZE the use of this publication/article as part of the Doctoral Thesis.

Additionally, I declare that I have NEITHER ACCEPTED NOR AUTHORIZED NOR USED this publication/article as part of the documents of a different Doctoral Thesis at the University of Granada or at any other University. Furthermore, I RESIGN myself to accept/authorize/use it in a future Doctoral Thesis at the University of Granada and or any other University.

DALILA MIELE

Department of Drug Sciences, Faculty of Pharmacy, University of Pavia, Pavia, 27100, Italy

ACEPTACIONES Y RENUNCIAS TRABAJO 8



UNIVERSIDAD
DE GRANADA



ACEPTACION Y RENUNCIA DE LOS COAUTORES DE LA PUBLICACION

Publicación: **Safety of nanoclay/spring water hydrogels: Assessment and mobility of hazardous elements.** Pharmaceutics, 12, 8, 764, 1-17. DOI: 10.3390/pharmaceutics12080764

Los coautores:

D/D ^a .	Rita Sánchez Espejo
D/D ^a .	Ana Borrego Sánchez
D/D ^a .	Pilar Cerezo González
D/D ^a .	César Viseras

declaran que:

ACEPTAN y AUTORIZAN la utilización de dicha publicación/artículo como parte de la documentación de depósito y defensa de la tesis doctoral de D./D^a. Fátima García Villén titulada **Aplicaciones Farmacéuticas de aluminosilicatos mesoporosos: estudio de arcillas fibrosas (sepiolita y palygorskita) en geles con agua mineromedicinal,**

NO HAN UTILIZADO dicha publicación/artículo como parte de la documentación de depósito y defensa de otra tesis doctoral y/ o RENUNCIAN a utilizarlo en una futura tesis doctoral.

En Granada, a 03 de noviembre de 2020

Fdo.:

Fdo.:

Fdo.:

Fdo.:

Asunto: R: artículo di Fatima

De: Luana Perioli <luana.perioli@unipg.it>

Fecha: 04/11/2020 12:14

Para: César Viseras <cviseras@ugr.es>

AUTHORIZATION AND WITHDRAWAL FROM CO-AUTHORS OF A SCIENTIFIC PUBLICATION SUBMITTED AS PART OF A DOCTORAL THESIS

TO: International School for Postgraduate Studies, University of Granada

Regarding the deposit and defense of the Doctoral Thesis of Ms. Fátima García Villén entitled Aplicaciones Farmacéuticas de aluminosilicatos mesoporosos: estudio de arcillas fibrosas (sepiolita y palygorskita) en geles con agua mineromedicinal (**Pharmaceutical Applications of mesoporous aluminosilicates: study of fibrous clay minerals (sepiolite and palygorskite) in spring water hydrogels**) which contains the publication/article **Safety of nanoclay/spring water hydrogels: Assessment and mobility of hazardous elements. Pharmaceutics, 12, 8, 764, 1-17. DOI: 10.3390/pharmaceutics12080764**, I declare, as co-author that:

I ACCEPT and AUTHORIZE the use of this publication/article as part of the Doctoral Thesis.

Additionally, I declare that I have NEITHER ACCEPTED NOR AUTHORIZED NOR USED this publication/article as part of the documents of a different Doctoral Thesis at the University of Granada or at any other University. Furthermore, I RESIGN myself to accept/authorize/use it in a future Doctoral Thesis at the University of Granada and or any other University.

Luana Perioli

Department of I s, University of Perugia, via del Liceo 1, Perugia, 06123, Italy

ACEPTACIONES Y RENUNCIAS TRABAJO 9



UNIVERSIDAD
DE GRANADA

Escuela
Internacional
de Posgrado

ACEPTACION Y RENUNCIA DE LOS COAUTORES DE LA PUBLICACION

Publicación: **Correlation between elemental composition/mobility and skin cell proliferation of fibrous nanoclay/spring water hydrogels.** Pharmaceutics, 12, 9, 891, 1-20, 2020. DOI: 10.3390/pharmaceutics12090891

Los coautores:

D/D ^a .	Rita Sánchez Espejo
D/D ^a .	Ana Borrego Sánchez
D/D ^a .	Pilar Cerezo González
D/D ^a .	César Viseras

declaran que:

ACEPTAN y AUTORIZAN la utilización de dicha publicación/artículo como parte de la documentación de depósito y defensa de la tesis doctoral de D./D^a. Fátima García Villén titulada **Aplicaciones Farmacéuticas de aluminosilicatos mesoporosos: estudio de arcillas fibrosas (sepiolita y palygorskita) en geles con agua mineromedicinal,**

NO HAN UTILIZADO dicha publicación/artículo como parte de la documentación de depósito y defensa de otra tesis doctoral y/ o RENUNCIAN a utilizarlo en una futura tesis doctoral.

En Granada, a 03 de noviembre de 2020

Fdo.:

Fdo.:

Fdo.:

Fdo.:

Asunto: Re: terza mail
De: Sandri Giuseppina <g.sandri@unipv.it>
Fecha: 04/11/2020 7:43
Para: César Viseras <cviseras@ugr.es>

Ahia scusa
Provvedo
Dobbiamo anche sentirci per Ele
Più tardi?

Inviato da iPhone

AUTHORIZATION AND WITHDRAWAL FROM CO-AUTHORS OF A SCIENTIFIC PUBLICATION SUBMITTED AS PART OF A DOCTORAL THESIS

TO: International School for Postgraduate Studies, University of Granada

Regarding the deposit and defense of the Doctoral Thesis of Ms. Fátima García Villén entitled Aplicaciones Farmacéuticas de aluminosilicatos mesoporosos: estudio de arcillas fibrosas (sepiolita y palygorskita) en geles con agua mineromedicinal (**Pharmaceutical Applications of mesoporous aluminosilicates: study of fibrous clay minerals (sepiolite and palygorskite) in spring water hydrogels**) which contains the publication/article **Correlation between elemental composition/mobility and skin cell proliferation of fibrous nanoclay/spring water hydrogels. *Pharmaceutics*, 12, 9, 891, 1-20, 2020. DOI: 10.3390/pharmaceutics12090891**, I declare, as co-author that:

I ACCEPT and AUTHORIZE the use of this publication/article as part of the Doctoral Thesis.

Additionally, I declare that I have NEITHER ACCEPTED NOR AUTHORIZED NOR USED this publication/article as part of the documents of a different Doctoral Thesis at the University of Granada or at any other University. Furthermore, I RESIGN myself to accept/authorize/use it in a future Doctoral Thesis at the University of Granada and or any other University.

Giuseppina Sandri

Department of Pharmaceutical Sciences, Faculty of Pharmacy, University of Pavia, viale Taramelli 12, Pavia, 27100, Italy

Asunto: Re: Articolo da Granada per Tesi di dottorato
De: Lucia Cucca <luca.cucca@unipv.it>
Fecha: 04/11/2020 9:23
Para: César Viseras <cviseras@ugr.es>

Gentilissimo buongiorno,

ecco la dichiarazione
Cordiali saluti

Lucia Cucca

AUTHORIZATION AND WITHDRAWAL FROM CO-AUTHORS OF A SCIENTIFIC PUBLICATION SUBMITTED AS PART OF A DOCTORAL THESIS

TO: International School for Postgraduate Studies, University of Granada

Regarding the deposit and defense of the Doctoral Thesis of Ms. Fátima García Villén entitled Aplicaciones Farmacéuticas de aluminosilicatos mesoporosos: estudio de arcillas fibrosas (sepiolita y palygorskita) en geles con agua mineromedicinal (**Pharmaceutical Applications of mesoporous aluminosilicates: study of fibrous clay minerals (sepiolite and palygorskite) in spring water hydrogels**) which contains the publication/article **Correlation between elemental composition/mobility and skin cell proliferation of fibrous nanoclay/spring water hydrogels. Pharmaceutics, 12, 9, 891, 1-20, 2020. DOI: 10.3390/pharmaceutics12090891**, I declare, as co-author that:

I ACCEPT and AUTHORIZE the use of this publication/article as part of the Doctoral Thesis.

Additionally, I declare that I have NEITHER ACCEPTED NOR AUTHORIZED NOR USED this publication/article as part of the documents of a different Doctoral Thesis at the University of Granada or at any other University. Furthermore, I RESIGN myself to accept/authorize/use it in a future Doctoral Thesis at the University of Granada and or any other University.

Lucia Cucca

Department of Chemistry, University of Pavia, viale Taramelli 12, Pavia, 27100, Italy